

**AD-A277 925**



94-10832



**1995 GRADUATE HANDBOOK**

374-8 (1)

**SEASOAR and CTD Observations During a COARE Surveys Cruise,  
W9211C, 22 January to 22 February 1993.**

A. Huyer, P.M. Kosro,  
R. O'Malley, J. Fleischbein

College of Oceanic and Atmospheric Sciences  
Oregon State University  
Corvallis, Oregon 97331-5503

Data Report 154  
Reference 93-2  
October 1993

Accesion For	
NTIS	CRA&I
DTIC	TAB
U.announced	<input type="checkbox"/>
Justification .....	
By .....	
Distribution / .....	
Availability Codes	
Dist	Avail and / or Special
A-1	

DTIC QUALITY INSPECTED 3

## Table of Contents

<b>Introduction</b>	<b>1</b>
<b>Cruise Narrative</b>	<b>6</b>
<b>CTD Data Acquisition, Calibration and Data Processing</b>	<b>13</b>
<b>Seasoar Data Acquisition and Preliminary Processing</b>	<b>15</b>
<b>Seasoar Conductivity Calibration</b>	<b>15</b>
<b>Post-Processing of Seasoar Data</b>	<b>21</b>
<b>Background</b>	<b>21</b>
<b>Procedures</b>	<b>28</b>
<b>Data Presentation</b>	<b>31</b>
<b>CTD/Seasoar Comparison</b>	<b>31</b>
<b>Acknowledgments</b>	<b>32</b>
<b>References</b>	<b>32</b>
<b>CTD Data</b>	<b>33</b>
<b>Seasoar Trajectories</b>	<b>47</b>
<b>Ensemble Profiles of Seasoar Temperature and Salinity</b>	<b>99</b>
<b>N2S</b>	<b>100</b>
<b>W2E</b>	<b>124</b>
<b>E2N</b>	<b>136</b>
<b>SBN to Equator</b>	<b>148</b>
<b>Vertical Sections of Temperature, Salinity and Sigma-t</b>	<b>149</b>
<b>N2S Temperature</b>	<b>150</b>
<b>Salinity</b>	<b>162</b>
<b>Sigma-t</b>	<b>174</b>
<b>S2W Temperature</b>	<b>186</b>
<b>Salinity</b>	<b>198</b>
<b>Sigma-t</b>	<b>210</b>

<b>Vertical Sections of Temperature, Salinity and Sigma-t (Cont'd)</b>	
<b>W2E Temperature</b>	<b>222</b>
<b>Salinity</b>	<b>234</b>
<b>Sigma-t</b>	<b>246</b>
<b>E2N Temperature</b>	<b>258</b>
<b>Salinity</b>	<b>270</b>
<b>Sigma-t</b>	<b>282</b>
<b>SBN to Equator</b>	<b>294</b>
<b>Appendix A:</b>	
<b>Time Series of Maximum T/C Correlations and Lags for Seasoar Tows 2-6</b>	<b>297</b>
<b>Appendix B:</b>	
<b>T-S Diagrams from CTD and Seasoar at Start and End of Tows 2-6.</b>	<b>315</b>

## SEASOAR and CTD Observations During a COARE Surveys Cruise, W9211C, 22 January to 22 February 1993.

### Introduction

An international Coupled Ocean-Atmosphere Response Experiment (COARE) was conducted in the warm-pool region of the western equatorial Pacific Ocean over a four-month period from November 1992 through February 1993 (Webster and Lukas, 1992). Most of the oceanographic and meteorological observations were concentrated in the Intensive Flux Array (IFA) centered at 1° 45'S, 156°00'E. As part of this experiment, the R/V Wecoma conducted three survey cruises on the R/V Wecoma; each cruise included measurements of the temperature, salinity and velocity distribution in the upper 300 m of the ocean, and continuous meteorological measurements of wind, air temperature, humidity, etc. Most of these measurements were along a butterfly pattern that was sampled repeatedly during the three COARE Surveys cruises, W9211A and W9211B, and W9211C.

Coordinates of the Standard Butterfly Pattern were chosen to measure zonal and meridional gradients across the center of the IFA, spanning the profiling current meter array, while avoiding moorings and stationary ships without frequent deviations from our track (Figure 1). The standard coordinates of the butterfly apexes are:

SBN	1°14'S	156°06'E
SBS	2°26'S	156°06'E
SBW	1°50'S	155°30'E
SBE	1°50'S	156°42'E,

and sampling was done sequentially along the track joining these four points, i.e. along a meridional section (N2S) from SBN to SBS, a diagonal section (S2W) from SBS to SBW, a zonal section (W2E) from SBW to SBE, and a diagonal section (E2N) from SBE to SBN to complete the pattern. Along this track, we measured the upper ocean temperature and salinity by means of a towed undulating Seasoor vehicle (Figure 2) equipped with a SeaBird CTD system, while underway at 7-8 knots. CTD casts were made at the beginning and end of each tow, primarily to check calibration of the Seasoor sensors. Water velocity along the ship's track was measured by means of the ship-borne acoustic Doppler current profiler.

This report summarizes the Seasoor and CTD observations from Wecoma's third COARE Surveys cruise, W9211C. It also provides a cruise narrative, and a brief description of the data processing procedures.

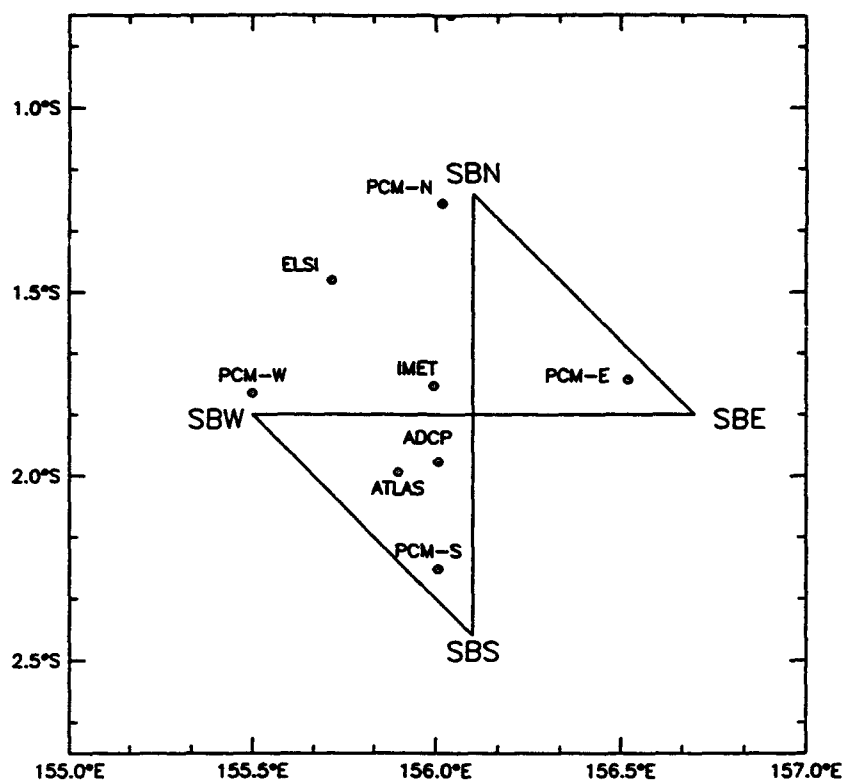


Figure 1. The Standard Butterfly Pattern in relation to the moorings of the COARE Intensive Flux Array.

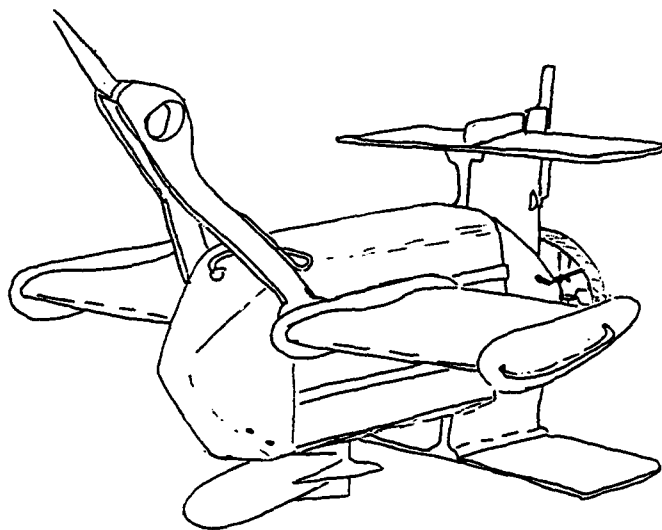


Figure 2. Sketch of the Seasoor vehicle used during W9211C.

Table 1. Summary of CTD stations during W9211C.

Date	Time (UTC)	Station No.	Latitude	Longitude	Wind Dir. (T)	Wind Spd. (kts)	Atmos. P. (mbar)
26 Jan	1439	1	03°07.4'N	156°07.1'E	260	10	1005.8
27 Jan	0725	2	01°14.0'S	156°06.0'	310	8	1006.8
29 Jan	0540	3	02°27.2'	156°07.8'	300	9	1007.2
29 Jan	0750	4	02°22.0'	156°02.0	320	11	1008.3
3 Feb	2035	5	01°51.3'	155°30.3'	340	20	1010.8
3 Feb	2159	6	01°51.2'	155°34.1'	350	19	1012.3
7 Feb	0003	7	01°17.2'	156°09.6'	340	10	1010.7
7 Feb	1930	8	01°14.0'	156°06.0'	340	12	1008.4
12 Feb	2059	9	02°00.4'	155°40.4'	335	13	1009.6
12 Feb	2320	10	02°00.3'	155°40.7'	330	15	1010.0
13 Feb	0440	11	01°59.3'	155°43.4'	310	10	1007.2
16 Feb	2130	12	00°08.7'S	156°06.1'E	070	10	1010.3

Table 2. Instruments and sensors used for CTD, Seasoar, and underway salinity sampling, W9211C, and date of most recent manufacturer's pre-cruise calibration.

System (Instrument)	Sensor	Pre-Cruise Calibration Date	
CTD (SBE 9/11 plus SN 0256)	P	50130	5 Mar 92
	T1	1364	6 Oct 92 (modified 2 Dec 92)
	T2	1366	6 Oct 92 (modified 2 Dec 92)
	C1	1018	16 Sept 92
	C2	1021	16 Sept 92
Seasoar (SBE 9/11 plus SN 2843) (Tows 1-6)	P	39107	5 Mar 92
	C1	1030	17 Apr 92
	C2	1041	24 Apr 92
	T1	1367	27 Mar 92 (modified 2 Dec 92)
	T2	1369	27 Mar 92 (modified 2 Dec 92)
(Tows 4-6)	T1	997	6 Oct 92 (modified 2 Dec 92)
	T2	1384	6 Oct 92 (modified 2 Dec 92)
5-m Intake (MIDAS)	T	854	10 Aug 90
	C	1070	23 Sept 92

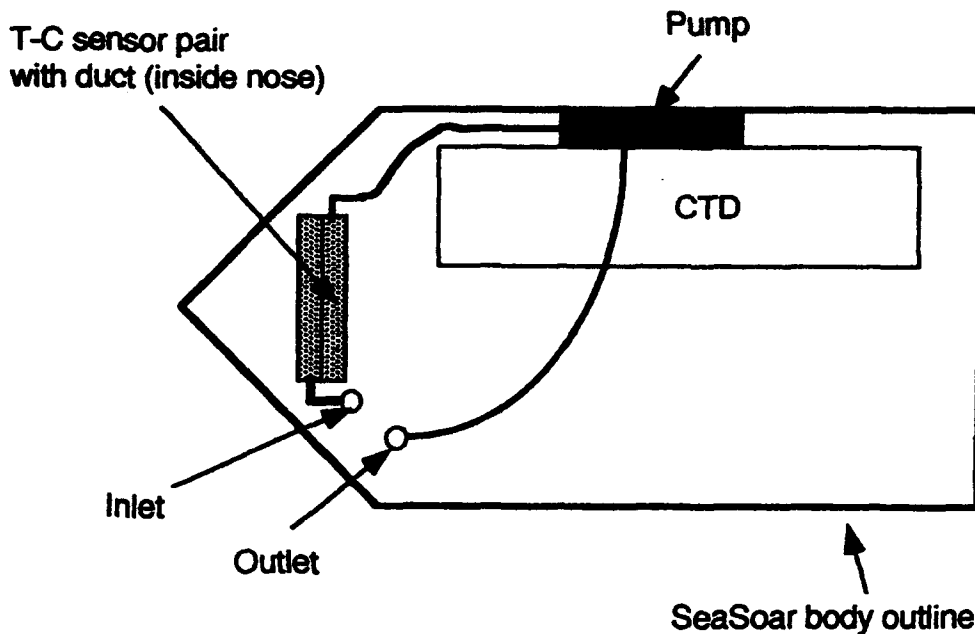


Figure 3. Schematic of the plumbing of the ducted T/C sensors inside the SeaSoar vehicle. Primary sensor inlet and outlet ports were on the starboard side of the SeaSoar nose; secondary sensor ports were on the port side. During Tow 2, both ducts were disconnected at the outlet from the pump; during Tow 4, the secondary sensor duct was disconnected at the outlet port.

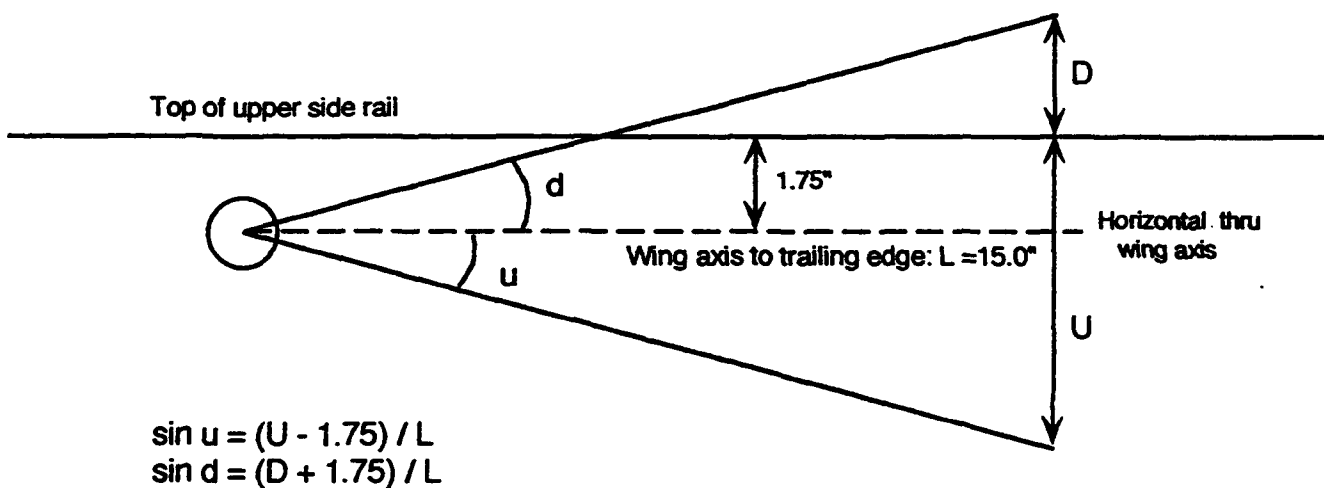


Figure 4. Schematics of SeaSoar wing angle settings. During Tows 1 and 2, the value of D was  $2\frac{3}{8}$ " and U was  $7\frac{5}{8}$ ", yielding an up-angle of  $23^\circ$  and a down-angle of  $16^\circ$ . During Tows 3 through 6, D was  $2\frac{5}{8}$ " and U was  $7\frac{3}{8}$ ", yielding an up-angle of  $22^\circ$  and a down-angle of  $17^\circ$ .

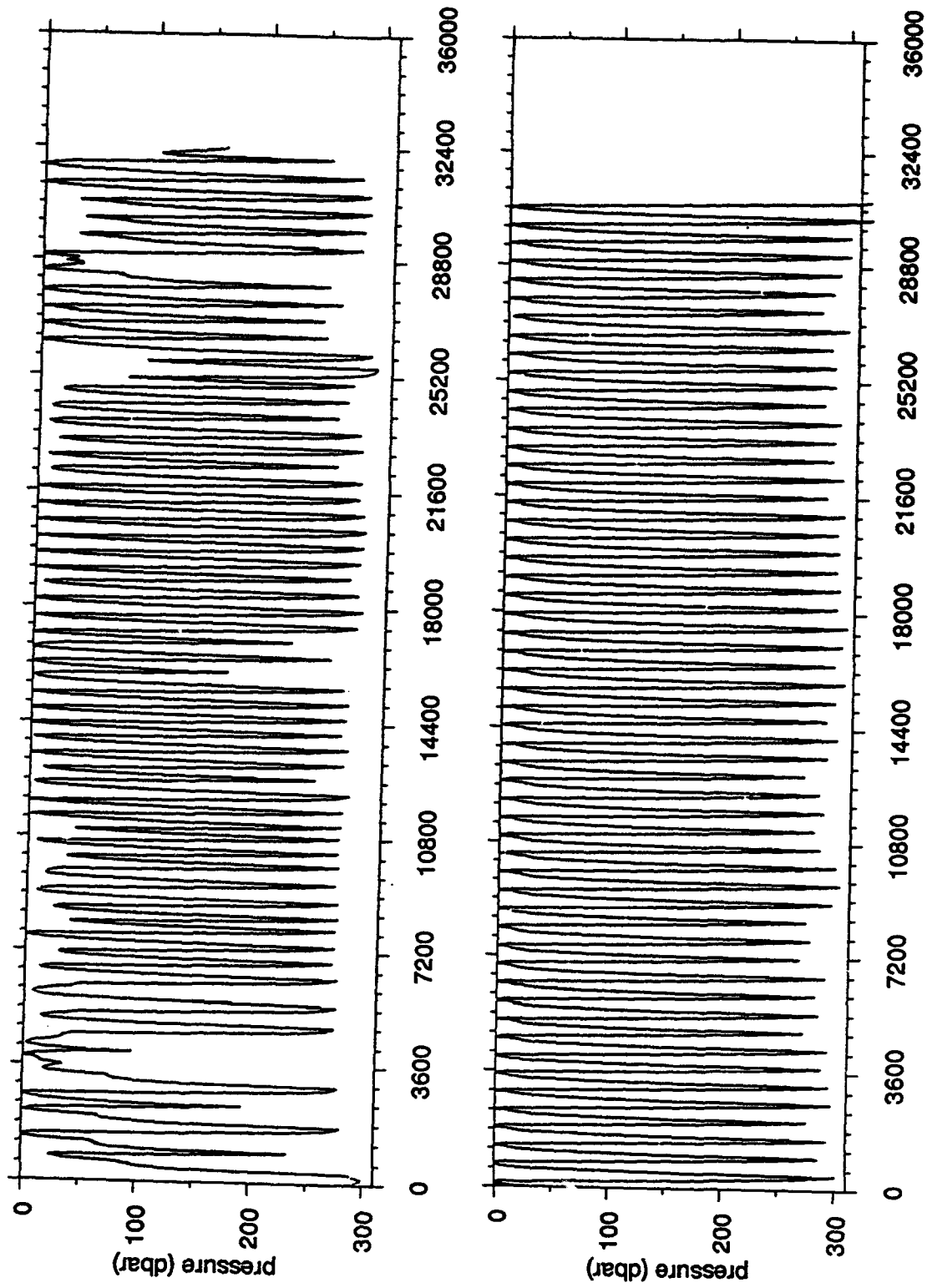


Figure 5. Examples of Seasoor trajectory (pressure vs. time in seconds) before and after changing the wing angle setting to from a maximum down-angle of  $16^\circ$  to a maximum down-angle of  $17^\circ$ .  
Top: the N2S section on 28 January during Tow 2. Bottom: the W2E section on 31 January during Tow 3.

## Cruise Narrative, W9211C

We coma departed from Guam about 0000 UTC, 22 Jan 1993, and began a transit to 3°N, 156°E where we intended to begin a cross-equatorial Seasoar section. After arrival on 26 January, we made a pre-tow CTD cast (Station 1, Table 1) with an SBE 9/11 plus CTD with dual ducted temperature and conductivity sensors (Table 2). Seasoar was deployed for Tow 1 at about 0600 UTC, 26 Jan at 3°08'N, 156°07'E; the Seasoar vehicle (Figure 2) was equipped with an SBE 9/11plus CTD (SN 0256) with dual ducted temperature and conductivity sensors (Table 2; Figure 3). Tow 1 began normally, but in about 10 minutes the vehicle stopped responding to the control signal, and Seasoar was recovered on deck about 0845 UTC, 26 Jan. There was no evidence of a leak in the hydraulic unit, but it had definitely lost its power (after working successfully for more than 800 hours of consecutive towing in W9211A and W9211B). We then proceeded directly to the COARE Intensive Flux Array to begin sampling along the Standard Butterfly Pattern (Figure 1).

A new hydraulic unit (SN 011) was installed in the Seasoar vehicle, and the pushrods were adjusted to set the wing-angle so that the maximum up-angle was 23° and the maximum down-angle was 16° (Figure 4).

When we arrived at SBN, the northern apex of the Standard Butterfly Pattern, we made a pre-tow CTD cast to 500 m (Station 2, Table 1) and then deployed Seasoar at about 0845 UTC, 27 January. Tow 2 began southward toward SBS along the N2S line and continued along the Standard Butterfly in the usual direction (Table 3); for a 12-km portion of the line between SBE and SBN, the Seasoar was kept at depths below 30 m to avoid contamination from emptying the ship's tanks. The Seasoar vehicle was very difficult to control in the presence of strong vertical shear, so the resulting trajectories were quite irregular (e.g., Figure 5); we tentatively concluded that the 16° down-angle was too shallow. Preliminary temperature and salinity profiles and T-S diagrams showed there was a flow-rate problem through both T-C ducts from about the beginning of Tow 2, particularly during descent. Seasoar was recovered at SBS at about 0500 UTC, 29 January and we found that the outflow from the pumps was not connected to the tubes leading to the outlet ports through the nose of the vehicle (Figure 3); instead, the outflow from both sensor ducts was about 10 inches above the intake and into the interior of the Seasoar vehicle during Tow 2. CTD Station 3 (Table 1) was completed immediately after recovery.

After Tow 2, we changed the Seasoar wing angle setting to yield a maximum up-angle of 22° and a maximum down-angle of 17° (Figure 4) and reinstalled the CTD, checking the continuity of both sensor ducts with running

**Table 3. Times (UTC) of standard waypoints during Tow 2 of W9211C.**  
 Positions of these waypoints are: SBN ( $1^{\circ}14'S$ ,  $156^{\circ}06'E$ ); SBS ( $2^{\circ}26'S$ ,  $156^{\circ}06'E$ );  
 SBW ( $1^{\circ}50'S$ ,  $155^{\circ}30'E$ ); SBE ( $1^{\circ}50'S$ ,  $156^{\circ}42'E$ ).

	Begin/End	SBN	SBS	SBW	SBE
27 January	0846	0917	1827		
28 January				0143	1207
28 January		1930			
29 January			0430		
29 January	0503				

**Table 4. Times (UTC) of standard waypoints during Tow 3 of W9211C.**

	Begin/End	SBN	SBS	SBW	SBE
29 January	0920			1646	
30 January					0225
30 January		0945	1926		
31 January				0238	1112
31 January		1827			
1 February			0358	1124	2015
2 February		0320	1221	1925	
2 February	2004				

**Table 5. Times (UTC) of standard waypoints during Tow 4 of W9211C.**

	Begin/End	SBN	SBS	SBW	SBE
3 February	1306			1410	2304
4 February		0604	1524	2230	
5 February					0719
5 February		1425			
6 February			0015	0747	1641
6 February	2315				

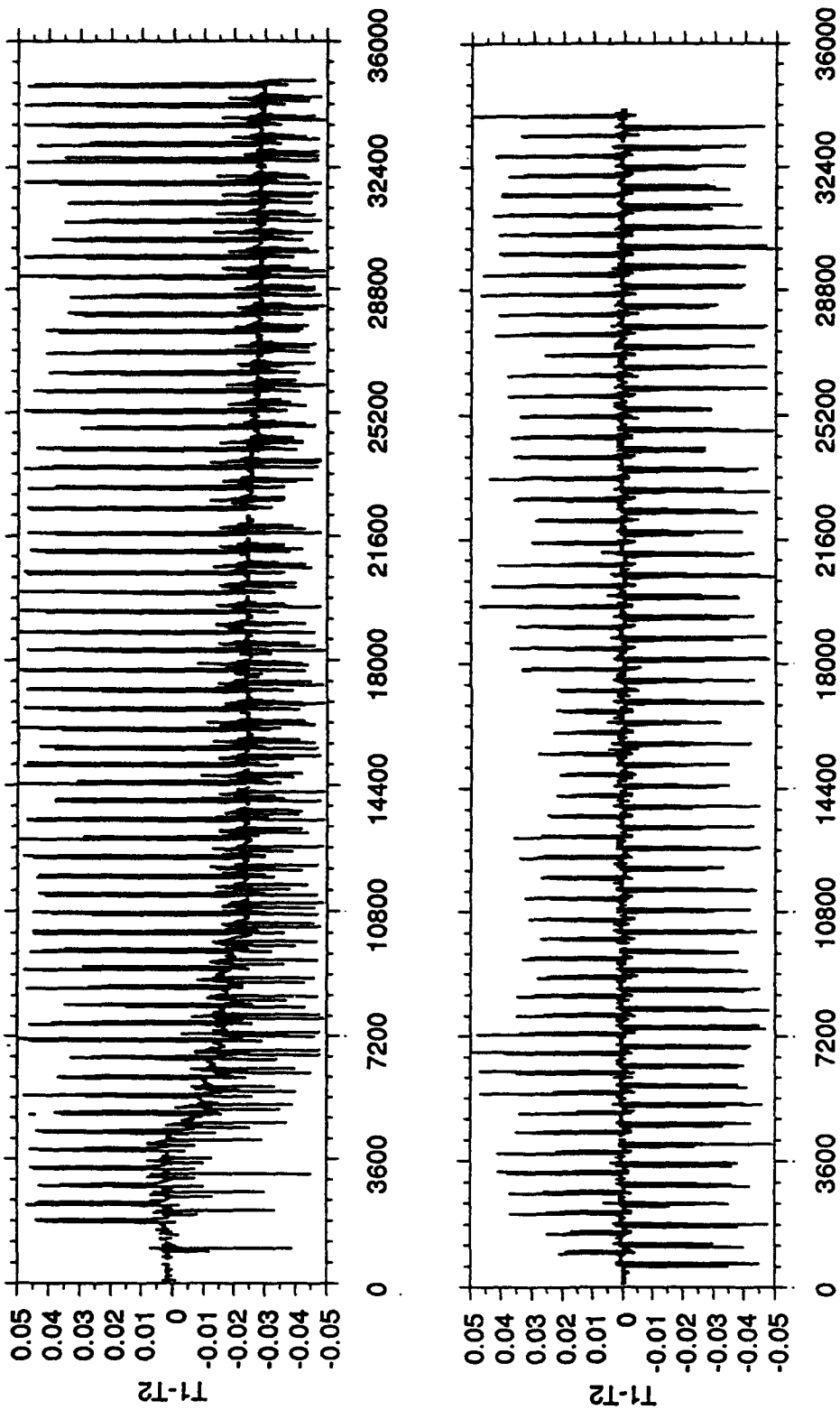


Figure 6. Time series of the preliminary temperature differences before and after changing both primary and secondary temperature sensors in *Seasoar*; high frequency fluctuations seem to be due to vehicle roll, i.e., to small differences in the depth of the two sensors. Top: the difference between sensors SN 1364 and 1366 during the W2E section on 29 January; sensor 1366 malfunctioned. Bottom: the difference between sensors SN 997 and 1384 during the W2E section on 11 February.

**Table 6.** Times (UTC) of standard waypoints during Tow 5 of W9211C.

	Begin/End	SBN	SBS	SBW	SBE
7 February	2058	2200			
8 February			0820	1524	
9 February					0114
9 February		0803	1824, 1921		
10 February				0200	1128
10 February		1819			
11 February			0452	1207	2135
12 February		0433	1456		
12 February	2036				

**Table 7.** Times (UTC) of standard waypoints during Tow 6 of W9211C.

	Begin/End	SBN	SBS	SBW	SBE
13 February	0551			0845	1856
14 February		0151	1139	1833	
15 February					0456
15 February		1137			
15 February	2047				

**Table 8.** Summary of Seasoor Tows, W9211C. Parameter values in the last column (for the T/C alignment offset, and for the amplitude and time constant of the thermal mass of the conductivity cell) were used for the preliminary (at-sea) data processing.

Tow No.	Start Time	Stop Time	Duration (hrs)	Parameters Measured	T/C Pair (and Parameter used for At-Sea Analysis)
1	01/26/0605	01/26/0840	0	P, T1, C1, T2, C2	T2, C2 (3.25, 0.045, 8.0)
2	01/27/0846	01/29/0500	50	P, T1*, C1*, T2*, C2*	T2, C2 (3.25, 0.045, 8.0)
3	01/29/0920	02/02/2004	106	P, T1, C1, T2, C2	T2, C2 (3.25, 0.045, 8.0)
4	02/03/1306	02/06/2315	80	P, T1, C1, T2*, C2*	T1, C1 (2.00, 0.045, 5.0)
5	02/07/2059	02/12/2033	118	P, T1, C1, T2, C2	T2, C2 (2.00, 0.045, 5.0)
6	02/13/0551	02/15/2045	62	P, T1, C1, T2, C2	T2, C2 (2.00, 0.045, 9.0)

\*Use data from ascending profiles only; outlet of T-C duct was into the interior of the Seasoor vehicle.

water. Tow 3 was deployed at about 0915 UTC, 29 January at  $2^{\circ}22'S$ ,  $156^{\circ}02'E$  near SBS immediately after CTD Station 4. Tow 3 began northwestward toward SBW along the S2W line, and continued along the Standard Butterfly Pattern in the usual direction (Table 4). The Seasoar trajectory (Figure 5) was greatly improved over the previous tow, presumably because of the  $1^{\circ}$  change in the wing-angle setting. Preliminary T-S diagrams showed that data quality from both sensor pairs was also greatly improved. Preliminary time series of the temperature difference between T1 and T2 showed both drift and offsets larger than expected from SBE specifications (Figure 6). Tow 3 continued for more than 4 days (Table 4). Seasoar was recovered near SBW at about 2010 UTC, 2 February and CTD Station 5 (Table 1) was completed immediately after recovery.

After Tow 3, we replaced both primary and secondary temperature sensors with sensors without a reed-switch assembly (SN 997 and 1384) to reduce the likelihood of damage from vibration, and reterminated the tow cable. Wecoma ran at full speed for a few hours to clear the exhaust system.

Seasoar was deployed near SBW at about 1300 UTC, 3 February immediately after CTD Station 6, and Tow 4 proceeded along the Standard Butterfly pattern in the usual direction (Table 5). Preliminary salinity data from the secondary sensor pair were very noisy during ascending profiles, and we suspected a problem with the sensor duct. Preliminary time series of the difference between the two temperature sensors showed no evidence of drift or offset (Figure 6). The temperature and conductivity data became intermittent during the E2N section of 6 February, so the vehicle was recovered near SBN at about 2315, 6 Feb and CTD Station 7 was made soon afterward. We found that the outlet tube for the secondary sensors had become detached from the nose, so the actual outlet from these sensors was inside the vehicle.

After Tow 4, we reterminated the Seasoar cable again, using a modified wire grip instead of the standard tapered plastic cow-tail to reduce cable flexing. We also repaired the secondary outlet duct, so that this outlet was once again directly through the nose of the Seasoar vehicle. Seasoar was deployed near SBN at about 2100, 7 February, immediately after CTD Station 8 (Table 1). Tow 5 began southward toward SBS and continued along the Standard Butterfly in the usual direction for almost five days (Table 6), when it was terminated at about  $2^{\circ}$  on the S2W line to allow the ship to make a high-speed run to clear the exhaust system; CTD Station 9 was made immediately after recovery. The Seasoar vehicle, instrument and termination were apparently in excellent condition. During CTD Station 10, as we were preparing to deploy Seasoar for Tow 6, we found a broken strand in the Seasoar cable adjacent to the loop attached for

crane handling. We therefore cut the cable above this point and reterminated the cable.

Seasoar was deployed for Tow 6 at about 0545 UTC, 13 February at 1°59'S, 155°43'E on the S2W line, immediately after CTD Station 11. Tow 6 began northwestward toward SBW and continued along the Standard Butterfly in the usual direction (Table 7) until 1137 UTC, 15 February, when we turned northward toward the equator. Seasoar was recovered just south of the equator at about 2045 UTC, 15 February, and CTD Station 12 was completed immediately afterward. We then ceased operations in the COARE IFA, and Wecoma proceeded to Pohnpei.

In all, we completed six Seasoar tows during W9211C (Table 8), for a total towing time of 416 hours. The overall Seasoar sampling included 12 occupations each of the N2S and W2E lines (Table 9) and the S2W and E2N lines (Table 10).

Wecoma arrived in Pohnpei at about 2300 UTC, 17 Feb, to disembark some personnel and departed there at about 0600 UTC, 18 Feb for the transit to Guam. En route to Guam, we conducted an 8-hour test of Seasoar flight characteristics with an optical plankton counter attached to the vehicle. Wecoma arrived in Guam at 0400 UTC, 22 Feb.

Underway measurements were made continuously through most of the cruise. These include: Acoustic Doppler Current Profile measurements of water velocity relative to the ship and accompanying GPS position data (contact Eric Firing et al., Univ. of Hawaii); temperature and salinity of water at 5 m depth and 2 m depth (contact Clayton Paulson, Oregon State Univ.); near-surface salinity of water pumped from a buoyant hose (contact Gary Lagerloef, SAIC); microwave radiometer estimates of surface salinity (contact Gary Lagerloef, SAIC); and a broad spectrum of meteorological observations (contact Clayton Paulson, OSU) including sonic inertial dissipation (contact Jim Edson, WHOI).

Members of the scientific party included Marc Willis, Tim Holt (both Wecoma Marine Technicians), Adriana Huyer, Robert L. Smith, Fred Bahr, Pip Courbois, Jane Fleischbein (all from Oregon State University), Eric Firing, Fred Bingham, Tung Le, Dail Rowe, and Joanna Muench, (all from University of Hawaii), Clay Wilson (SAIC) and Jonas Aleksa (University of Massachusetts). Additional persons on the Pohnpei-Guam transit were Mike Hill (Oregon State University), Meng Zhou, and Walter Nordhausen (both from Scripps Institution of Oceanography).

Table 9. Times (UTC) of meridional and zonal sections of the Standard Butterfly pattern. All N2S sections were southward along 156°06'E from SBN (1°14'S) to SBS (2°26'S), and all W2E sections were eastward along 1°50'S from SBW (155°30'E) to SBE (156°42'E). Number in parentheses indicates intake of preferred sensor T/C sensor pair was on port (1) or starboard (0) side of Seasoor)

N2S (SBN to SBS) along 156°06'E	W2E (SBW to SBE) along 1°50'S
0917, 27 Jan to 1827, 27 Jan* (0)	0143, 28 Jan to 1207, 28 Jan* (0)
1930, 28 Jan to 0430, 29 Jan* (0)	1646, 29 Jan to 0225, 30 Jan** (0)
0945, 30 Jan to 1926, 30 Jan (0)	0238 to 1112, 31 Jan (0)
1827, 31 Jan to 0358, 1 Feb (0)	1124 to 2015, 1 Feb (0)
0320, 2 Feb to 1221, 2 Feb (0)	1410 to 2304, 3 Feb (0)
0604, 4 Feb to 1524, 4 Feb (0)	2230, 4 Feb to 0719, 5 Feb (0)
1425, 5 Feb to 0015, 6 Feb (0)	0747 to 1641, 6 Feb (0)
2200, 7 Feb to 0820, 8 Feb (1)	1524, 8 Feb to 0114, 9 Feb (1)
0803 to 1824, 9 Feb <sup>1</sup> (1)	0200 to 1128, 10 Feb (1)
1819, 10 Feb to 0452, 11 Feb (1)	1207 to 2135, 11 Feb (1)
0433 to 1456, 12 Feb (1)	0845 to 1856, 13 Feb (1)
0151 to 1139, 14 Feb (1)	1833, 14 Feb to 0456, 15 Feb (1)

\* Data from ascending profiles only.

\*\* Includes a 6 second data gap from 20:52:25 through 20:53:30 UTC, 29 January.

<sup>1</sup> Section extends past SBS to 2°29'S.

Table 10. Times (UTC) of diagonal sections of the Standard Butterfly pattern: S2W between SBS (2°26'S, 156°06'E) and SBW (1°50'S, 155°30'E); and E2N between SBE (1°50'S, 156°42'E) and SBN (1°14'S, 156°06'E). During most E2N sections Seasoor was kept at maximum depth for about 12 km.

S2W (SBS to SBW)	E2N (SBE to SBN)
1827, 27 Jan to 0142, 28 Jan* (0)	1207, 28 Jan to 1930, 28 Jan* (0)
1035, 29 Jan to 1646, 29 Jan (0)	0225 to 0945, 30 Jan (0)
1926, 30 Jan to 0238, 31 Jan (0)	1112 to 1827, 31 Jan (0)
0358, 1 Feb to 1124, 1 Feb (0)	2015, 1 Feb to 0320, 2 Feb (0)
1221, 2 Feb to 1925, 2 Feb (0)	2304, 3 Feb to 0604, 4 Feb (0)
1524 to 2230, 4 Feb (partial) (0)	0719 to 1425, 5 Feb (0)
0015 to 0747, 6 Feb (0)	1641 to 2315, 6 Feb (partial)** (0)
0820 to 1524, 8 Feb (1)	0114 to 0803, 9 Feb (1)
1824, 9 Feb to 0200, 10 Feb (1)	1128 to 1819, 10 Feb (1)
0452 to 1207, 11 Feb (1)	2135, 11 Feb to 0433, 12 Feb (1)
1456 to 2036, 12 Feb (partial) (1)	1856, 13 Feb to 0151, 14 Feb (1)
0641 to 0845, 13 Feb (partial) (1)	0456 to 1137, 15 Feb (1)
1139 to 1833, 14 Feb (1)	

\*Data from ascending profiles only.

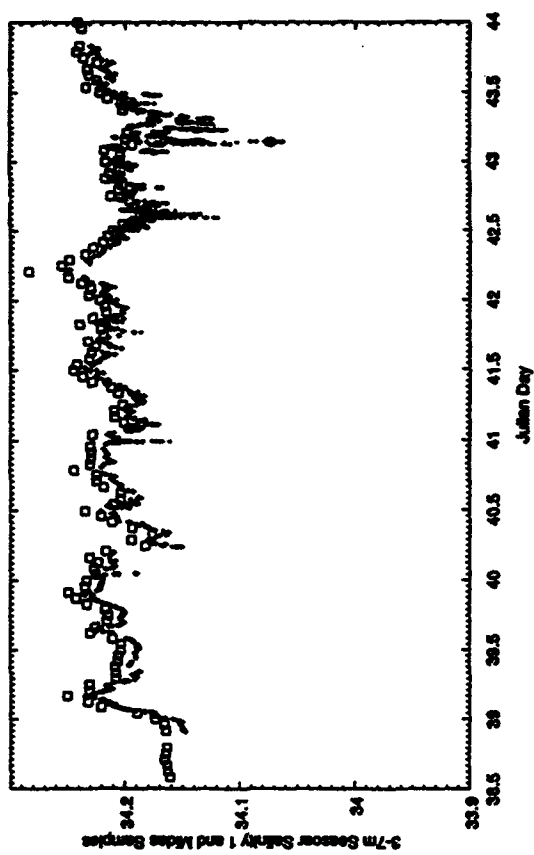
\*\* Includes numerous short gaps after 22:06:27 UTC, 6 February.

## CTD Data Acquisition, Calibration and Data Processing

All CTD/rosette casts were made with an SBE 9/11-plus CTD system equipped with dual ducted temperature and conductivity sensors (Table 2). CTD casts were made primarily to monitor the calibration of the Seasoor data, and were therefore made before and after each Seasoor tow, with as little delay as possible. Maximum sampling depth was about 500 m. Raw 24 Hz CTD data were acquired on an IBM compatible PC using the SEASAVE module of SEASOFT version 4.015 (Anon., 1992); temperature and conductivity data were recorded from both pumped sensor ducts. At each station a few salinity samples were collected for *in situ* calibration of the conductivity sensors; CTD values at the sample depth (calculated from the most recent manufacturer's pre-cruise calibration) were recorded both by pressing the F5 key at the time of rosette firing and manually on the station log sheets. Samples were analyzed on a Guildline Autosal salinometer that was standardized with IAPSO Standard Water P-119 at the beginning and end of each batch of about 36 samples. Sample salinity values were in essential agreement with the calculated CTD salinity values from both sensor pairs (average  $\Delta S_1=0.002$ , with standard deviation of 0.004, 36 samples; average  $\Delta S_2=0.002$ , with standard deviation of 0.005, 33 samples), and hence no conductivity correction was applied.

CTD data were processed on an IBM-compatible PC using applicable SEASOFT modules. Since there was no significant difference between the data from the two sensor pairs, we fully processed data from the primary sensors only. The DATCNV module of SEASOFT was used with the pre-cruise calibration constants to calculate 24 Hz values of pressure, temperature and conductivity from the raw frequencies. When necessary, the output data file was edited to remove any spikes and any values inadvertently recorded before the pressure minimum at the beginning of the cast. The CELLT<sup>M</sup> module was used to correct for the thermal mass of the conductivity cell, assumed to have a thermal anomaly amplitude of 0.03 and a time constant of 9 seconds. Ascending portions of the 24-Hz data file were removed by LOOPEDIT with the minimum velocity set to 0.0 m/s. The remaining data were averaged to 1 dbar values using BINAVG. The final processed data files consist of 1 dbar values of pressure, temperature and conductivity. These processed data files were transferred to a SUN computer where we used standard algorithms (Fofonoff and Millard, 1983) to calculate salinity, potential temperature, density anomaly (sigma-theta), specific volume anomaly, and geopotential anomaly (dynamic height).

Tow 3



Tow 2

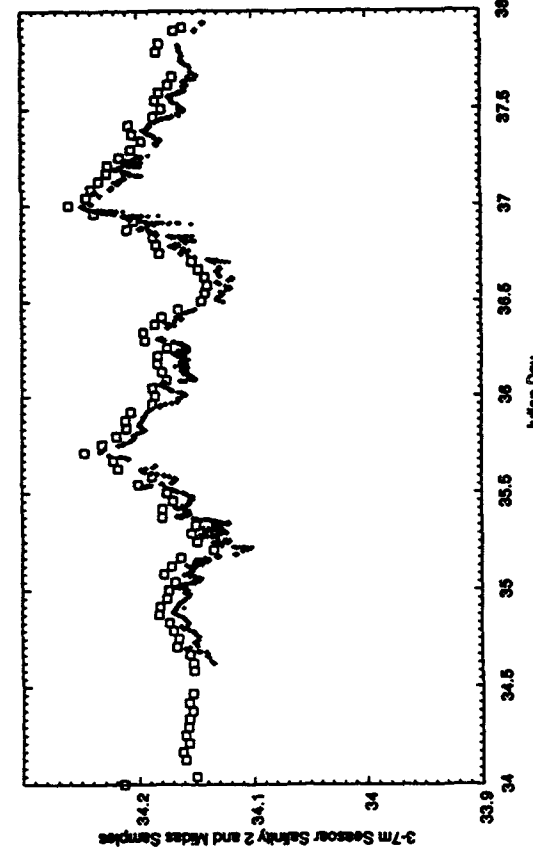
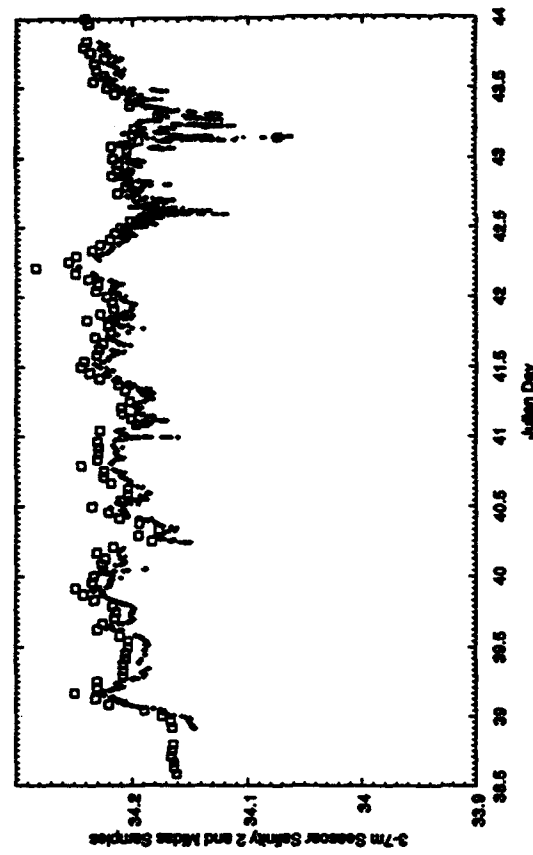
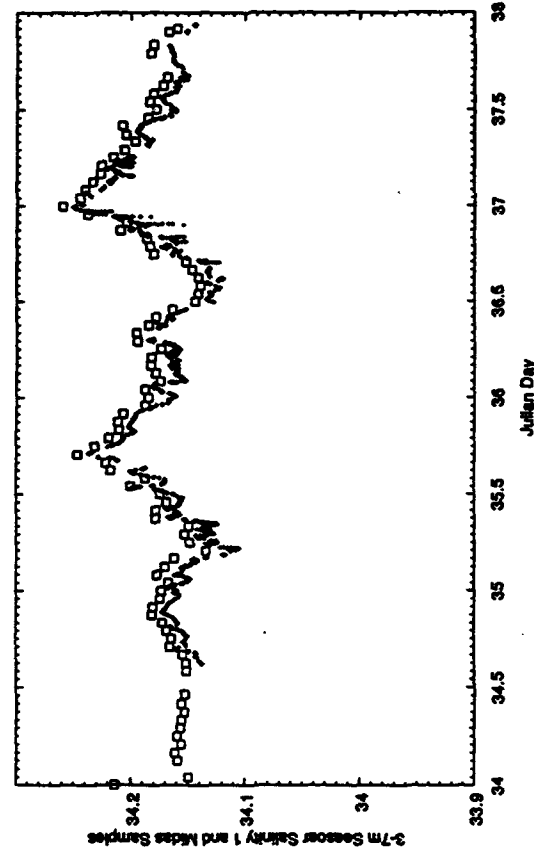


Figure 7(a). Time series of hourly salinity samples from the ship's intake at 5 m (squares), and of preliminary near-surface (3-7.99 m) Seasoar salinity data (dots) from both primary (upper panel) and secondary sensors (lower panel), for each Seasoar tow of W9211C: Tow 2 (left) and Tow 3 (right) of W9211C.

## Seasoar Data Acquisition and Preliminary Processing

Raw 24 Hz CTD data from the Seasoar vehicle and GPS position and time data were acquired by an IBM compatible PC, which also set flags to indicate missing GPS data and to mark the collection of a salinity sample. The raw data were simultaneously recorded on optical disk by PC and on a Sun Sparc workstation. The PC displayed time series of subsampled temperature (both sensors), conductivity (both sensors) and pressure in real time; it also displayed accumulated temperature data for 6-8 hours as a vertical section (color raster). One-second averages of ship's position, CTD temperature (both sensors), conductivity (both sensors), salinity (both sensor pairs), and pressure were calculated on the Sparc workstation, using the most recent manufacturer's calibration (Table 2). For each tow, the preliminary salinity for each sensor pair was calculated using a fixed offset between temperature and salinity, and a fixed value for the amplitude and time constant of the thermal mass of the conductivity cell, but these parameters were changed from one tow to another (Table 8). Time-series and vertical profile plots of the one-second data were made at the end of each hour. The 1-second preliminary data were used to calculate the average temperature and salinity data in bins extending 3 km in the horizontal and 2 dbar in the vertical, and these gridded values were used to plot vertical sections for each leg of the Standard Butterfly pattern.

## Seasoar Conductivity Calibration

Salinity samples were collected once per hour from a throughflow system in Wecoma's wetlab from 0000 UTC, 27 January until 2000 UTC, 15 February 1993. This system pumps water from the seachest at a depth of 5 m in the ship's hull, through a tank containing SBE temperature and conductivity sensors; samples are drawn from a point just beyond this tank. The 120 ml glass sample bottles were rinsed three times before filling, and closed with screw-on plastic caps with conical polyethylene liners. Samples were further sealed by wrapping parafilm around the base of the cap. Samples were analyzed at sea on an Autosal salinometer, usually within 2-3 days after collection; the salinometer was standardized with IAPSO Standard Water P-119 at the beginning and end of each batch of about 24 samples. Time series of these hourly salinity samples and time series of the preliminary Seasoar data from the 3-7 m depth range (Figure 7) show very similar variations, especially during Tows 4-6.

For a quantitative comparison between the salinity samples and the Seasoar data, we selected Seasoar values that were both within 7 minutes of the time of the salinity sample and within a depth range of 3.0 to 5.5 m. For each salinity sample, we calculated a bottle conductivity using the measured salinity and the temperature from each Seasoar sensor duct, and then compared this sample conductivity to the directly

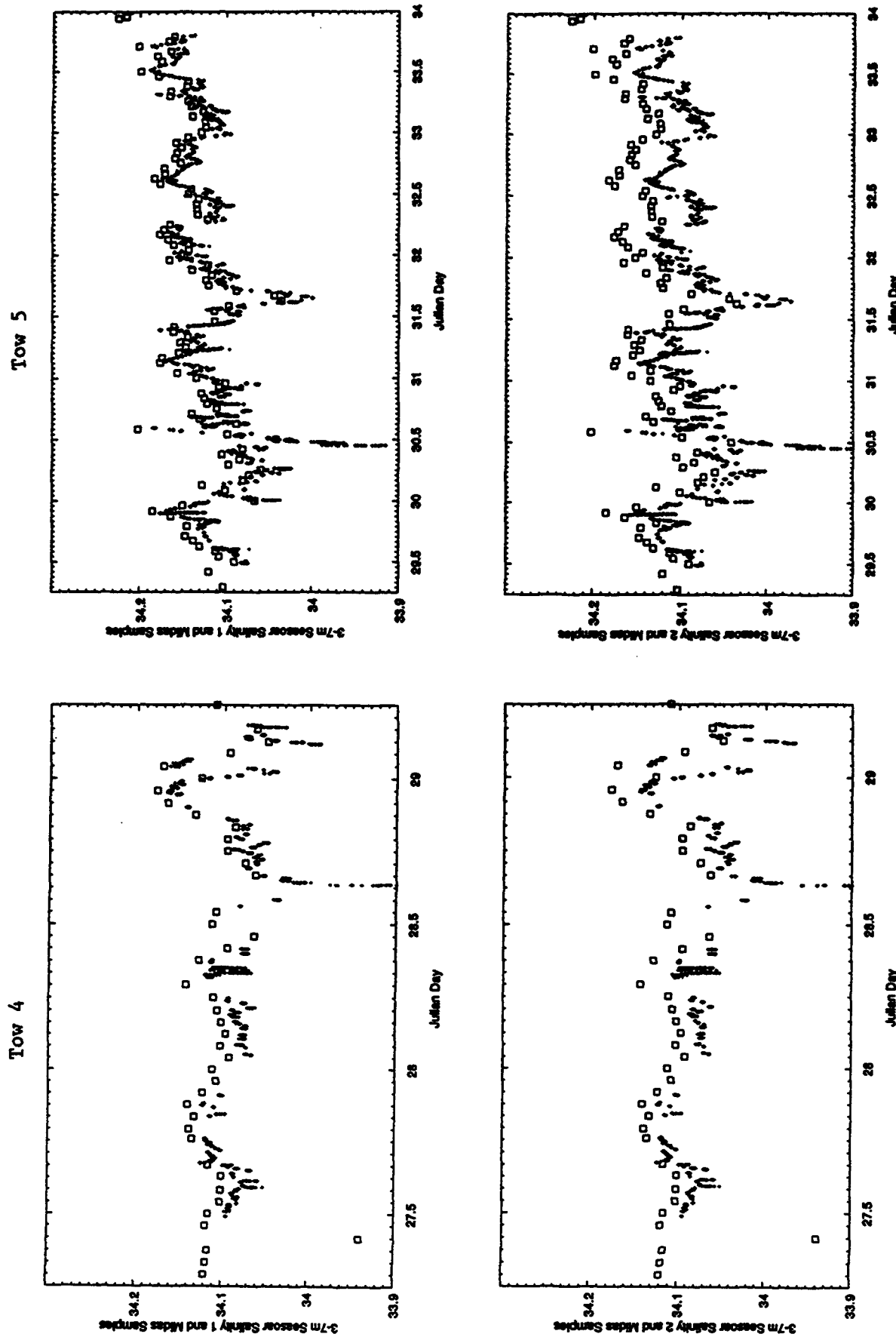


Figure 7(b). Time series of hourly salinity samples from the ship's intake at 5 m (squares), and of preliminary near-surface (3-7.99 m) Seasoar salinity data (dots) from both primary (upper panel) and secondary sensors (lower panel), during Tow 4 (left) and Tow 5 (right) of W9211C.

Tow 6

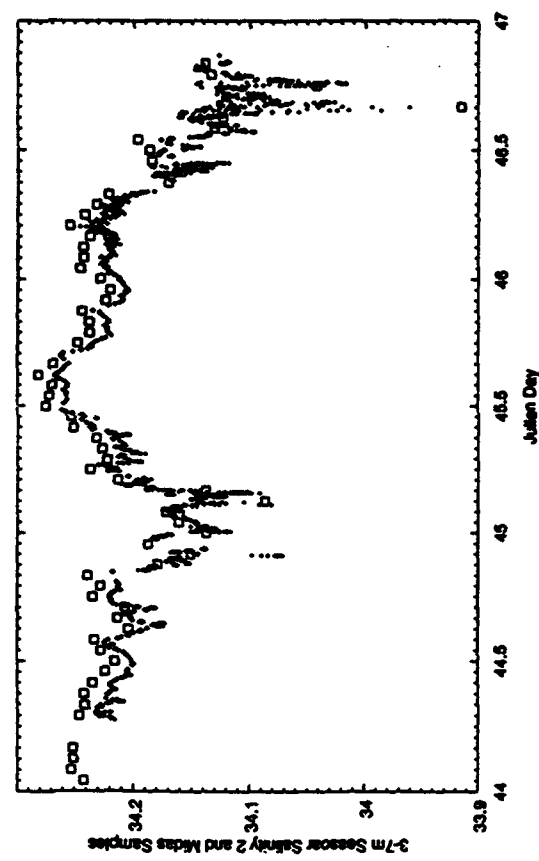
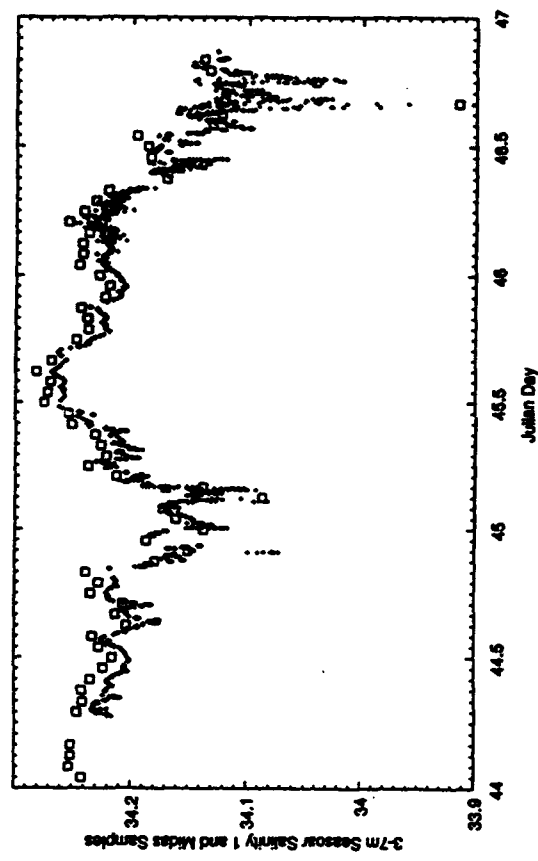


Figure 7(c): Time series of hourly salinity samples from the ship's intake at 5 m (squares), and of preliminary near-surface (3-7.99 m) Seasoar salinity data (dots) from both primary (upper panel) and secondary sensors (lower panel), during Tow 6 of W9211C.

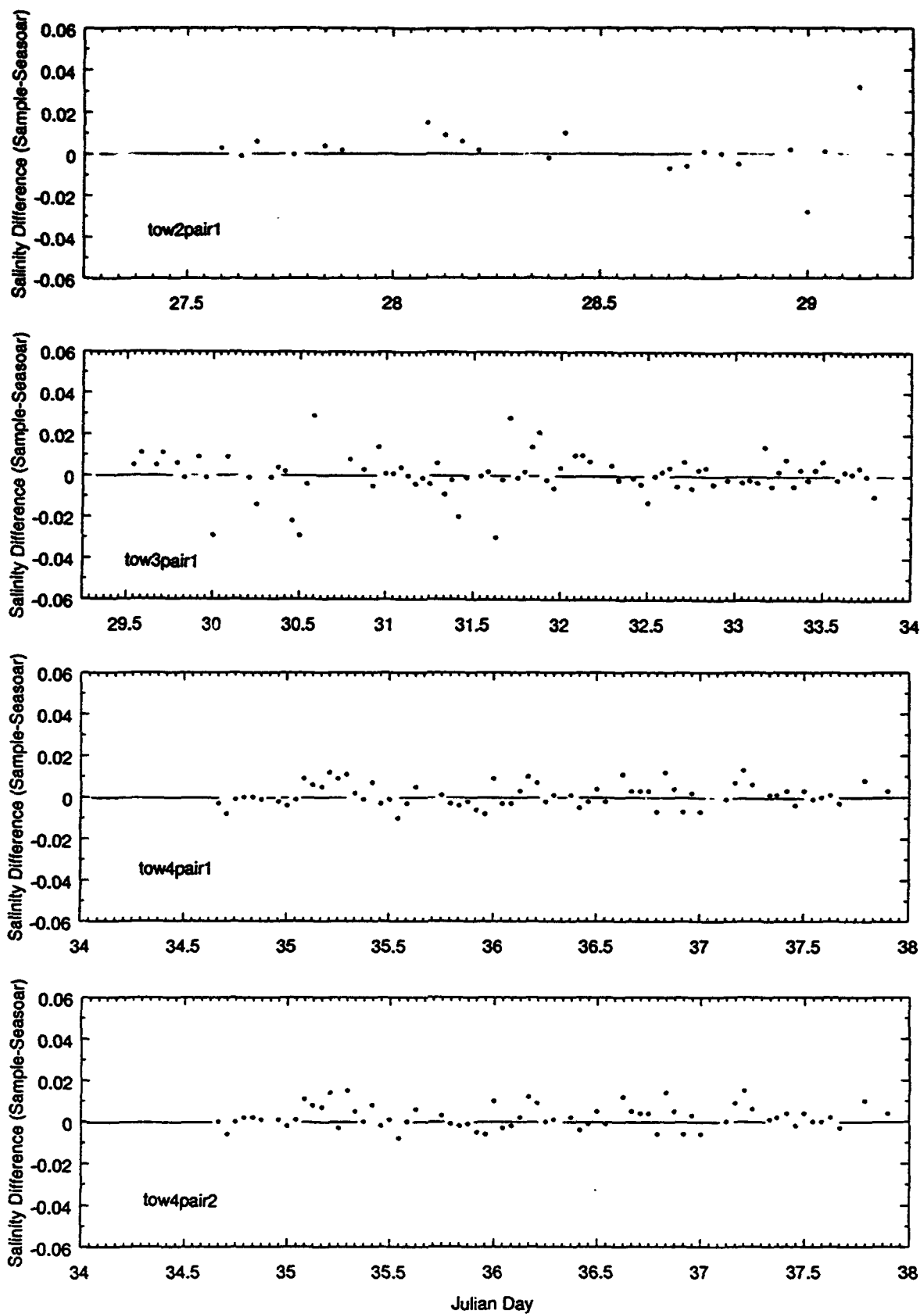


Figure 8 (a). Time series of salinity differences between the 5-m samples and the matching corrected SeaSoar data, for the primary T/C sensor pair during Tows 2 and 3, and for both primary and secondary sensors during Tow 4 of W9211C.

measured conductivity from the same sensor duct; a very few pairs with very large differences (only 5 out of a total of 329) were eliminated from the comparison. Assuming, as usual, that the measured conductivity should be corrected by a multiplier alone, we calculated the slope ( $m$ ) of the zero-intercept regression line between the measured conductivity and the sample conductivity separately for each sensor pair and for each Seasoor tow.

Between Tows 2 and 3, we found no significant difference in the multiplier for the primary sensor pair, and therefore we pooled the data, and used the same correction factor ( $k$ ) for both tows (Table 11). Since the secondary temperature sensor malfunctioned during Tows 2 and 3, we used the primary temperature data to determine the multiplier for secondary conductivity for these tows. Both primary and secondary sensors were replaced after Tow 3.

Between Tows 4, 5 and 6, we found no significant difference in the multiplier ( $m$ ) for either the primary or secondary conductivity data, and therefore we adopted the values determined from the pooled data as the correction factors (Table 11).

Applying these multipliers to the Seasoor conductivity data before recalculating salinity allows us to compare the corrected Seasoor salinity values from both primary and secondary sensor ducts to the sample salinity (Figure 8, Table 11). The time series of the differences (Figure 8) show reasonable agreement between sample and near-surface Seasoor data for the primary sensor pairs during Tows 2 and 3, and for both sensor pairs during Tows 4, 5 and 6. In general, largest sample-Seasoor differences occur when the surface layer is stratified, so the standard deviations of the salinity differences (Table 11) primarily reflect sampling errors rather than instrumental noise.

Table 11. Conductivity multipliers ( $m_1$  and  $m_2$ ) for primary and secondary sensors, determined (separately for each tow) from comparison of near-surface Seasoor data with 5-m intake samples, and the conductivity correction factors ( $k_1$  and  $k_2$ ) adopted for reprocessing the Seasoor conductivity data. Also shown are the average and standard deviations of the salinity differences between the sample values and the corrected Seasoor data.

Tow	N	$m_1$	$m_2$	$k_1$	$k_2$	Average		Std. Dev.	
						S1	S2	S1	S2
1	0	—	—	1.000433	1.000449	—	—	—	—
2	21	1.000470	—	1.000433	1.000449	0.001	—	0.007	—
3	84	1.000424	—	1.000433	1.000449	0.000	—	0.009	—
4	67	1.000388	1.000460	1.000368	1.000418	0.001	0.002	0.004	0.004
5	100	1.000354	1.000396	1.000368	1.000418	-0.001	-0.001	0.007	0.008
6	52	1.000396	1.000420	1.000368	1.000418	0.002	0.000	0.012	0.012

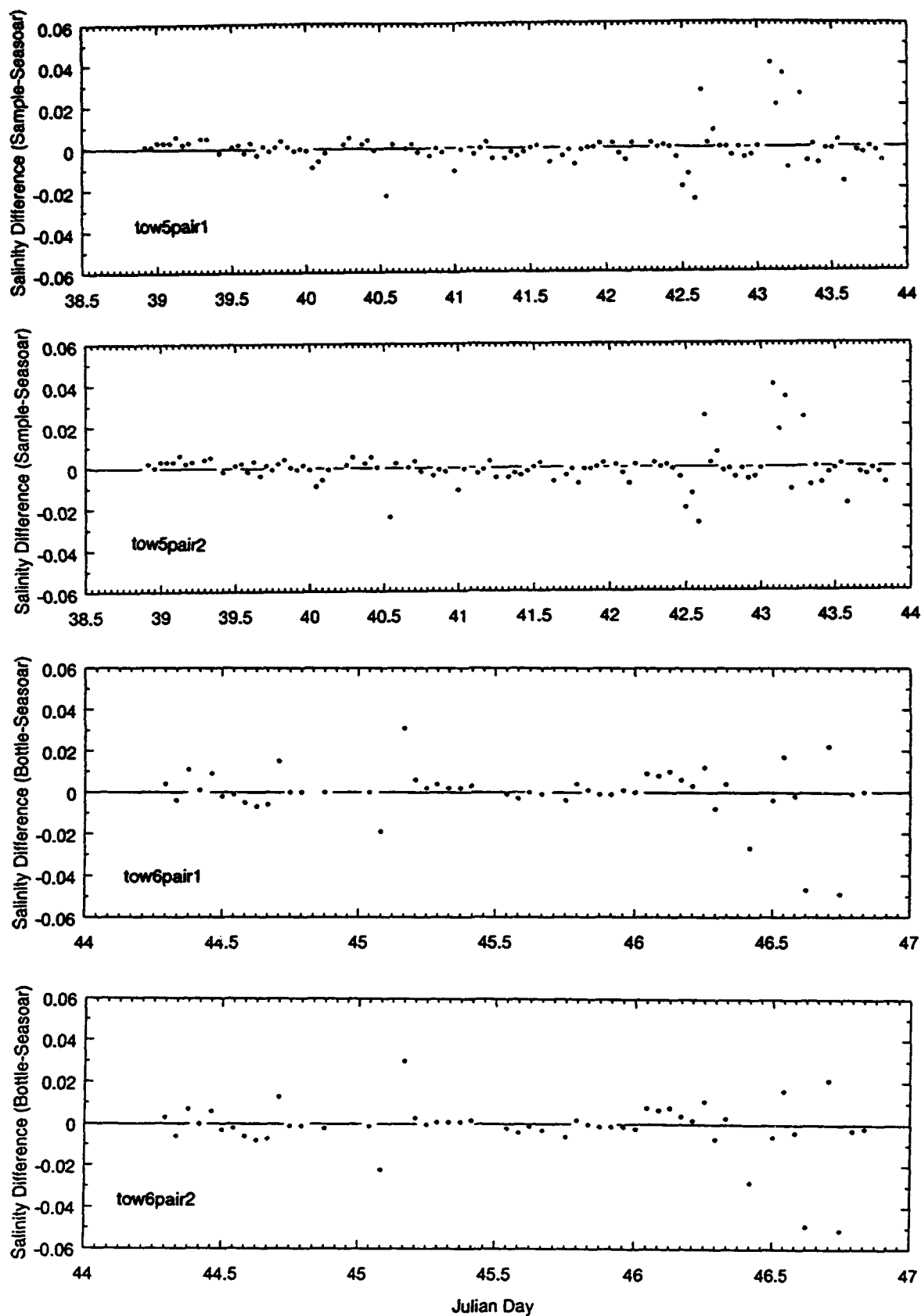


Figure 8 (b). Time series of salinity differences between the 5-m samples and the matching corrected Seasoor data, for both primary and secondary sensor pairs during Tows 5 and 6 of W9211C.

## Post-processing of Seasoar Data

**Background** Salinity data derived from SeaBird ducted temperature and conductivity sensors are subject to errors from three separate sources (Larson, 1992): (1) poor alignment of the 24 Hz temperature and conductivity data, (2) poor compensation for the transfer of heat between the mantle of the conductivity cell and the water flowing through it, and (3) mismatch of the effective time constants of the temperature and conductivity measurements. These sources of error are minimized in a normal SeaBird CTD, by pumping the water through the ducted pair at a fixed rate, by software algorithms for changing the T/C alignment and the thermal mass parameters, and by matching the thermistor to the effective time constant of the conductivity measurement through the fixed-length duct. With sensors mounted inside a towed Seasoar vehicle, these error sources need to be considered anew.

While at sea, we noticed that there was often a significant difference in data quality between ascending and descending profiles, with salinity data from descending profiles generally noisier than salinity data from ascending profiles; descending profiles frequently showed a large and variable positive salinity bias (e.g. Figure 9). These systematic up/down differences were observed in data from both sensor pairs, though sometimes more pronounced in one of the sensor pairs. We therefore suspected that there might be variations in the flow-rate of water through the pumped T/C sensor ducts, leading to variations in the optimum alignment offset between the 24-Hz temperature and conductivity data.

To check this hypothesis, we applied the general procedures outlined by Nordeen Larson (1992) to a segment of raw data from the hour beginning at 0000 UTC, 9 February. We first reprocessed the data from both sensor pairs without applying any T/C offset, retaining 24-Hz output; data from the first ascending profile (about 0001 to 0006 UTC) and the first descending profile (0006 to 0010 UTC) were read into separate files. These served as input to a program which realigns the temperature and conductivity data from both sensor pairs by a specified offset and recalculates salinity; for each scan it also determines a "median salinity",  $S_m$ , using a centered nine-point median filter, and a "spike salinity",  $S'$ , as the anomaly from the median salinity. The time integral of this spike salinity, normalized by the sign of the temperature gradient,

$$ISS = \sum (S'_n / \text{sgn}(T_{n+1} - T_{n-1})),$$

changes sign at the optimum offset value (Larson, 1992). Calculations were repeated for a range of offsets, and spike salinity profiles were plotted for each (e.g., Figure 10). For these profiles, we found that the optimum alignment offset,  $\xi$ , during

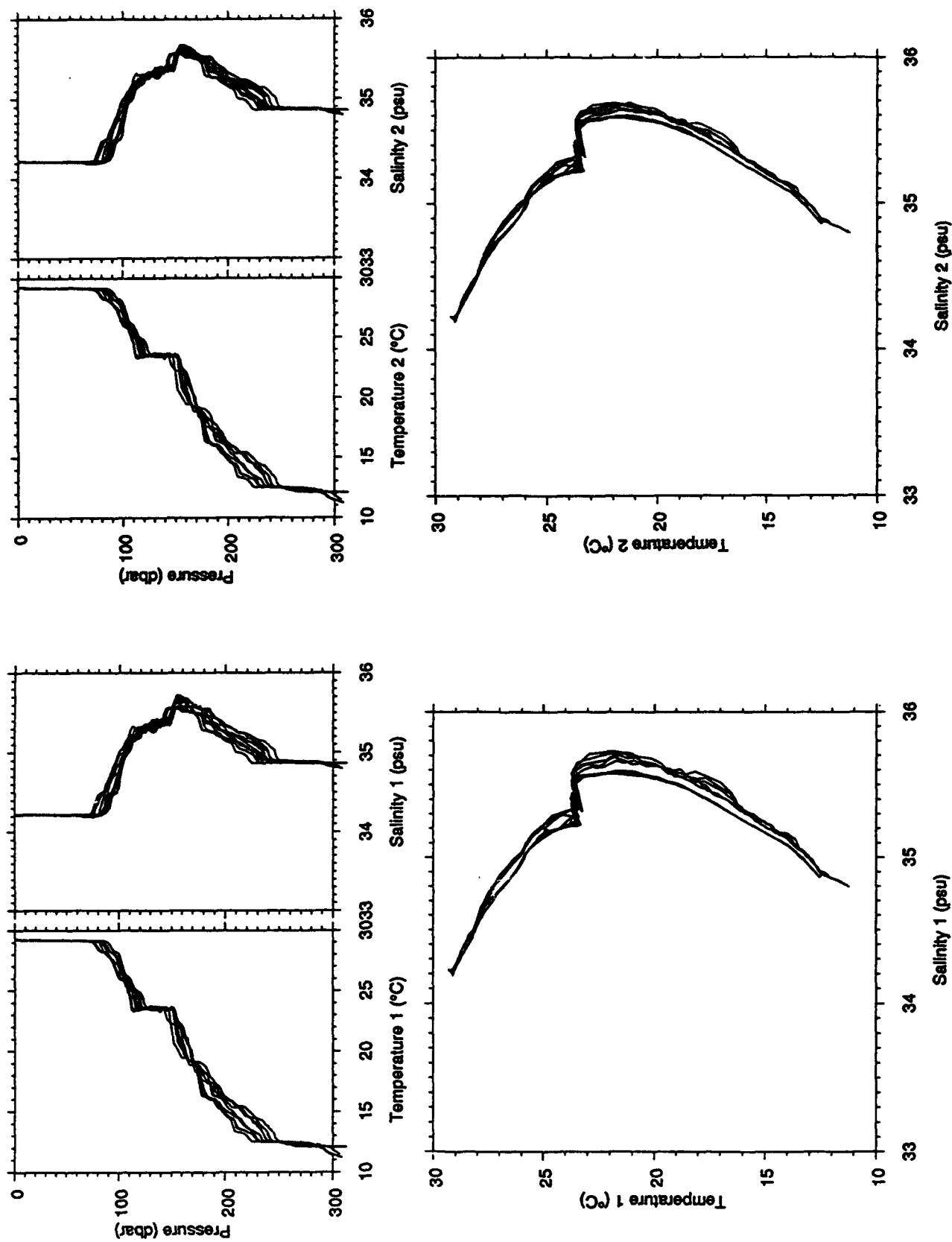


**Figure 9.** Preliminary profiles and T-S diagrams for both Seasoar T/C sensor pairs, for the hour beginning 0000 UTC on 9 February 1993. Data were processed with constant values of the T/C offset ( $\xi_1 = 0.0$  and  $\xi_2 = 2.0$ ) and thermal mass parameters ( $\alpha = 0.045$  and  $\tau = 5$  sec). For both sensor pairs, splitting of the T-S characteristics into two groups reflects systematic differences between ascending and descending profiles.

ascent was essentially the same as those for ducted sensors in a normal profiling SBE9/11 plus CTD, i.e. 0.0 scans for primary sensors and 1.75 scans for secondary sensors. (The SBE 11/plus deck unit previously applies a T/C alignment offset of 1.75 scans to data from primary sensors but not secondary sensors). Optimum values of the offset during descent were larger: 1.75 scans for primary sensors, and 2.75 scans for secondary sensors (Figures 10, 11).

We independently calculated lagged correlation coefficients between the temperature and conductivity data from each sensor pair, using first differencing to remove low frequency trends in both, and obtained the same results, and found that the lag of maximum correlation was in essential agreement with the alignment offset determined by Larson's spike salinity method. Alternating between two values of the alignment offset (one for descent, one for ascent) significantly improved the processed salinity data, but systematic up/down differences remained during portions of some Seasoar tows (e.g. Figure 12).

Further study of the 24-Hz Seasoar CTD data has shown that the optimum T/C alignment offset,  $\xi$ , varies on several different time scales: within each undulation, from section to section, gradually over the length of a tow, and from one tow to another (e.g., Figure 13). In most cases, the optimum alignment offset during ascent is near the default values of 0.0 scans for T1/C1 and 1.75 scans for T2/C2, while the optimum offset during descent is longer. We attribute these variations in optimum offset to reductions in the rate of pumped flow through the sensors, and believe these variations in flow rate are the result of dynamic pressure differences, partly between the inside and outside of the vehicle, and partly along the exterior of the vehicle nose (though inlet and outlet ports are separated by only a few centimeters). Possible sources of such pressure gradients include high rates of ascent and descent (sometimes  $>3$  m/s, superimposed on a horizontal tow speed of 4 m/s), and local small perturbations of the flow field around the vehicle, associated perhaps with a persistent roll angle or strong cross-currents. Whatever their source, the variations in offset alignment are a major source of potential error in calculating salinity, and must be taken into account in reprocessing the data. After some trial and error, we chose to determine the optimum lag in three depth ranges (excluding the surface mixed layer) for each ascending and descending profile; calculating lags for successive 10-second segments proved to be less satisfactory in minimizing salinity noise and bias.

Still further study of the preliminary Seasoar data showed that systematic up/down salinity differences were particularly strong near sharp thermoclines, even though we had attempted to correct for the thermal mass of the conductivity cell (Lueck, 1990), using constant values for the time constant ( $\tau$ ) and amplitude ( $\alpha$ ) parameters in the recursive algorithm provided by SeaBird:

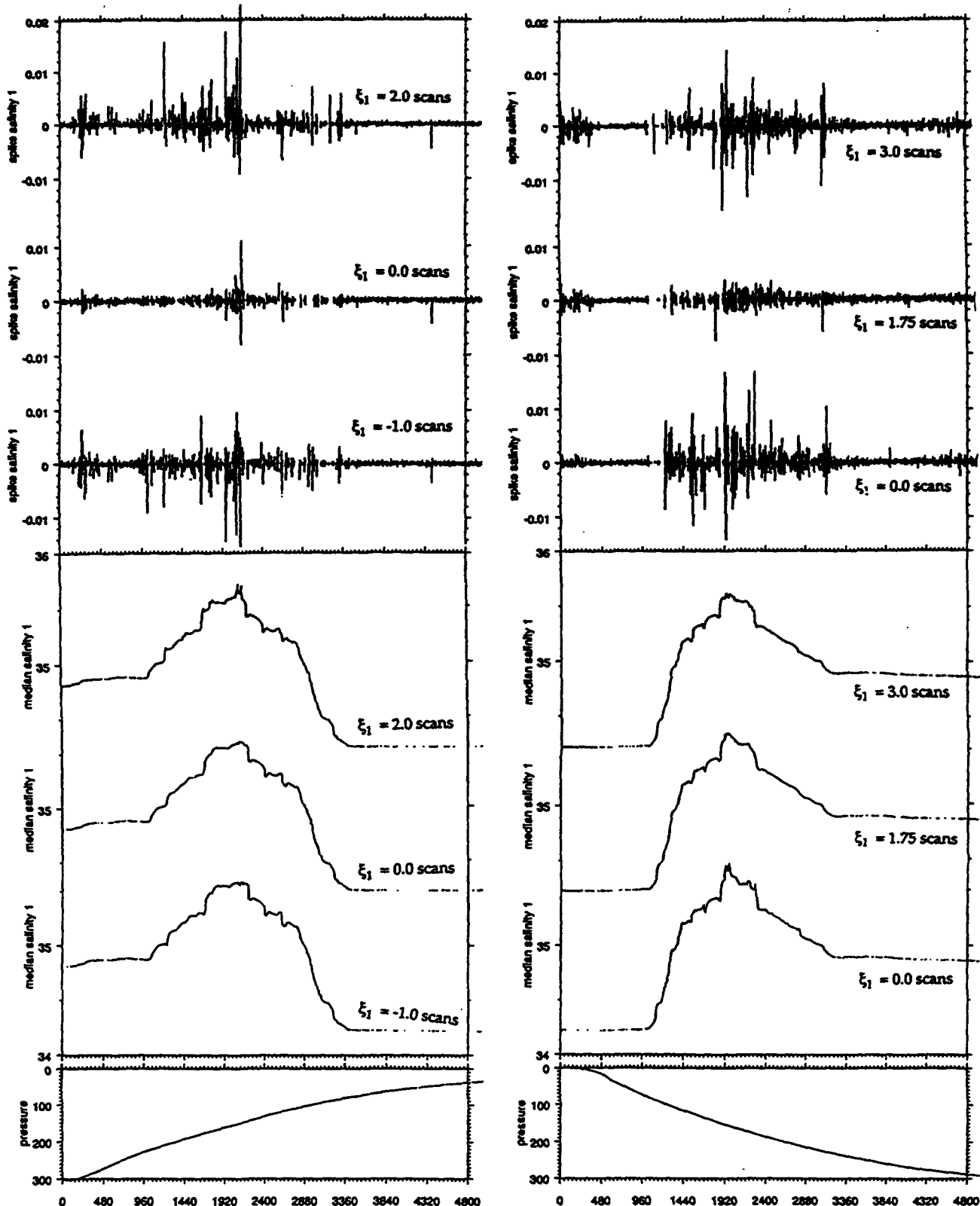


Figure 10. Time-series of 24-Hz "median salinity" and "spike salinity" from ascending (left) and descending (right) segments of Seasoar data between 0001 and 0010 UTC, 9 February, calculated for three different values of T/C alignment offsets  $\xi_1$ . The "median salinity" is the median of 9 scans, and the "spike salinity" is the anomaly from this median.

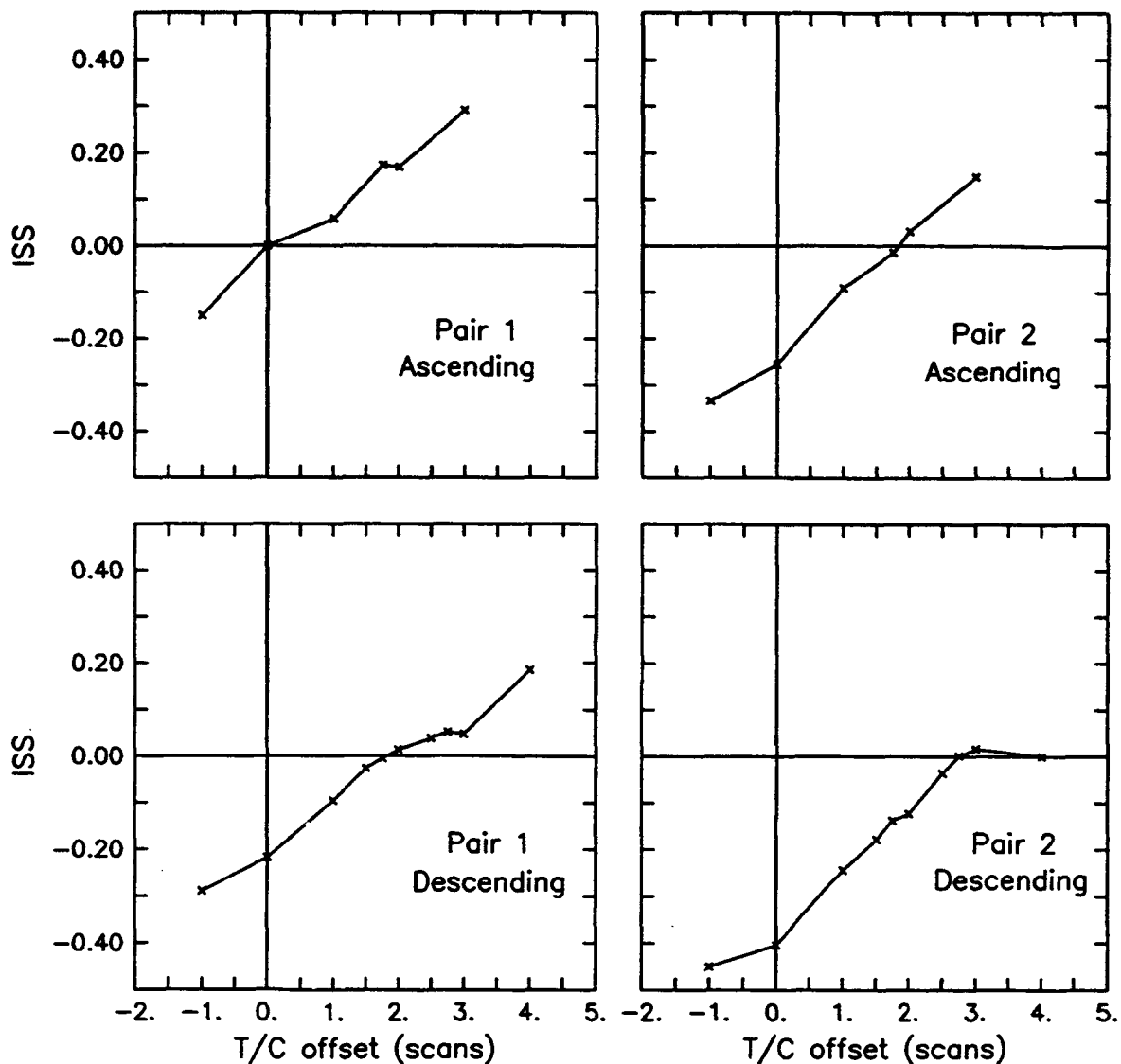
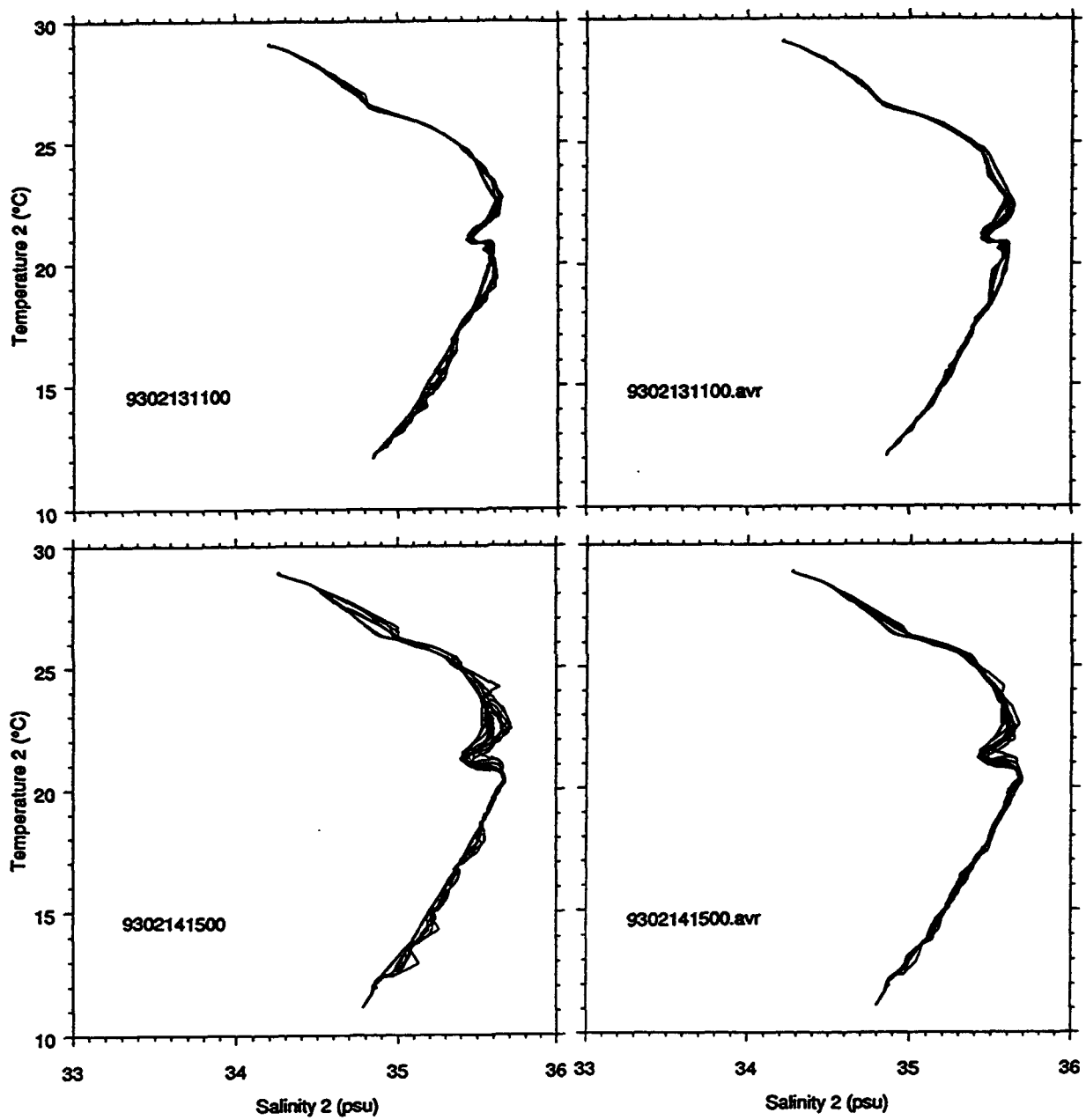


Figure 11. Values of the integral of spike salinity, ISS, for ascending and descending segments of data from both T/C sensor pairs, during 0001 and 0010 UTC, 9 February 1993; note that the value of the optimum offset (at ISS = 0) is larger during descent.



**Figure 12.** T-S characteristics for Seasoor data from two different hours, processed by two different methods: with constant values of the T/C alignment offset (left,  $\xi_2 = 2.0$  scans), and with alternating values of the offset (right;  $\xi_2 = 2.5$  scans during ascent and  $\xi_2 = 5.0$  scans during descent). In both methods, we used constant values of the thermal mass parameters ( $\alpha = 0.045$  and  $\tau = 9$  sec).

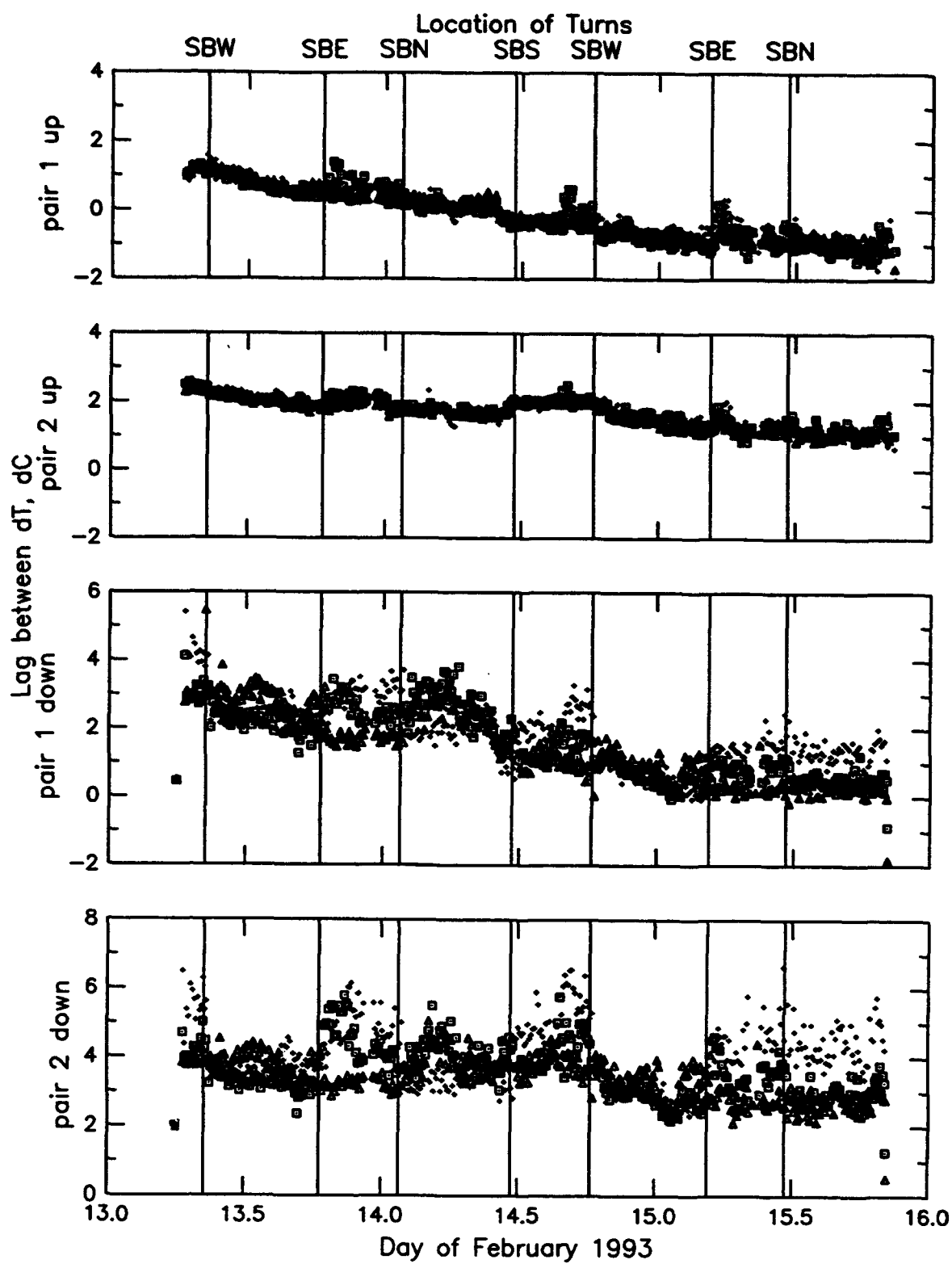


Figure 13. Time series of the lag at maximum cross-correlation between 24-Hz temperature and conductivity data (detrended by first-differencing), for both primary and secondary sensor pairs during Seasoor Tow 6. Correlations were calculated for three different layers (50-120 dbar, plus signs; 120-180 dbar, squares; 180-240 dbar, triangles), and separately for ascending and descending profiles; times of turns in the ship's track are indicated by vertical lines.

$$\begin{aligned}
 dt &= \text{temperature} - \text{previous temperature} \\
 ctm &= -b * \text{previous } ctm + a * dcdt * dt \\
 \text{corrected conductivity} &= \text{conductivity} + ctm
 \end{aligned}$$

where  $a = 2\alpha / (0.0417\beta + 2)$ ,  $dcdt = 0.1 + 0.0006$  (temperature - 20),  $\beta = 1/\tau$  and  $b = 1 - 2a/\alpha$ . Constant values of  $\alpha$  and  $\tau$  had been chosen by two different methods: by comparing CTD casts with Seasoar deployment and recovery profiles, and by minimizing differences between ascending and descending salinity data near the top of the thermocline for some data segments with exceptionally steep gradients at the bottom of the surface mixed layer; both methods indicated the best constant values were  $\alpha = 0.04$  for the thermal anomaly amplitude and  $\tau = 10$  sec for the time constant. The association of residual salinity bias with sharp thermoclines suggested that variations in flow rate through the ducted sensors effectively altered the rate of heat transferred from the walls of the conductivity cell. Experimenting with different values of  $\alpha$  indicated that larger values of  $\alpha$  are appropriate for larger values of the alignment offset (Figure 14).

Finally, we considered the effect of elongating the intake duct (from about 1 cm on a standard SeaBird T/C ducted pair to about 5 cm) by adding Tygon tubing between the sensor duct and inlet in the Seasoar nose. In principle, elongating the intake could slow the response time of the conductivity measurement through turbulent mixing within the duct (Nordeen Larson, personal communication). We compared conductivity spectra from conventional CTD casts with those from the Seasoar deployment and recovery profiles, and found no significant difference: both were similar to the temperature spectra. We conclude that any change in sensor time constant due to intake elongation is negligible, at least with the present choice of tubing.

**Procedures** The first step in reprocessing is to incorporate temperature and conductivity corrections determined from in-situ calibration or post-cruise calibration in a new configuration file for each tow. Except for temperature sensor #1369, which clearly malfunctioned during the cruise, the post-cruise temperature calibrations of the Seasoar sensors showed little or no drift from the pre-cruise calibrations, so no temperature corrections were applied. The conductivity correction factors determined from the *in situ* calibration data (Table 11) were incorporated in the configuration files for each tow.

The next step is to compute lagged correlations between temperature and conductivity for each sensor pair, separately for ascending and descending profiles, and separately for three depth ranges: 50 to 120 dbar, 120 to 180 dbar, and 180 to 240 dbar, provided the segment contains at least 72 scans. Cross-correlations are calculated after detrending both temperature and conductivity by first-differencing

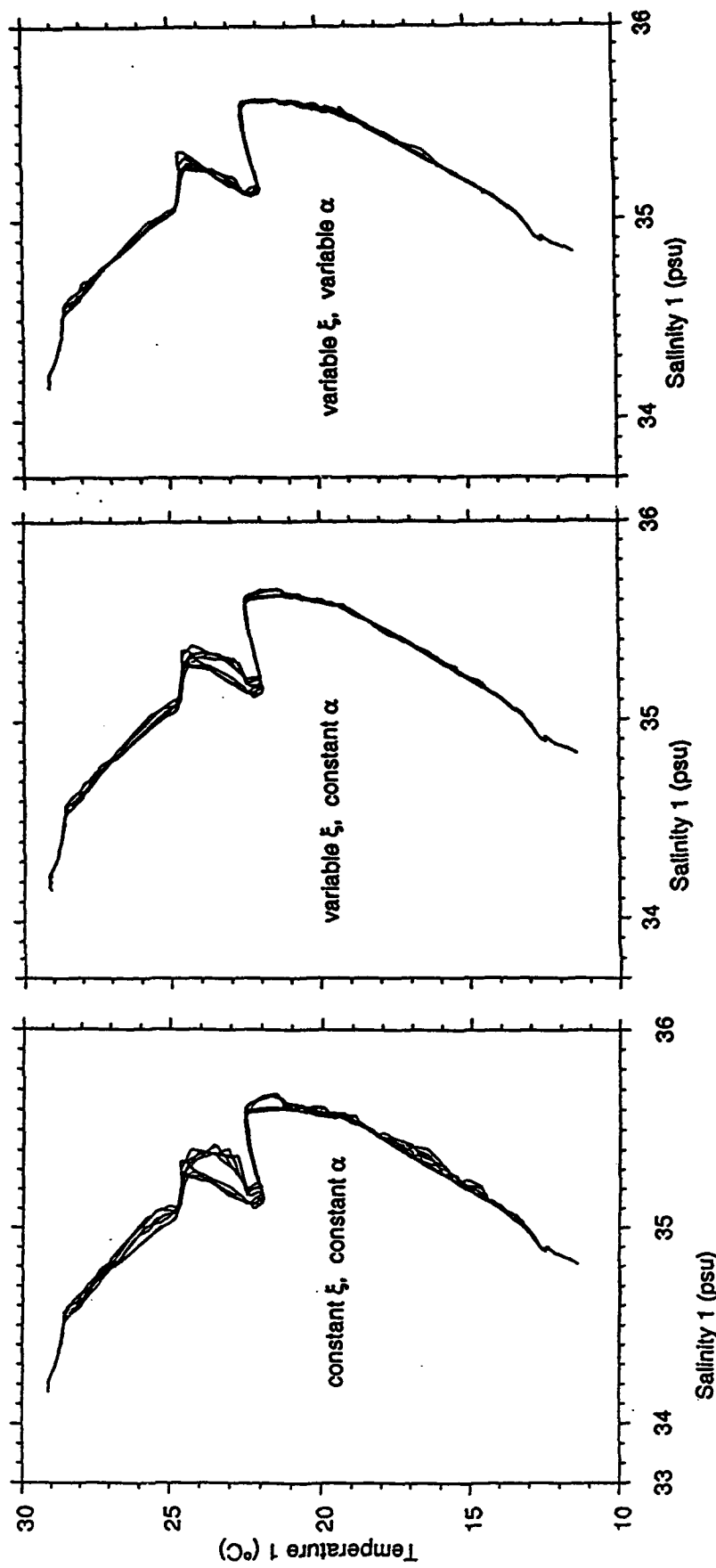


Figure 14. T-S characteristics for Seasoar data from the same hour (2000-2100 UTC, 13 Feb 1993), processed by three different methods: left, using a constant T/C offset ( $\xi_1 = 0.0$ ), and a constant thermal anomaly amplitude ( $\alpha = 0.045$ ); center, using variable  $\xi$  determined from T-C cross-correlation and constant  $\alpha$ ; right, using both variable  $\xi$  and a variable  $\alpha$  which increases with  $\xi$ .

the 24-Hz data. Correlations are calculated for  $\pm 12$  lags; the maximum correlation is almost always  $\geq 0.85$ . The fractional value of the lag at maximum correlation is determined by fitting a parabola to the cross-correlation values. The resulting time series of the optimum primary and secondary alignment offsets ( $\xi_1$  and  $\xi_2$ ) for each tow are shown in Appendix A. Lag values greater than 12 and other outliers (obtained occasionally for data segments lasting <10 seconds) were not used in processing the data. Very large lags were obtained for many descending profiles of Tow 2) when the pump outlets were not properly connected, and hence data from descending profiles from this tow were discarded.

The edited values of the alignment offset were applied sequentially in reprocessing the 24-Hz T/C data. To reprocess data from depths shallower than 50 m, we used the  $\xi$  value determined from the preceding 120 to 50 dbar layer; for data deeper than 240 m, we used the  $\xi$  value determined from the preceding 180 to 240 dbar layer. Short segments with unreasonably large lags were processed with the lag obtained for the succeeding data segment.

To correct the 24 Hz conductivity data for the thermal mass of the conductivity cell, we used the standard algorithm with a fixed value for the thermal anomaly time constant ( $\tau = 10$  sec), and variable values for the thermal anomaly amplitude depending on the alignment offset:

$$\begin{aligned}\alpha_1 &= 0.03 && \text{if } \xi_1 \leq 0 \\ \alpha_1 &= 0.03 + 0.03(\xi_1/2.75) && \text{if } \xi_1 > 0 \\ \alpha_2 &= 0.03 && \text{if } \xi_2 \leq 1.75 \\ \alpha_2 &= 0.03 + 0.03(\xi_2 - 1.75)/2.75) && \text{if } \xi_2 > 0,\end{aligned}$$

where the subscripts denote primary or secondary sensors. The corrected and realigned 24 Hz temperature and conductivity data are used to calculate 24-Hz salinity, and these are averaged to yield 1-second averages stored in hourly files. These procedures greatly reduce the systematic salinity differences (both bias and noise) between ascending and descending profiles (e.g. Figure 14). However, salinity data from descending profiles remains somewhat noisy, while the ascending data is almost always free of significant noise.

The reprocessed data from both sensor pairs were plotted to determine which pair provided the better data for each Seasor tow. During Tow 2, with both sensor ducts disconnected from the outlet, there is evidence of stalling in the pumped sensor ducts during descent, but data from ascending profiles is apparently of good quality. For both Tows 2 and 3, with the malfunctioning secondary temperature sensor, data from the primary sensors is clearly preferable. During Tow 4, the

secondary sensor duct was disconnected from the outlet, and data from the primary sensors is clearly preferable. For Tows 5 and 6, the data from the two sensor pairs was of essentially the same quality, with only very subtle reasons to prefer the secondary sensors over the primary sensors.

## Data Presentation

Successive hourly files of the reprocessed one-second average data were joined and clipped to yield a single data file for each section of the Standard Butterfly Pattern (Tables 9 and 10). Final processed data files contain unfiltered GPS latitude and longitude; pressure; temperature, salinity and sigma-t from the better sensor pair; date and time; and an integer representing flags (to indicate collection of a water sample from 5-m intake (thousands digit set to 1), missing GPS data filled by linear interpolation (tens digit set to 1), and to indicate port or starboard intake for the T/C sensor pair (ones digit set to 1 or 0, respectively)). We present consecutive figures of the Seasoar trajectory (time series of pressure, latitude and longitude) along each section. We also present summary figures of all of the 1-second data for each of the four standard sections as follows: ensembles of temperature profiles (both ascending and descending, except for Tow 2), salinity profiles (ascending profiles only), and T-S diagrams (for ascending profiles only). Vertical distributions of the temperature, salinity and sigma-t along each section were plotted using Don Denbo's PPlus program with a vertical grid spacing of 2 dbar and a horizontal spacing of 1 nm, and with a value of CAY= 5 for the smoothing parameter (combined spline and laplacian filter). For the temperature sections, we used both ascending and descending data, for all tows except Tow 2 where we used ascending data only. For the salinity and sigma-t sections, we used only ascending data for all tows.

## CTD/Seasoar Comparison

T-S diagrams for the beginning and end of each Seasoar Tow are shown in Appendix B. Each diagram shows the T-S curve from both the conventional CTD cast and the preferred Seasoar sensors during Seasoar deployment or recovery. Seasoar deployment profiles are generally noisier than either the CTD profiles or Seasoar recovery profiles, probably because the Seasoar vehicle is tilted nose-upward during both deployment and recovery; since the ship is moving very slowly, observations during deployment are sometimes within the turbulent wake of the descending vehicle.

## Acknowledgments

COARE Survey cruises on Wecoma were undertaken jointly by scientists from the University of Hawaii (R. Lukas, P. Hacker, and E. Firing) and Oregon State University (A. Huyer, M. Kosro and C. Paulson). Seasoor watchstanders on this cruise included personnel from both institutions (Eric Firing, Fred Bingham, Joanna Muench and Dail Rowe from UH; Jane Huyer, Bob Smith, Tim Holt, Jane Fleischbein, Marc Willis from OSU). We are deeply indebted to Wecoma's Marine Technicians: Marc Willis, Brian Wendler, Mike Hill and Tim Holt; this work would not have been possible without their skill and dedication. We are grateful to Nordeen Larson of SeaBird Electronics for his advice on installing the SeaBird sensors in the Seasoor vehicle and on data processing principles. Dail Rowe analyzed most of the salinity samples. Our COARE Survey cruises were supported by the National Science Foundation through its Ocean Sciences Division and by NOAA's Office of Global Programs under TOGA.

## References

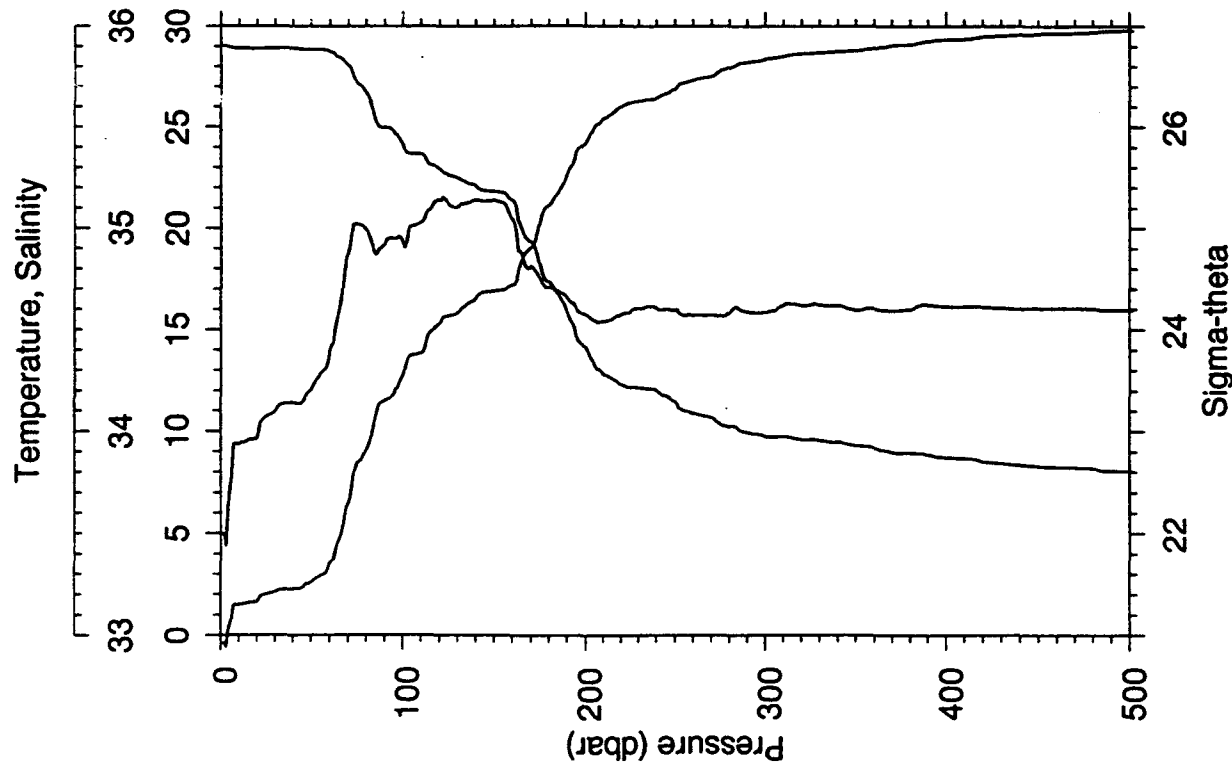
- Anonymous, 1992. *CTD Data Acquisition Software, SEASOFT Version 4.015*. Sea-Bird Electronics, Inc., Bellevue, Washington, USA.
- Fofonoff, N. P., and R. C. Millard. 1983. *Algorithms for computation of fundamental properties of seawater*. Unesco Technical Papers in Marine Science, 44, 53 pp.
- Larson, N. 1992. *Oceanographic CTD Sensors: Principles of Operation, Sources of Error, and Methods for Correcting Data*. Sea-Bird Electronics, Inc., Bellevue, Washington, USA.
- Lueck, R. 1990. Thermal inertia of conductivity cells: *Theory*. *J. Atmos. Oceanic Tech.*, 7, 741-755.
- Lueck, R., and J. J. Picklo. 1990. Thermal inertia of conductivity cells: *Observations with a Sea-Bird cell*. *J. Atmos. Oceanic Tech.*, 7, 756-768.
- Webster, P. J., and R. Lukas, 1992. TOGA COARE: The Coupled Ocean-Atmosphere Response Experiment. *Bull. Amer. Met. Soc.*, 73, 1378-1416.

**CTD DATA**

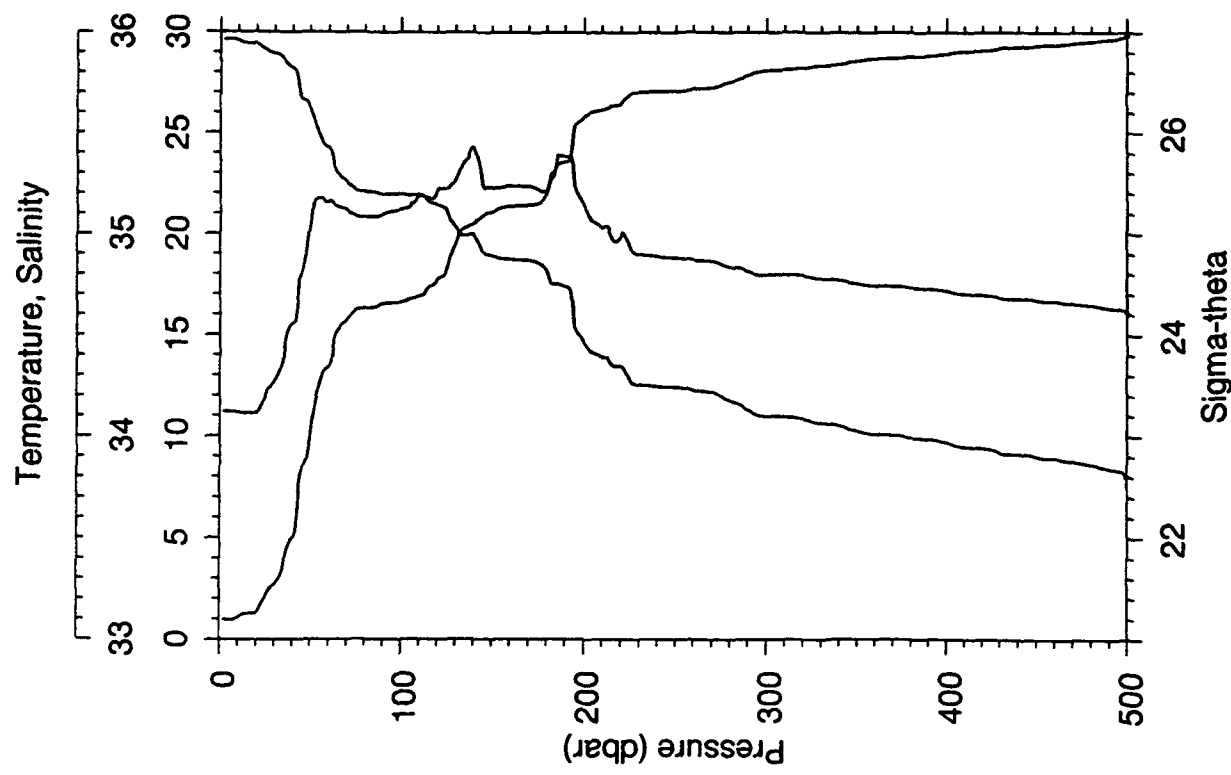
### CTD DATA

For each station, we present a plot of the vertical temperature, salinity, and sigma-t profiles, and a listing of the observed and derived variables at standard pressures. Header data includes the CTD Station Number, Latitude (in degrees and minutes; a negative degree integer indicates southern hemisphere), Longitude (degrees and minutes East), Date and Time (UTC), and Bottom Depth (in meters).

STA NO	1	LAT:	3	7.5	LONG: 156 7.1
26 JAN 1993	1439 GMT	DEPTH	2700		
P	T (C)	S	POT T (C)	SIGMA (CL/T)	DYN HT (J/KG)
(DB)				THETA	
1	29.042	33.492	29.041	20.920	684.7
10	28.910	33.935	28.908	21.298	648.9
20	28.896	33.961	28.891	21.323	647.0
30	28.900	34.096	28.893	21.423	637.8
40	28.916	34.143	28.907	21.454	635.4
50	28.864	34.206	28.852	21.520	629.5
60	28.739	34.397	28.725	21.705	612.3
70	28.066	34.877	28.049	22.288	556.9
80	26.707	34.993	26.688	22.813	507.1
90	24.973	34.918	24.954	23.295	461.3
100	24.144	34.930	24.123	23.554	437.0
110	23.668	35.028	23.645	23.769	416.9
120	22.954	35.139	22.930	24.061	389.4
130	22.487	35.104	22.461	24.168	379.5
140	22.105	35.140	22.077	24.304	366.9
150	21.829	35.138	21.799	24.380	360.0
160	21.361	35.043	21.330	24.437	354.9
170	19.310	34.811	19.279	24.806	319.7
180	17.328	34.707	17.298	25.219	280.2
190	15.823	34.656	15.793	25.531	250.5
200	14.161	34.578	14.132	25.834	221.5
225	12.173	34.585	12.143	26.240	182.9
250	11.497	34.596	11.466	26.376	170.4
275	10.349	34.570	10.317	26.562	152.8
300	9.746	34.586	9.712	26.678	142.0
325	9.596	34.623	9.559	26.732	137.4
350	9.306	34.597	9.267	26.760	135.1
375	8.951	34.596	8.911	26.816	130.0
400	8.717	34.615	8.674	26.868	125.4
425	8.469	34.608	8.425	26.902	122.5
450	8.296	34.606	8.249	26.927	120.4
475	8.226	34.606	8.177	26.938	119.8
500	8.049	34.596	7.997	26.957	118.2
502	8.048	34.596	7.996	26.957	118.3



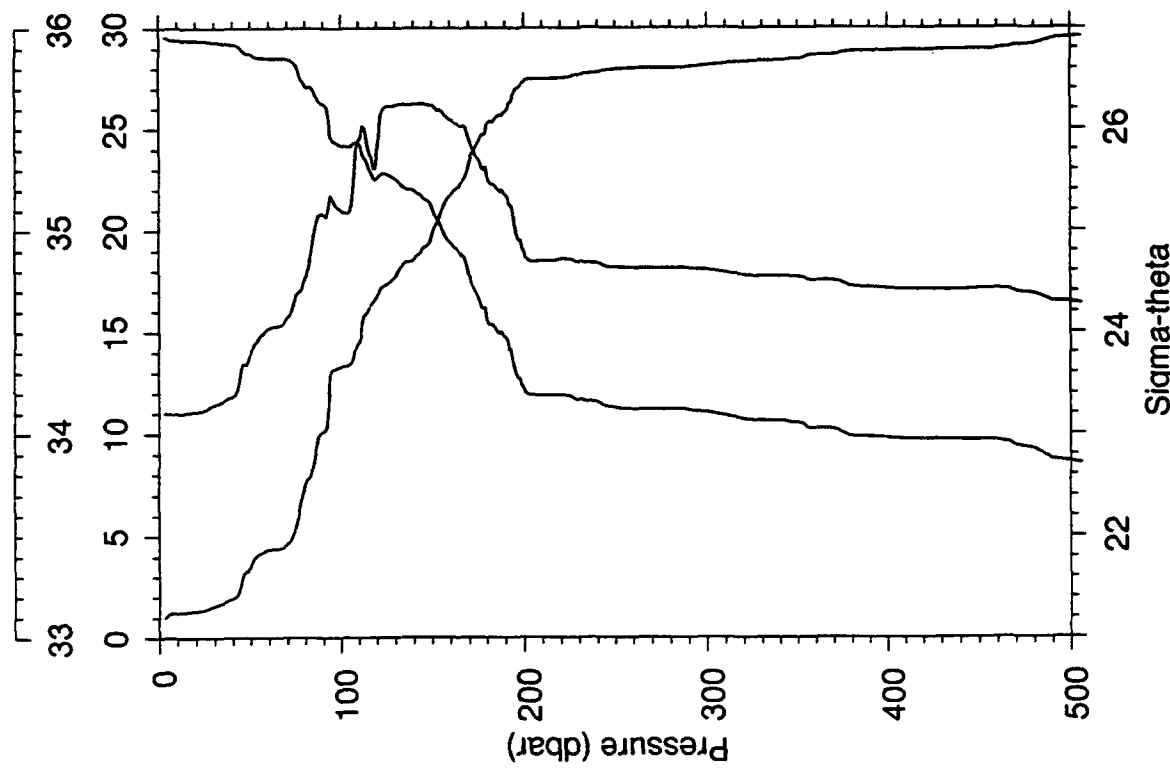
Before Tow 1

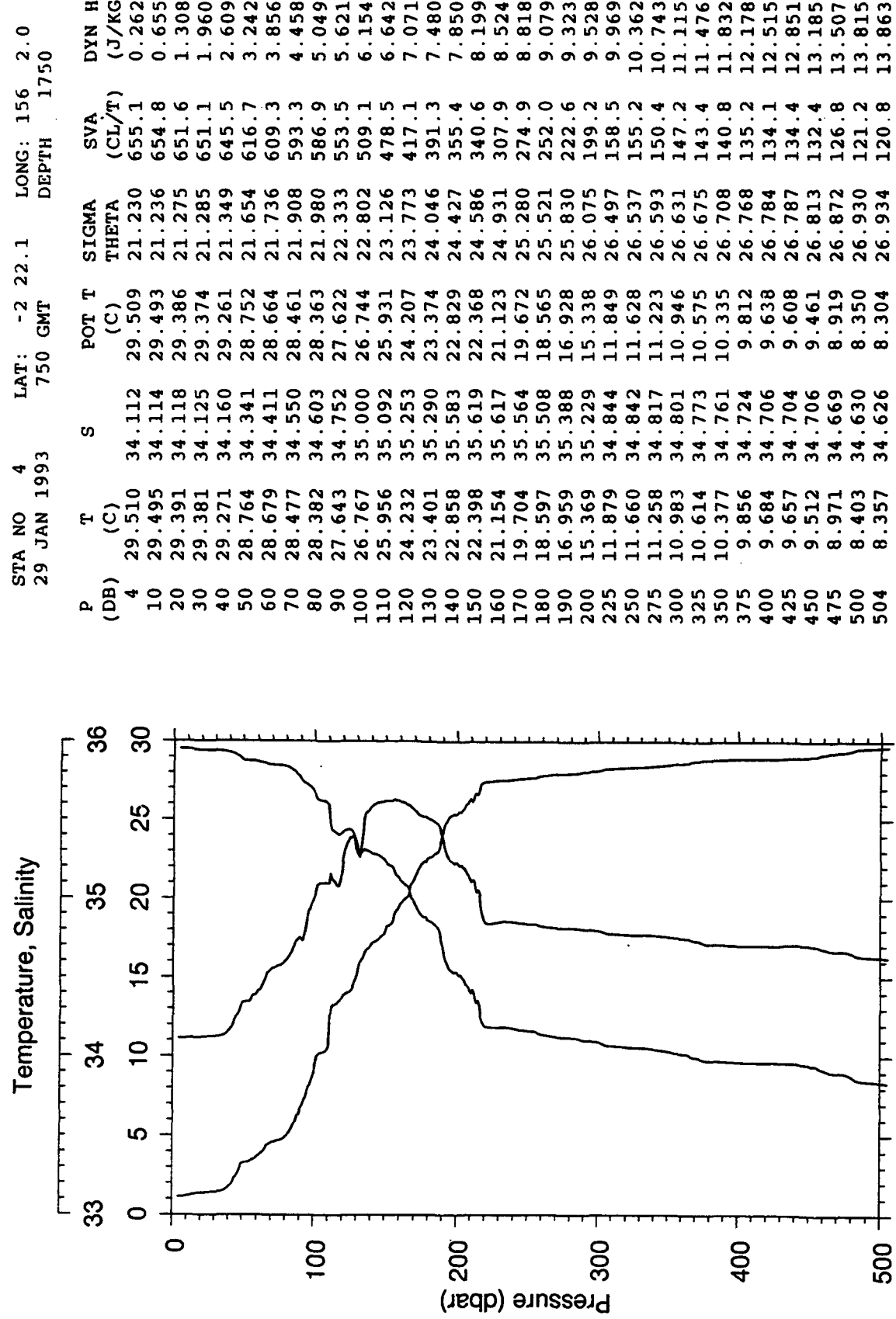


STA NO	27 JAN 1993	2	LAT:	-1	14.0	LONG:	156	5.9
			725	GMT	DEPTH	2020		
P	(DB)	T (C)	S	POT T (C)	SIGMA THETA	SVA (CL/T)	DYN HT	(J/KG)
2	29.636	34.119	29.635	21.192	658.7	0.132		
10	29.573	34.116	29.570	21.212	657.2	0.659		
20	29.424	34.113	29.419	21.260	653.0	1.313		
30	28.949	34.267	28.942	21.535	627.1	1.951		
40	28.209	34.557	28.200	21.999	583.2	2.558		
50	26.256	35.036	26.244	22.986	489.1	3.092		
60	24.288	35.158	24.275	23.681	423.1	3.537		
70	22.587	35.118	22.573	24.147	379.0	3.932		
80	22.081	35.082	22.065	24.263	368.3	4.303		
90	21.958	35.097	21.940	24.309	364.3	4.671		
100	21.976	35.121	21.956	24.324	363.4	5.034		
110	21.949	35.190	21.927	24.384	358.0	5.395		
120	21.424	35.215	21.401	24.549	342.6	5.747		
130	20.330	35.269	20.306	24.887	310.7	6.077		
140	20.012	35.431	19.986	25.096	291.2	6.374		
150	18.953	35.230	18.926	25.217	279.8	6.657		
160	18.750	35.239	18.722	25.276	274.6	6.934		
170	18.702	35.238	18.672	25.288	273.8	7.208		
180	18.179	35.214	18.148	25.400	263.4	7.479		
190	17.422	35.385	17.390	25.717	233.5	7.721		
200	14.649	35.136	14.619	26.161	190.7	7.931		
225	12.819	34.940	12.789	26.389	169.1	8.385		
250	12.447	34.883	12.414	26.419	166.8	8.802		
275	12.034	34.855	11.998	26.477	161.8	9.215		
300	11.023	34.798	10.986	26.622	148.2	9.601		
325	10.746	34.786	10.707	26.662	144.8	9.969		
350	10.298	34.756	10.257	26.718	139.8	10.326		
375	10.061	34.743	10.017	26.748	137.3	10.671		
400	9.733	34.720	9.687	26.787	133.9	11.010		
425	9.371	34.695	9.323	26.827	130.3	11.339		
450	9.000	34.672	8.951	26.870	126.5	11.659		
475	8.696	34.651	8.645	26.902	123.7	11.972		
500	8.028	34.613	7.977	26.974	116.7	12.276		
499	7.965	34.610	7.914	26.981	115.9	12.264		

STA NO 29 JAN 1993	3	LAT: 540	27.2	LONG: 1720	156	7.8
P (DB)	T (C)	S	POT T (C)	SIGMA THETA	SVA (CL/T)	DYN HT (J/KG)
3	29.585	34.103	29.584	21.197	658.2	0.197
10	29.424	34.099	29.421	21.249	653.6	0.656
20	29.404	34.110	29.399	21.265	652.6	1.309
30	29.322	34.144	29.314	21.319	647.8	1.960
40	29.203	34.184	29.193	21.390	641.5	2.604
50	28.740	34.391	28.728	21.700	612.3	3.231
60	28.517	34.519	28.503	21.870	596.5	3.832
70	28.462	34.571	28.445	21.929	591.3	4.427
80	27.137	34.769	27.119	22.508	536.3	4.997
90	26.248	35.080	26.228	23.025	487.3	5.508
100	24.217	35.101	24.196	23.661	426.8	5.955
110	24.296	35.447	24.273	23.900	404.5	6.376
120	22.576	35.378	22.552	24.350	361.8	6.753
130	22.538	35.616	22.512	24.543	343.9	7.104
140	21.988	35.623	21.960	24.704	328.9	7.438
150	21.133	35.619	21.104	24.938	306.9	7.757
160	19.399	35.544	19.370	25.343	268.4	8.042
170	17.857	35.453	17.828	25.663	238.0	8.299
180	15.594	35.263	15.566	26.050	200.9	8.518
190	14.733	35.173	14.707	26.170	189.6	8.714
200	12.264	34.896	12.238	26.463	161.2	8.887
225	11.840	34.857	11.810	26.515	156.8	9.281
250	11.279	34.818	11.248	26.589	150.1	9.664
275	11.184	34.812	11.150	26.602	149.5	10.038
300	11.035	34.804	10.998	26.624	147.9	10.411
325	10.649	34.774	10.610	26.670	143.9	10.775
350	10.519	34.769	10.477	26.689	142.7	11.134
375	9.985	34.735	9.941	26.756	136.5	11.483
400	9.778	34.712	9.732	26.773	135.3	11.821
425	9.718	34.708	9.669	26.780	135.1	12.159
450	9.681	34.713	9.629	26.790	134.7	12.496
475	9.327	34.692	9.274	26.833	130.9	12.830
500	8.645	34.647	8.591	26.906	123.7	13.146
502	8.575	34.641	8.521	26.913	123.1	13.171

Temperature, Salinity



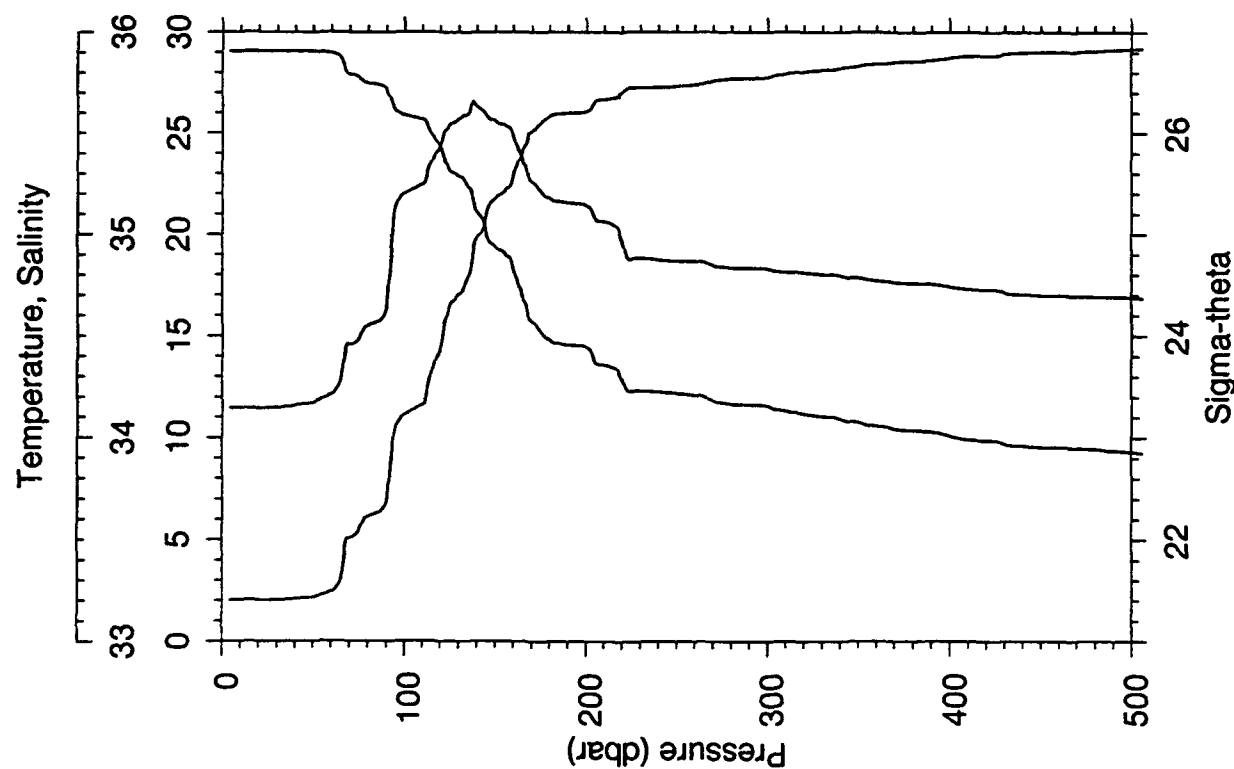


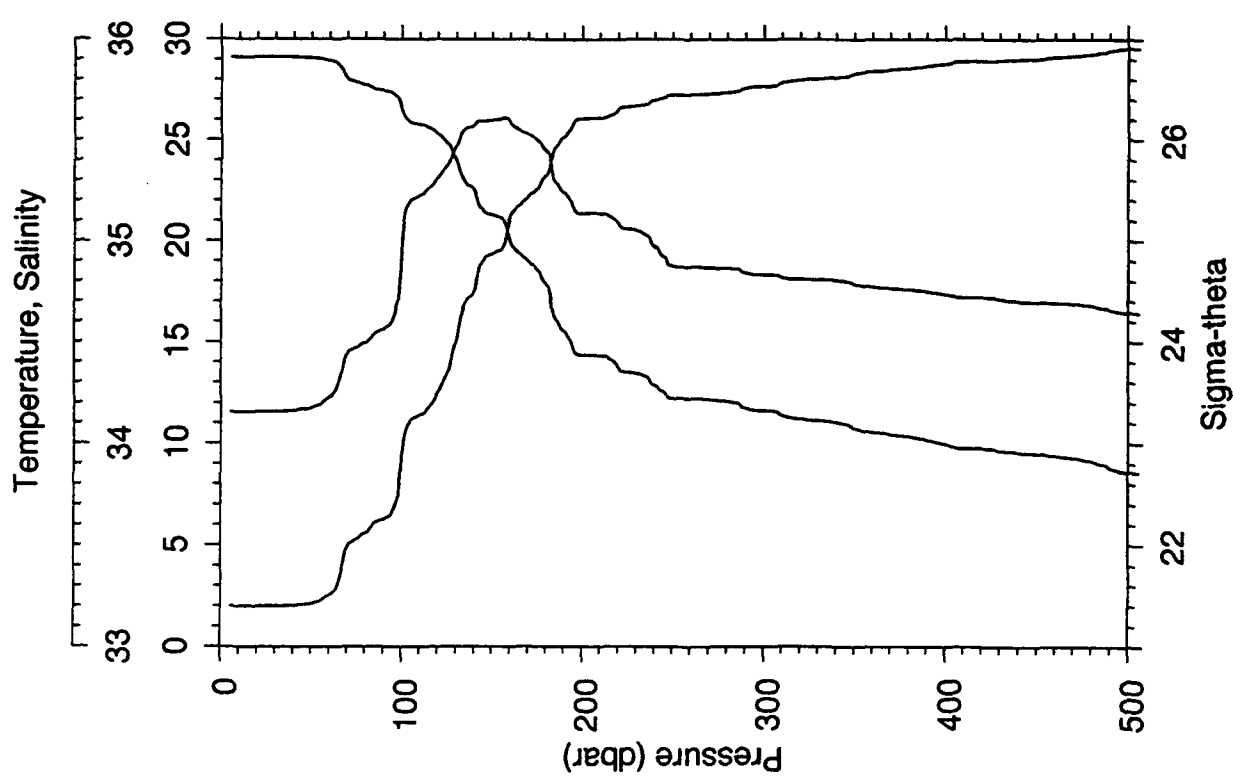
22      24      Sigma-theta

22      24

22      24

STA NO 02 FEB 1993	LAT: 5 2035 GMT	LONG: 155 30.3		DEPTH 1940			
		P (DB)	T (C)	S	POT T	SIGMA (C)	SVA (CL/T)
4	29.062	34.145	29.061	21.404	638.4	0.255	
10	29.052	34.146	29.049	21.409	638.2	0.638	
20	29.059	34.146	29.054	21.407	638.9	1.277	
30	29.063	34.150	29.056	21.410	639.1	1.916	
40	29.063	34.159	29.053	21.417	638.9	2.555	
50	29.057	34.170	29.045	21.428	638.3	3.194	
60	28.975	34.213	28.961	21.489	633.0	3.829	
70	27.936	34.461	27.919	22.018	582.8	4.444	
80	27.495	34.551	27.476	22.229	563.0	5.018	
90	27.234	34.631	27.213	22.374	549.6	5.577	
100	25.884	35.203	25.862	23.231	468.0	6.070	
110	25.687	35.247	25.662	23.326	459.4	6.534	
120	24.334	35.436	24.308	23.881	406.8	6.966	
130	22.866	35.571	22.839	24.415	356.1	7.340	
140	21.095	35.634	21.068	24.960	304.4	7.678	
150	19.410	35.562	19.383	25.353	267.0	7.962	
160	18.244	35.479	18.217	25.587	245.0	8.221	
170	15.702	35.258	15.676	26.021	203.4	8.444	
180	14.784	35.179	14.757	26.164	189.8	8.640	
190	14.540	35.156	14.512	26.199	186.8	8.828	
200	14.415	35.141	14.385	26.215	185.5	9.015	
225	12.277	34.876	12.247	26.446	163.5	9.448	
250	12.160	34.868	12.127	26.463	162.5	9.855	
275	11.694	34.838	11.658	26.528	156.7	10.256	
300	11.535	34.828	11.497	26.551	155.1	10.646	
325	11.084	34.806	11.043	26.617	149.3	11.025	
350	10.742	34.786	10.700	26.663	145.3	11.394	
375	10.377	34.761	10.332	26.709	141.3	11.751	
400	10.078	34.743	10.032	26.746	138.1	12.102	
425	9.866	34.728	9.816	26.771	136.1	12.443	
450	9.539	34.699	9.488	26.804	133.3	12.779	
475	9.467	34.695	9.413	26.812	132.9	13.112	
500	9.308	34.689	9.252	26.834	131.2	13.442	
505	9.263	34.685	9.207	26.839	130.9	13.508	

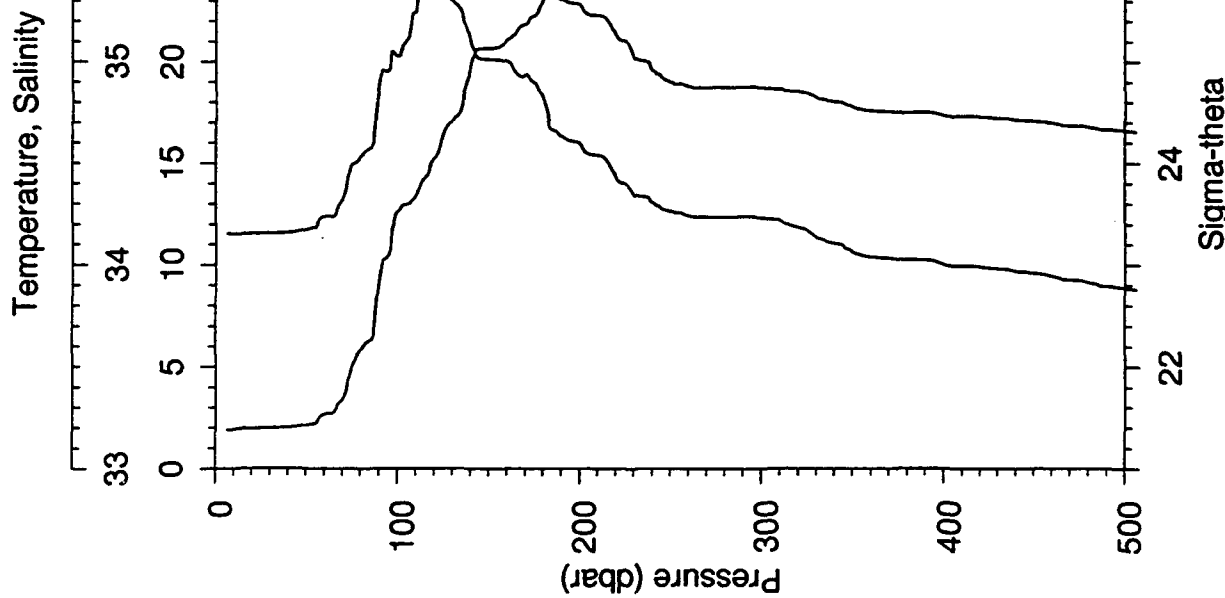


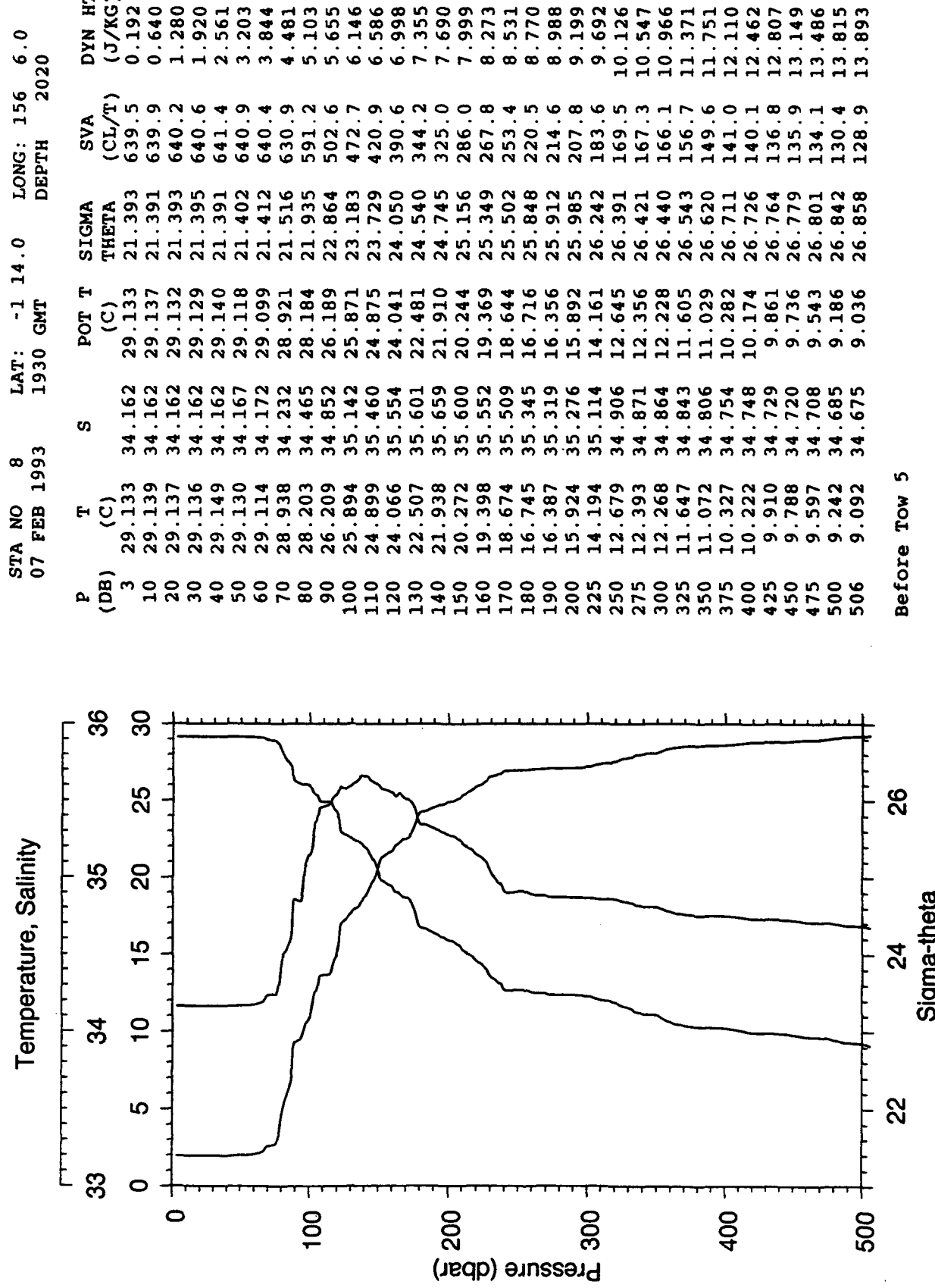


STA NO 03 FEB 1993	LAT: -1 51.9		LONG: 155 34.4		DEPTH 1900				
	6	2159 GMT	T (DB)	S (C)		POT T (C)	SIGMA (CL/T)	SVA	DYN HT (J/KG)
	5	29.095	34.154	29.093	21.400	638.9	0.319		
	10	29.098	34.153	29.096	21.399	639.2	0.639		
	20	29.104	34.154	29.099	21.399	639.7	1.278		
	30	29.102	34.156	29.095	21.401	639.9	1.918		
	40	29.101	34.158	29.091	21.404	640.2	2.558		
	50	29.069	34.174	29.056	21.427	638.4	3.198		
	60	28.927	34.230	28.913	21.517	630.3	3.833		
	70	28.016	34.441	28.000	21.977	586.7	4.447		
	80	27.712	34.495	27.693	22.117	573.7	5.026		
	90	27.456	34.562	27.435	22.251	561.4	5.592		
	100	26.438	34.996	26.416	22.902	499.5	6.140		
	110	25.771	35.226	25.747	23.284	463.4	6.612		
	120	25.274	35.315	25.248	23.505	442.7	7.068		
	130	23.966	35.478	23.938	24.023	393.6	7.489		
	140	22.516	35.576	22.488	24.519	346.6	7.852		
	150	21.315	35.599	21.286	24.873	313.1	8.174		
	160	19.879	35.585	19.850	25.249	277.5	8.476		
	170	18.973	35.527	18.943	25.440	259.4	8.744		
	180	17.853	35.444	17.822	25.657	238.9	8.994		
	190	15.586	35.243	15.556	26.036	202.6	9.210		
	200	14.396	35.138	14.366	26.217	185.4	9.402		
	225	13.548	35.061	13.516	26.336	174.5	9.857		
	250	12.268	34.875	12.235	26.448	164.0	10.282		
	275	12.139	34.866	12.103	26.466	162.9	10.691		
	300	11.647	34.834	11.609	26.535	156.7	11.090		
	325	11.163	34.811	11.122	26.607	150.3	11.474		
	350	10.756	34.786	10.713	26.661	145.5	11.846		
	375	10.397	34.762	10.352	26.706	141.6	12.205		
	400	9.988	34.736	9.941	26.756	137.0	12.553		
	425	9.755	34.720	9.706	26.783	134.8	12.891		
	450	9.511	34.697	9.460	26.807	133.0	13.225		
	475	9.226	34.685	9.173	26.844	129.7	13.553		
	500	8.607	34.645	8.553	26.911	123.3	13.869		
	505	8.575	34.641	8.521	26.913	123.1	13.931		

Before Tow 4

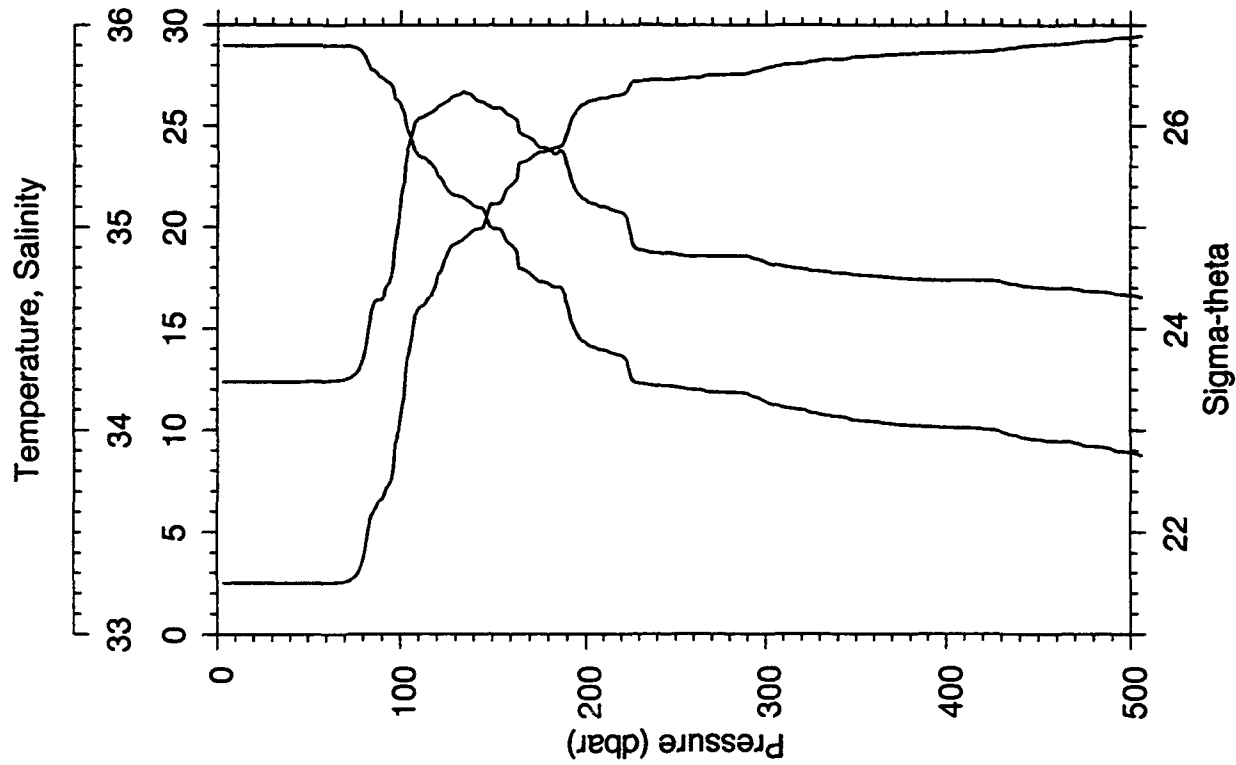
STA NO 07 FEB 1993	LAT: -1 17.2			LONG: 156 9.6		
	7	3	GMT	DEPTH	1980	
P (DB)	T (C)	S	POT T (C)	SIGMA THETA (CL/T)	DYN HT (J/KG)	
6	29.162	34.152	29.160	21.376	641.2	0.385
10	29.150	34.152	29.148	21.381	641.0	0.641
20	29.117	34.153	29.112	21.393	640.3	1.281
30	29.111	34.154	29.104	21.397	640.4	1.921
40	29.103	34.158	29.093	21.403	640.3	2.562
50	29.074	34.174	29.062	21.425	638.6	3.201
60	28.901	34.235	28.886	21.530	629.0	3.836
70	28.636	34.320	28.619	21.692	614.9	4.460
80	27.645	34.531	27.627	22.165	569.1	5.049
90	26.313	34.887	26.293	22.859	503.2	5.602
100	24.505	35.024	24.484	23.517	440.6	6.074
110	24.536	35.239	24.513	23.671	426.4	6.508
120	24.042	35.533	24.017	24.042	391.4	6.916
130	22.969	35.619	22.942	24.421	355.6	7.288
140	20.957	35.599	20.930	24.970	303.3	7.624
150	20.106	35.510	20.078	25.131	288.3	7.915
160	20.003	35.582	19.974	25.214	280.8	8.201
170	19.322	35.543	19.292	25.362	266.9	8.475
180	18.108	35.465	18.077	25.610	243.4	8.732
190	16.299	35.305	16.268	25.922	213.7	8.954
200	15.955	35.280	15.923	25.982	208.2	9.165
225	13.988	35.101	13.955	26.276	180.4	9.652
250	12.635	34.897	12.601	26.393	169.3	10.086
275	12.359	34.872	12.323	26.428	166.6	10.504
300	12.301	34.871	12.261	26.439	166.2	10.921
325	11.685	34.845	11.643	26.537	157.2	11.328
350	10.642	34.779	10.600	26.676	144.0	11.704
375	10.297	34.753	10.253	26.716	140.5	12.058
400	10.034	34.736	9.987	26.749	137.8	12.408
425	9.882	34.727	9.833	26.768	136.4	12.751
450	9.604	34.708	9.552	26.800	133.7	13.089
475	9.248	34.685	9.195	26.840	130.1	13.418
500	8.867	34.661	8.812	26.883	126.2	13.738
501	8.853	34.659	8.798	26.884	126.1	13.750

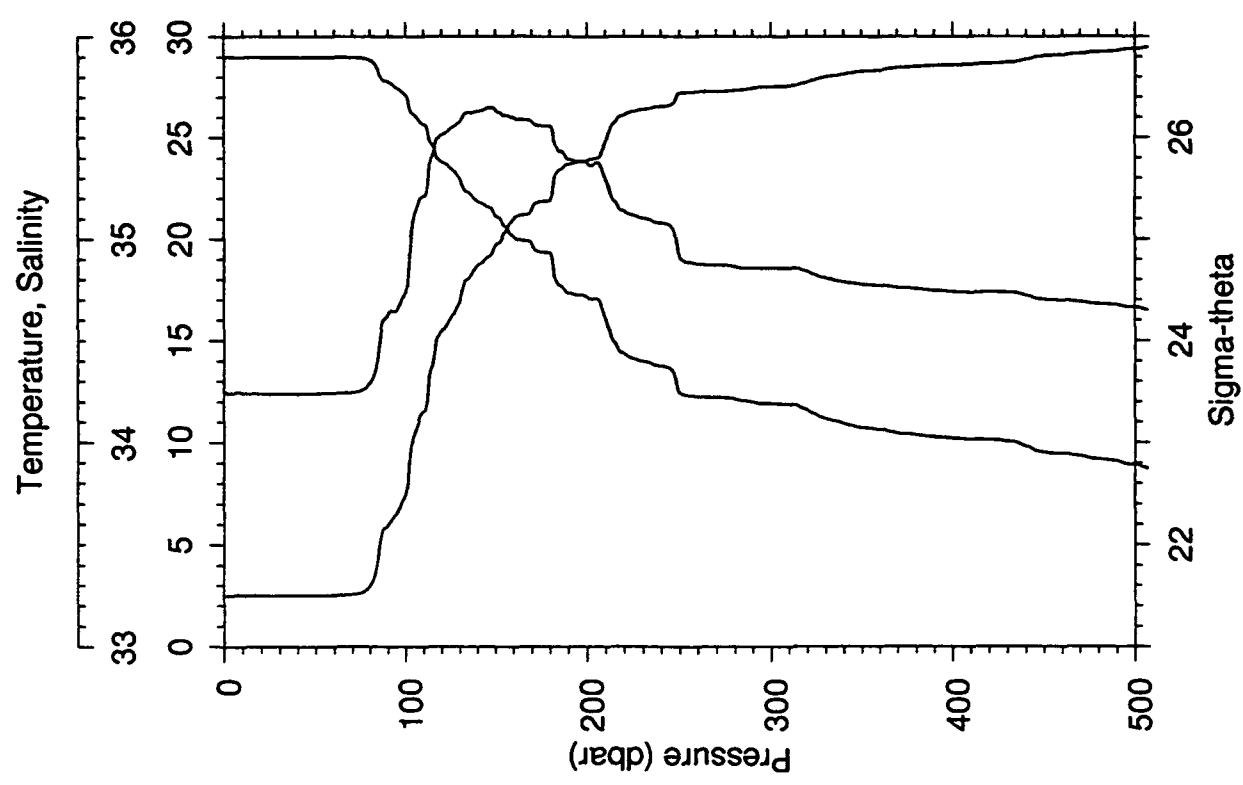




STA NO 9  
12 FEB 1993 LAT: -2 0.5 LONG: 155 40.4  
DEPTH 2059 GMT DEPTH 1890

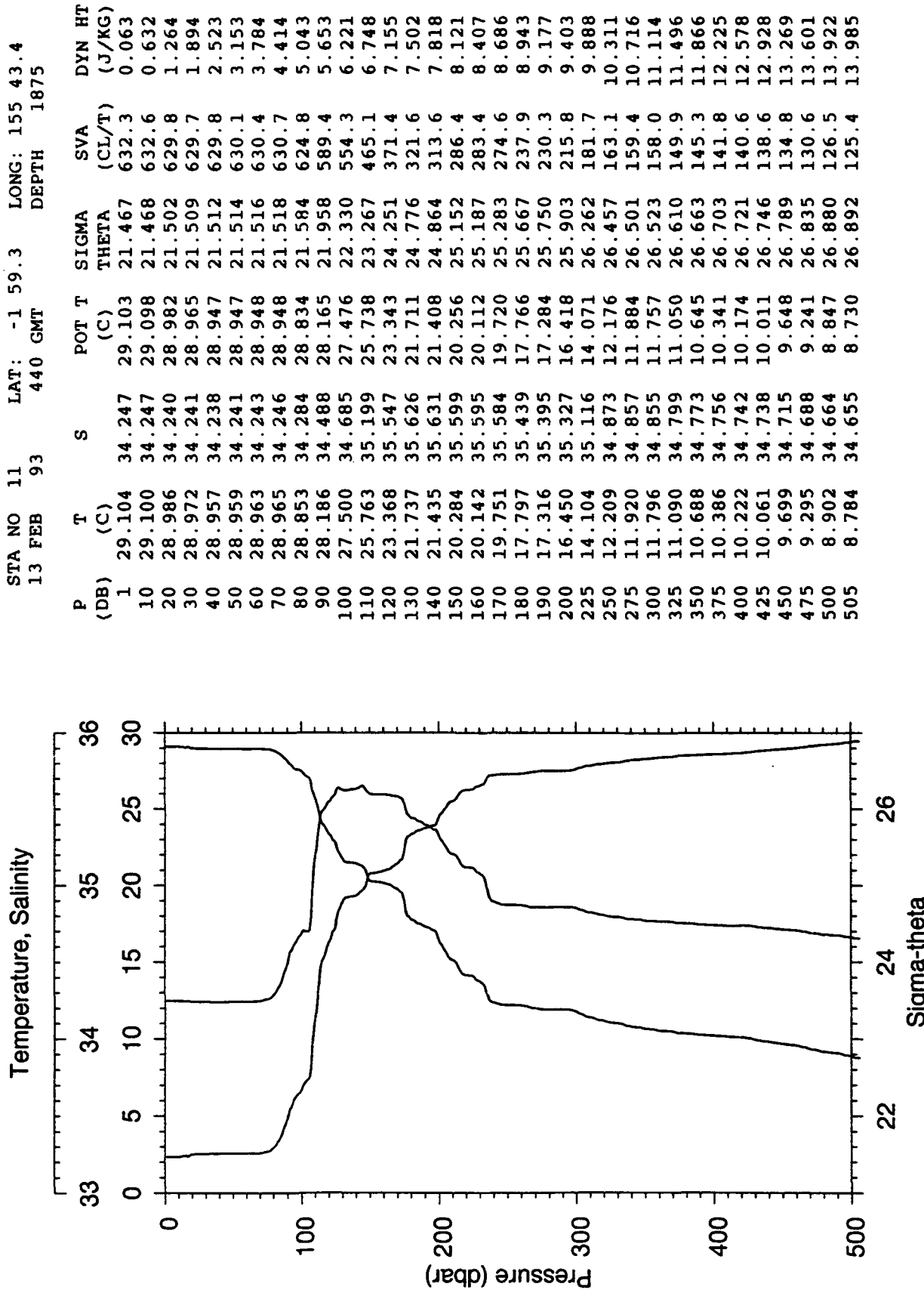
	P (DB)	T (C)	S	POT T	SIGMA (C)	SVA (CL/T)	DYN HT (J/KG)
3	28.975	34.235	28.974	21.501	629.1	0.189	
10	28.975	34.236	28.972	21.502	629.3	0.629	
20	28.973	34.236	28.968	21.504	629.7	1.259	
30	28.978	34.236	28.971	21.503	630.2	1.889	
40	28.981	34.237	28.971	21.503	630.7	2.519	
50	28.988	34.240	28.976	21.504	631.1	3.150	
60	28.991	34.241	28.976	21.505	631.5	3.781	
70	28.976	34.250	28.959	21.517	630.8	4.412	
80	28.574	34.354	28.555	21.729	610.9	5.038	
90	27.393	34.643	27.372	22.332	553.6	5.611	
100	26.043	35.130	26.021	23.127	478.0	6.135	
110	23.513	35.540	23.490	24.202	375.6	6.553	
120	22.660	35.594	22.635	24.491	348.5	6.919	
130	21.573	35.653	21.548	24.842	315.3	7.248	
140	21.067	35.640	21.041	24.972	303.3	7.558	
150	19.959	35.590	19.931	25.231	278.9	7.852	
160	19.149	35.550	19.120	25.412	261.8	8.125	
170	17.747	35.443	17.719	25.682	236.1	8.370	
180	17.217	35.384	17.187	25.766	228.4	8.601	
190	16.168	35.301	16.138	25.948	211.1	8.825	
200	14.314	35.136	14.285	26.232	183.8	9.018	
225	12.817	34.974	12.787	26.416	166.6	9.463	
250	12.146	34.867	12.113	26.465	162.3	9.871	
275	11.873	34.856	11.838	26.509	158.7	10.272	
300	11.402	34.826	11.364	26.574	152.9	10.665	
325	10.874	34.785	10.834	26.639	147.1	11.039	
350	10.514	34.766	10.472	26.688	142.8	11.402	
375	10.284	34.749	10.239	26.715	140.6	11.756	
400	10.158	34.738	10.111	26.728	139.8	12.107	
425	10.050	34.738	10.000	26.747	138.5	12.455	
450	9.560	34.706	9.509	26.805	133.1	12.794	
475	9.235	34.684	9.182	26.842	129.9	13.124	
500	8.915	34.664	8.860	26.878	126.7	13.445	
505	8.807	34.656	8.752	26.889	125.7	13.508	





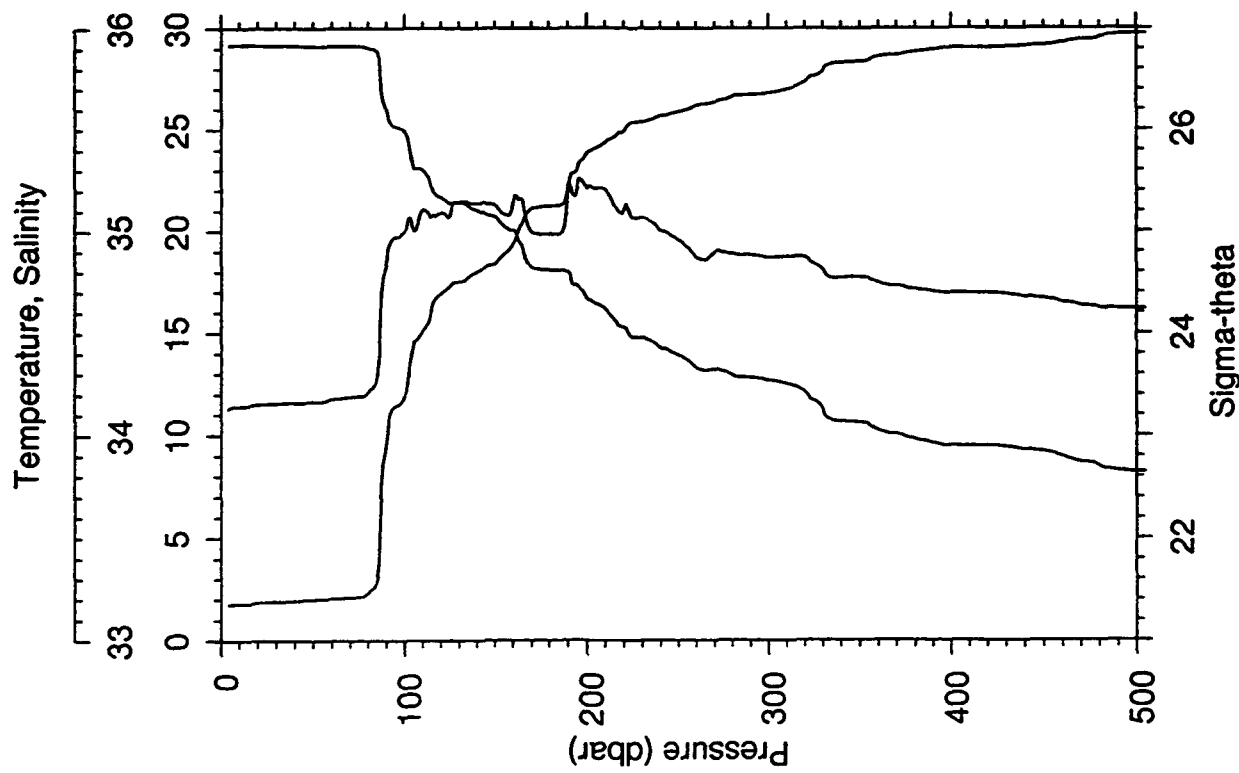
STA NO 12 FEB 1993	LAT: -2 0.4		LONG: 155 40.8		DEPTH 1880	
	P (DB)	T (C)	S	POT T (C)	SIGMA (CL/T)	DYN HT (J/KG)
1	29.003	34.249	29.003	21.502	629.0	0.063
10	28.977	34.239	28.975	21.503	629.2	0.629
20	28.975	34.239	28.970	21.505	629.5	1.258
30	28.976	34.237	28.969	21.504	630.1	1.888
40	28.977	34.238	28.968	21.505	630.5	2.519
50	28.979	34.239	28.967	21.506	630.8	3.149
60	28.979	34.242	28.964	21.509	631.0	3.780
70	28.971	34.249	28.954	21.518	630.7	4.411
80	28.831	34.294	28.812	21.599	623.4	5.040
90	27.768	34.628	27.747	22.199	566.3	5.632
100	27.097	34.741	27.074	22.501	537.9	6.186
110	25.655	35.210	25.630	23.308	461.1	6.674
120	23.789	35.513	23.764	24.101	385.7	7.092
130	22.994	35.578	22.967	24.383	359.2	7.466
140	21.868	35.630	21.840	24.743	325.2	7.804
150	21.161	35.639	21.132	24.946	306.1	8.122
160	20.165	35.605	20.135	25.189	283.2	8.418
170	19.711	35.581	19.679	25.291	273.8	8.696
180	19.324	35.559	19.292	25.375	266.1	8.964
190	17.347	35.392	17.316	25.741	231.2	9.204
200	17.158	35.376	17.125	25.774	228.3	9.434
225	14.107	35.116	14.075	26.262	181.8	9.942
250	12.410	34.905	12.376	26.443	164.5	10.386
275	12.195	34.870	12.159	26.458	163.6	10.795
300	11.899	34.855	11.860	26.504	159.8	11.199
325	11.372	34.822	11.331	26.577	153.2	11.594
350	10.734	34.777	10.691	26.658	145.8	11.966
375	10.424	34.758	10.379	26.698	142.3	12.326
400	10.213	34.741	10.166	26.722	140.5	12.680
425	10.111	34.739	10.061	26.738	139.4	13.030
450	9.523	34.703	9.471	26.809	132.7	13.371
475	9.224	34.683	9.171	26.843	129.8	13.700
500	8.913	34.664	8.859	26.878	126.7	14.021
504	8.782	34.654	8.728	26.891	125.4	14.072

Before Tow 6

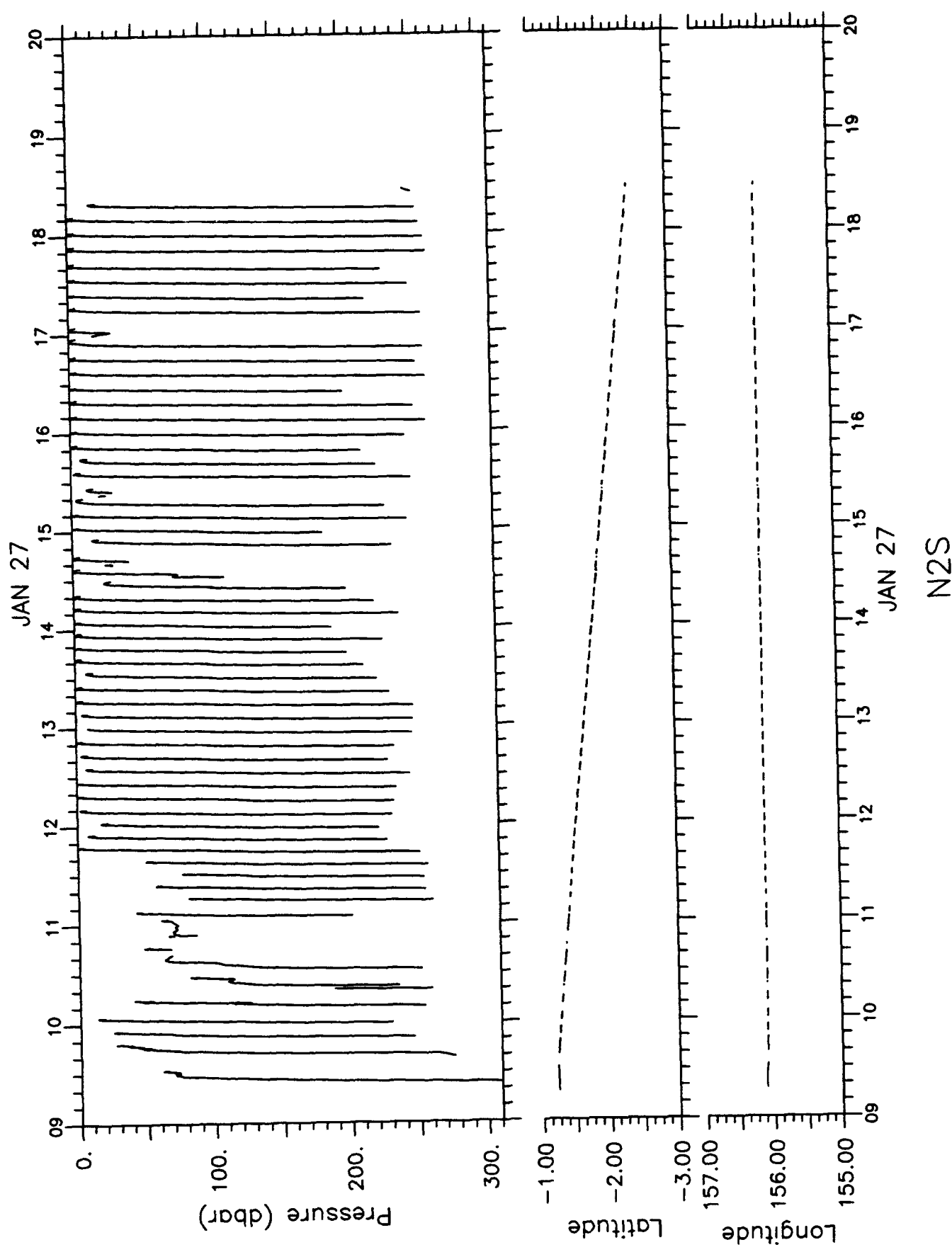


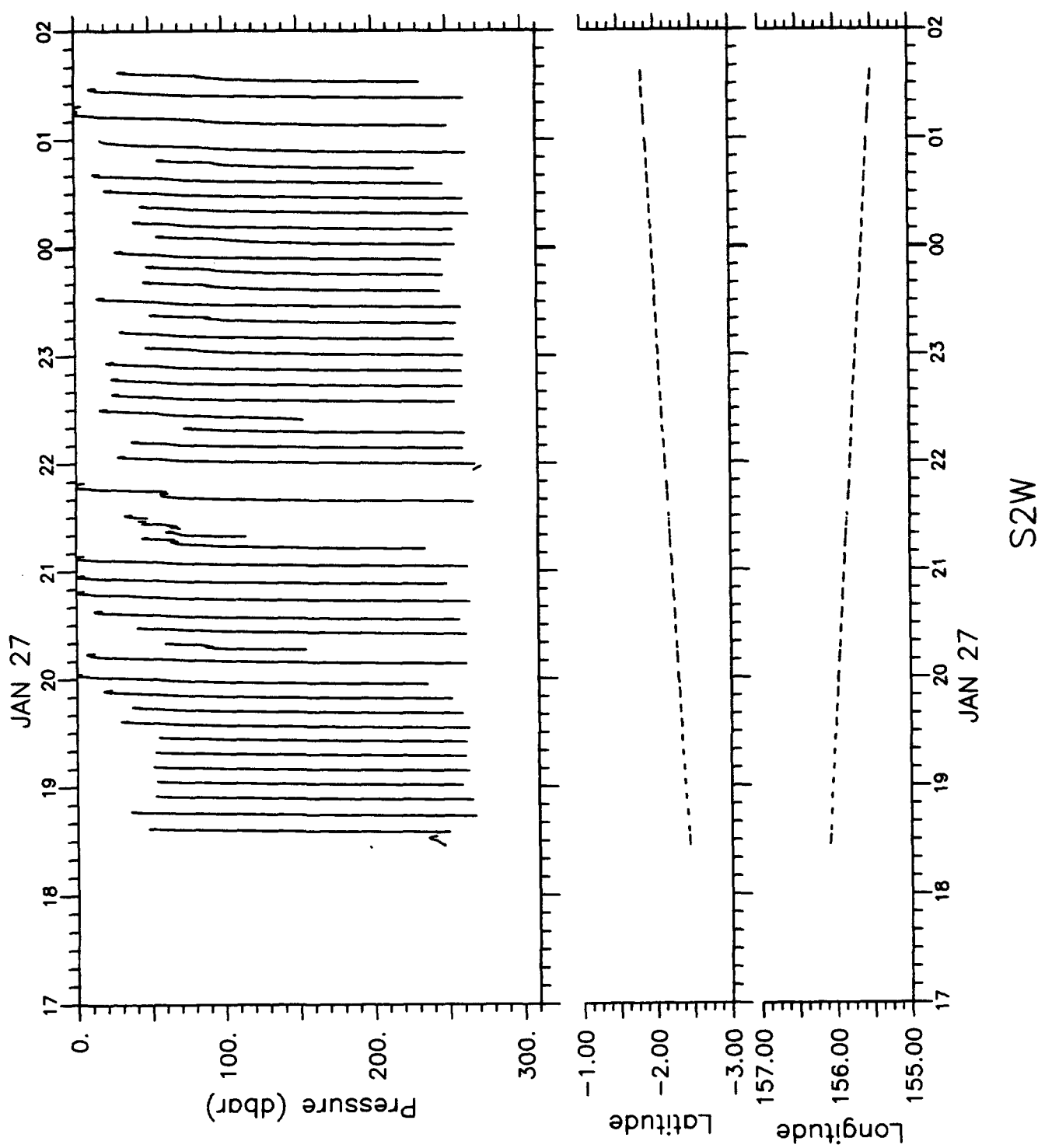
STA NO	12	LAT:	0	8.5	LONG: 156 5.9
	15 FEB 1993	2130 GMT	DEPTH		1925
P	T (C)	S	POT T (C)	SIGMA (CL/T)	DYN HT (J/KG)
(DB)					
4	29.177	34.126	29.176	21.351	643.5
10	29.192	34.141	29.189	21.358	643.1
20	29.165	34.151	29.160	21.376	641.9
30	29.163	34.156	29.156	21.381	641.9
40	29.146	34.159	29.136	21.390	641.5
50	29.122	34.165	29.110	21.403	640.8
60	29.127	34.177	29.112	21.412	640.4
70	29.127	34.186	29.110	21.419	640.2
80	29.039	34.211	29.020	21.467	636.0
90	25.943	34.846	25.923	22.943	495.0
100	24.866	34.998	24.845	23.388	452.9
110	23.011	35.109	22.989	24.022	392.7
120	21.659	35.089	21.635	24.389	358.0
130	21.393	35.145	21.368	24.505	347.2
140	21.028	35.137	21.001	24.599	338.6
150	20.722	35.128	20.693	24.676	331.7
160	20.049	35.143	20.020	24.867	313.7
170	18.208	34.995	18.179	25.225	279.6
180	18.096	34.986	18.065	25.246	277.9
190	18.018	35.225	17.985	25.449	259.0
200	16.651	35.207	16.619	25.765	229.0
225	14.802	35.064	14.768	26.073	199.9
250	13.913	34.955	13.877	26.179	190.2
275	13.130	34.896	13.091	26.295	179.6
300	12.697	34.871	12.656	26.362	173.7
325	11.708	34.840	11.666	26.529	158.0
350	10.639	34.774	10.597	26.672	144.4
375	9.910	34.721	9.866	26.757	136.3
400	9.498	34.696	9.452	26.807	131.9
425	9.474	34.694	9.426	26.810	132.1
450	9.211	34.670	9.161	26.834	130.1
475	8.661	34.632	8.610	26.892	124.6
500	8.226	34.618	8.174	26.948	119.3
505	8.227	34.619	8.175	26.948	119.4

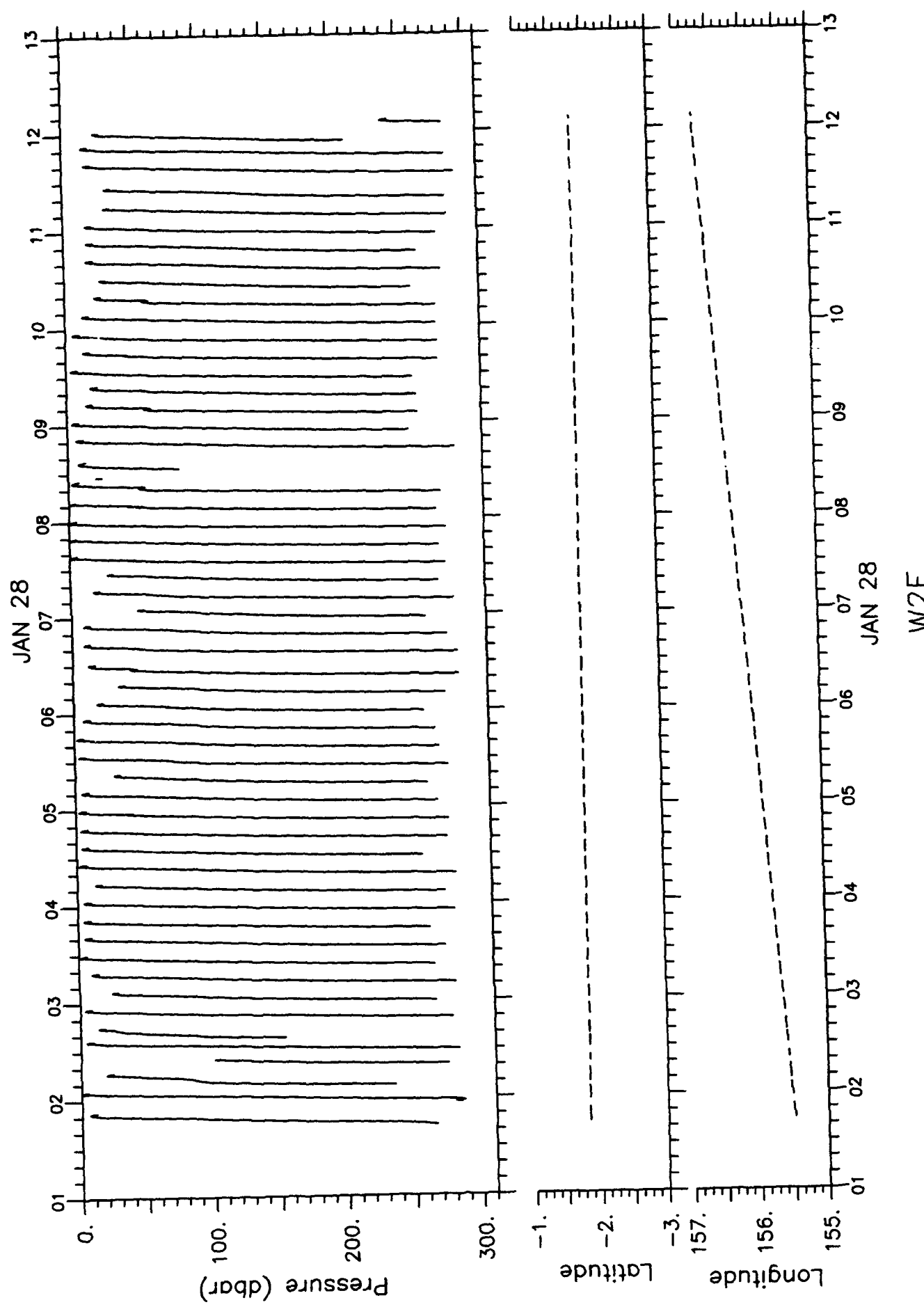
End of Tow 6

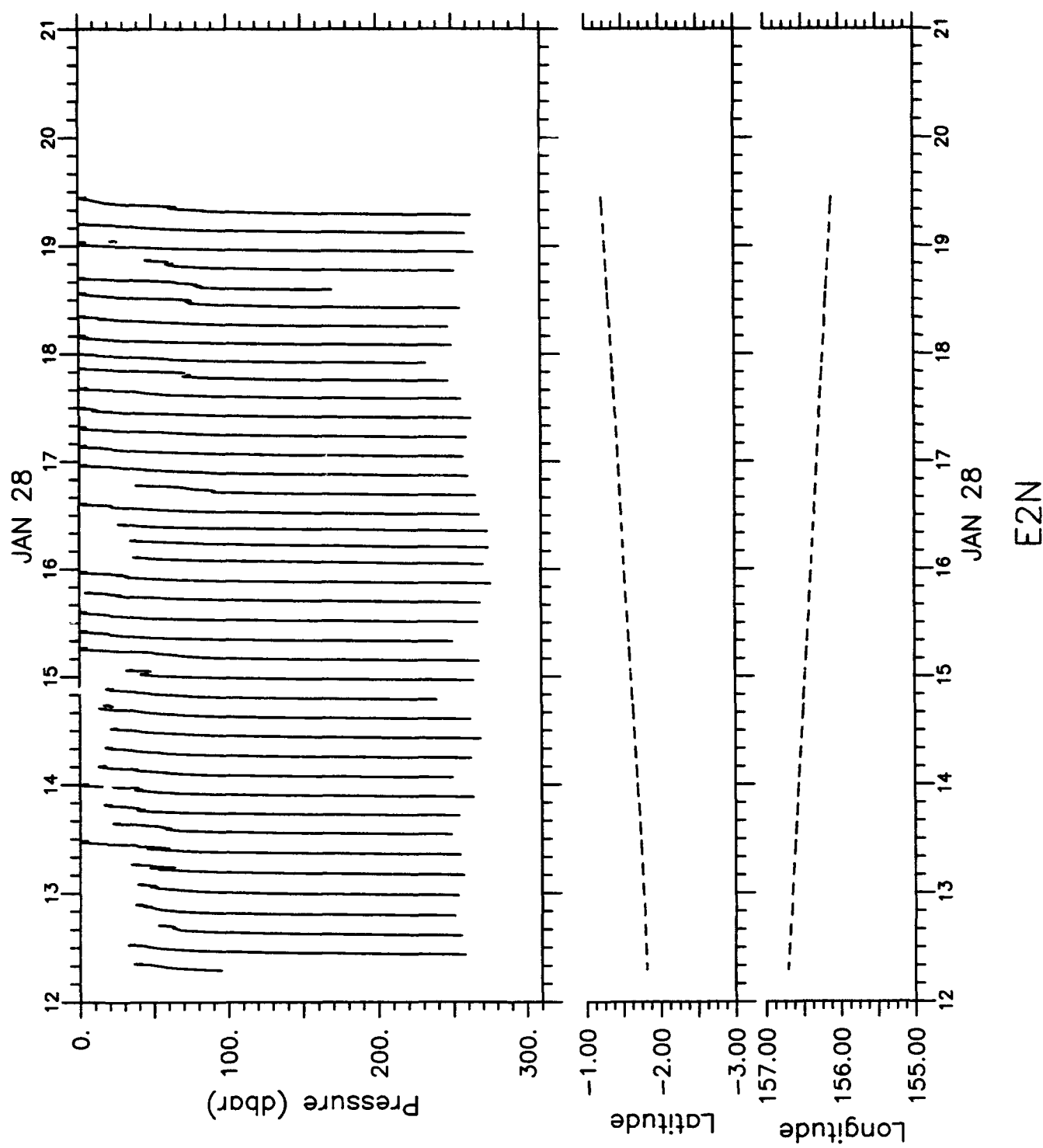


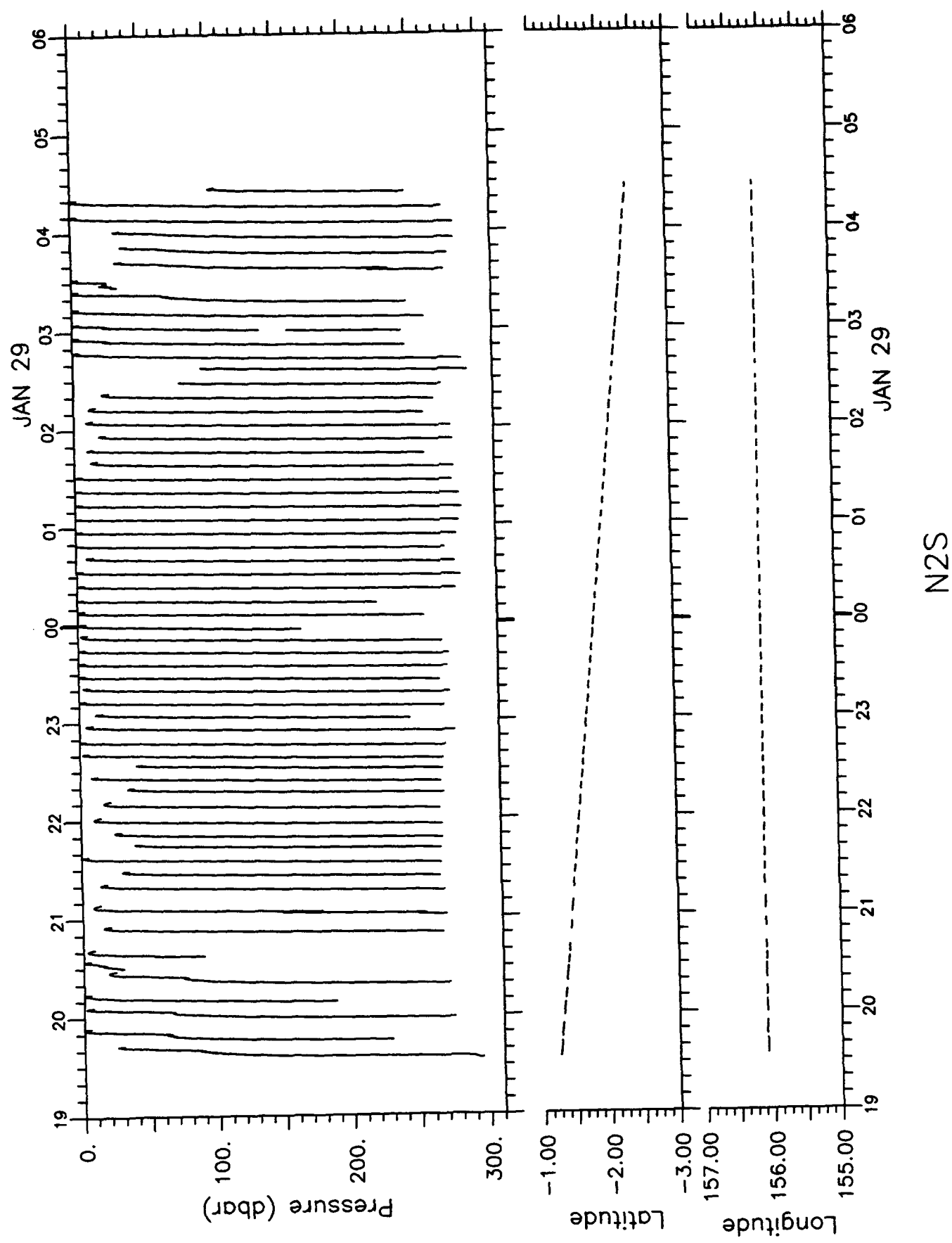
## **SEASOAR TRAJECTORIES**

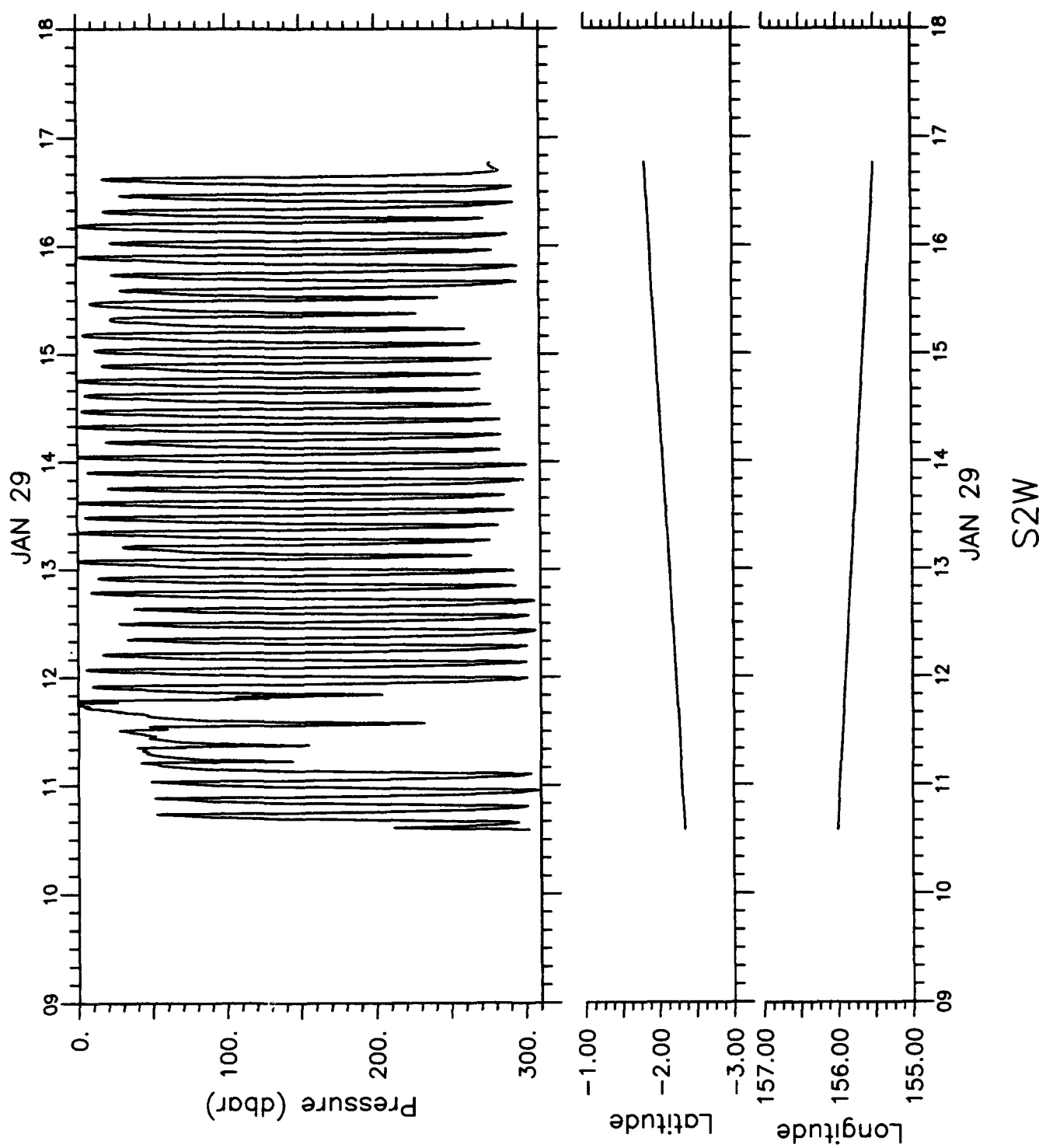


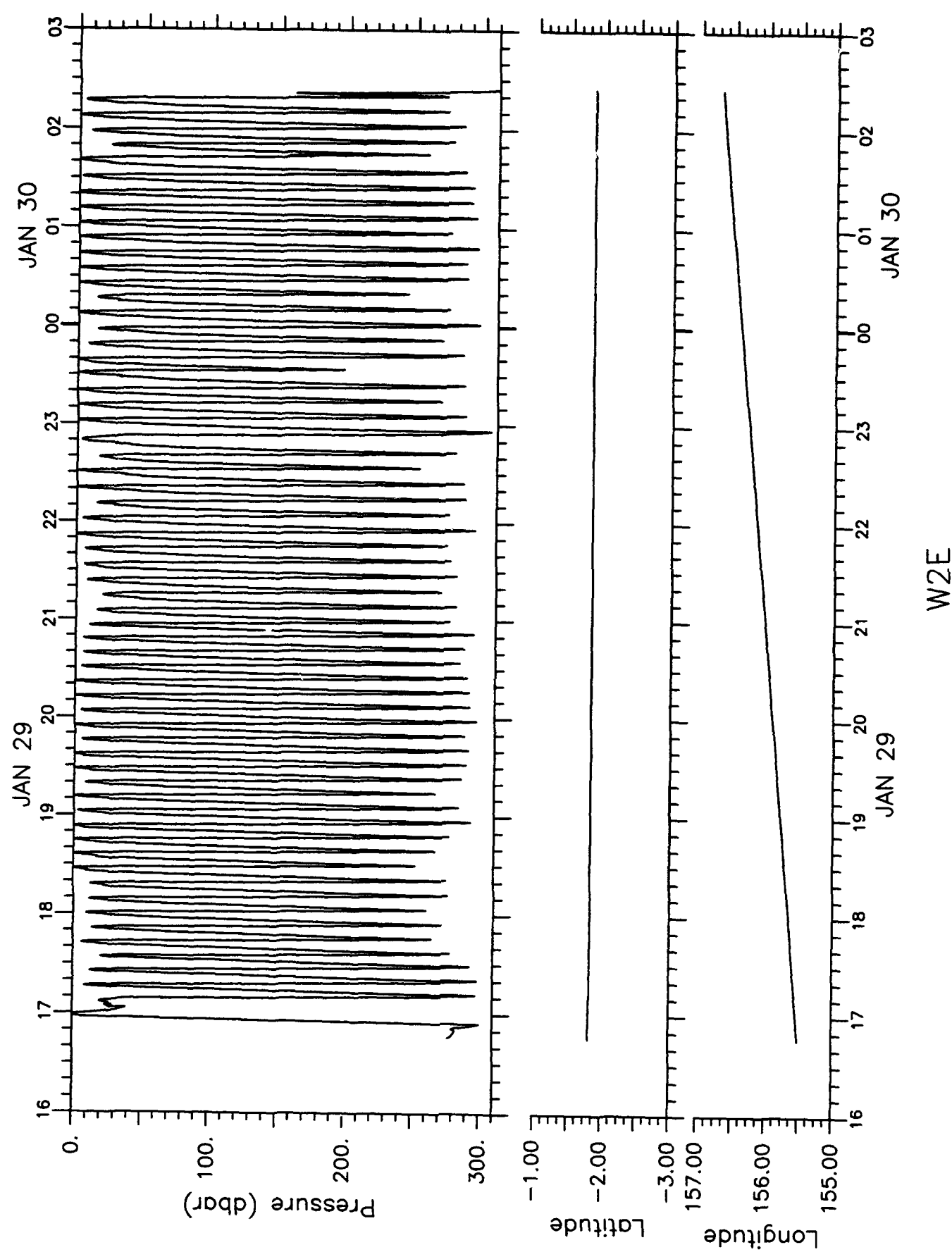


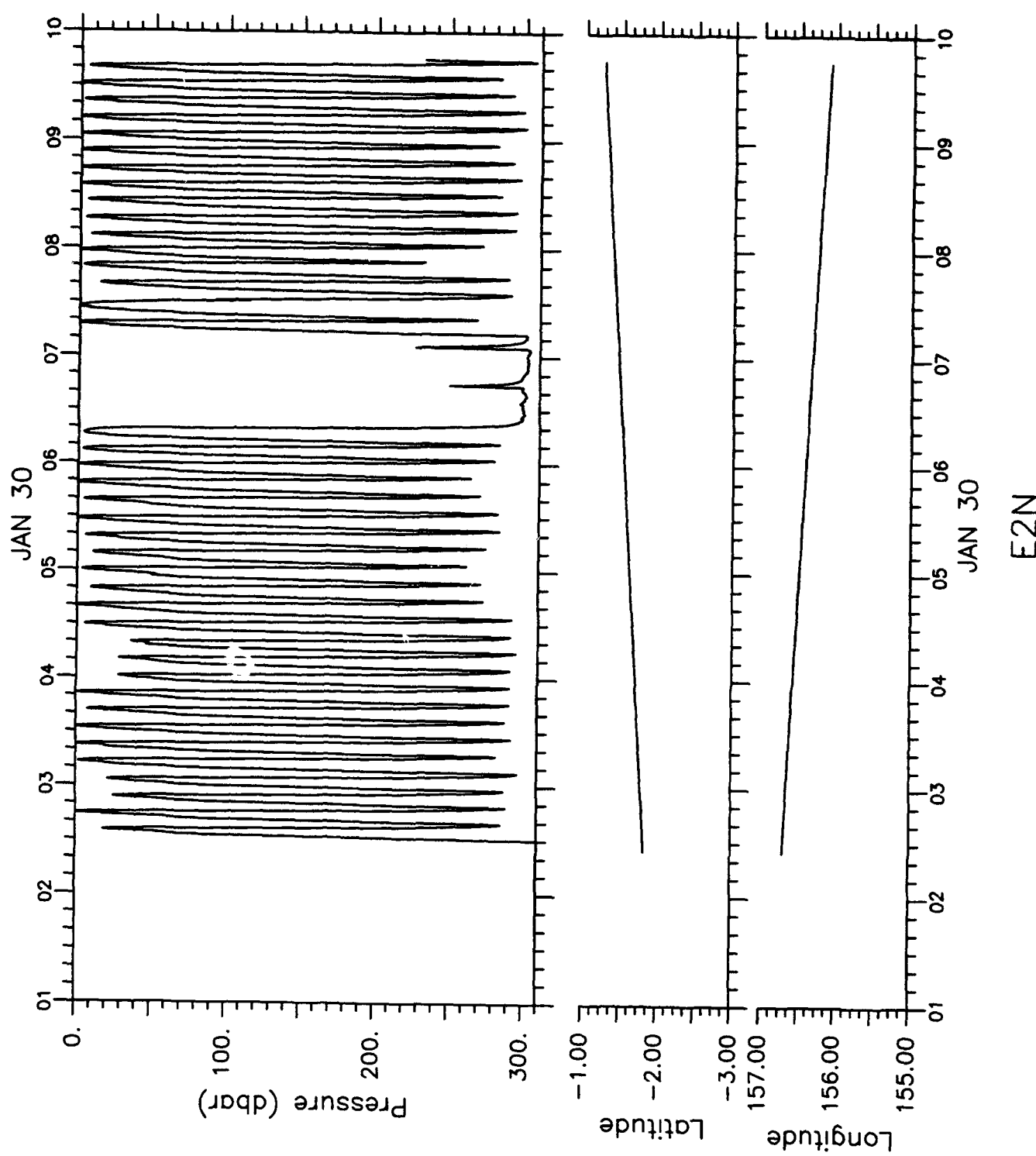


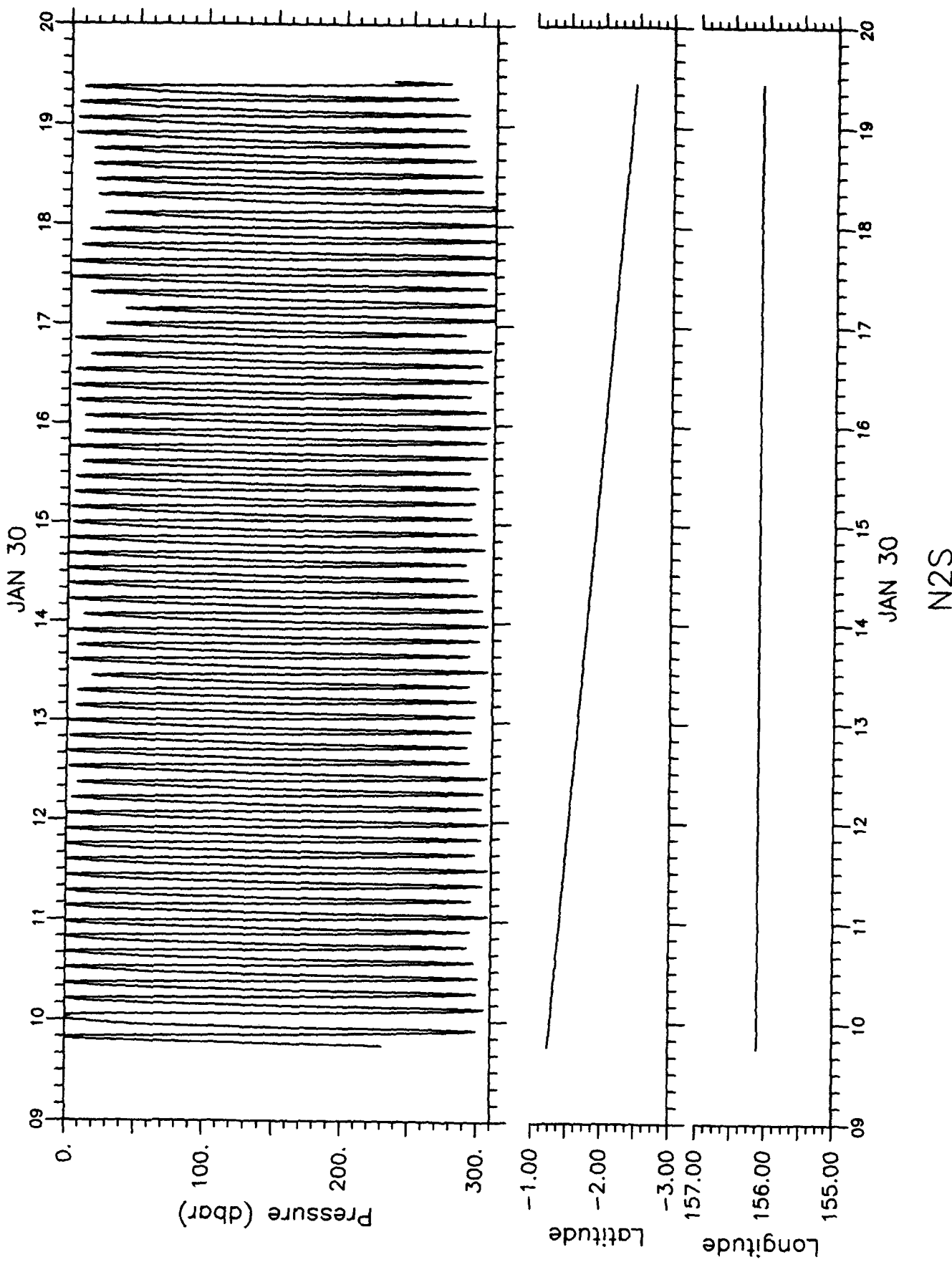


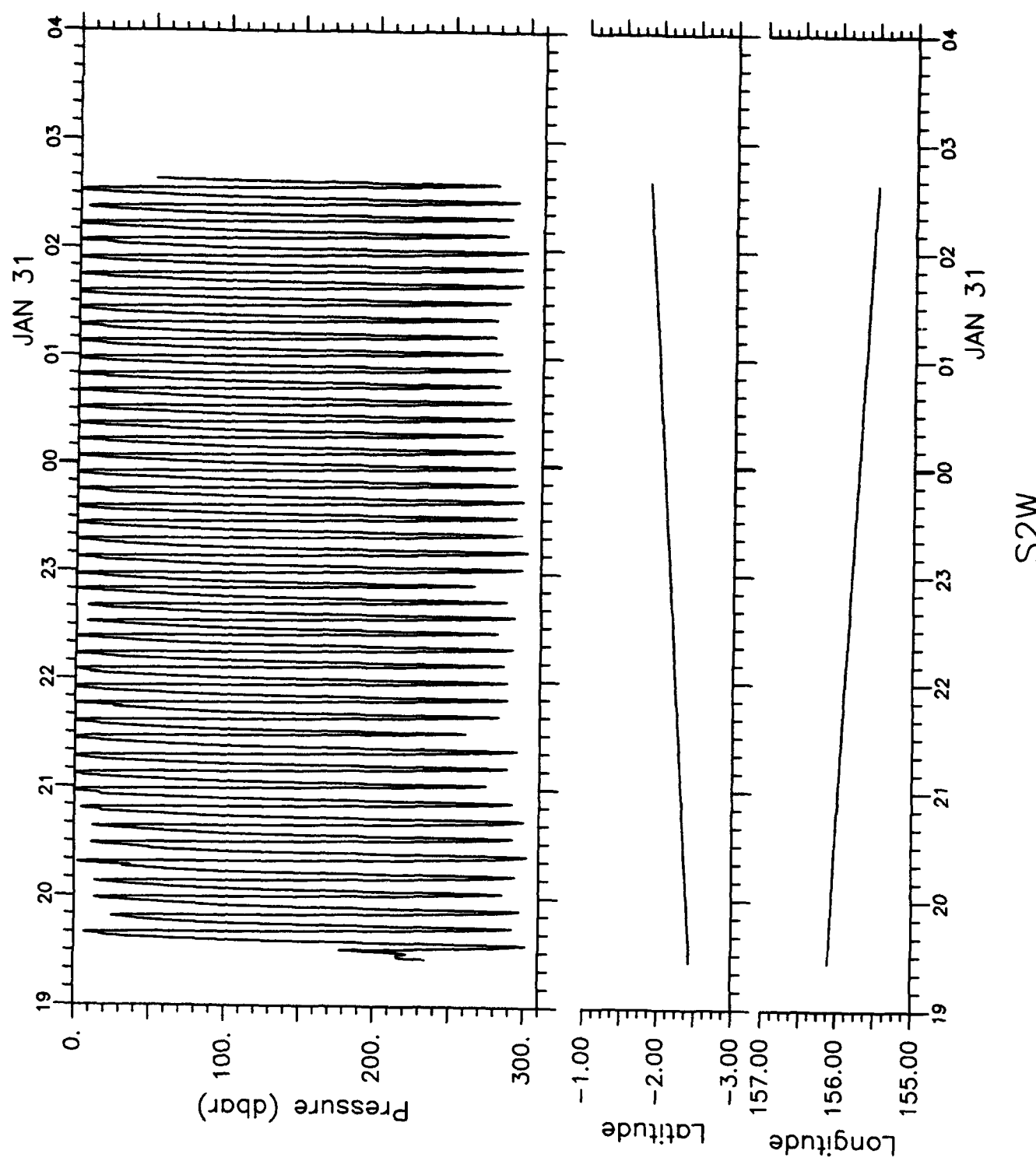


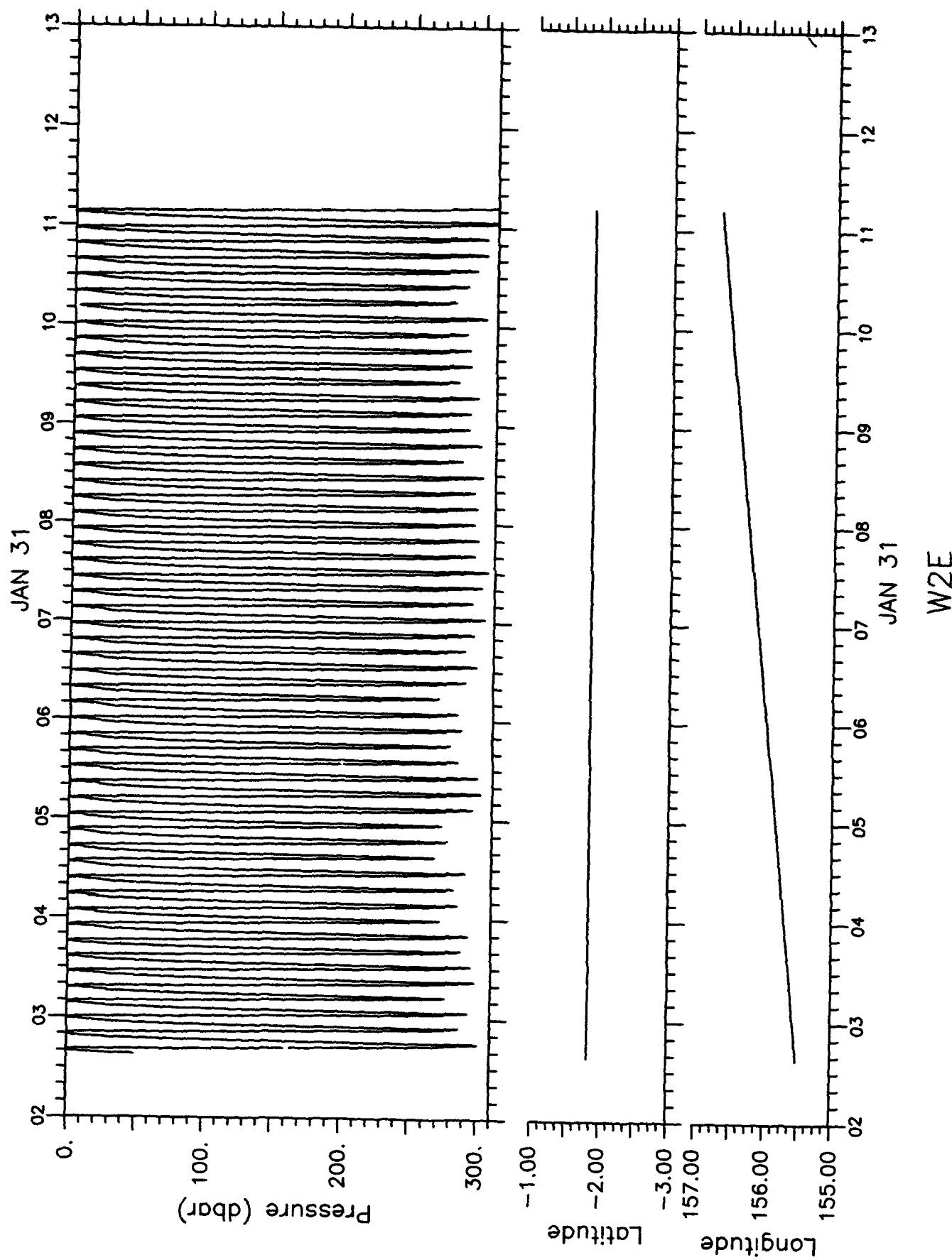


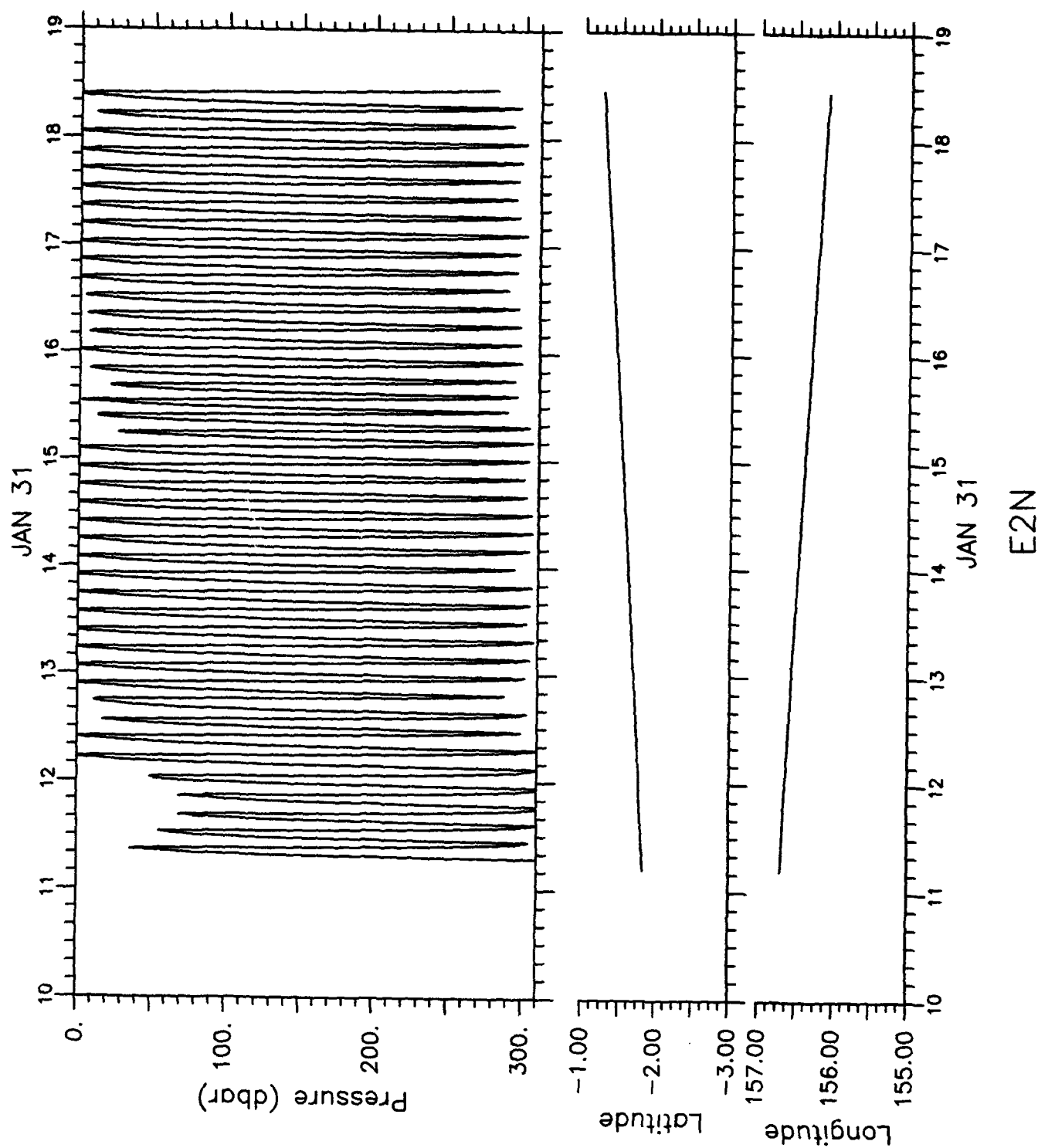


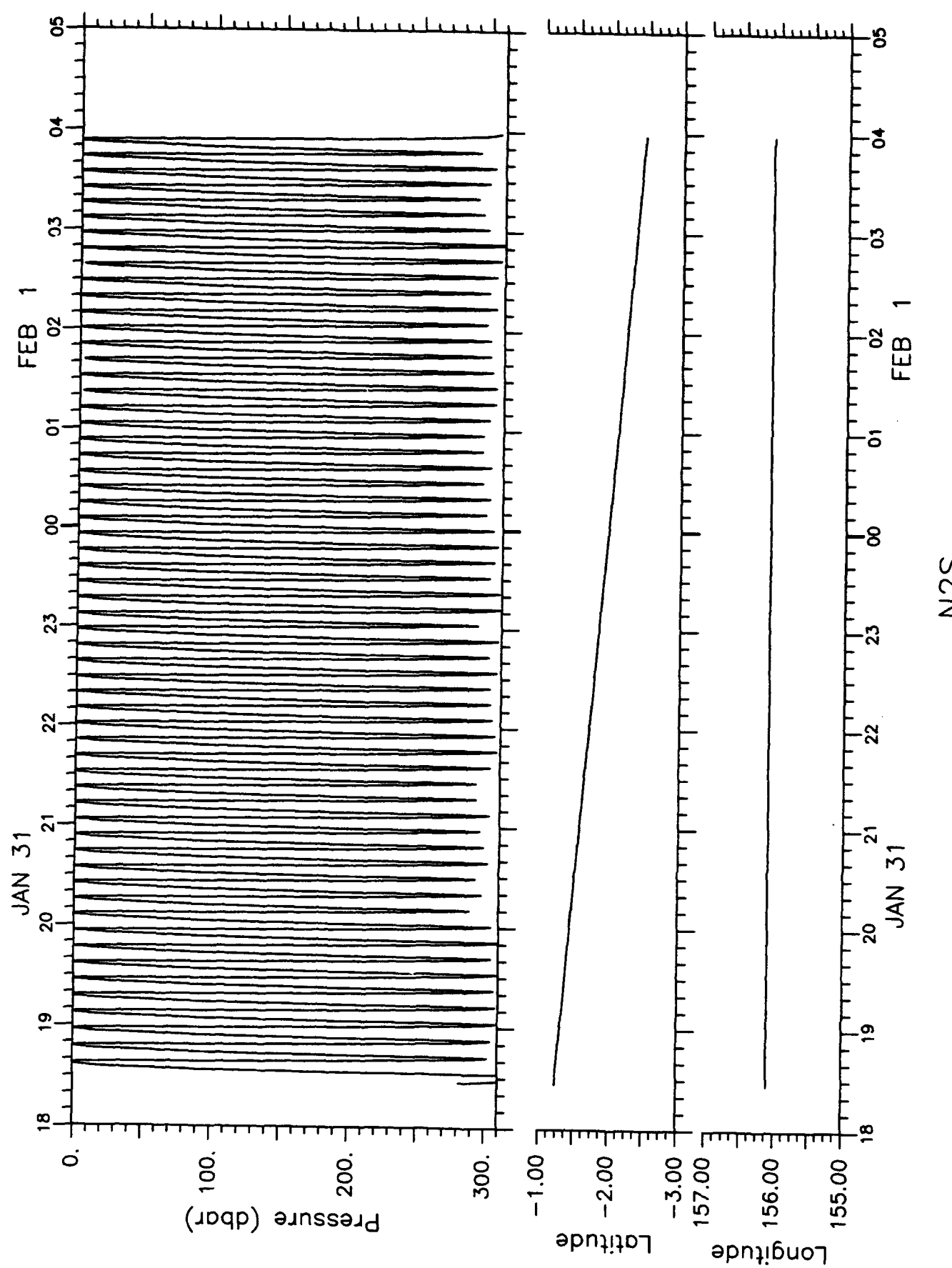




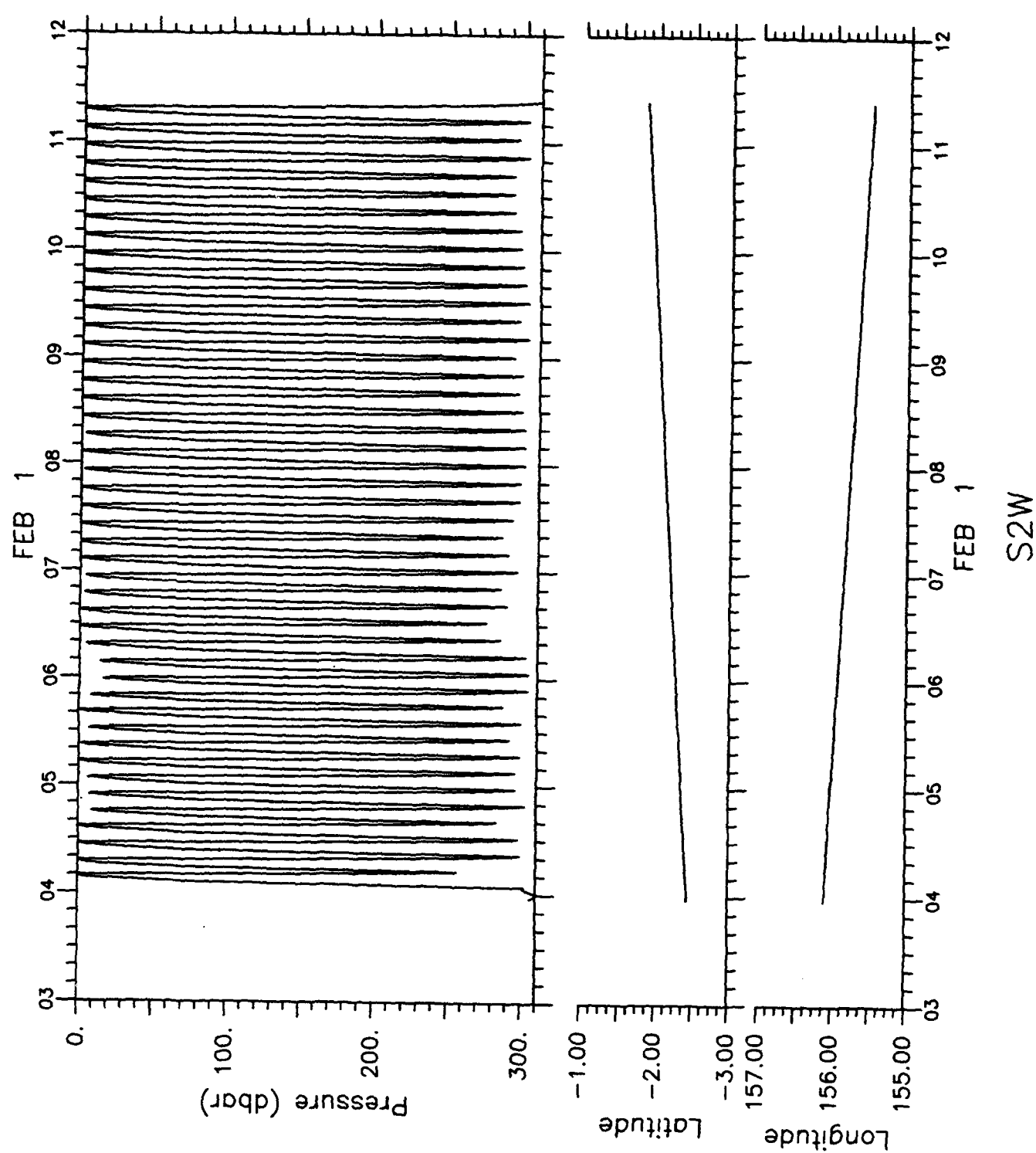


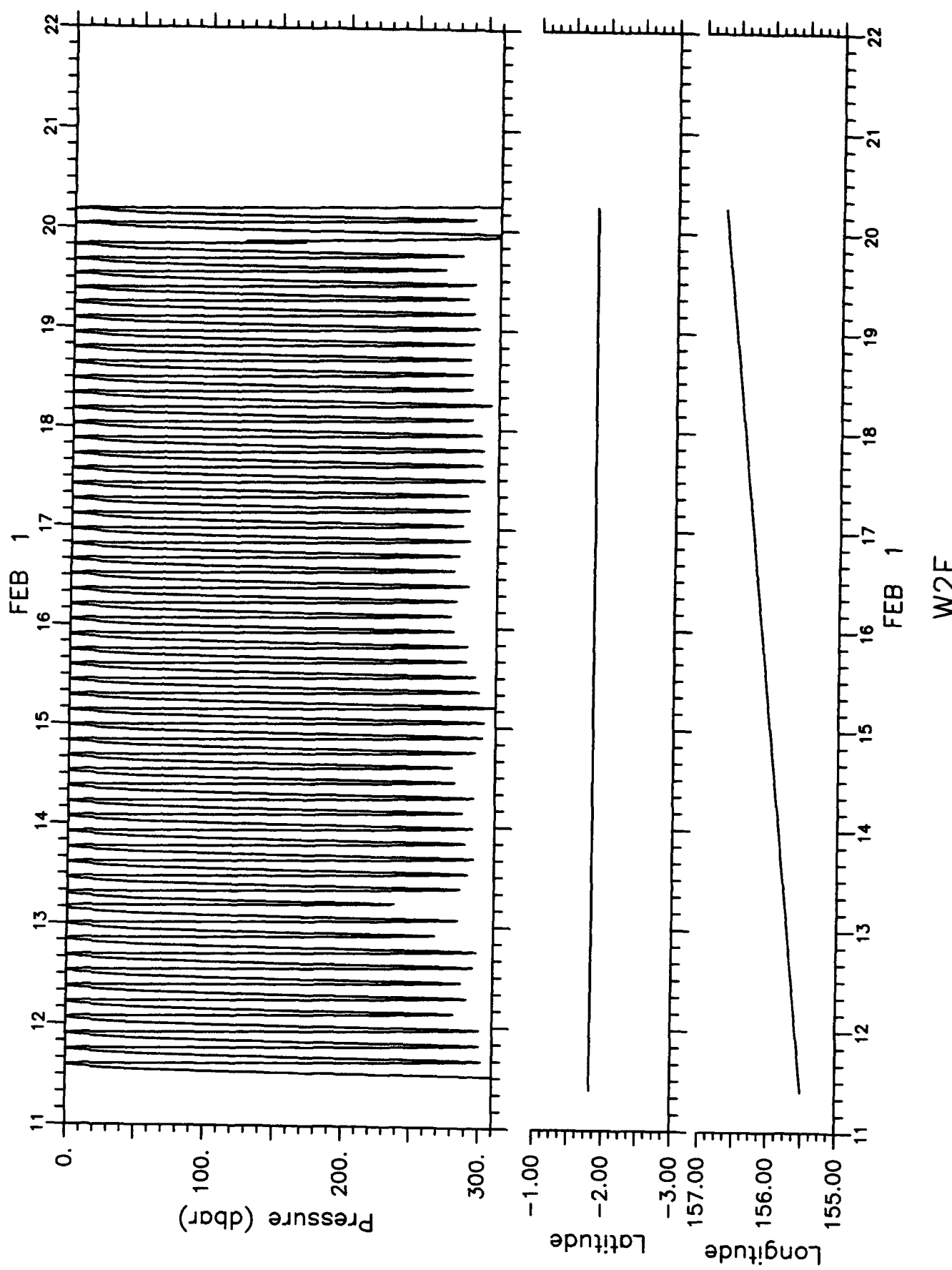


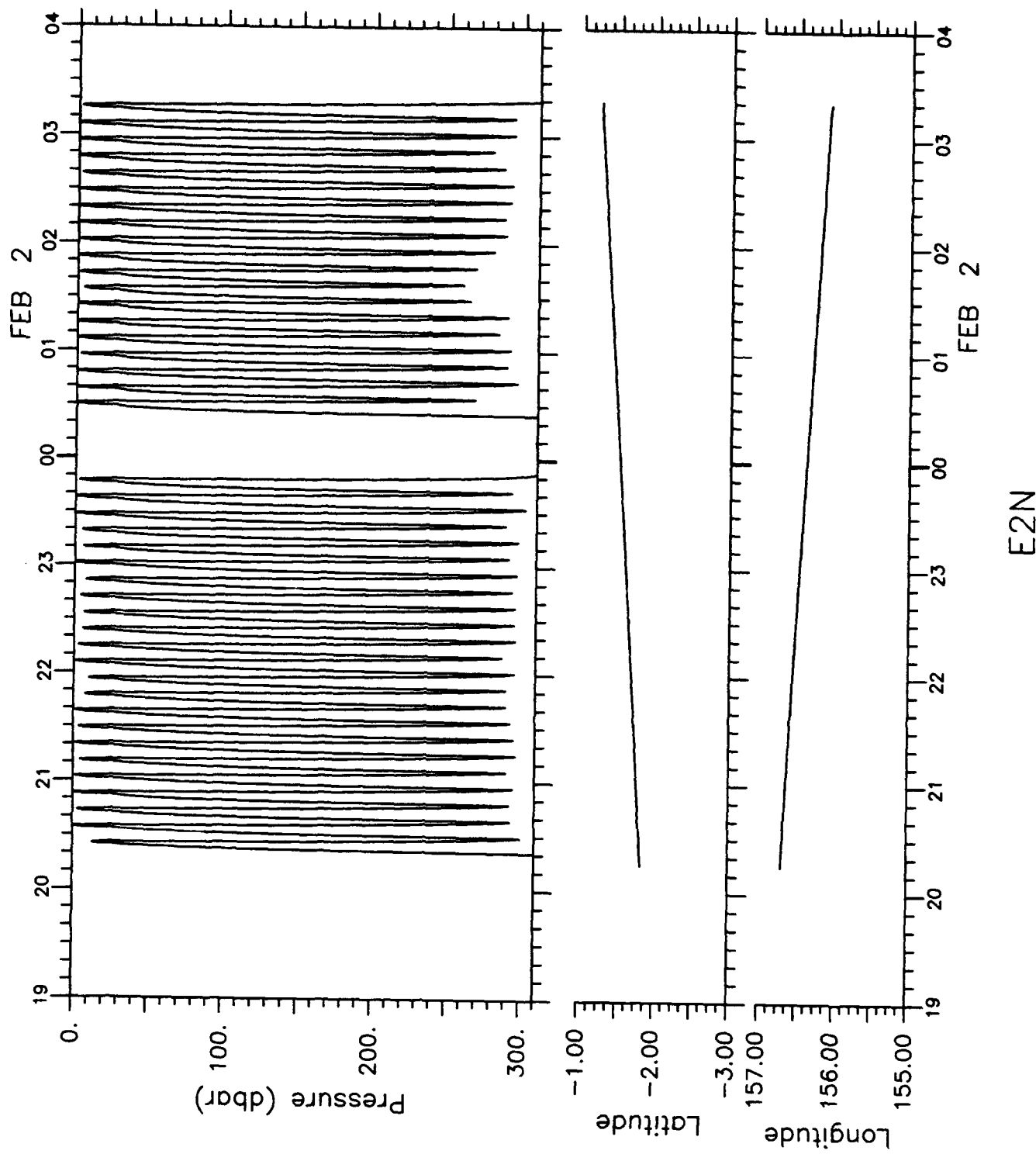


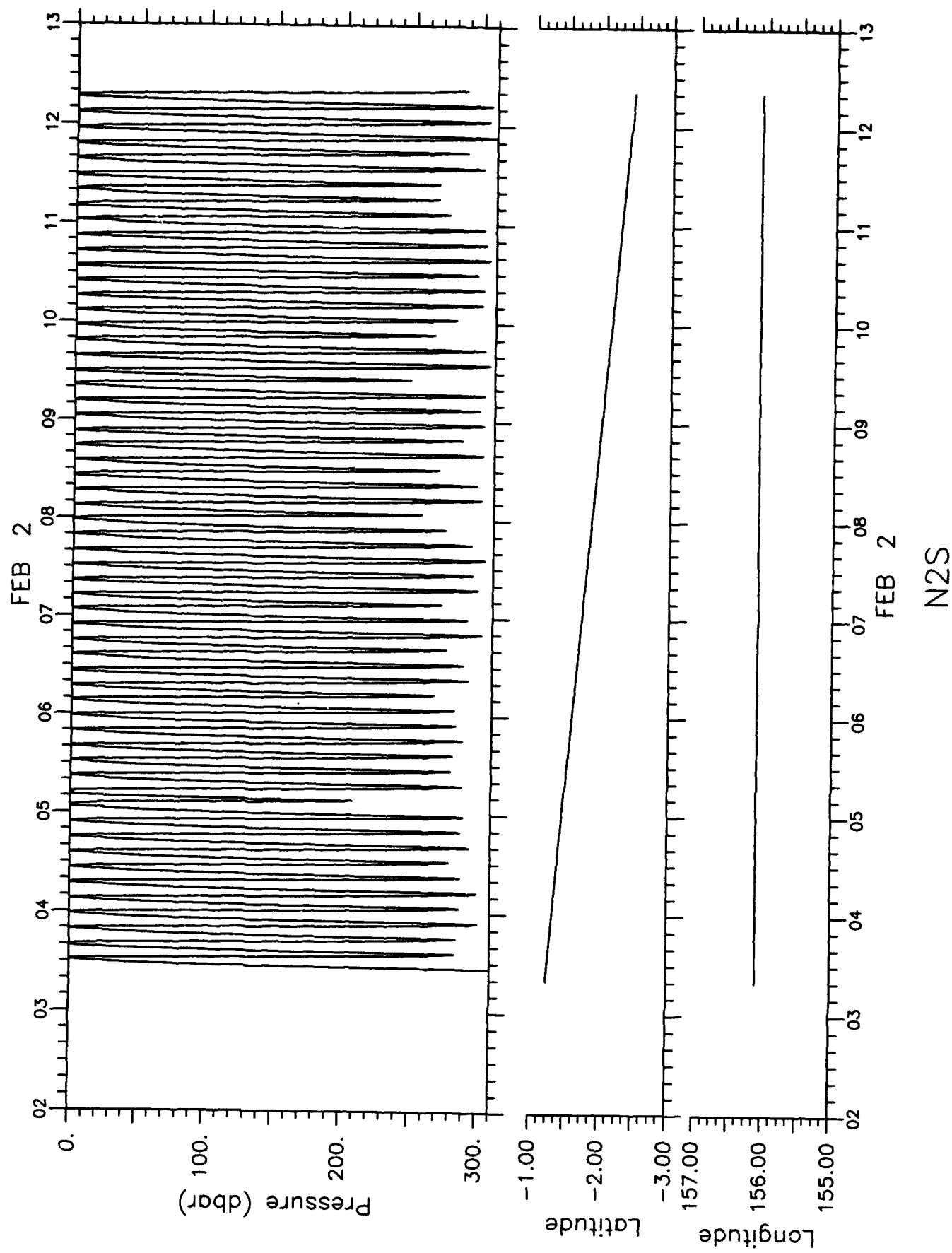


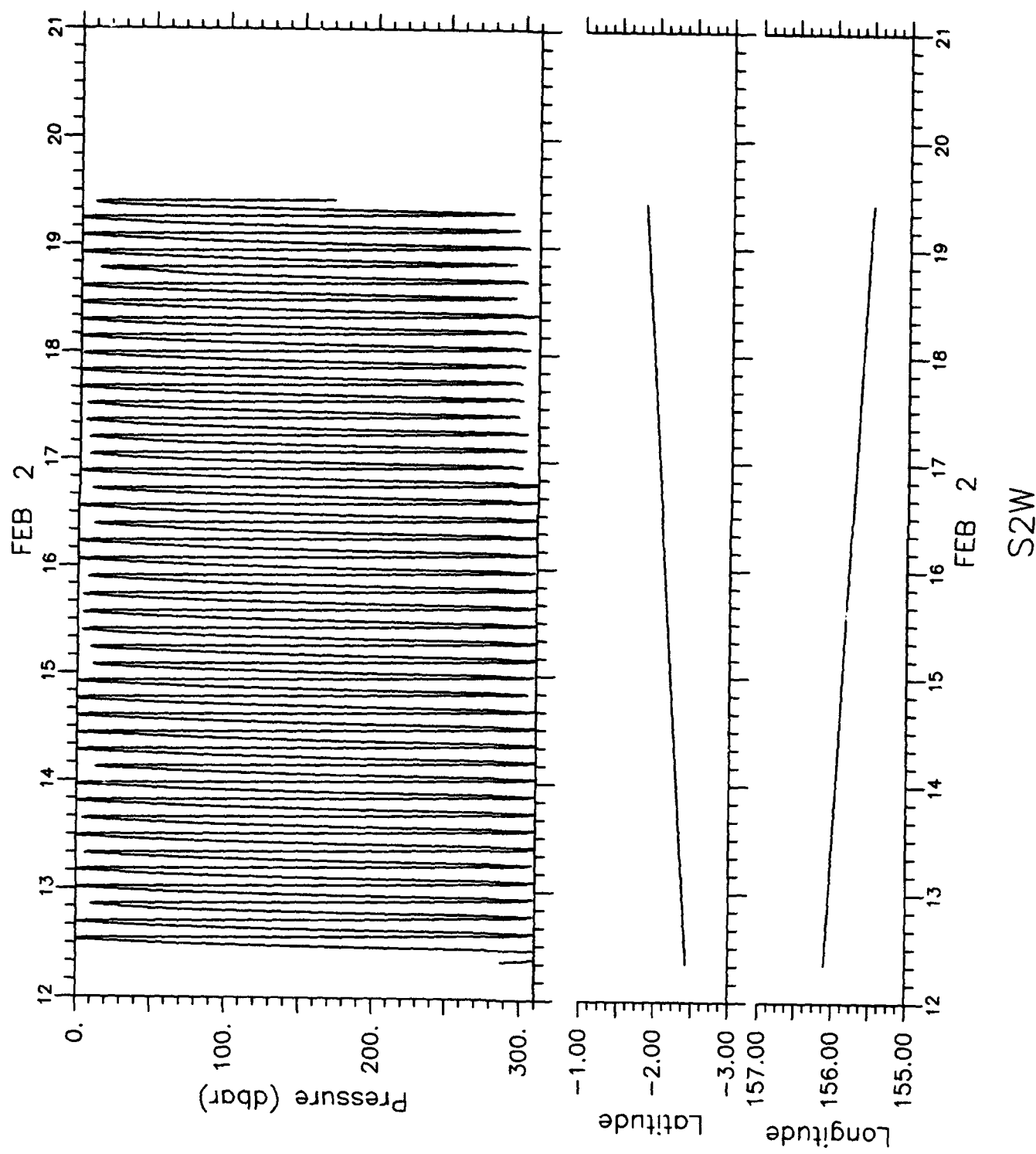
N2S

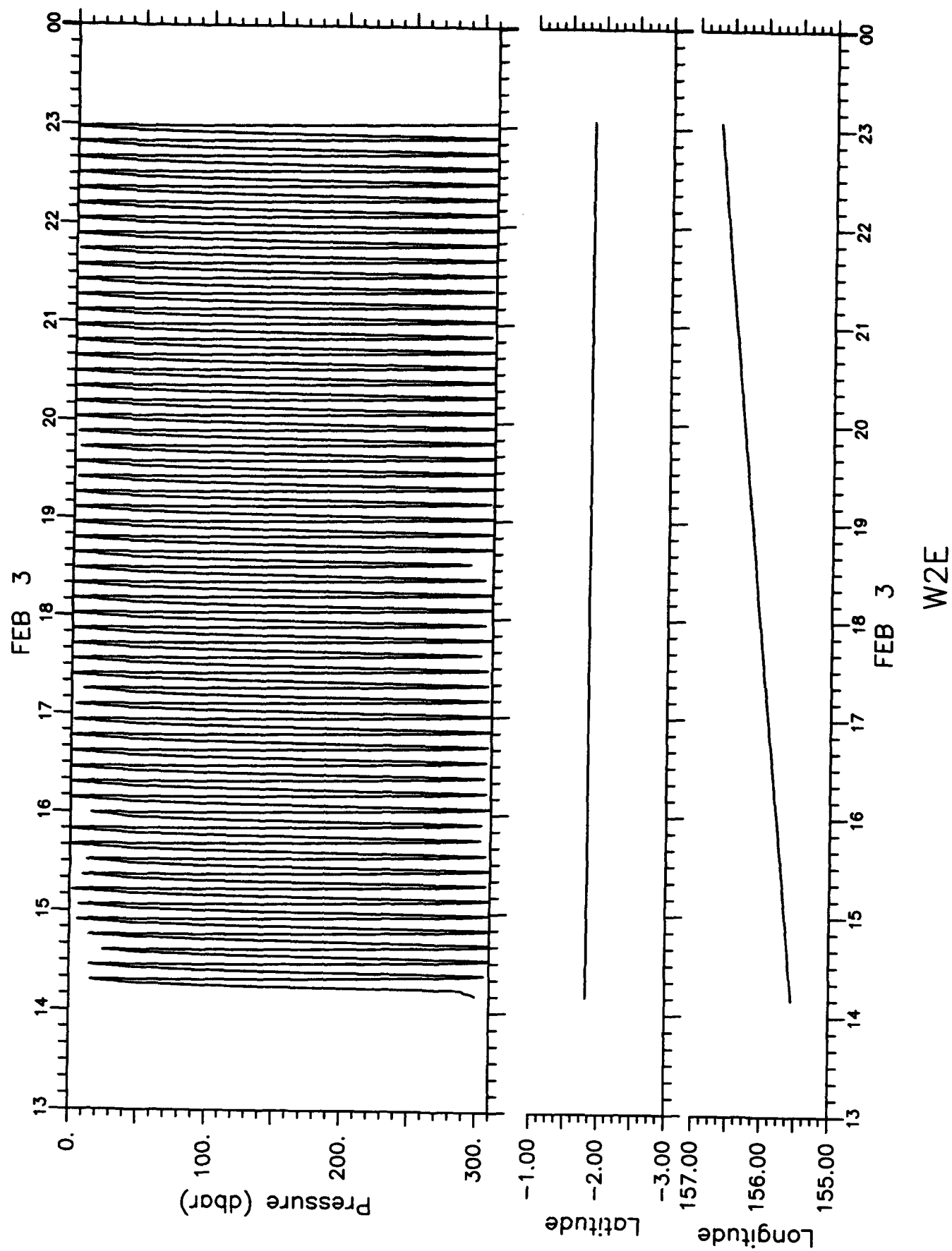


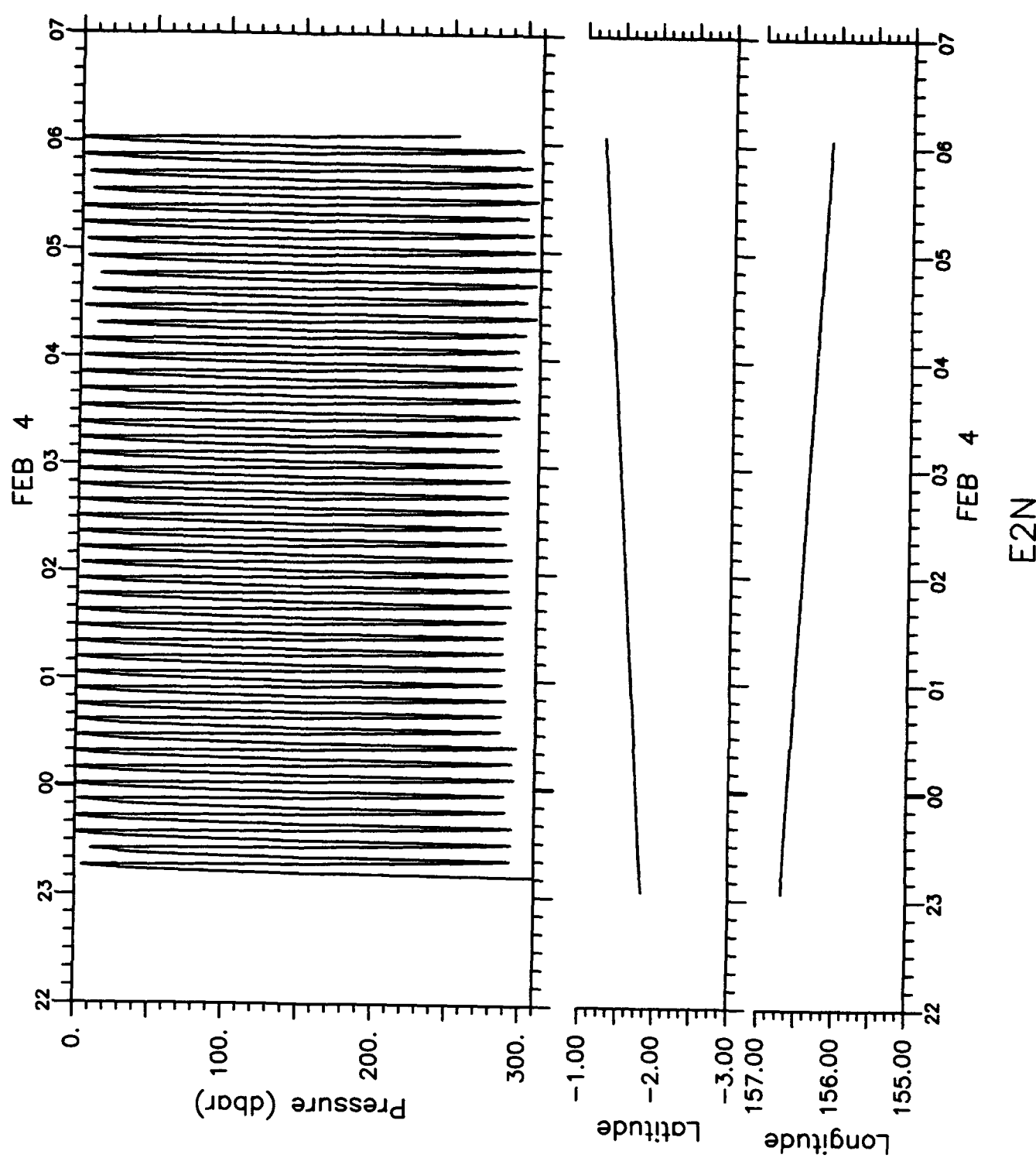


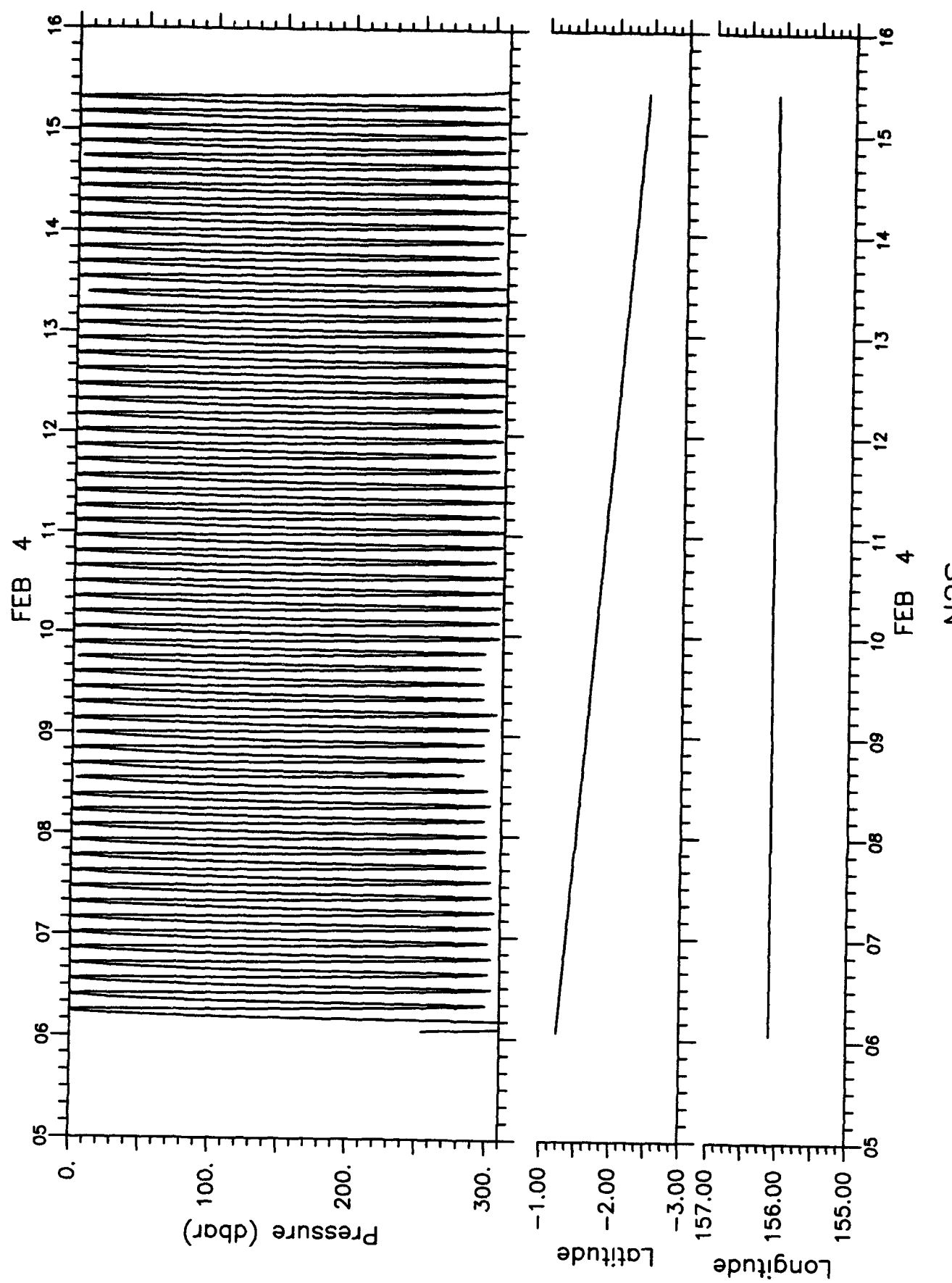




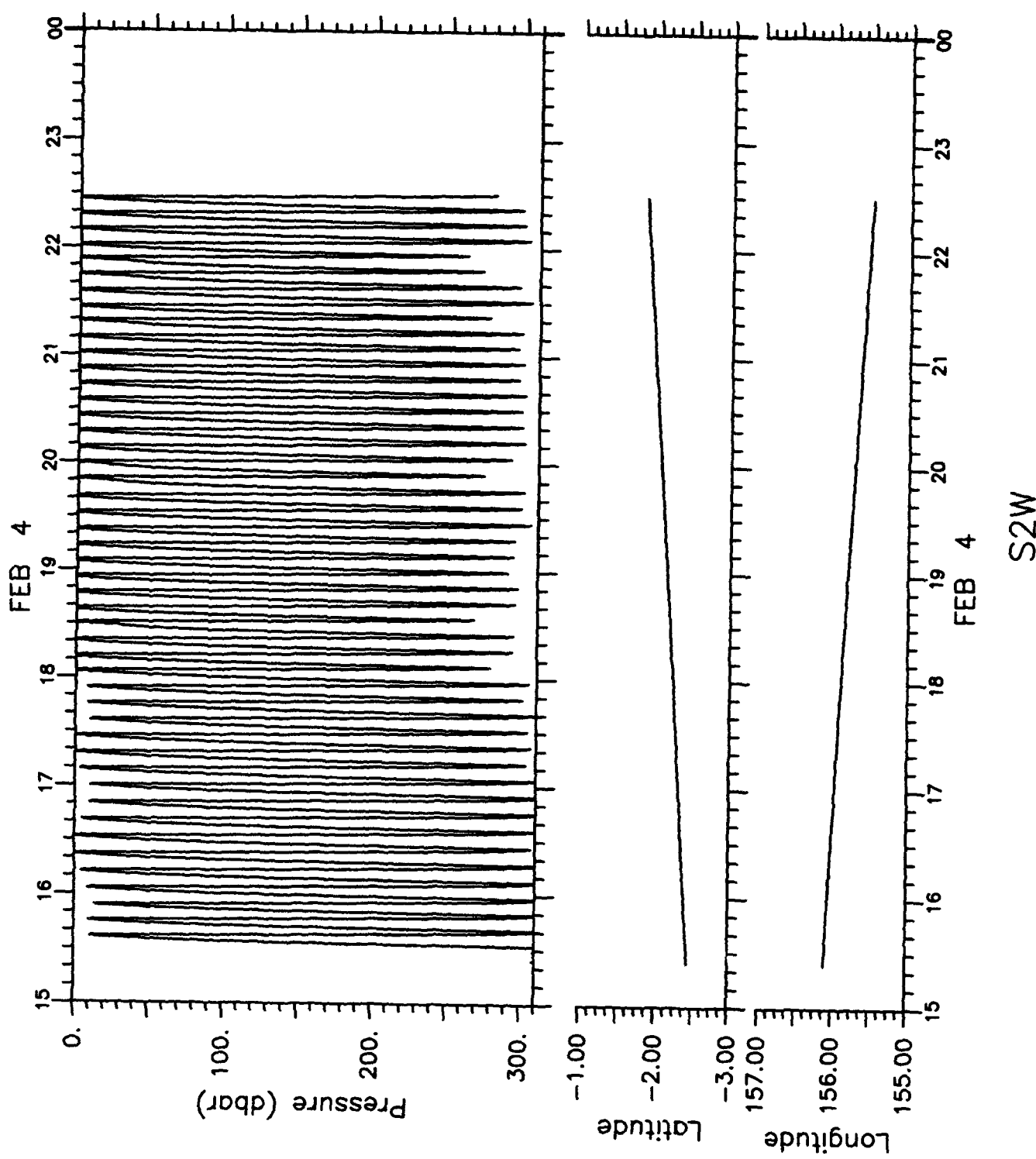


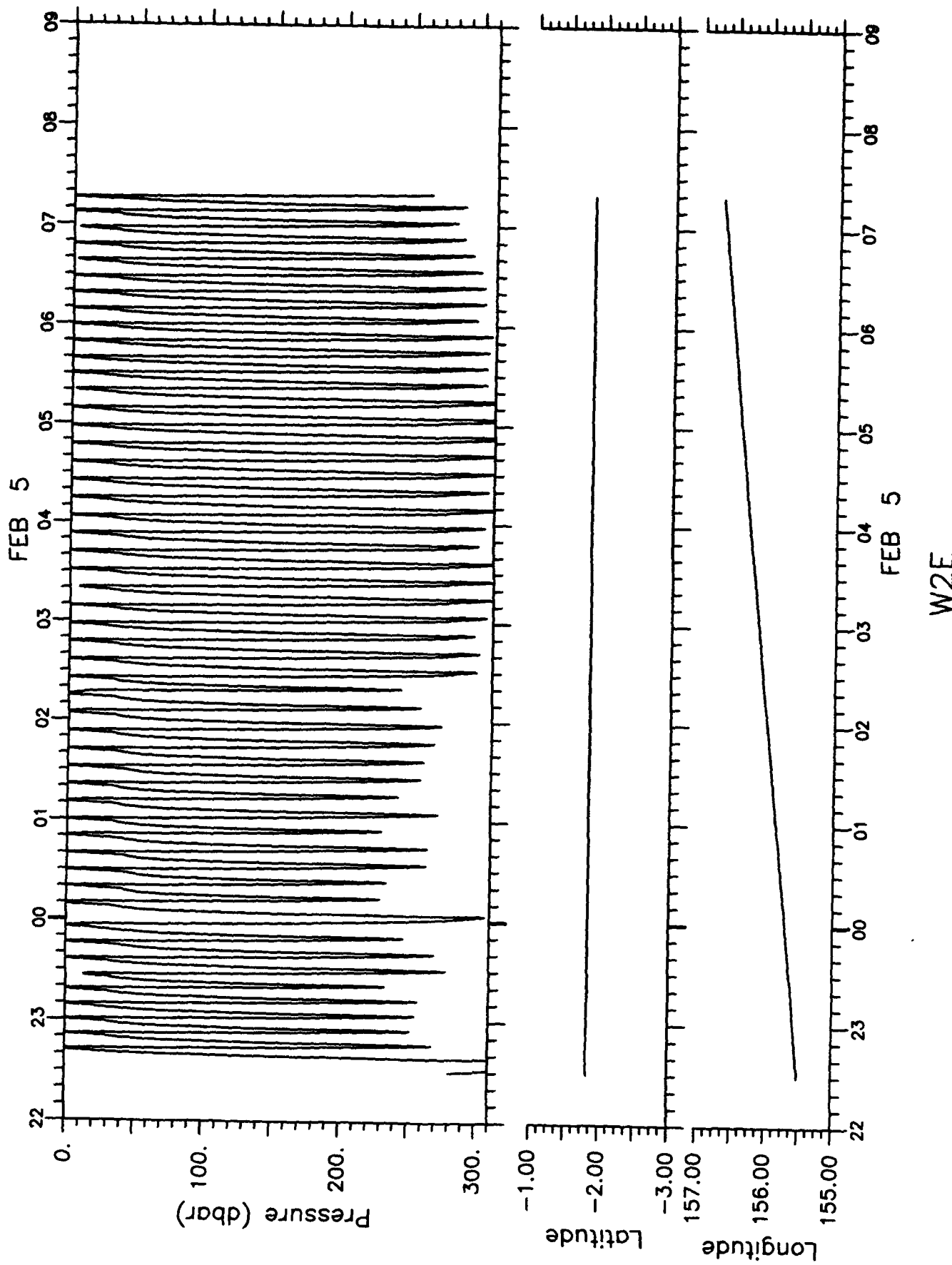


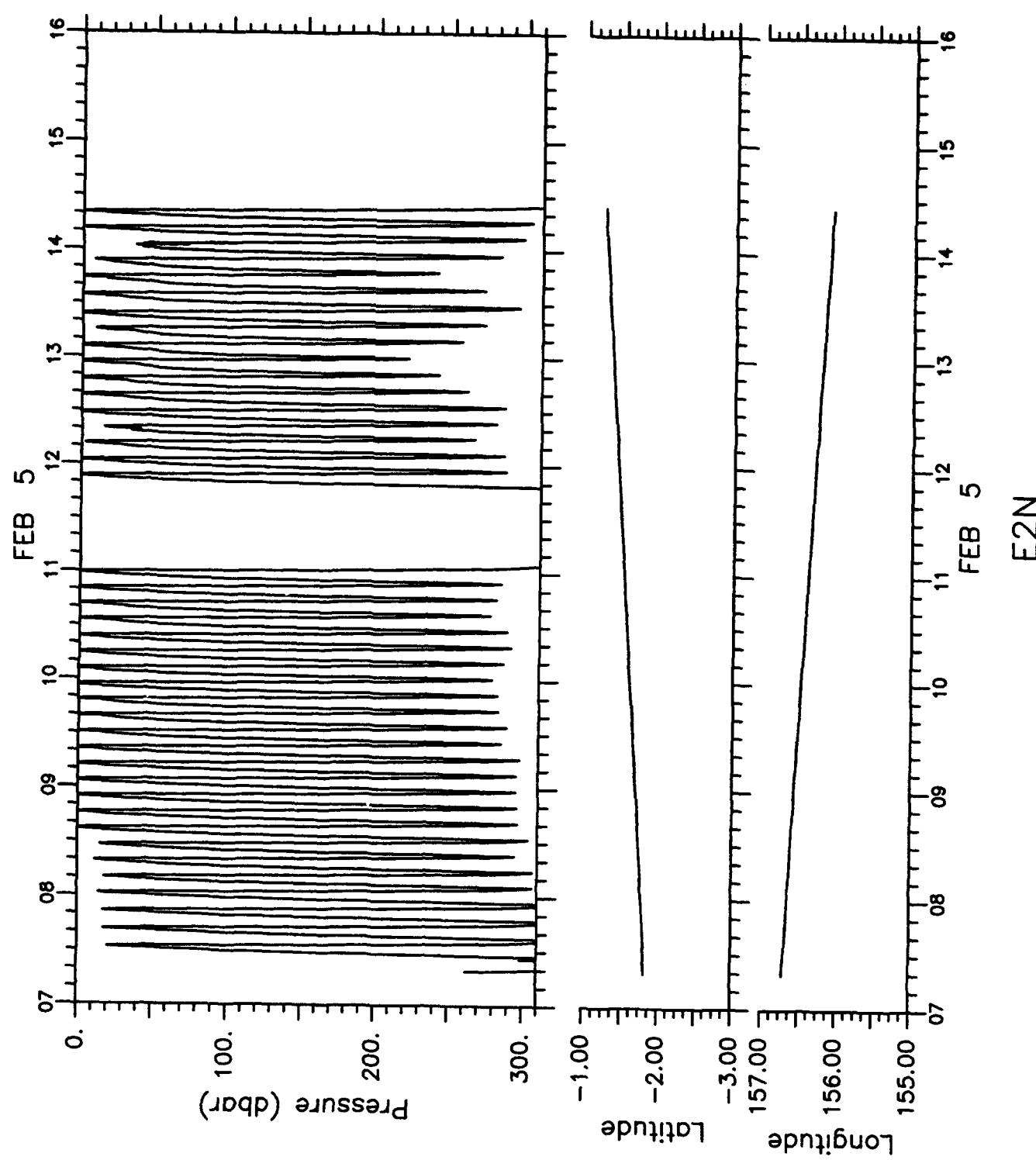


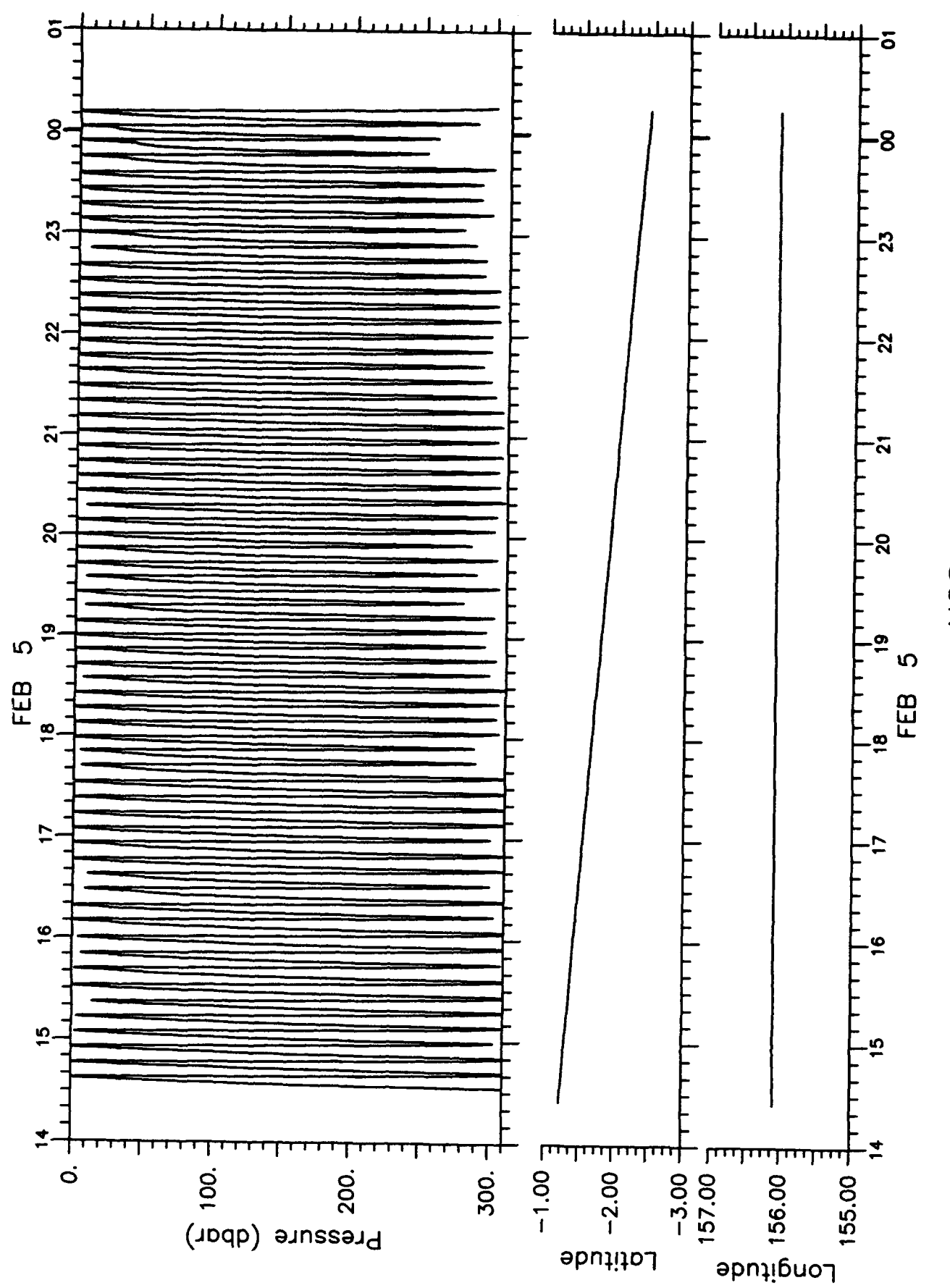


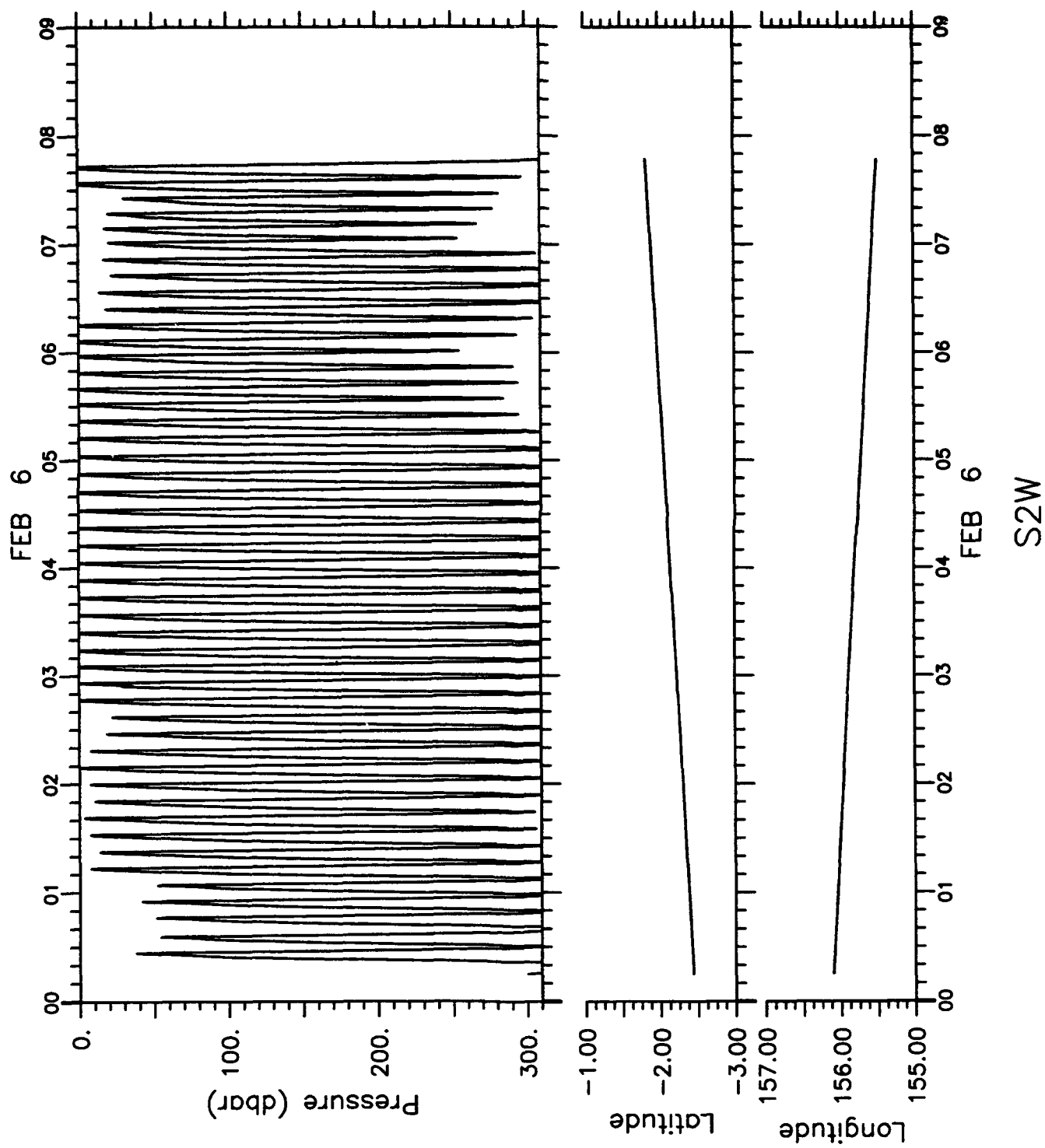
N2S

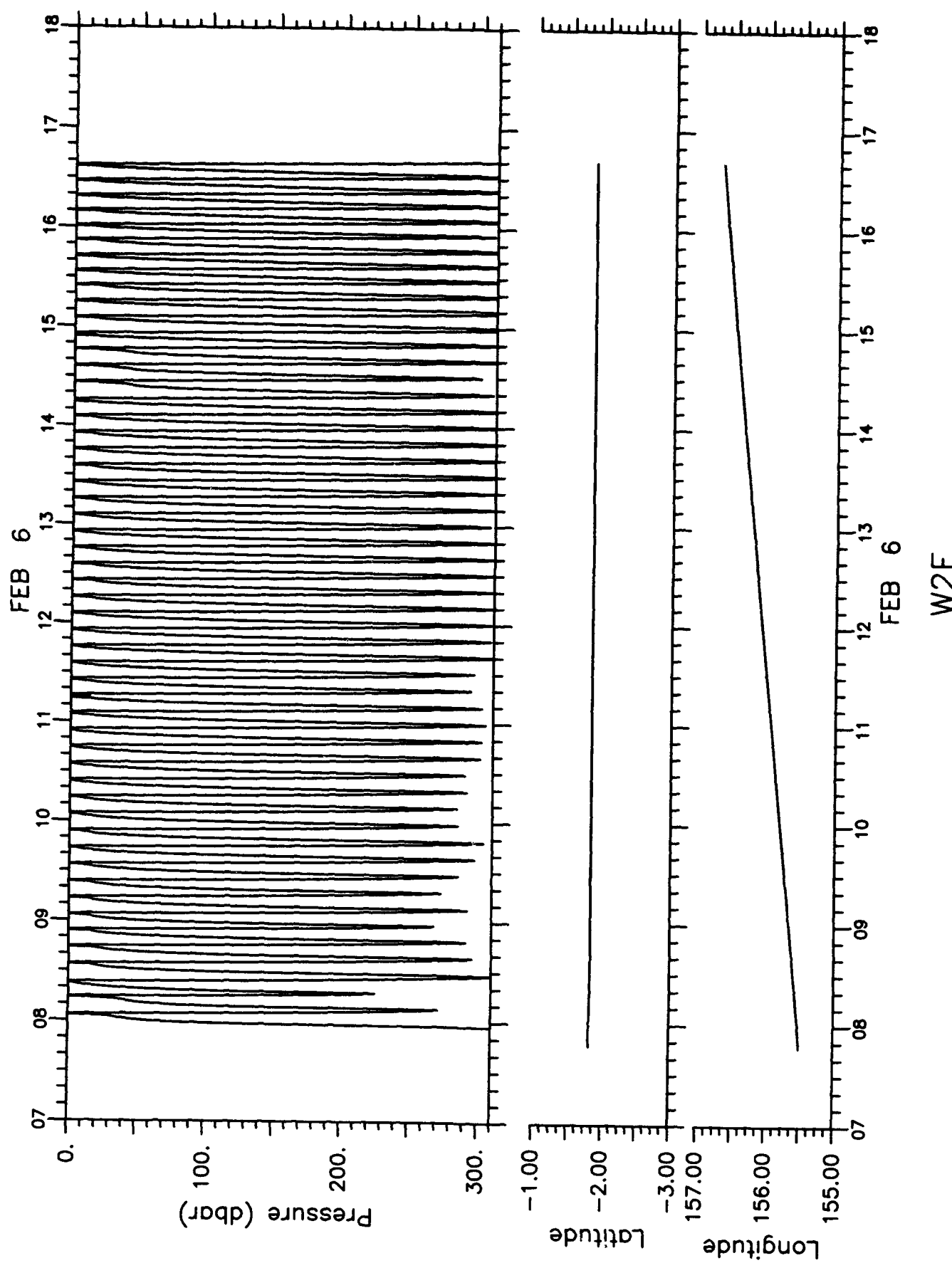


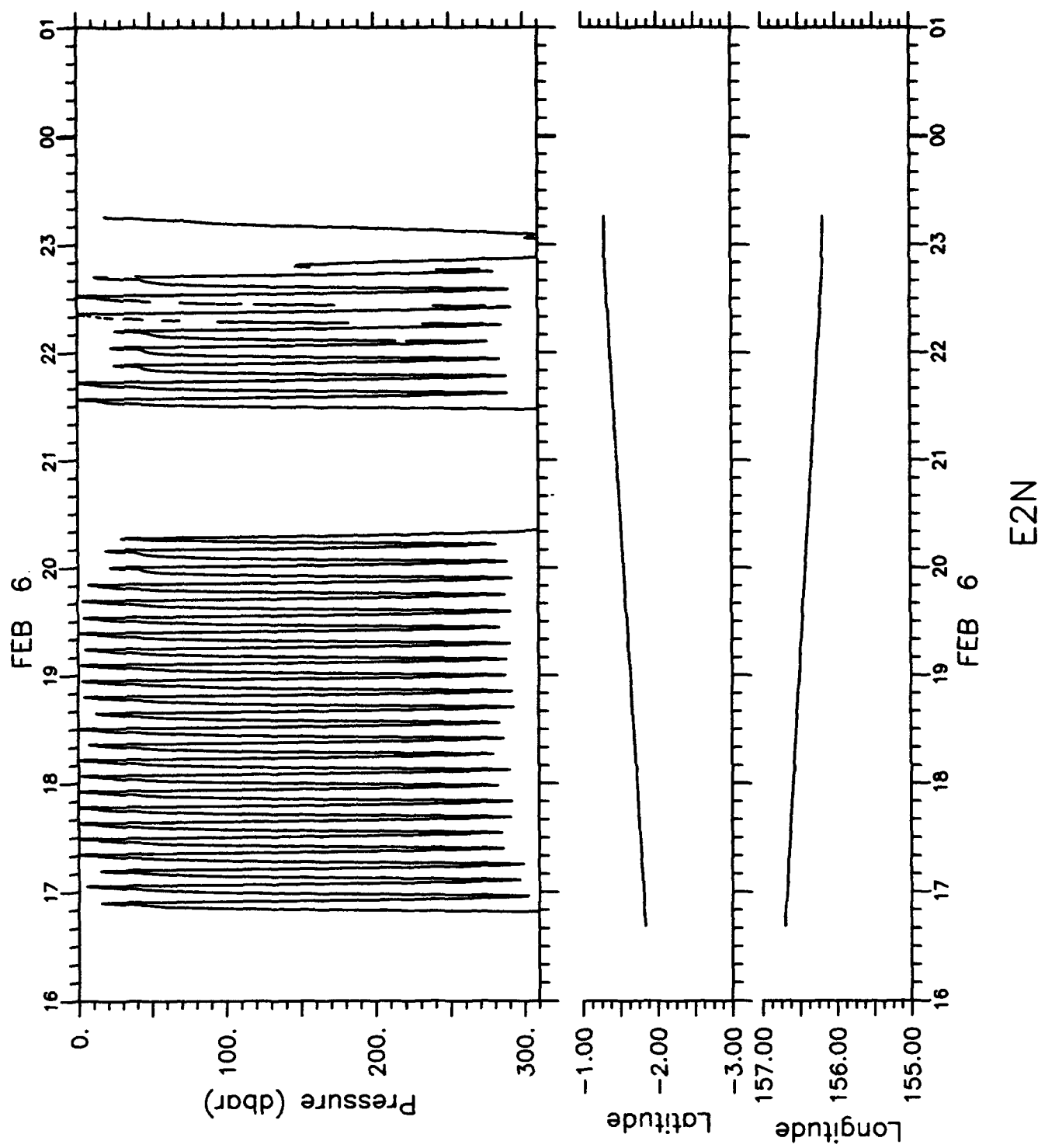


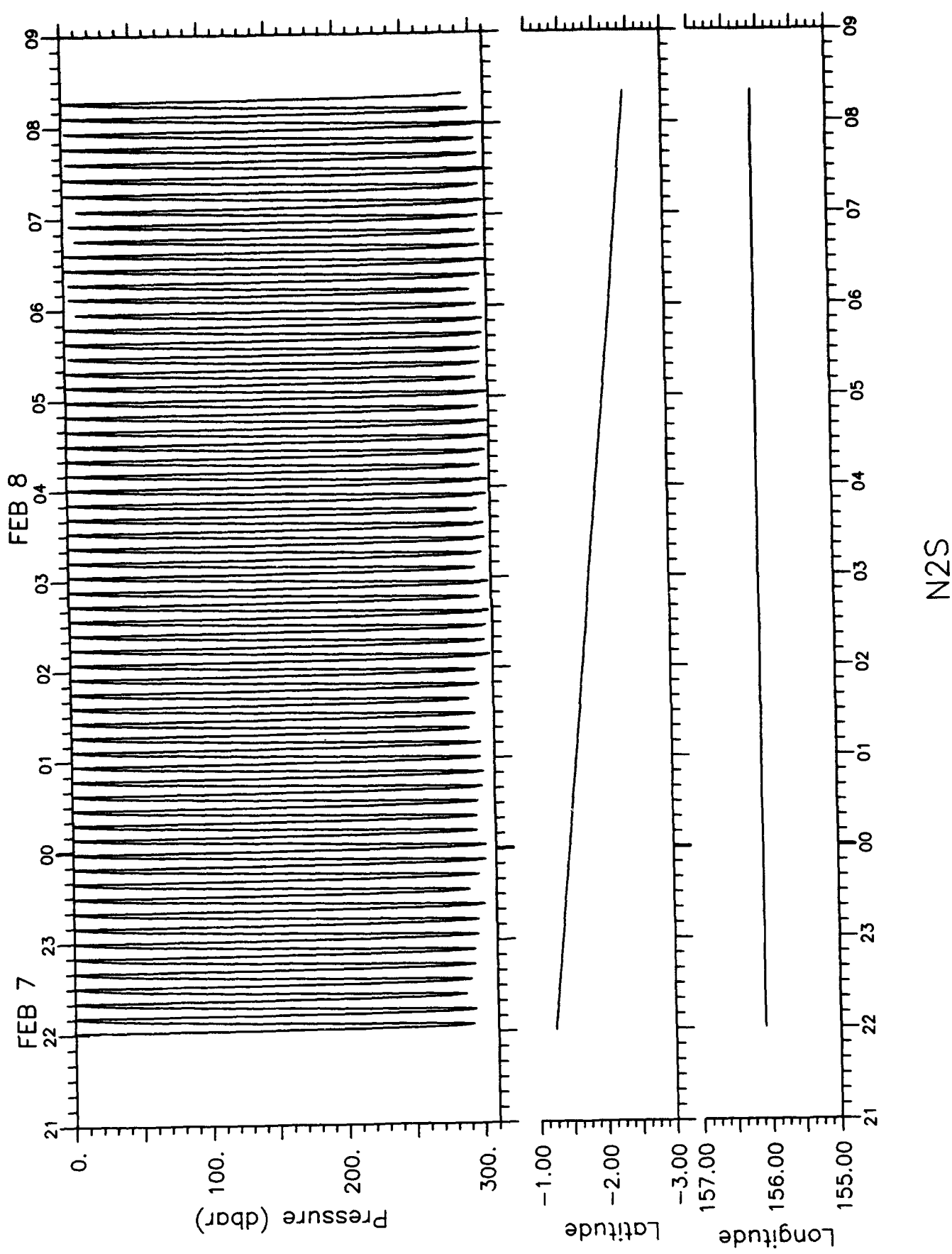


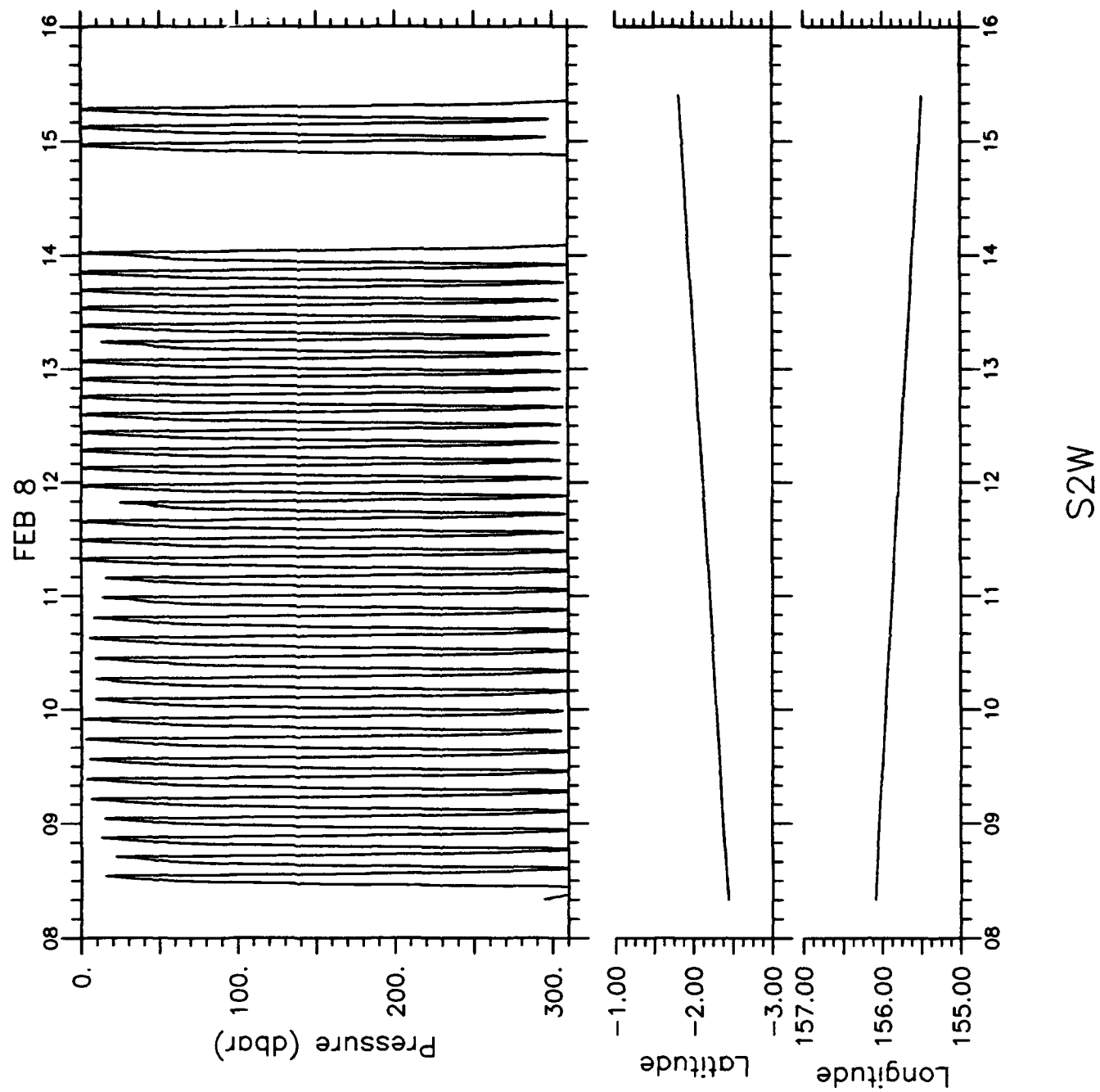


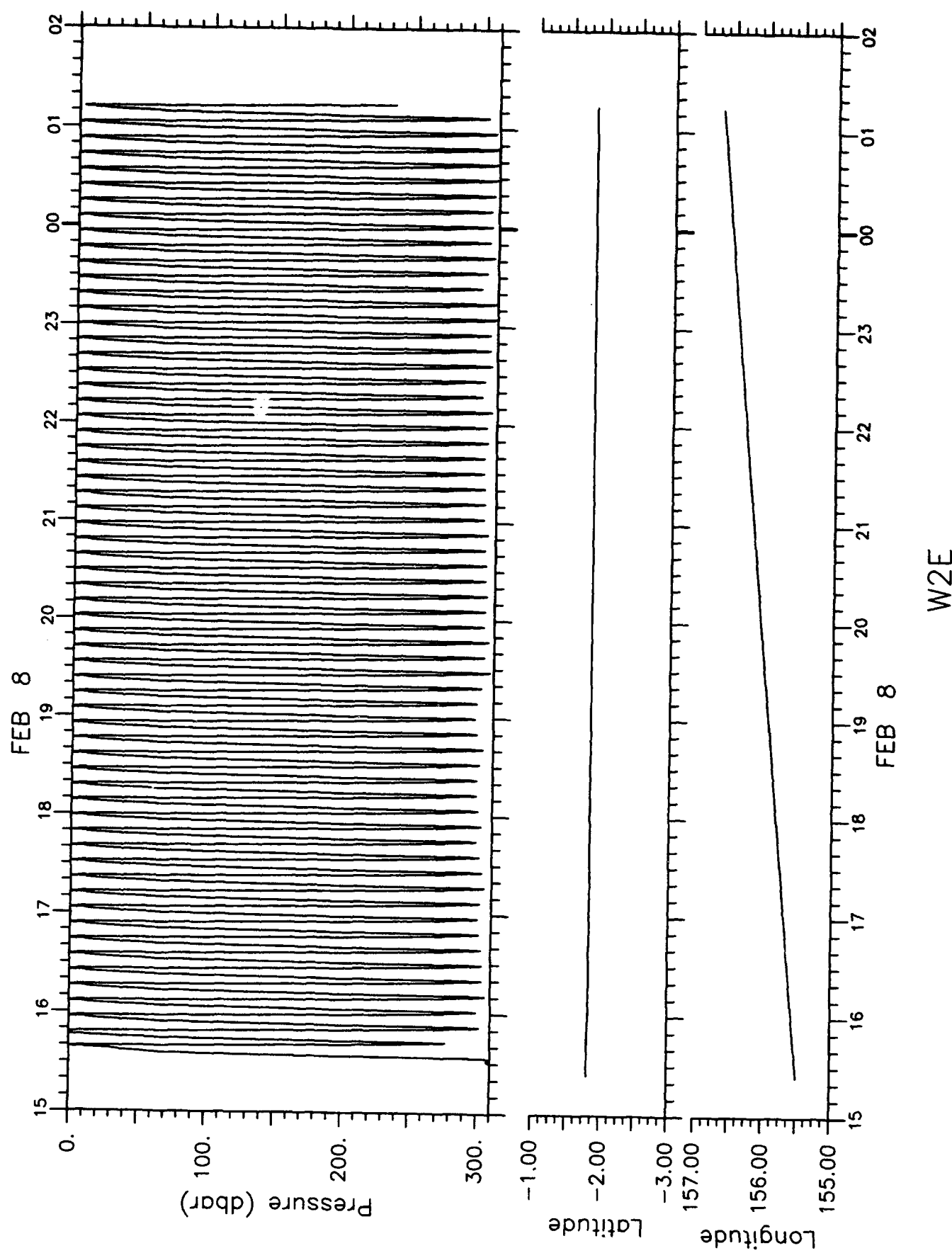


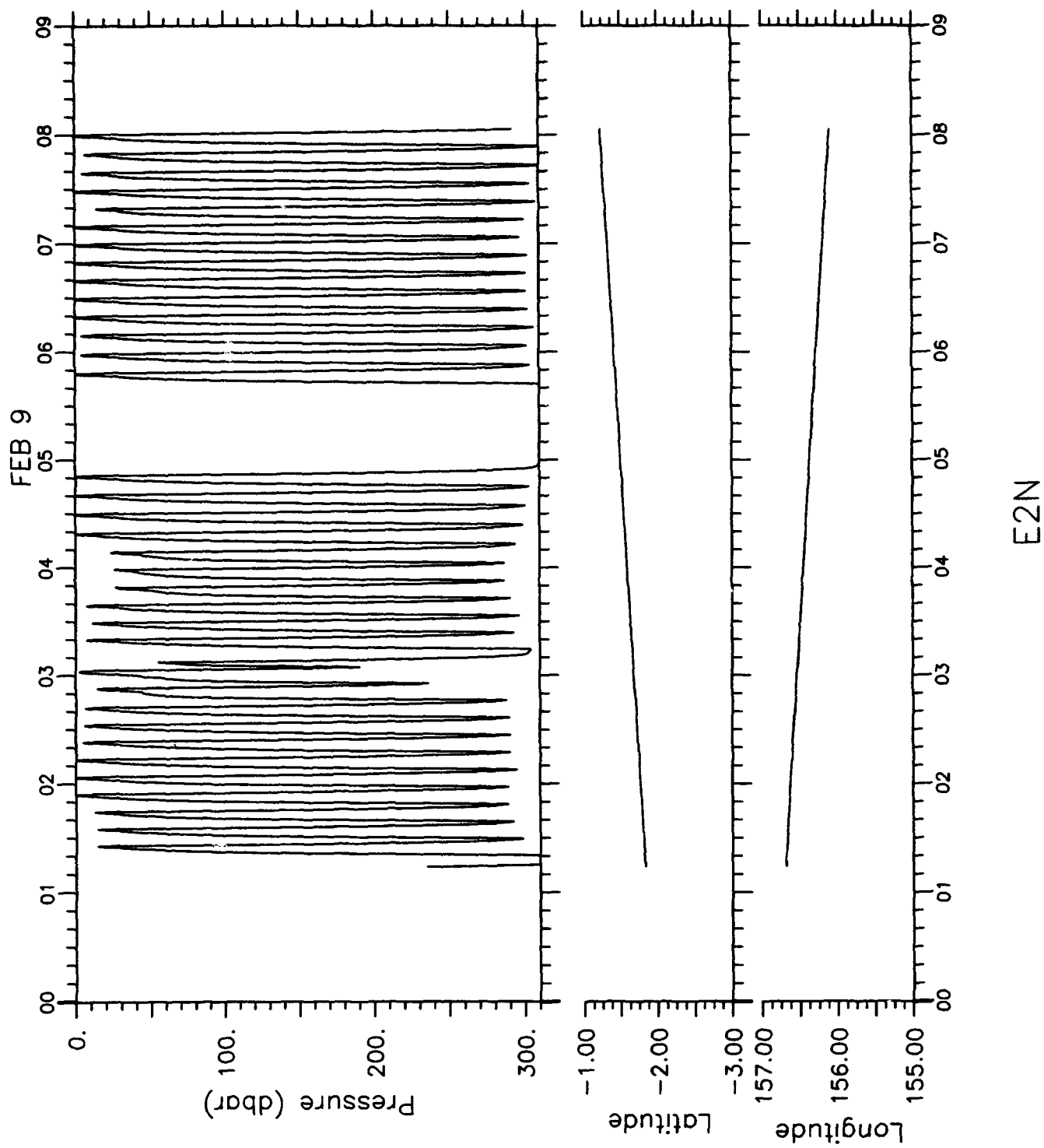


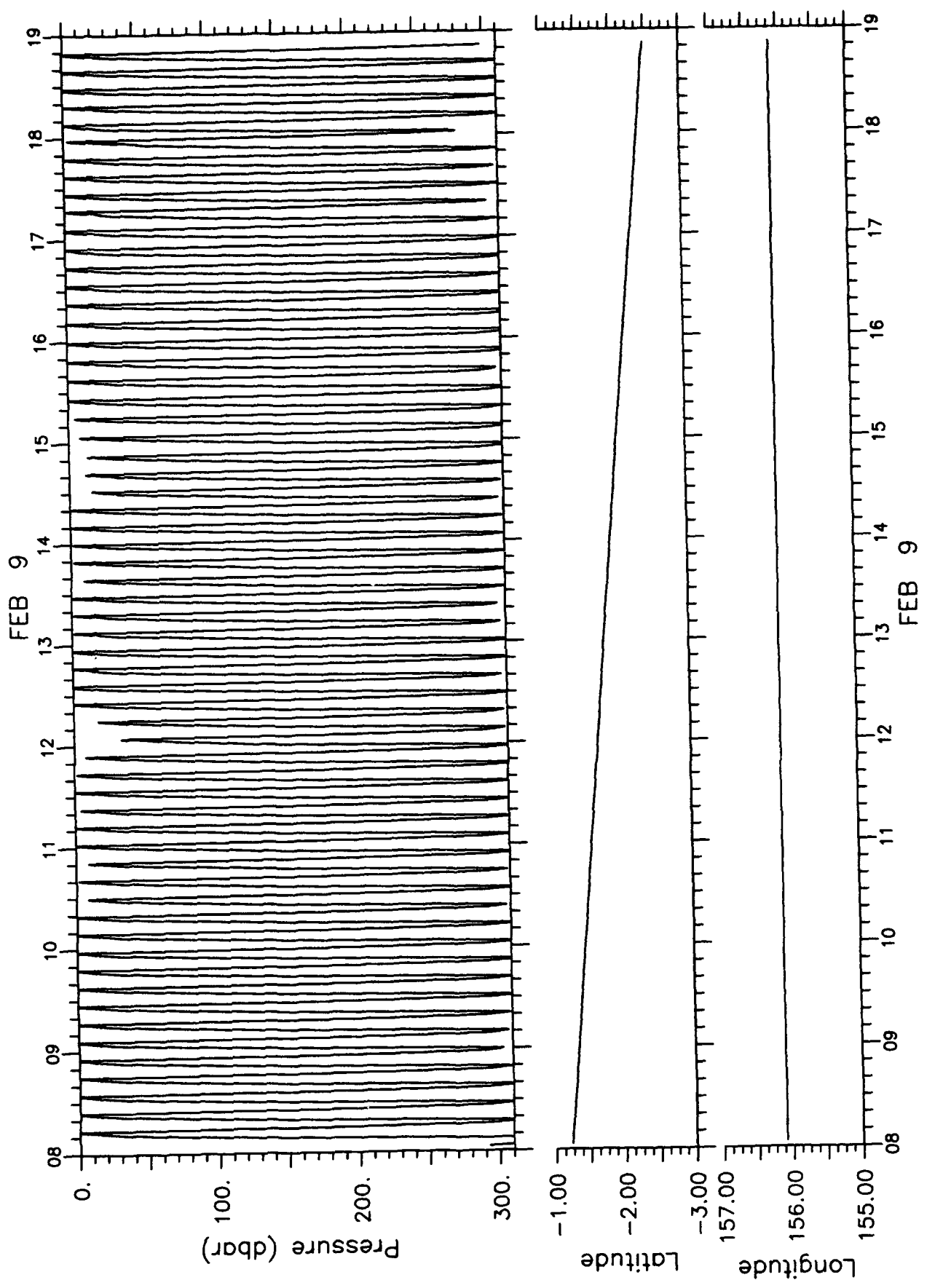




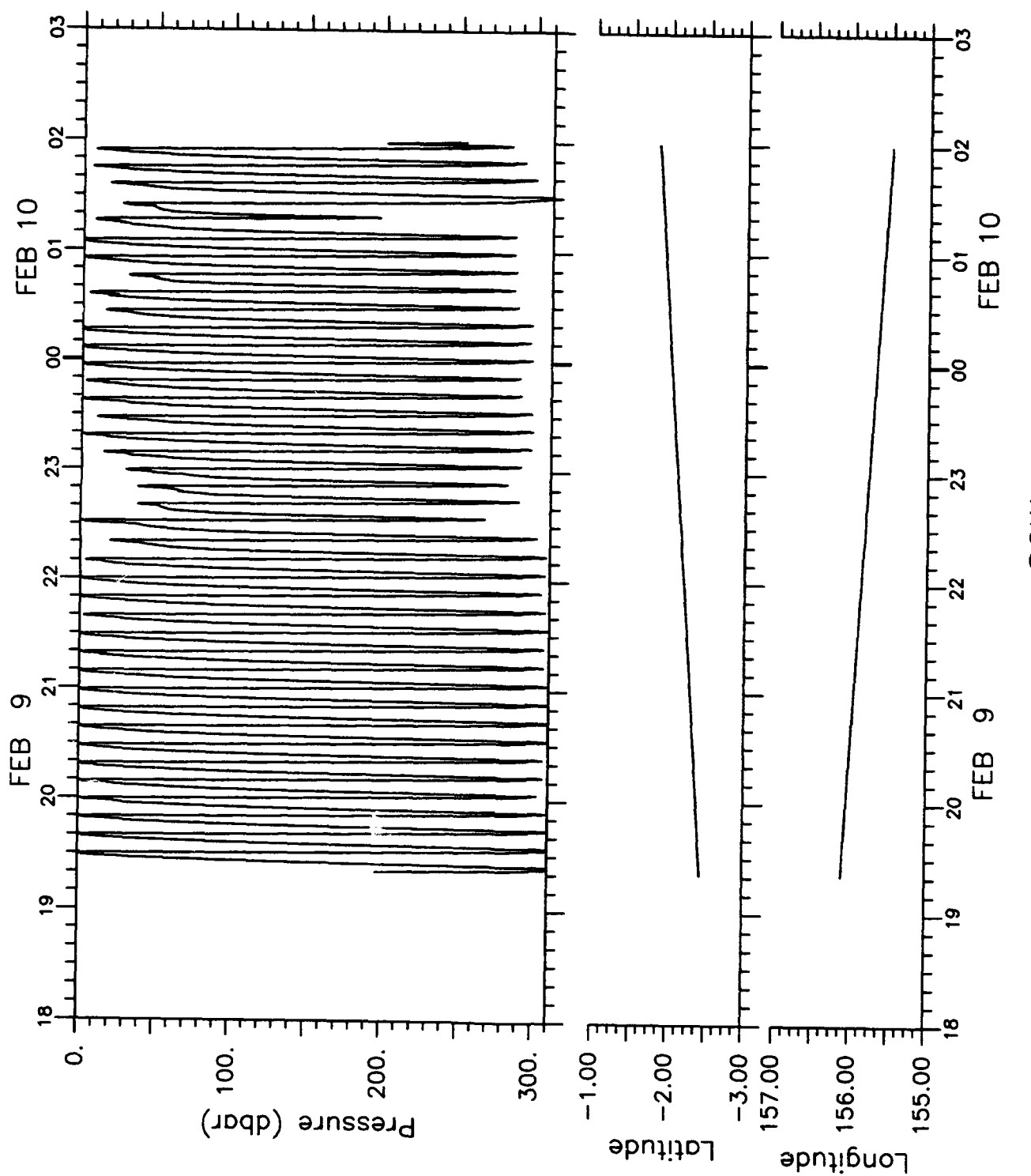


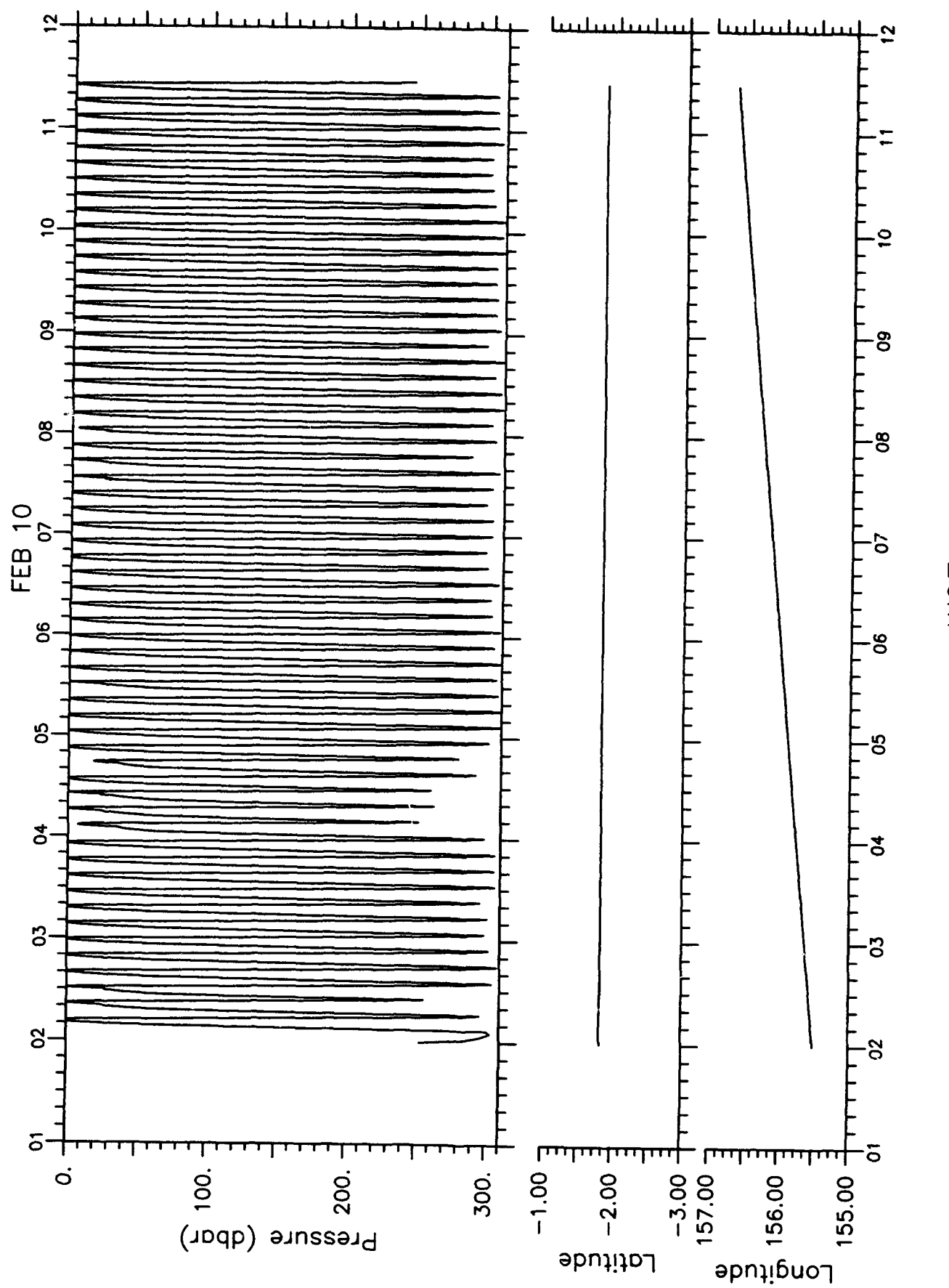


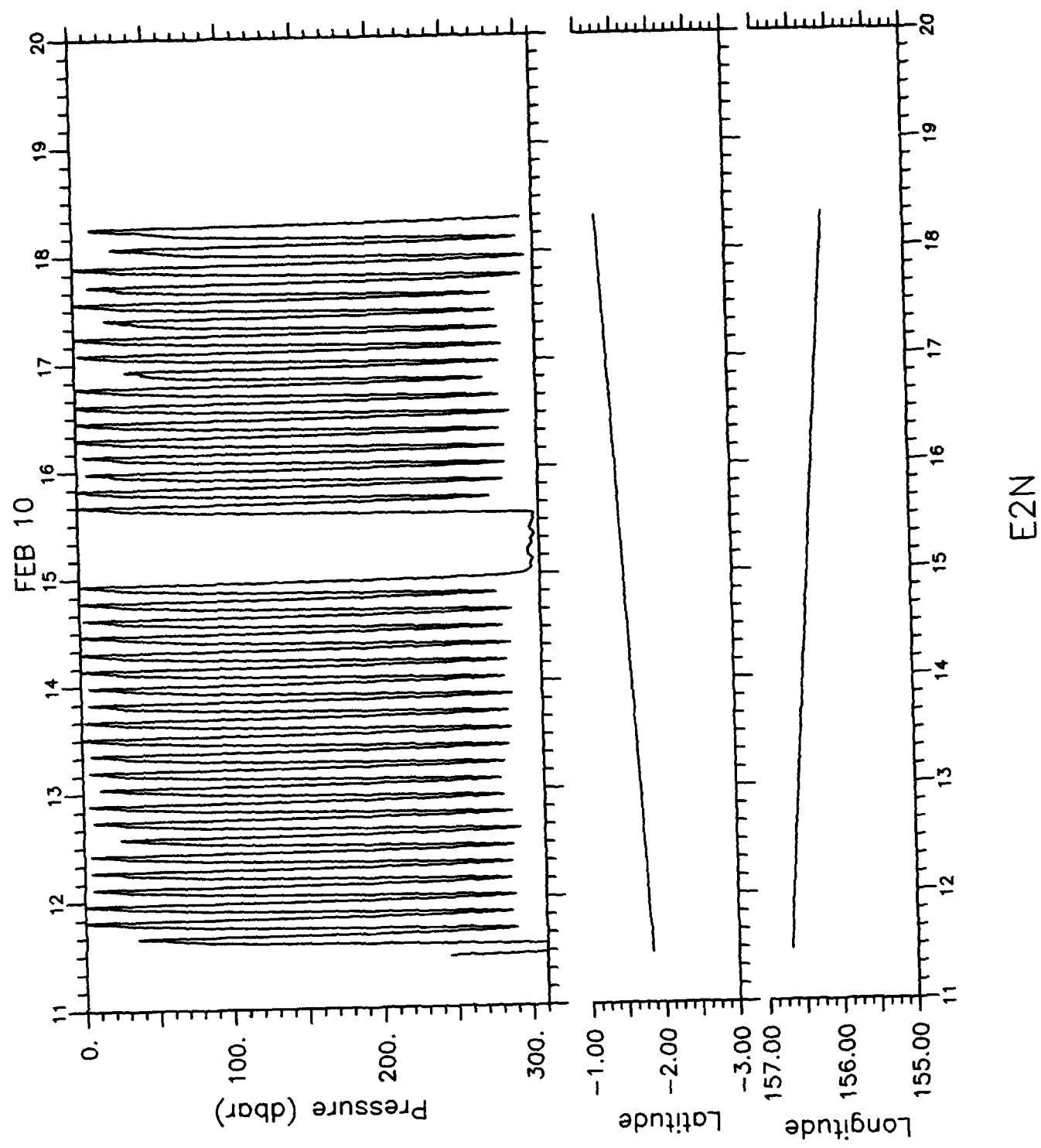


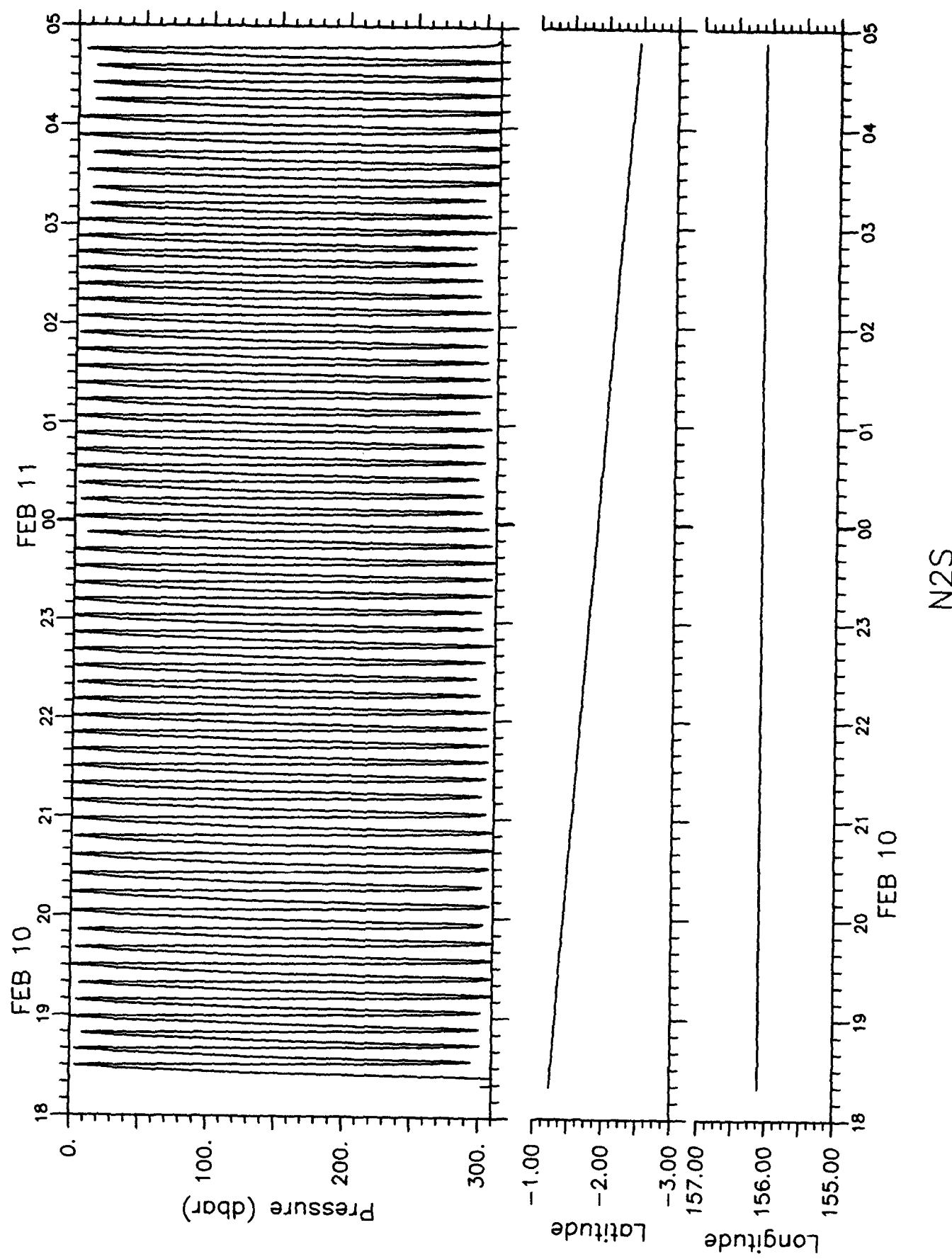


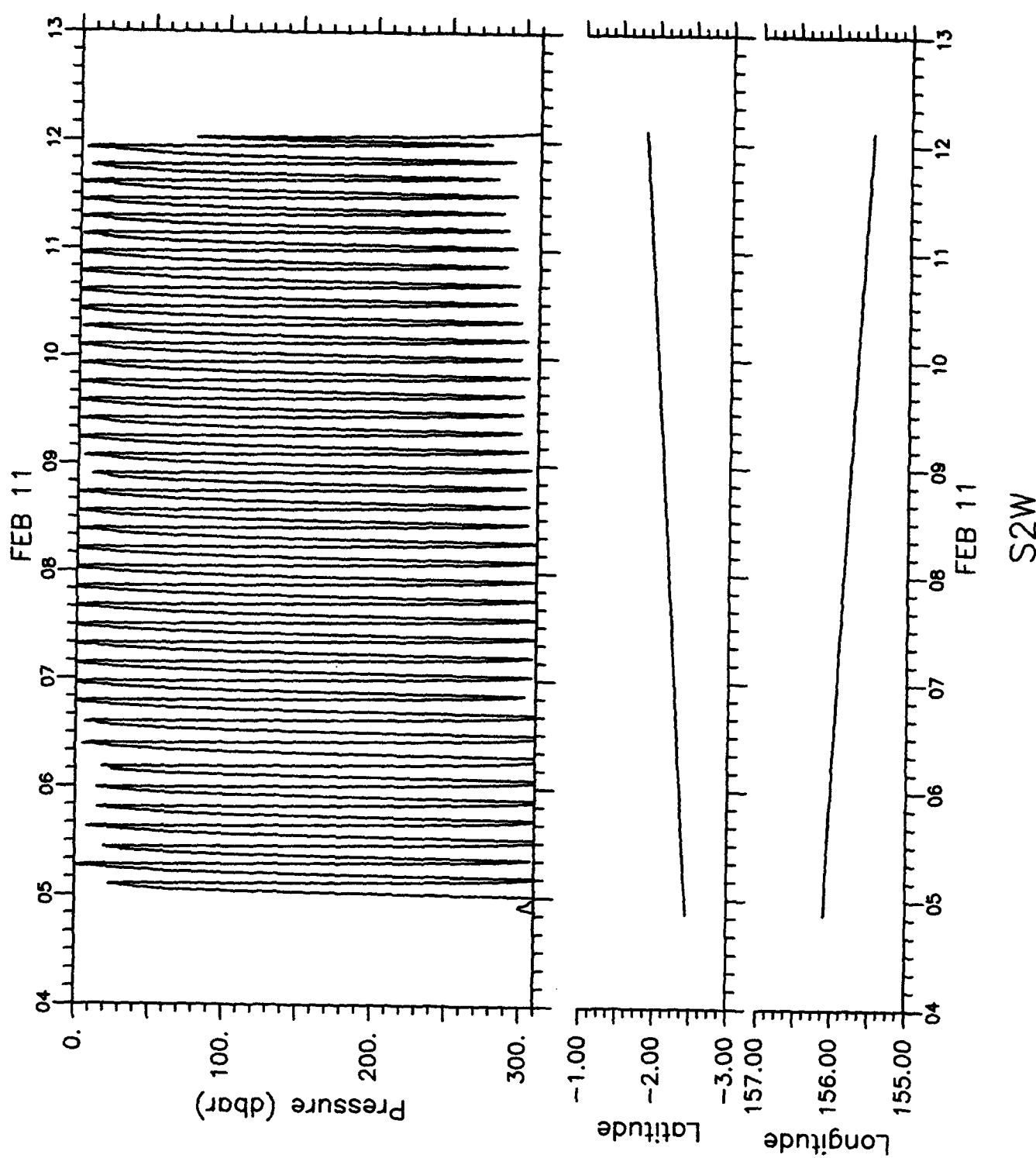
N2S

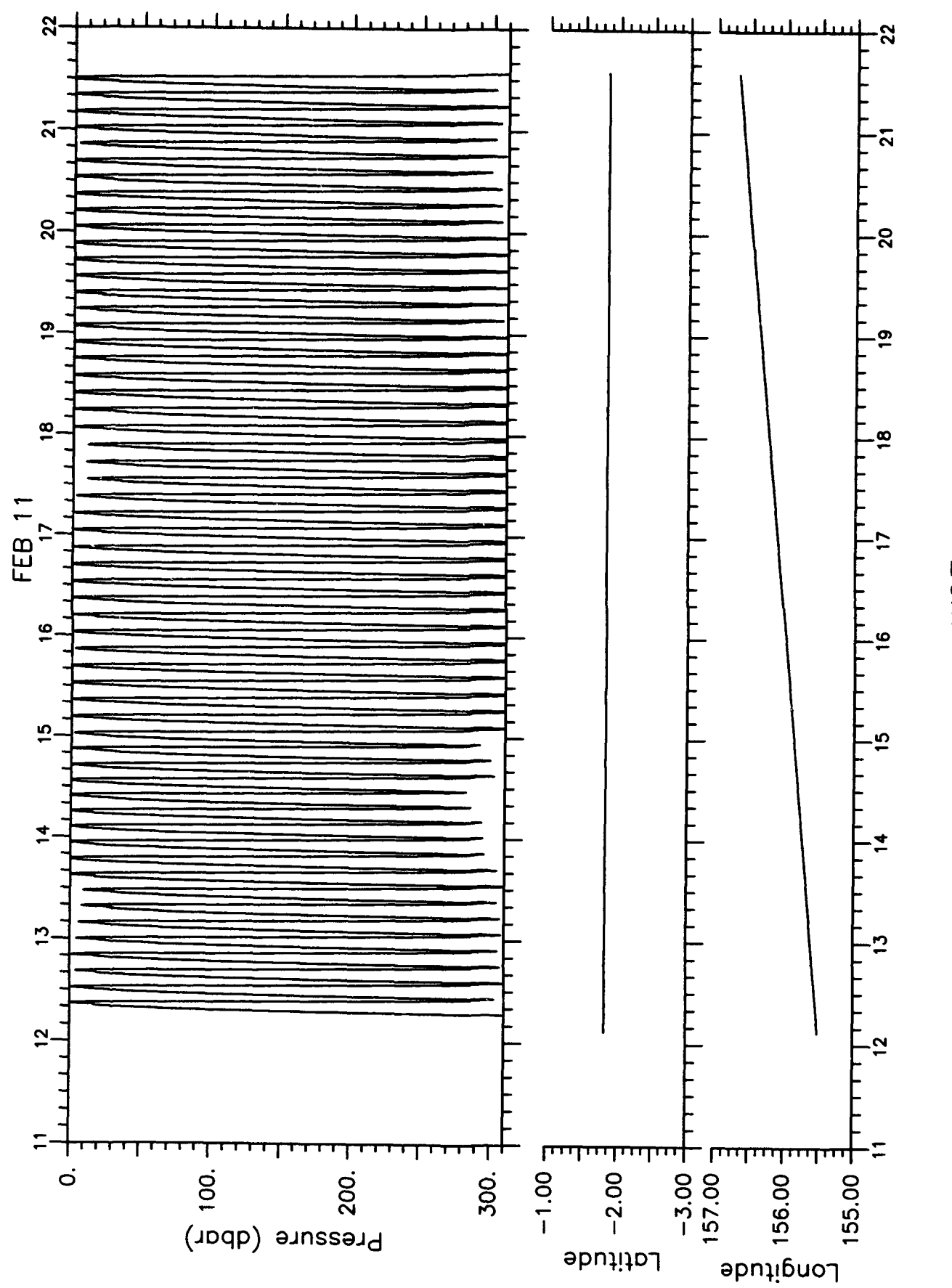


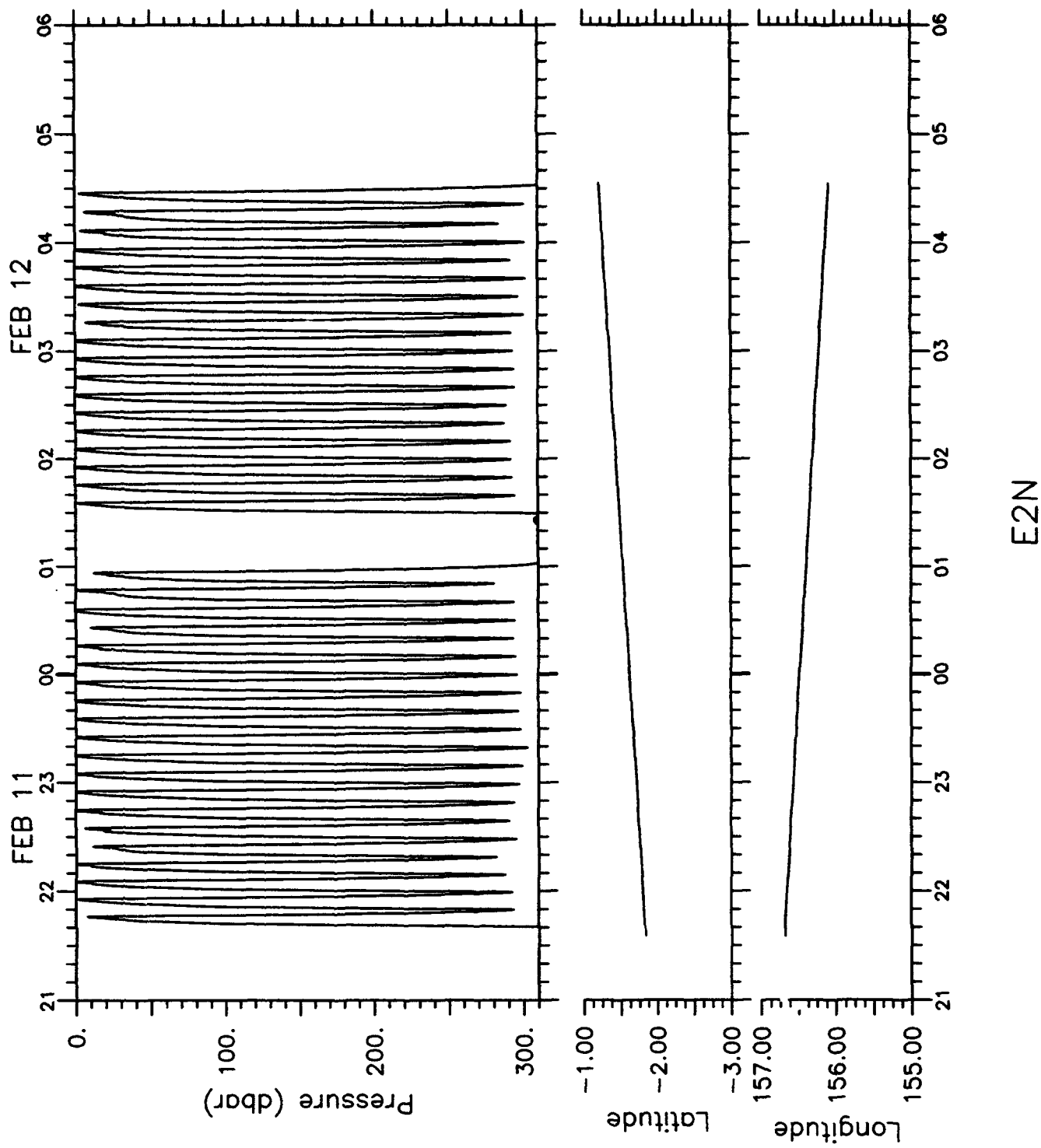


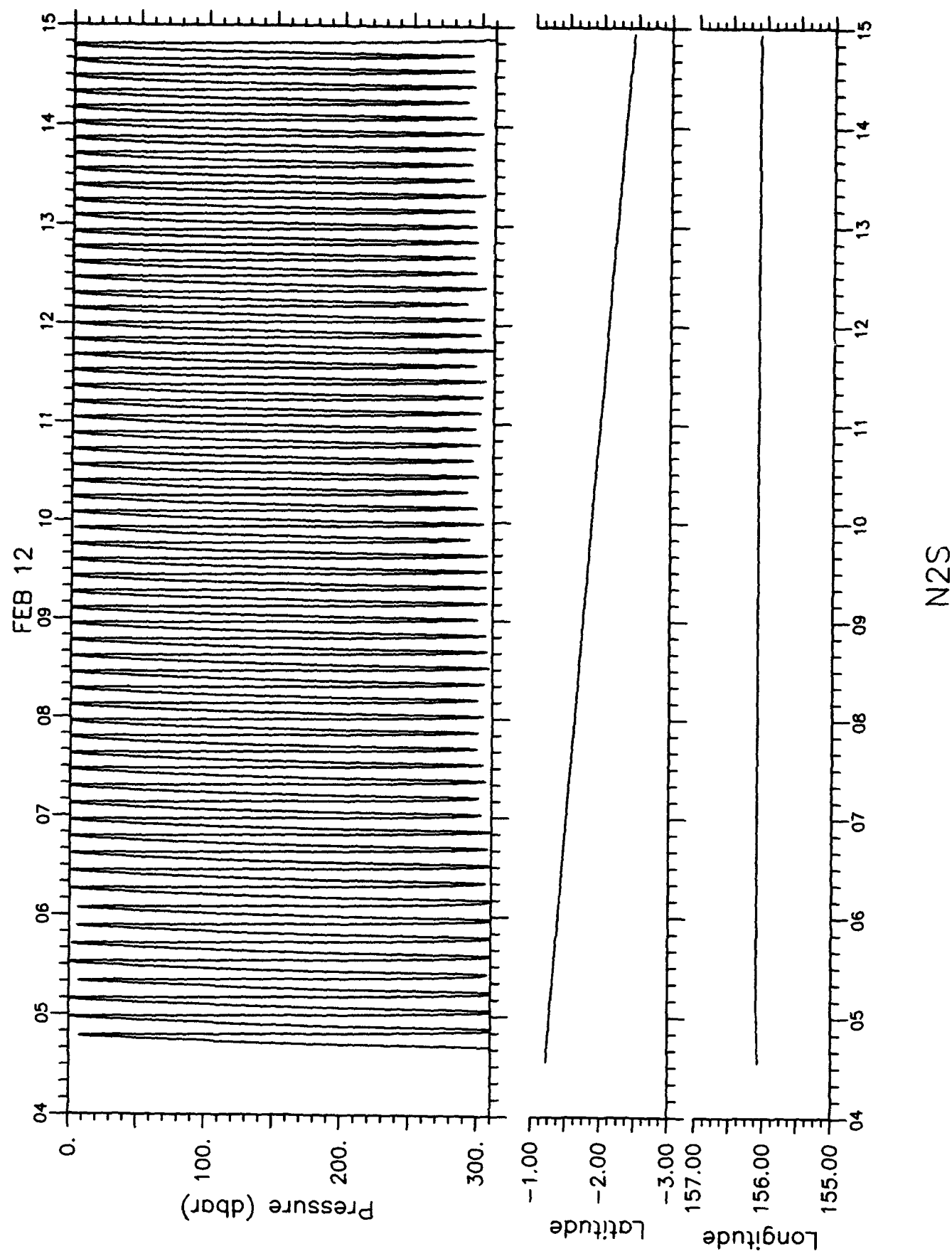


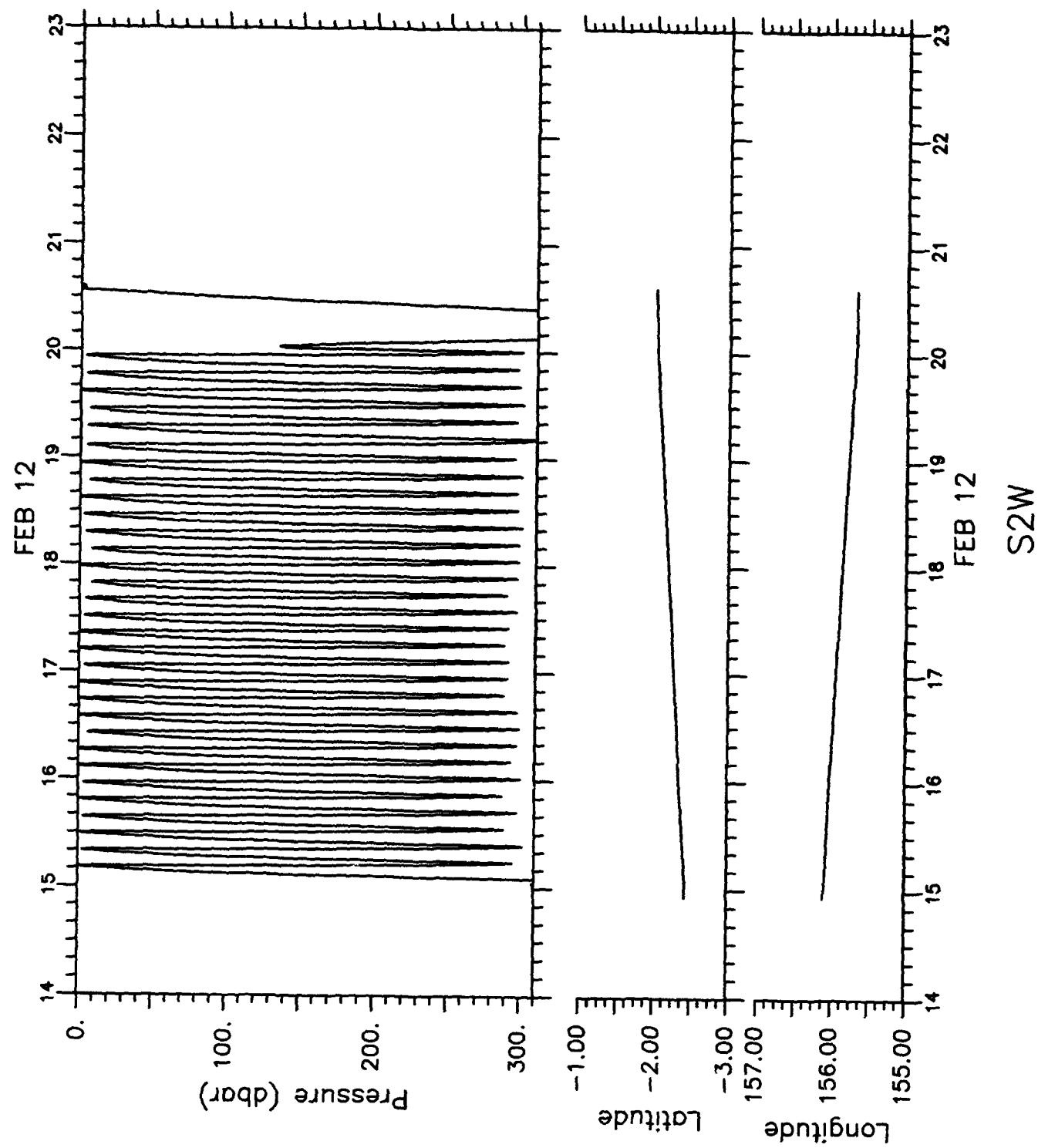


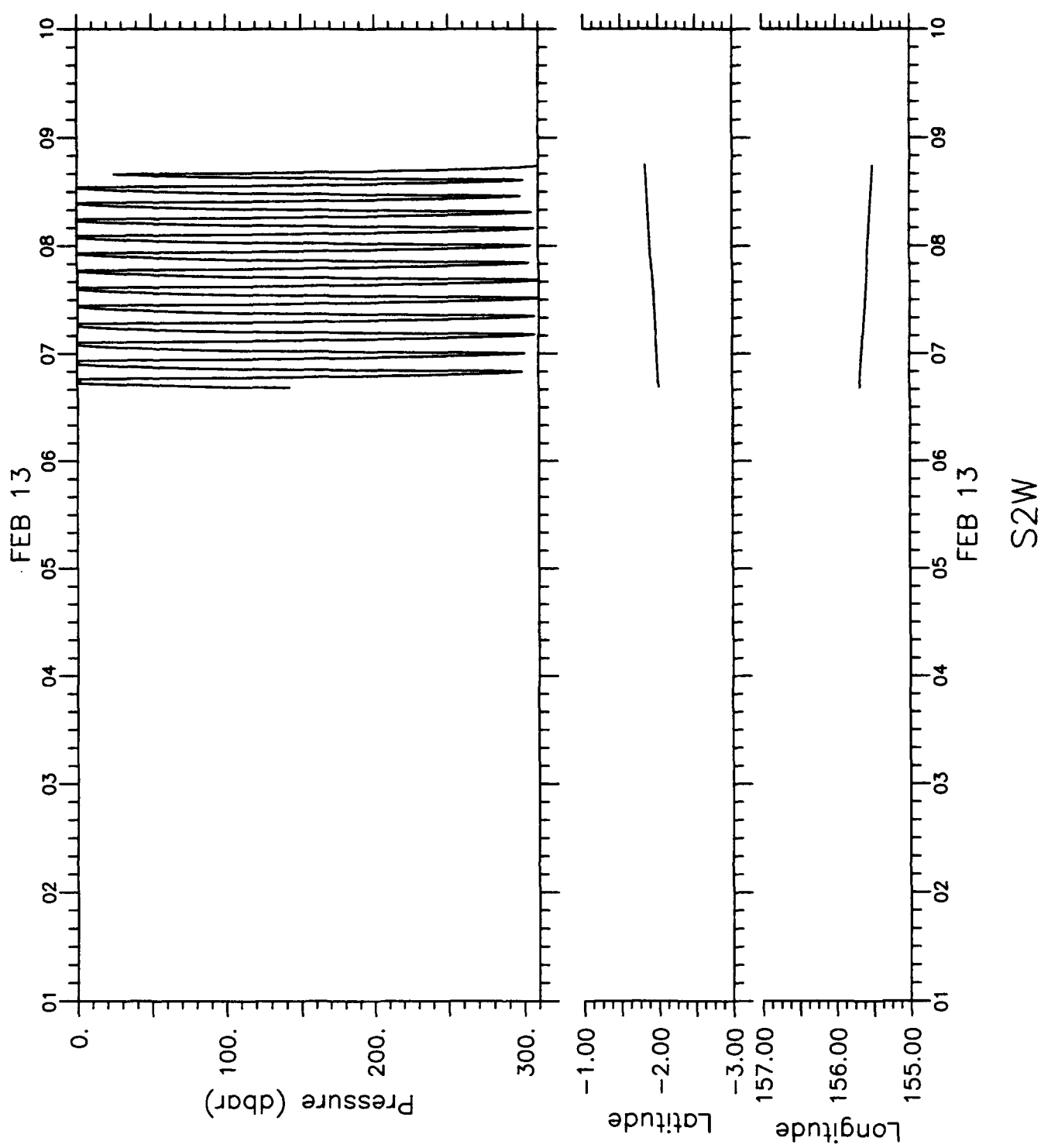


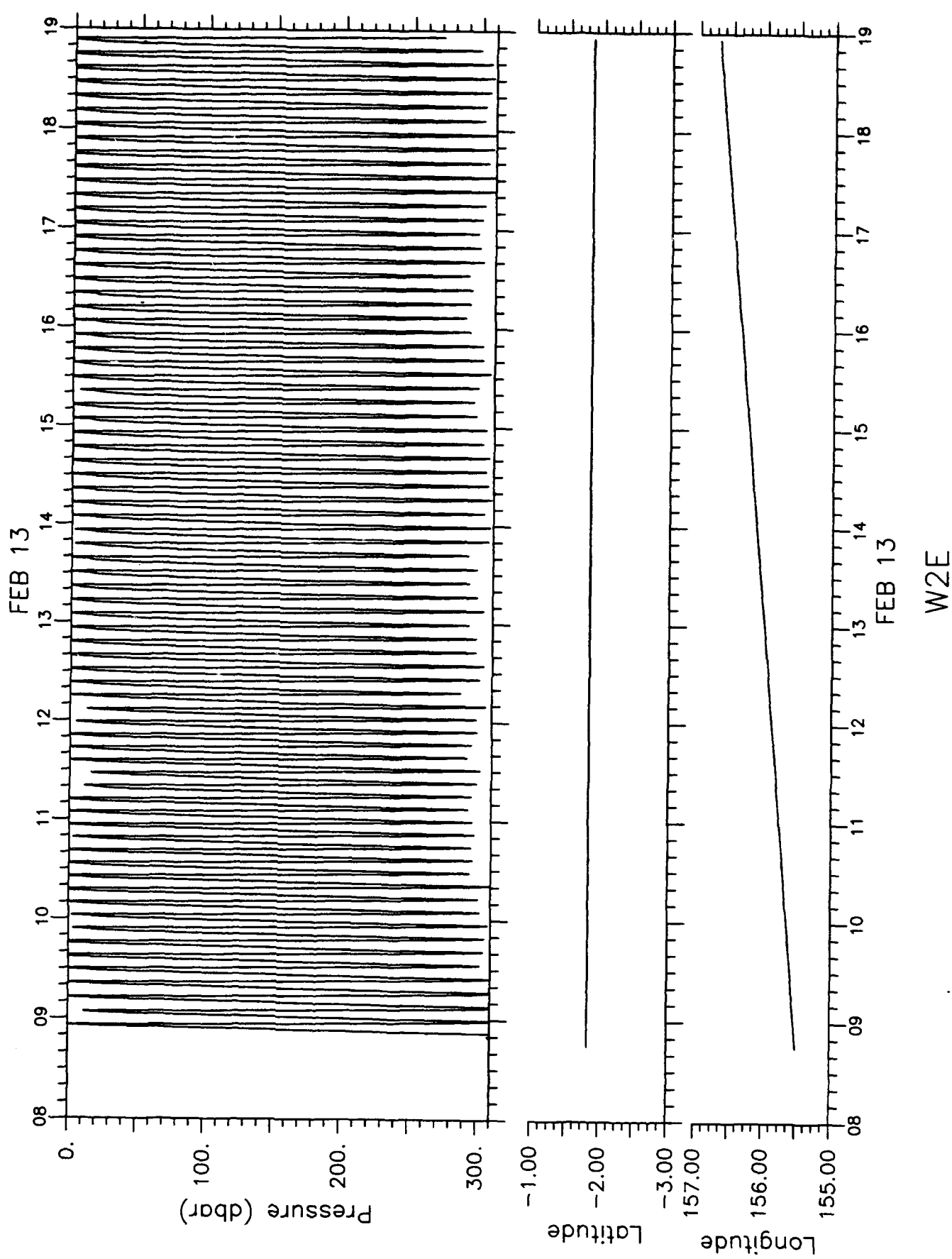


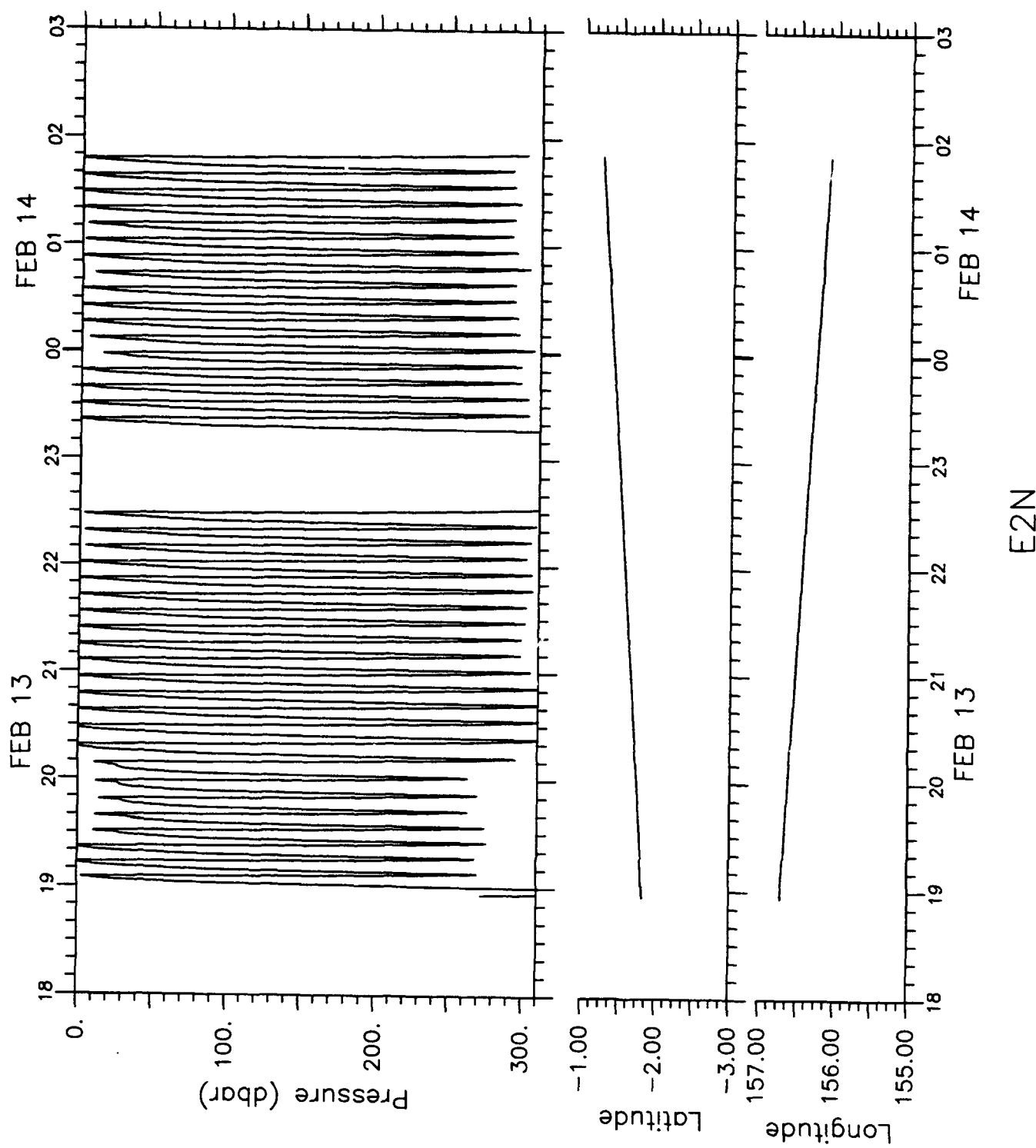


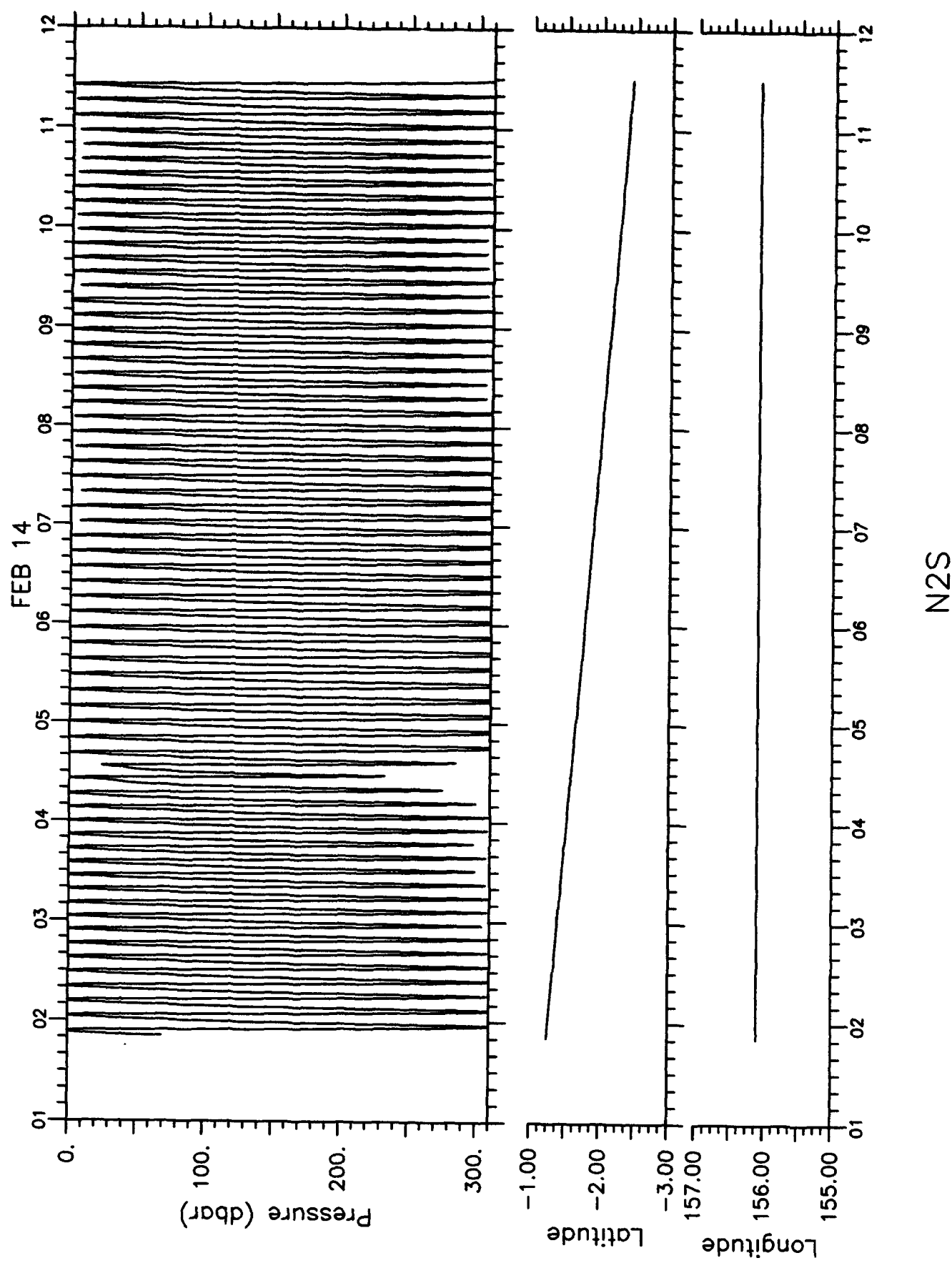


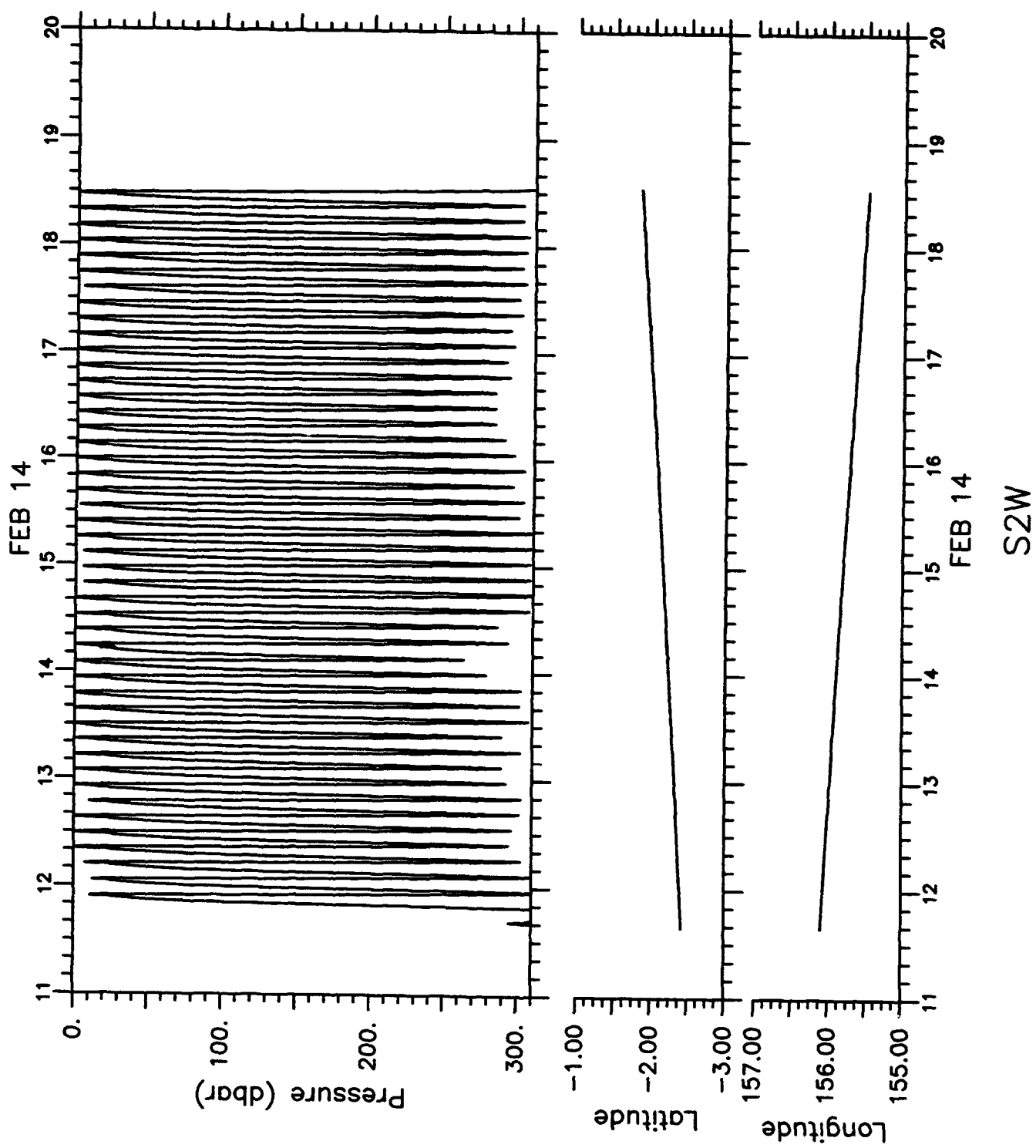


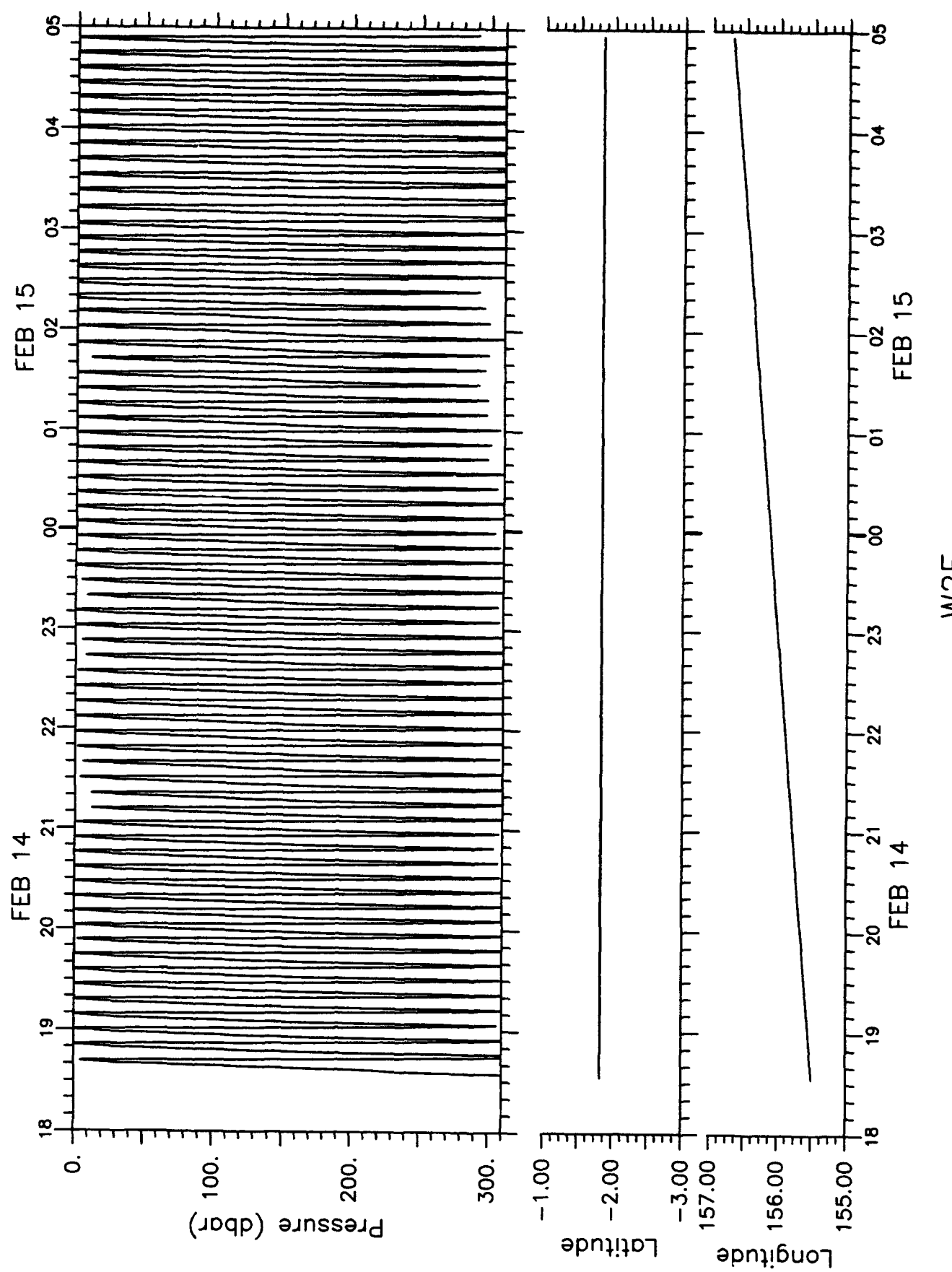


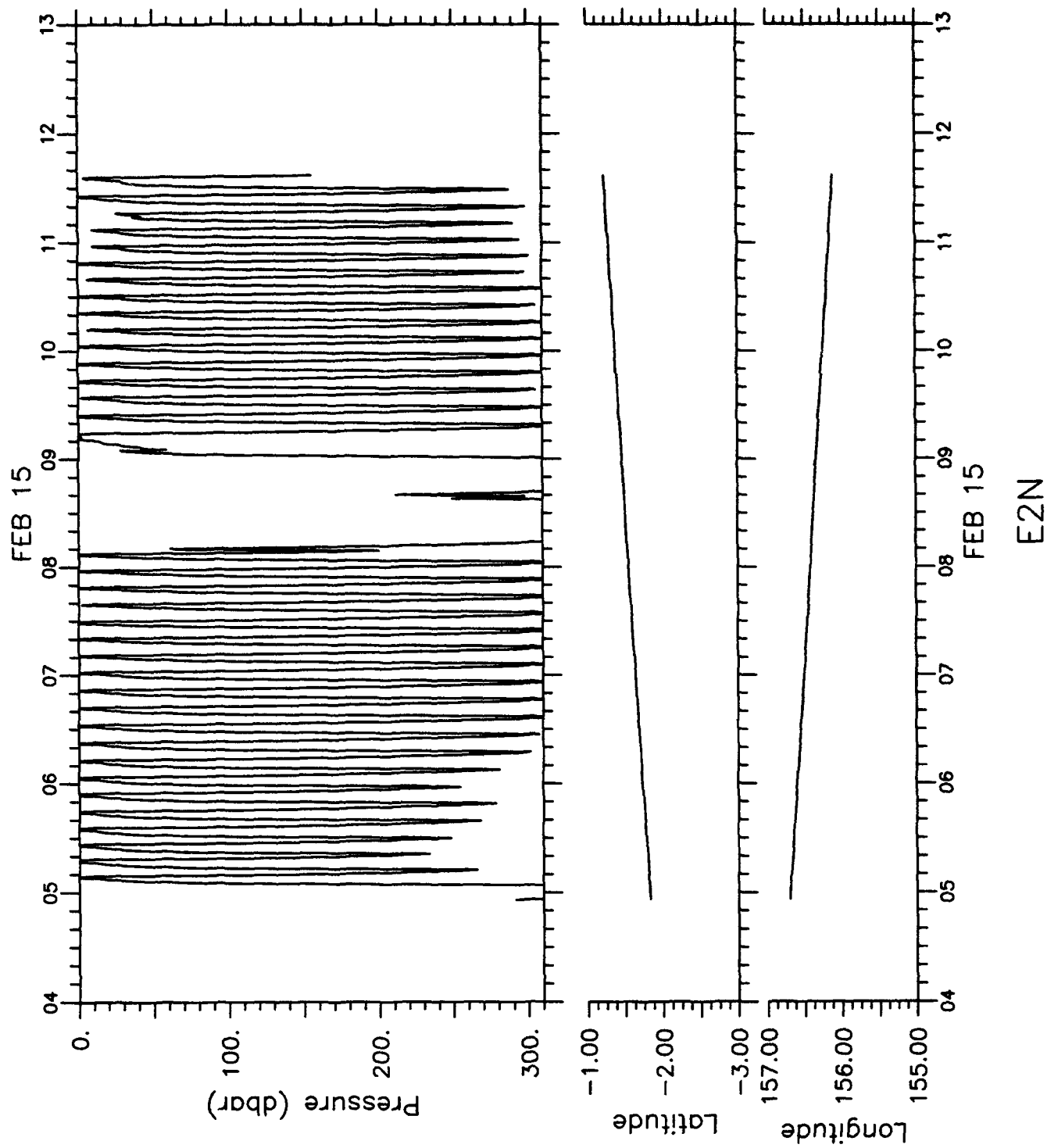


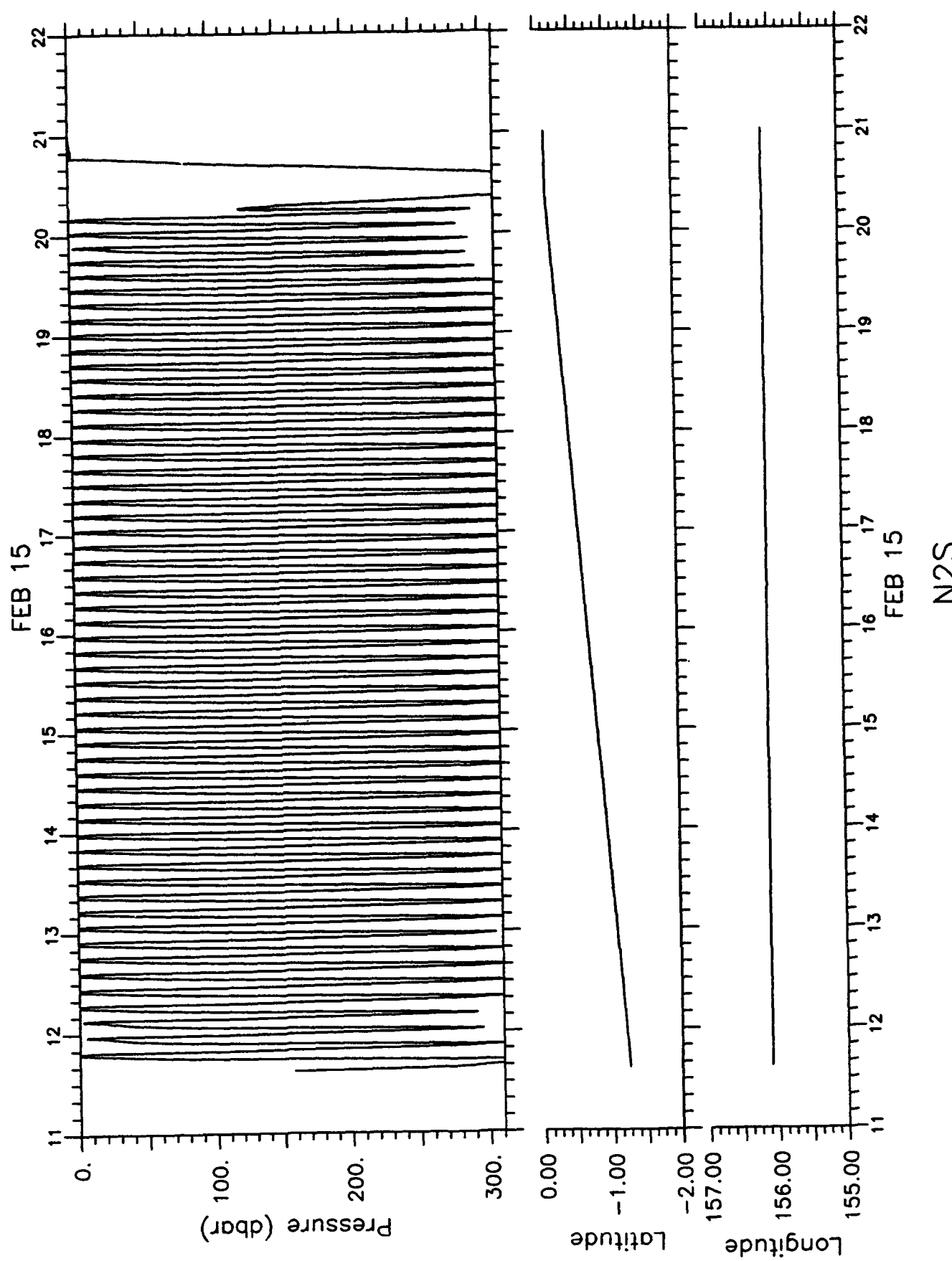










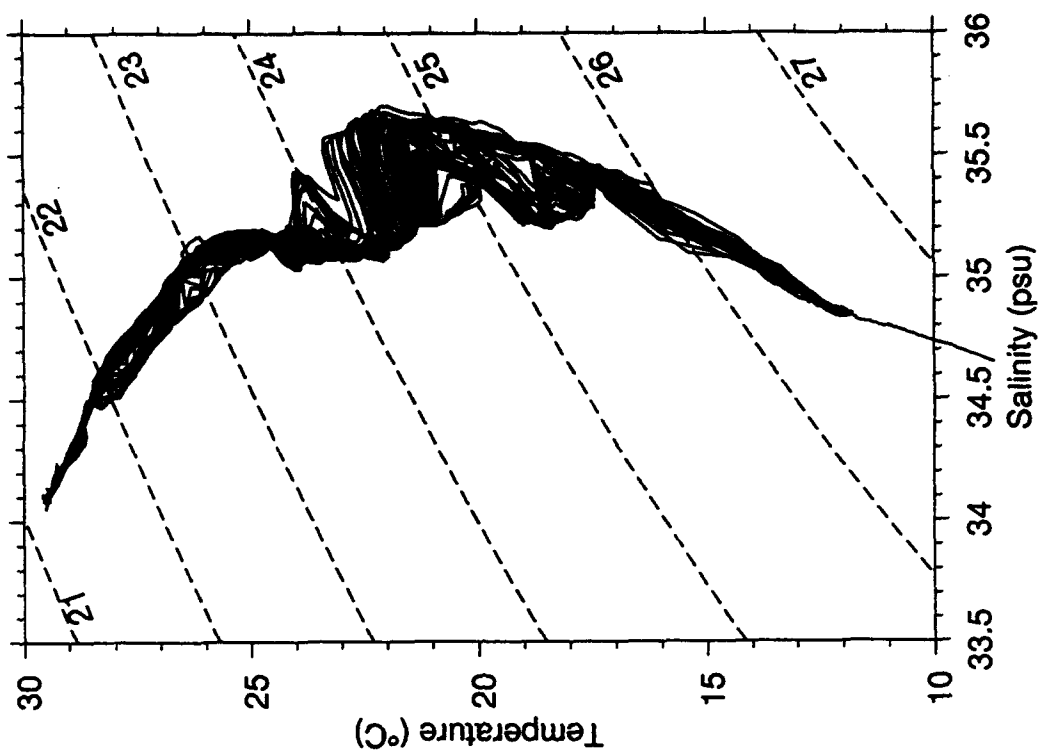




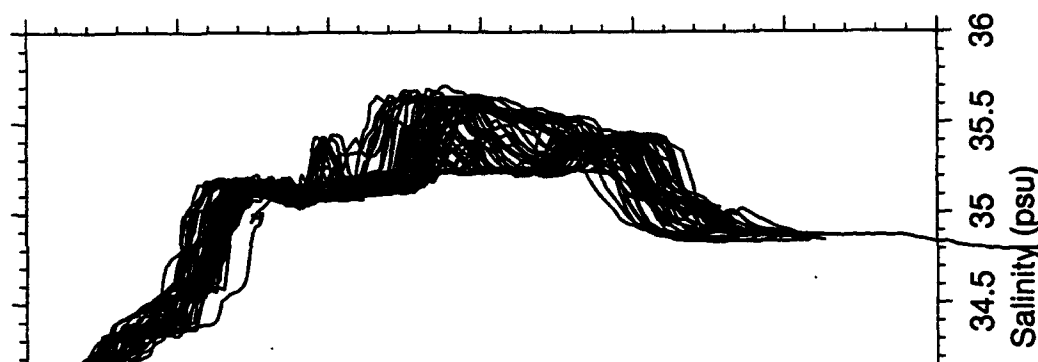
**ENSEMBLE PROFILES  
OF  
SEASOAR TEMPERATURE AND SALINITY**

100

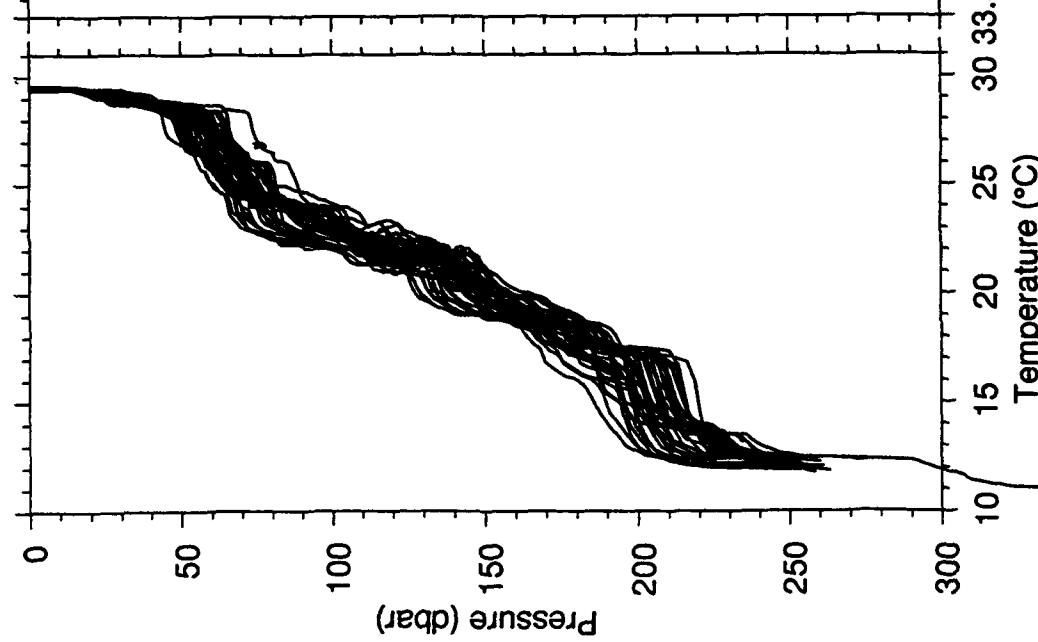
n2s27jan.up.data



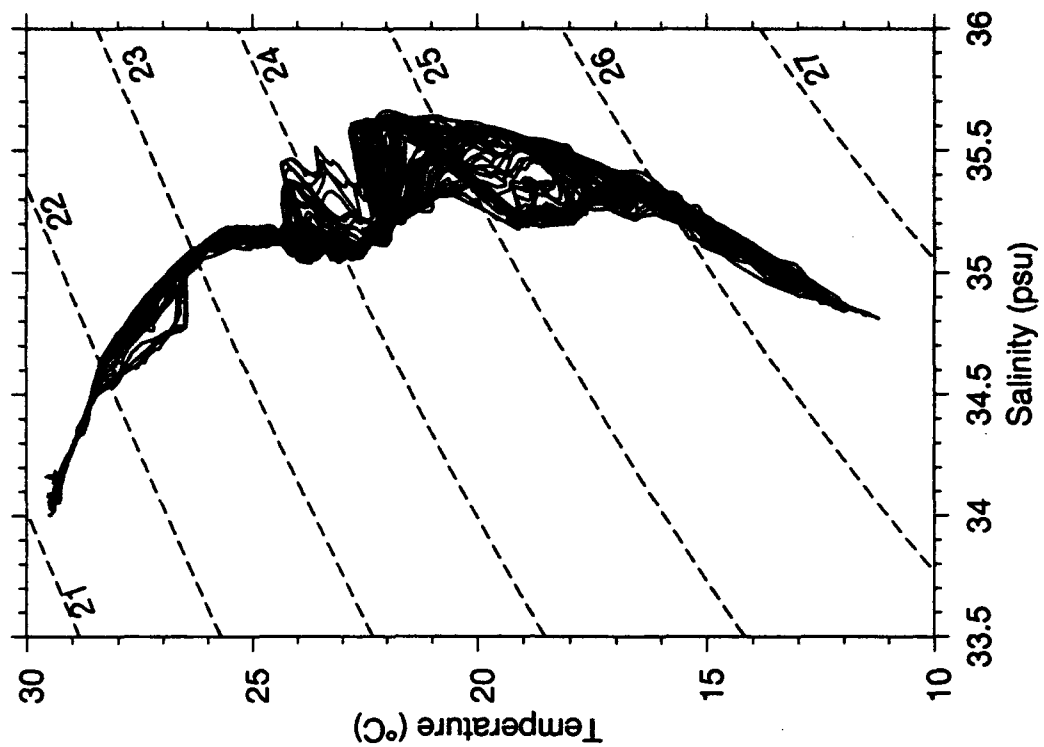
n2s27jan.up.data



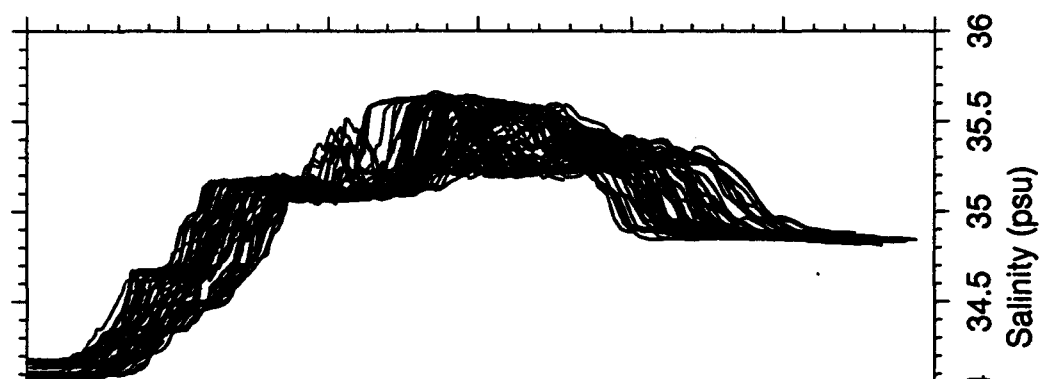
W9211C n2s27jan.up.data



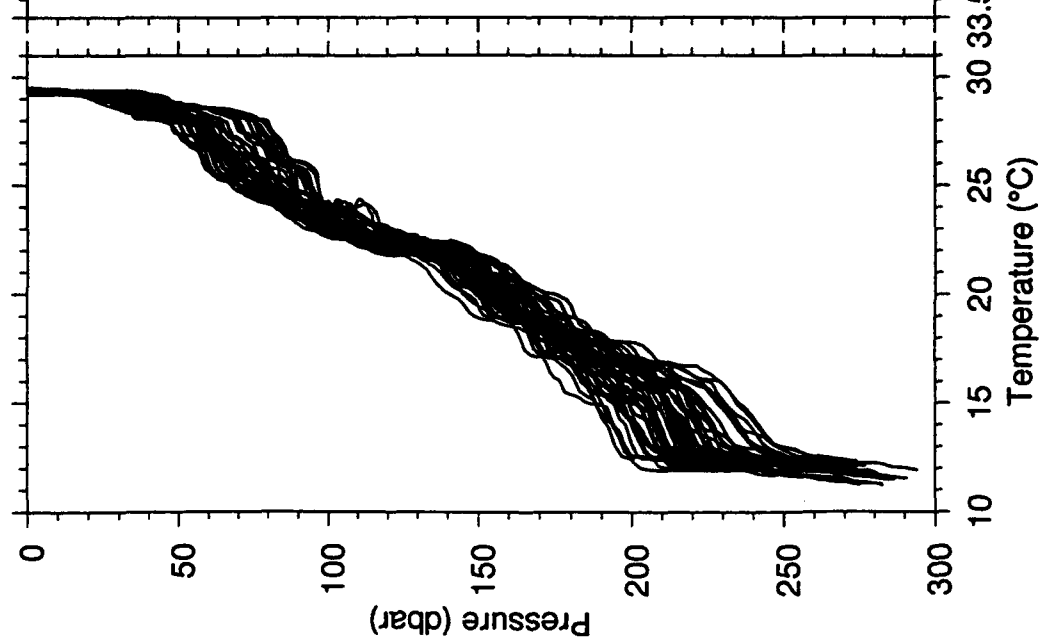
n2s28jan.up.data



n2s28jan.up.data

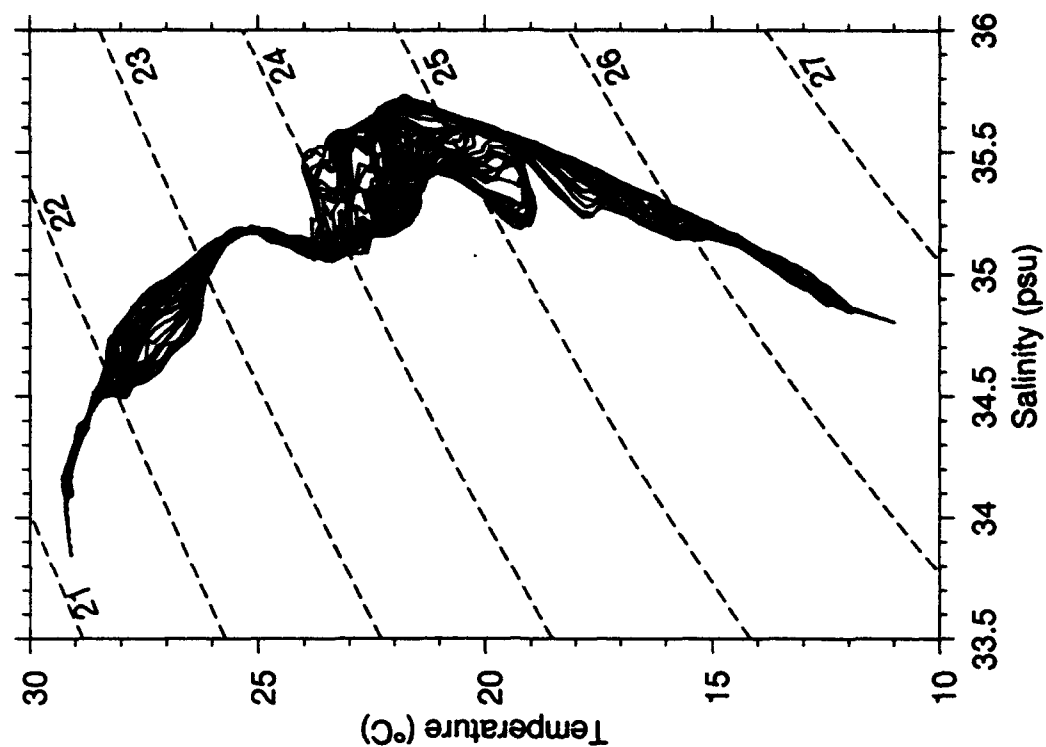


W9211C n2s28jan.up.data



102

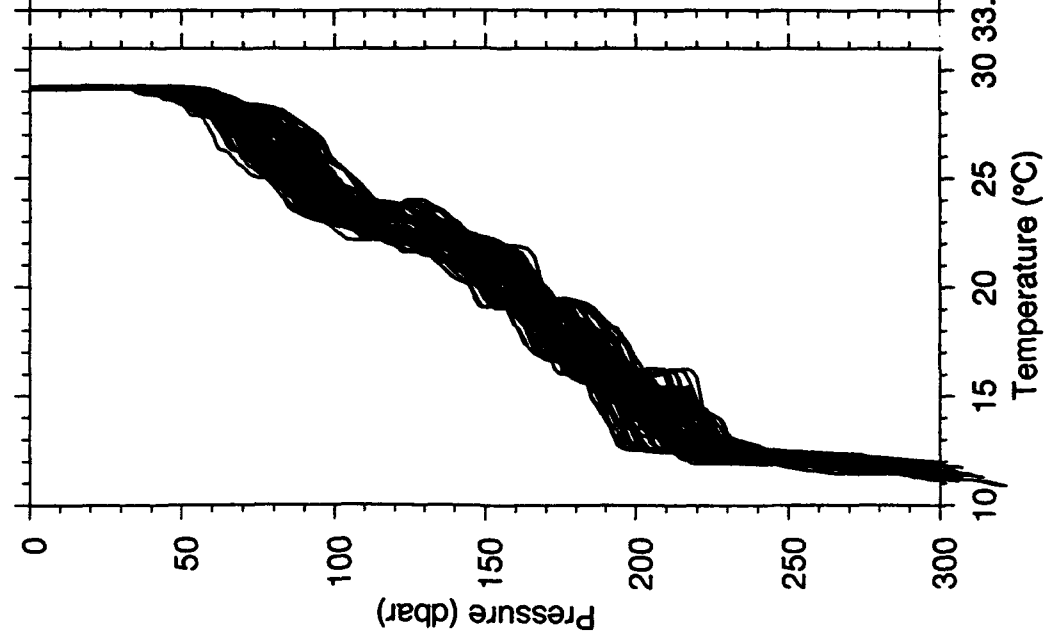
n2s30jan.up.data

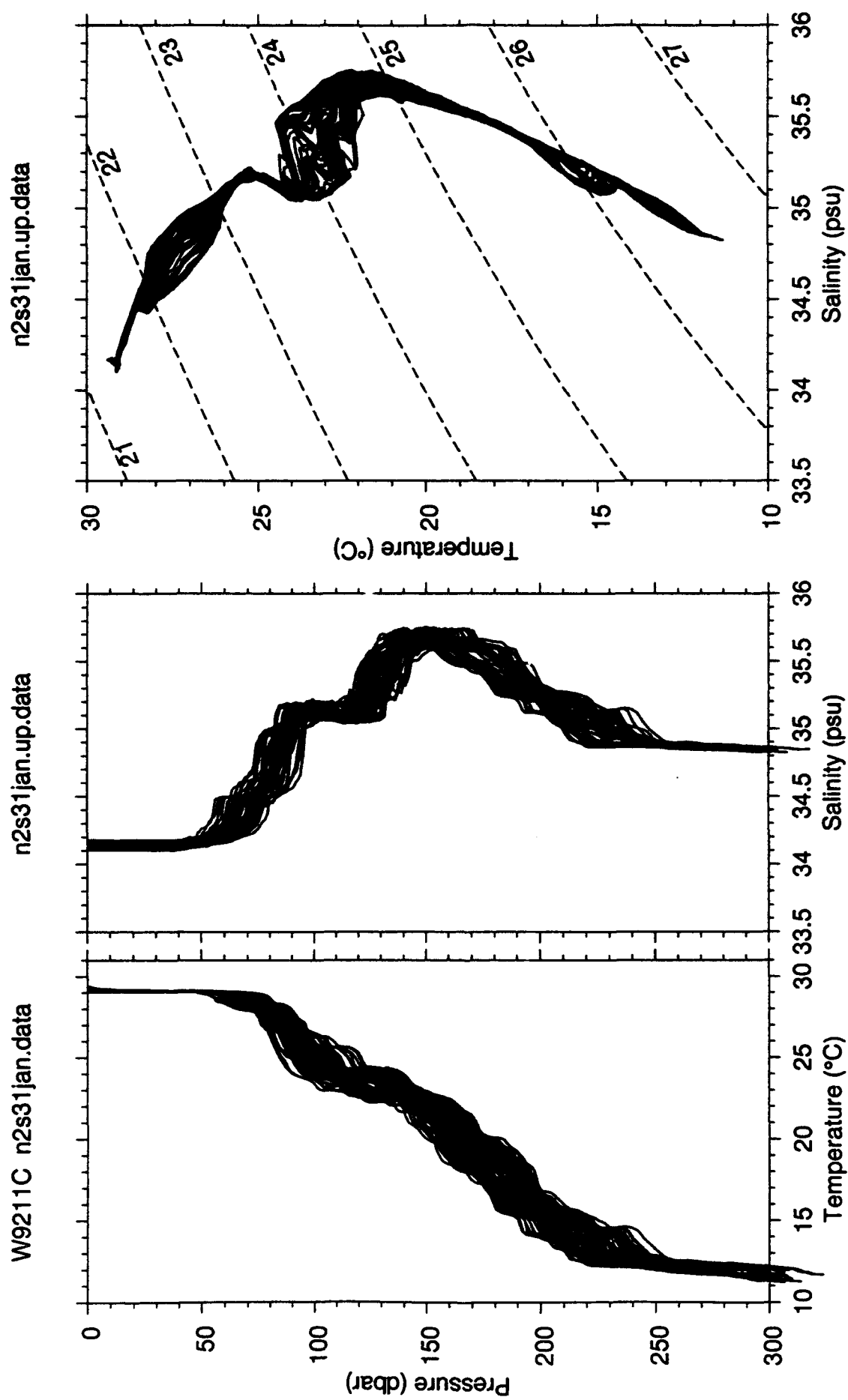


n2s30jan.up.data



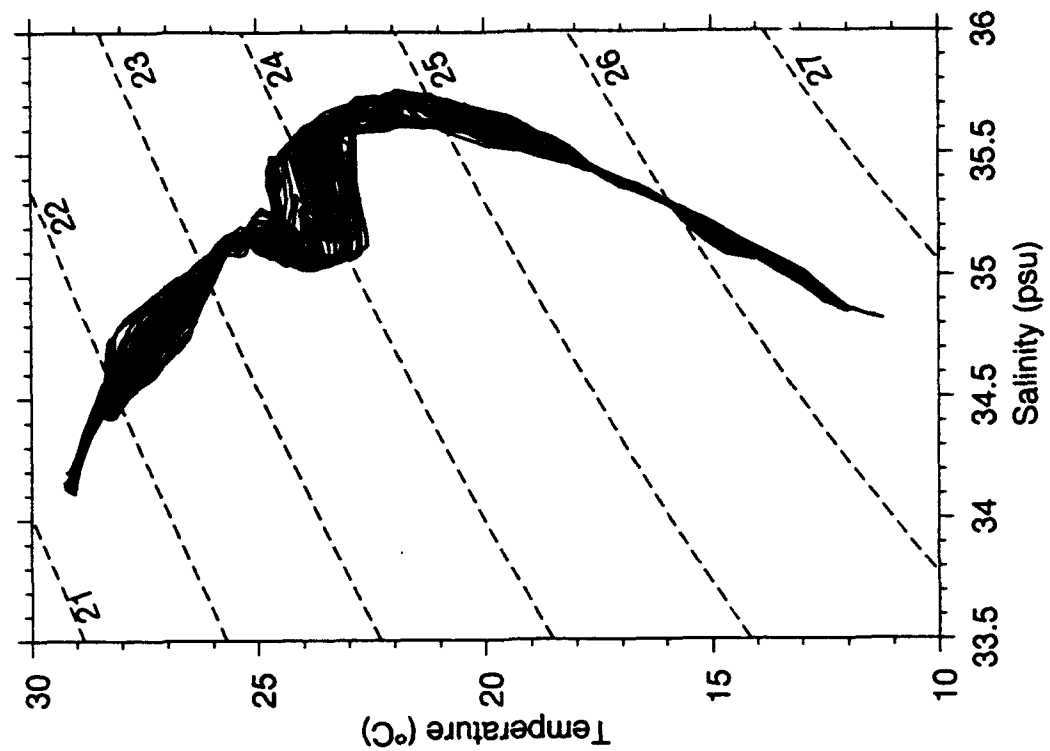
W9211C n2s30jan.data



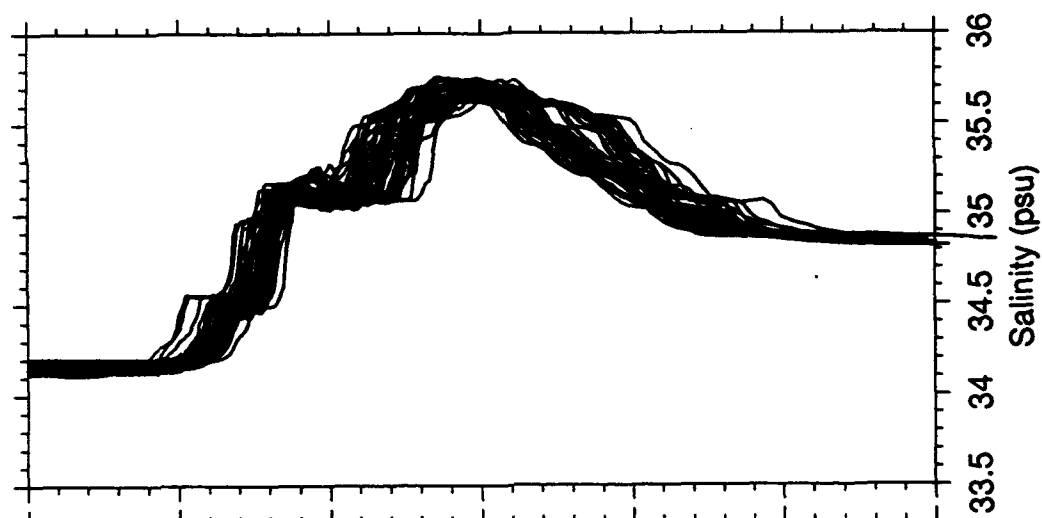


104

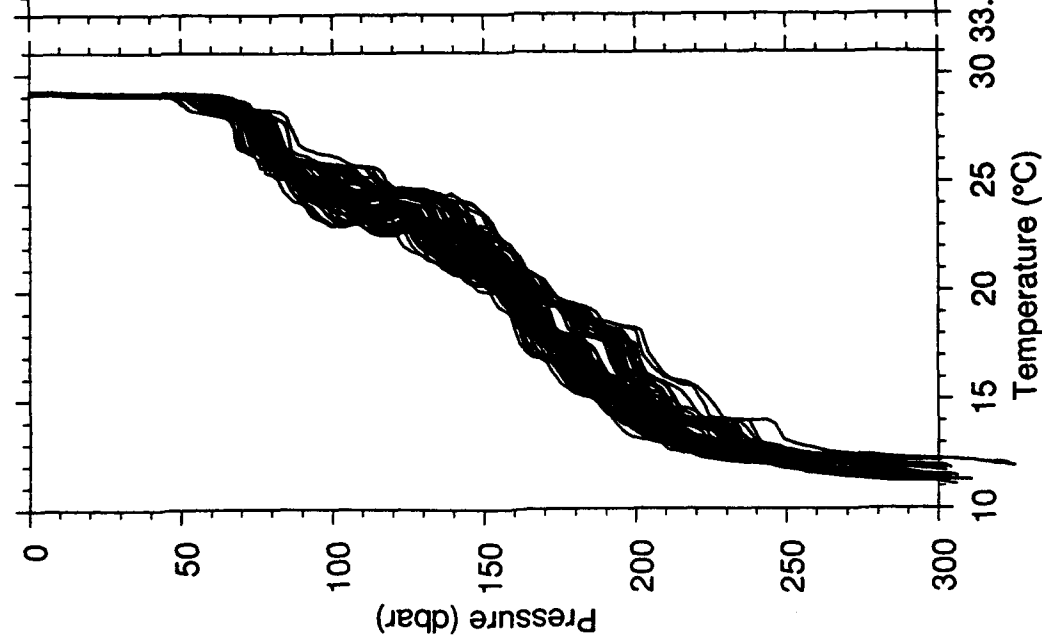
n2s02feb.up.data

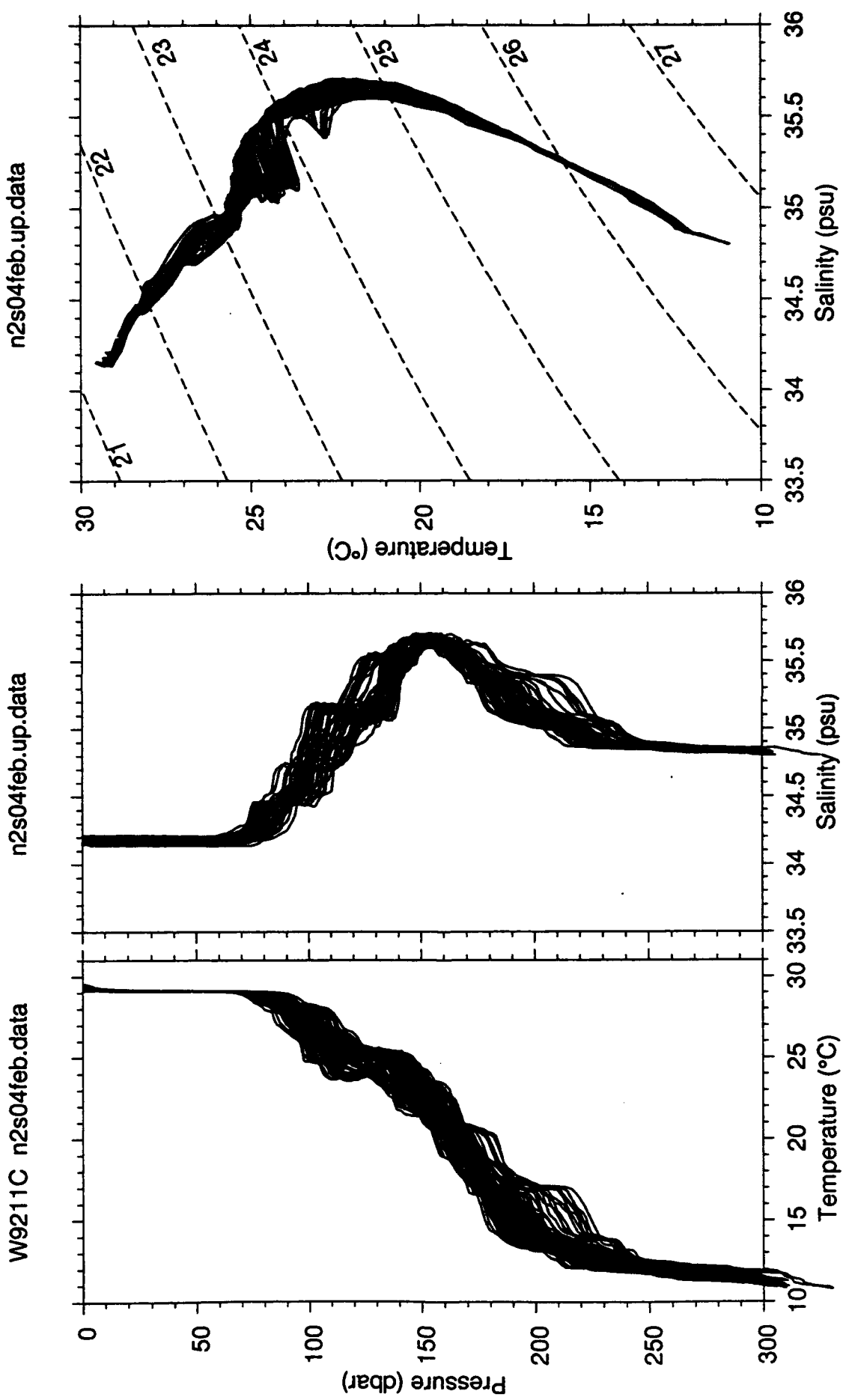


n2s02feb.up.data

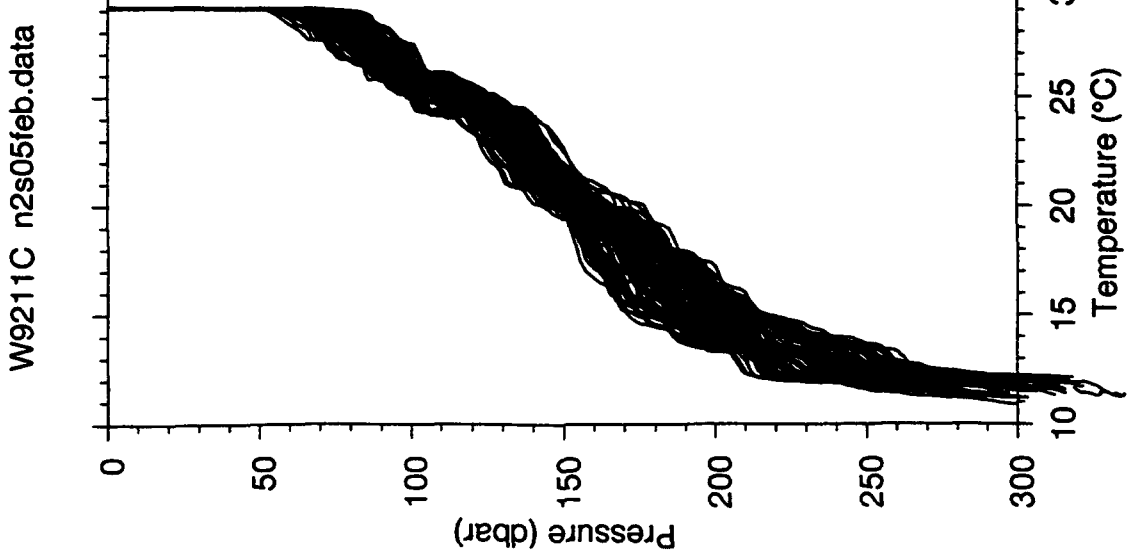
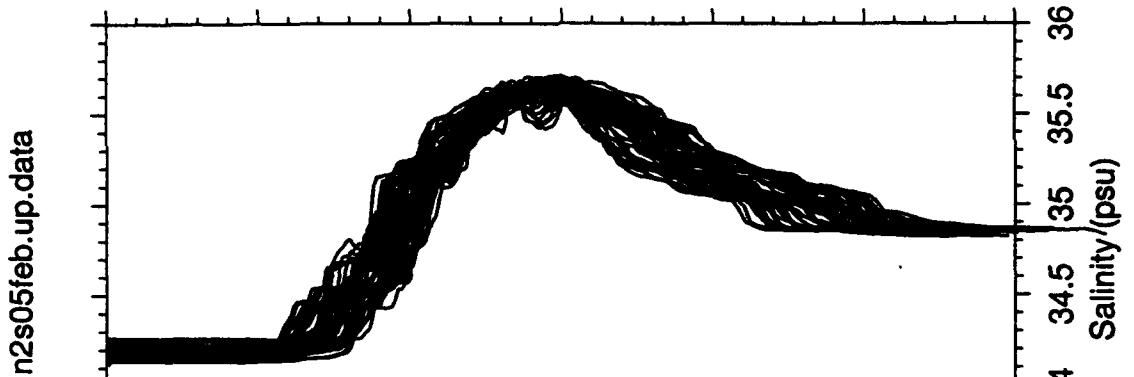
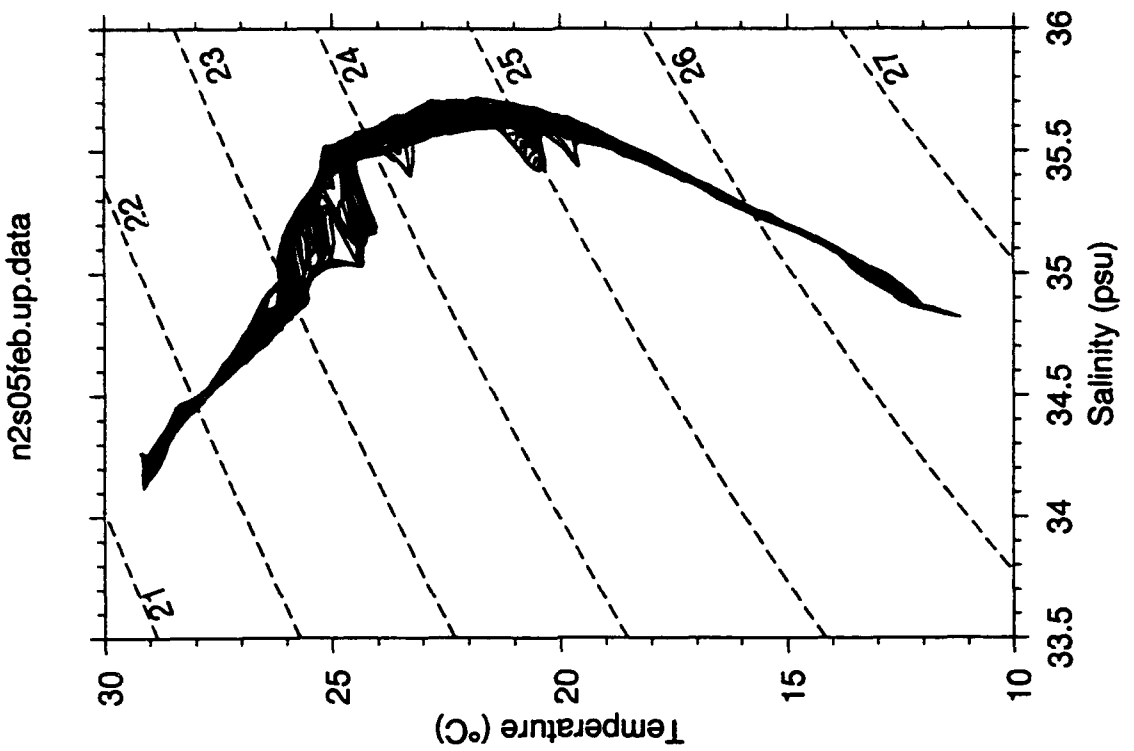


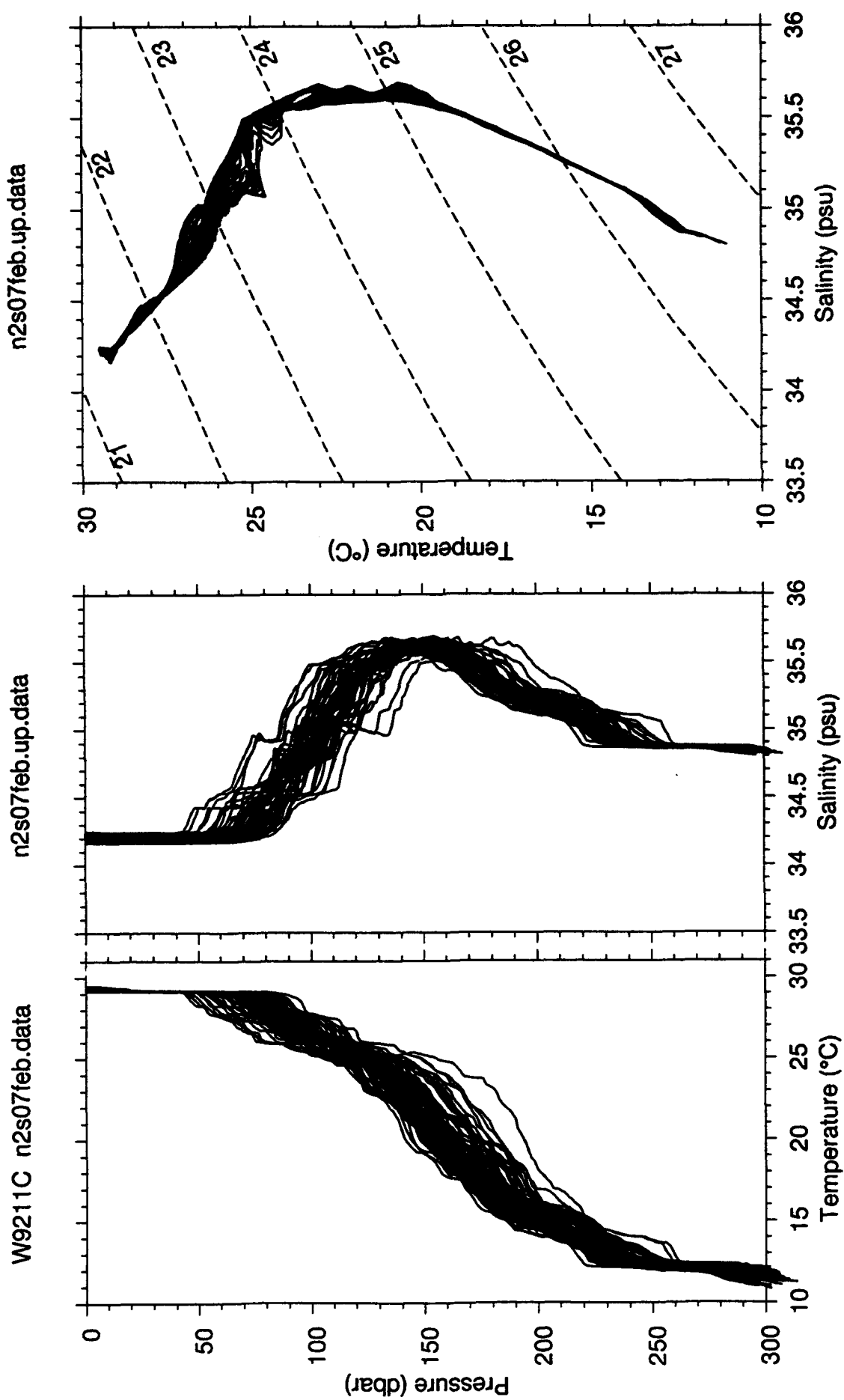
w9211C n2s02feb.data

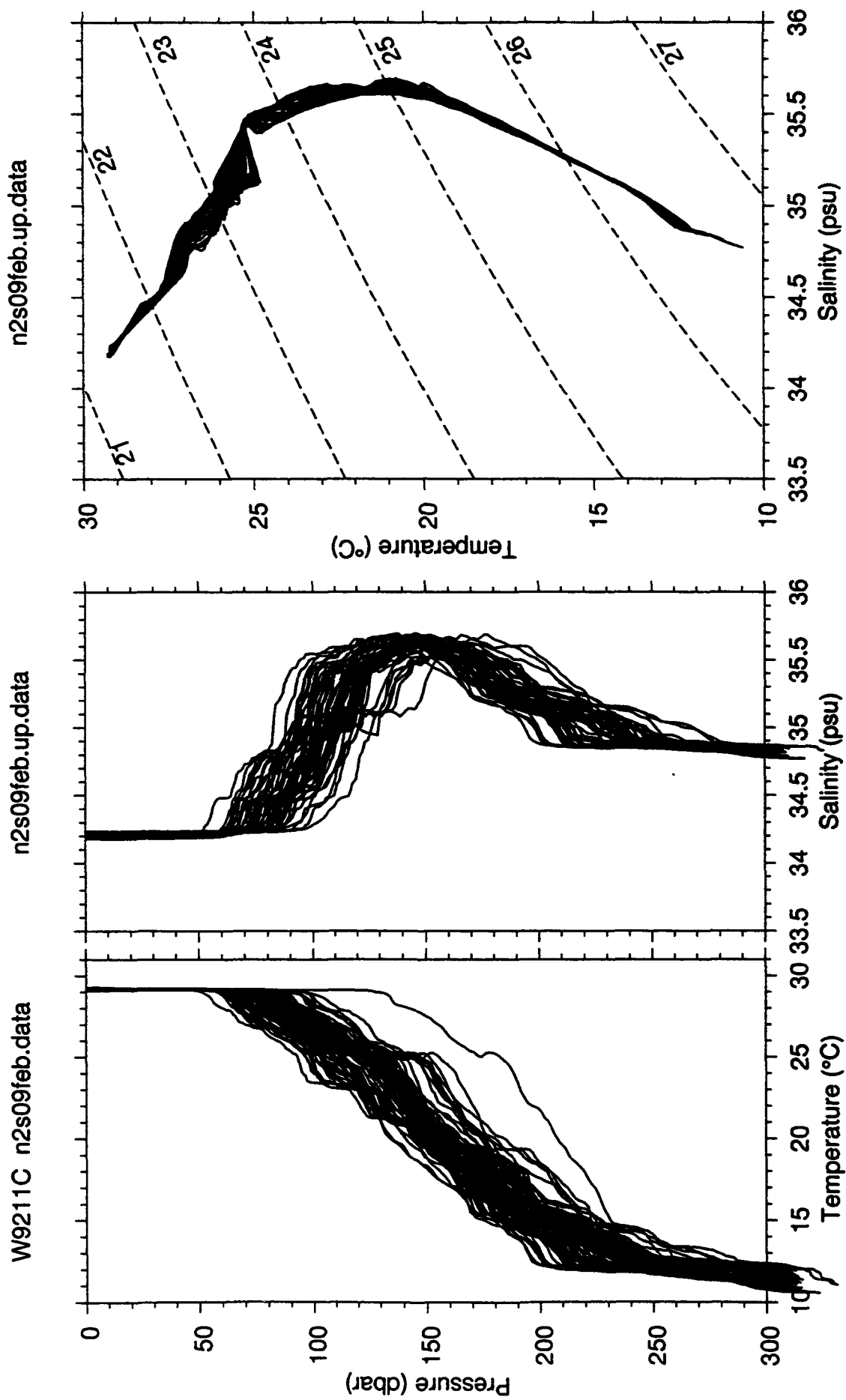


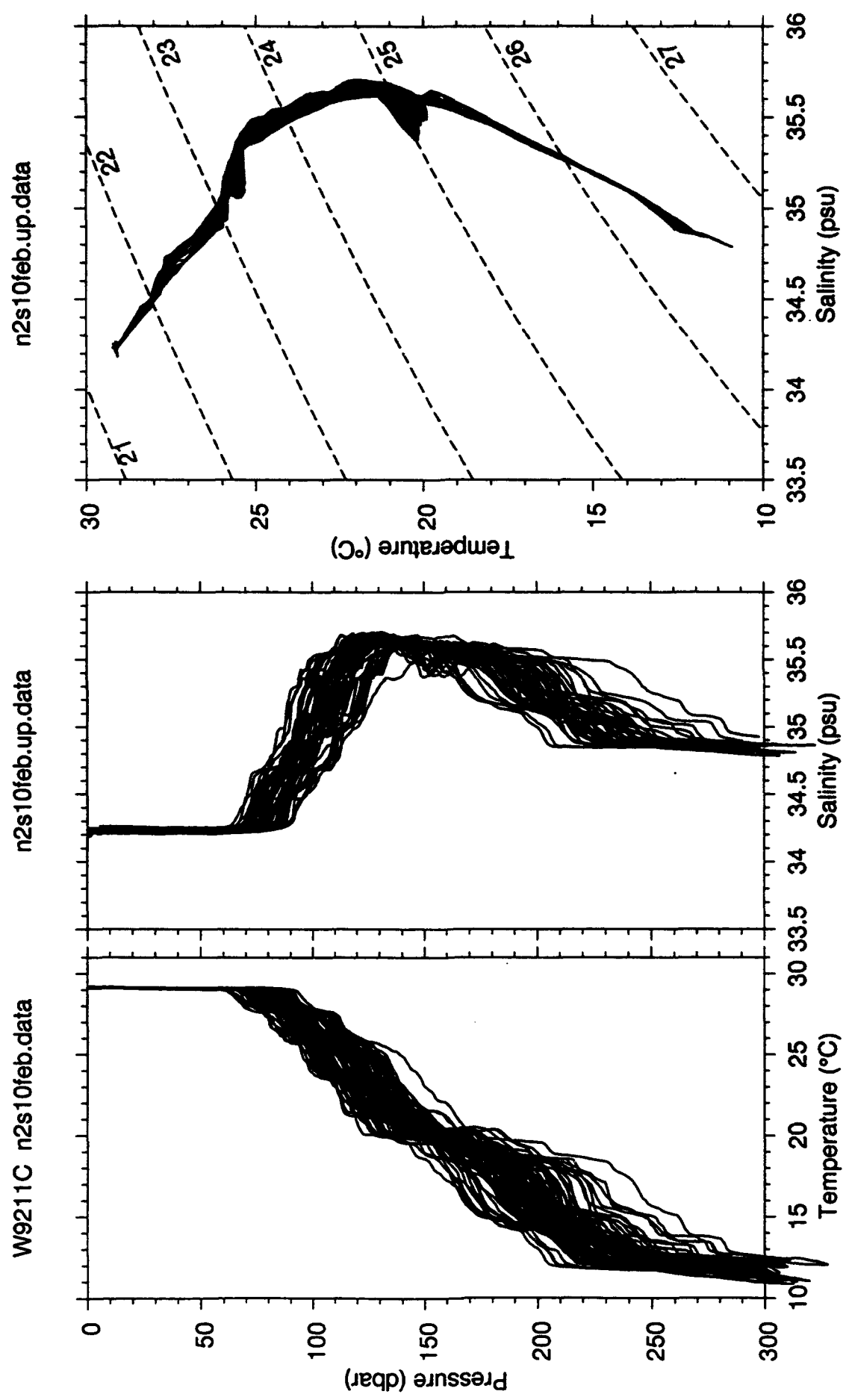


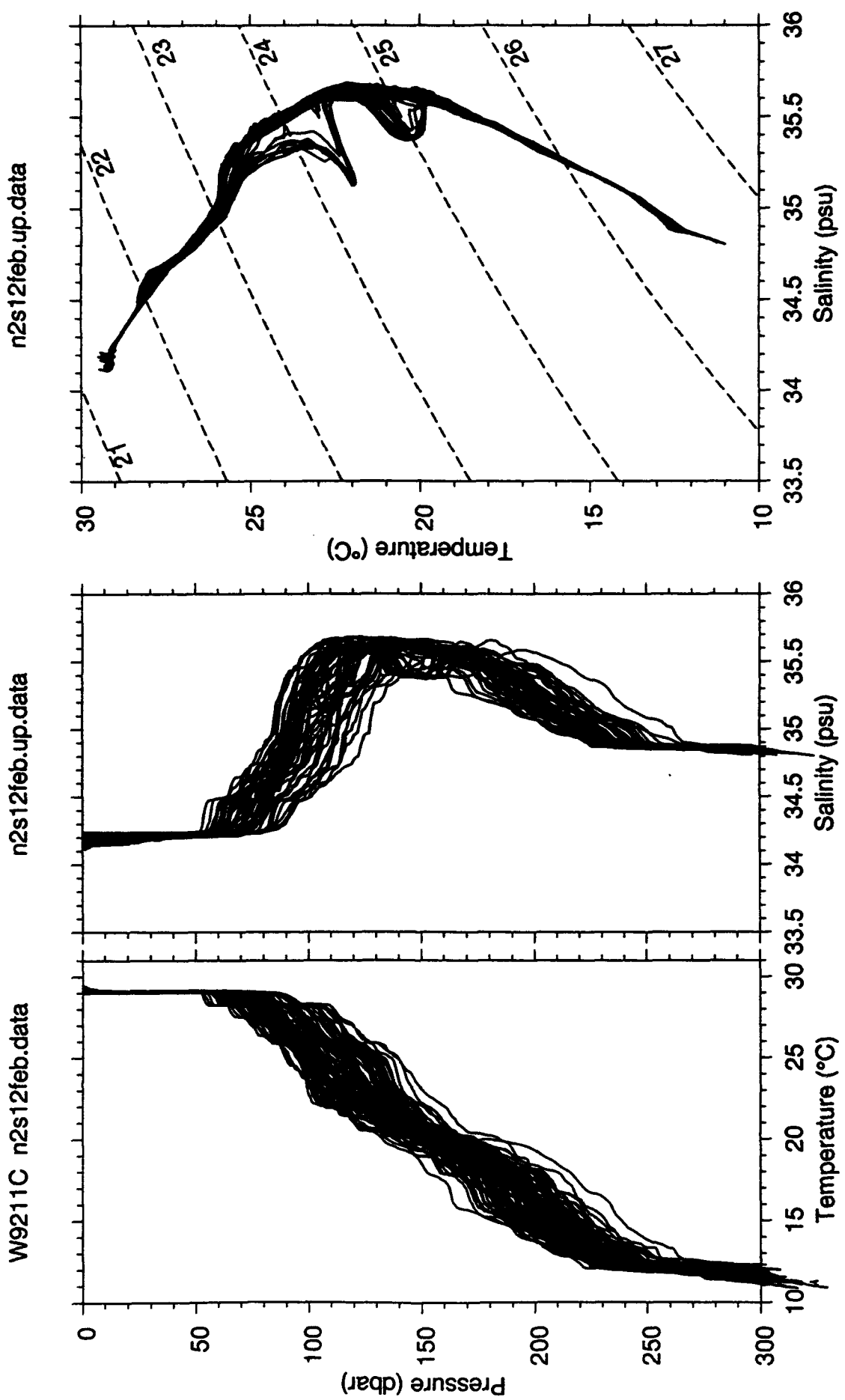
106

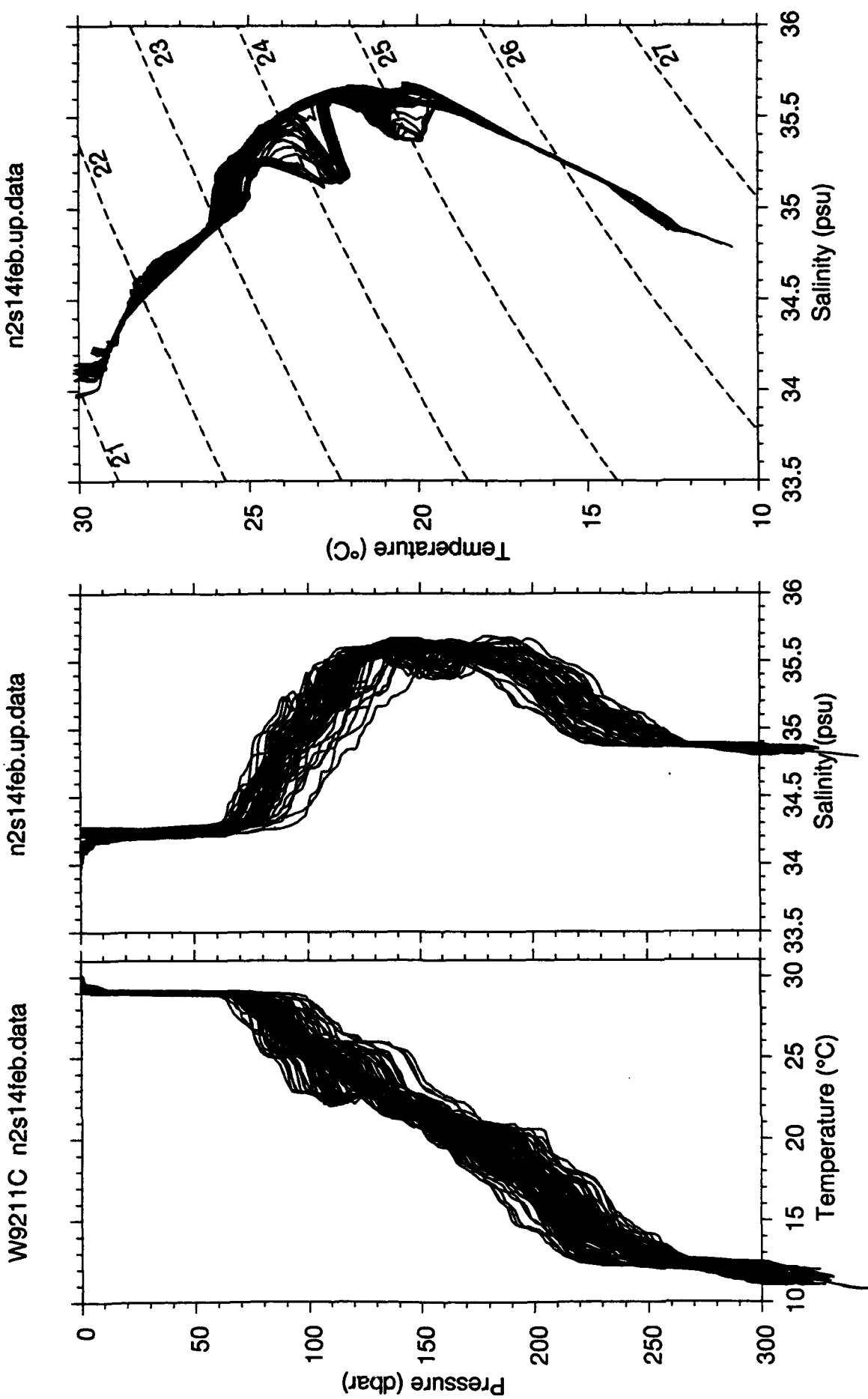


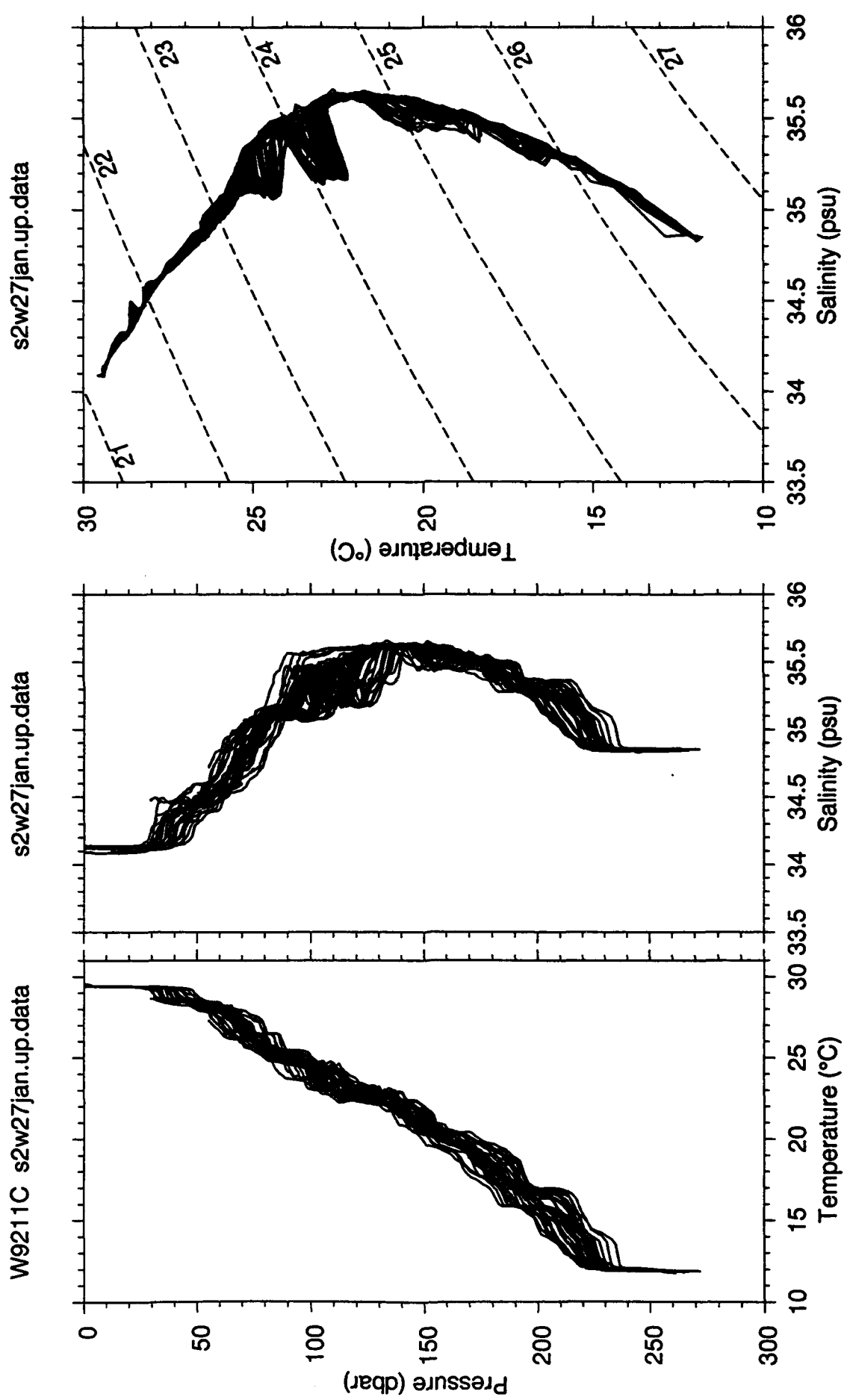




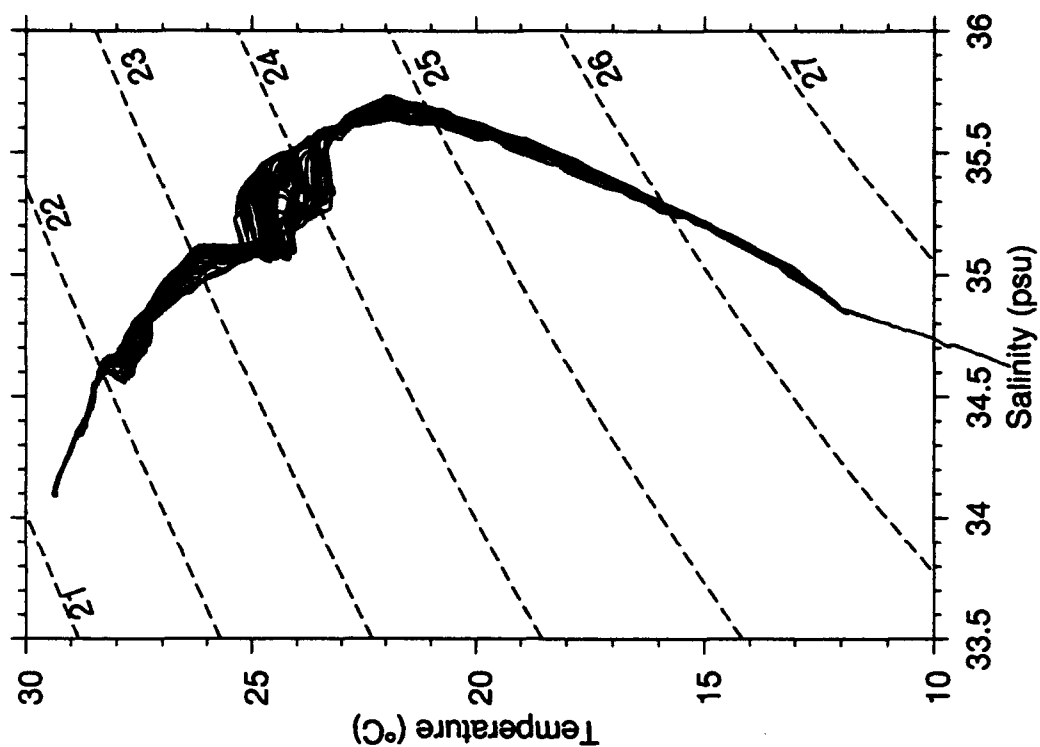




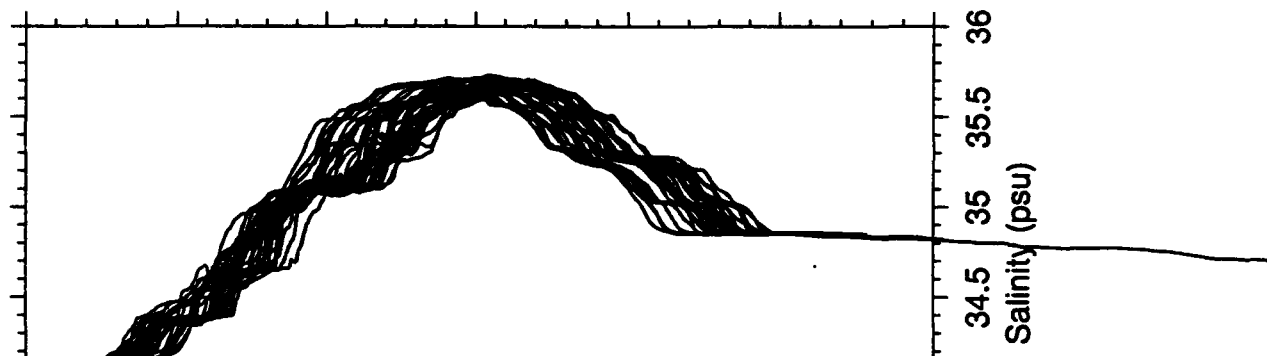




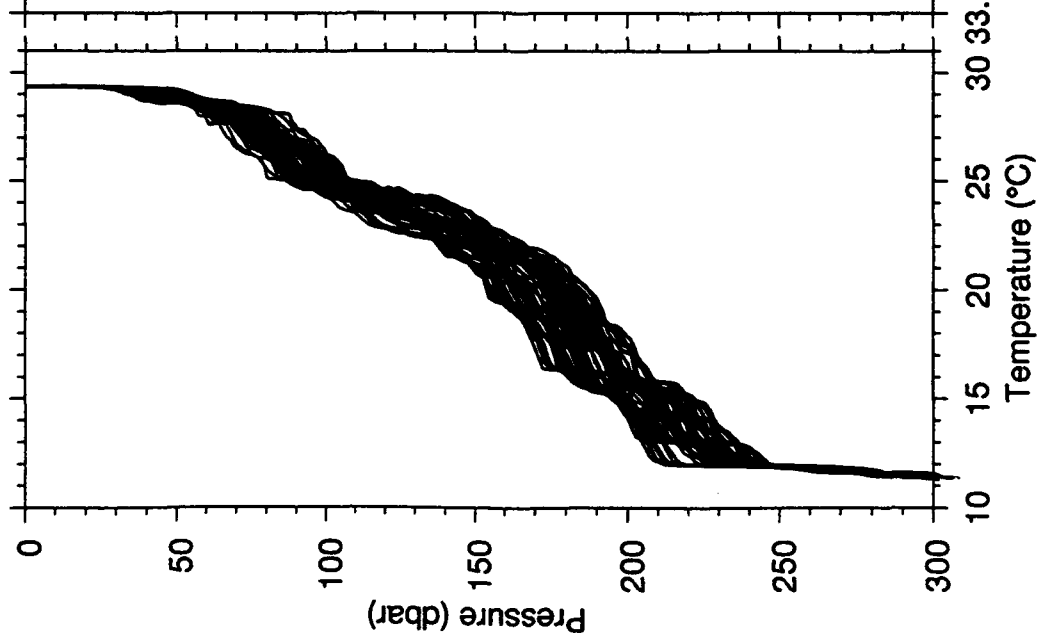
s2w29jan.up.data

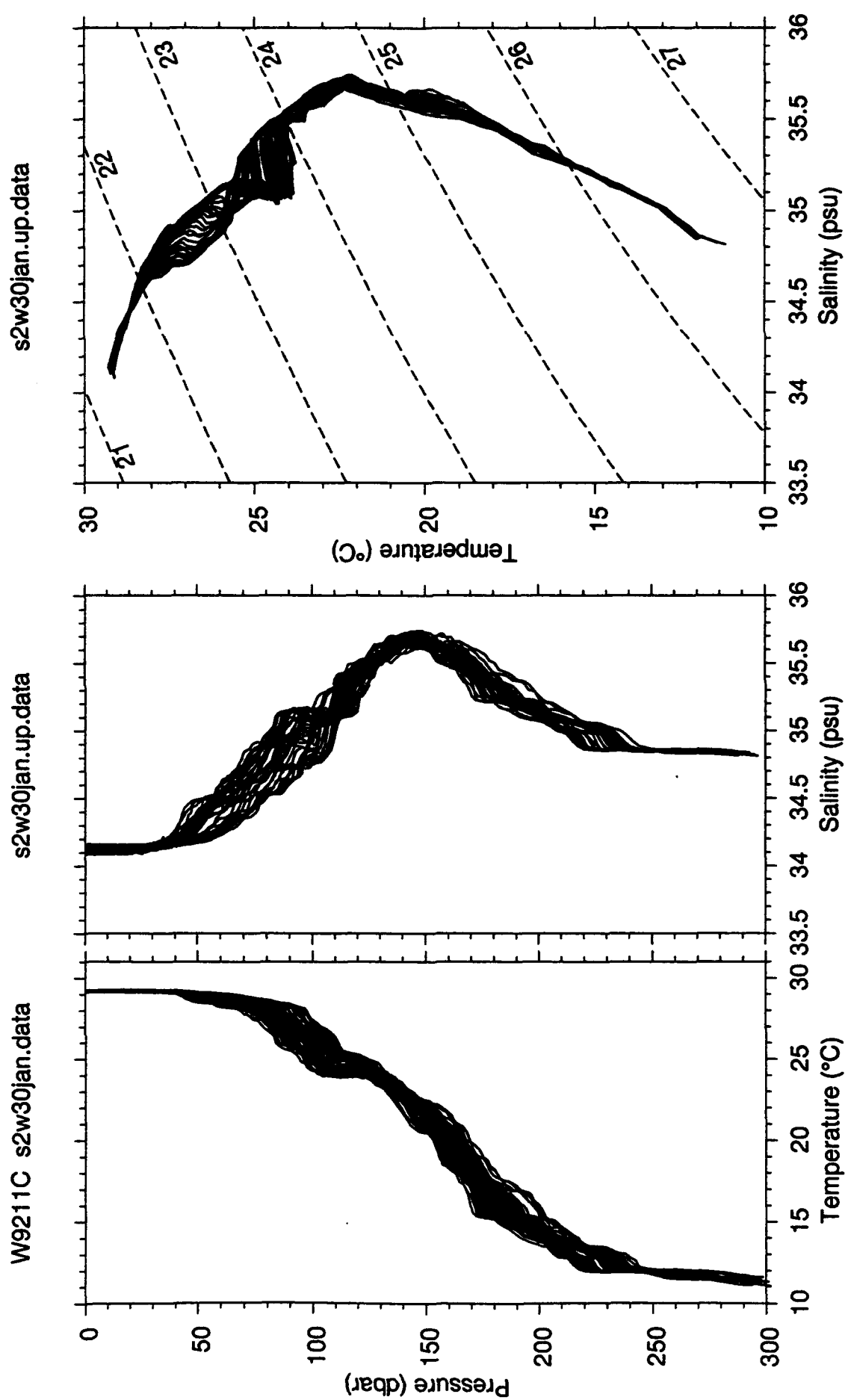


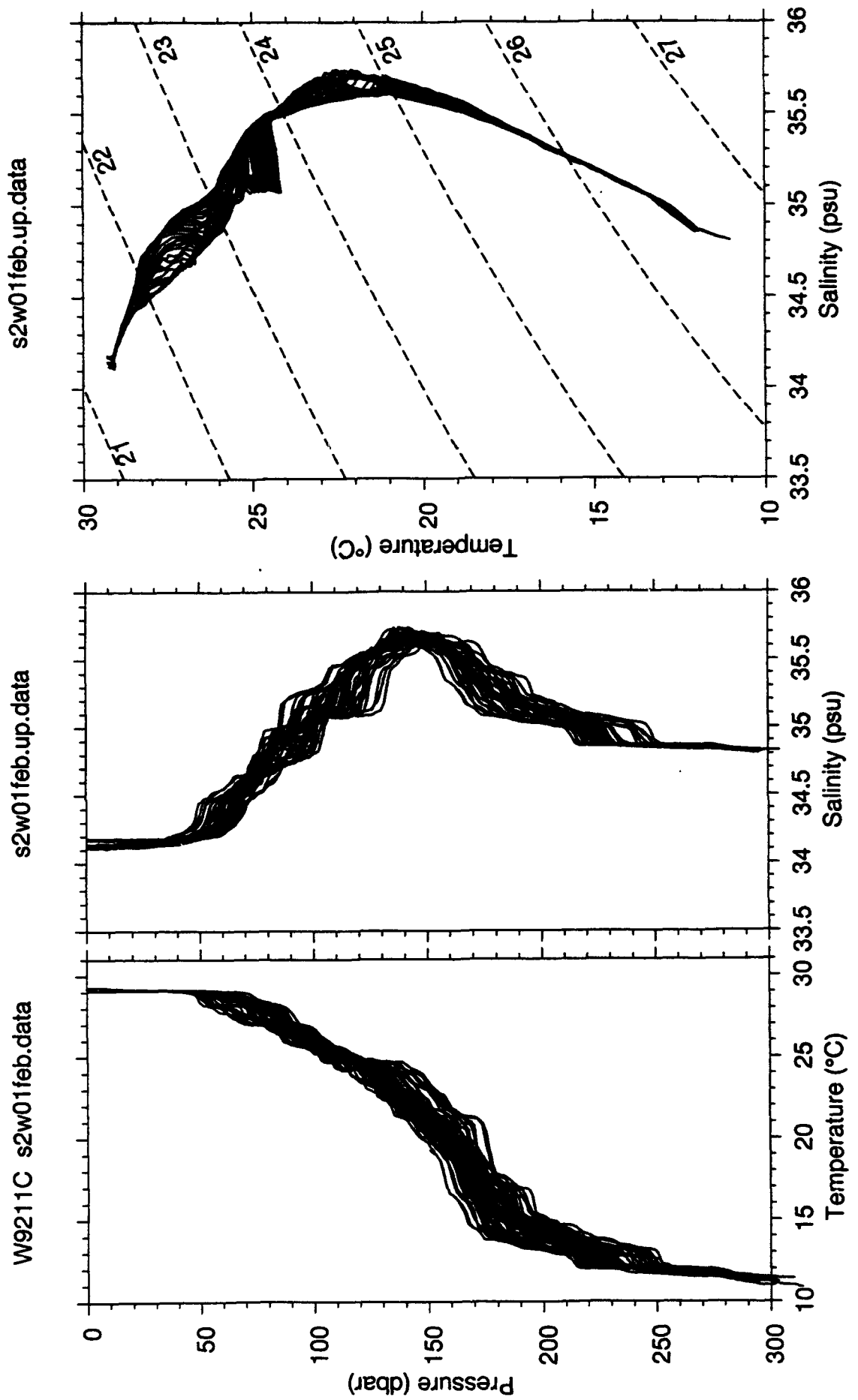
s2w29jan.up.data

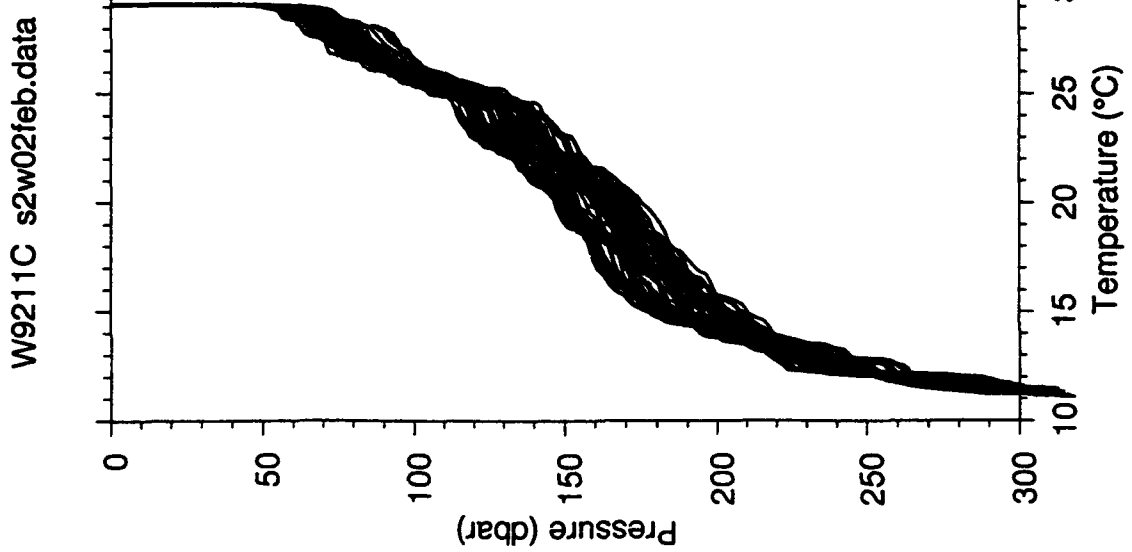
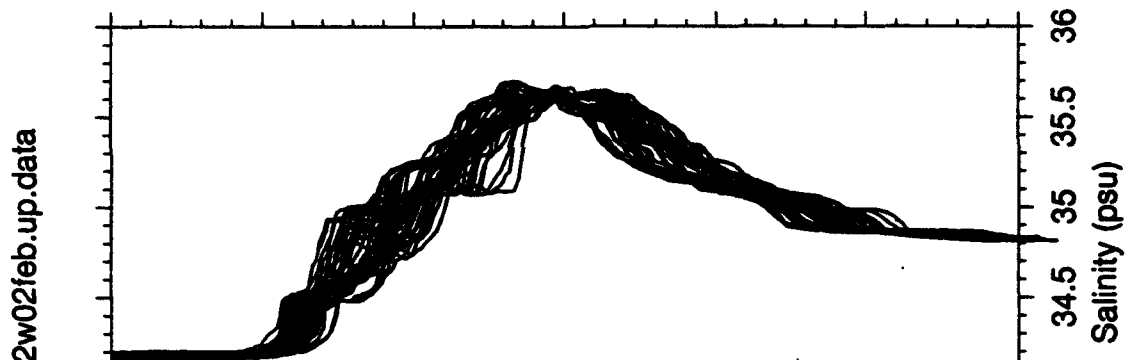
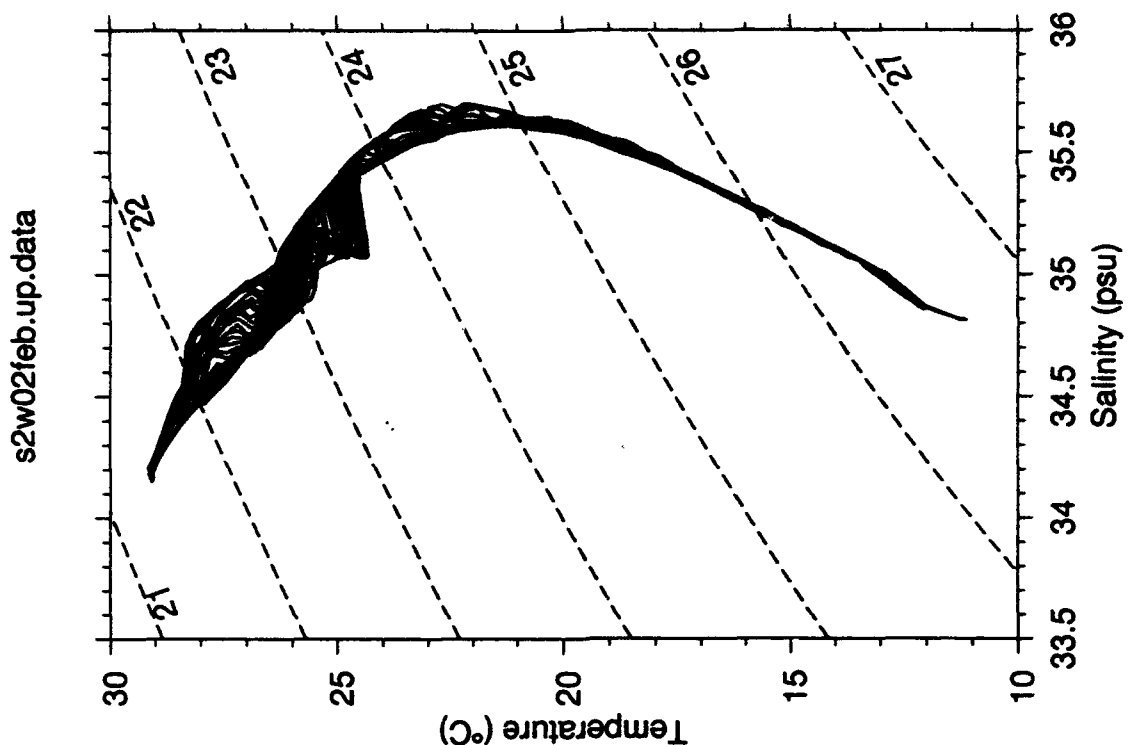


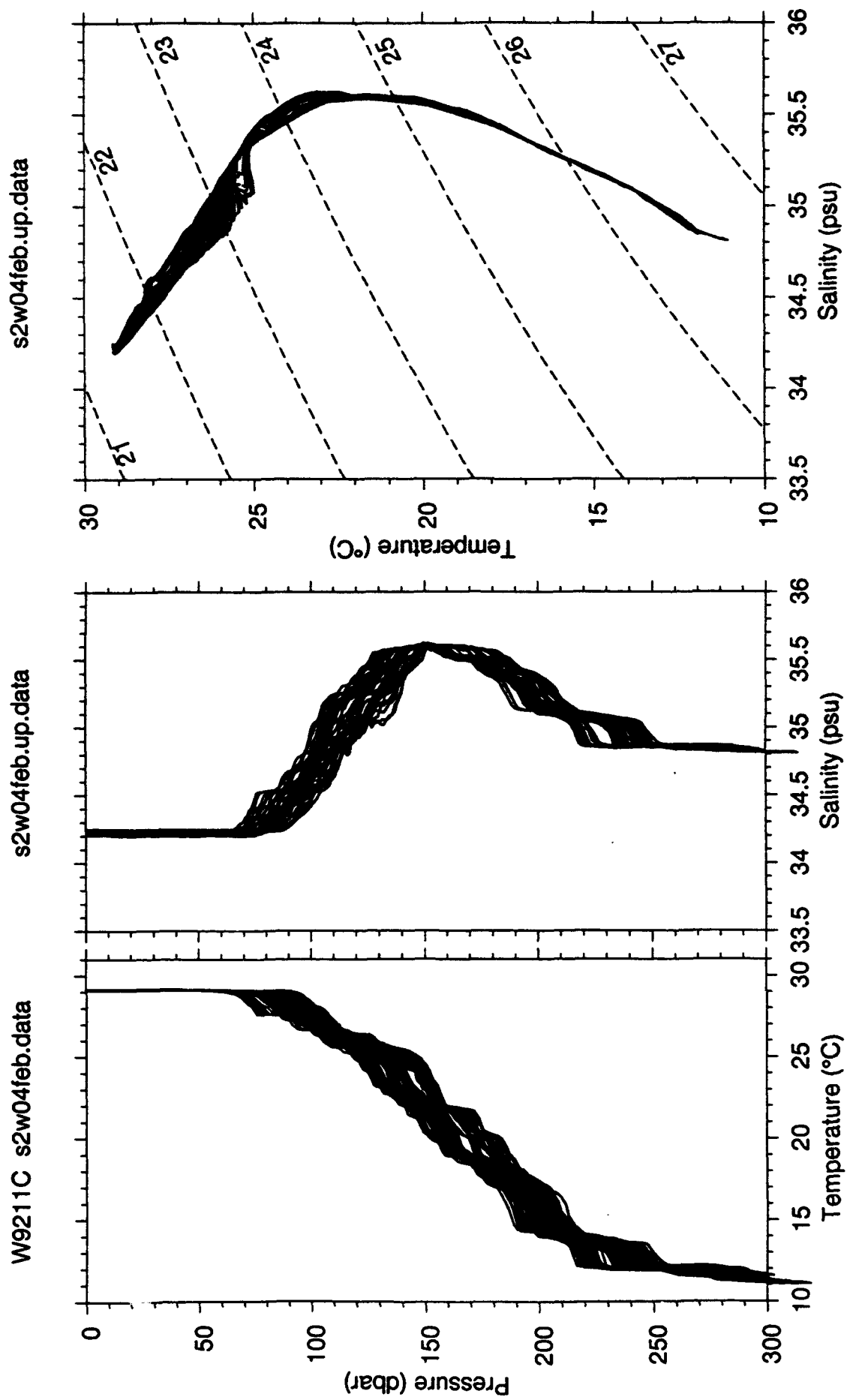
W9211C s2w29jan.data

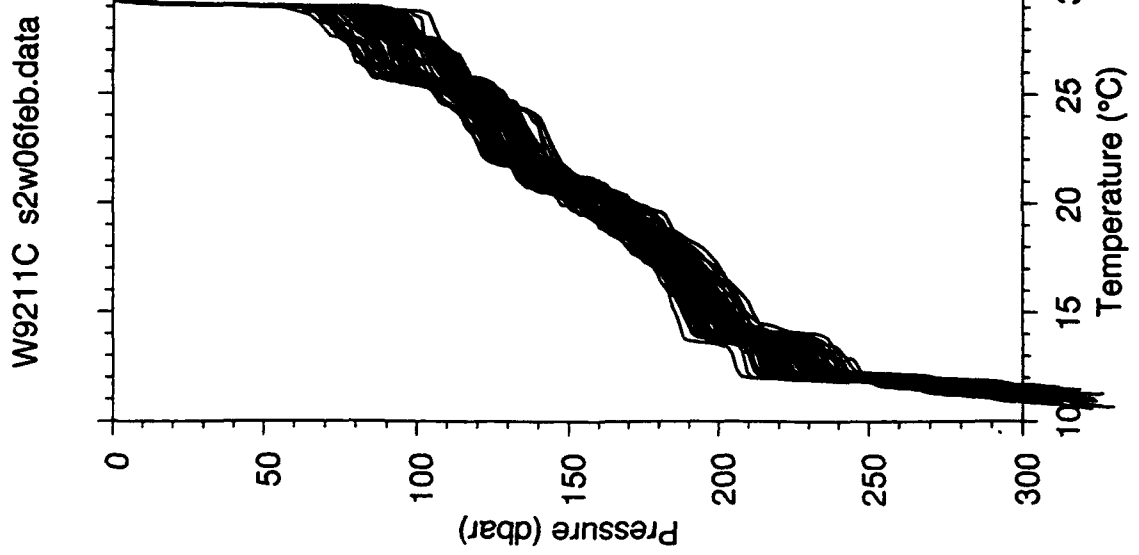
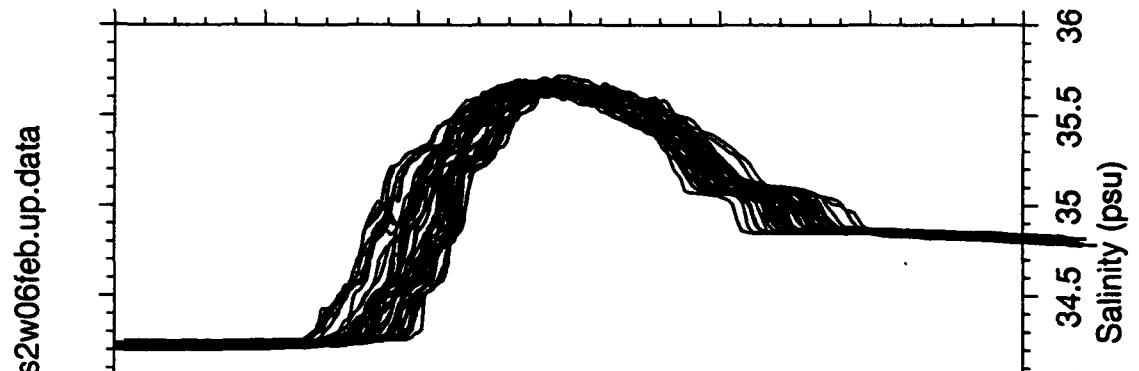
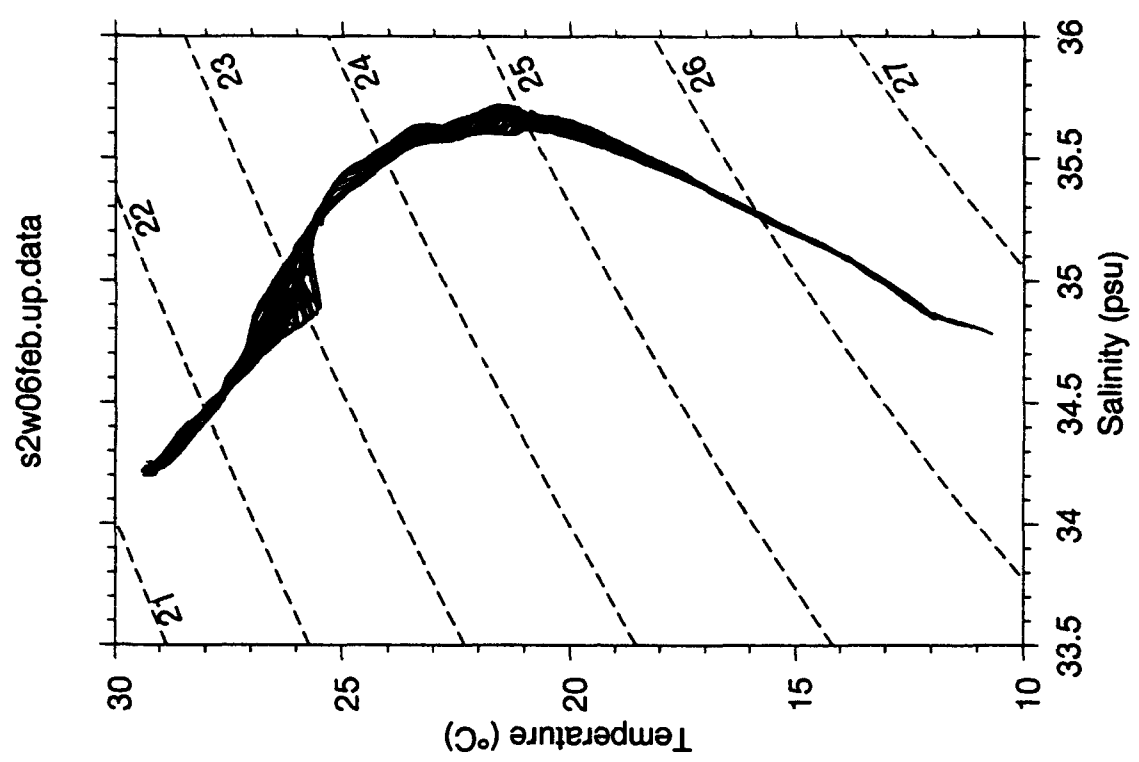




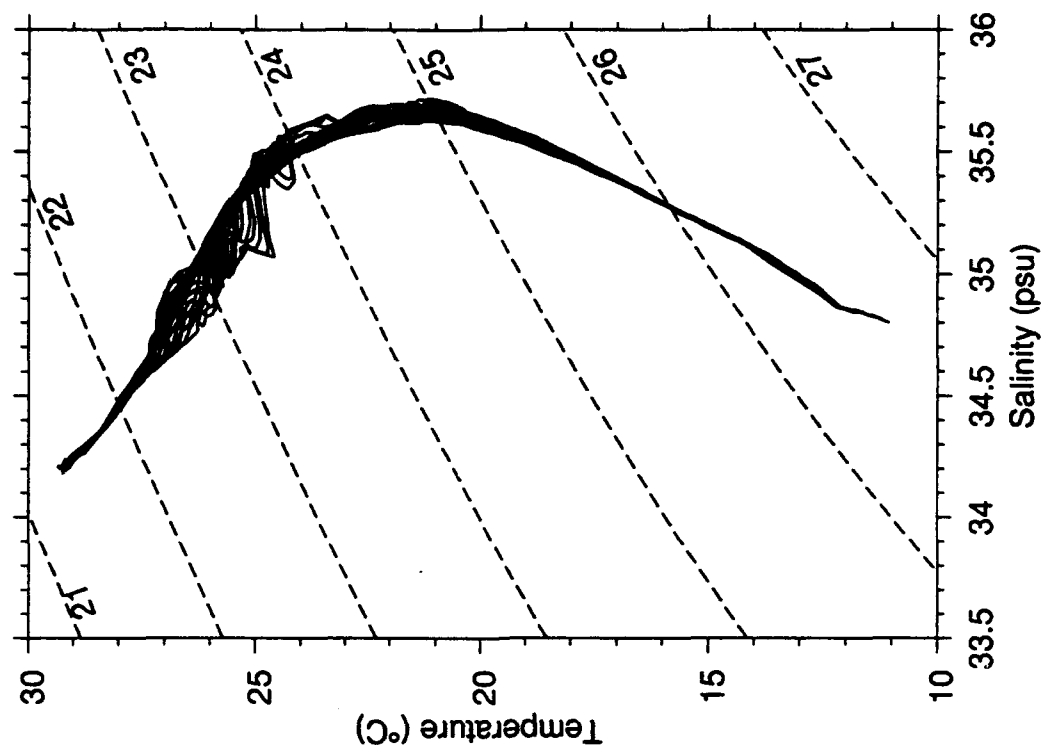




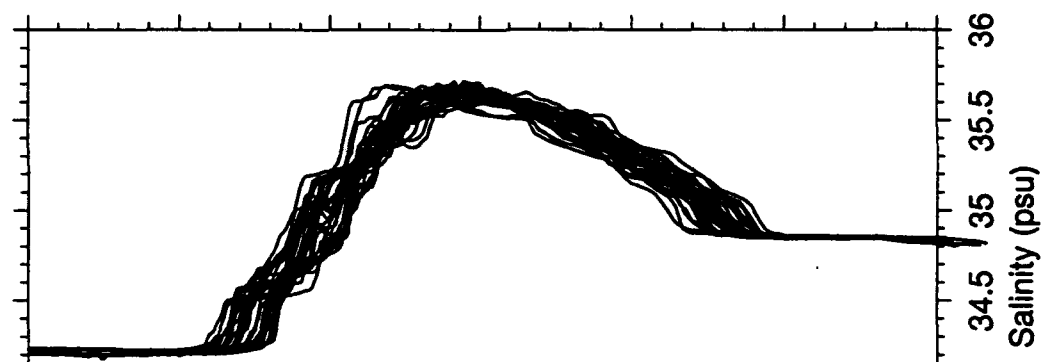




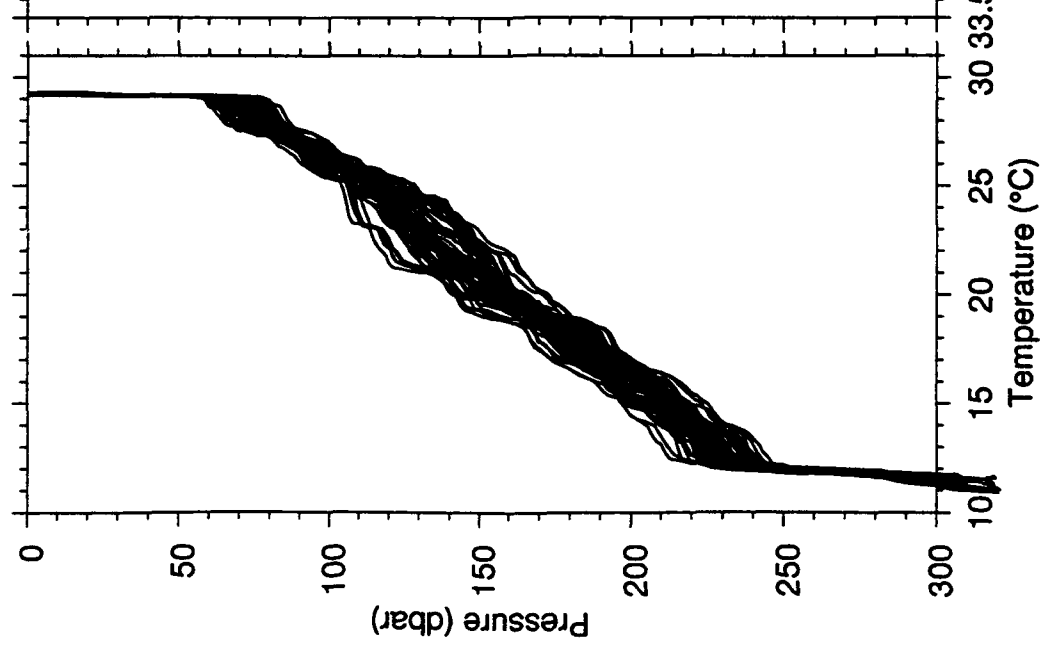
s2w08feb.up.data

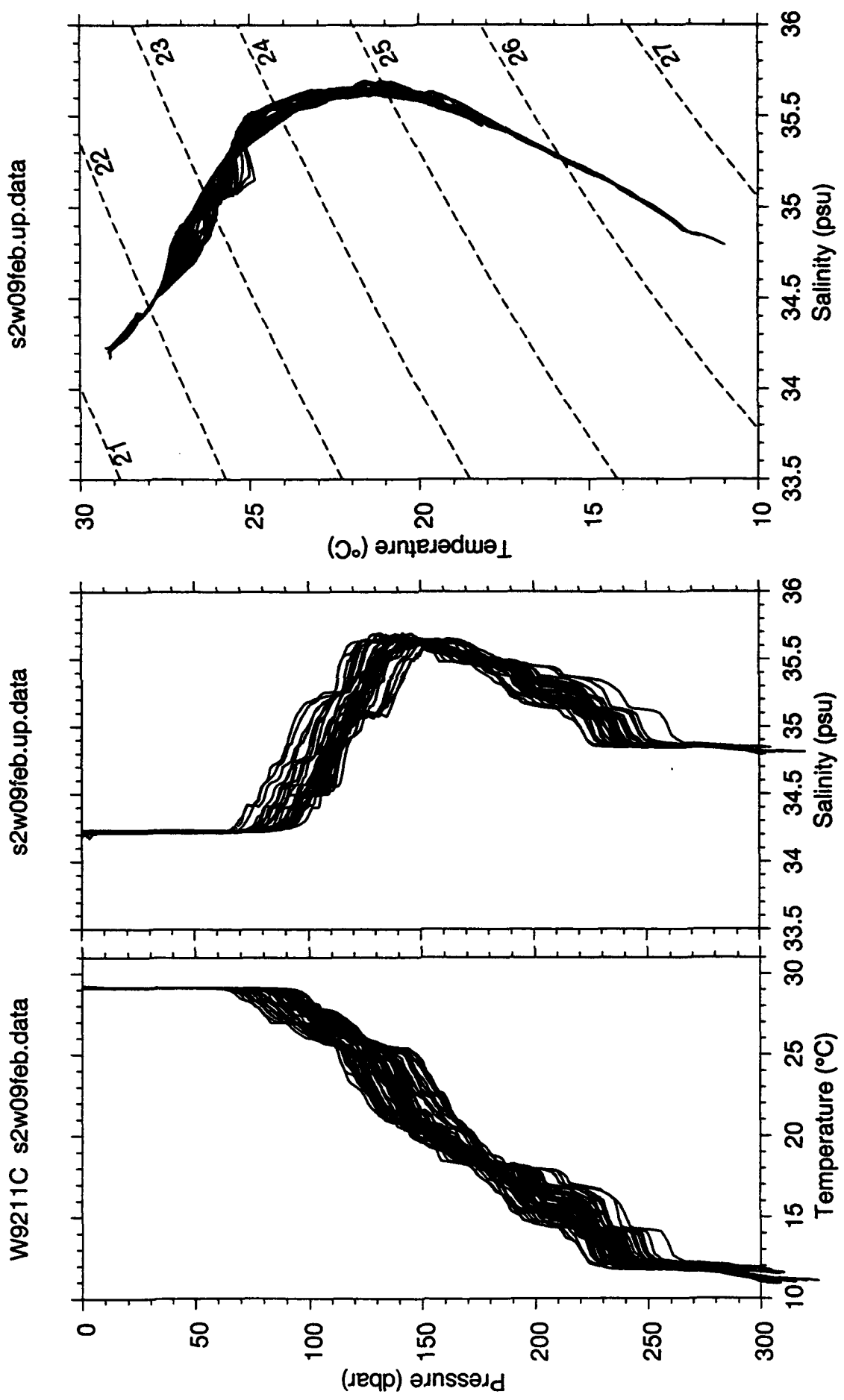


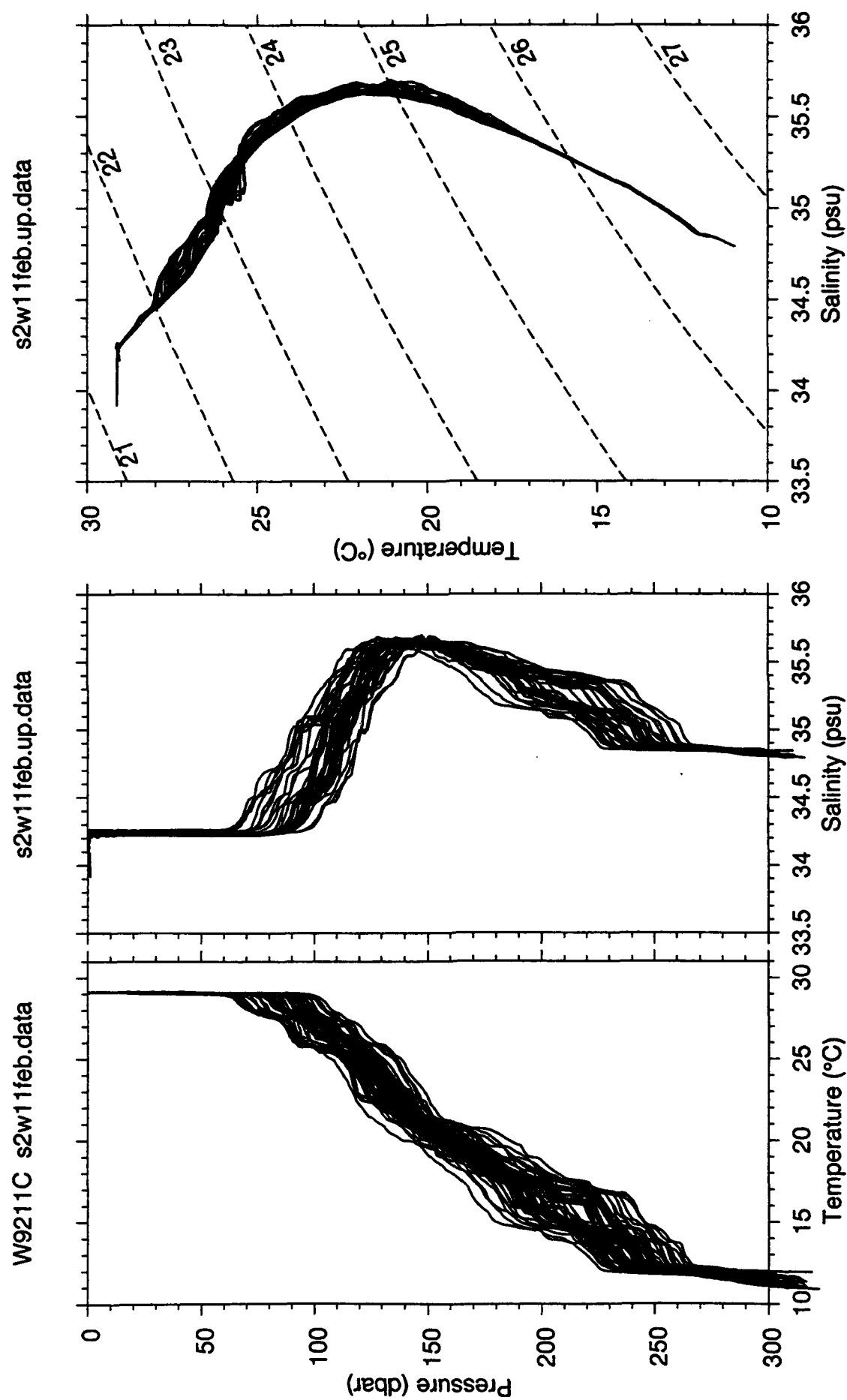
s2w08feb.up.data

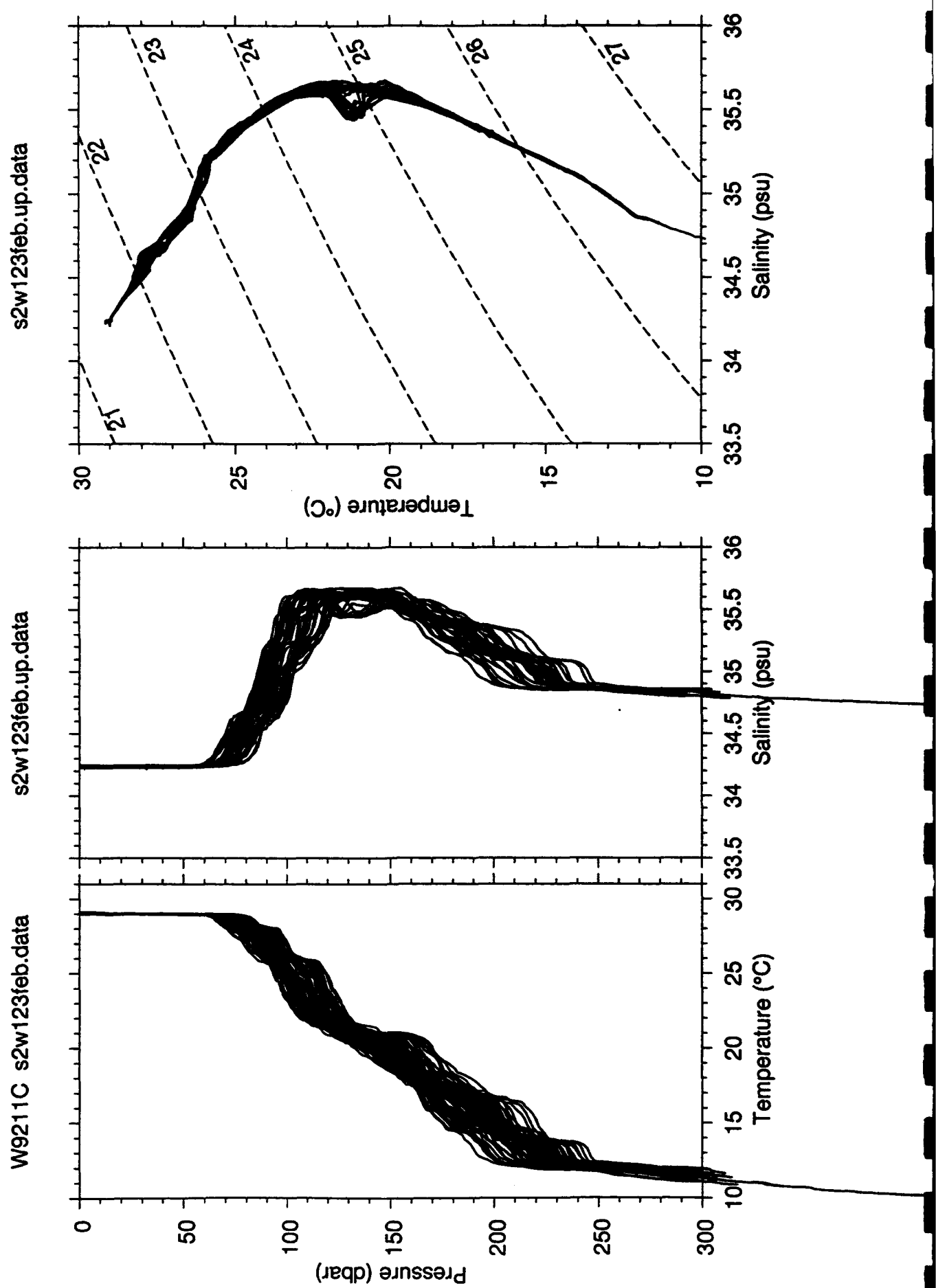


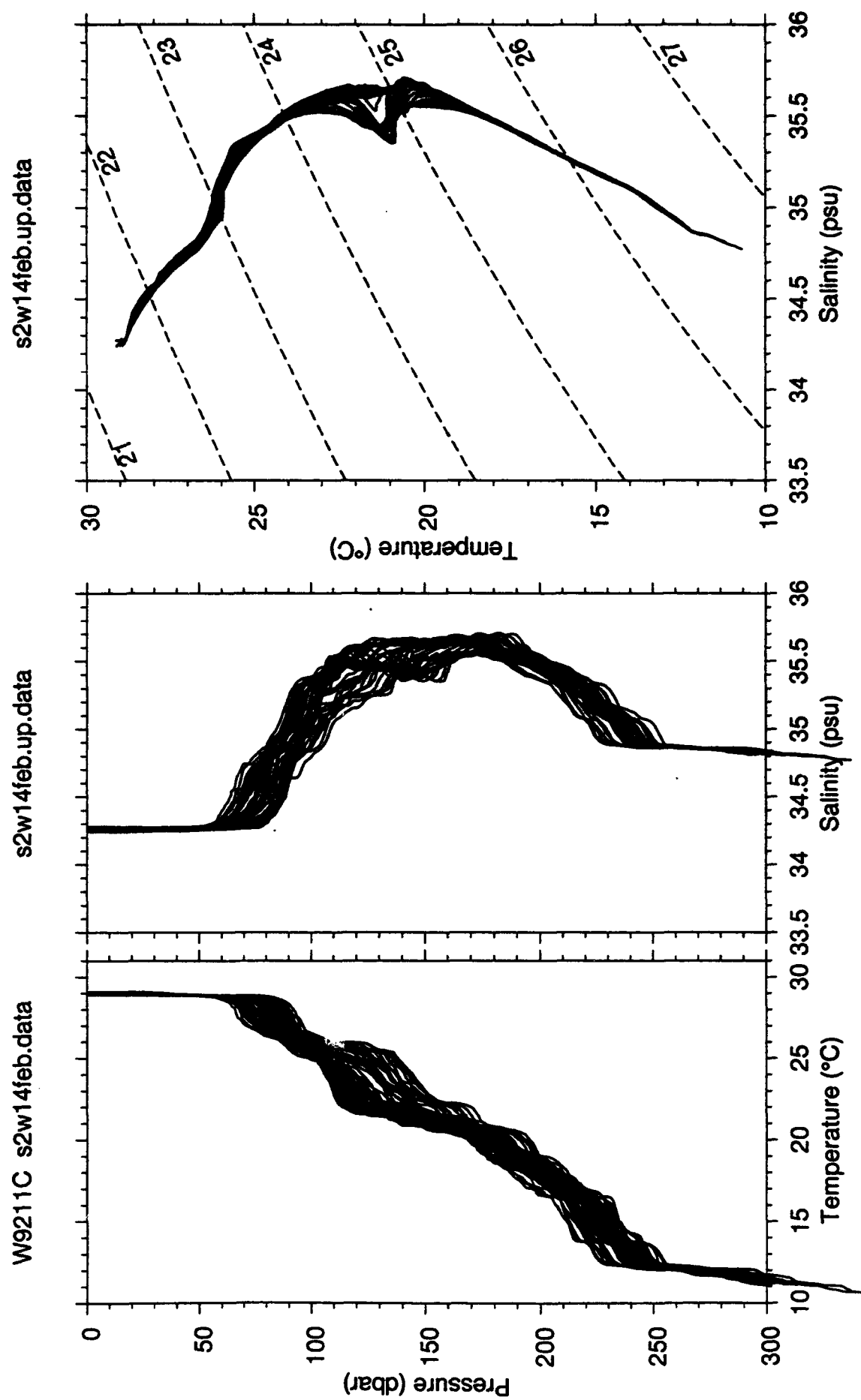
W9211C s2w08feb.data

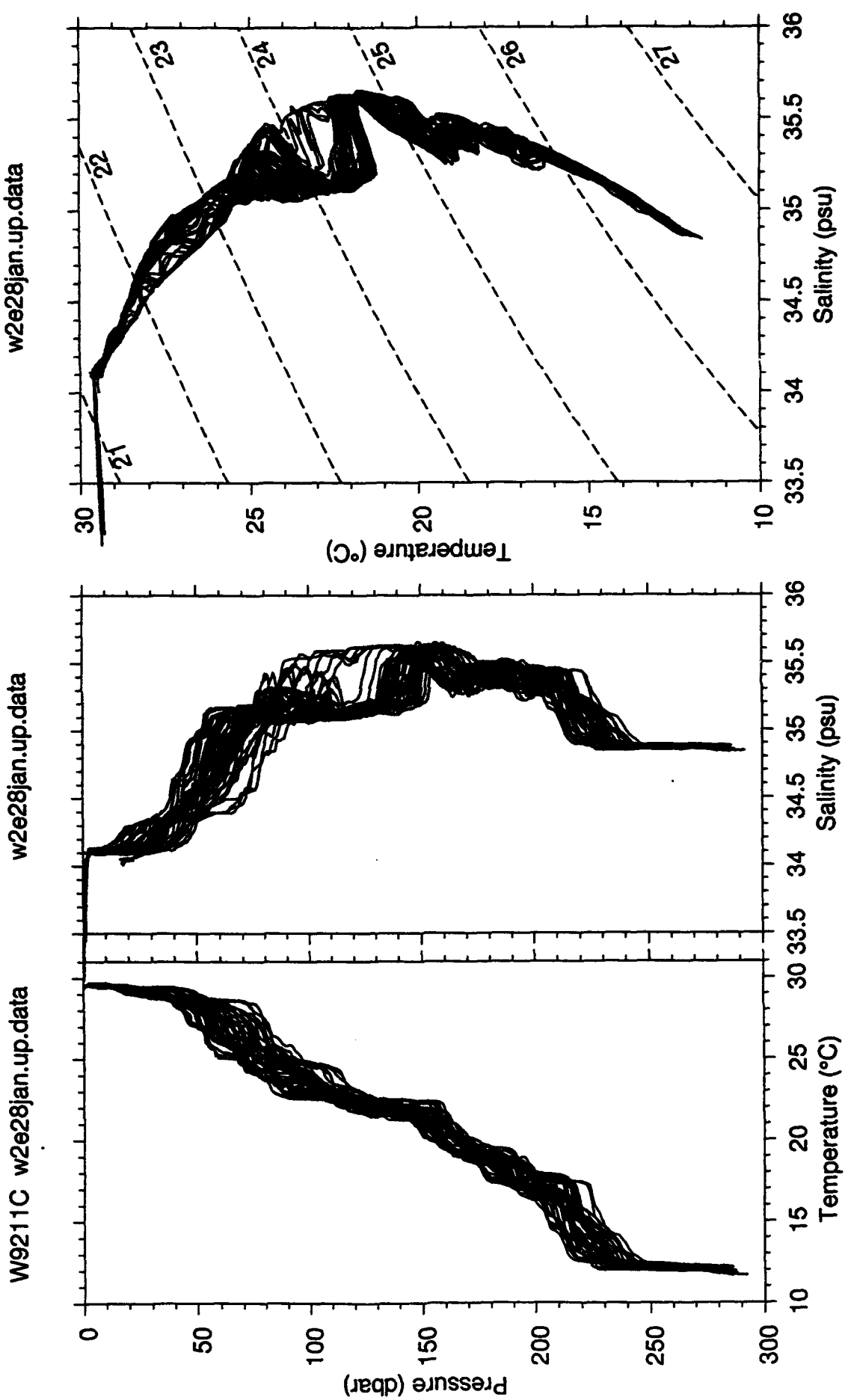


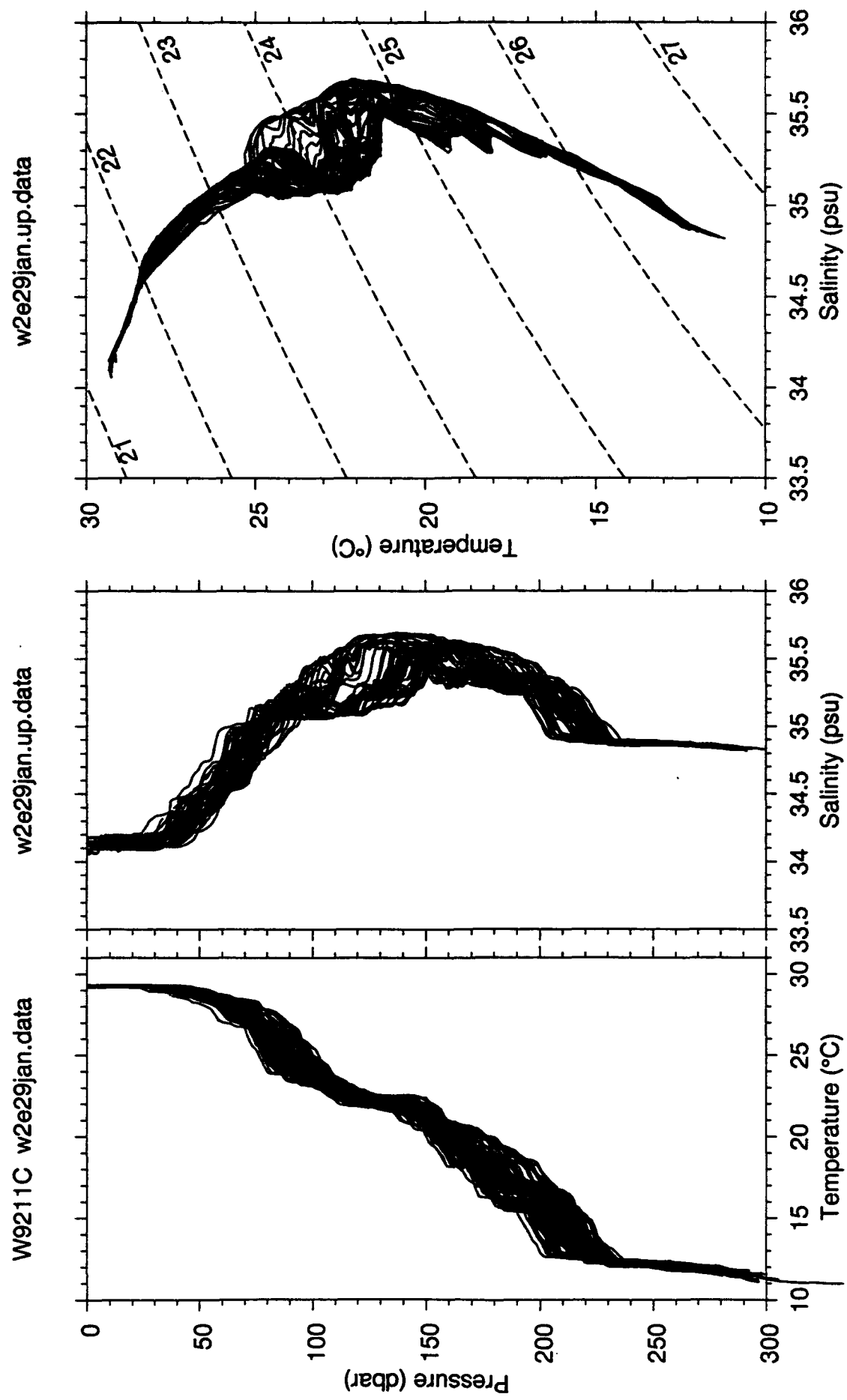


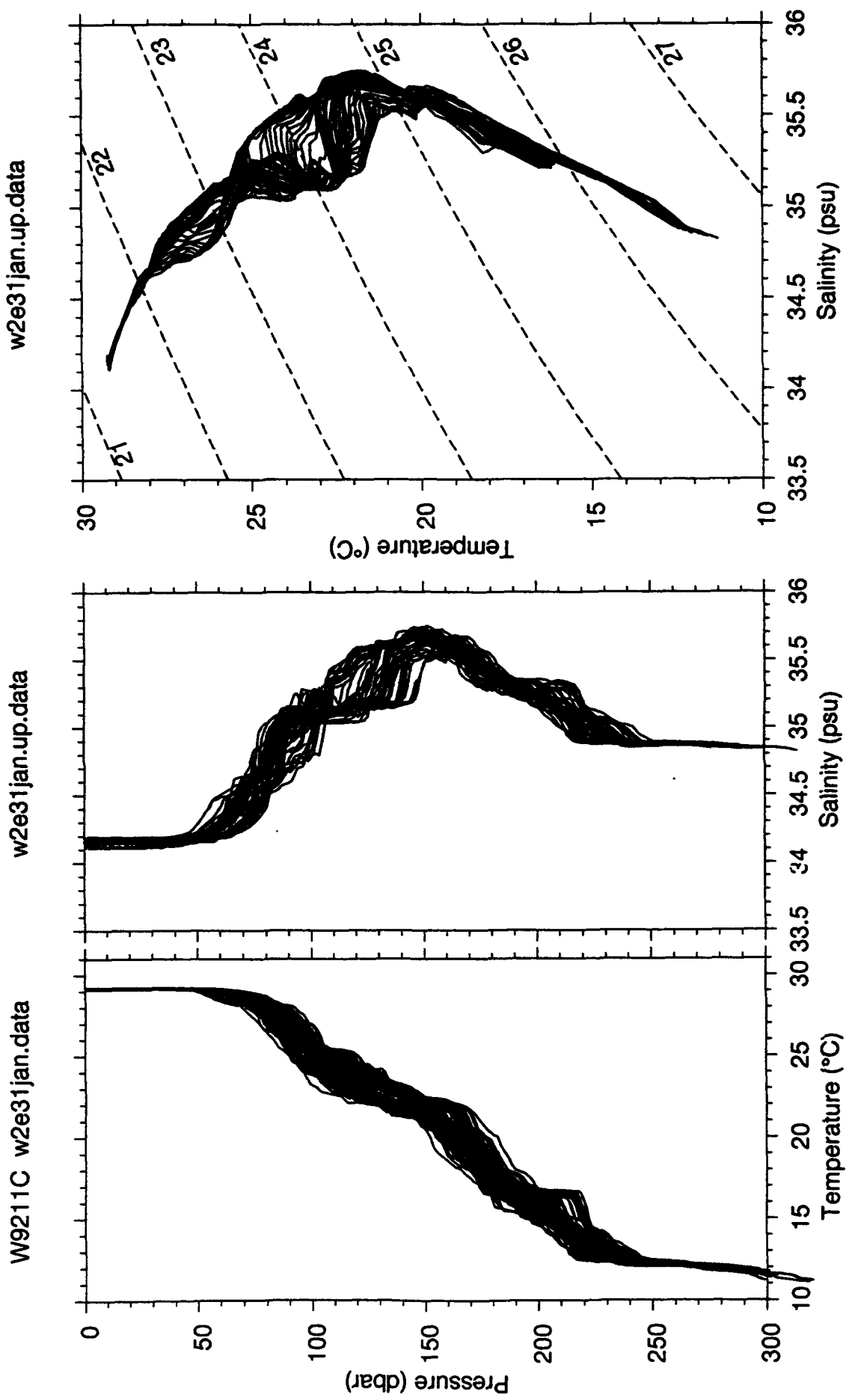




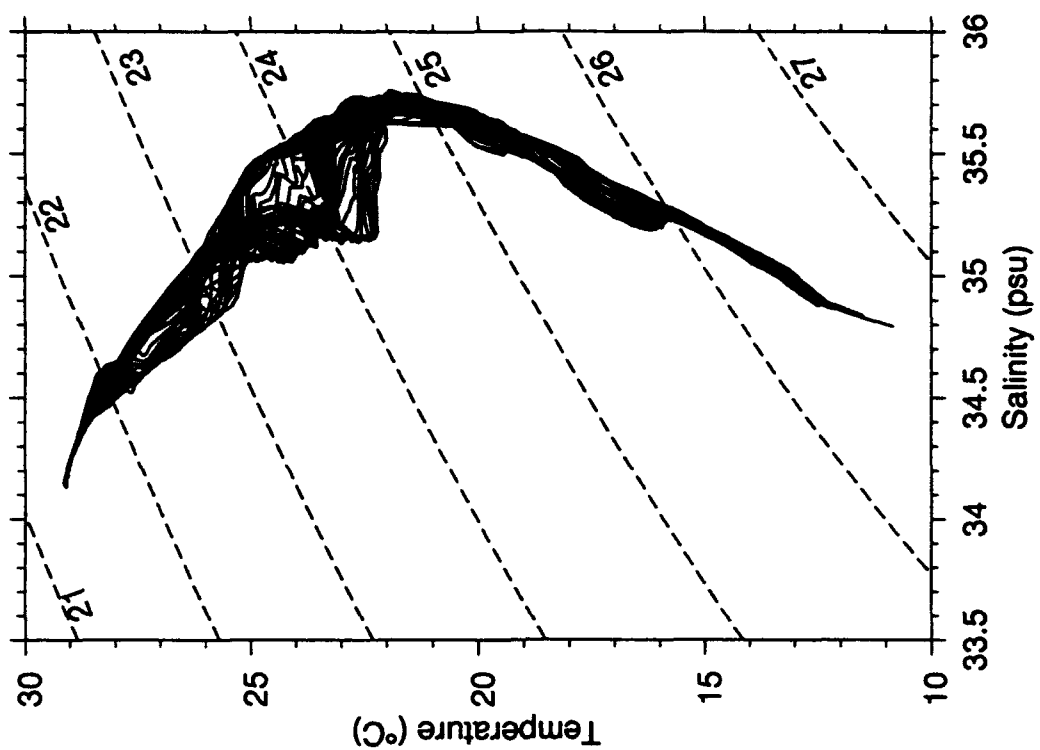




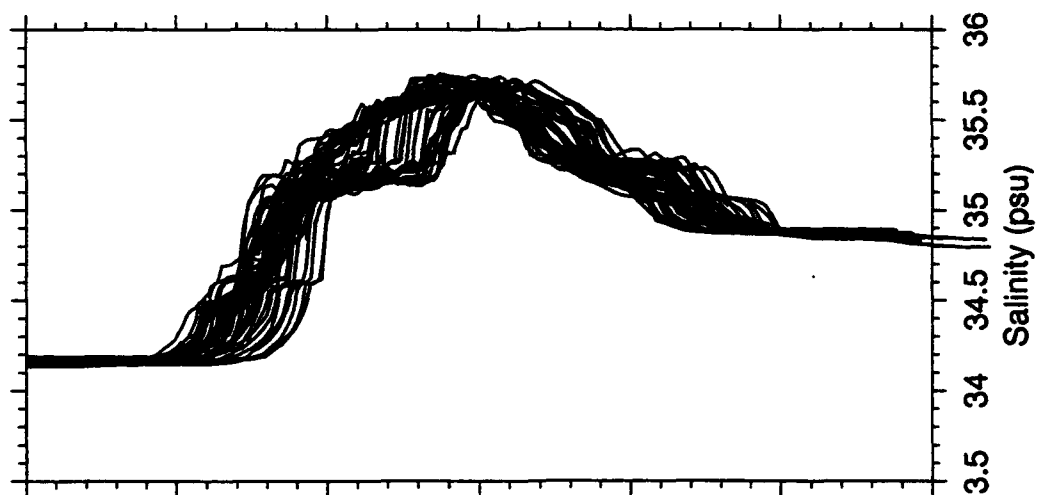




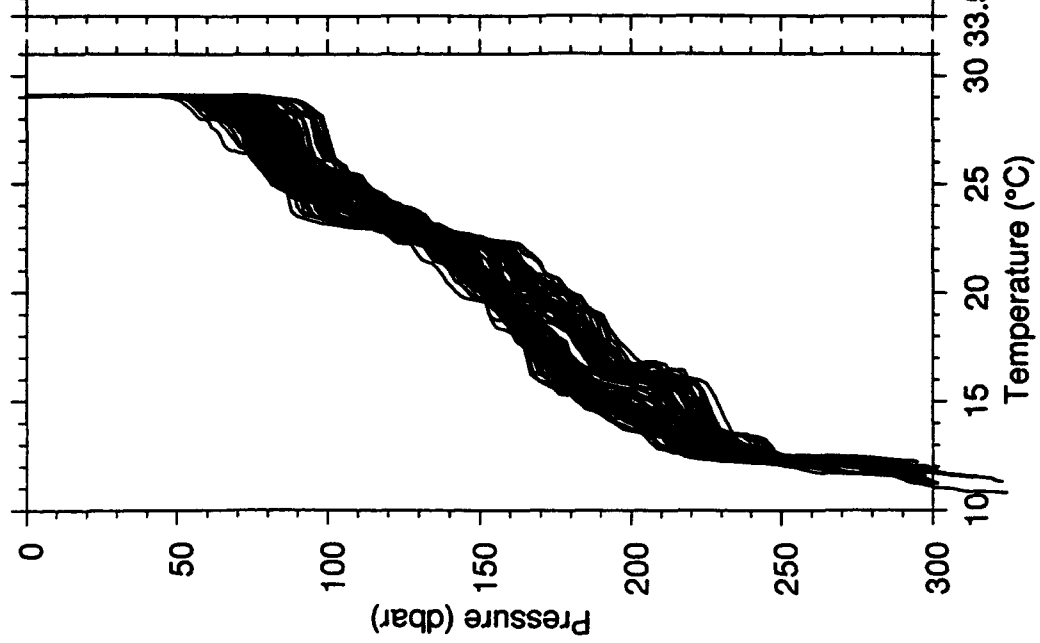
w2e01feb.up.data

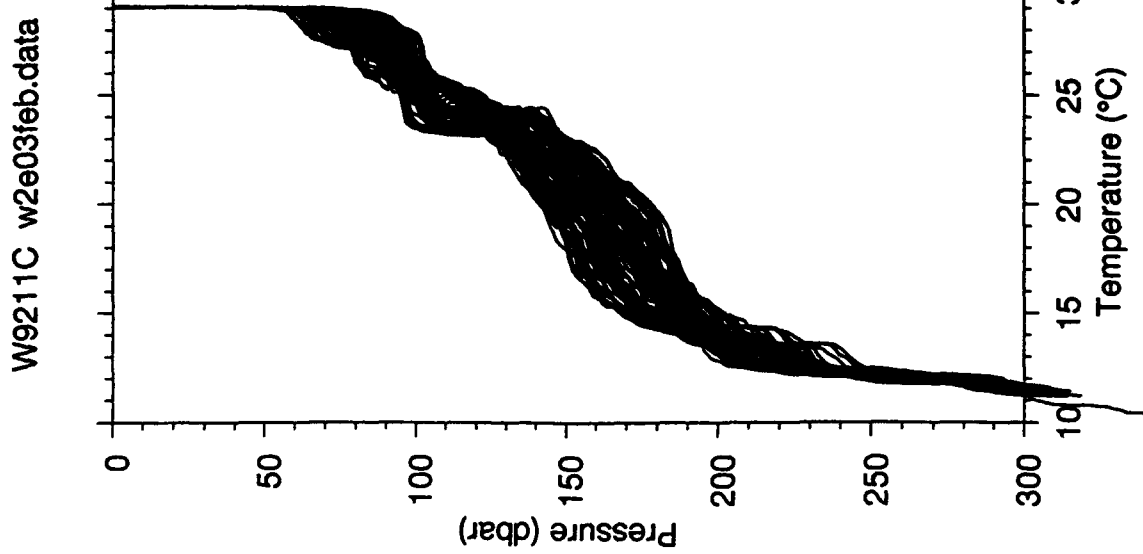
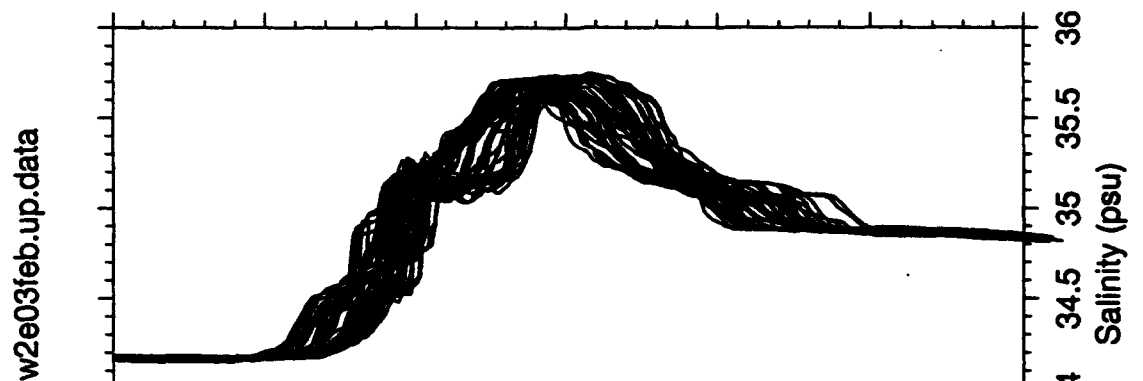
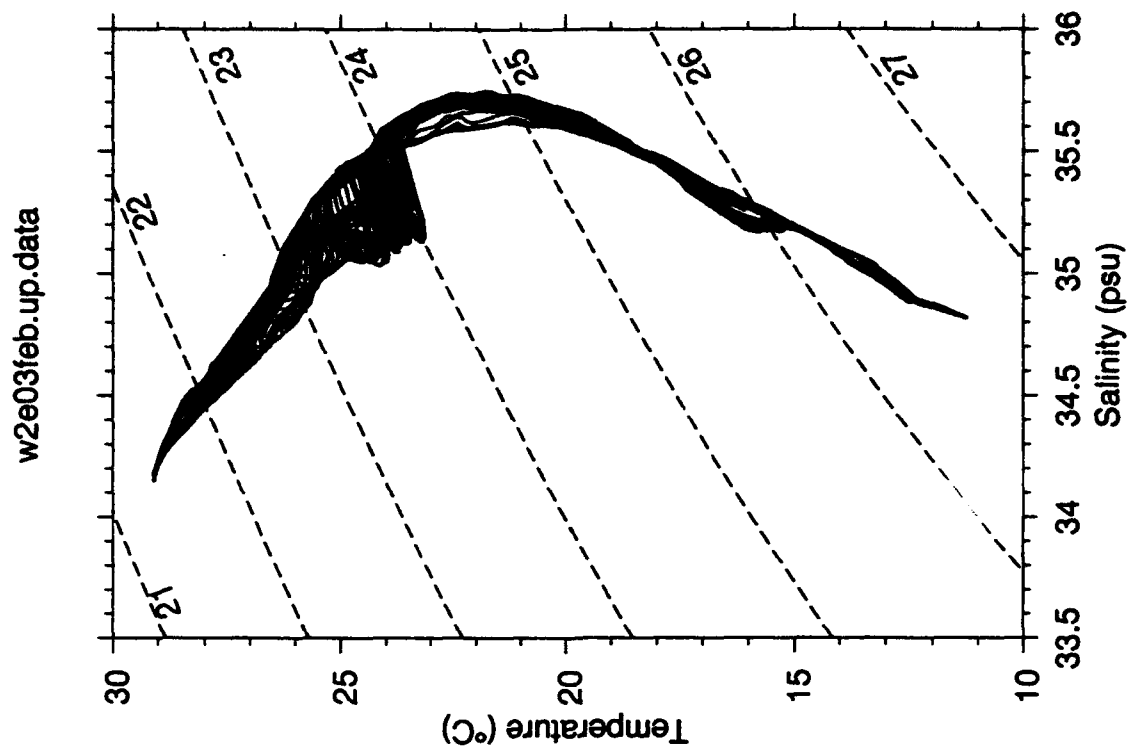


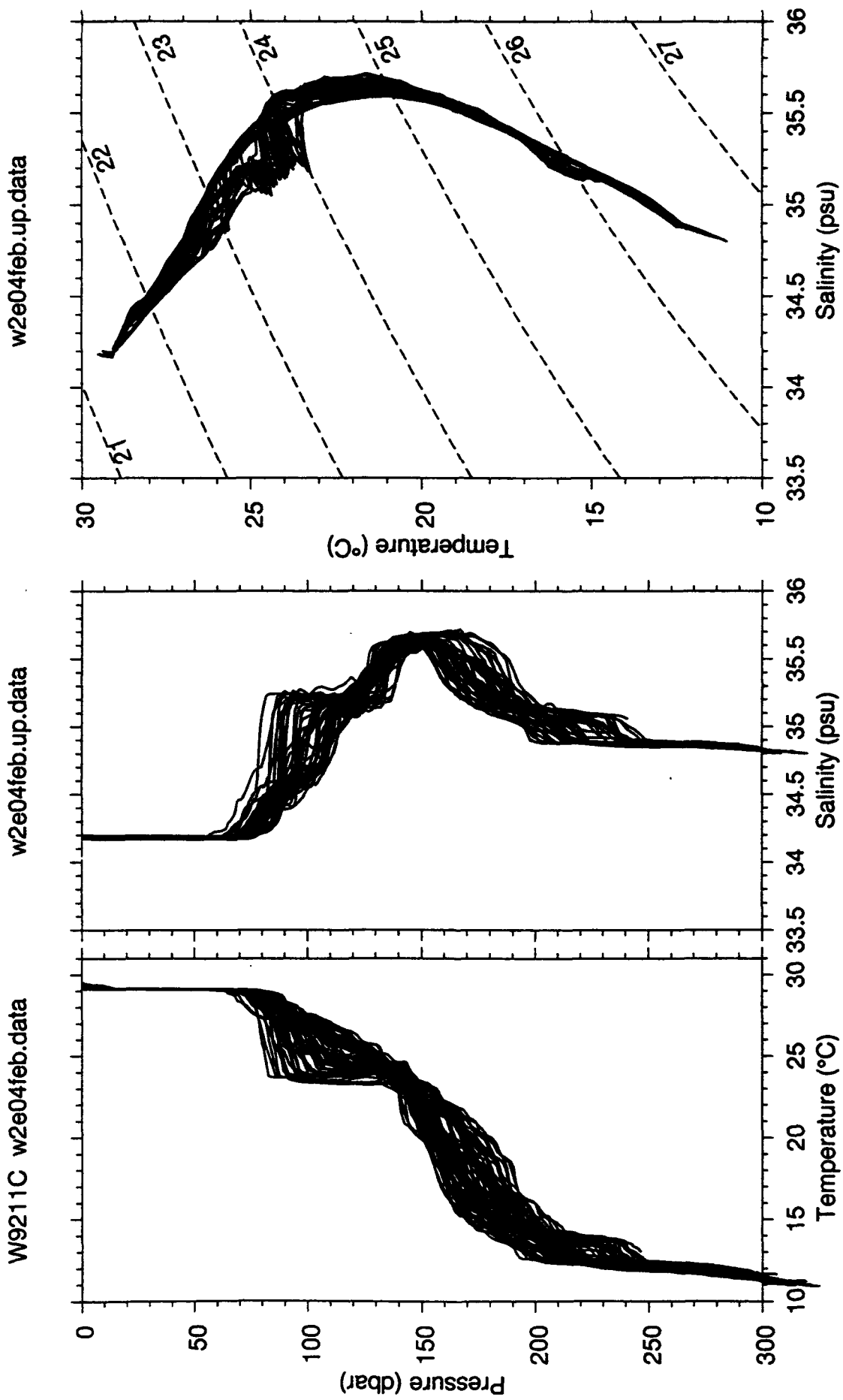
w2e01feb.up.data



w9211C w2e01feb.data

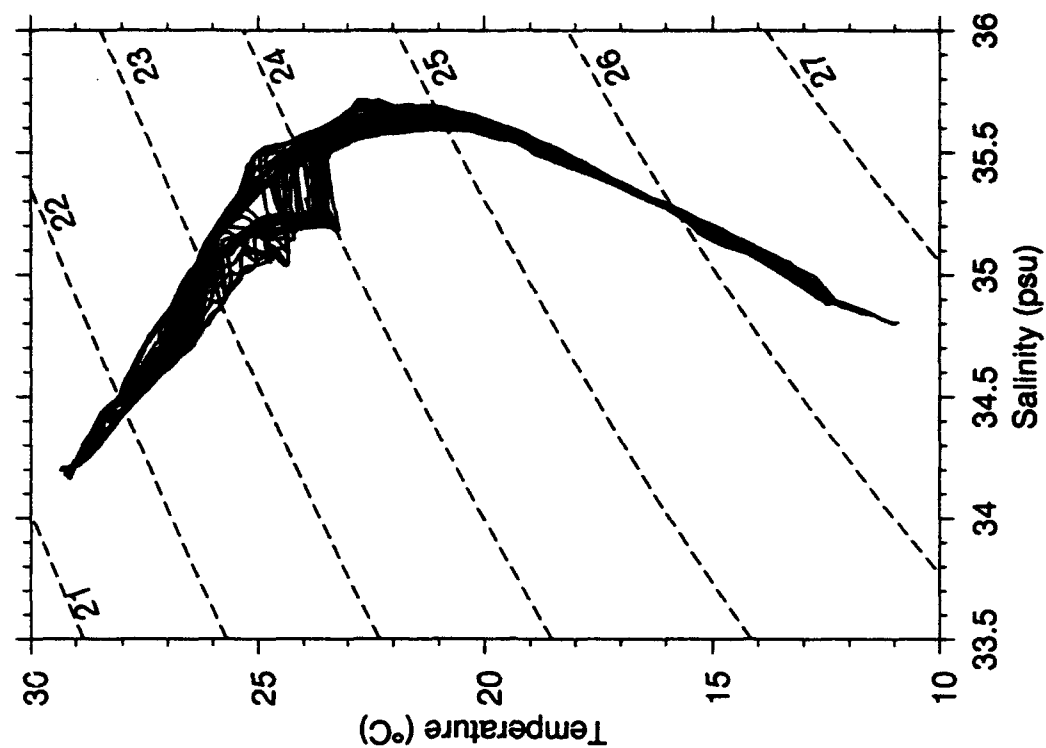




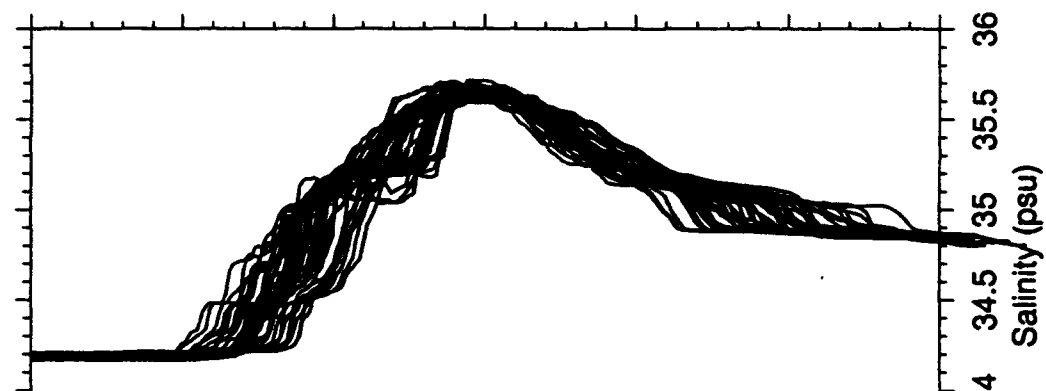


130

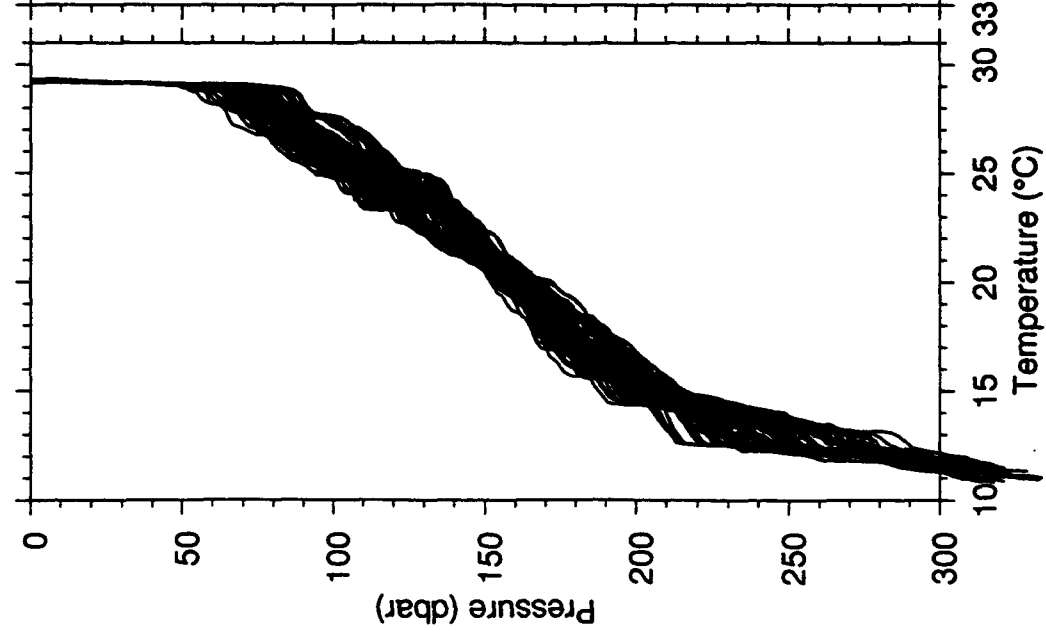
w2e06feb.up.data

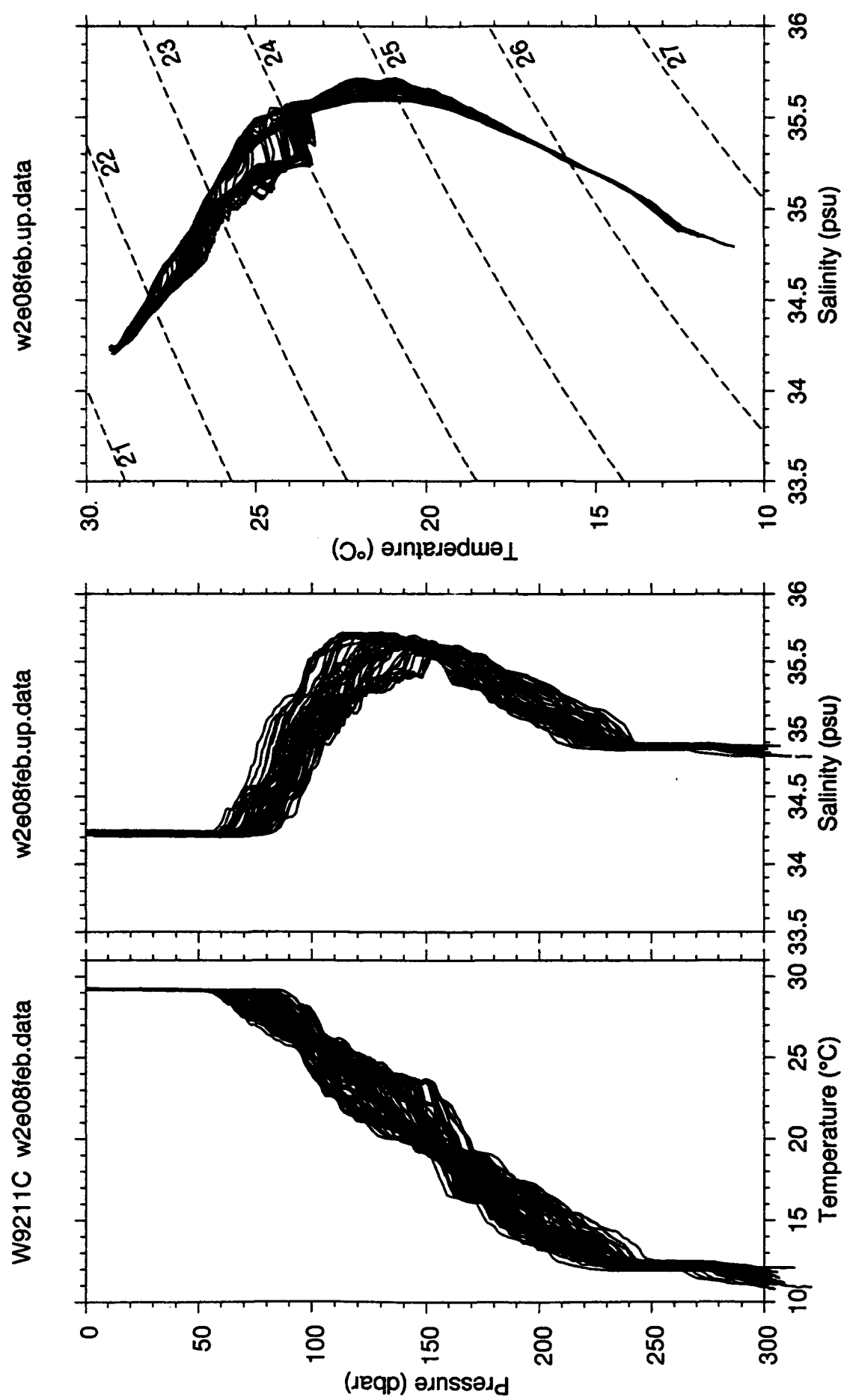


w2e06feb.up.data

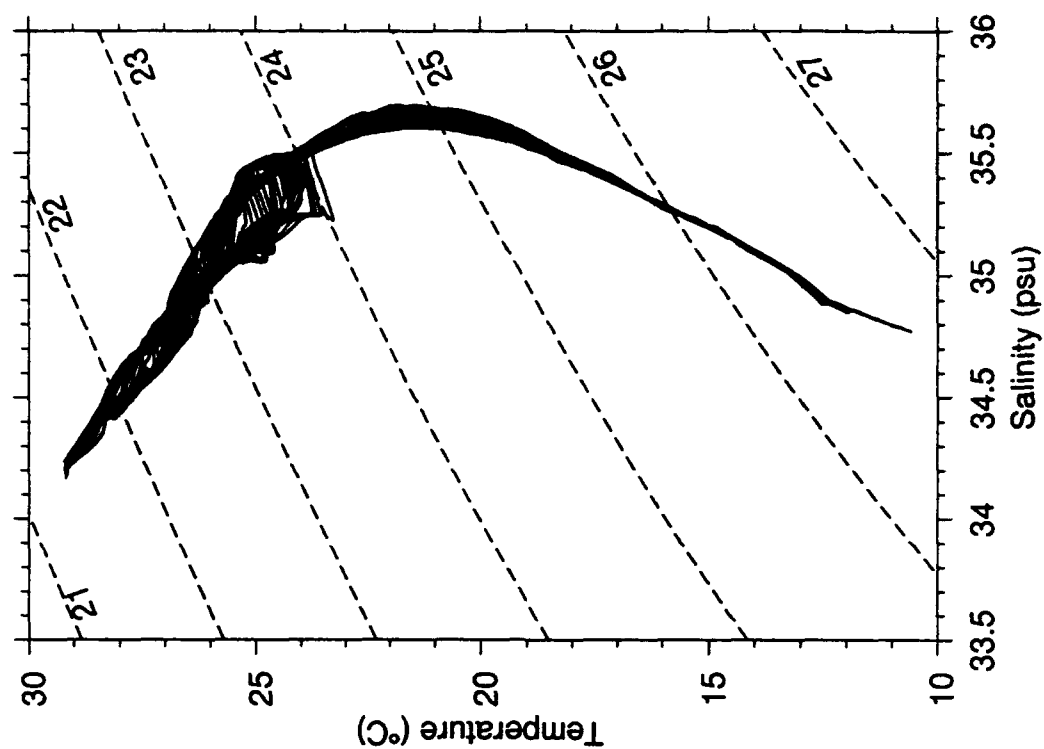


W9211C w2e06feb.data

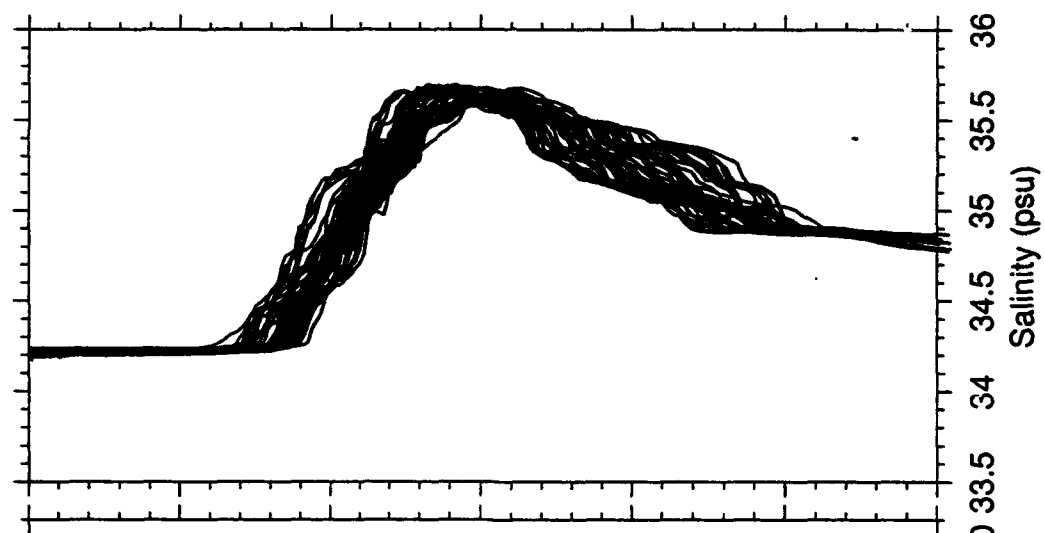




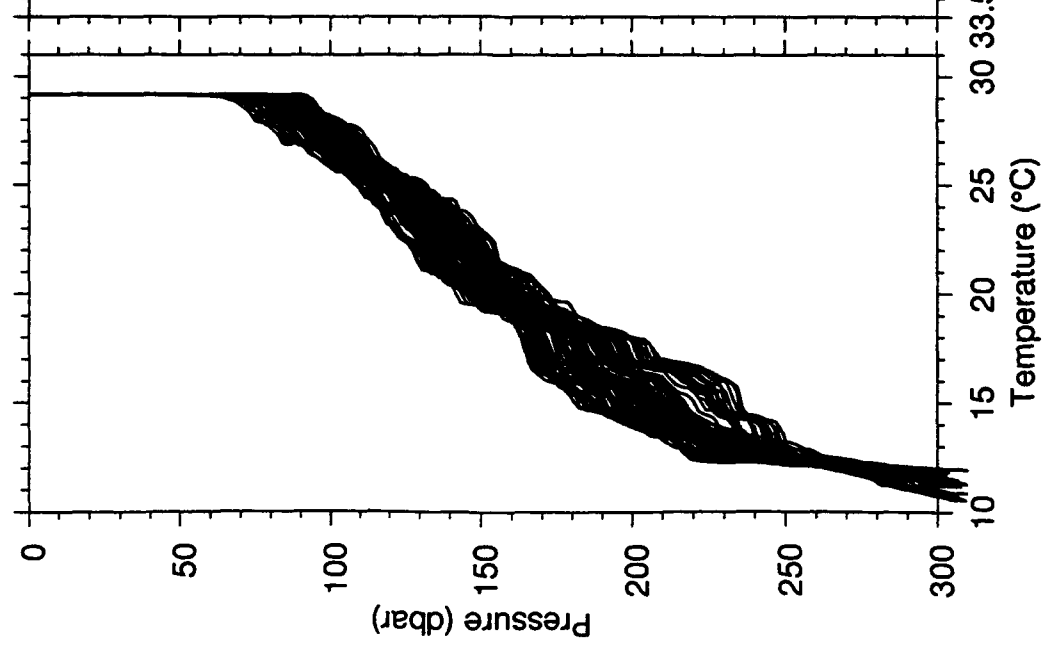
w2e10feb.up.data



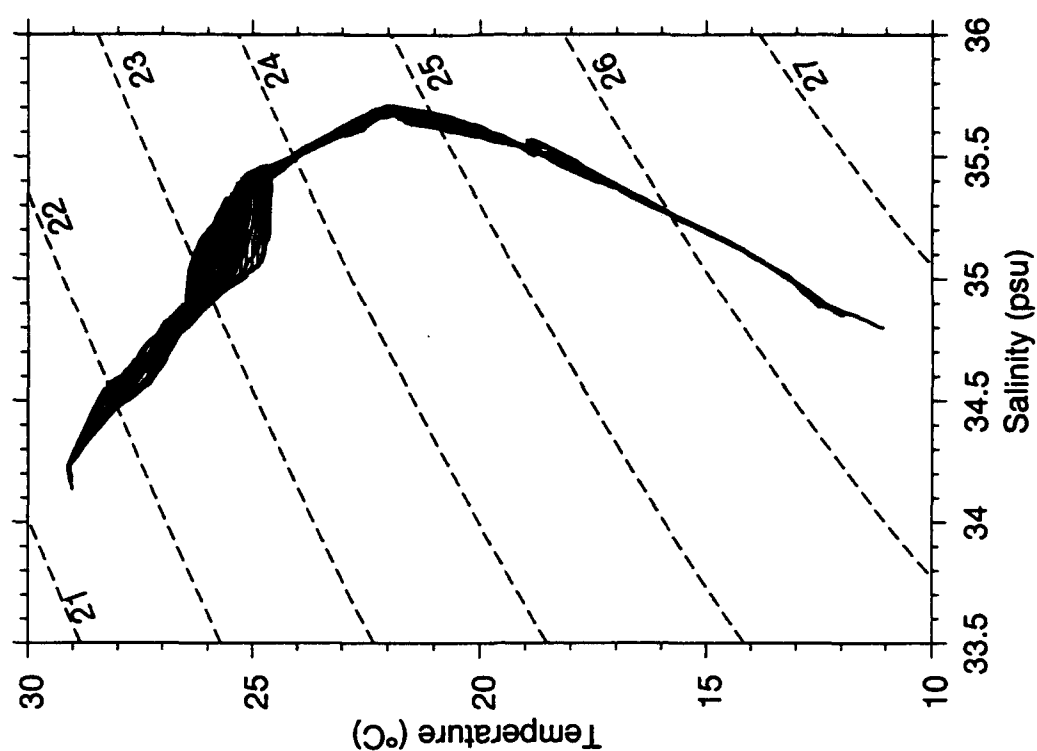
w2e10feb.m.p.data



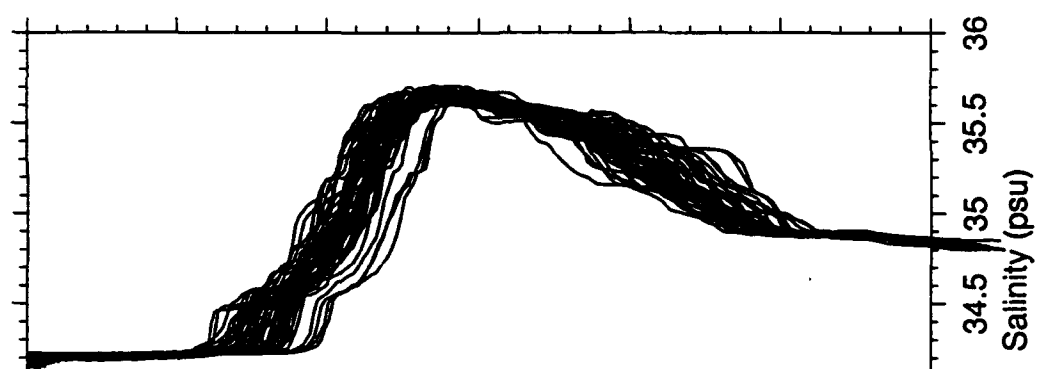
W9211C w2e10feb.data



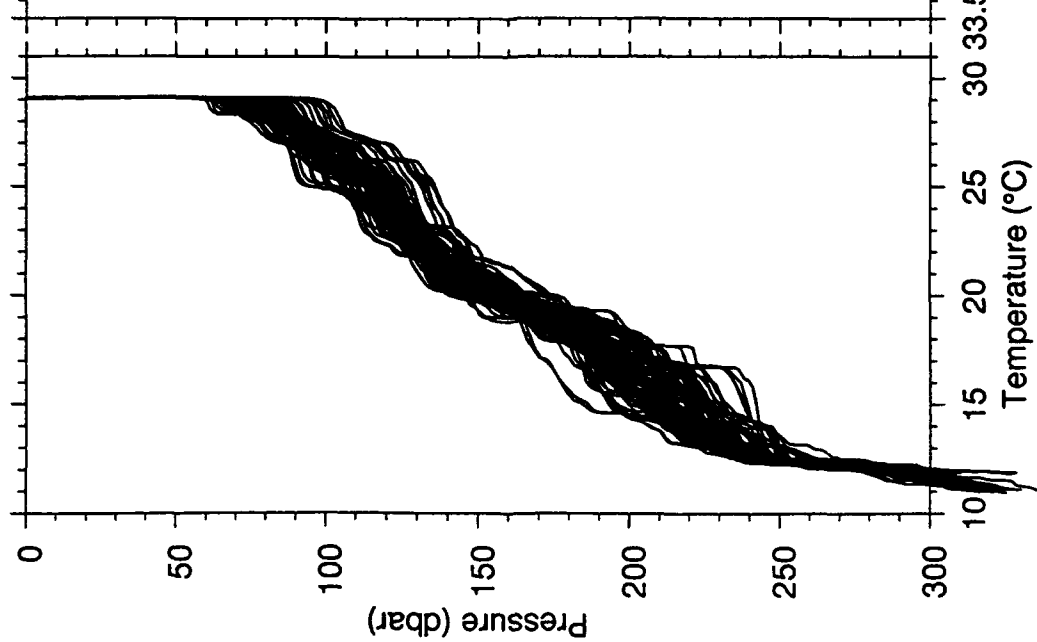
w2e11feb.up.data



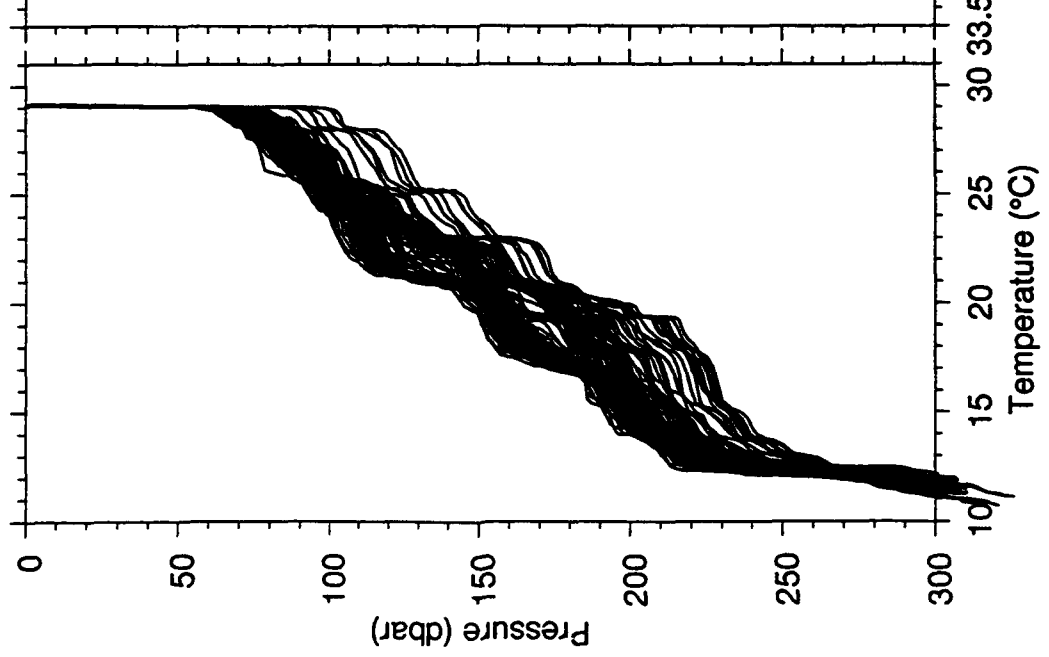
w2e11feb.up.data



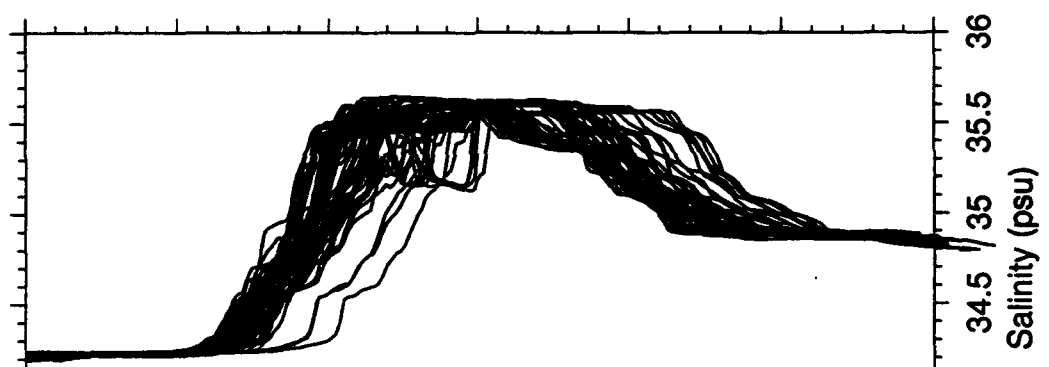
W9211C w2e11feb.data



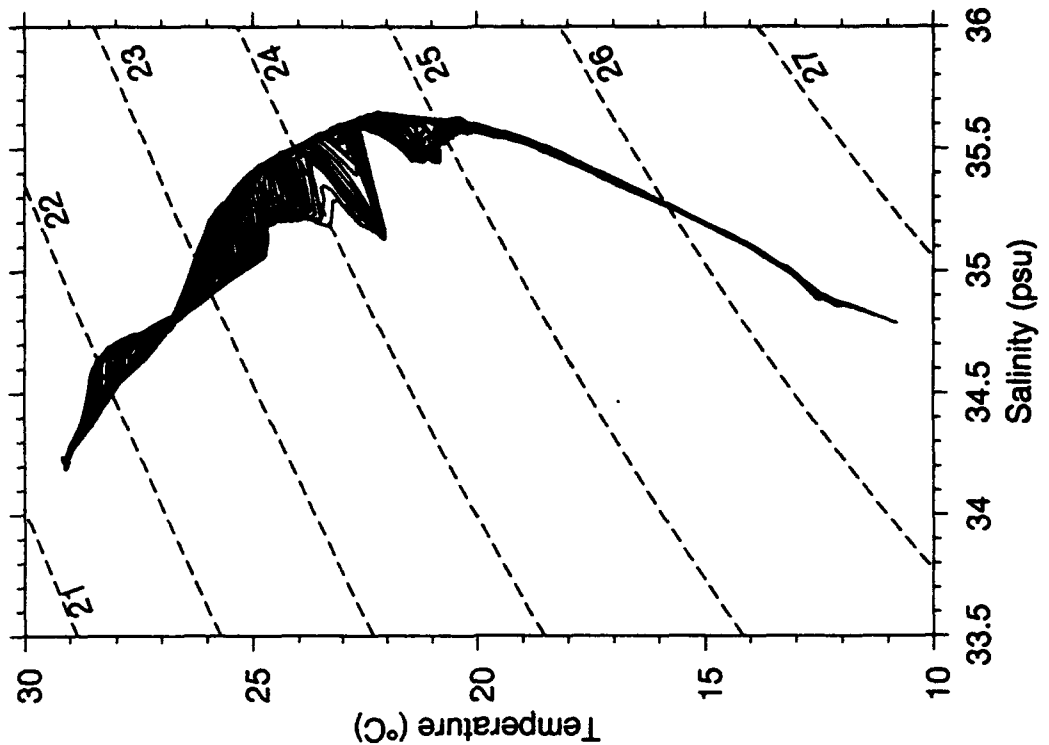
W9211C w2e13feb.data

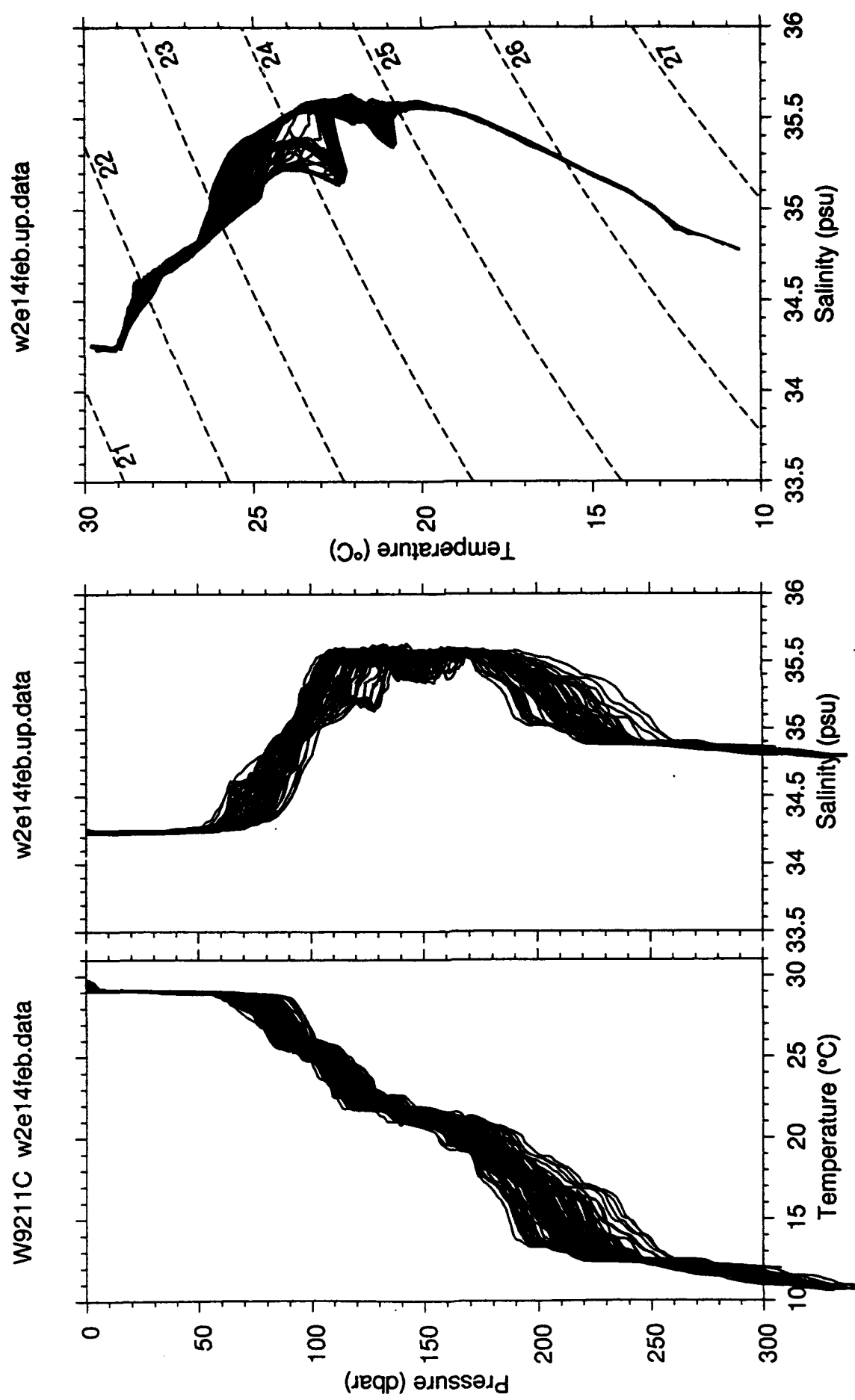


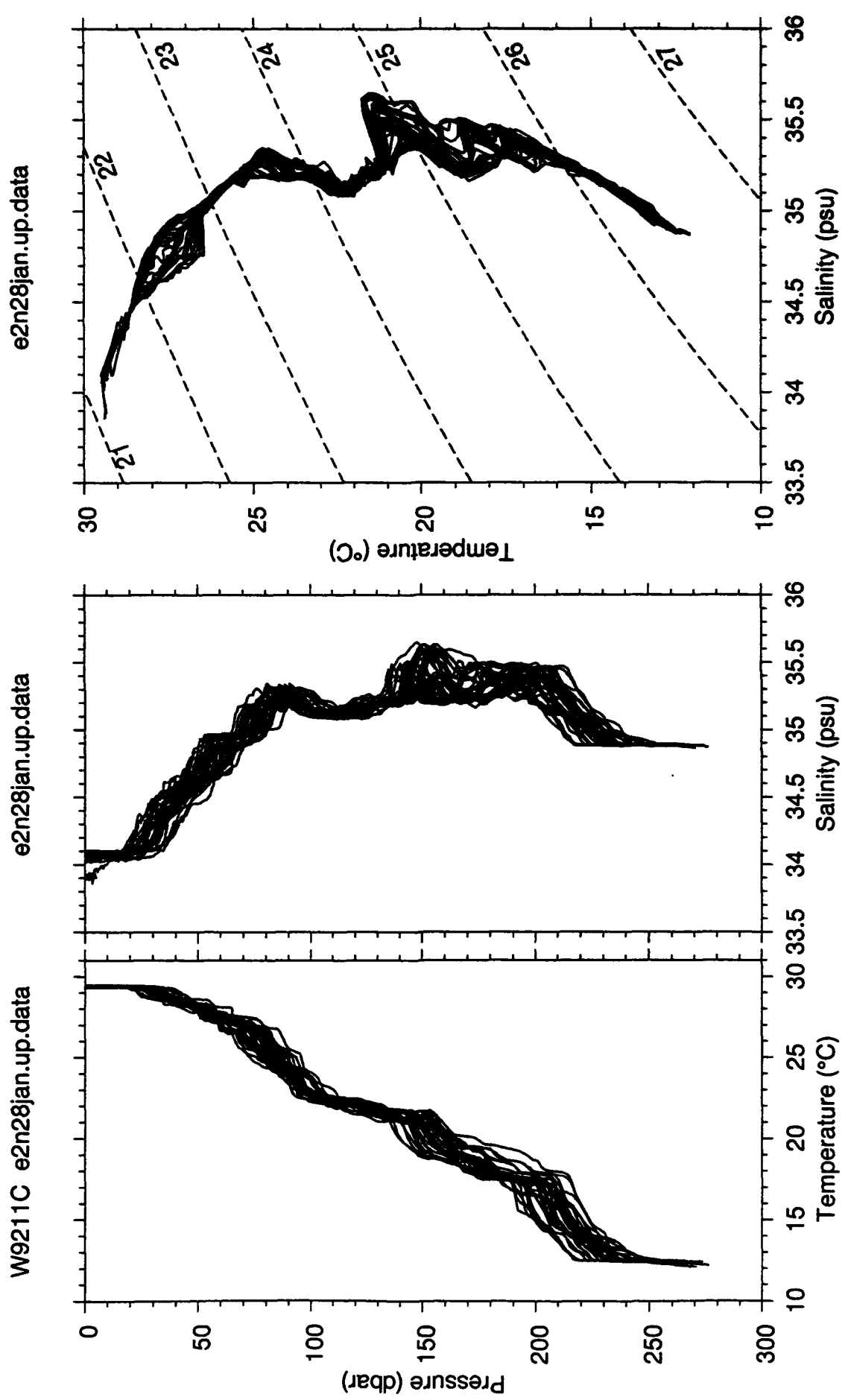
w2e13feb.up.data

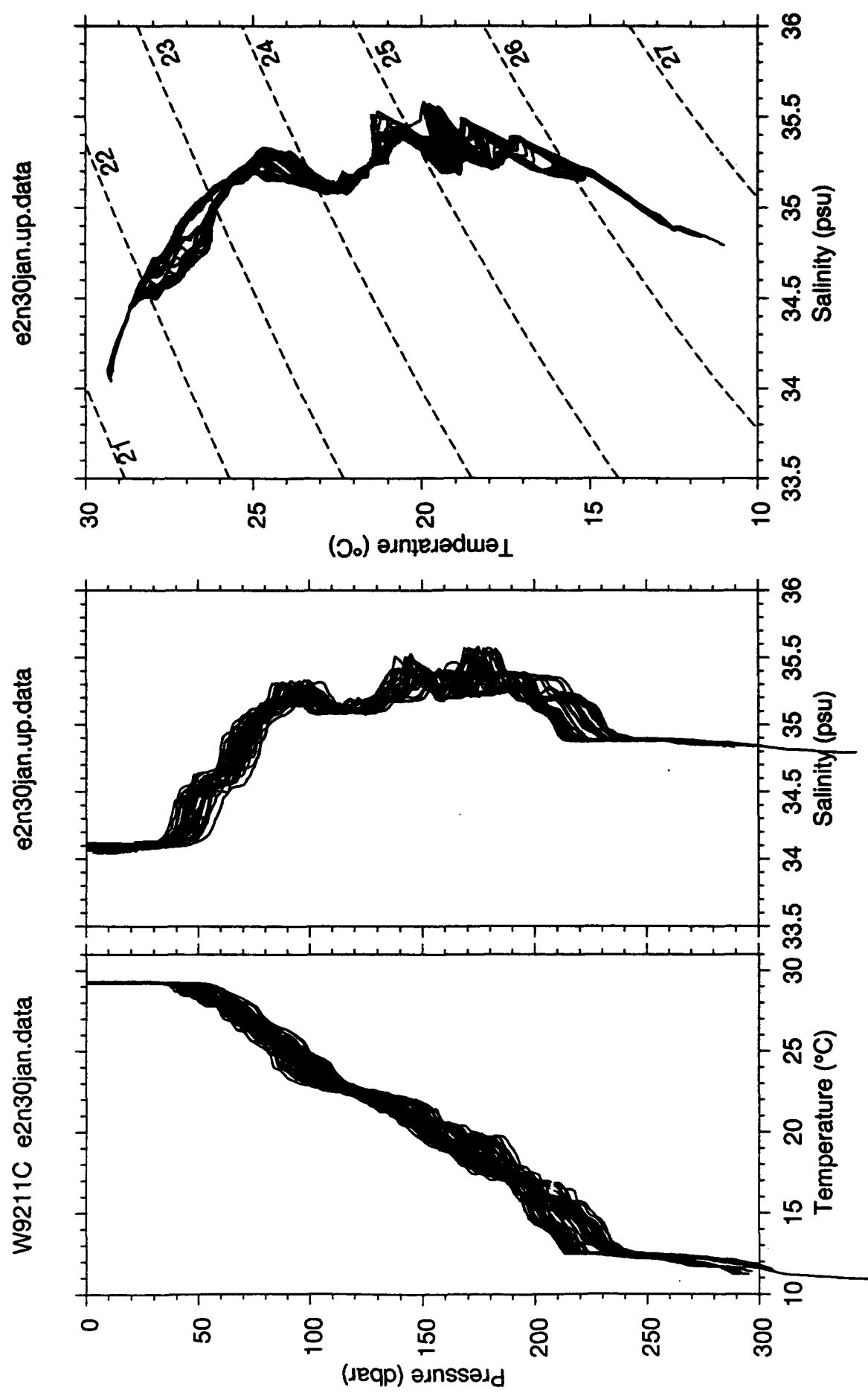


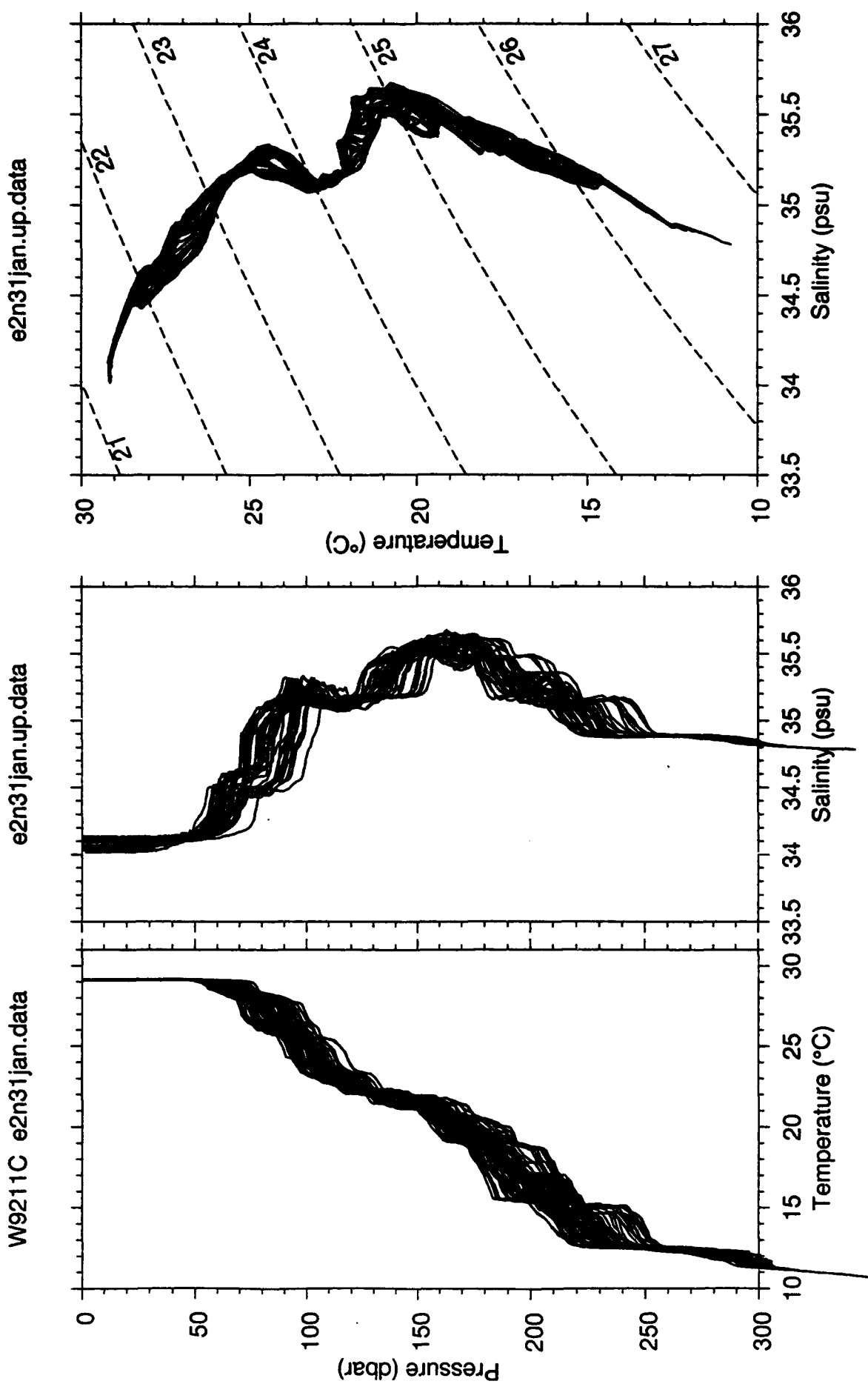
w2e13feb.up.data



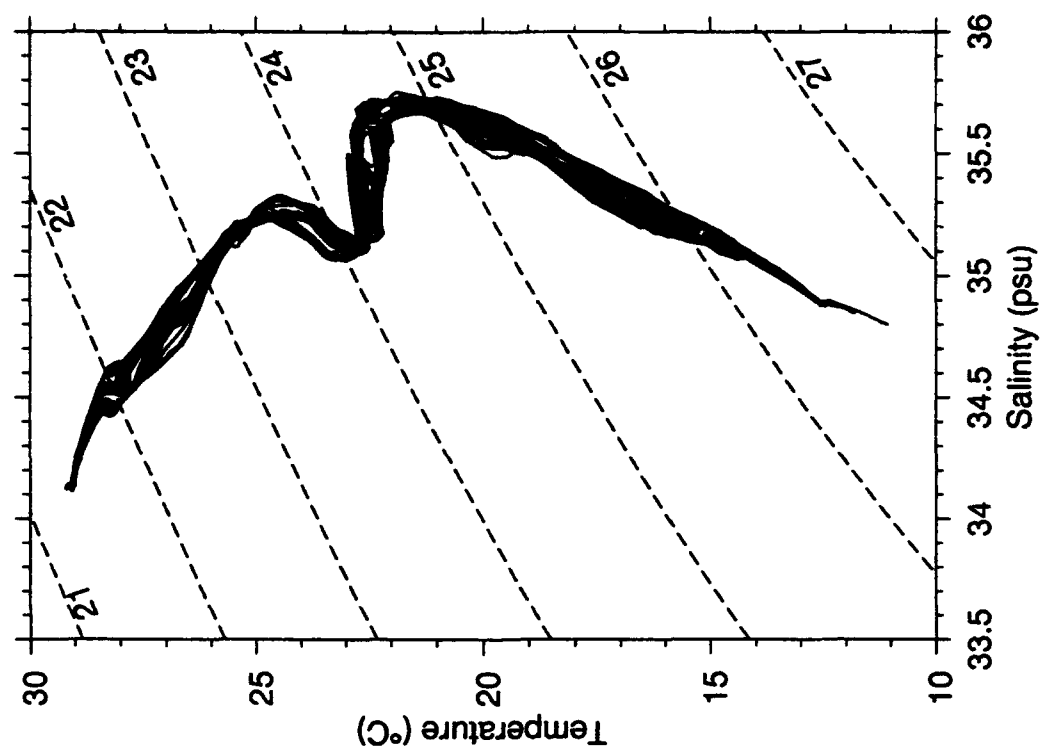




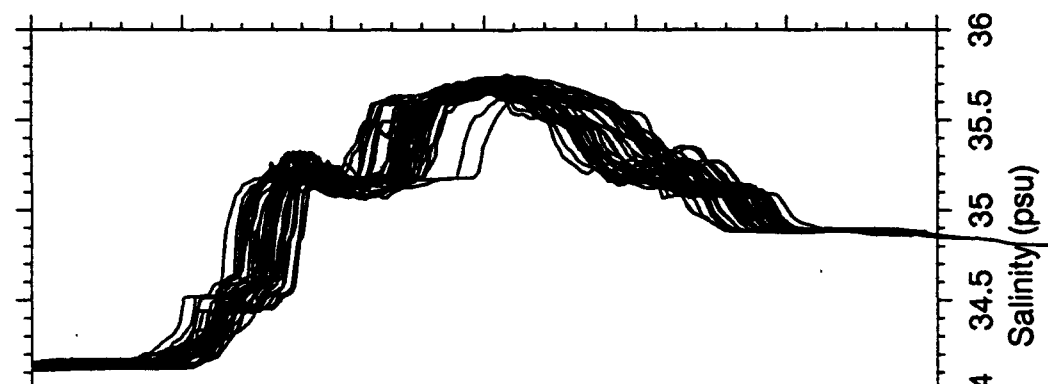




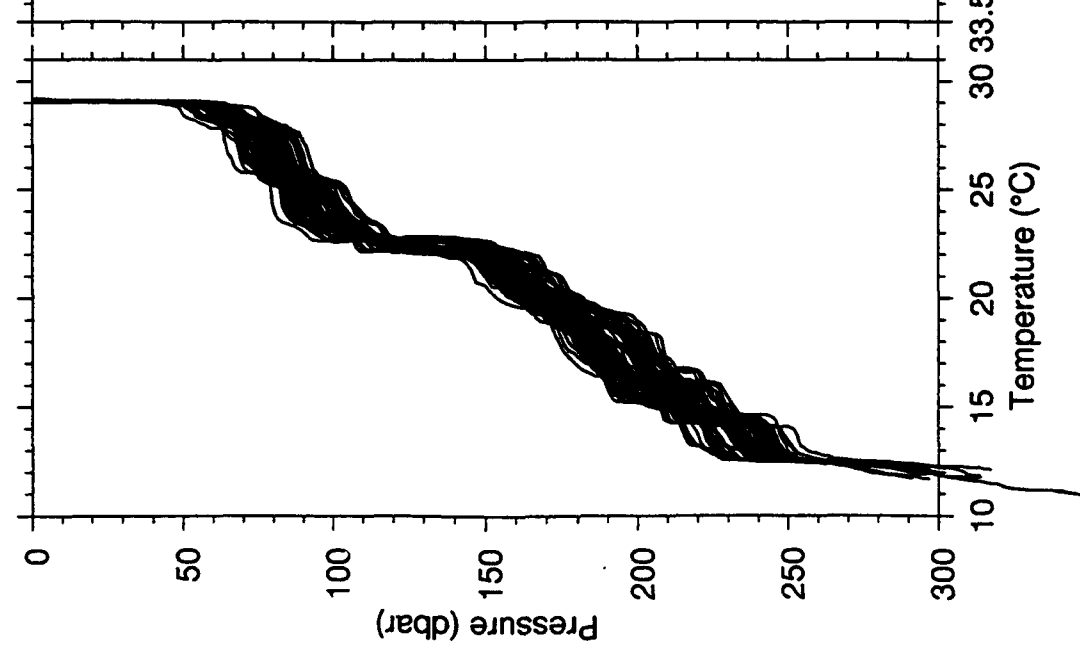
e2n01feb.up.data

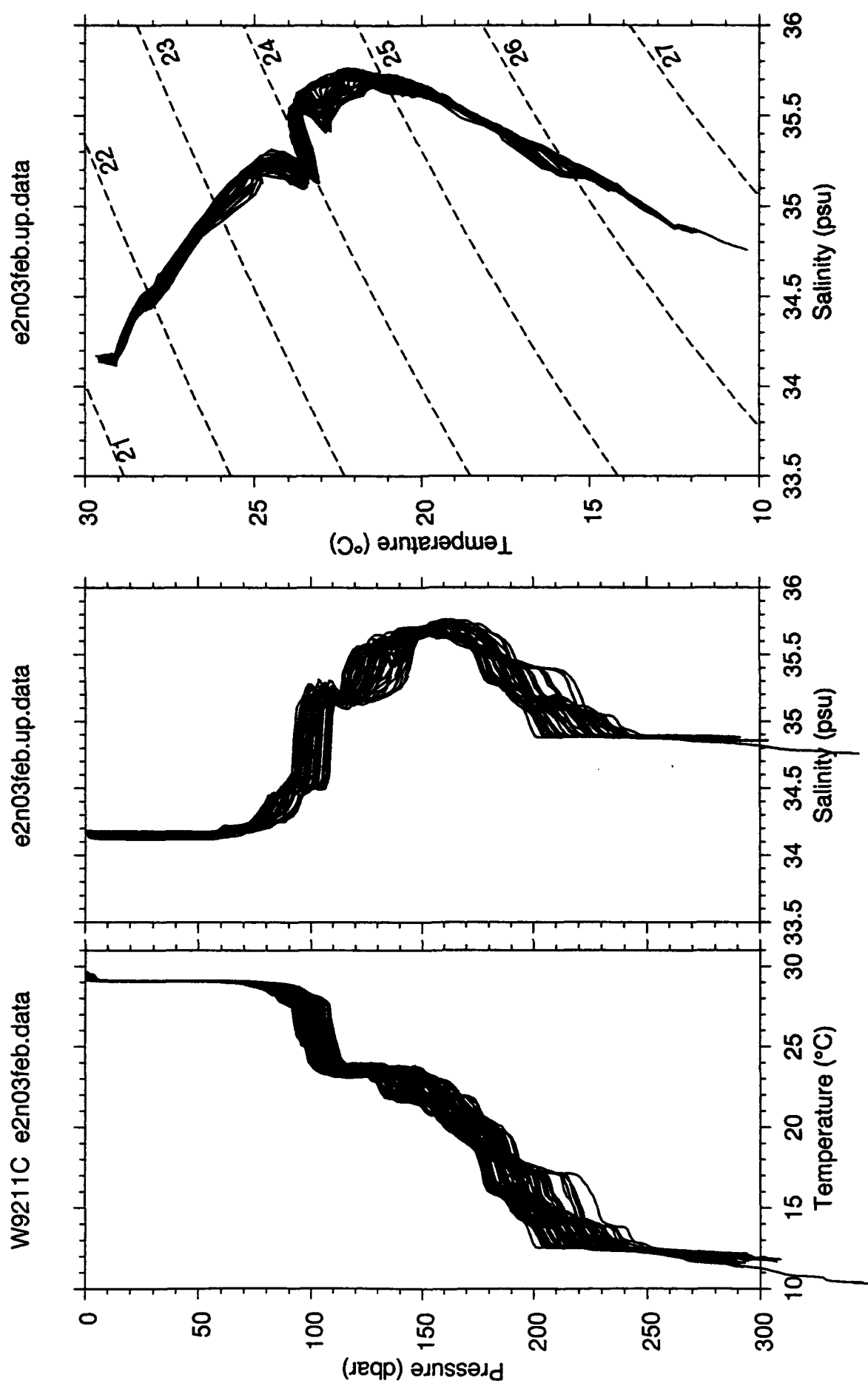


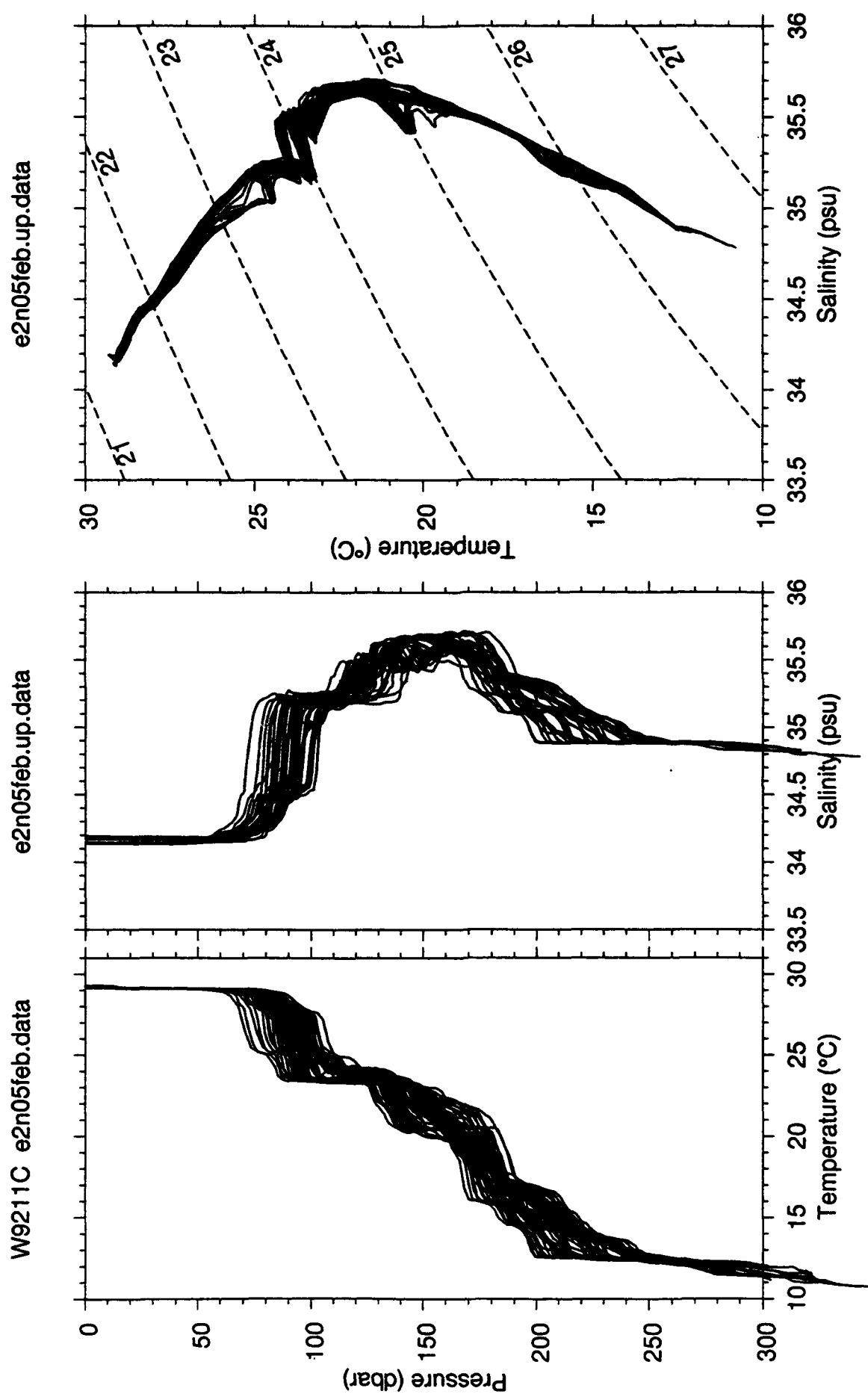
e2n01feb.up.data



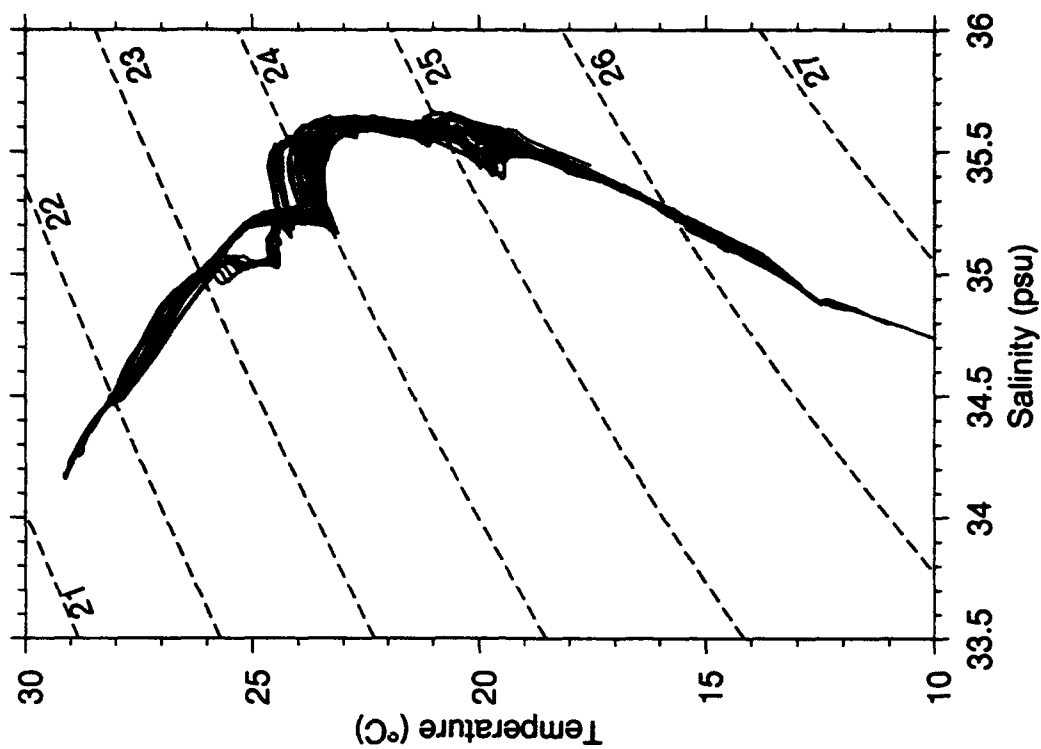
W9211C e2n01feb.data



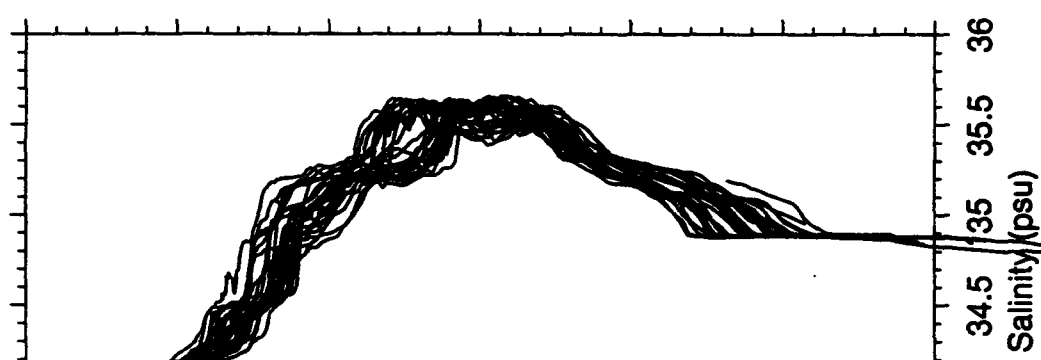




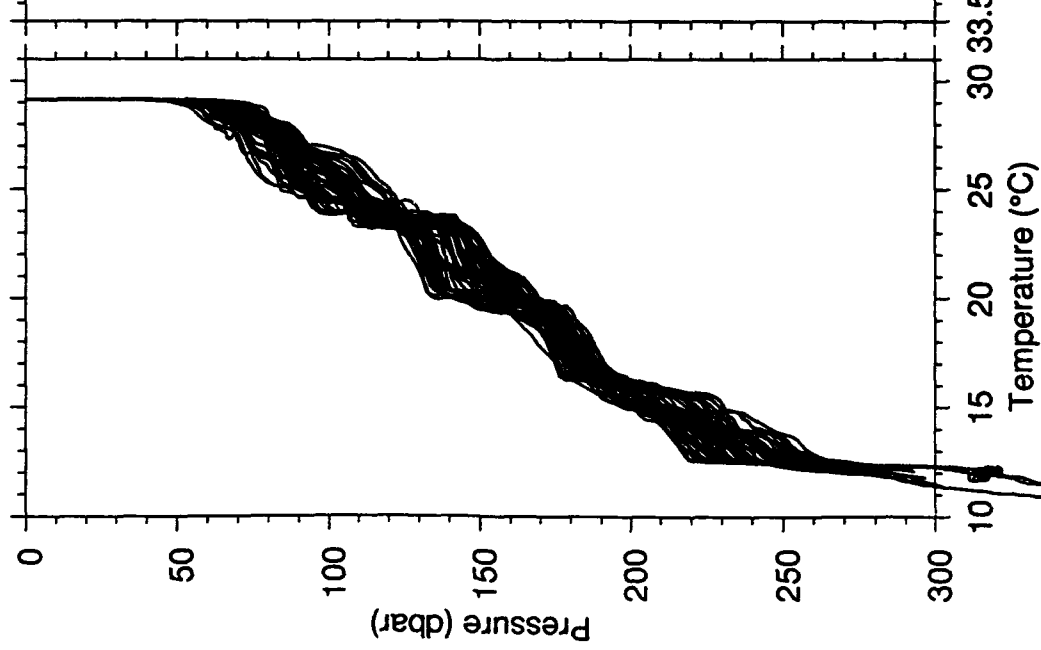
e2n06feb.up.data

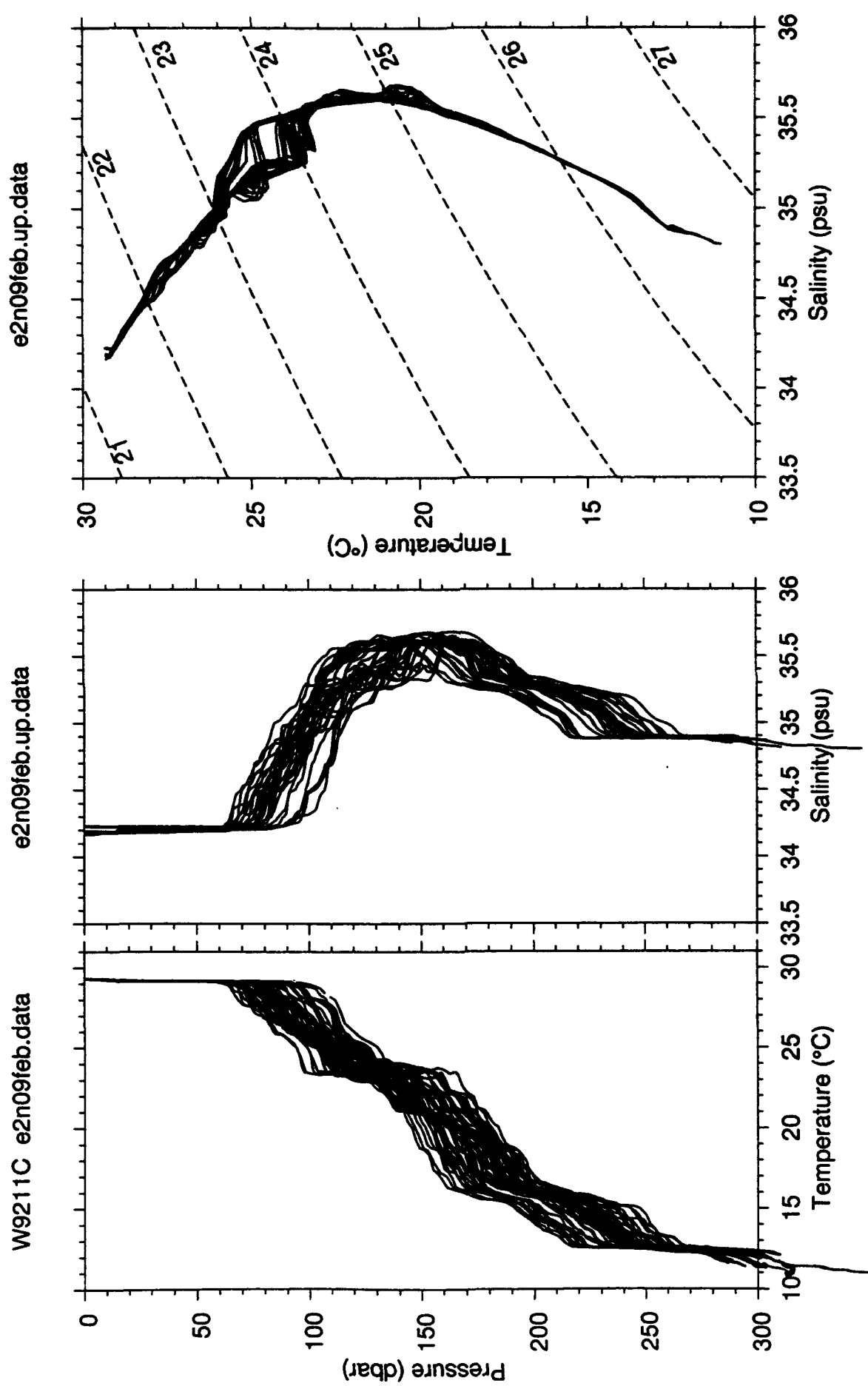


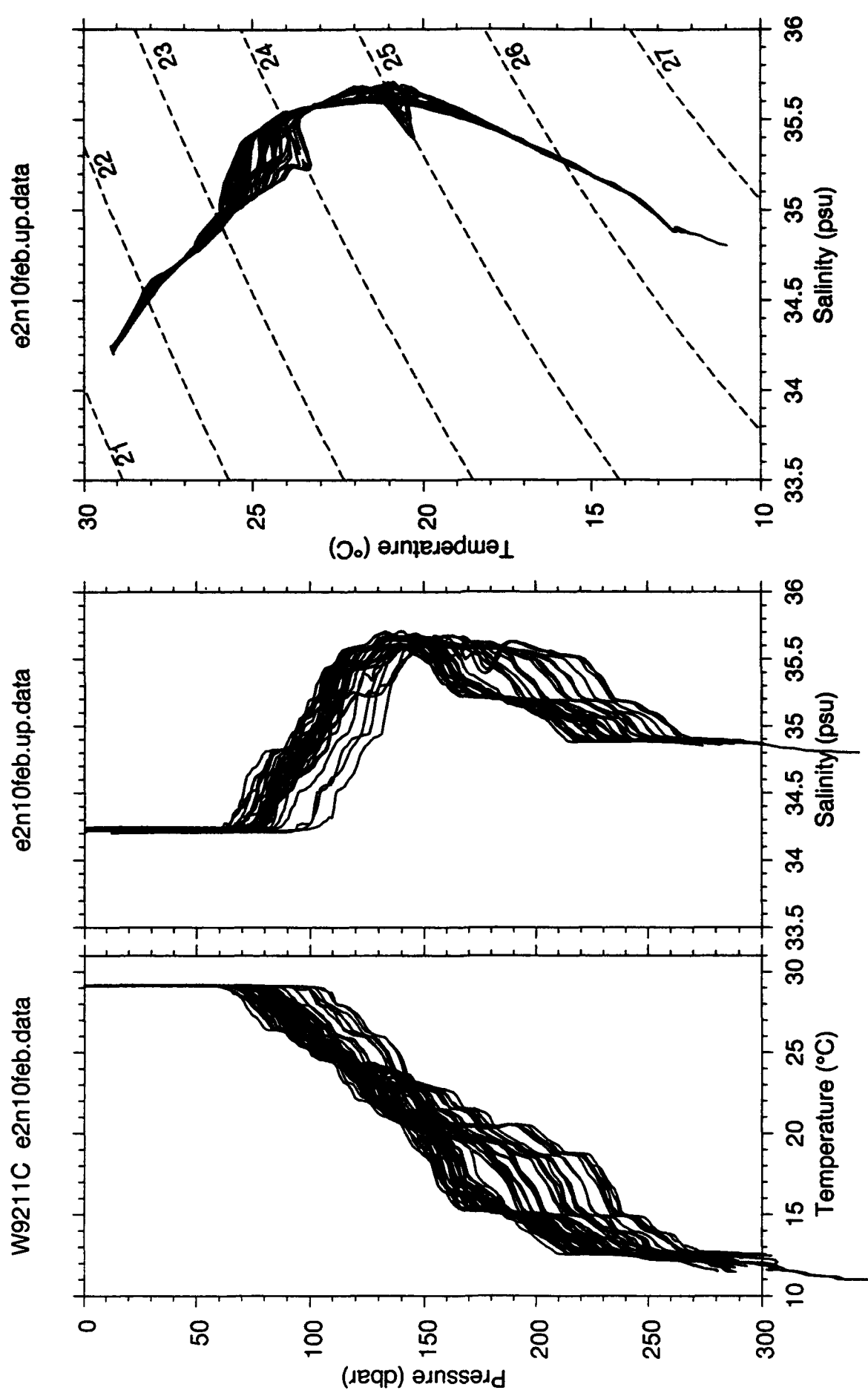
e2n06feb.up.data

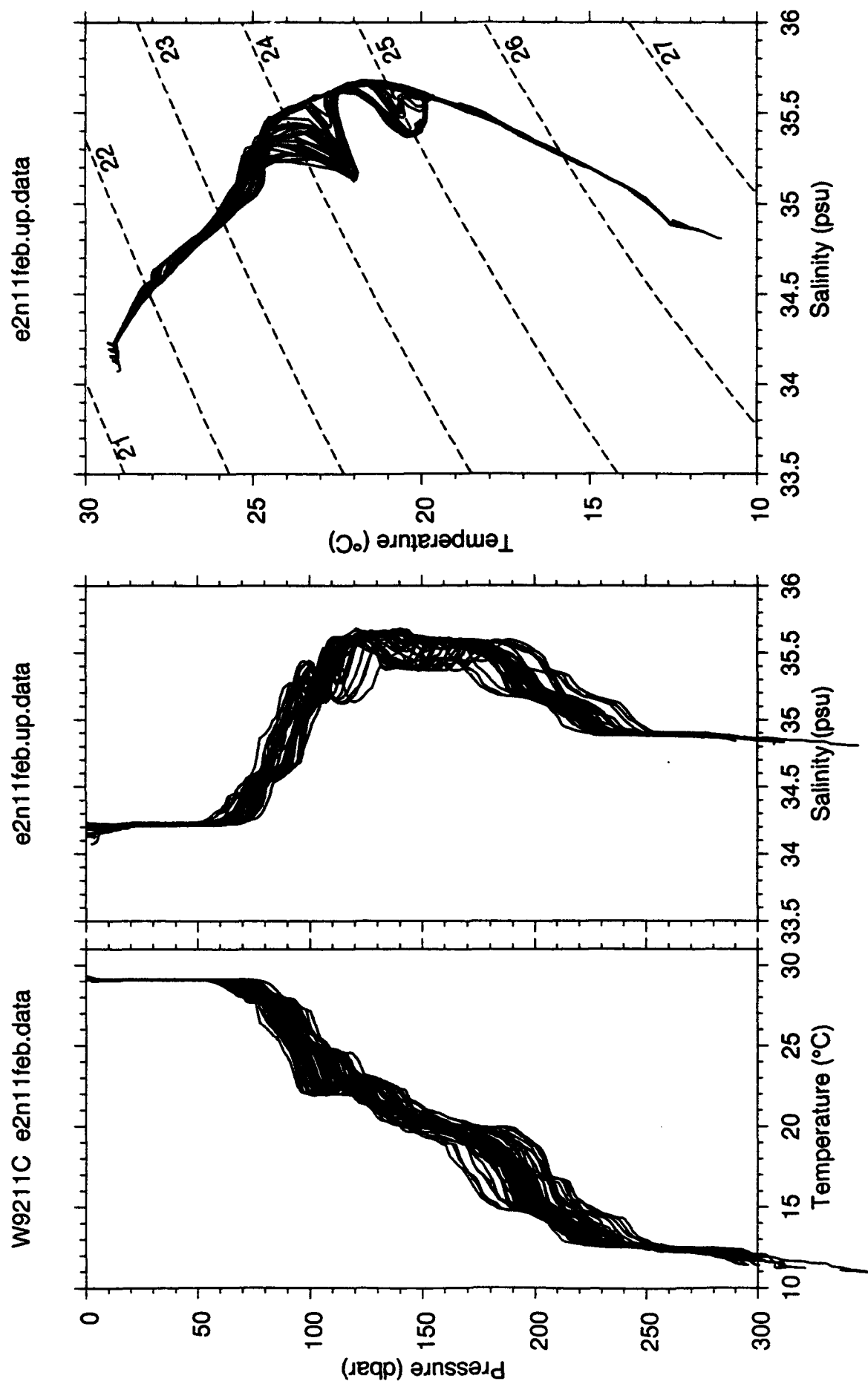


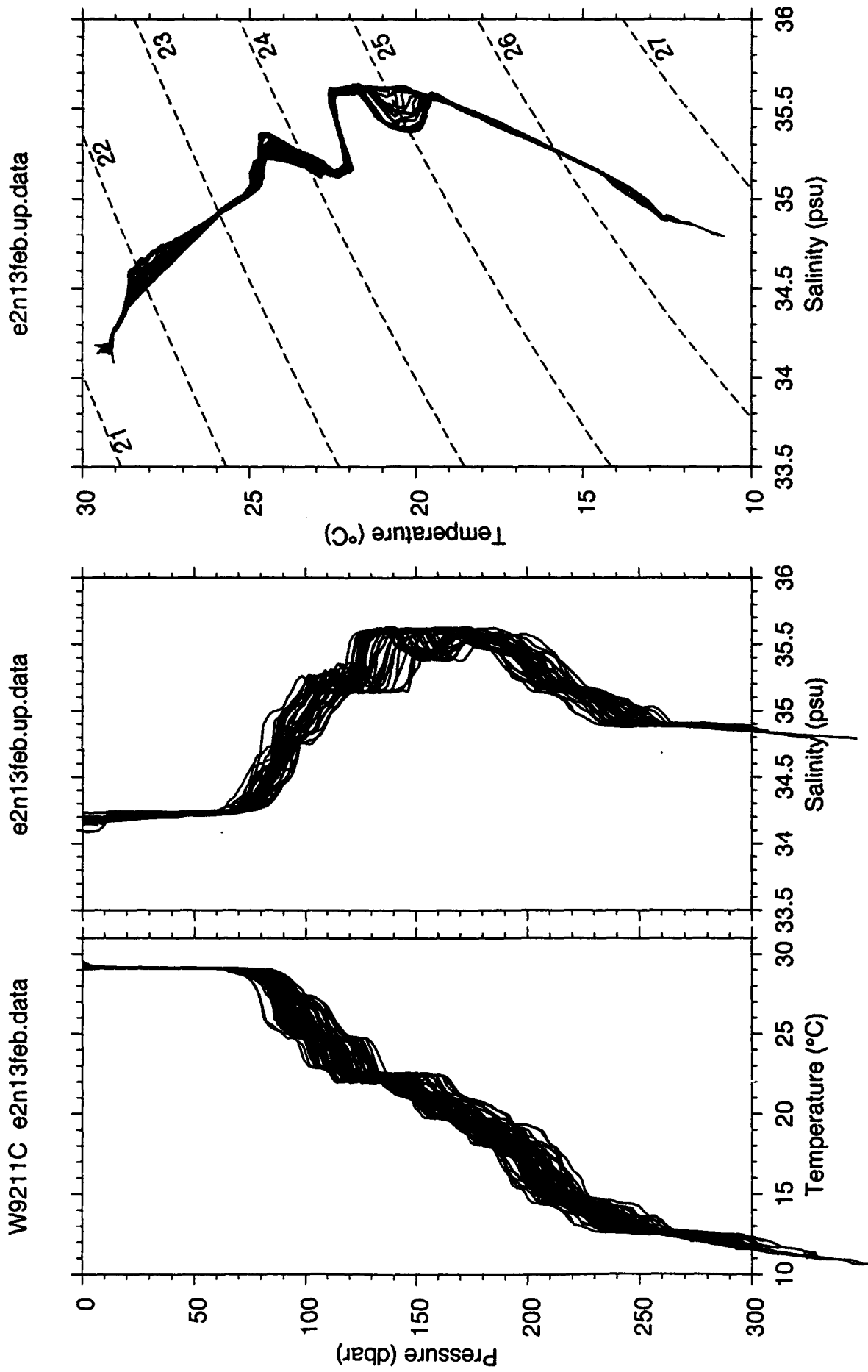
W9211C e2n06feb.data

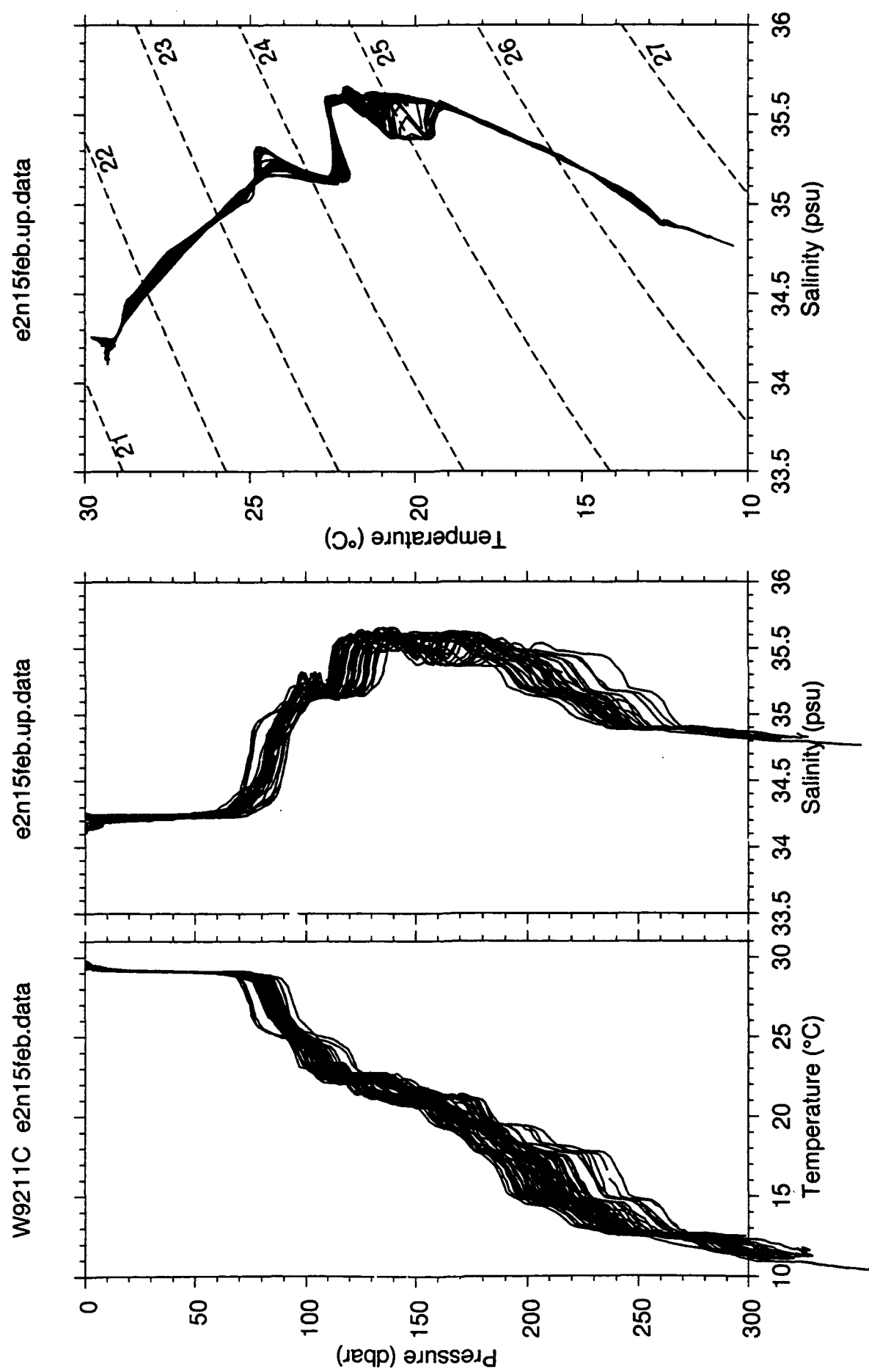


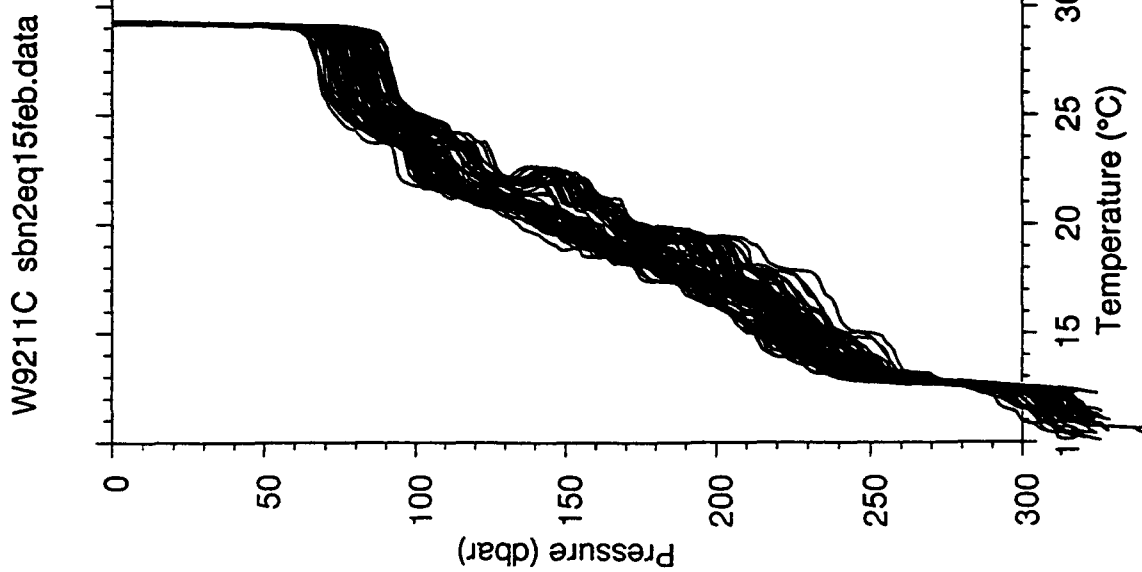
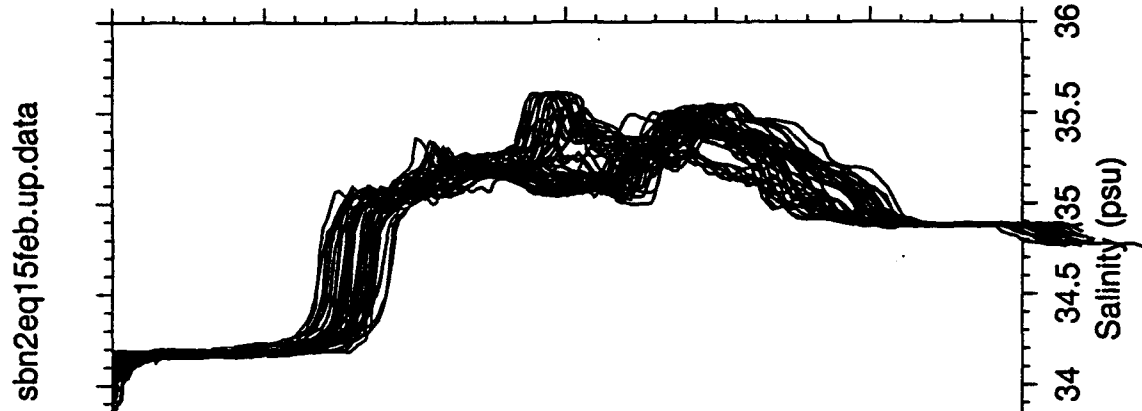
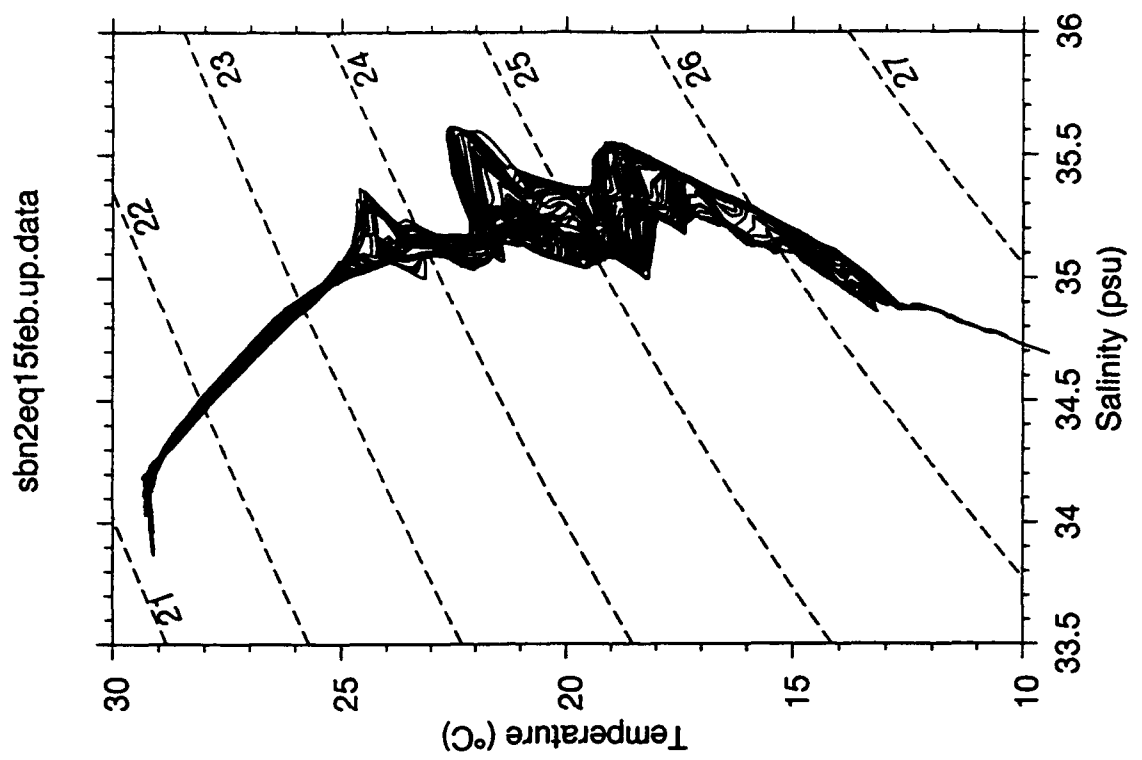




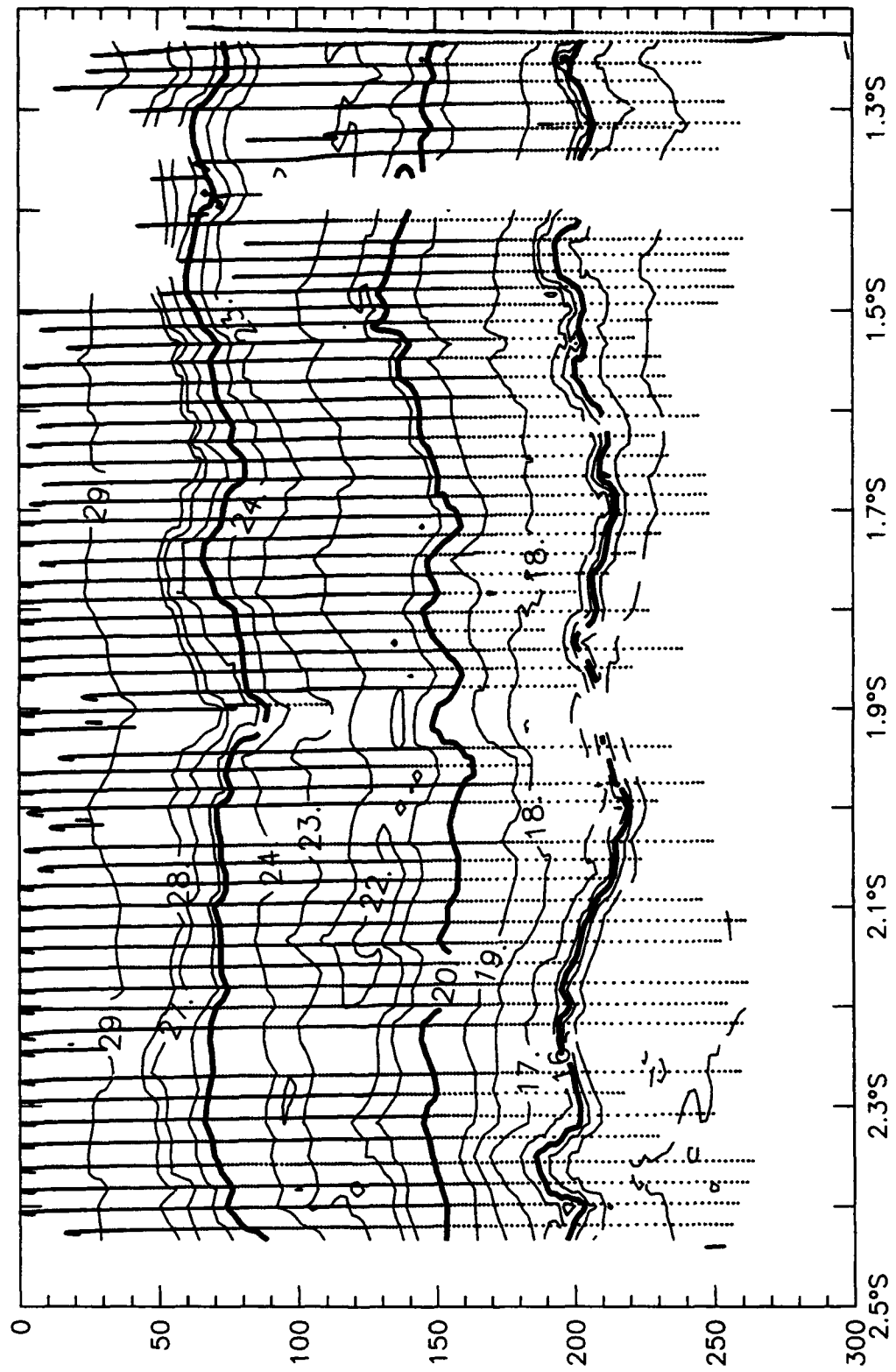




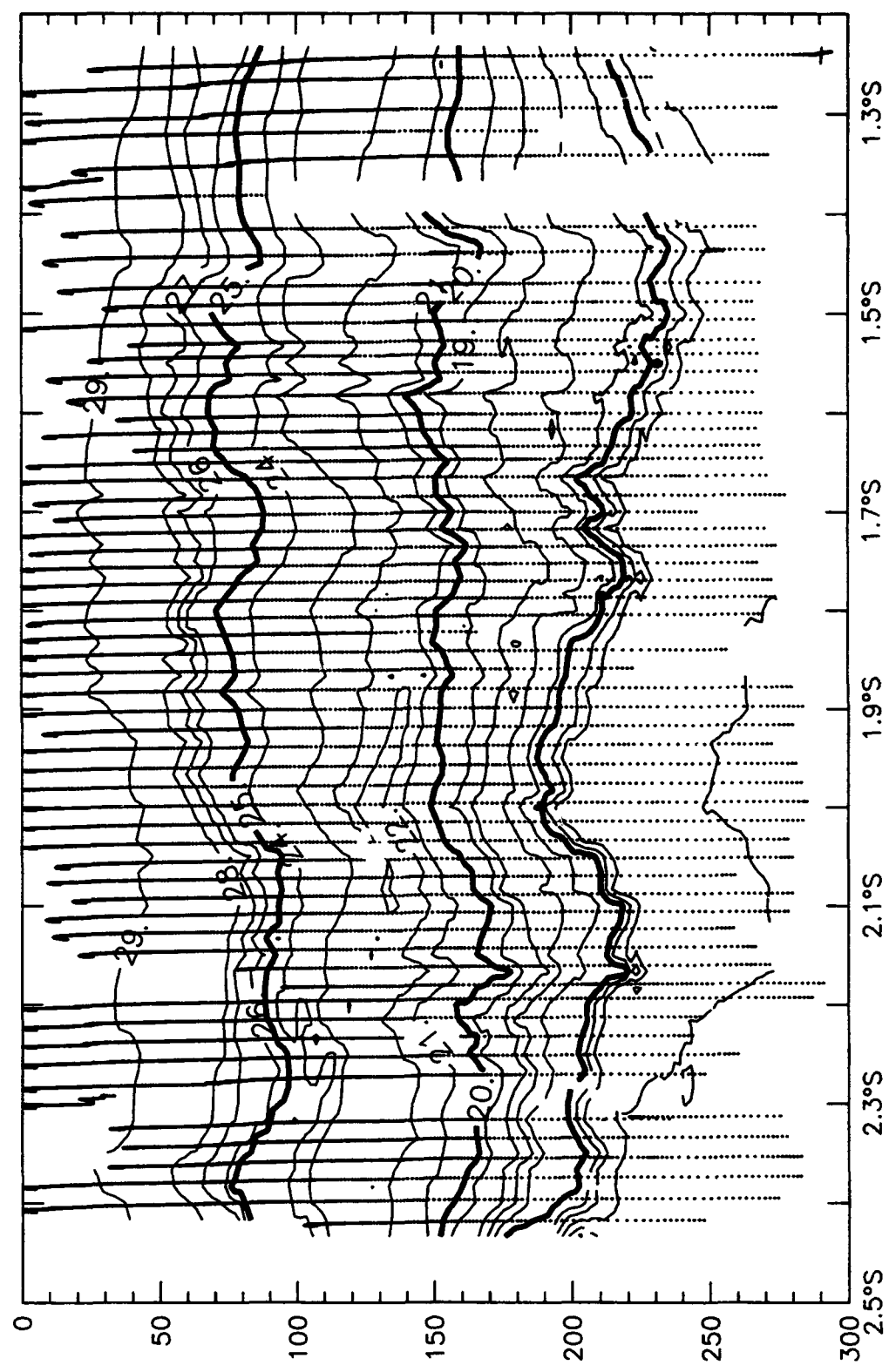




**VERTICAL SECTIONS  
OF  
TEMPERATURE, SALINITY AND SIGMA-T**

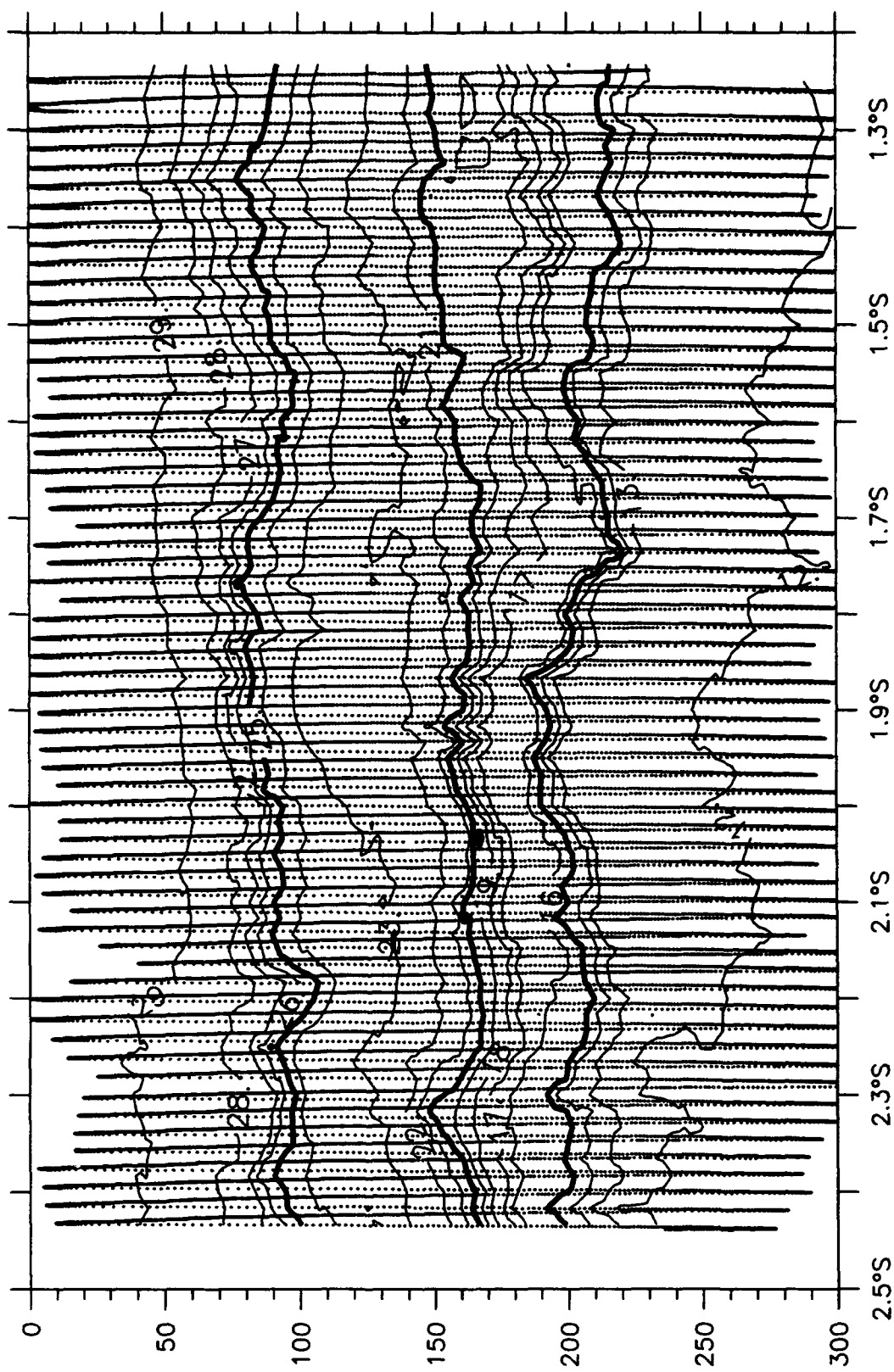


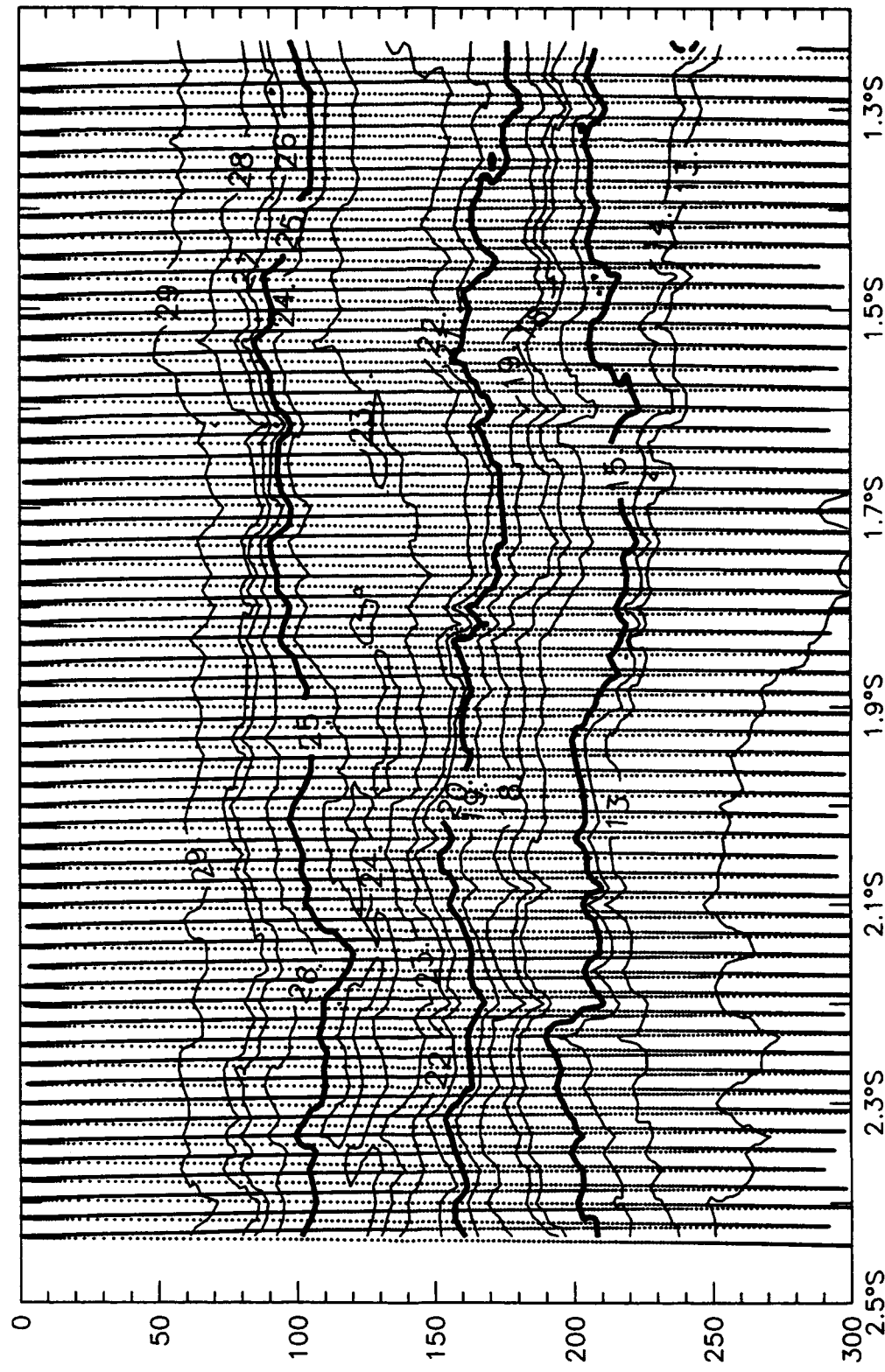
T( $^{\circ}$ C), N2S, 27 January 1993



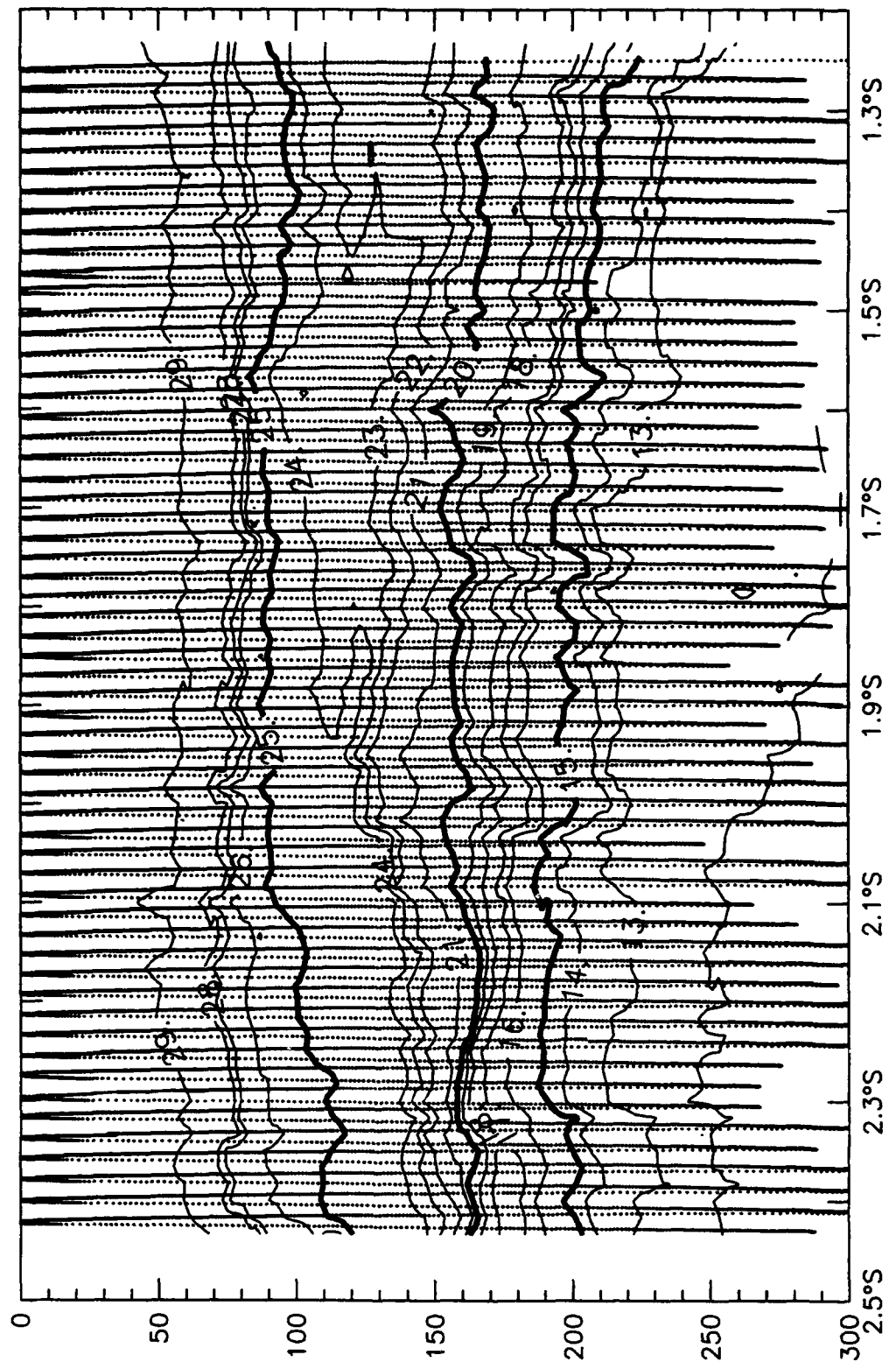
$T(^{\circ}\text{C})$ , N2S, 28 January 1993

T( $^{\circ}$ C), N2S, 30 January 1993

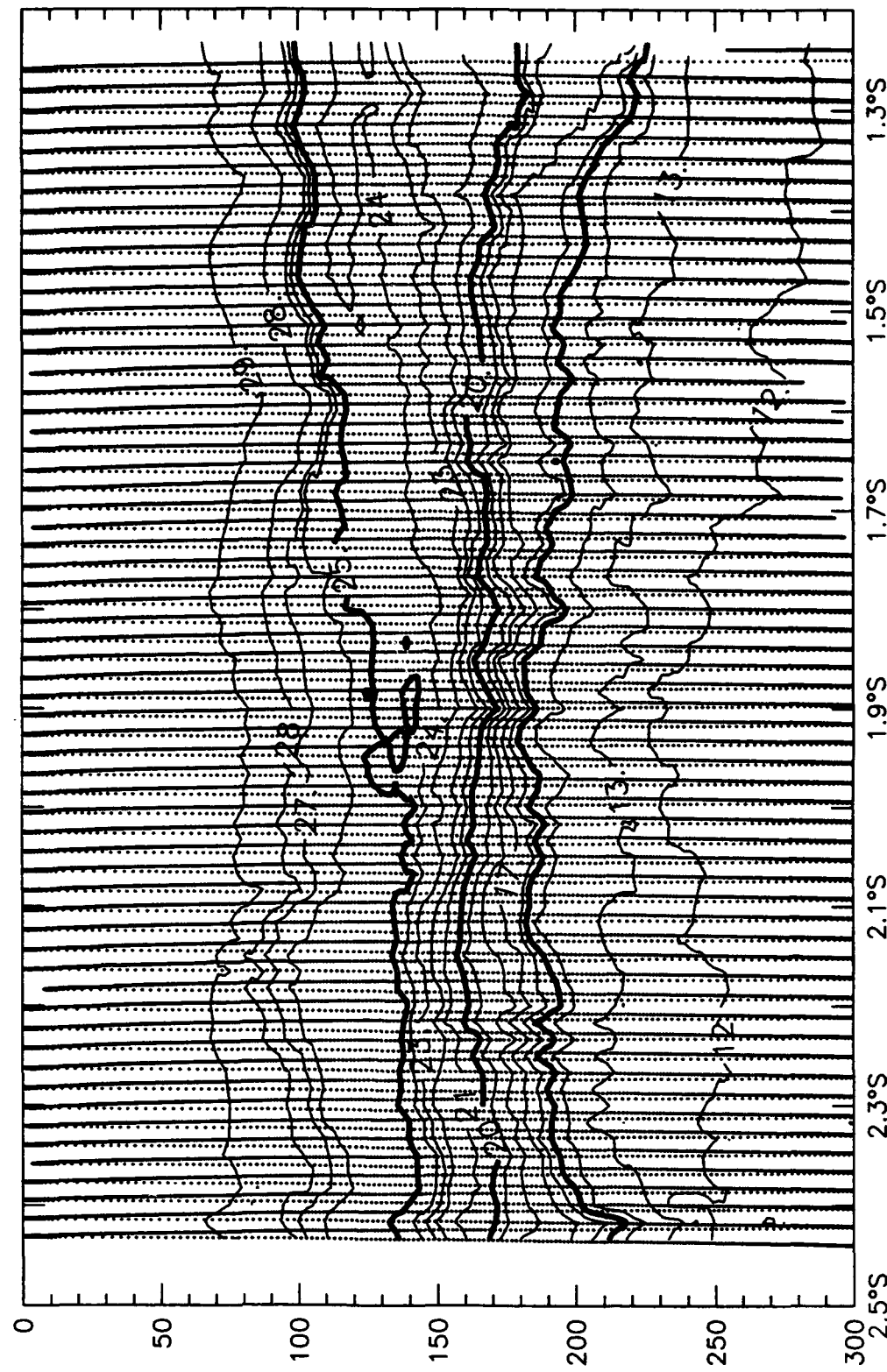




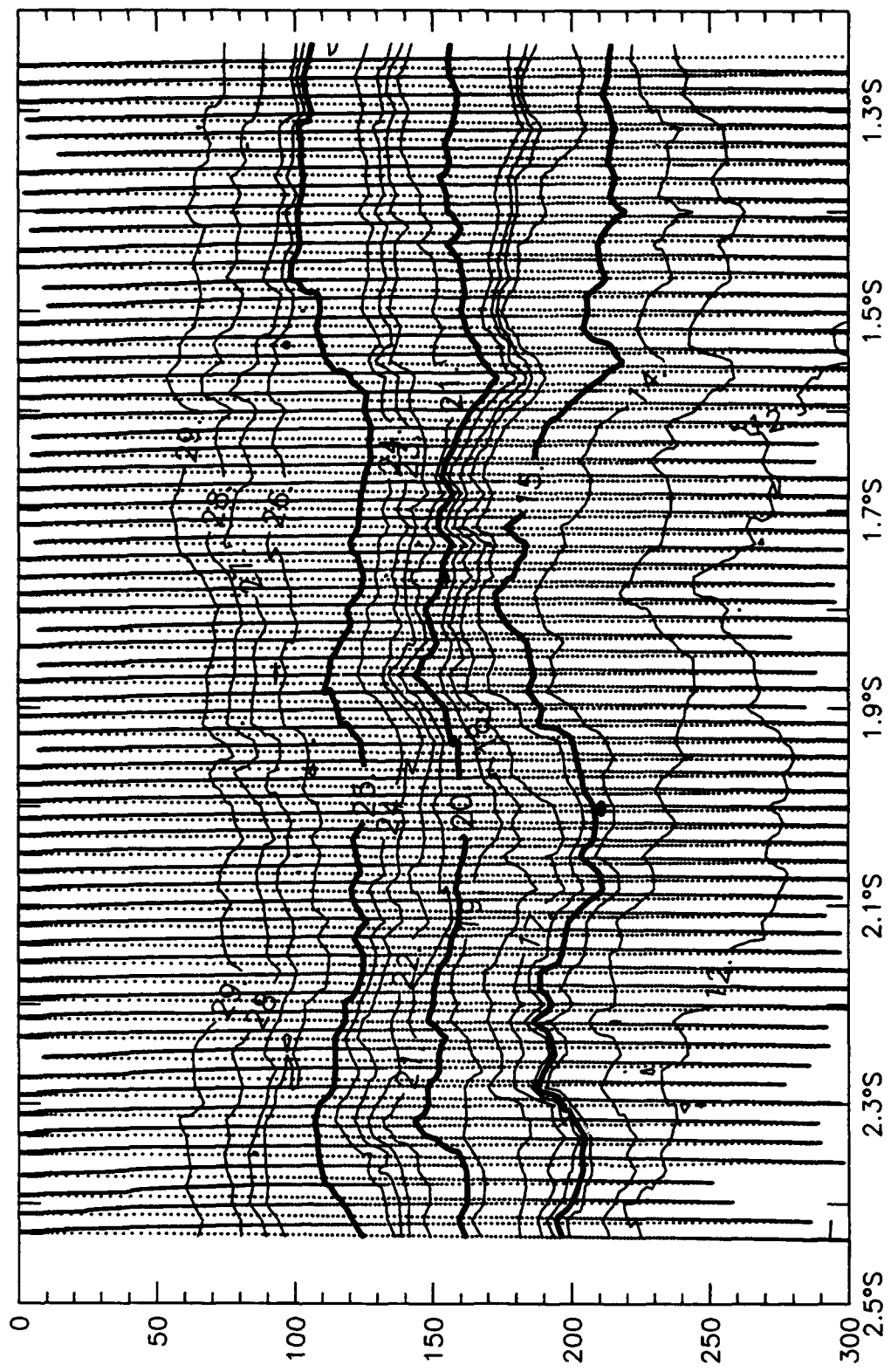
$T$  ( $^{\circ}\text{C}$ ), N2S, 31 January 1993



T( $^{\circ}\text{C}$ ), N2S, 2 February 1993

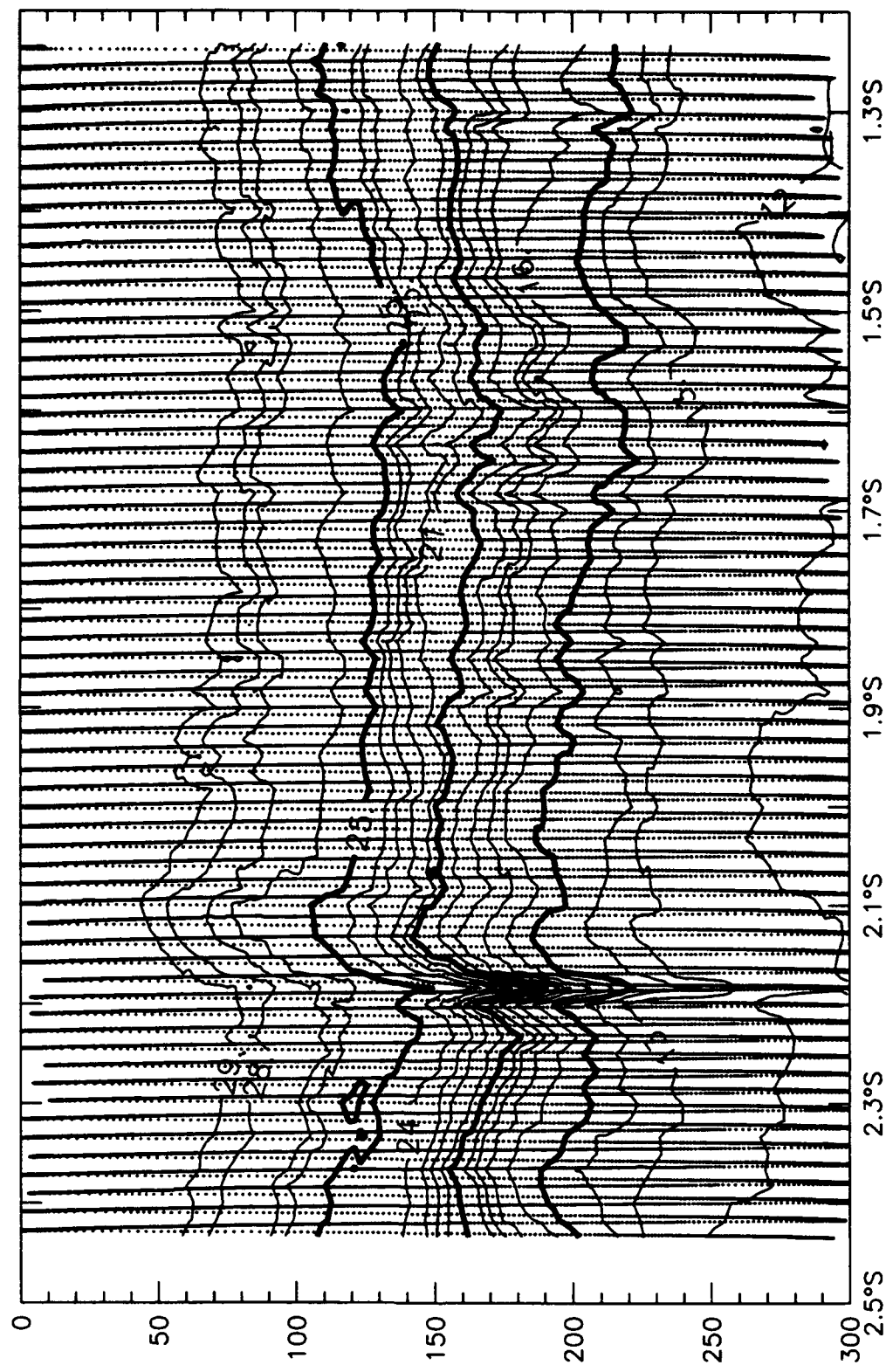


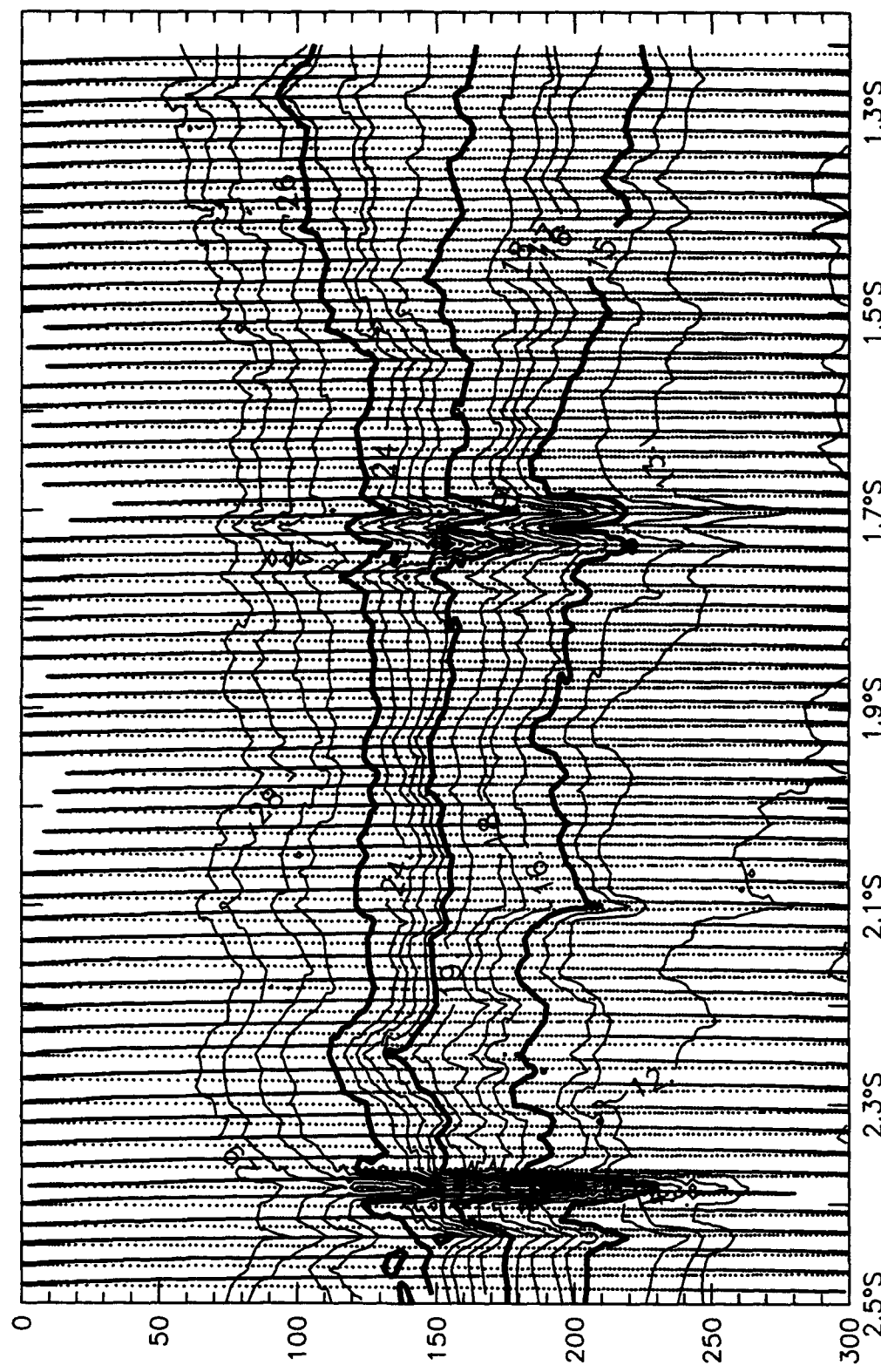
$T(^{\circ}\text{C})$ , N2S, 4 February 1993



$T(^{\circ}\text{C})$ , N2S, 5 February 1993

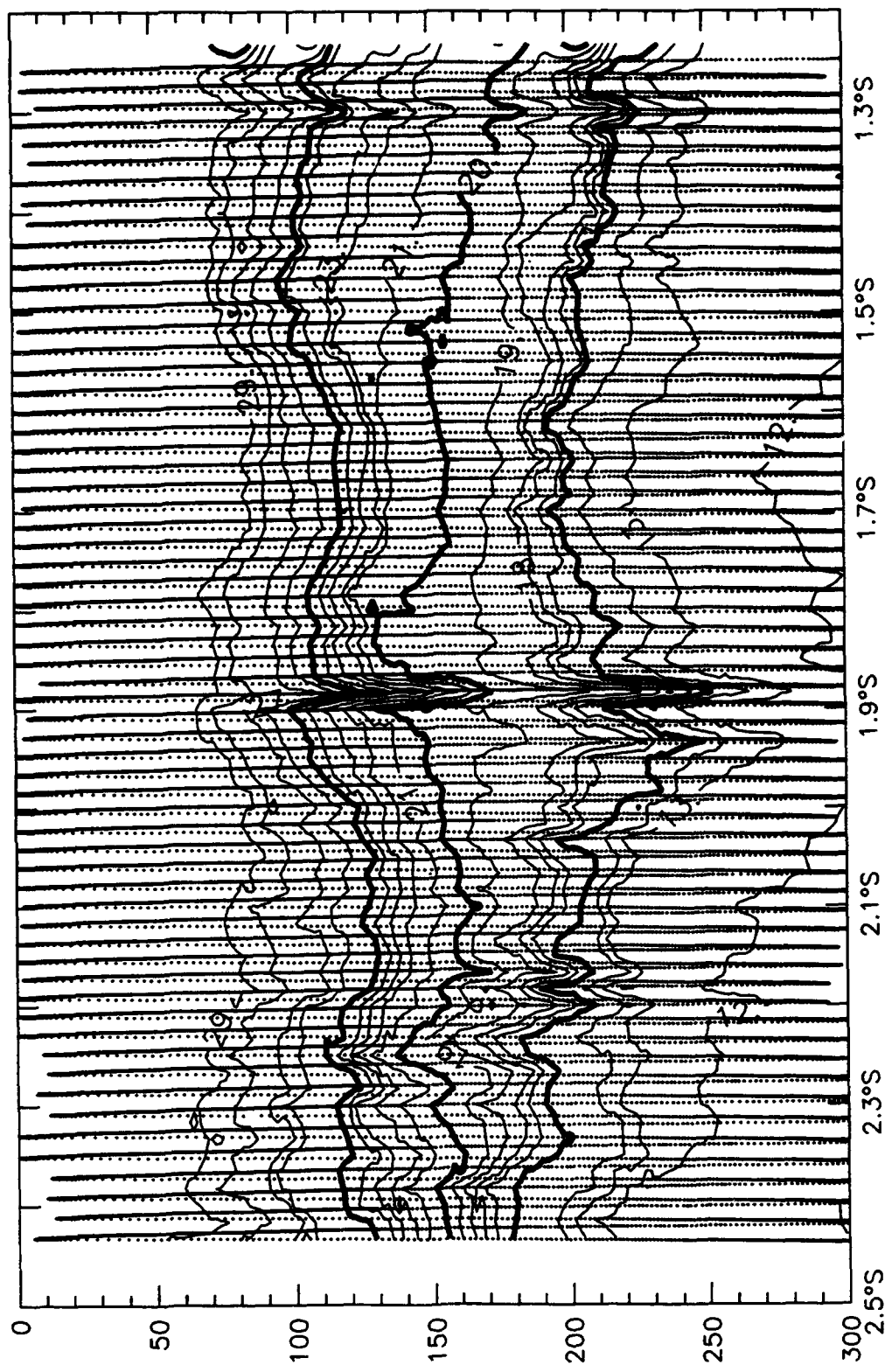
T( $^{\circ}$ C), N2S, 7 February 1993

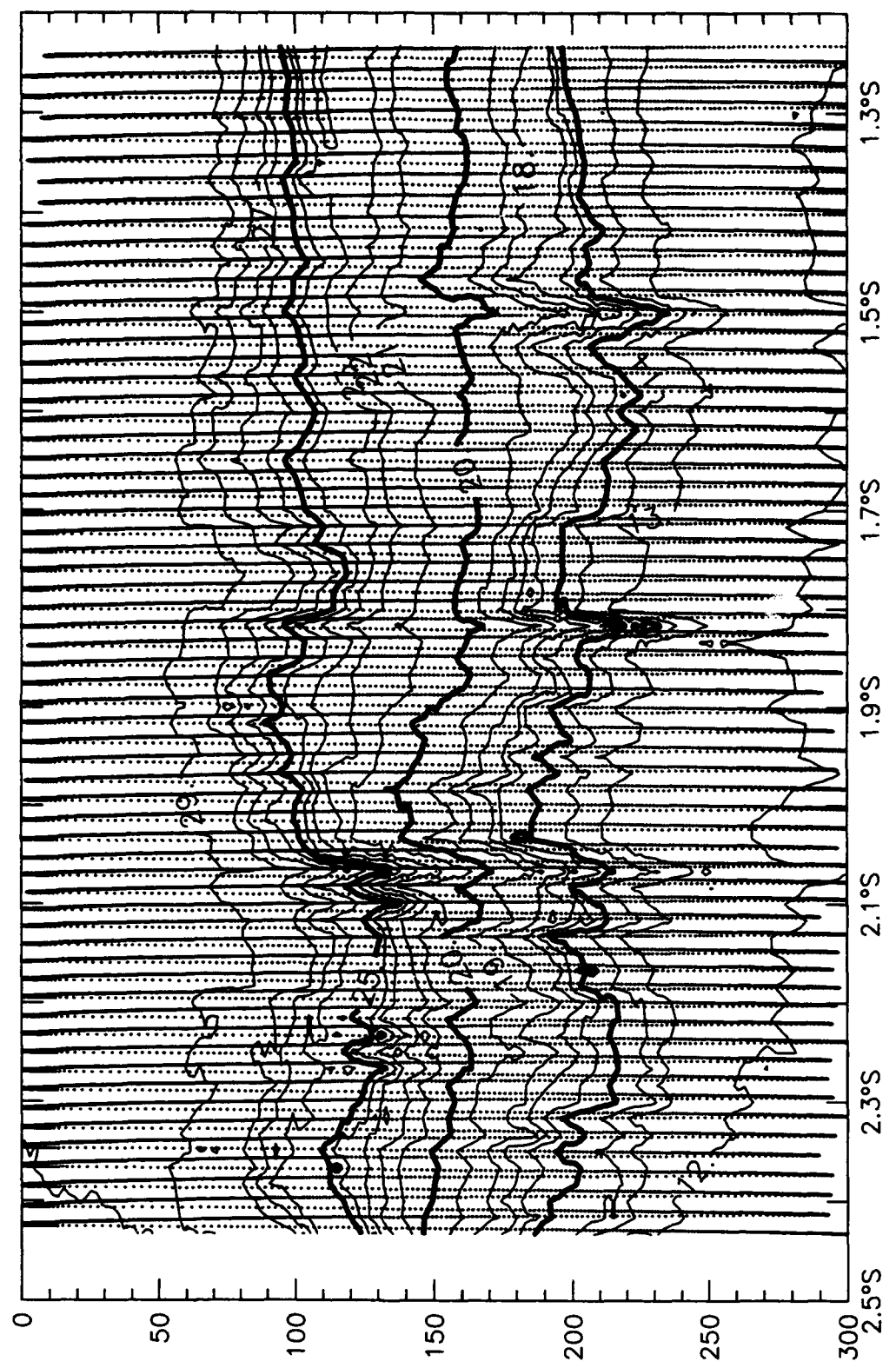




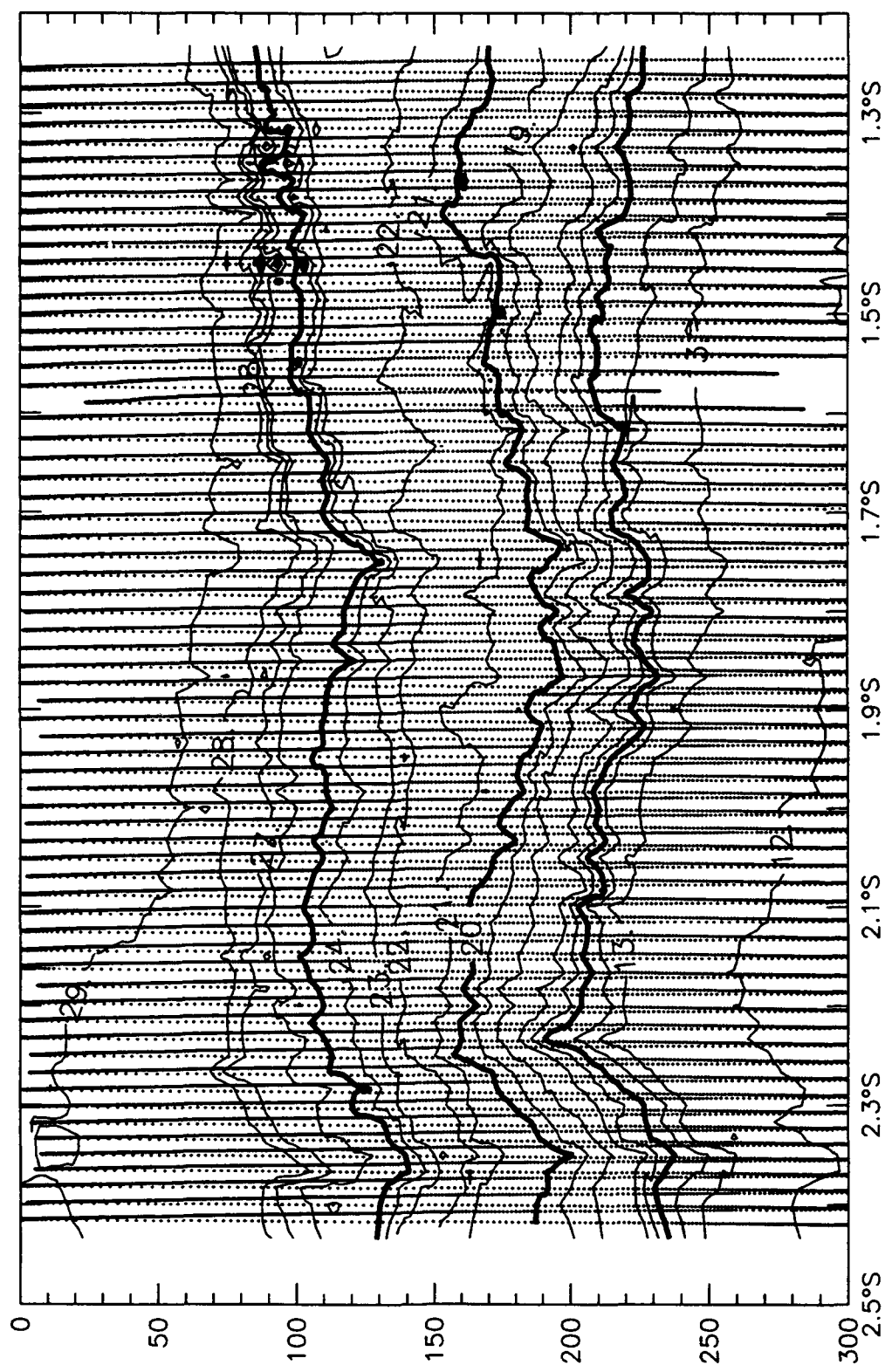
$T(^{\circ}\text{C})$ , N2S, 9 February 1993

$T(^{\circ}\text{C})$ , N2S, 10 February 1993

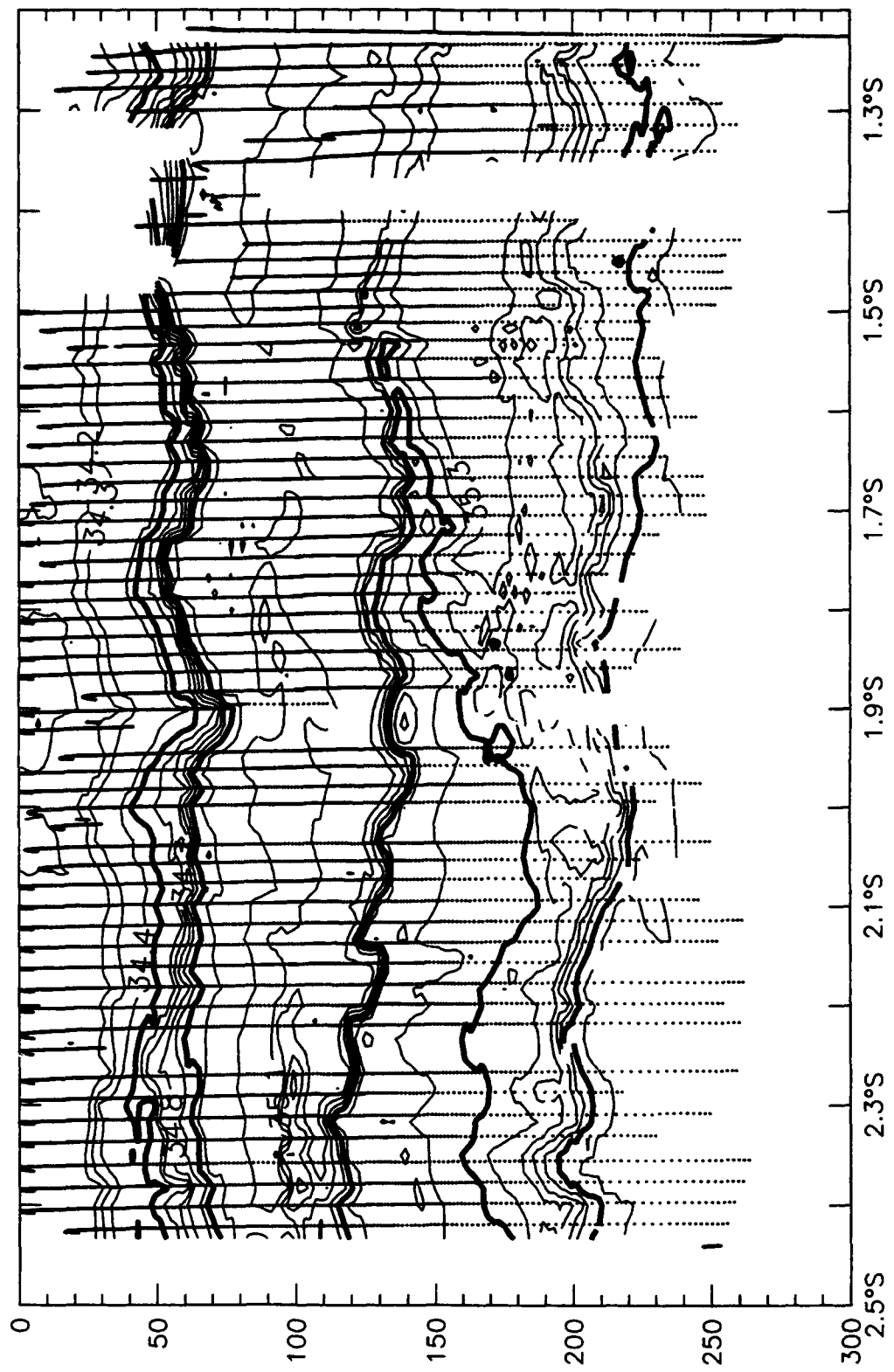




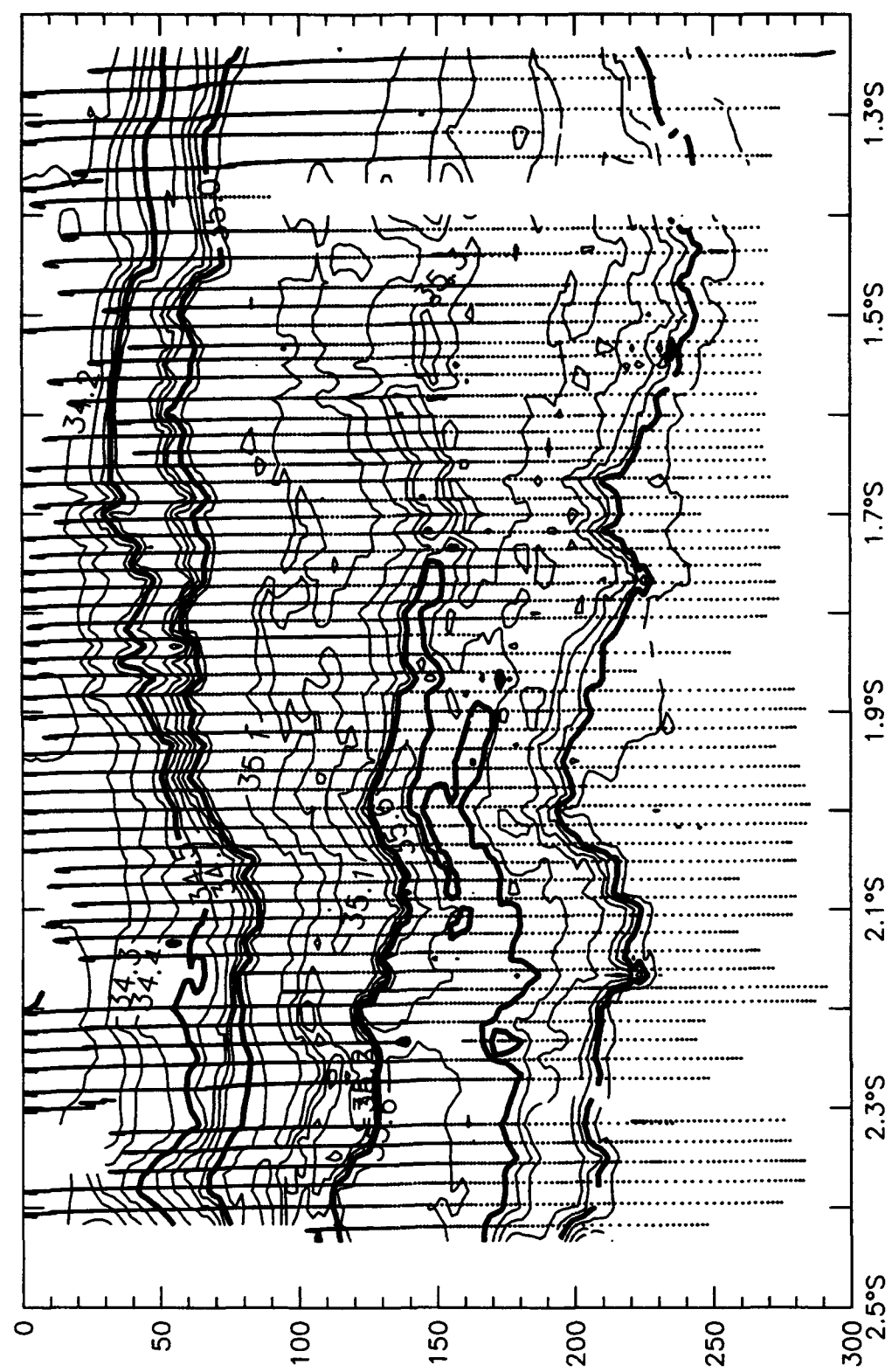
$T(^{\circ}\text{C})$ , N2S, 12 February 1993



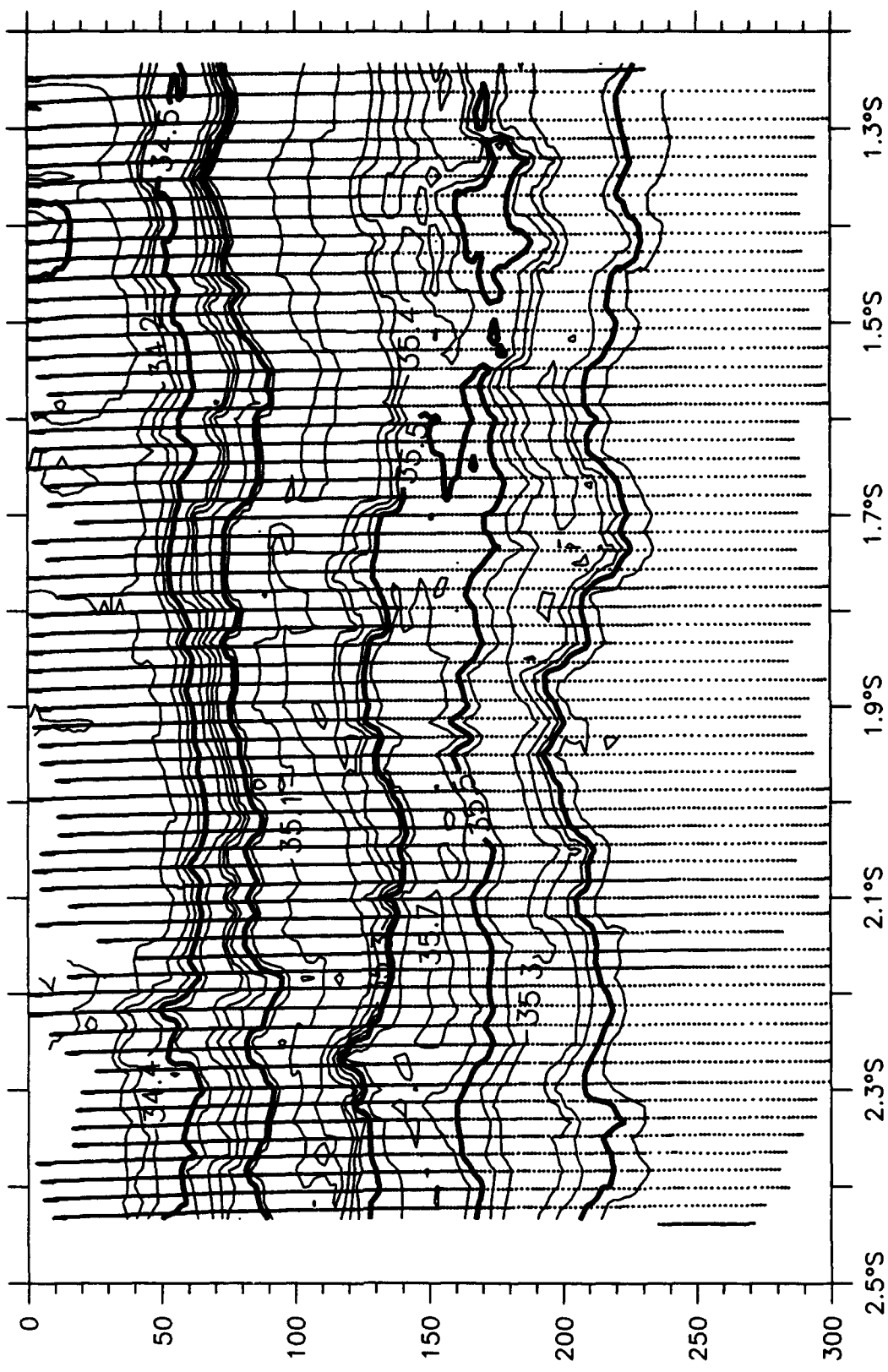
$T(^{\circ}\text{C})$ , N2S, 14 February 1993



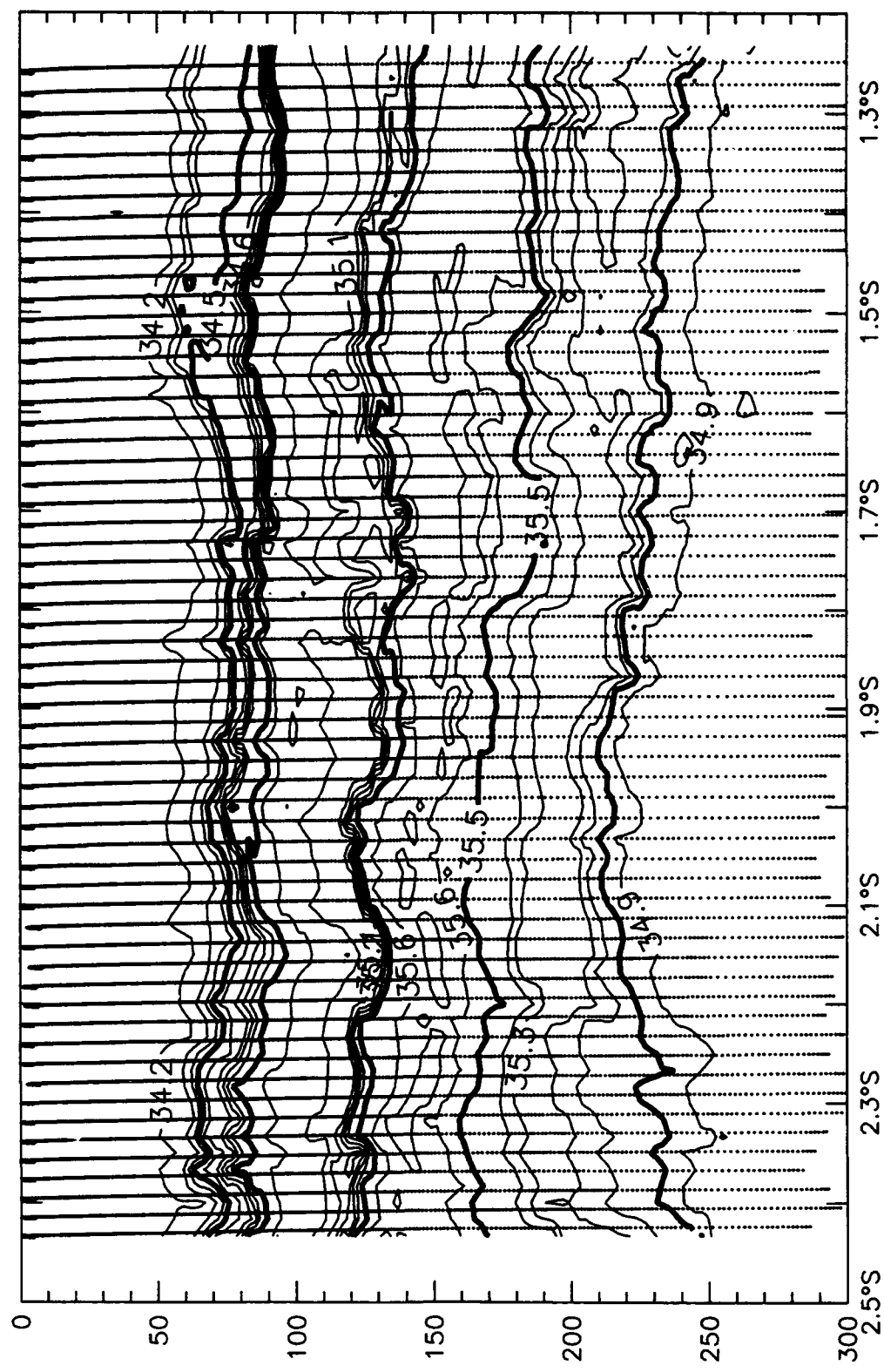
$S(\text{psu})$ , N2S, 27 January 1993



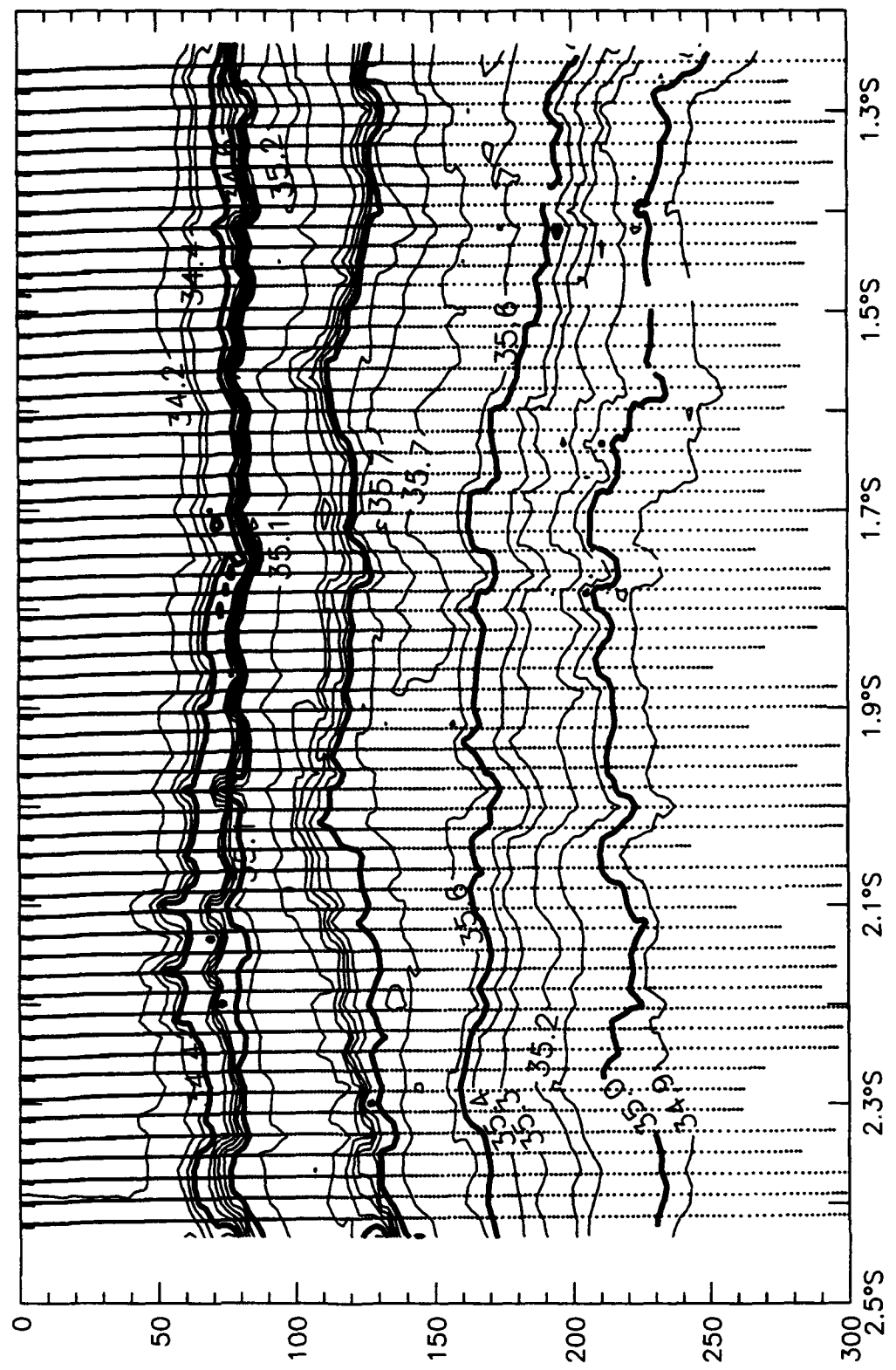
$S(\text{psu})$ ,  $N2S$ , 28 January 1993



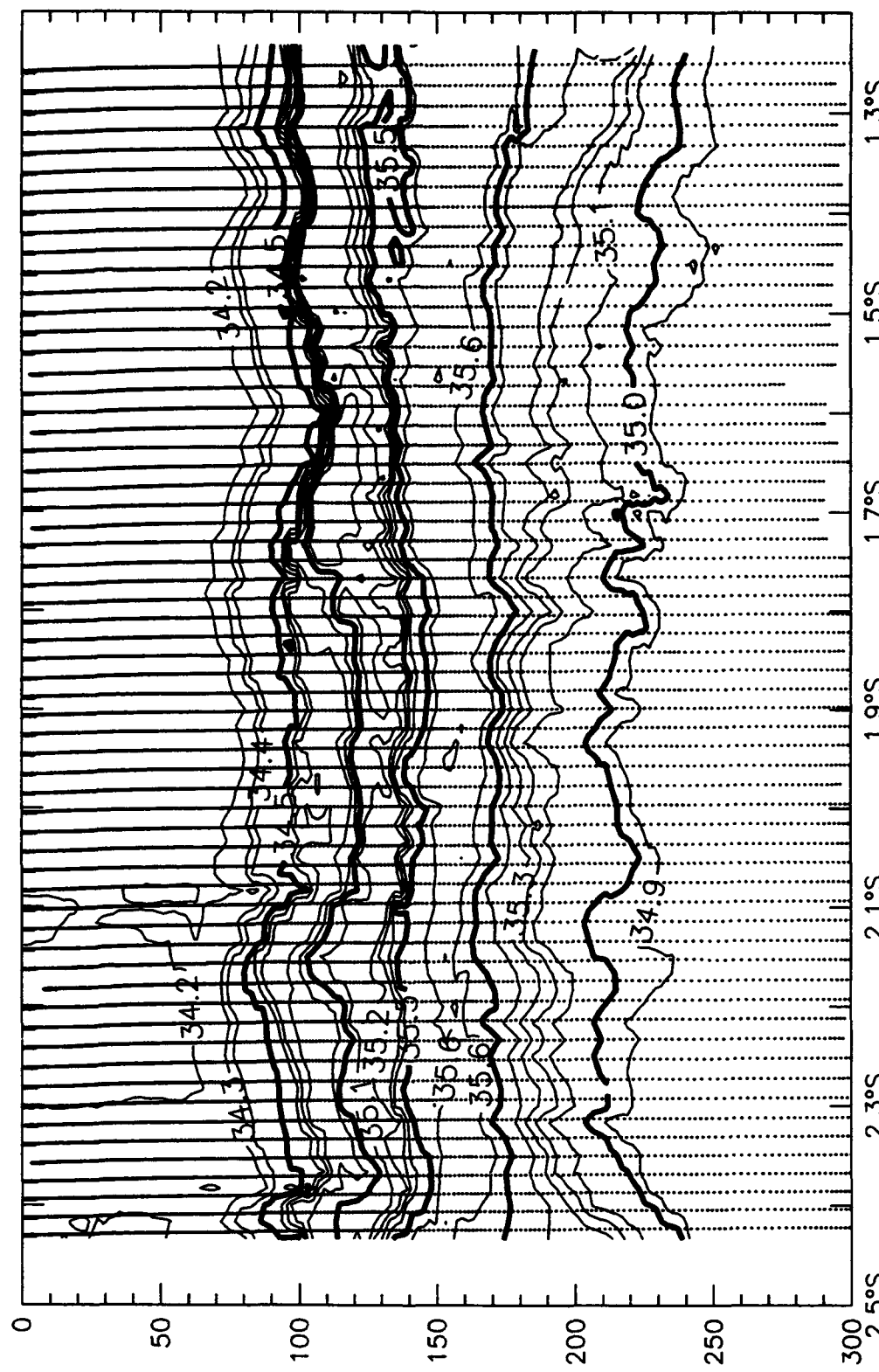
S(psu), N2S, 30 January 1993



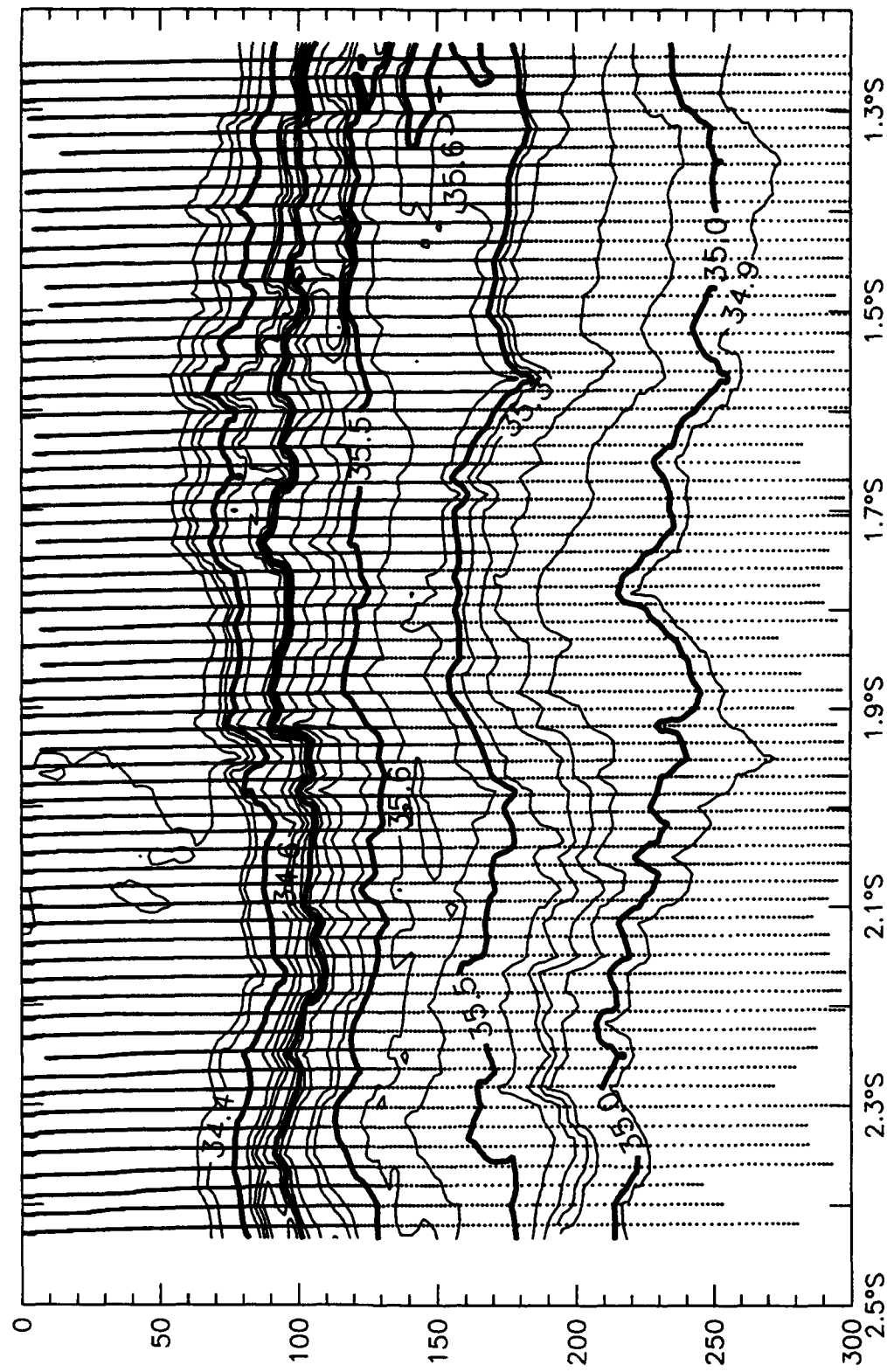
$S(\text{psu})$ , N2S, 31 January 1993



$S(\text{psu})$ , N2S, 2 February 1993

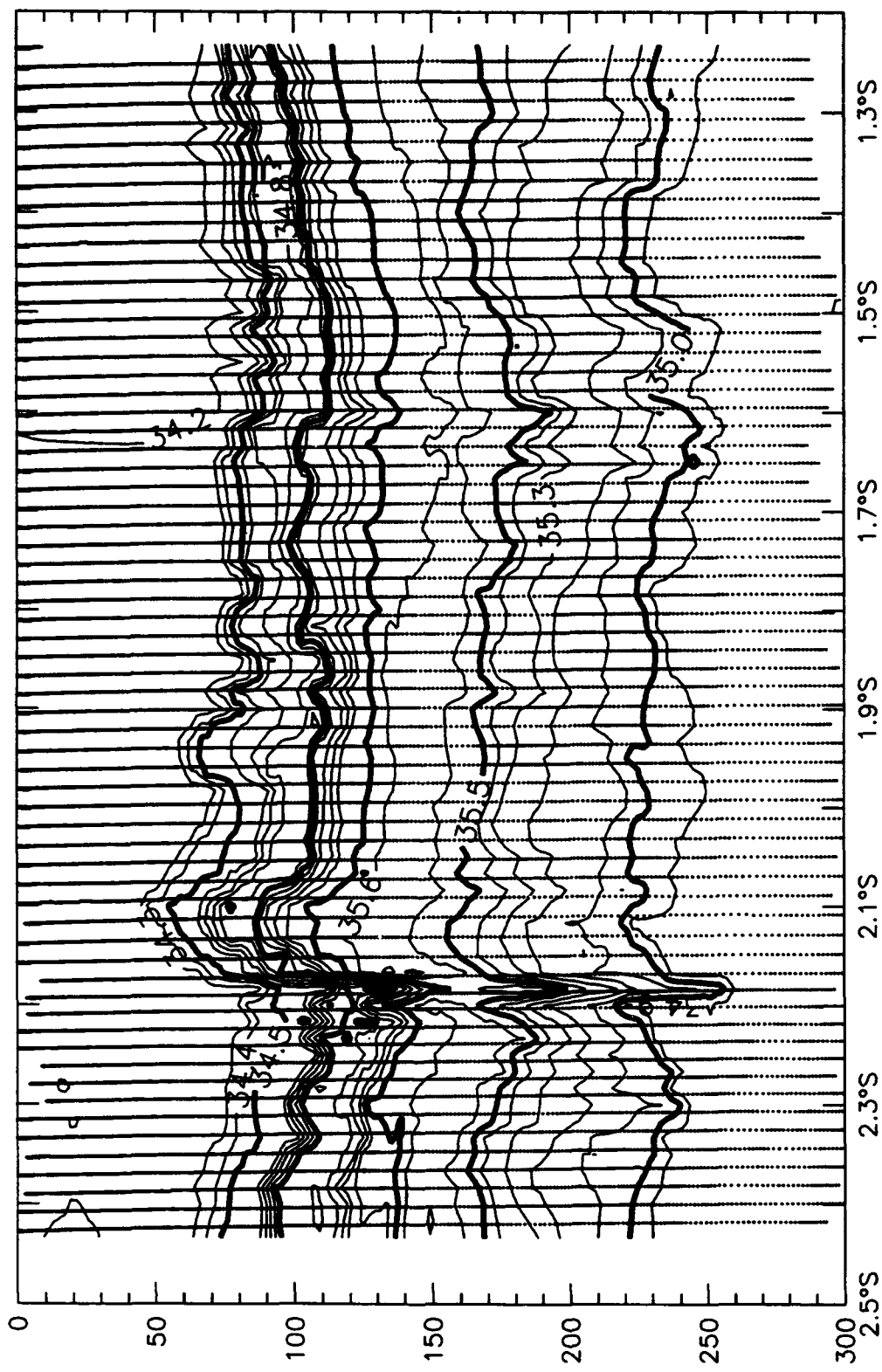


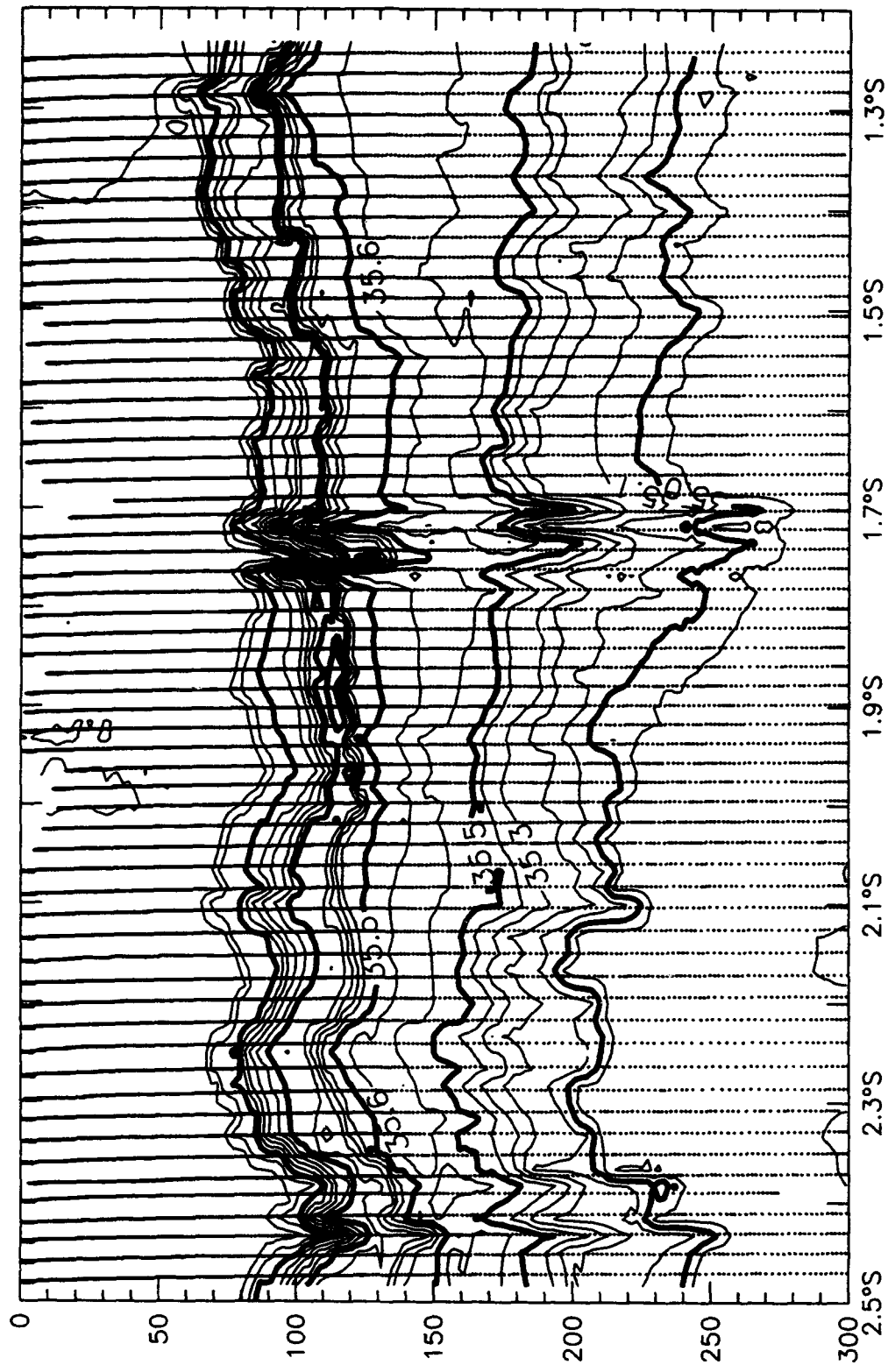
$S(\text{psu})$ , N2S, 4 February 1993



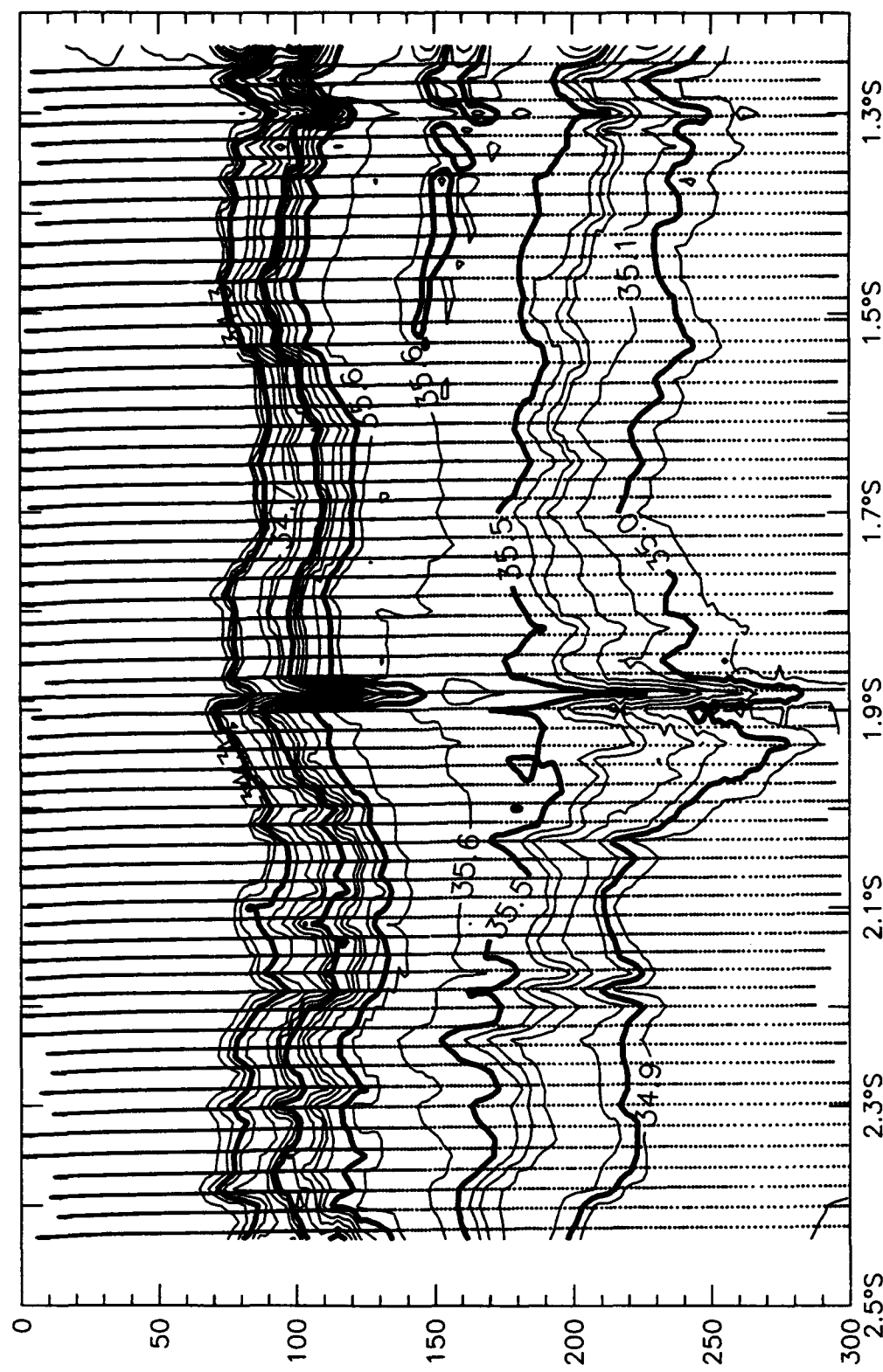
$S(\text{psu})$ , N2S, 5 February 1993

$S(\text{psu})$ , N2S, 7 February 1993

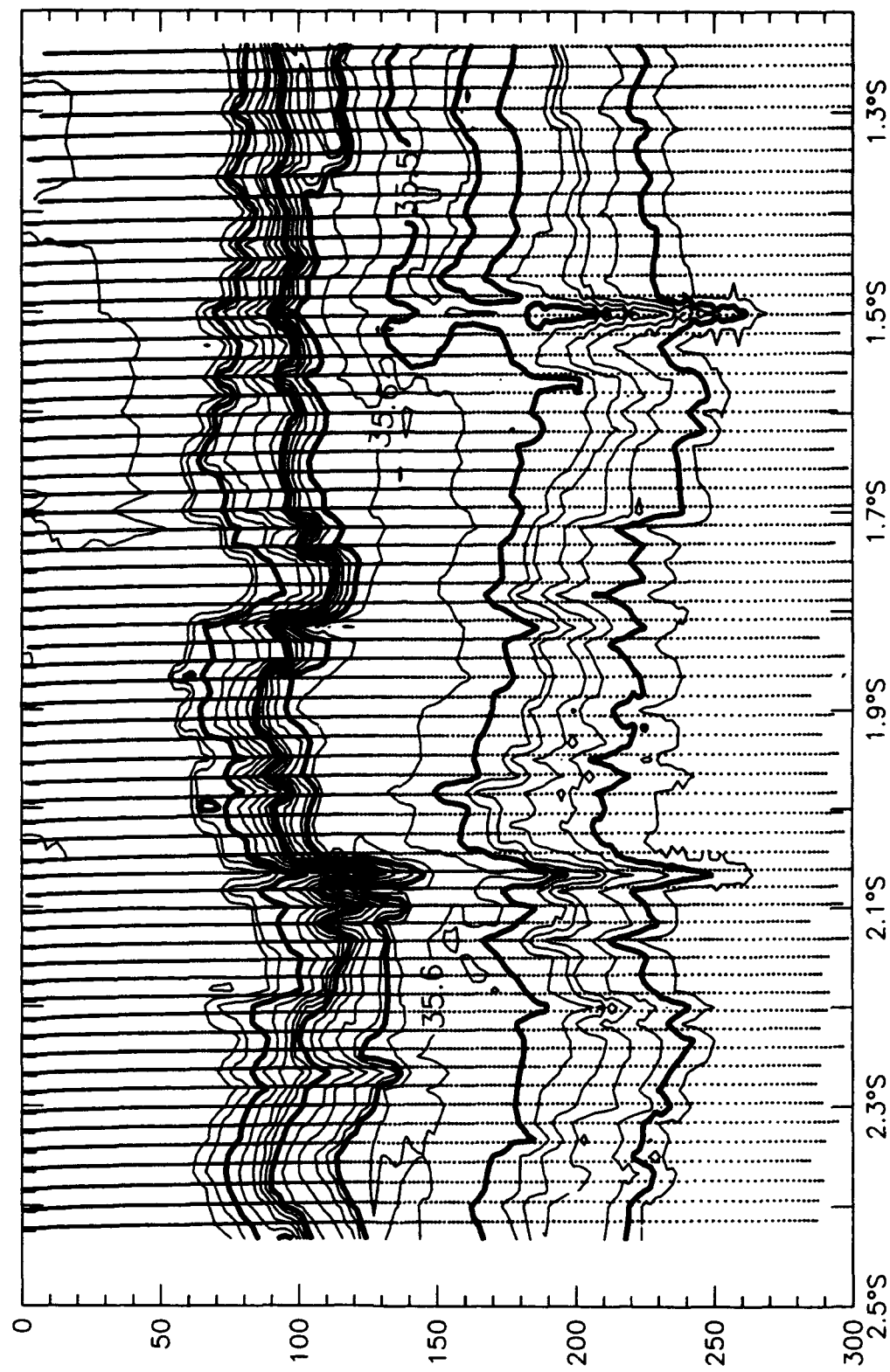




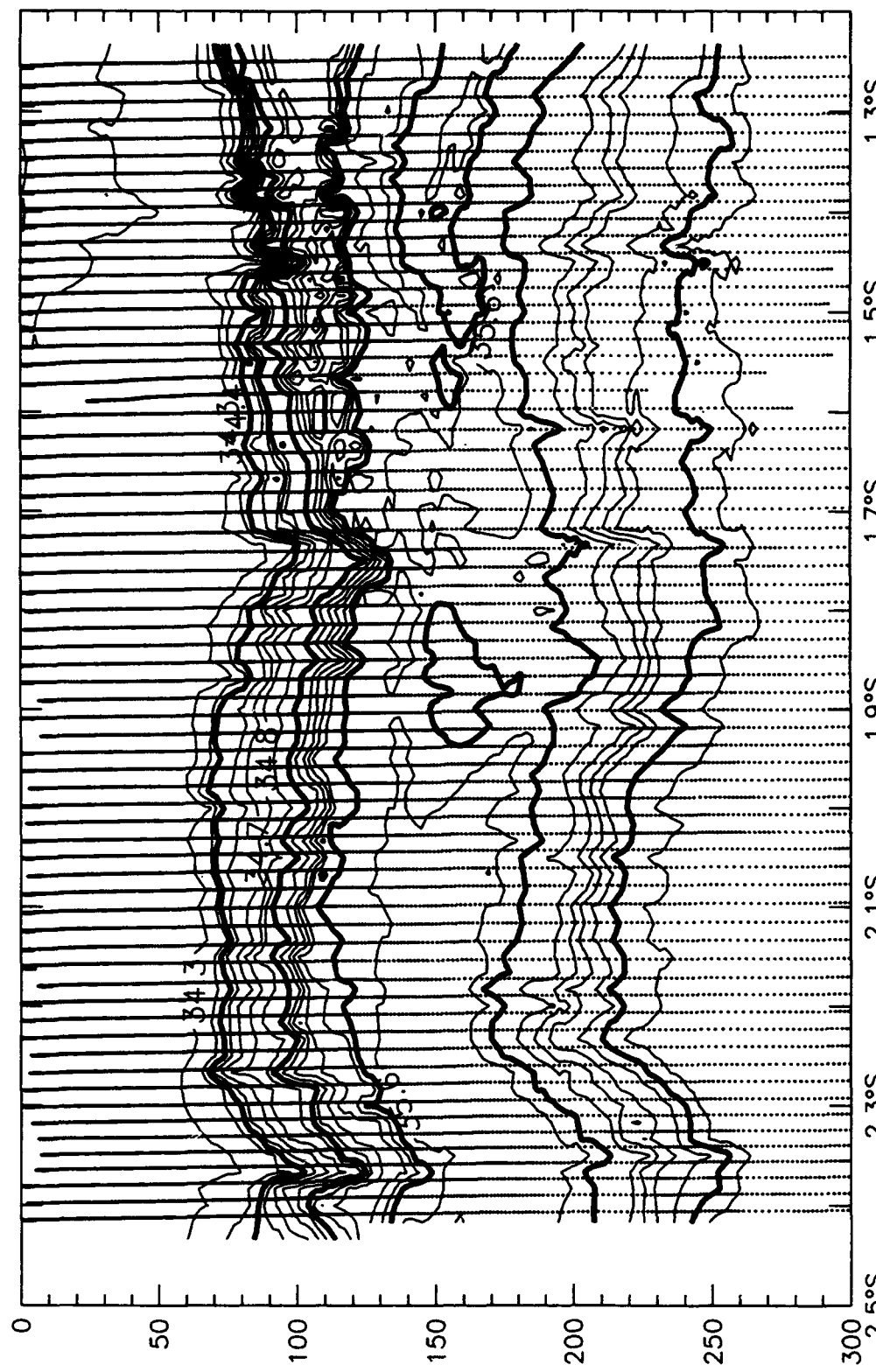
$S(\text{psu})$ , N2S, 9 February 1993



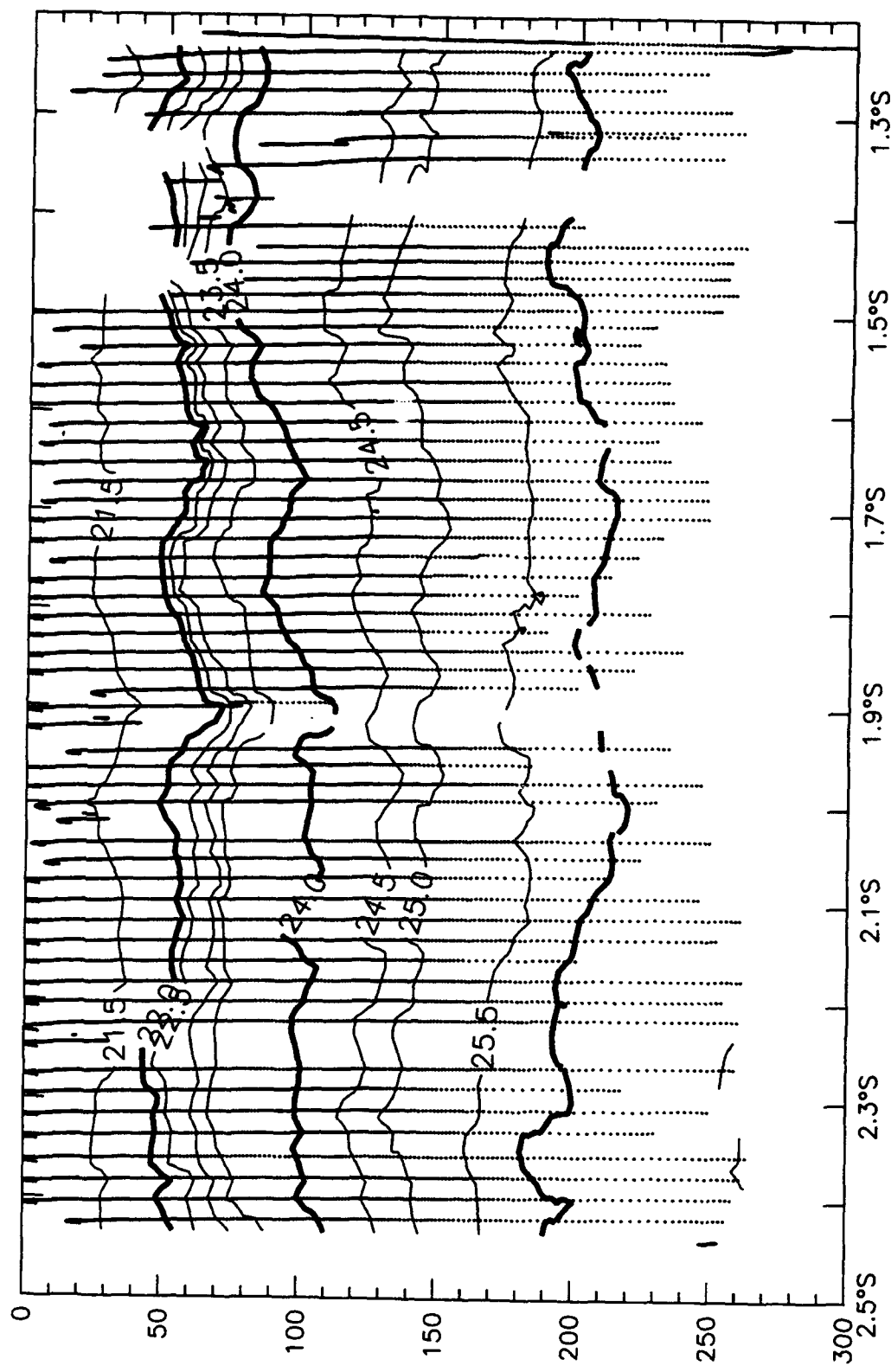
$S(\text{psu})$ , N2S, 10 February 1993



$S(\text{psu})$ , N2S, 12 February 1993

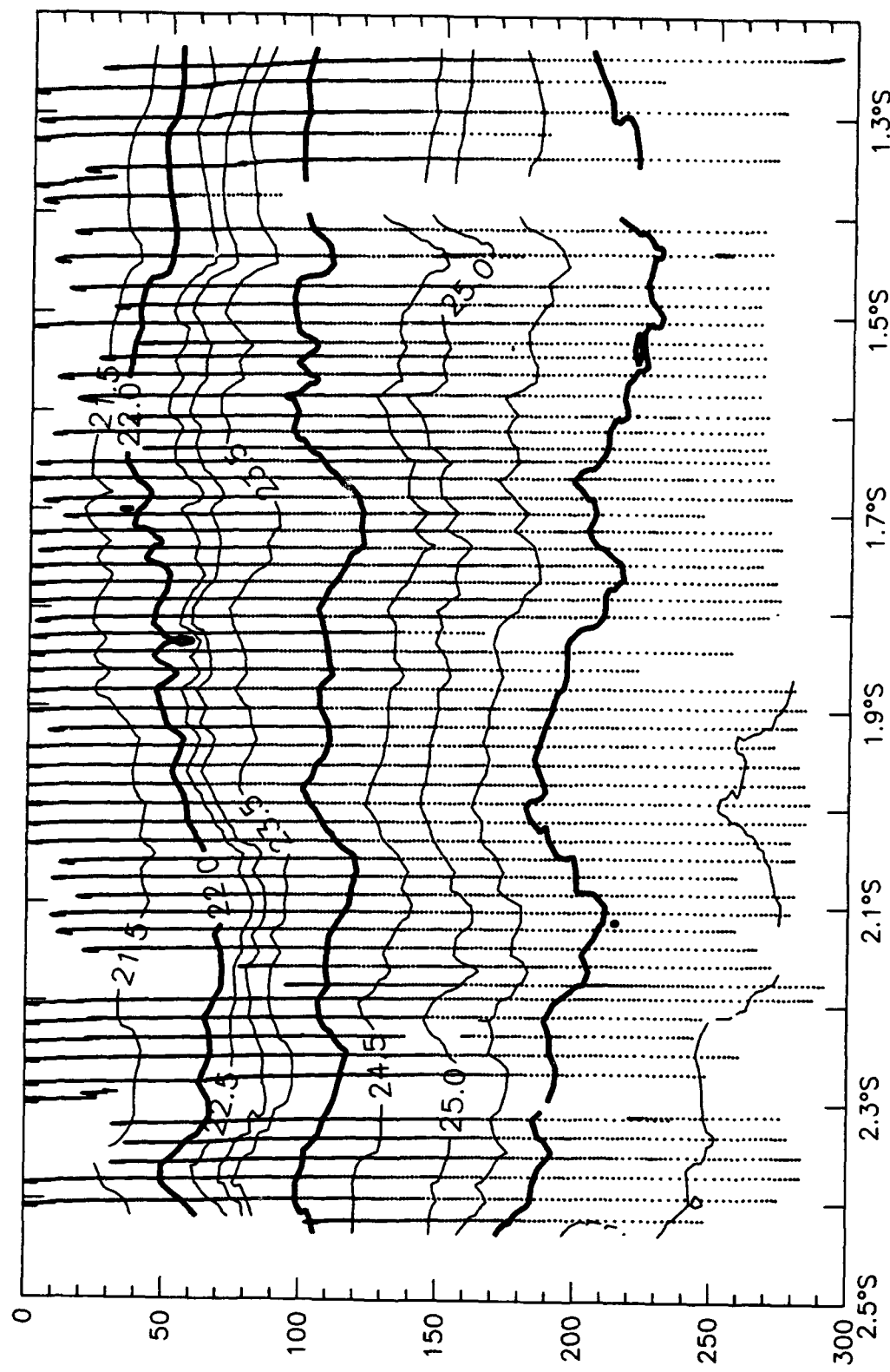


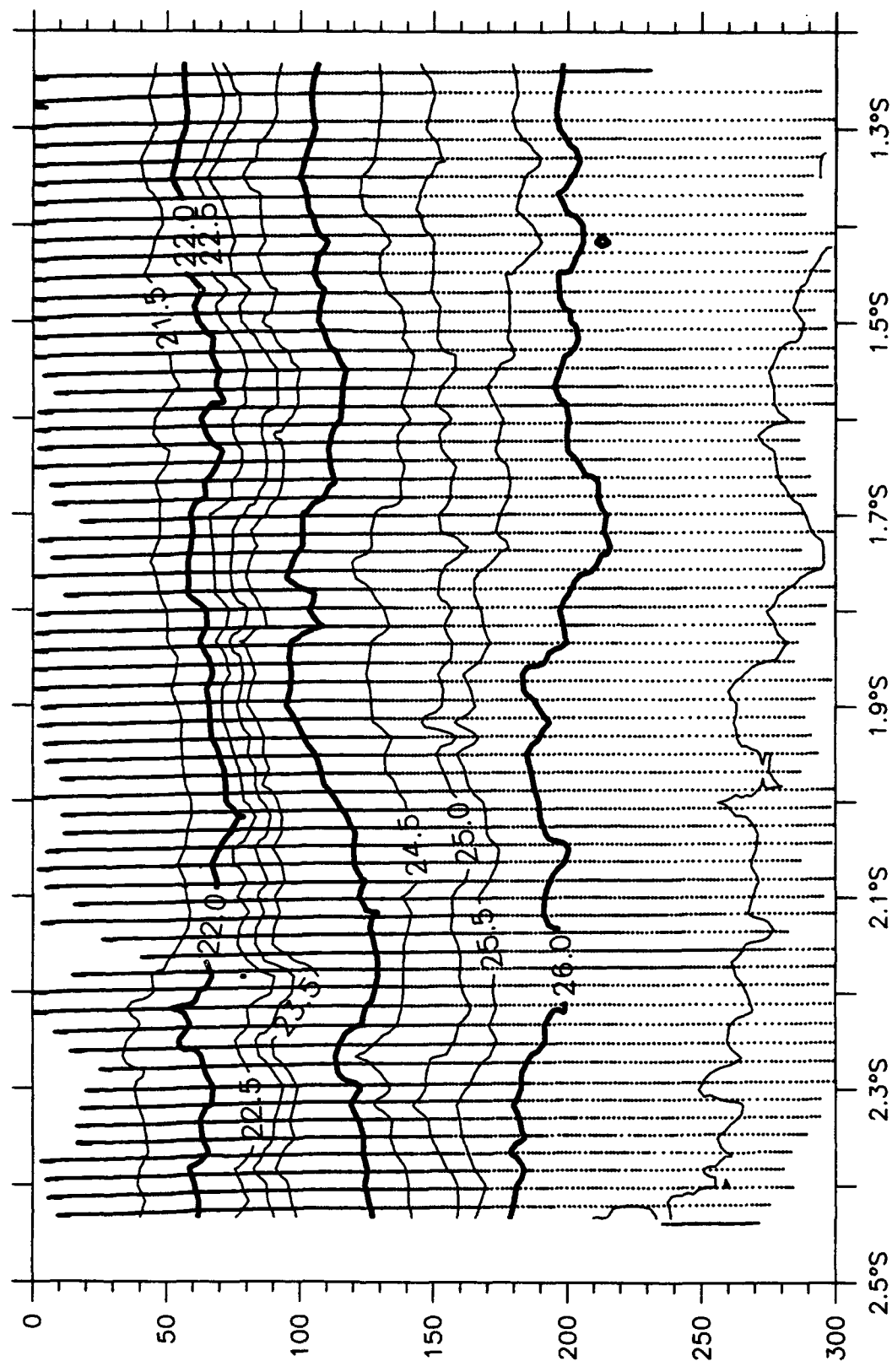
$S(\text{psu})$ ,  $\text{N}2\text{S}$ , 14 February 1993



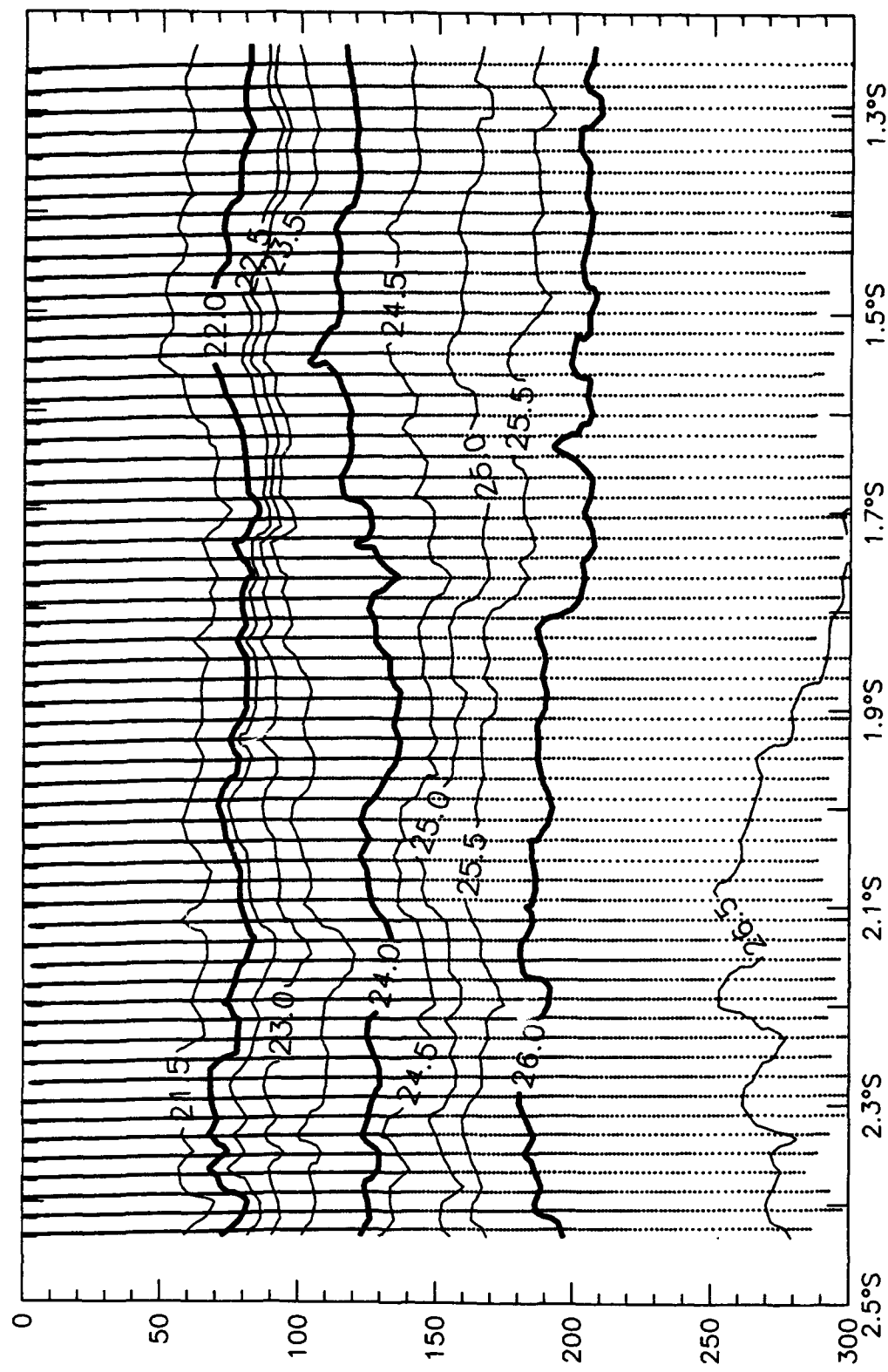
Sigma-t, N2S, 27 January 1993

Sigma-t, N2S, 28 January 1993

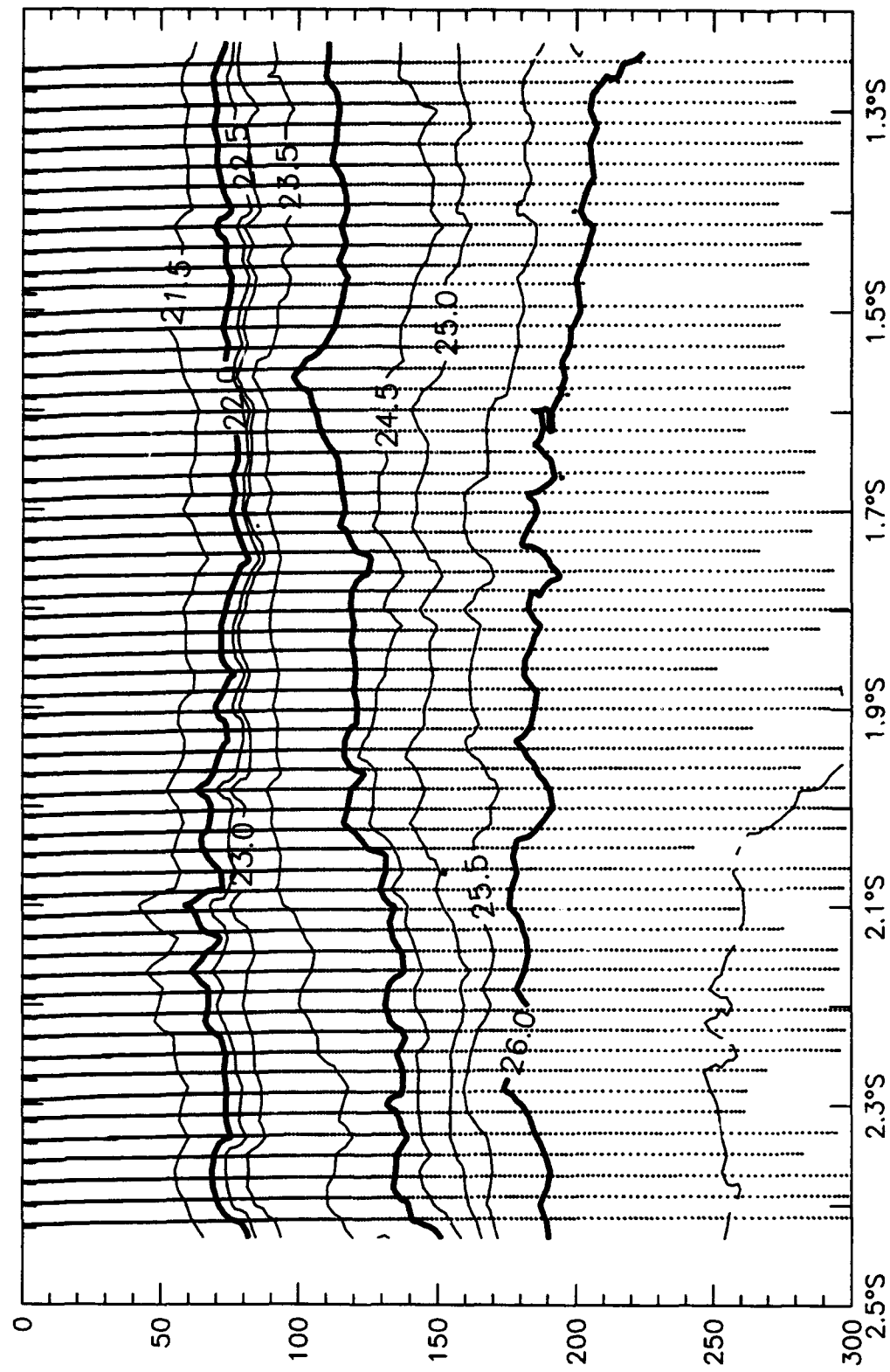




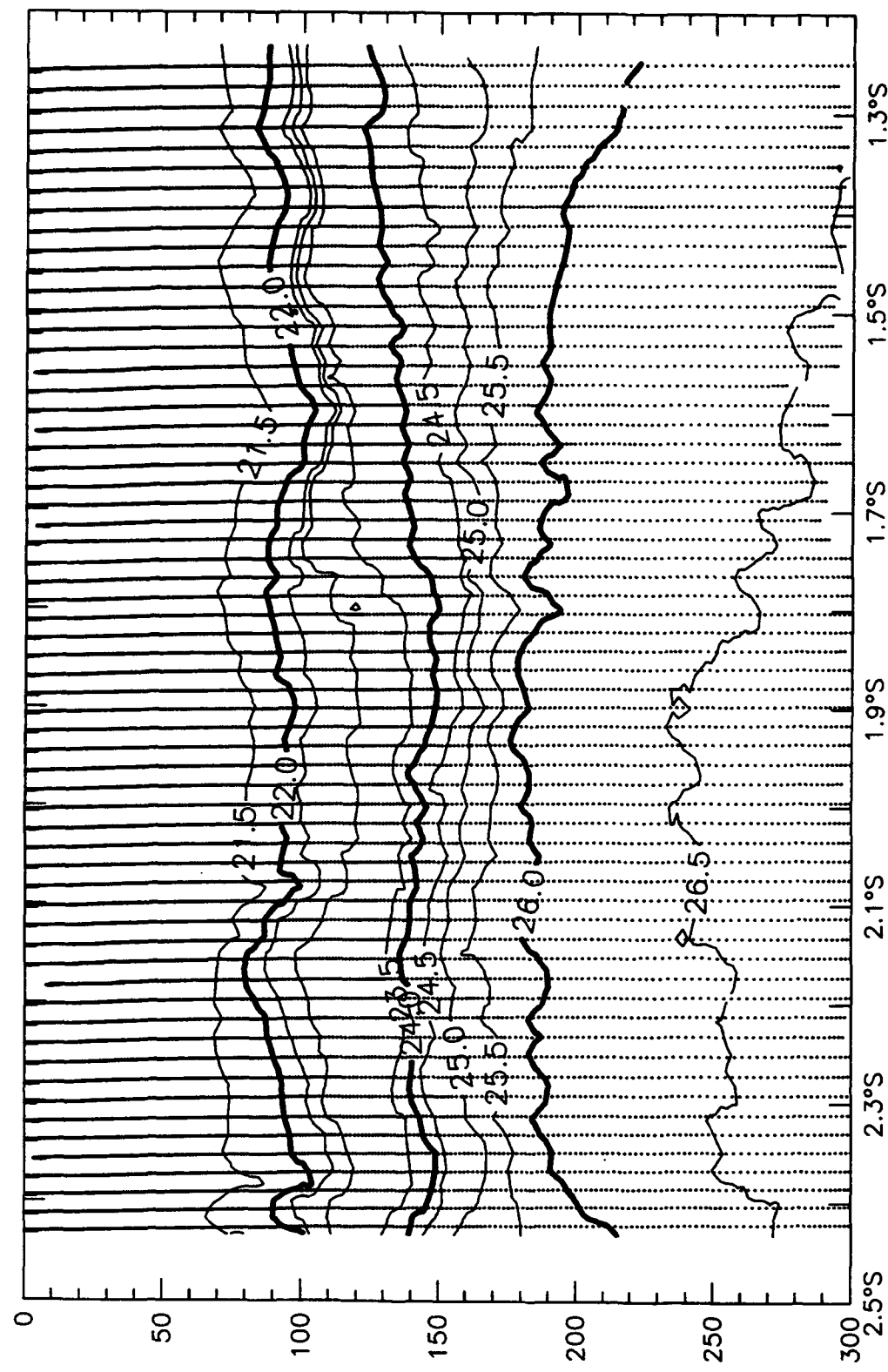
Sigma-t, N2S, 30 January 1993



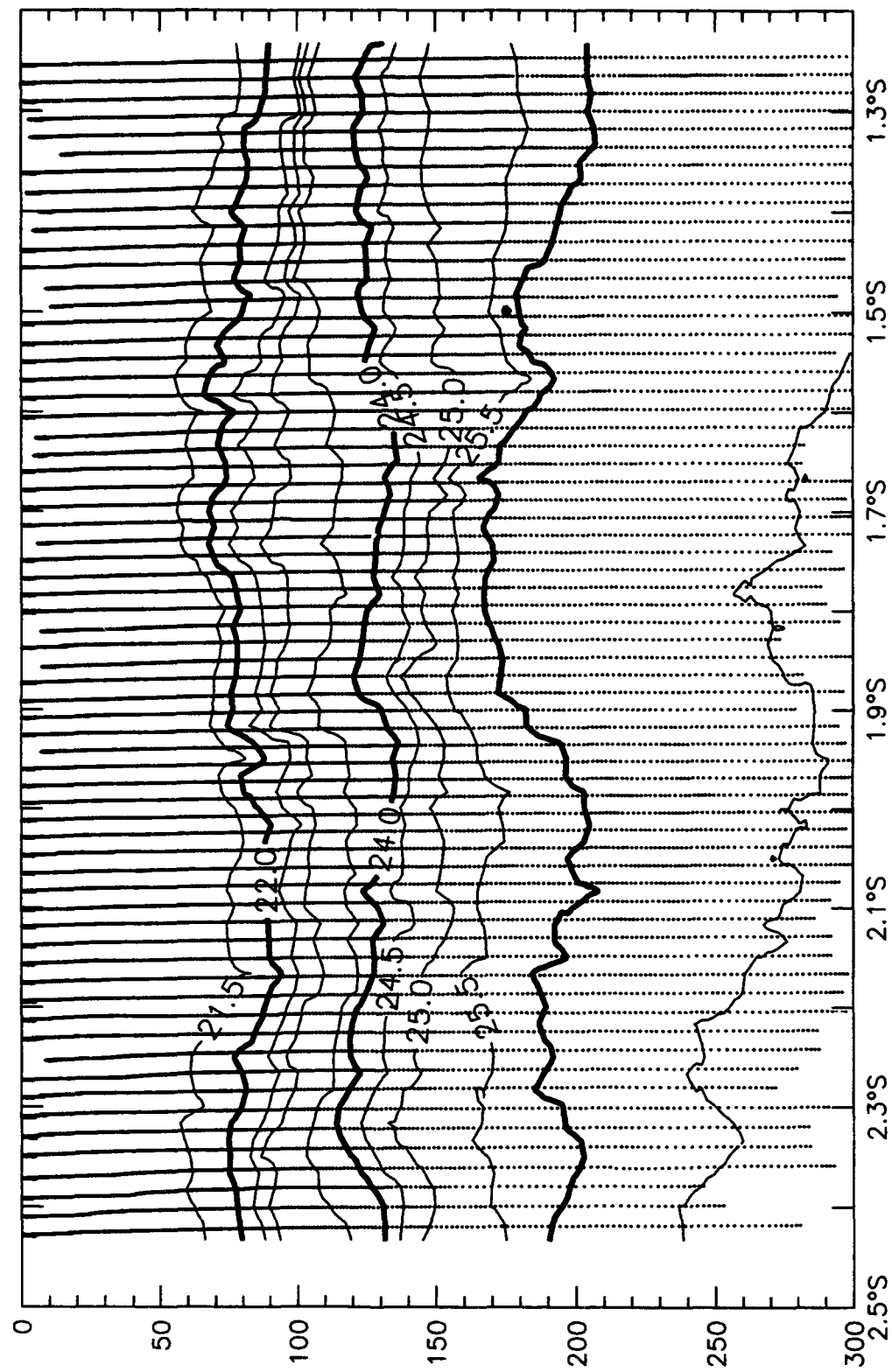
Sigma-t, N2S, 31 January 1993



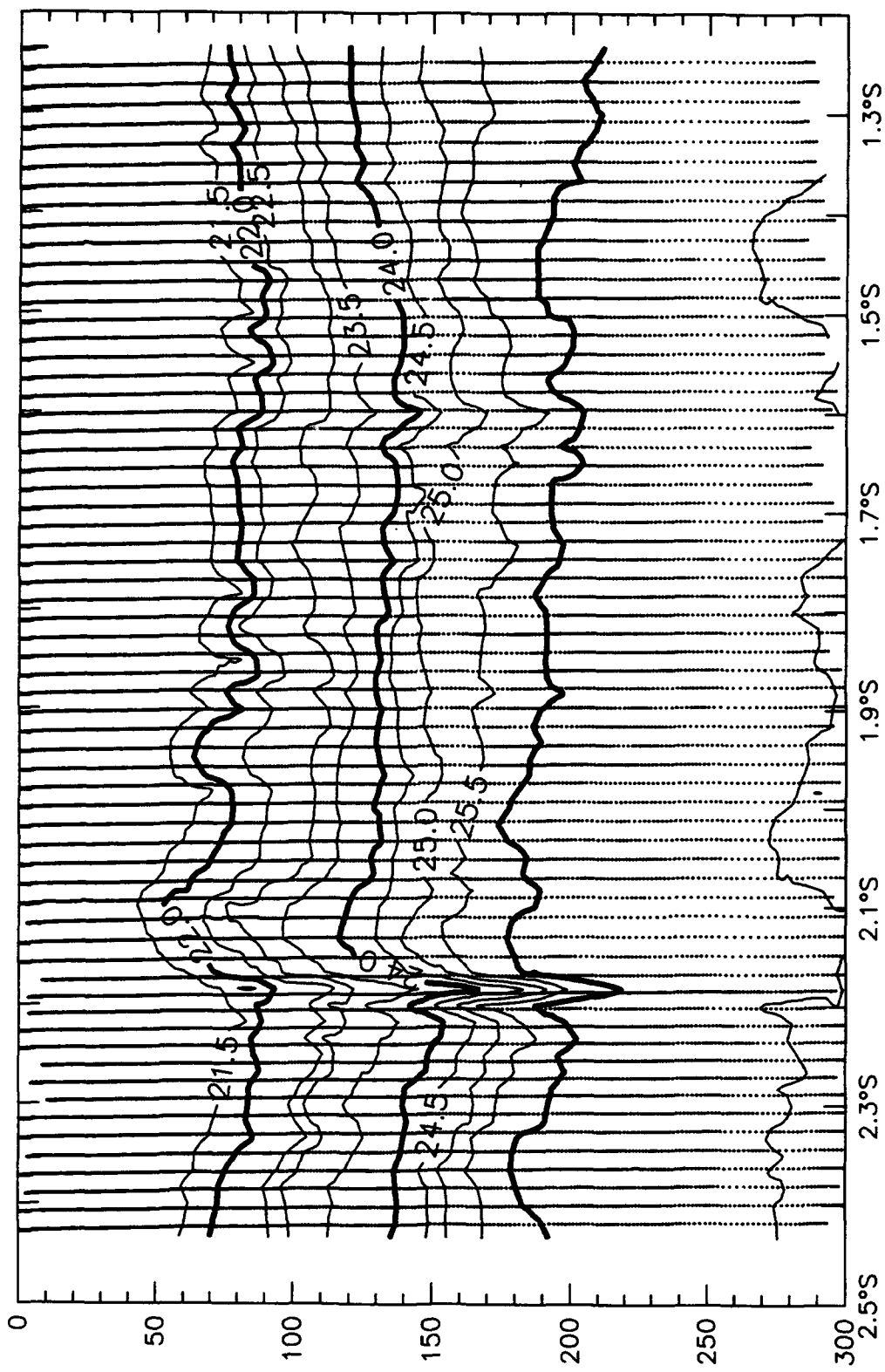
Sigma-t, N2S, ? February 1993



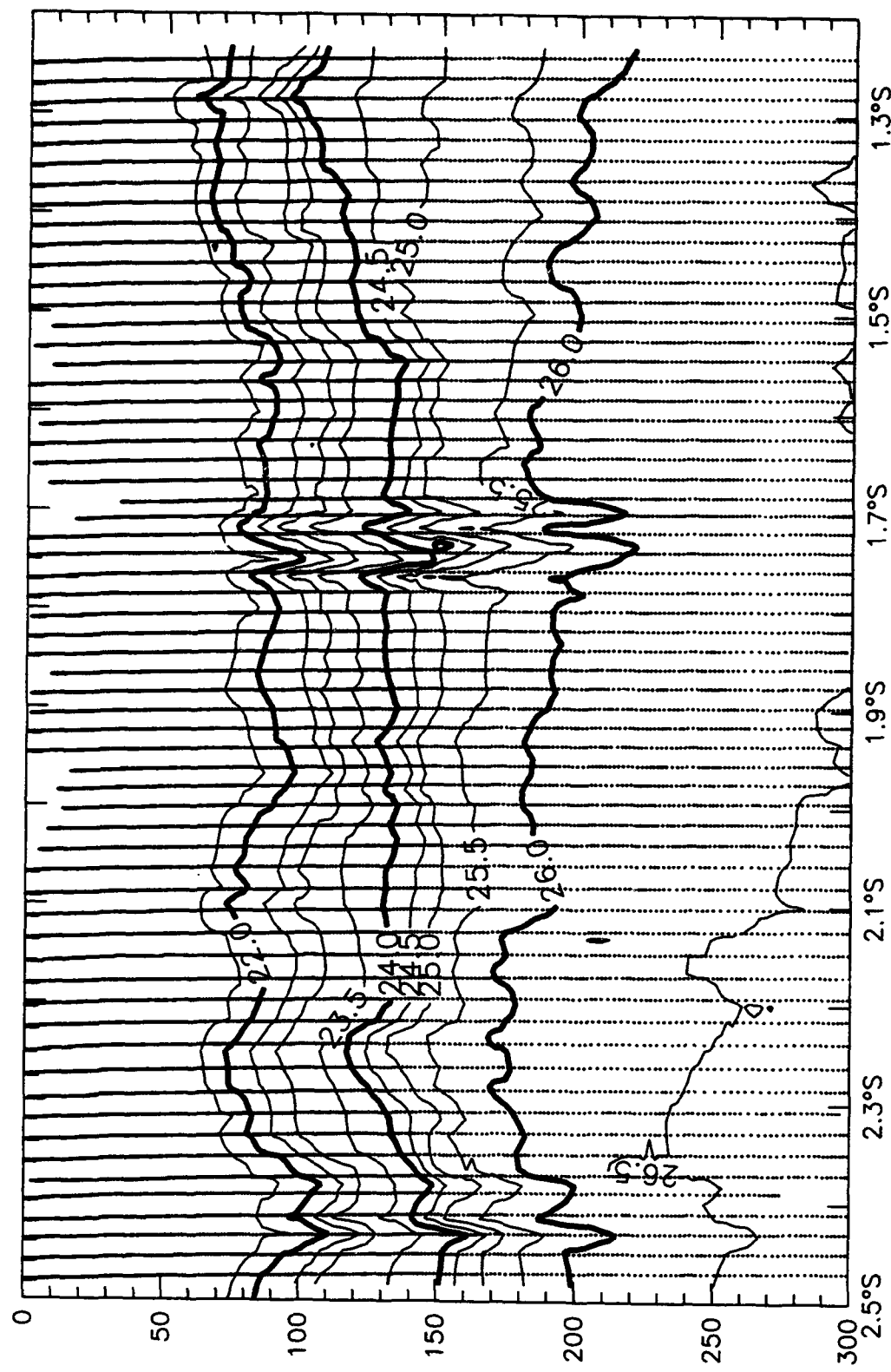
Sigma-t, N2S, 4 February 1993



Sigma-t, N2S, 5 February 1993

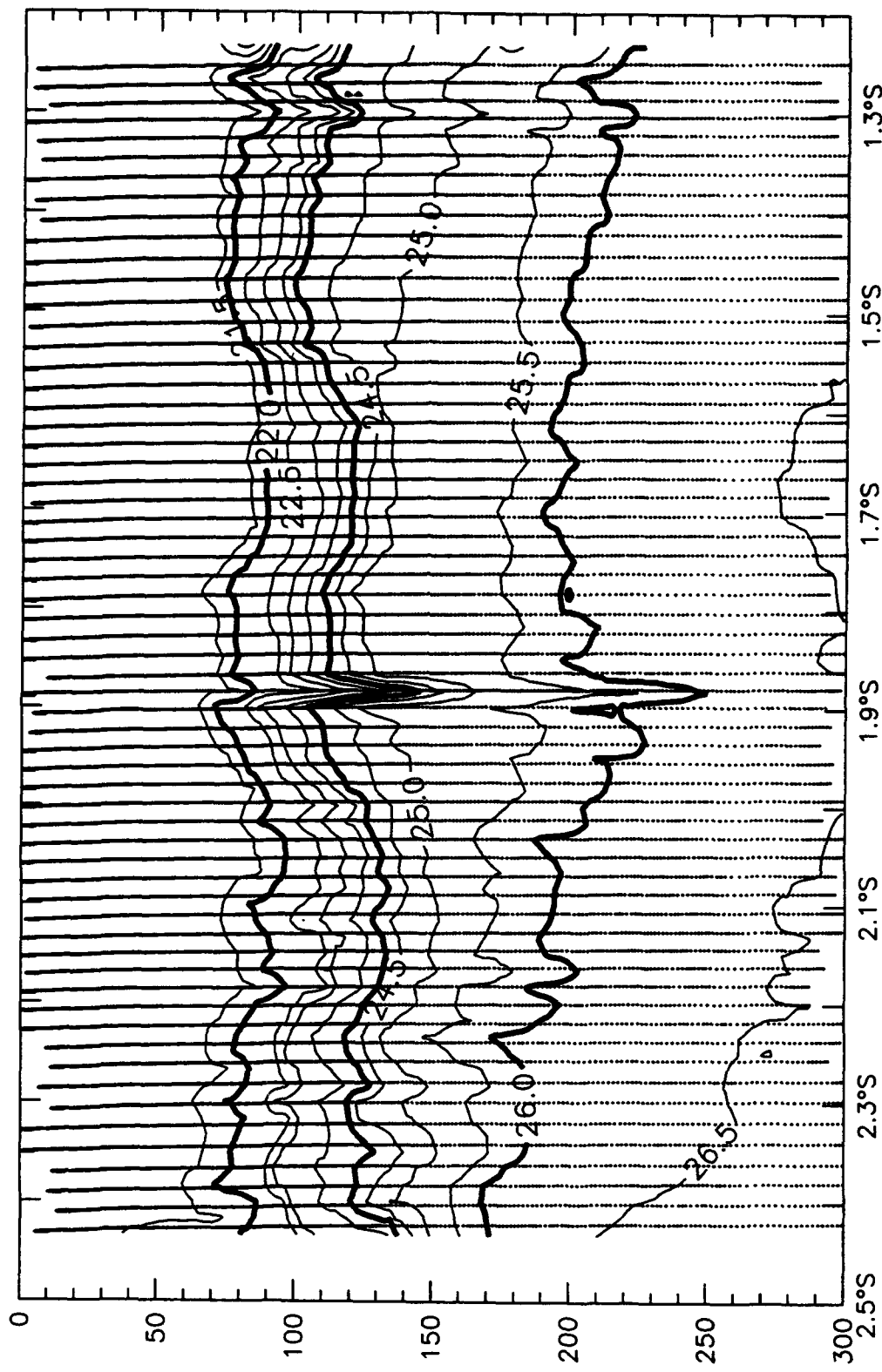


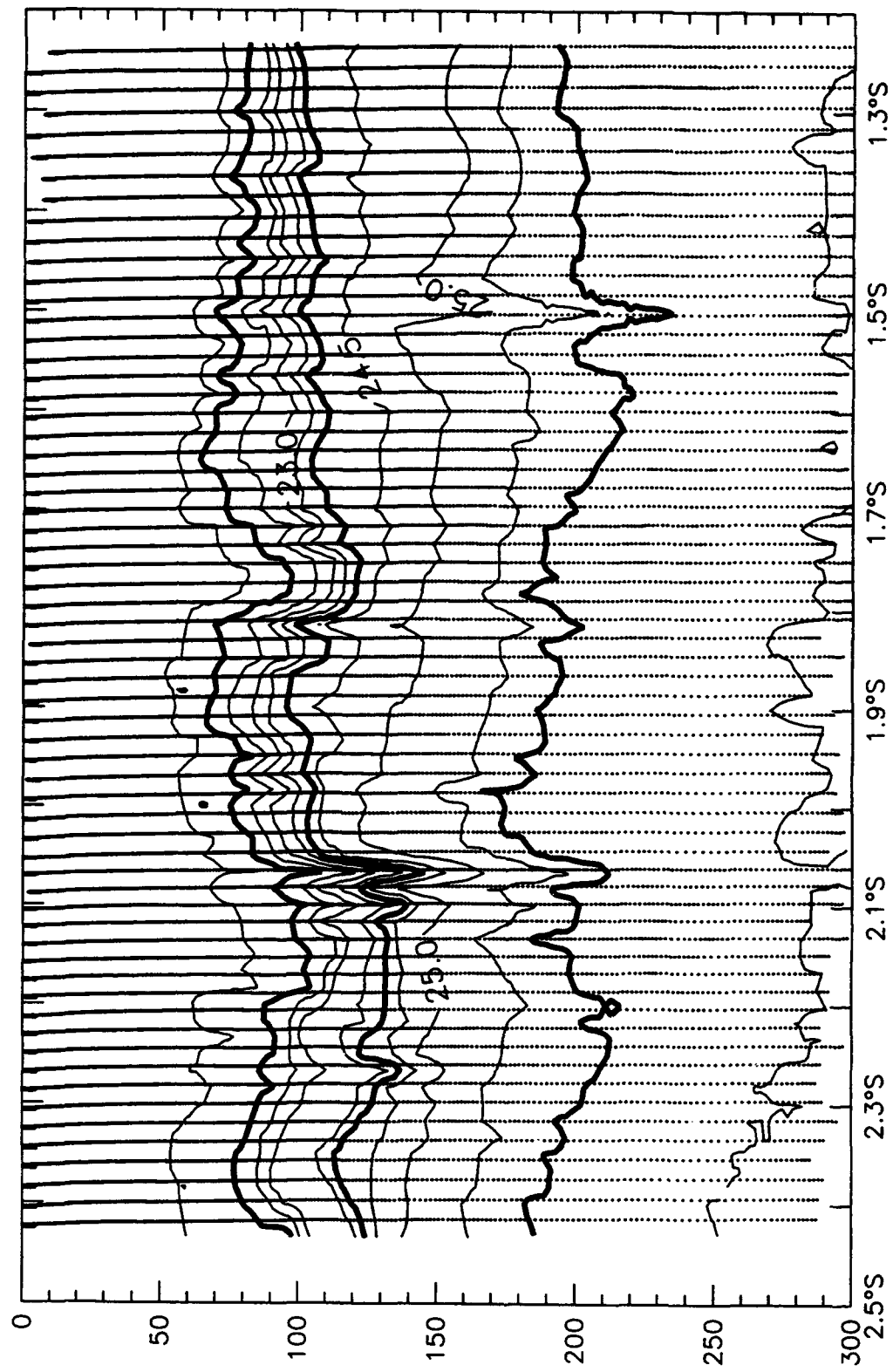
Sigma-t, N2S, 7 February 1993



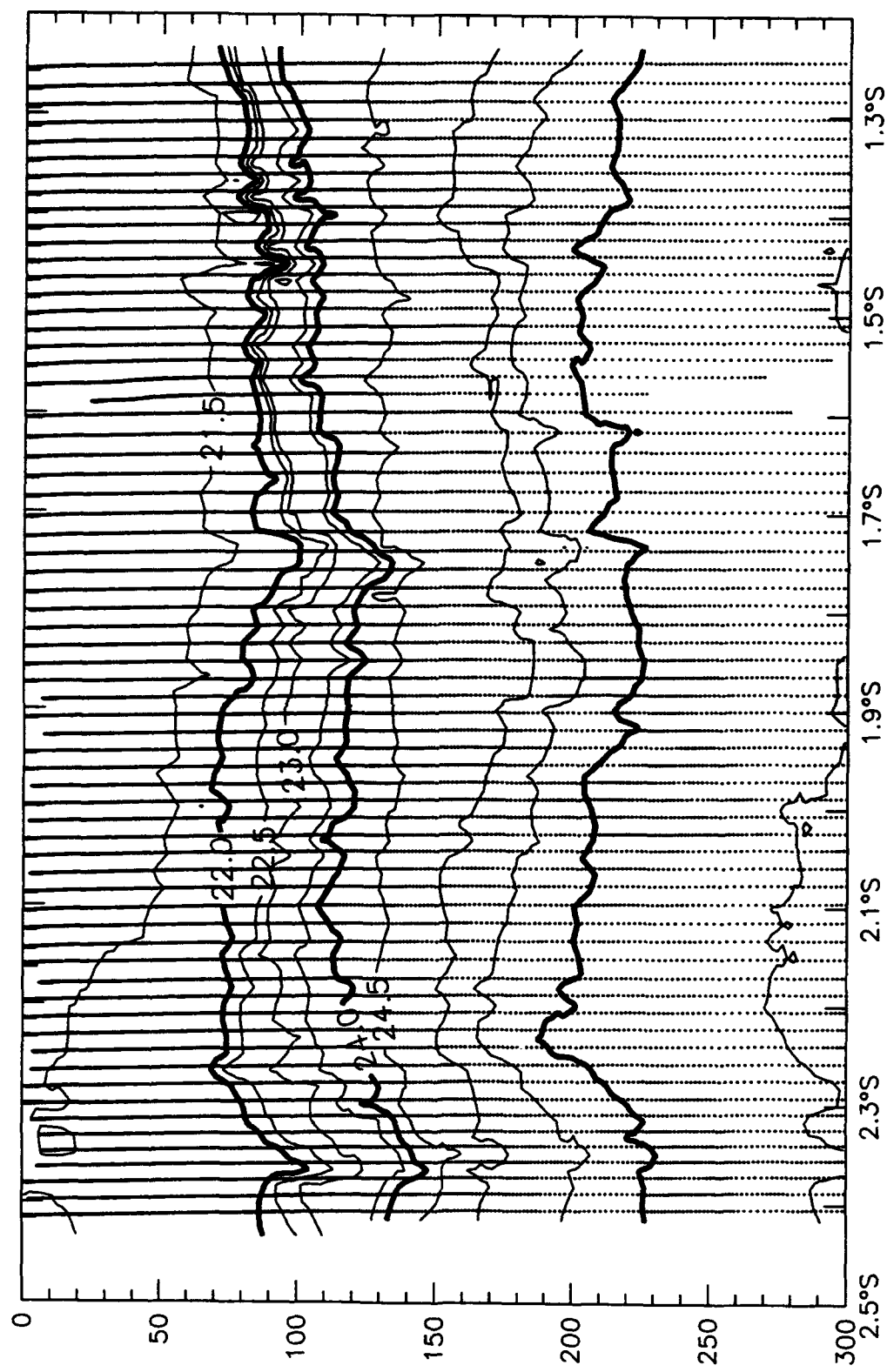
Sigma-t, N2S, 9 February 1993

Sigma-t, N2S, 10 February 1993

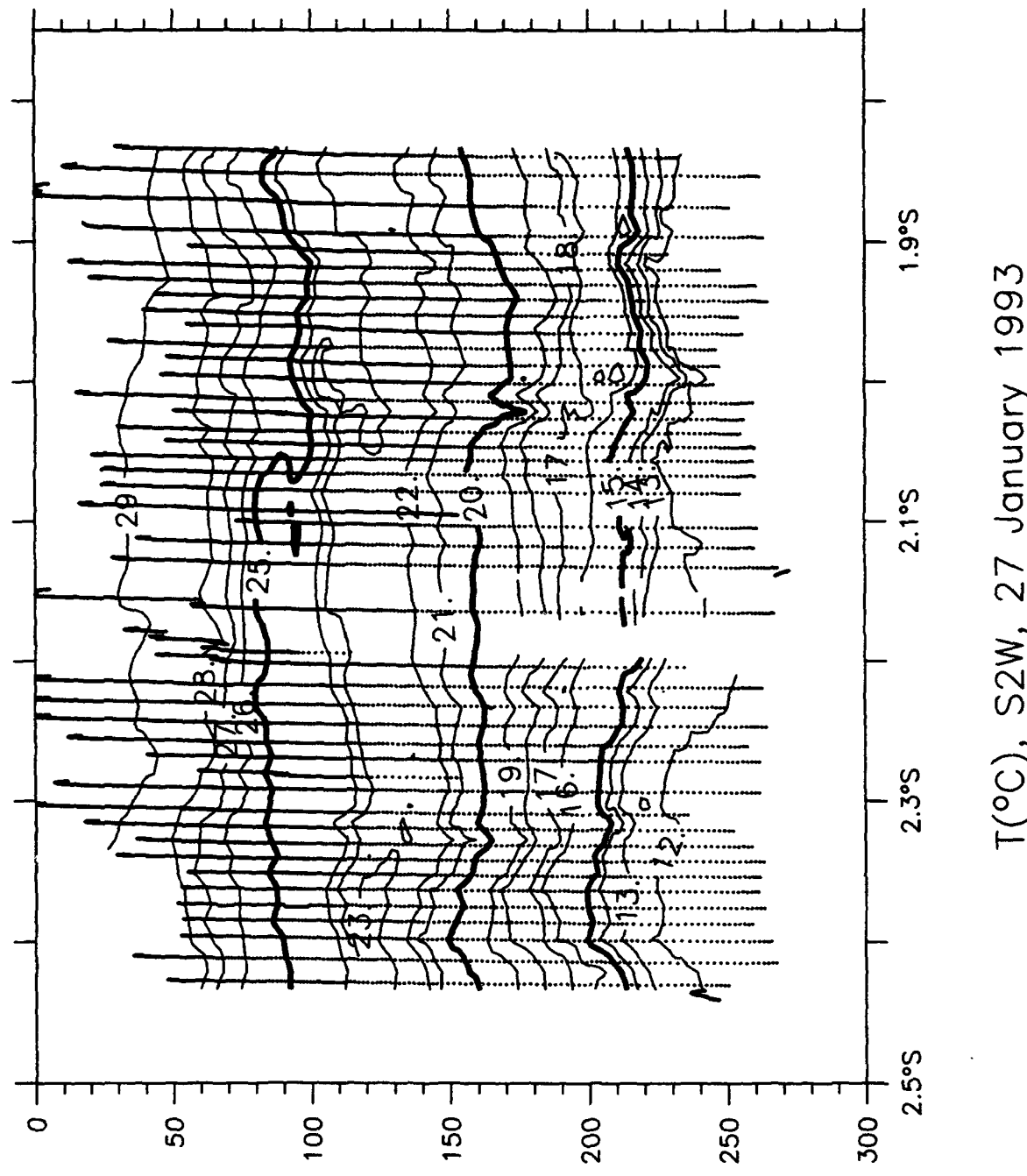


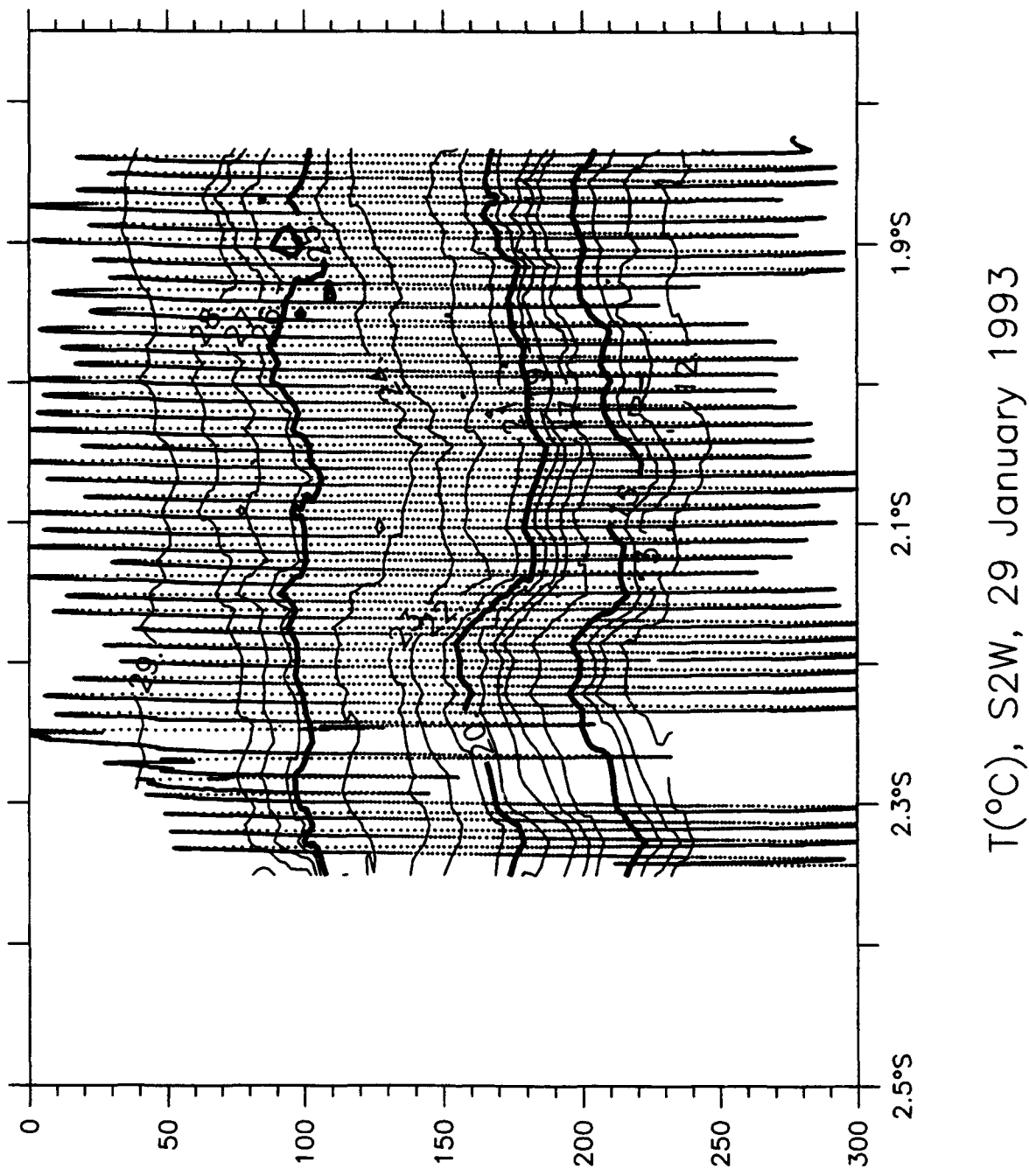


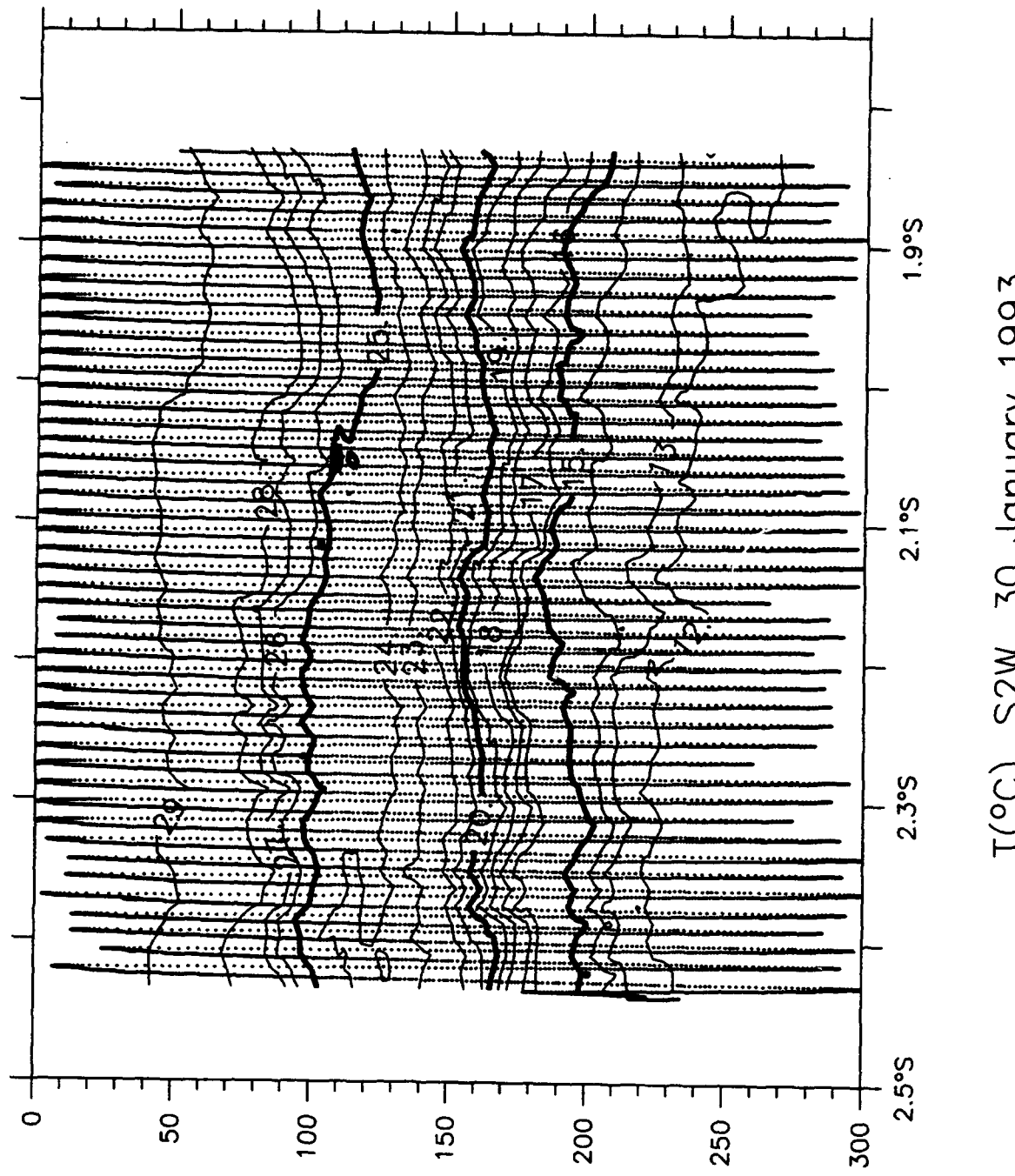
Sigma-t, N2S, 12 February 1993

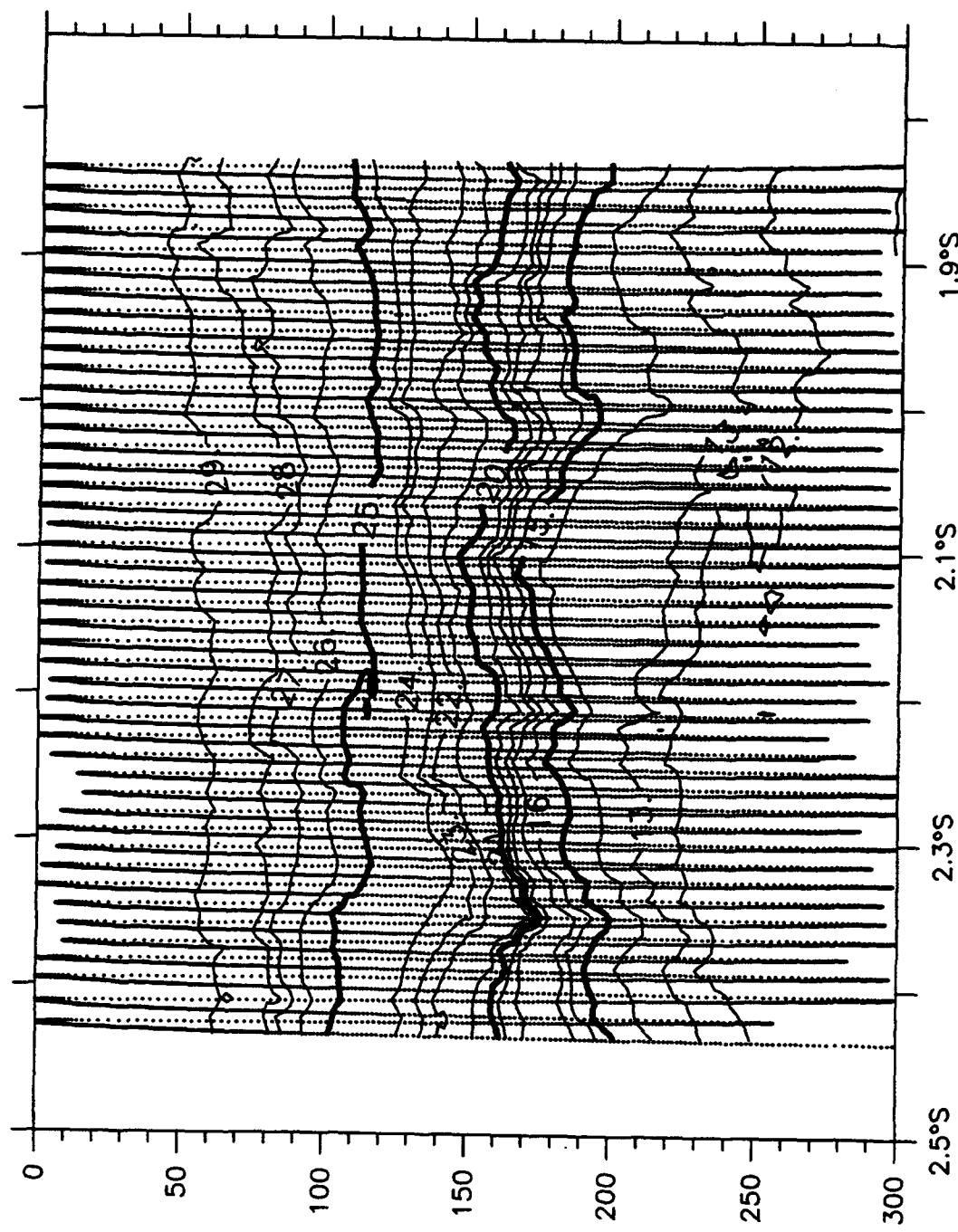


Sigma-t, N2S, 14 February 1993

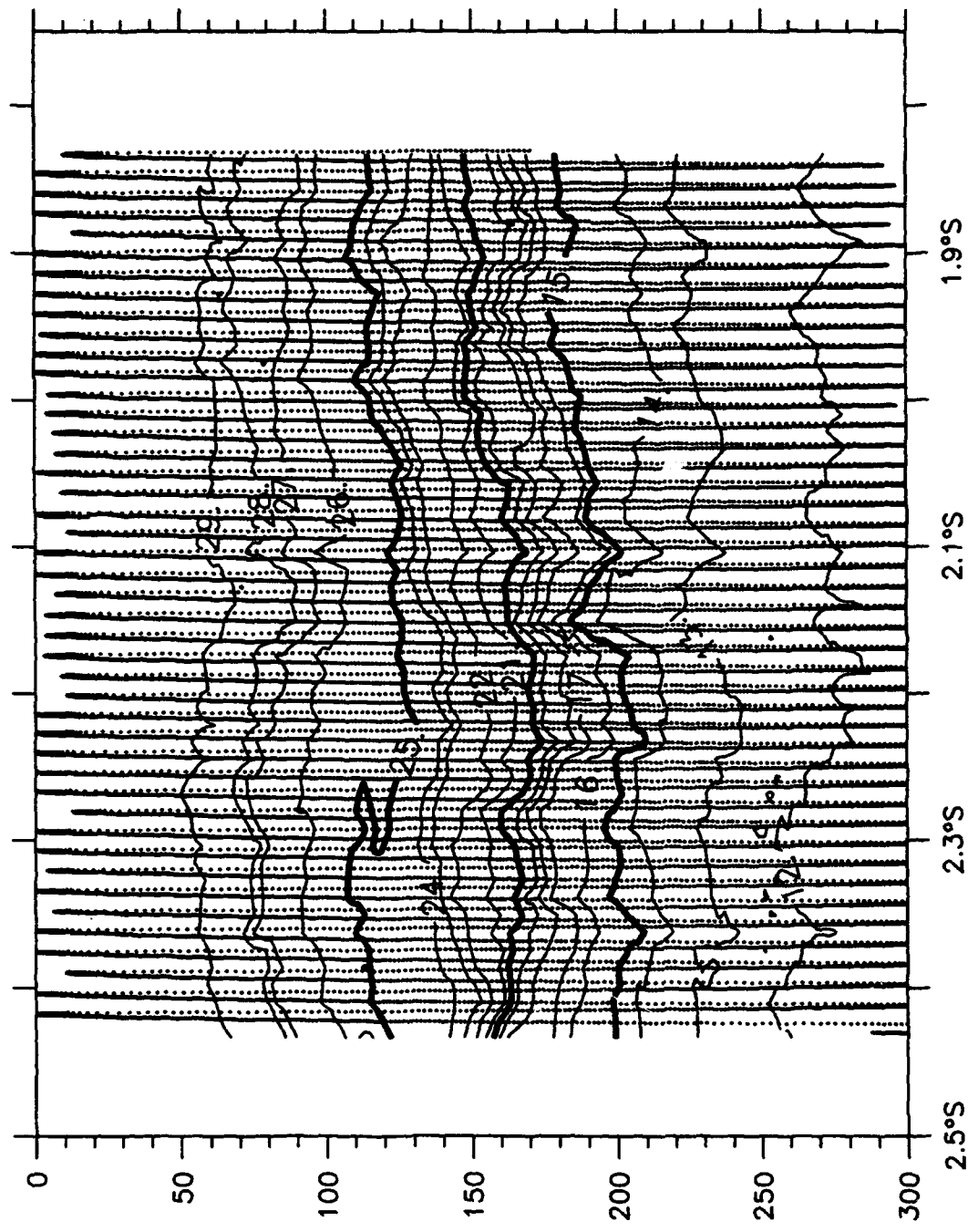




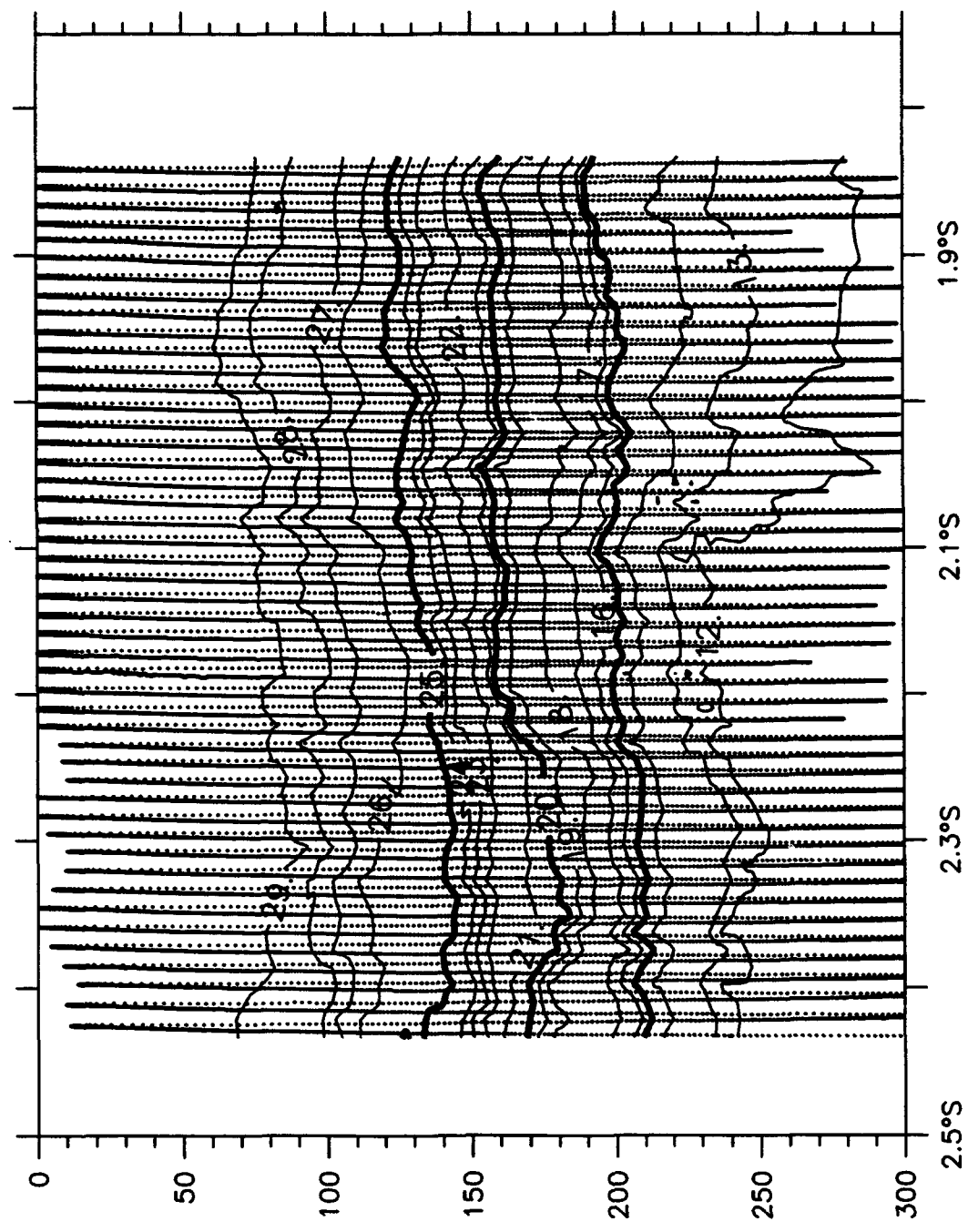




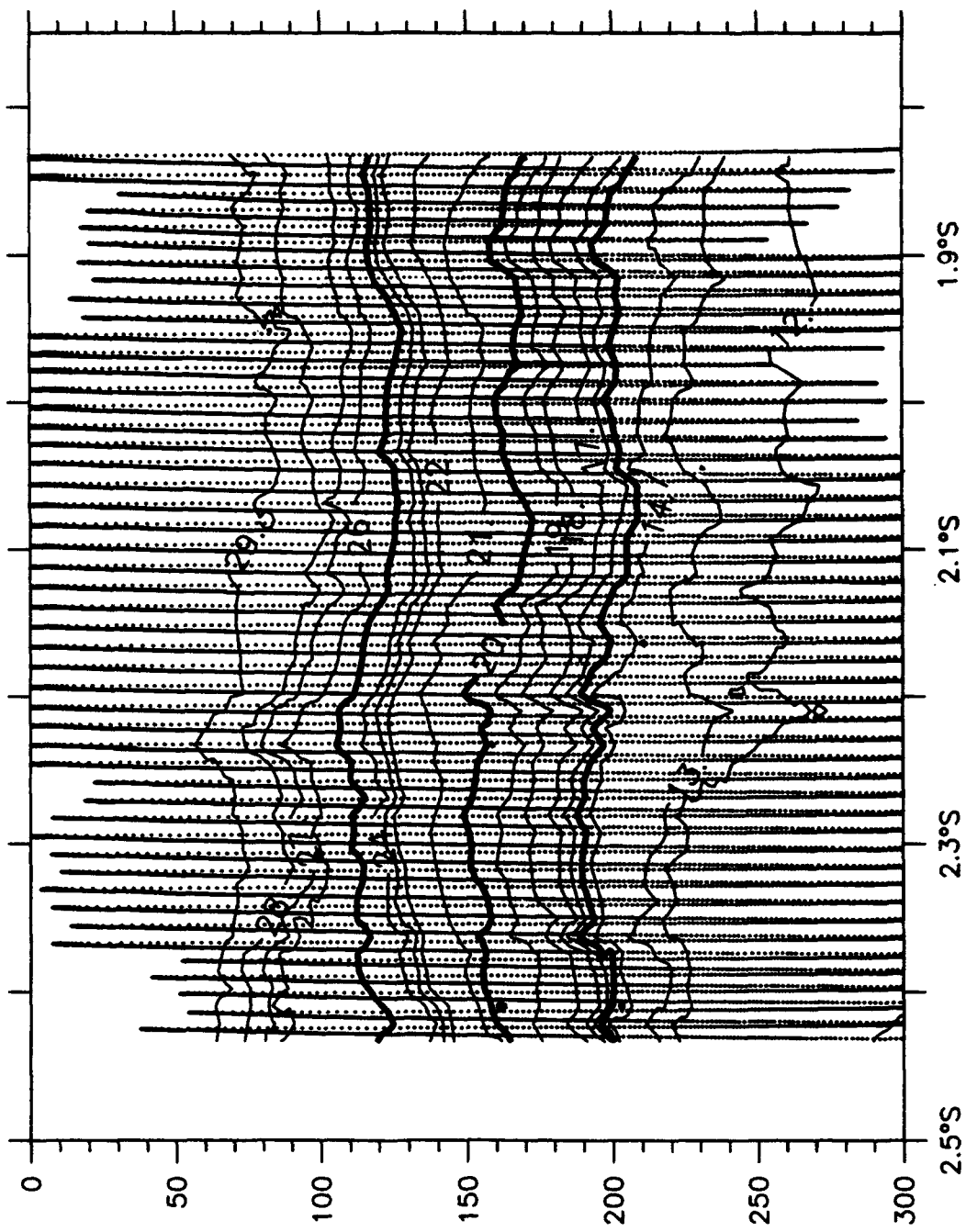
$T(^{\circ}\text{C})$ , S2W, 01 February 1993



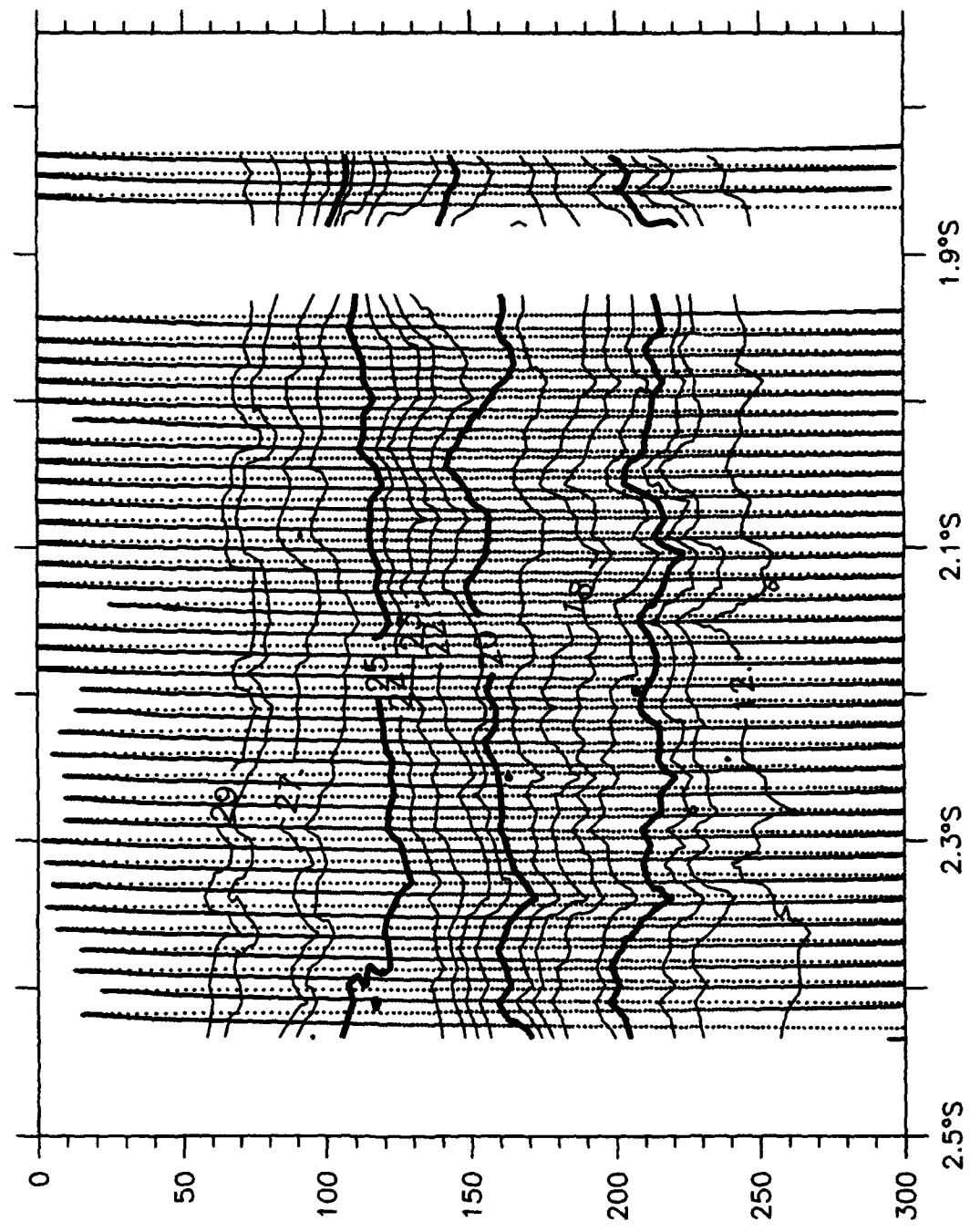
$T(^{\circ}\text{C})$ , S2W, 2 February 1993



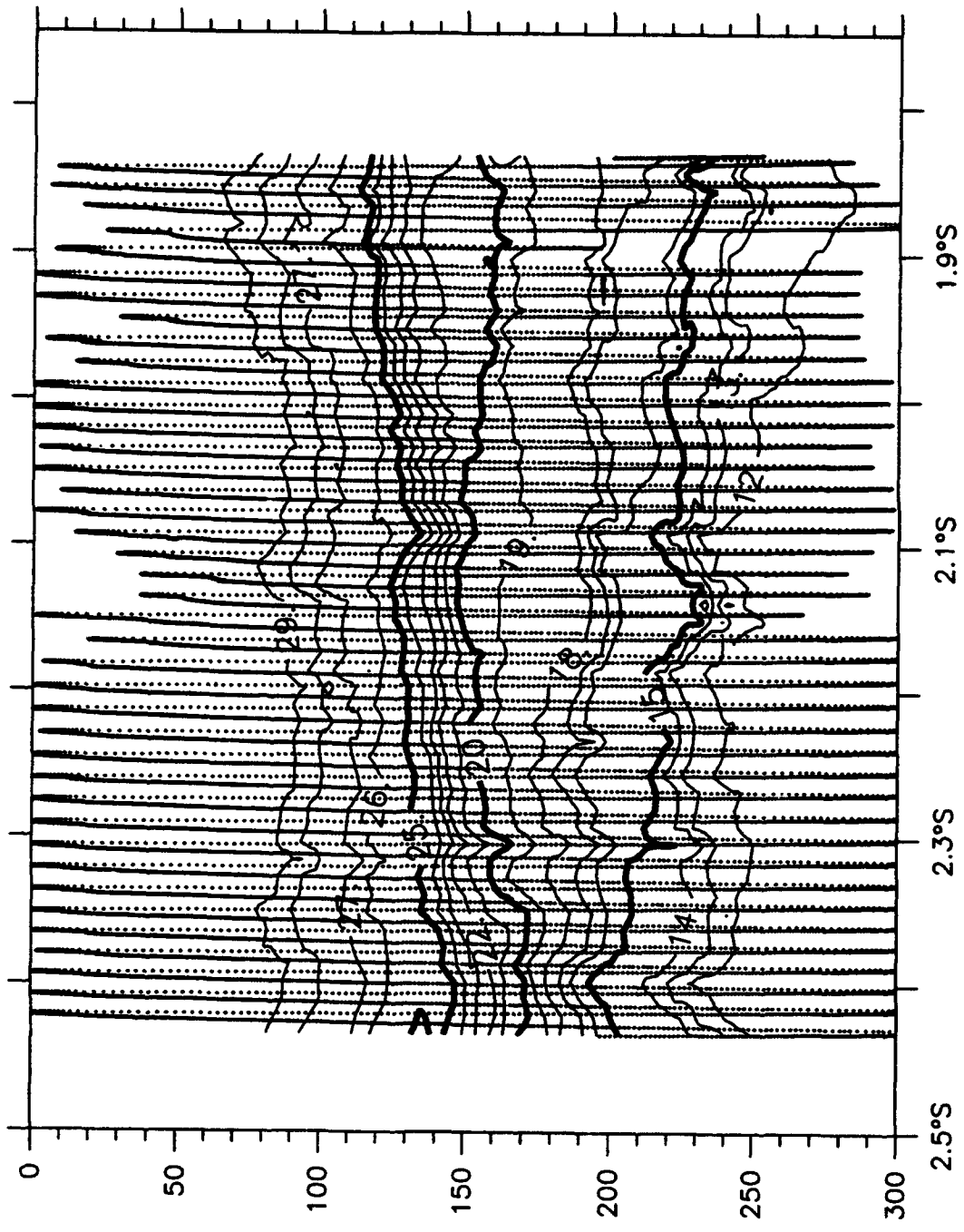
$T(^{\circ}\text{C})$ , S2W, 4 February 1993



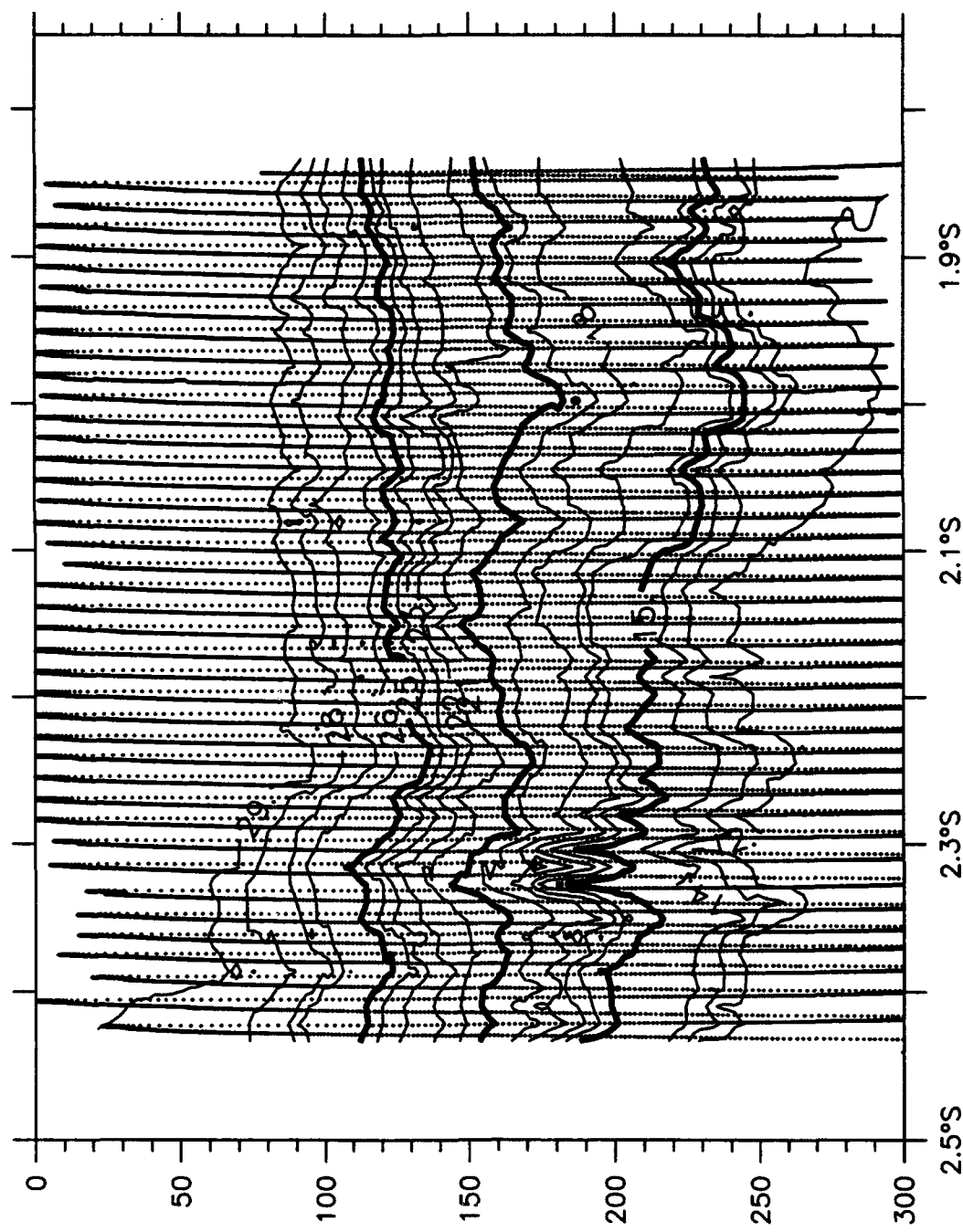
$T$ (°C), S2W, 6 February 1993

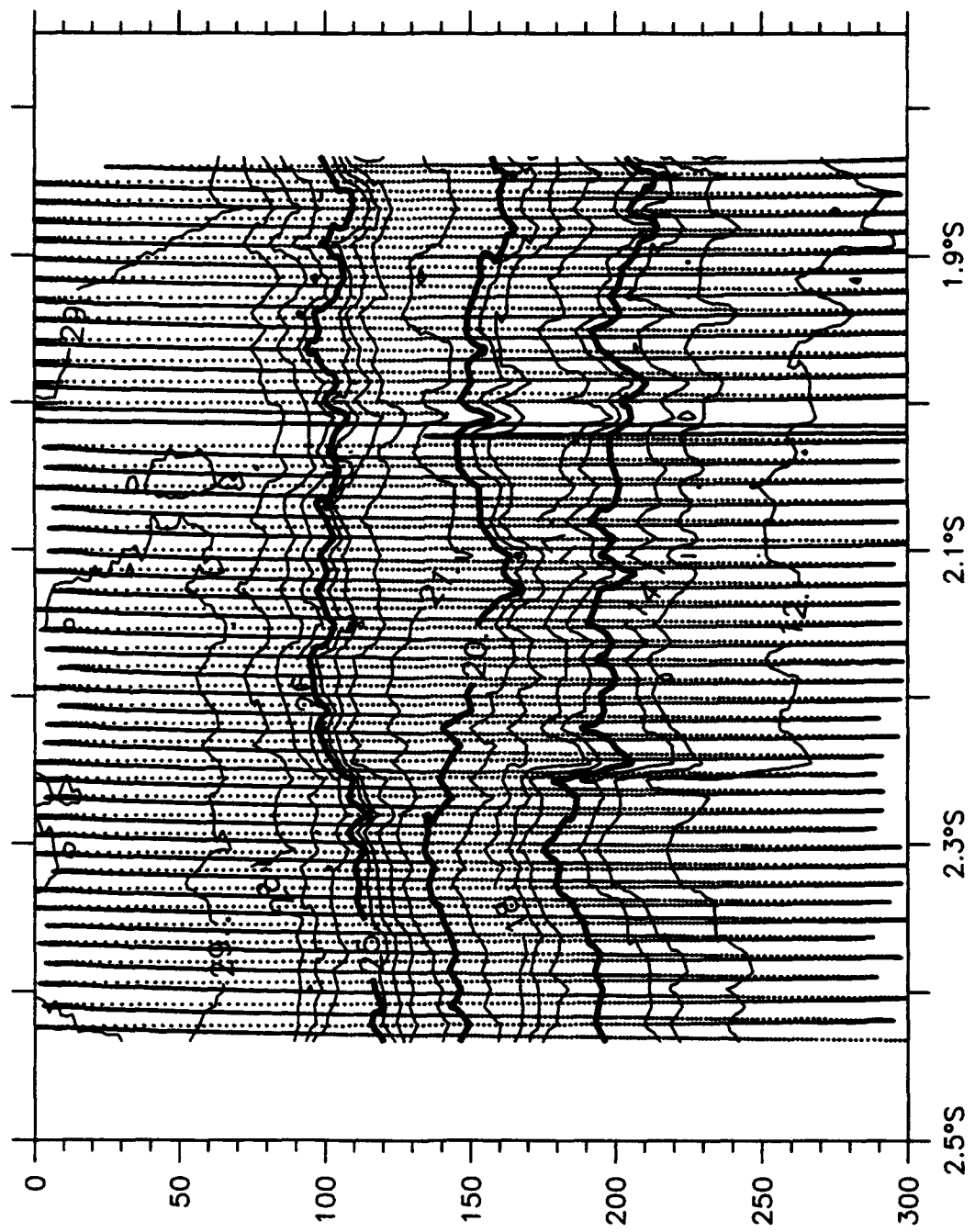


$T(^{\circ}\text{C})$ , S2W, 8 February 1993

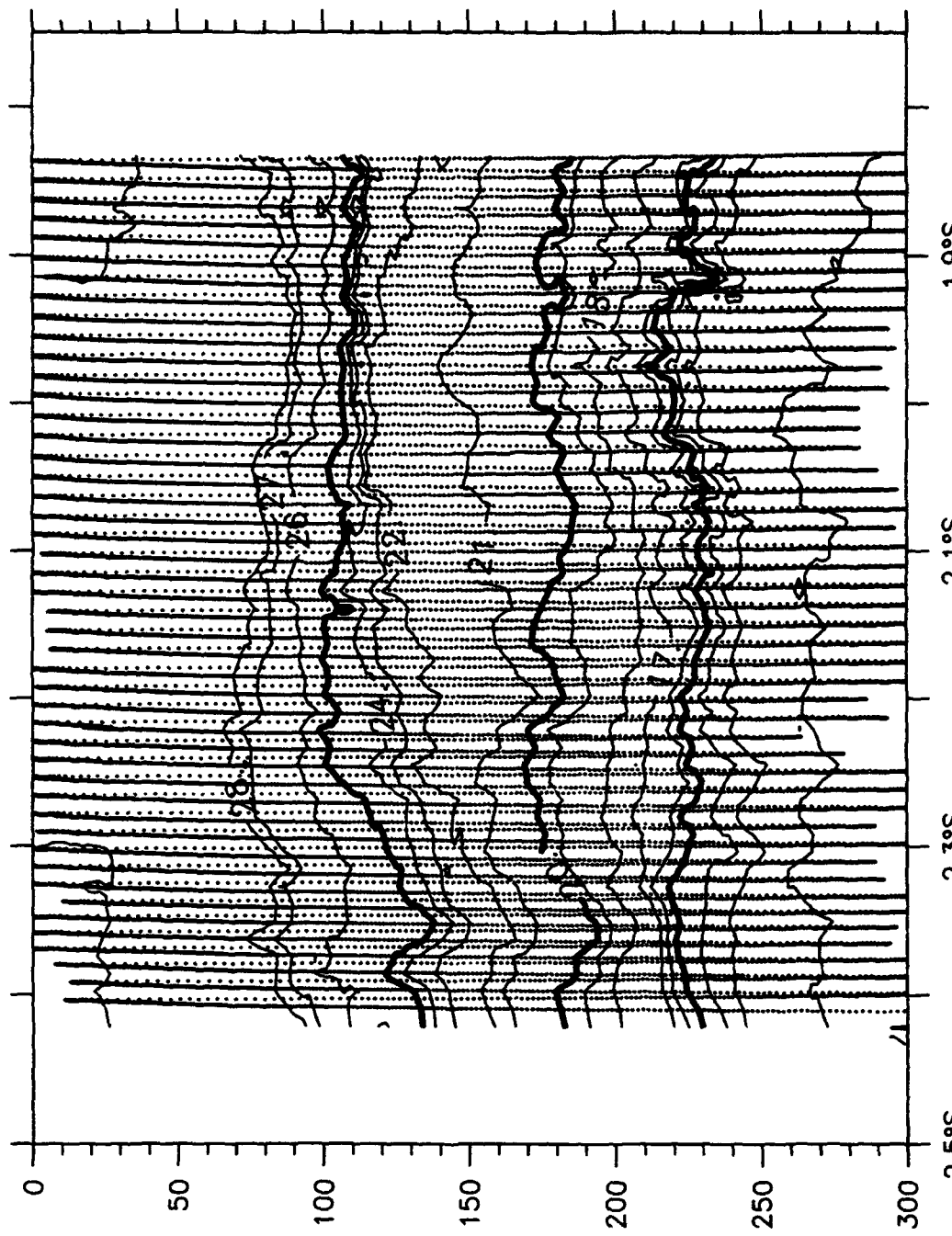


$T(^{\circ}\text{C})$ , S2W, 11 February 1993

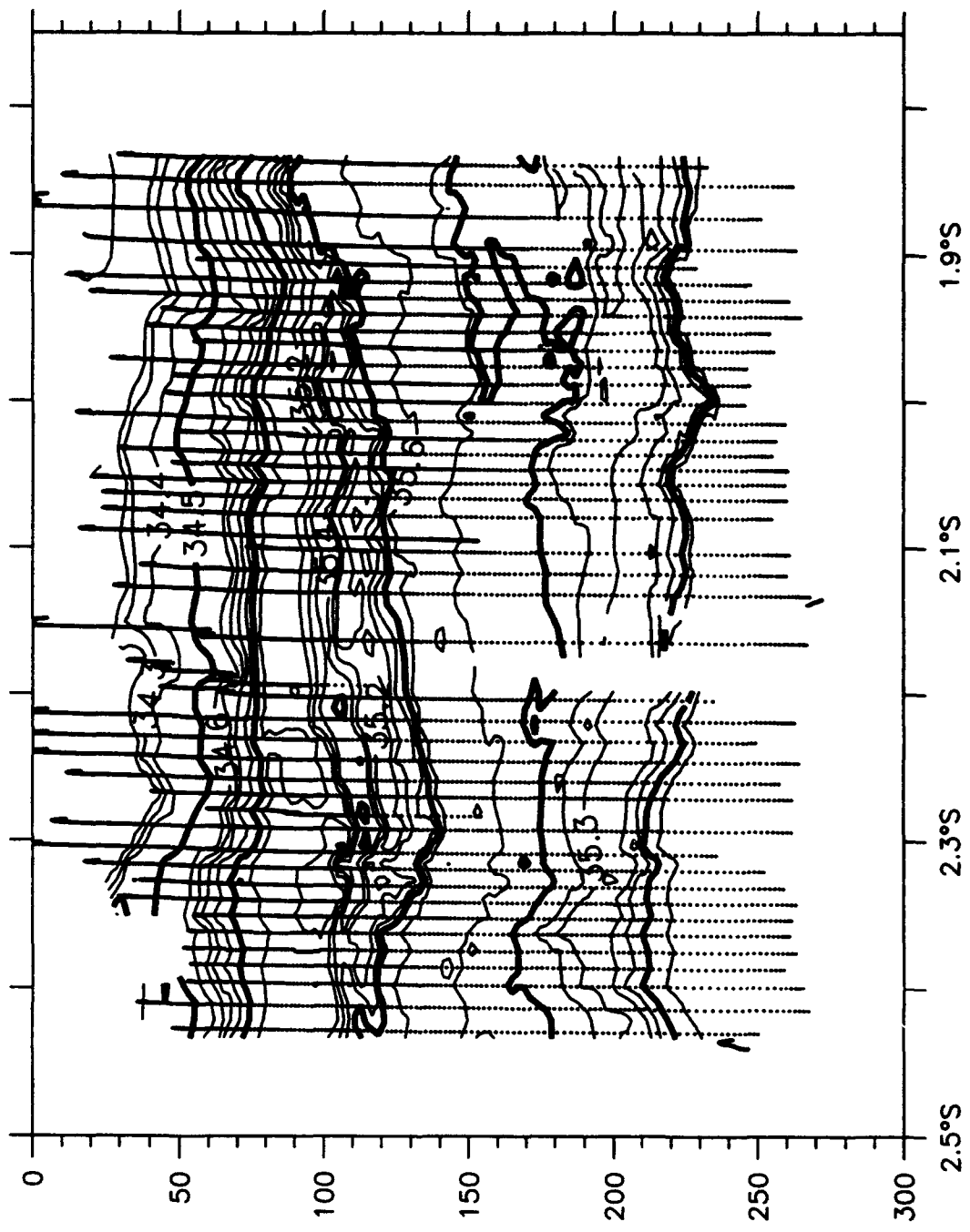




$T(^{\circ}\text{C})$ , S2W, 12–13 February 1993

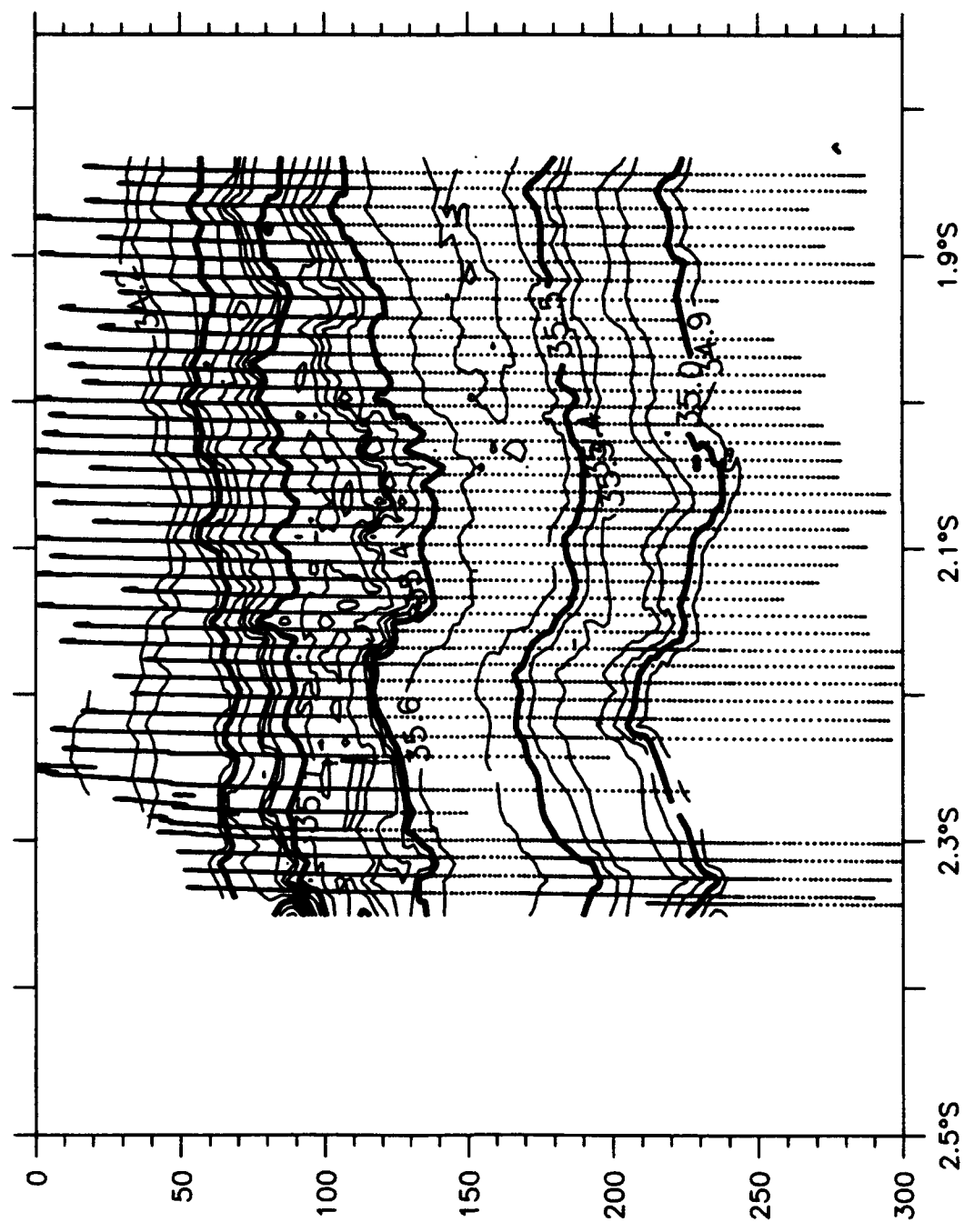


$T(^{\circ}\text{C})$ , S2W, 14 February 1993



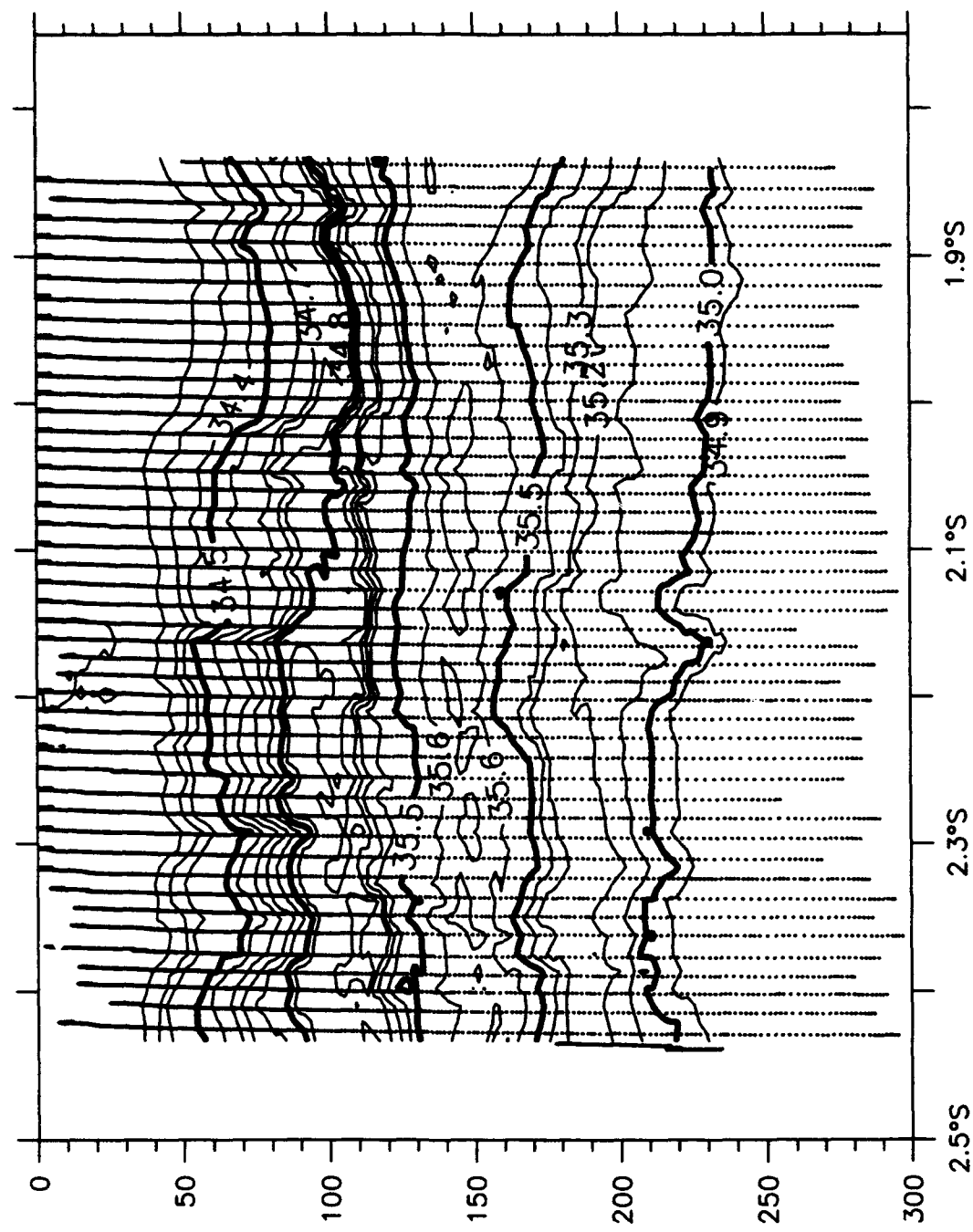
$S$ (psu), S2W, 27 January 1993

S(psu), S2W, 29 January 1993

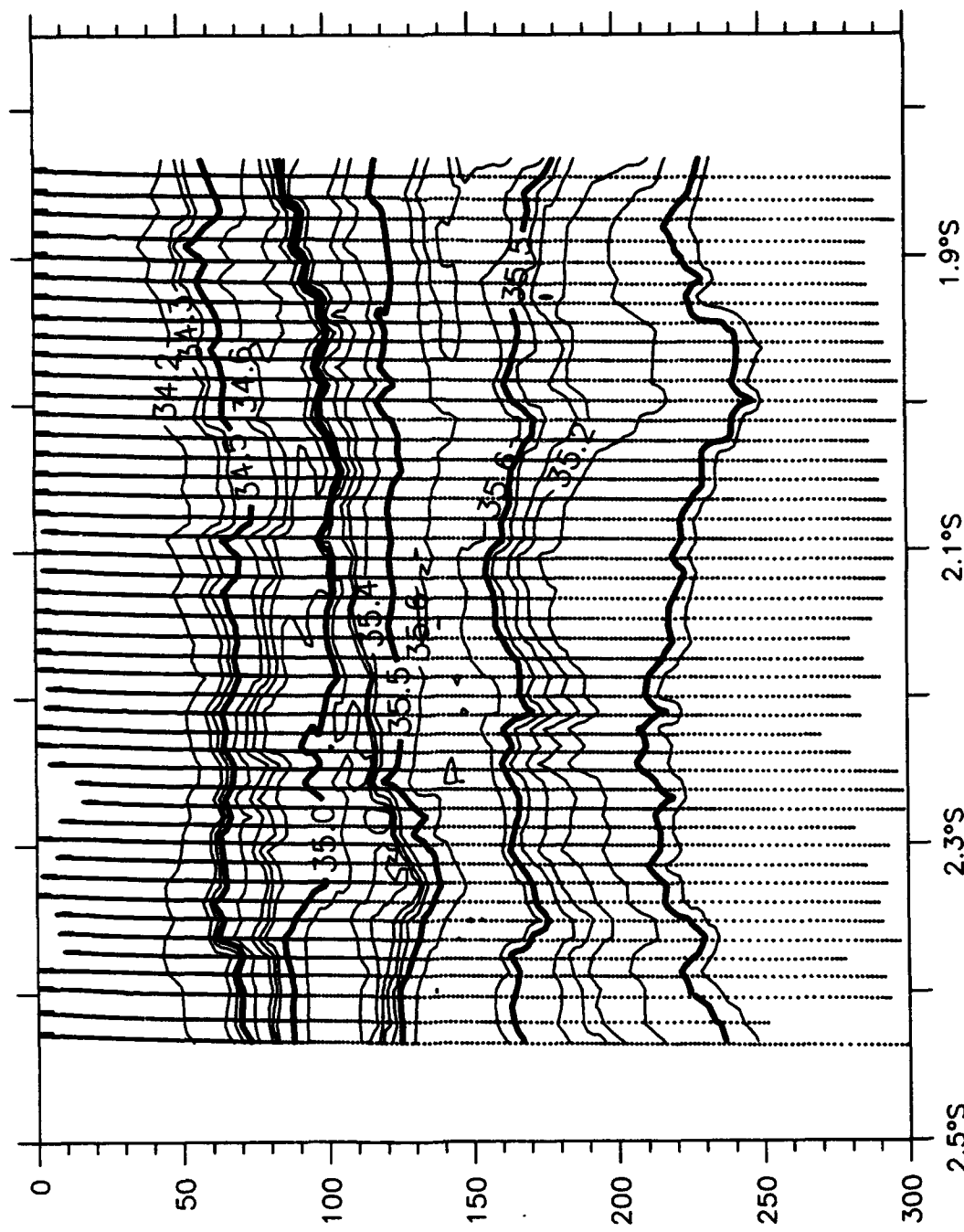


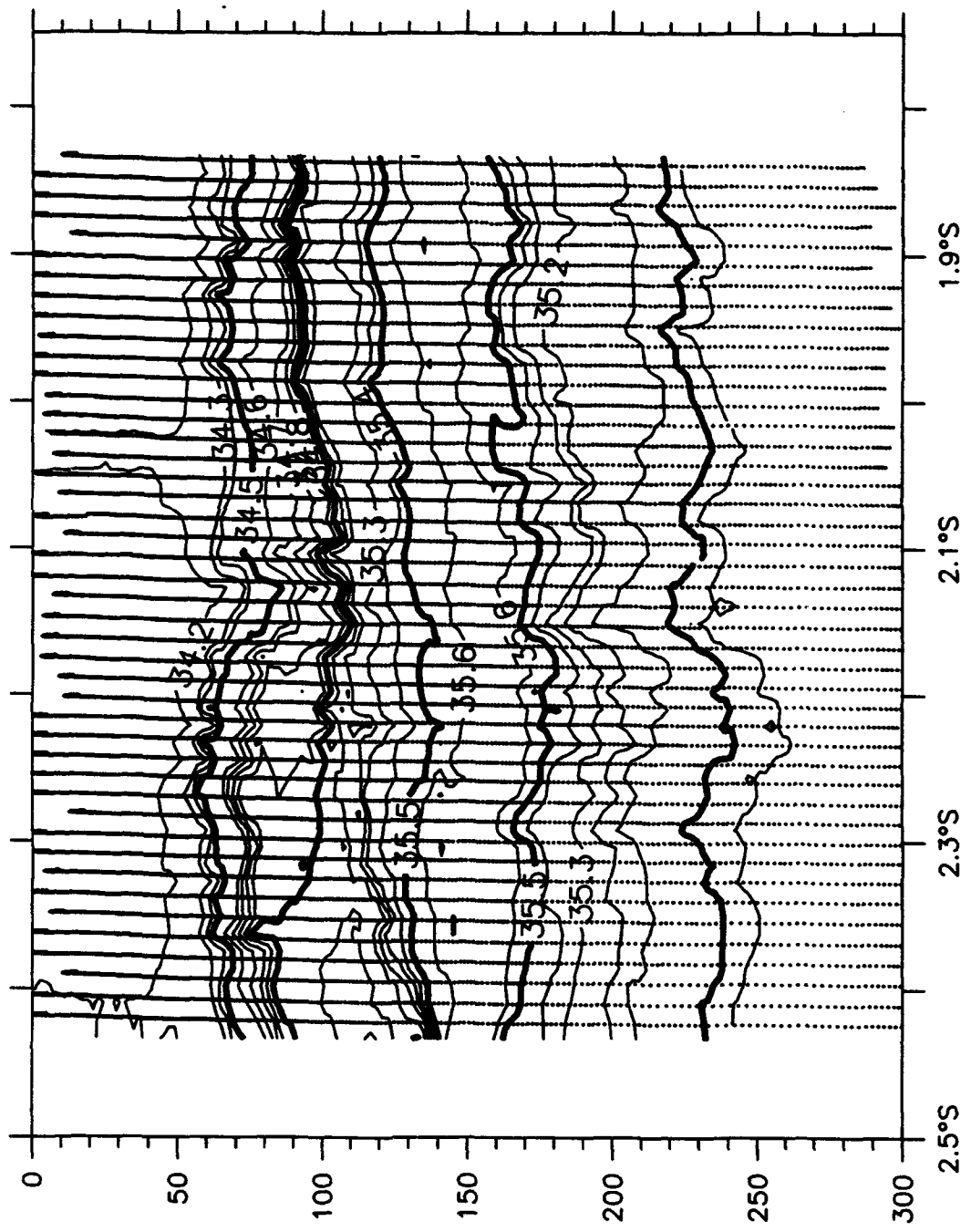
200

S(psu), S2W, 30 January 1993

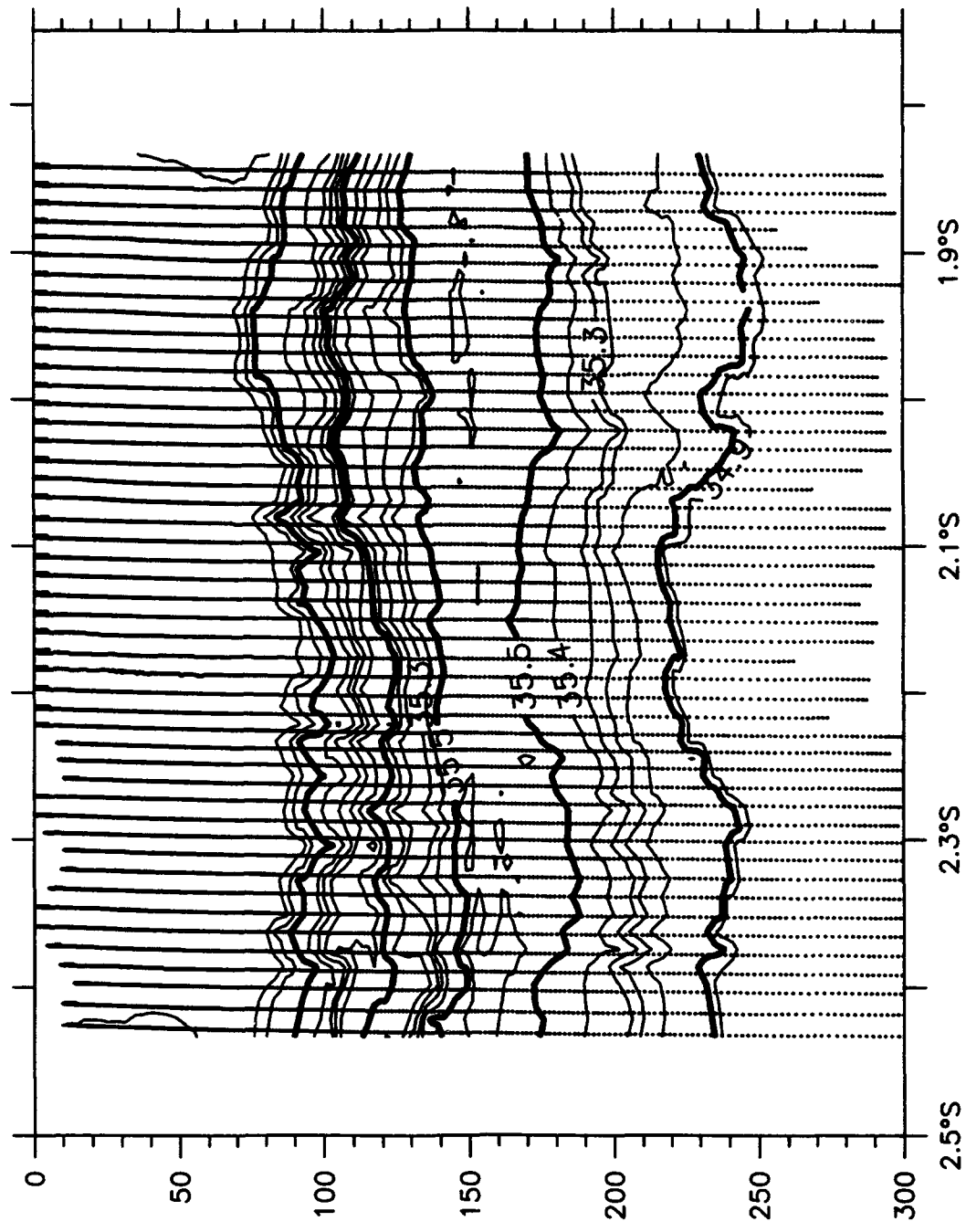


S(psu), S2W, 1 February 1993

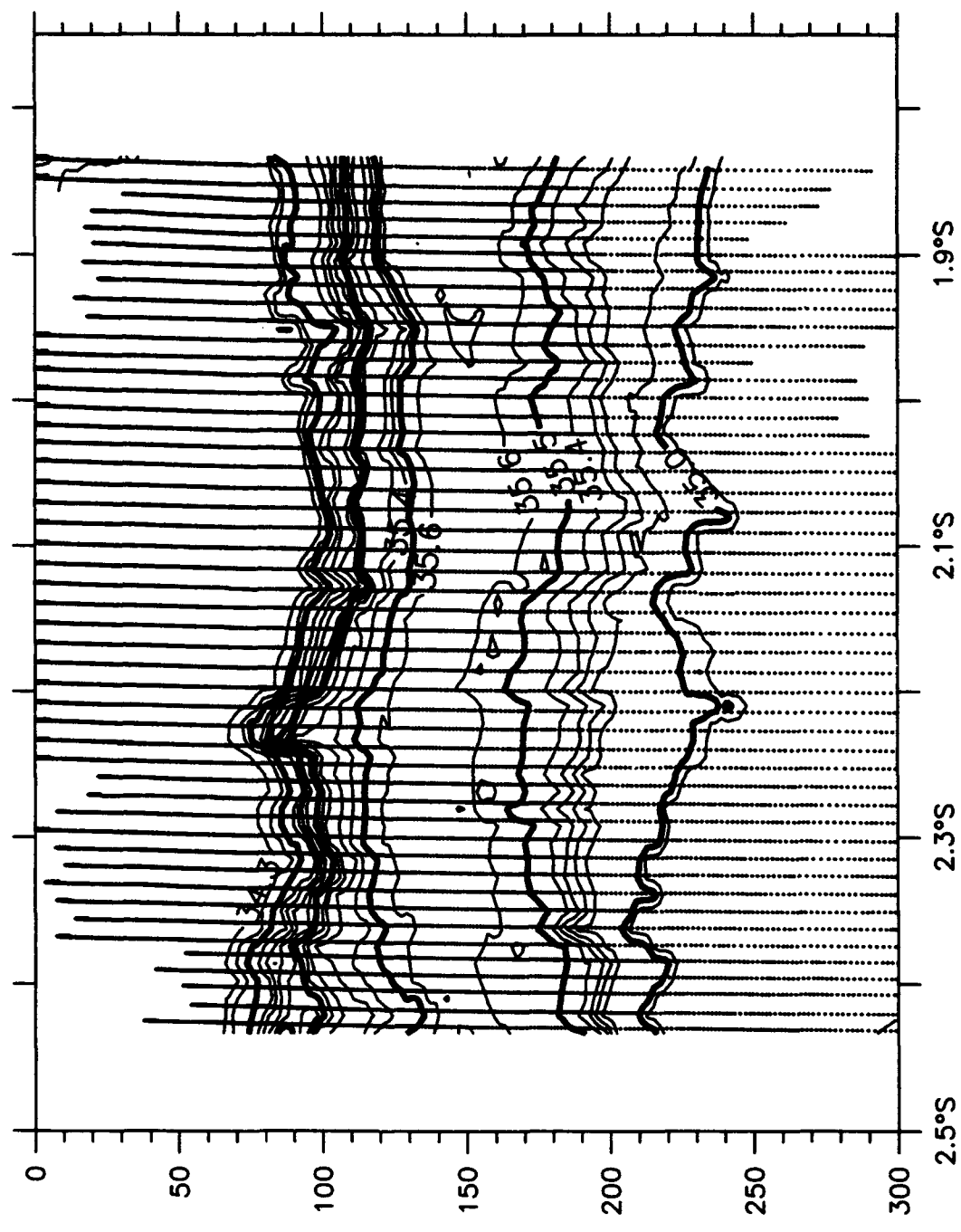




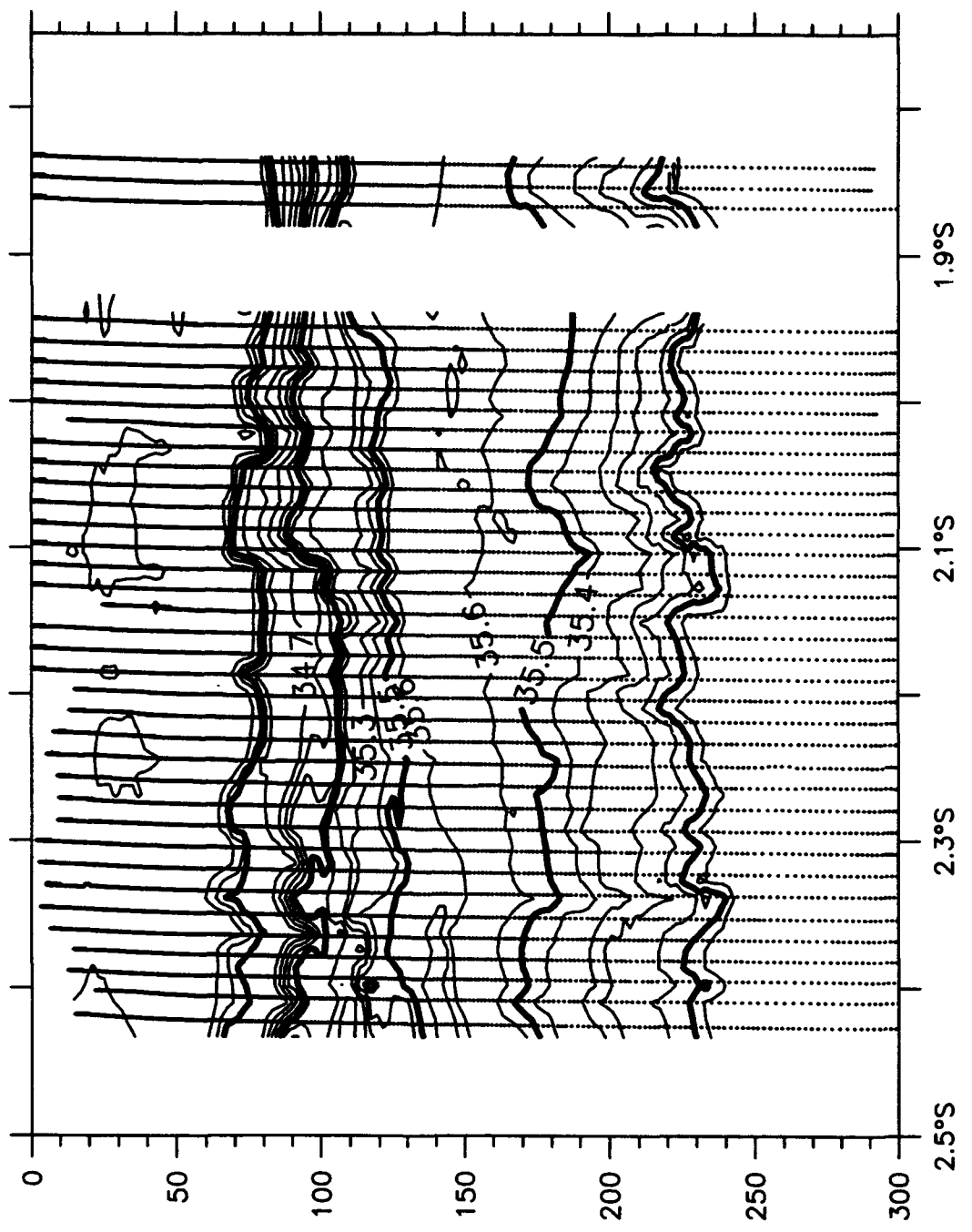
$S(\text{psu})$ , S2W, 2 February 1993



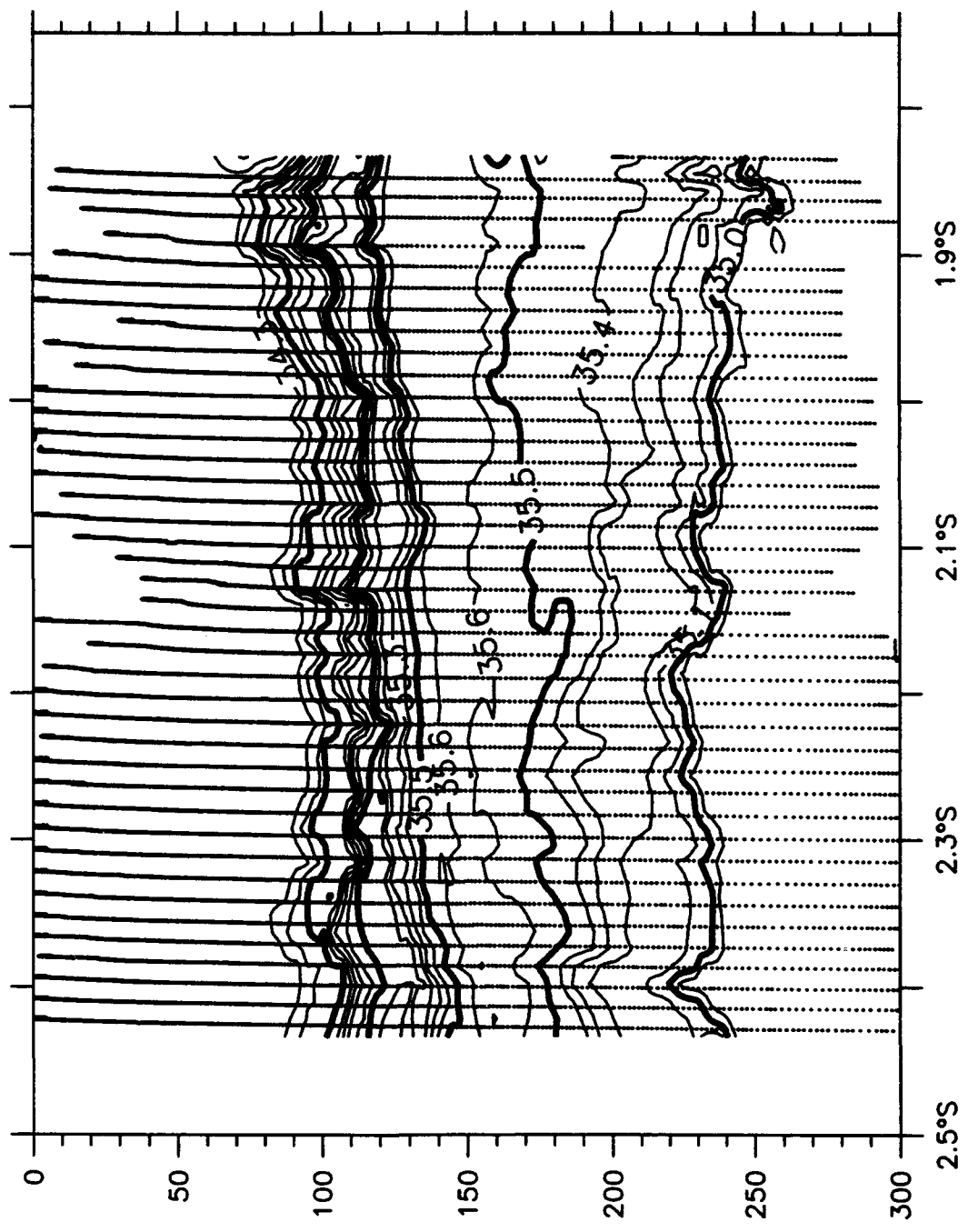
S(psu), S2W, 4 February 1993



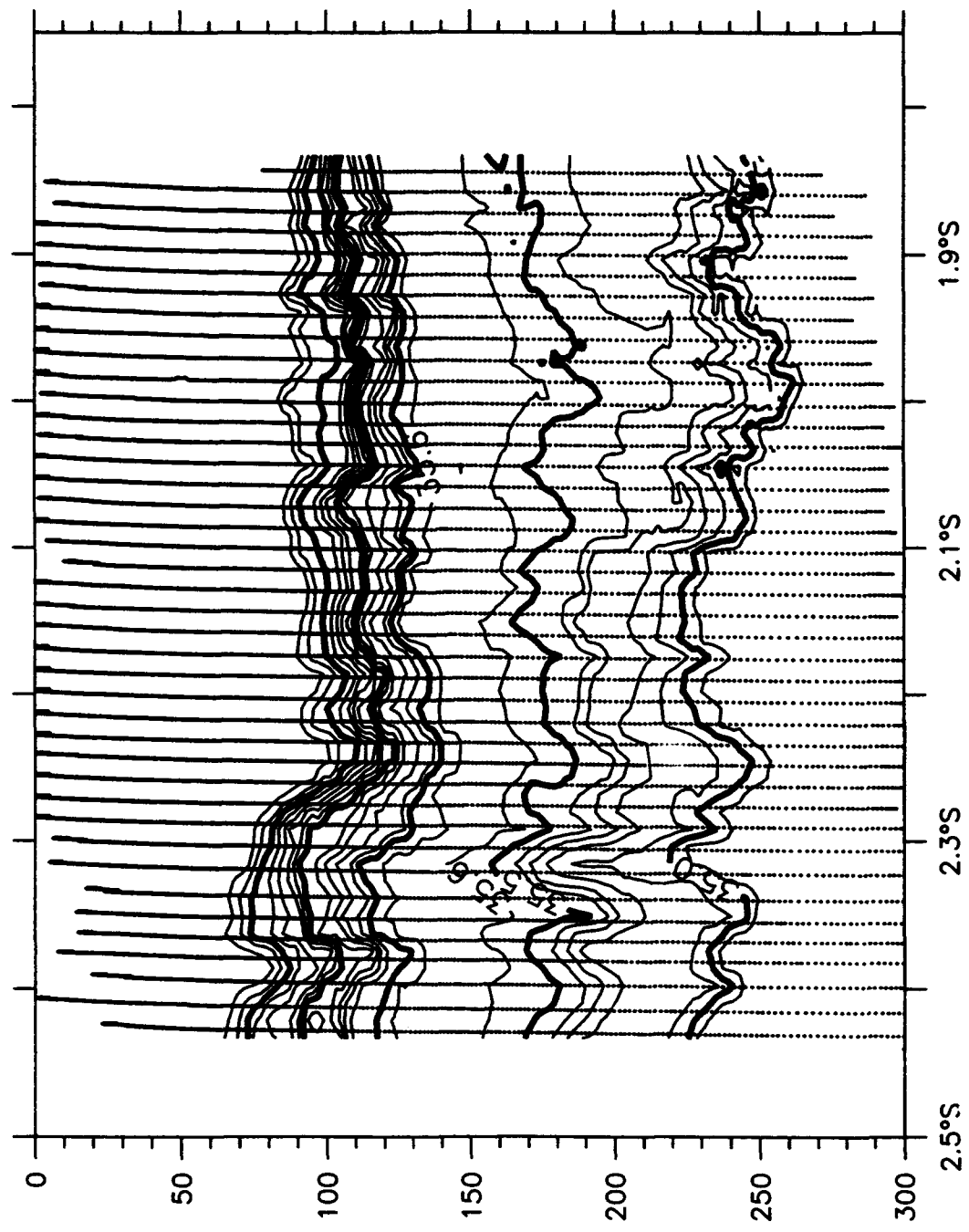
$S$ (psu), S2W, 6 February 1993



S (psu), S2W, 8 February 1993

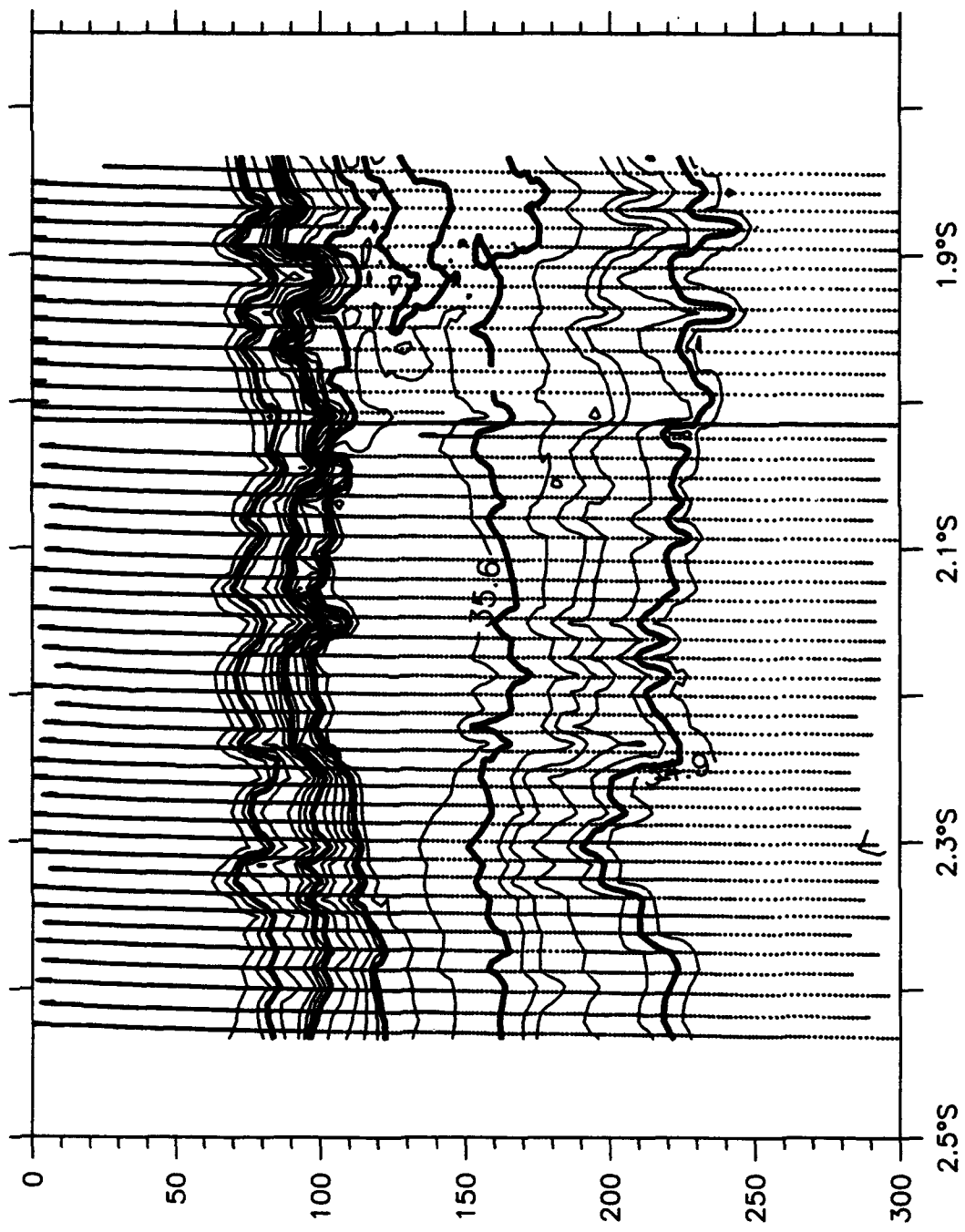


$S(\text{psu})$ , S2W, 9 February 1993

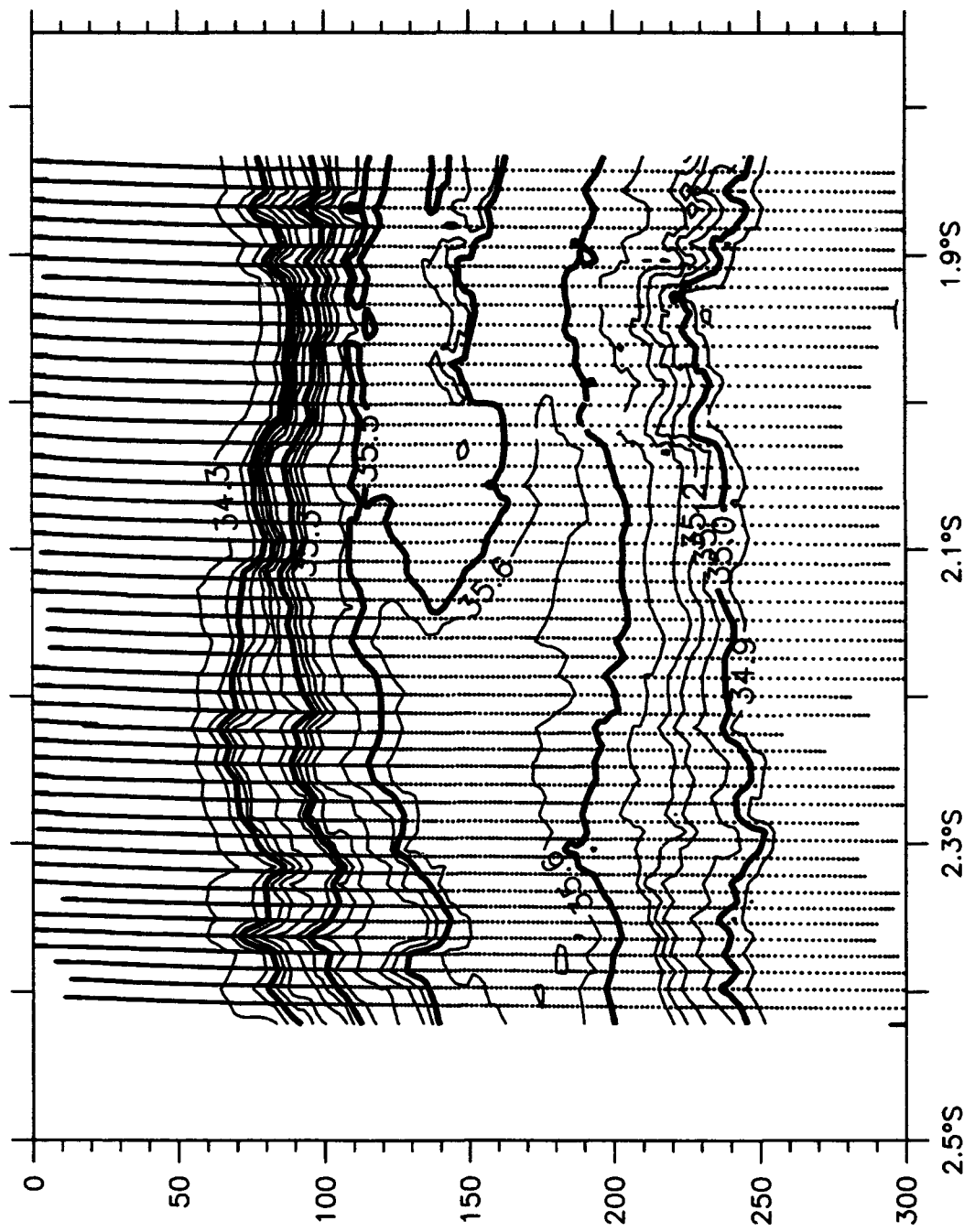


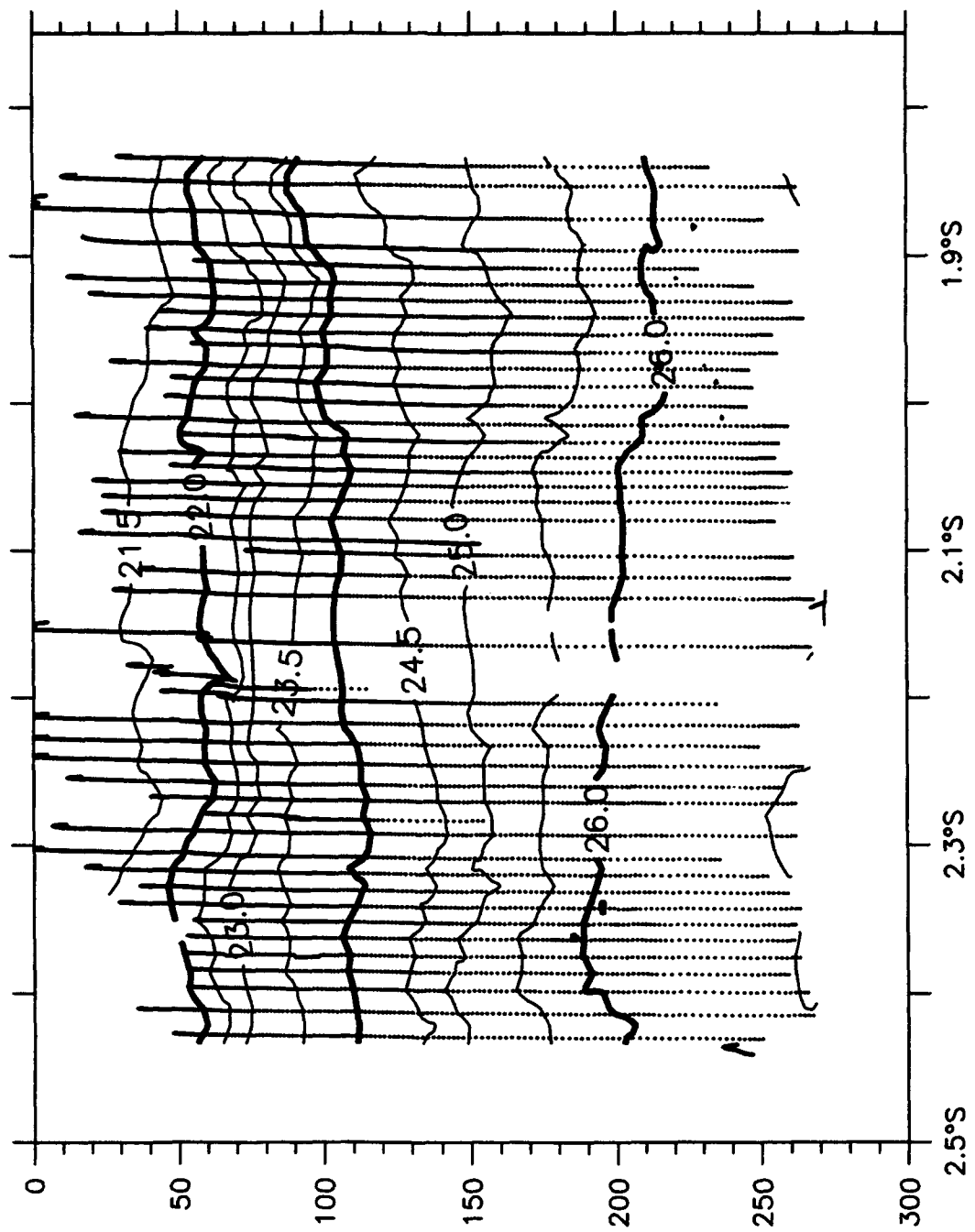
$S(\text{psu})$ , S2W, 11 February 1993

S(psu), S2W, 12–13 February 1993

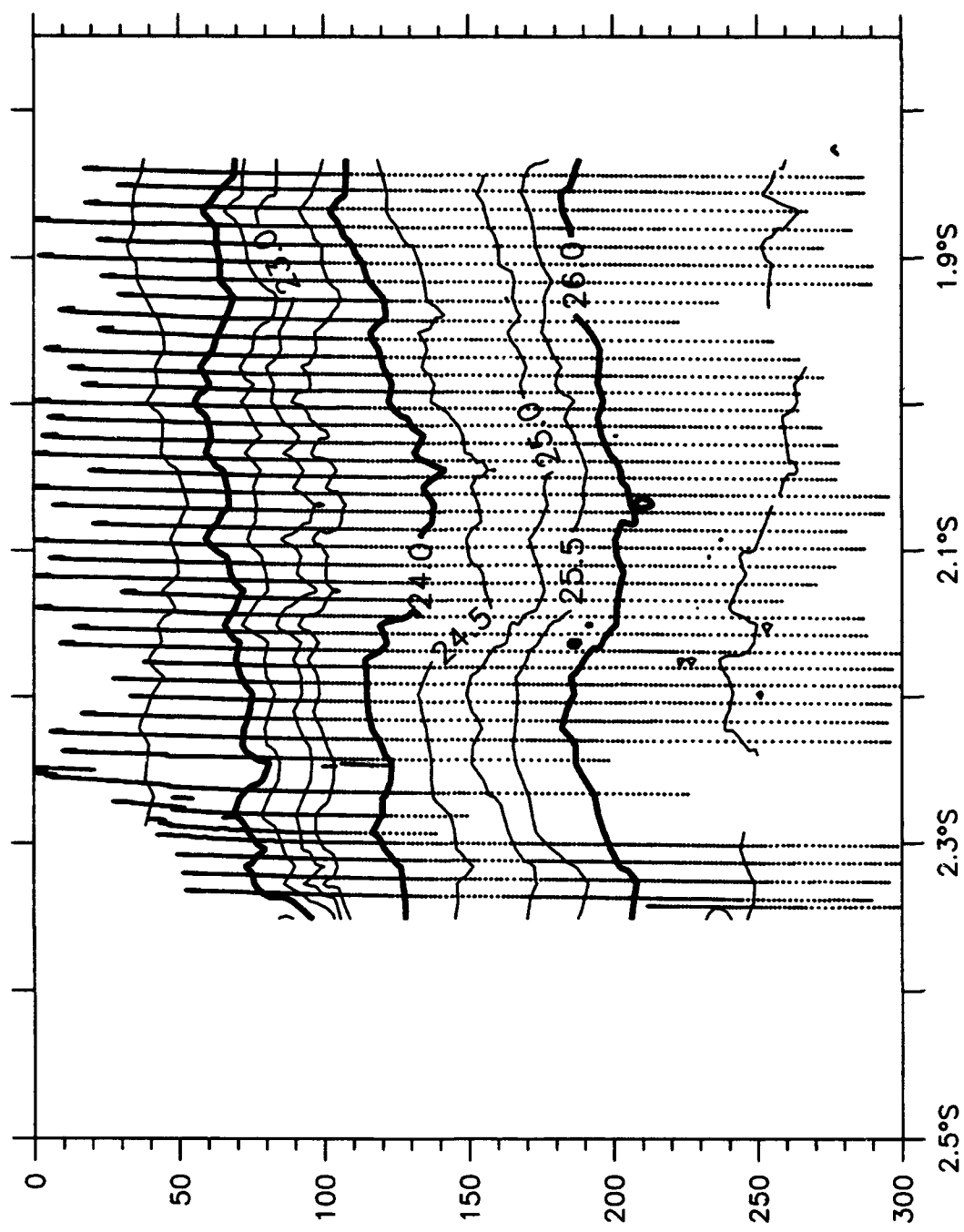


S(psu), S2W, 14 February 1993

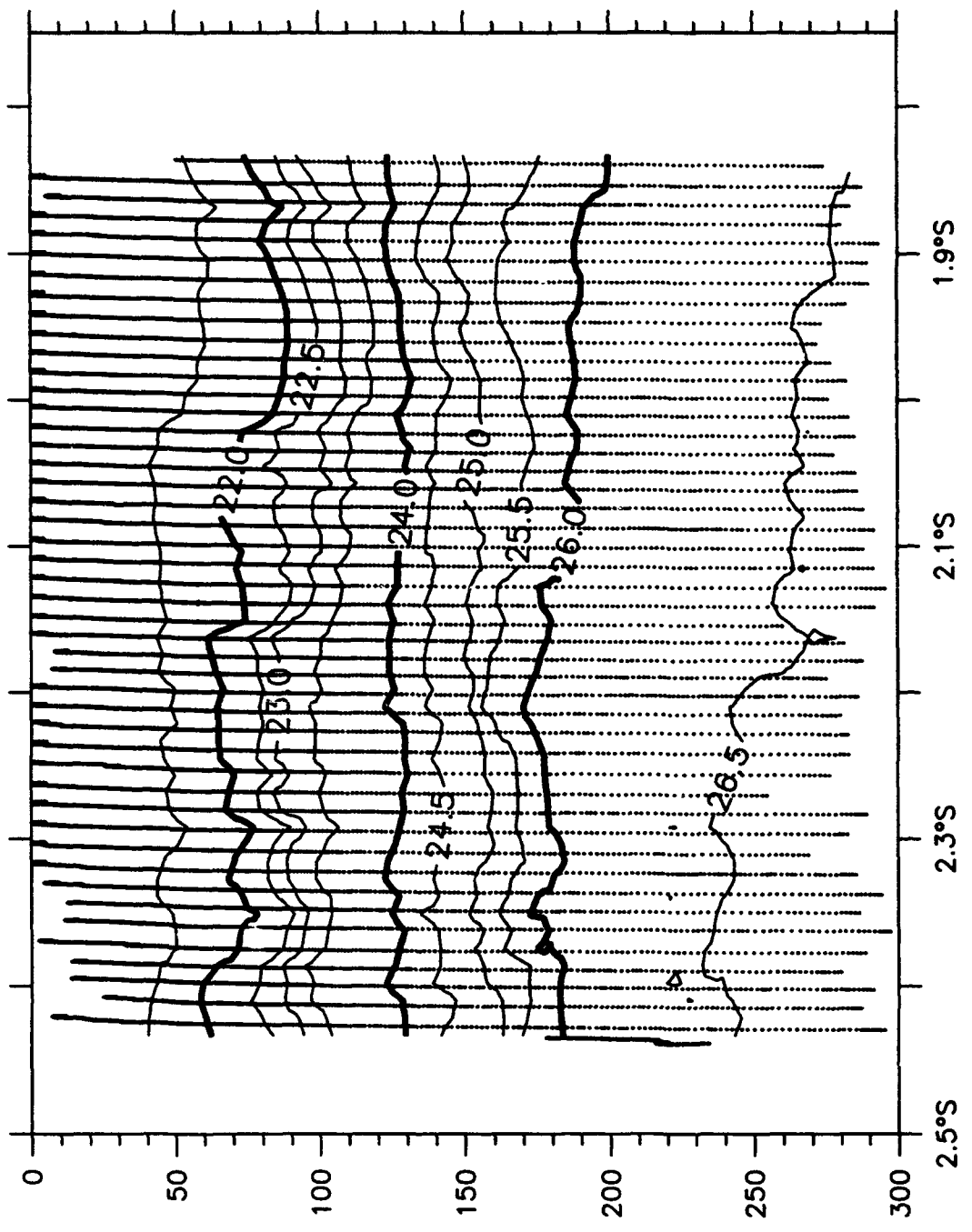




Sigma-t, S2W, 27 January 1993

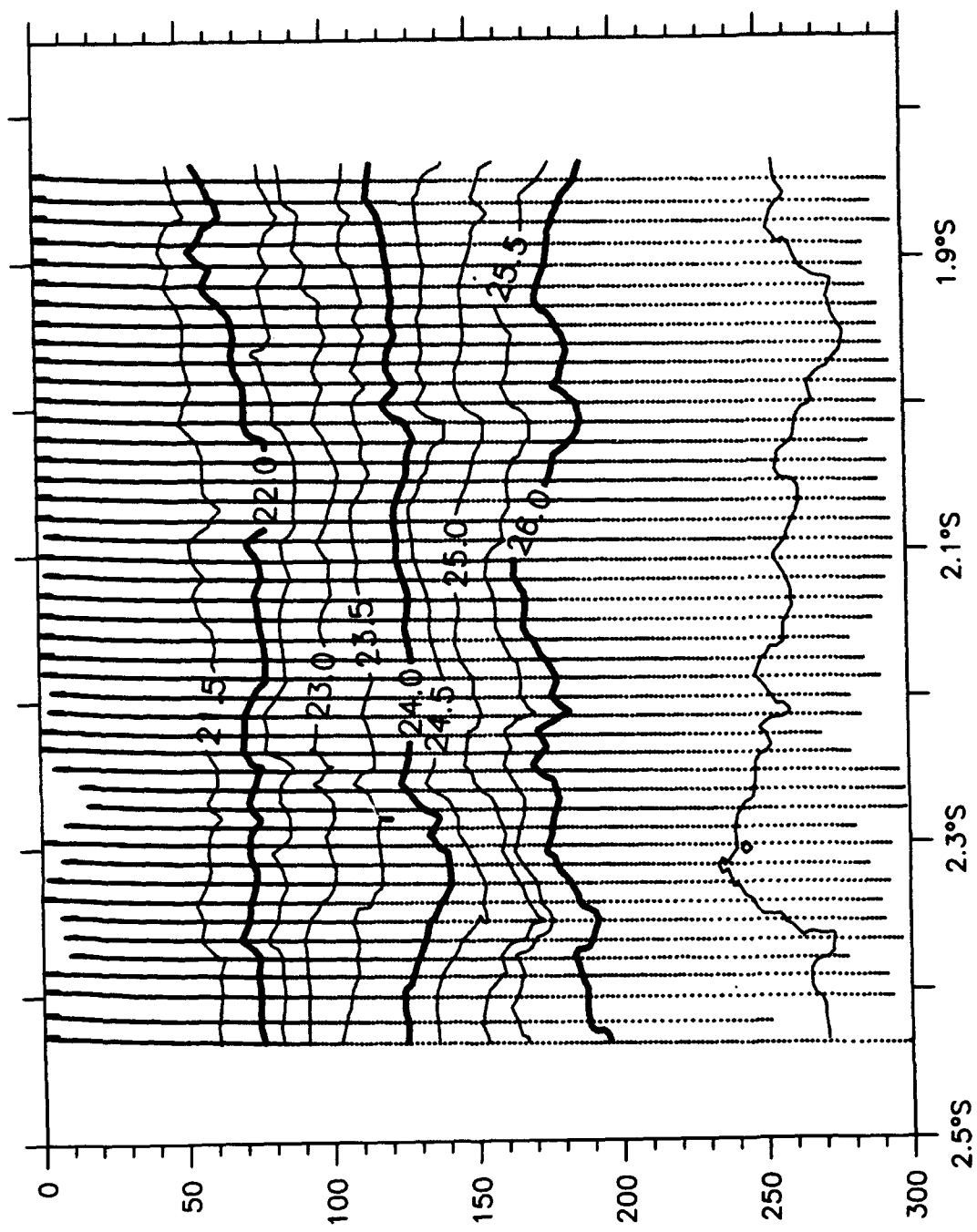


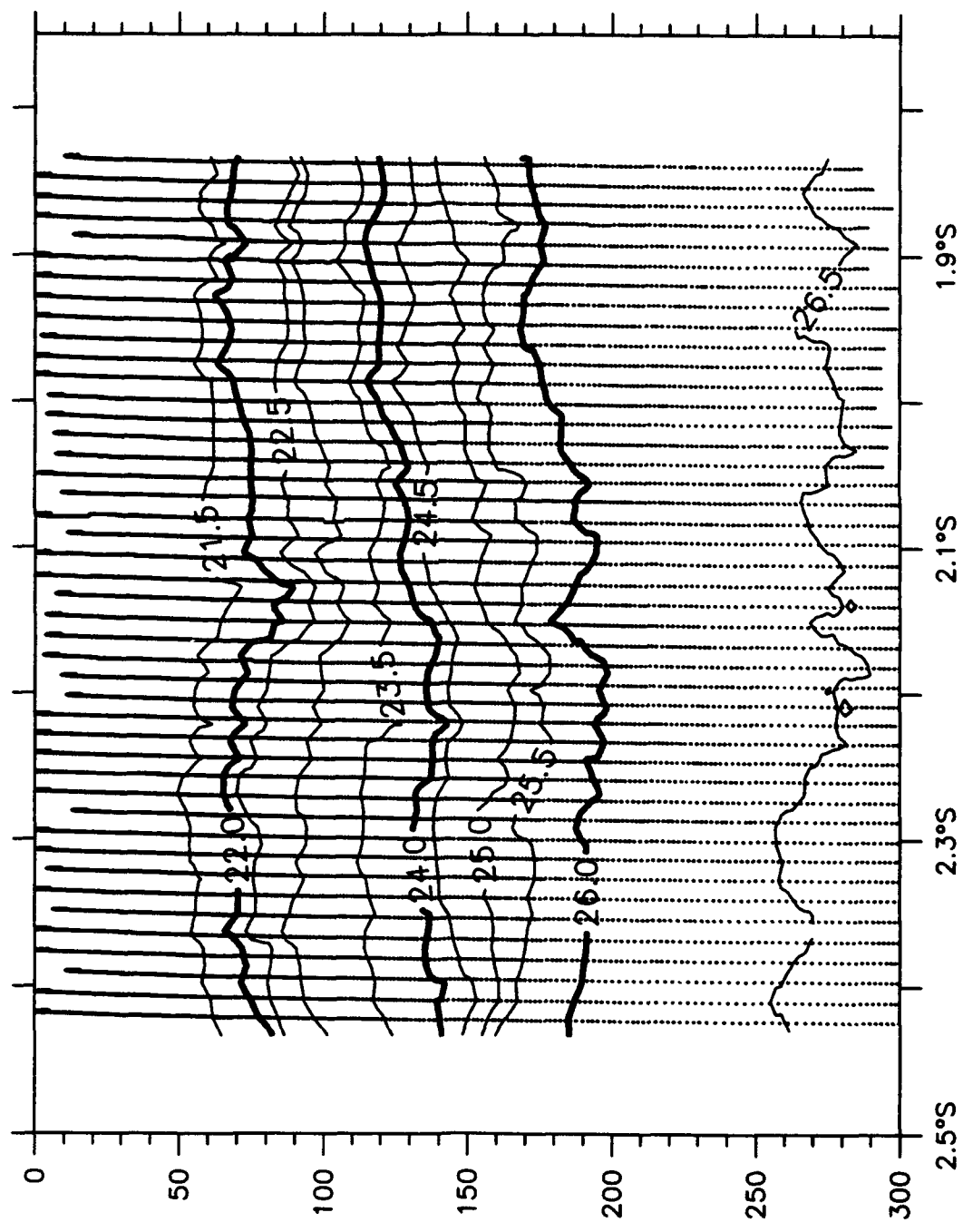
Sigma-t, S2W, 29 January 1993



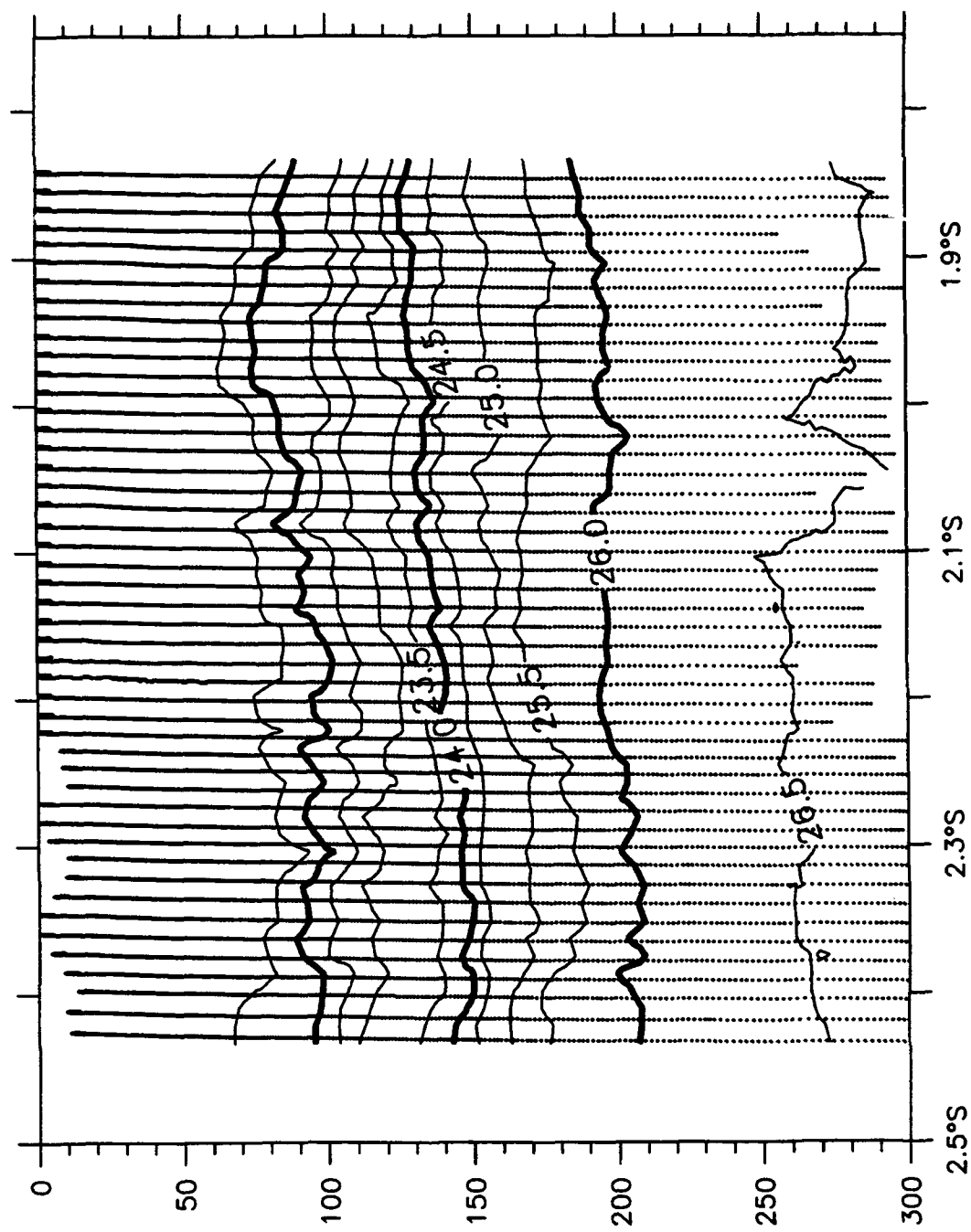
Sigma-t, S2W, 30 January 1993

Sigma-t, S2W, 1 February 1993

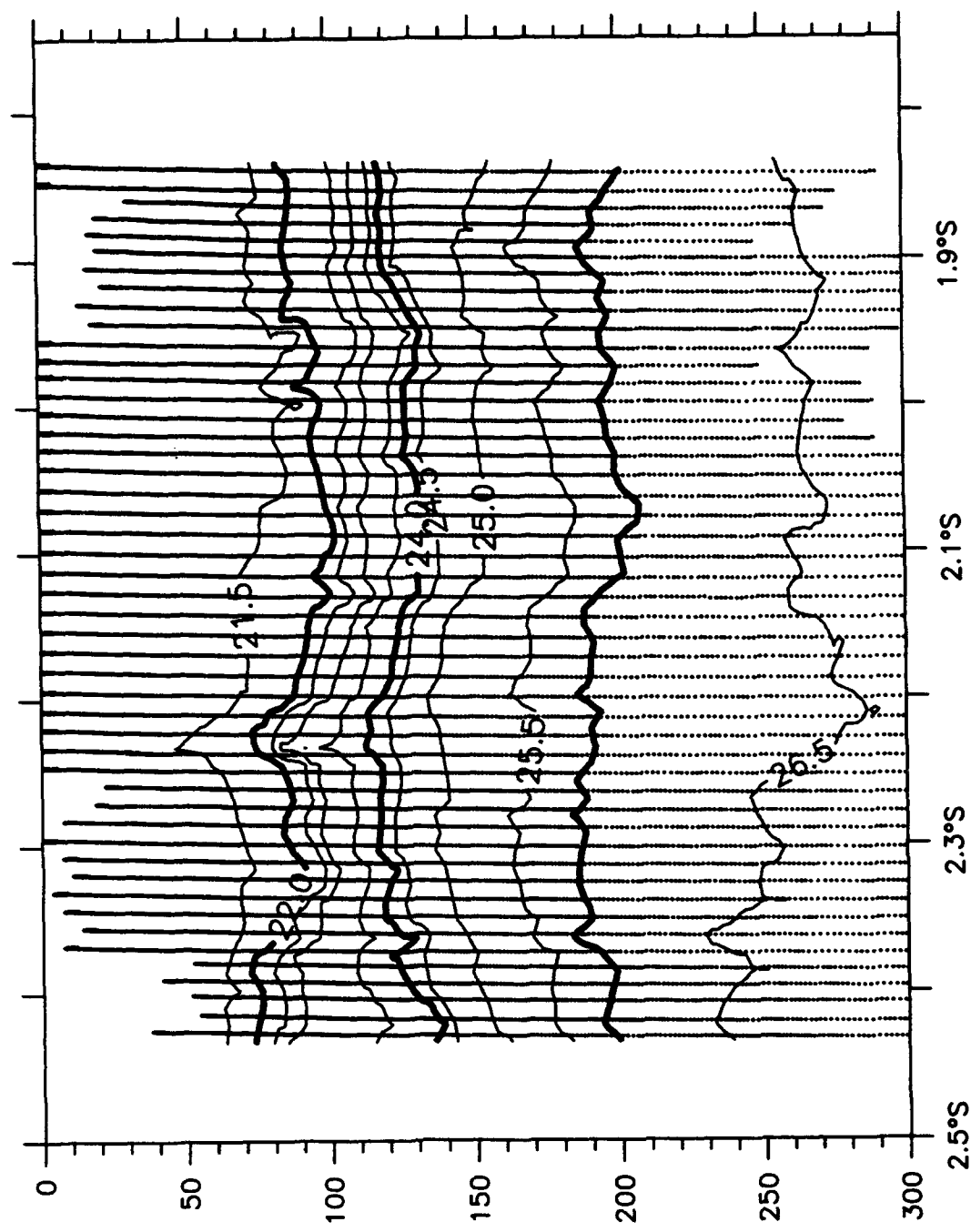




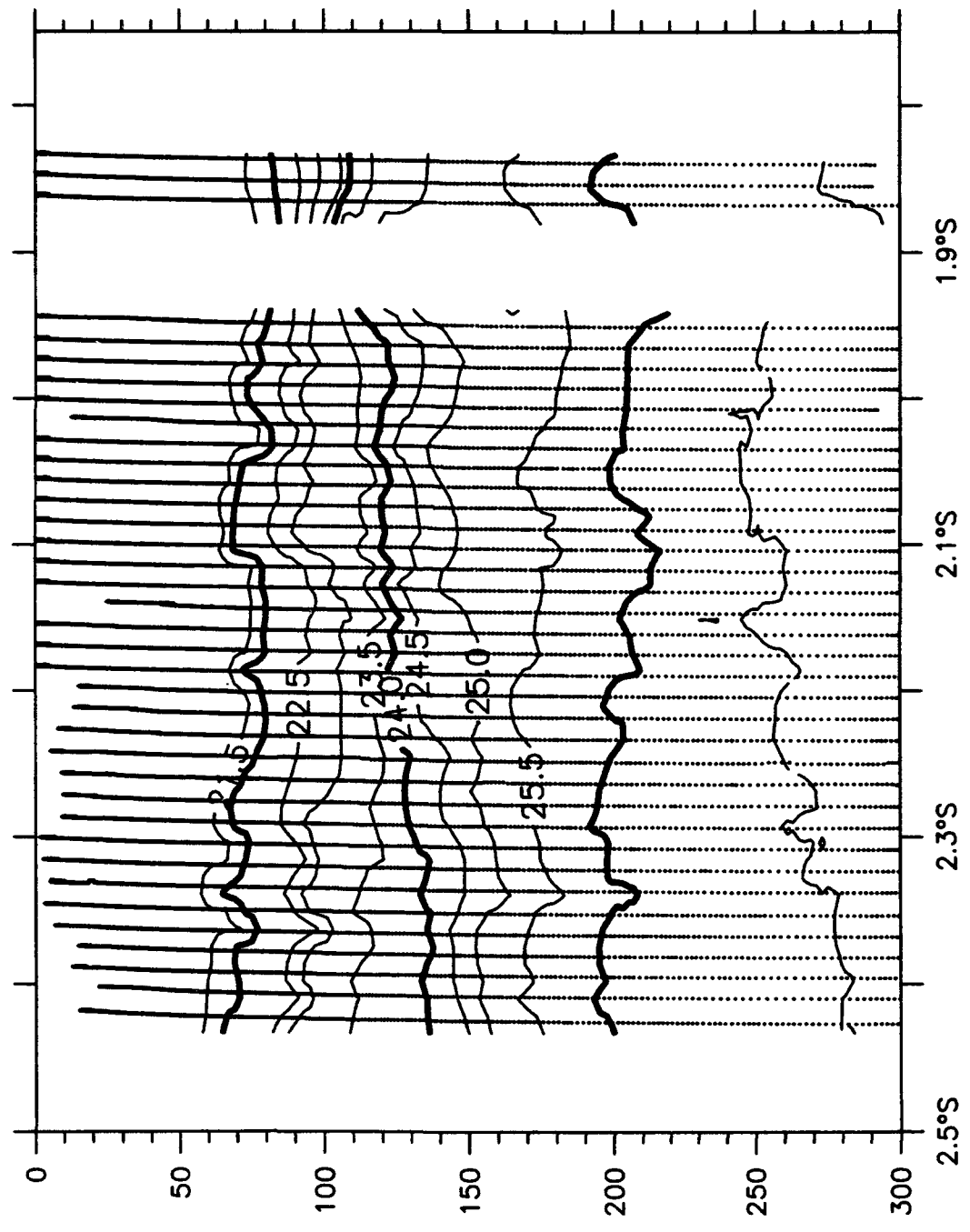
Sigma-t, S2W, 2 February 1993



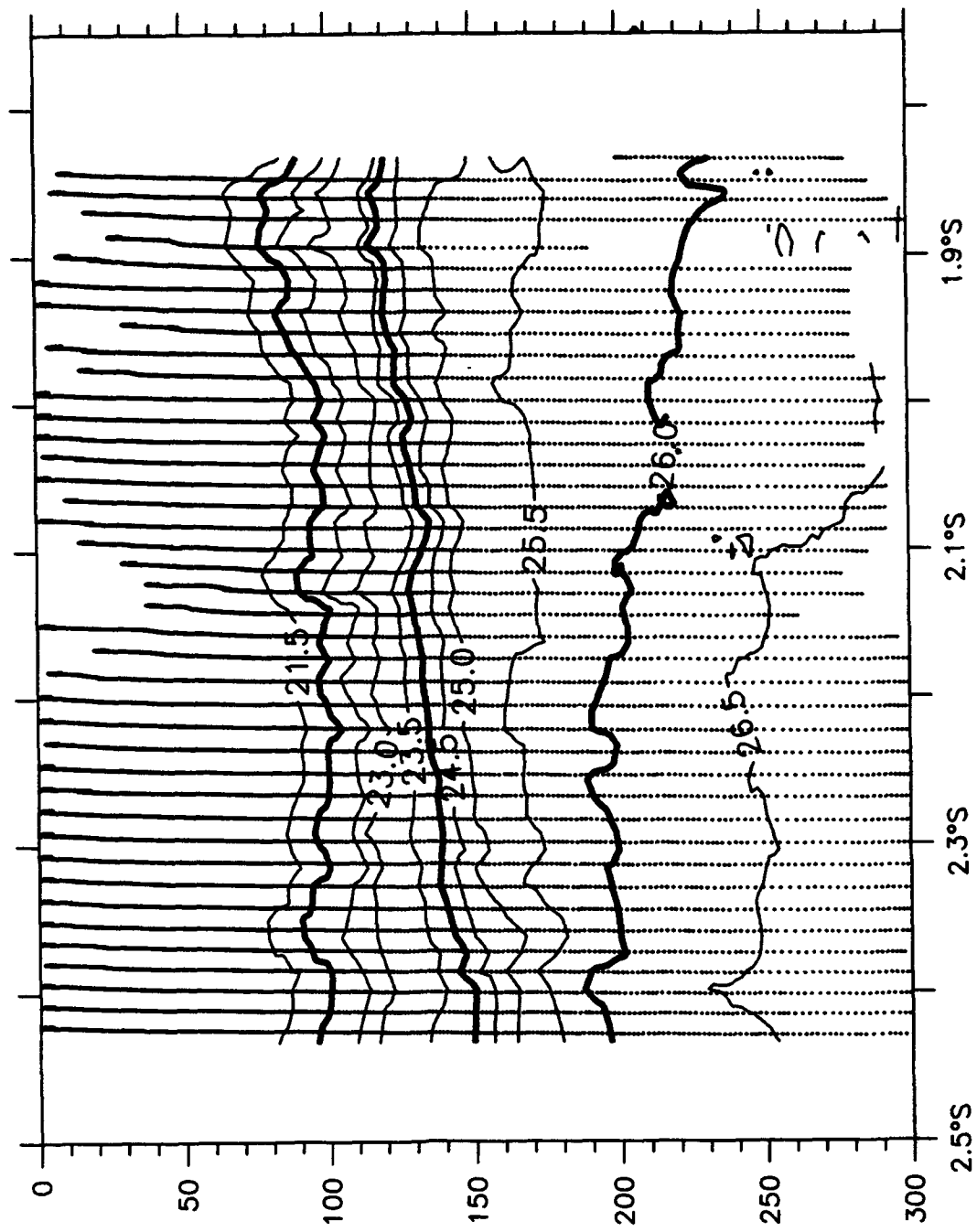
Sigma-t, S2W, 4 February 1993



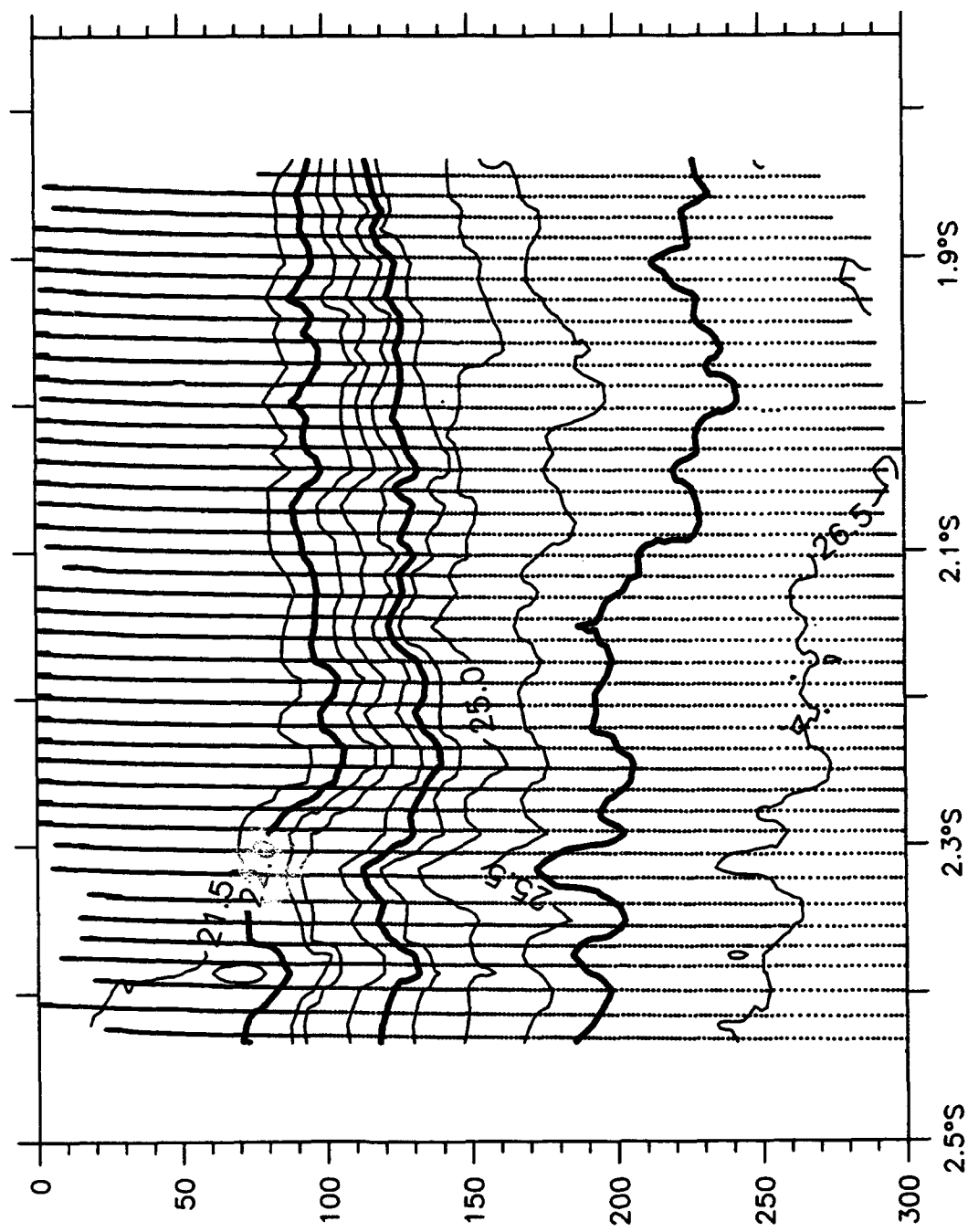
Sigma-t, S2W, 6 February 1993



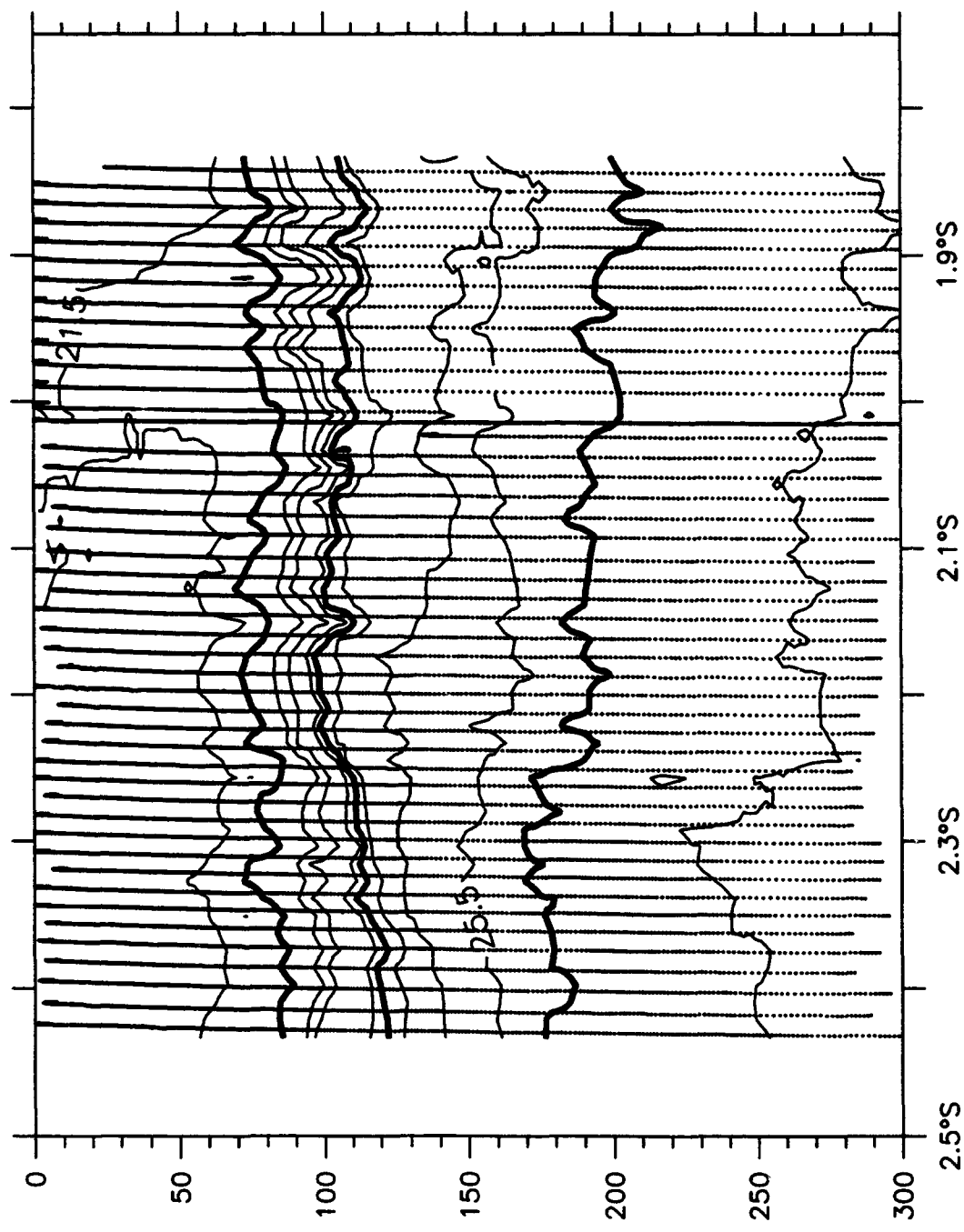
Sigma-t, S2W, 8 February 1993

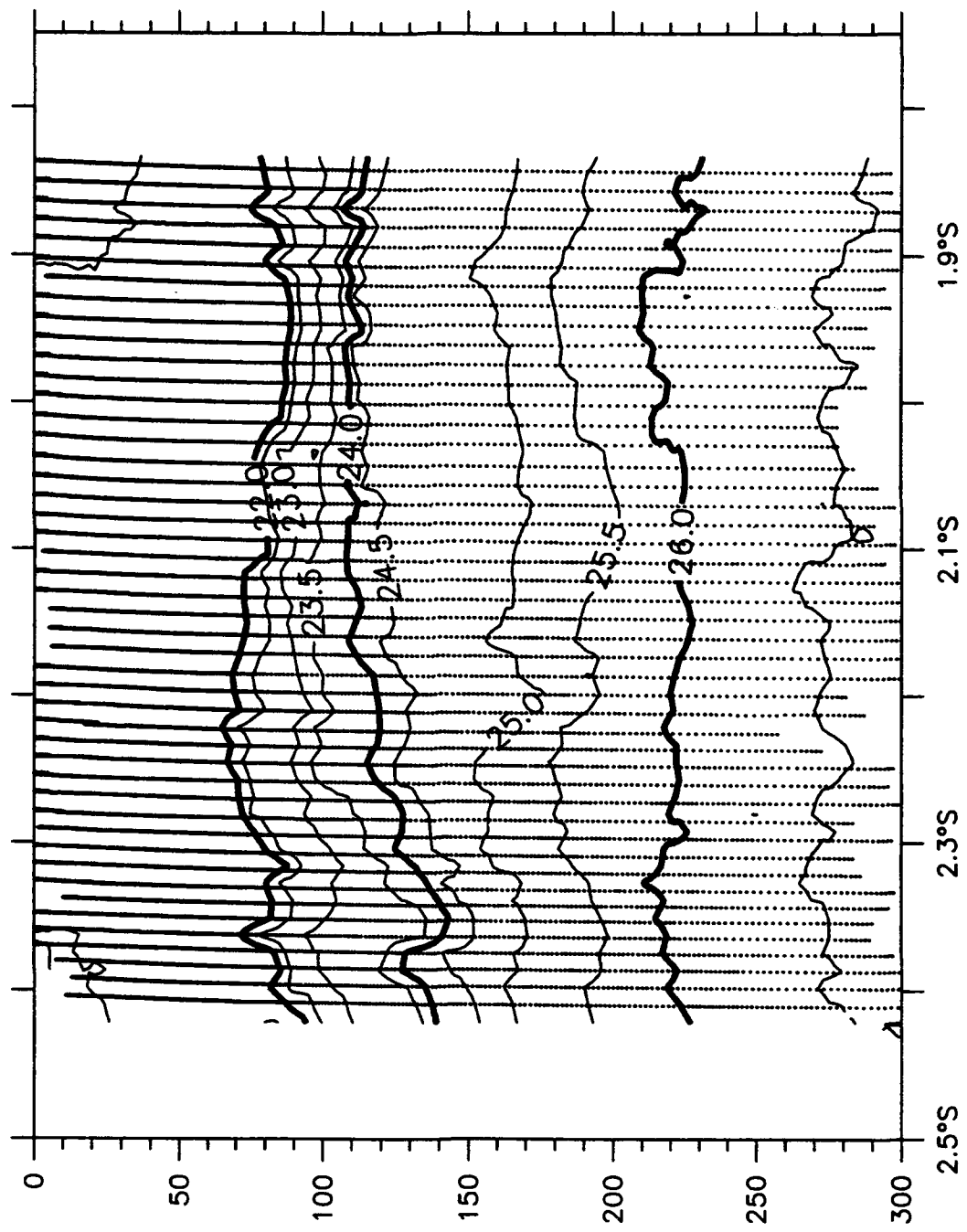


Sigma-t, S2W, 9 February 1993

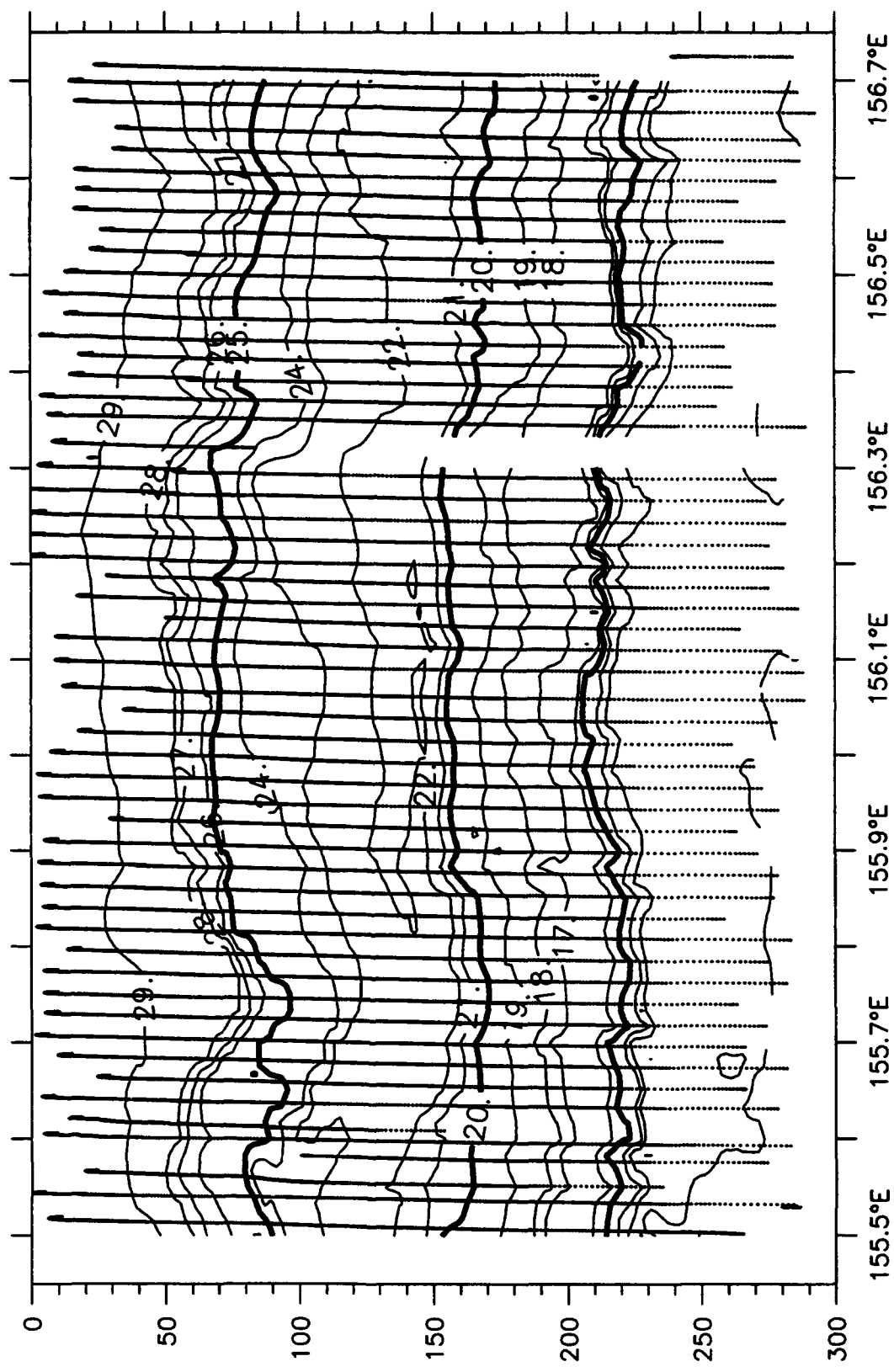


Sigma-t, S2W, 11 February 1993

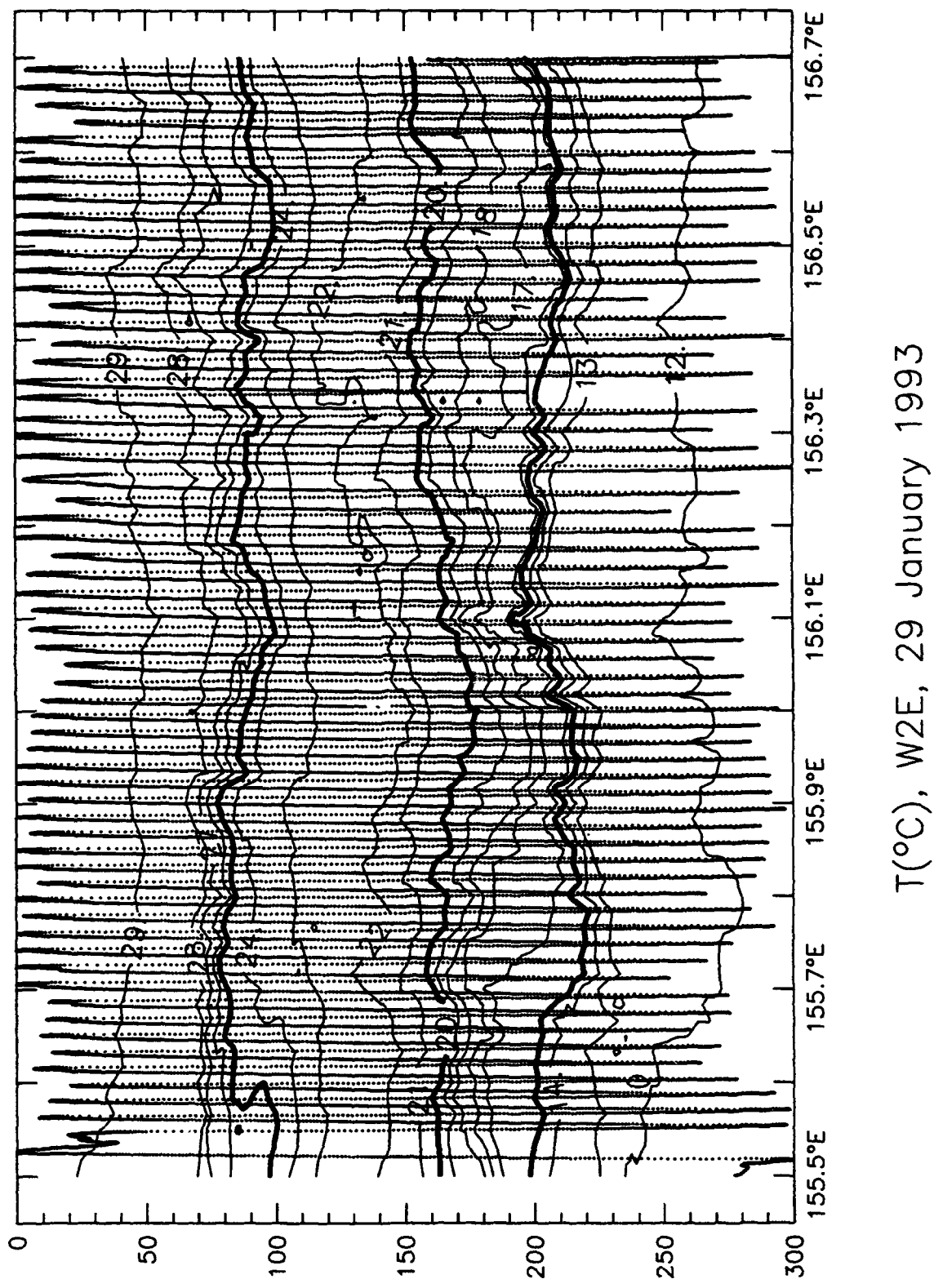


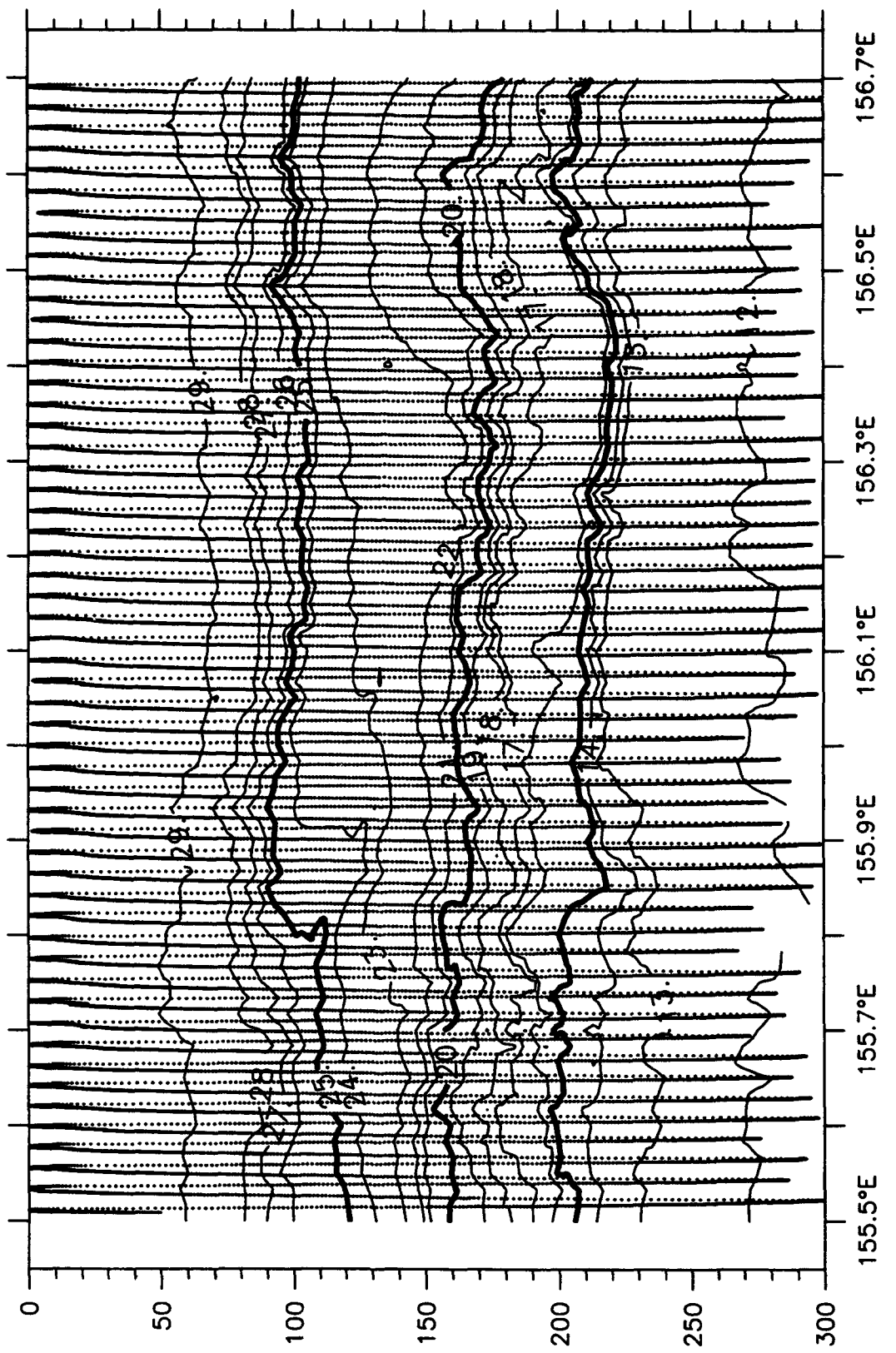


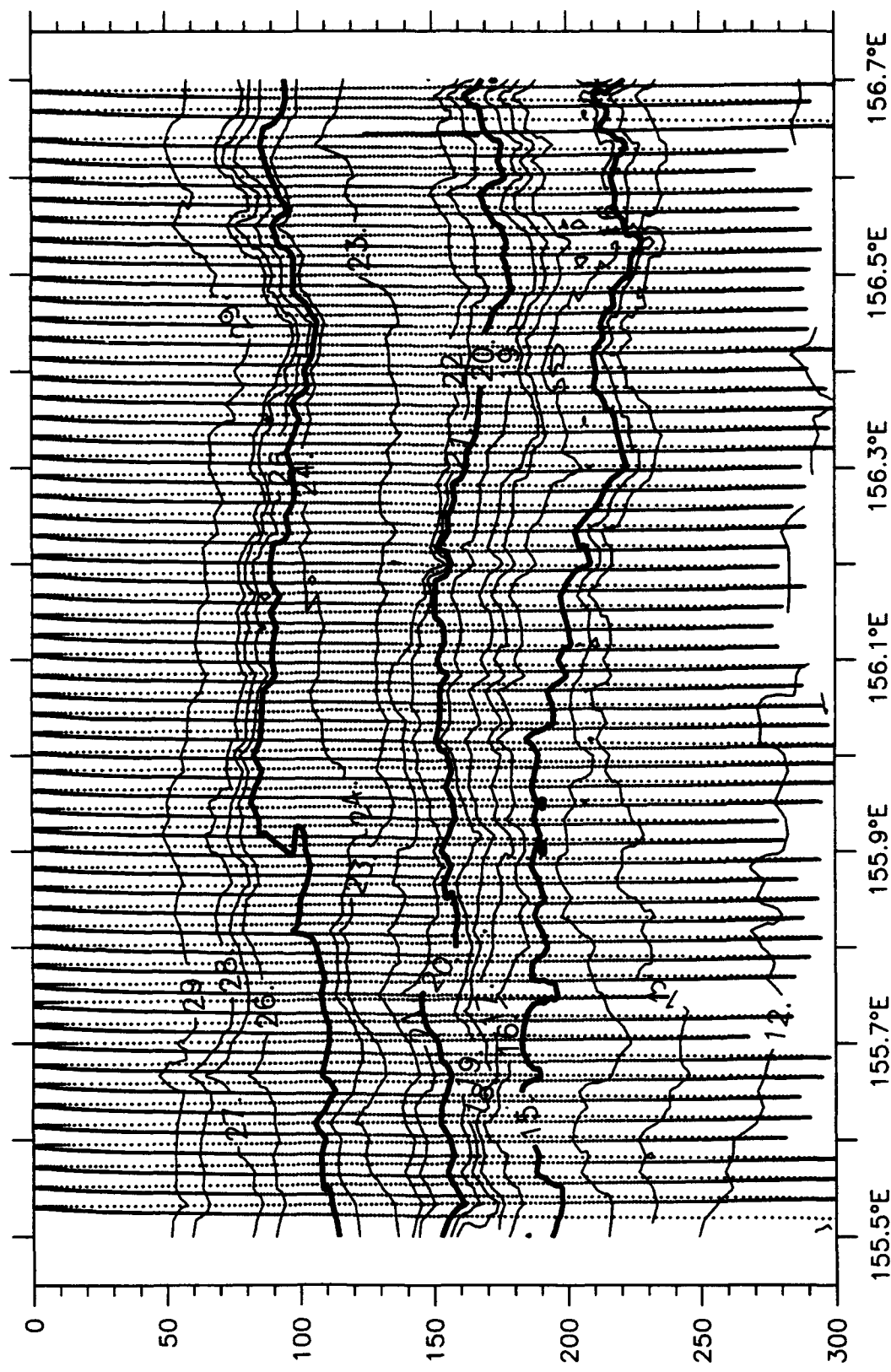
Sigma-t, S2W, 14 February 1993



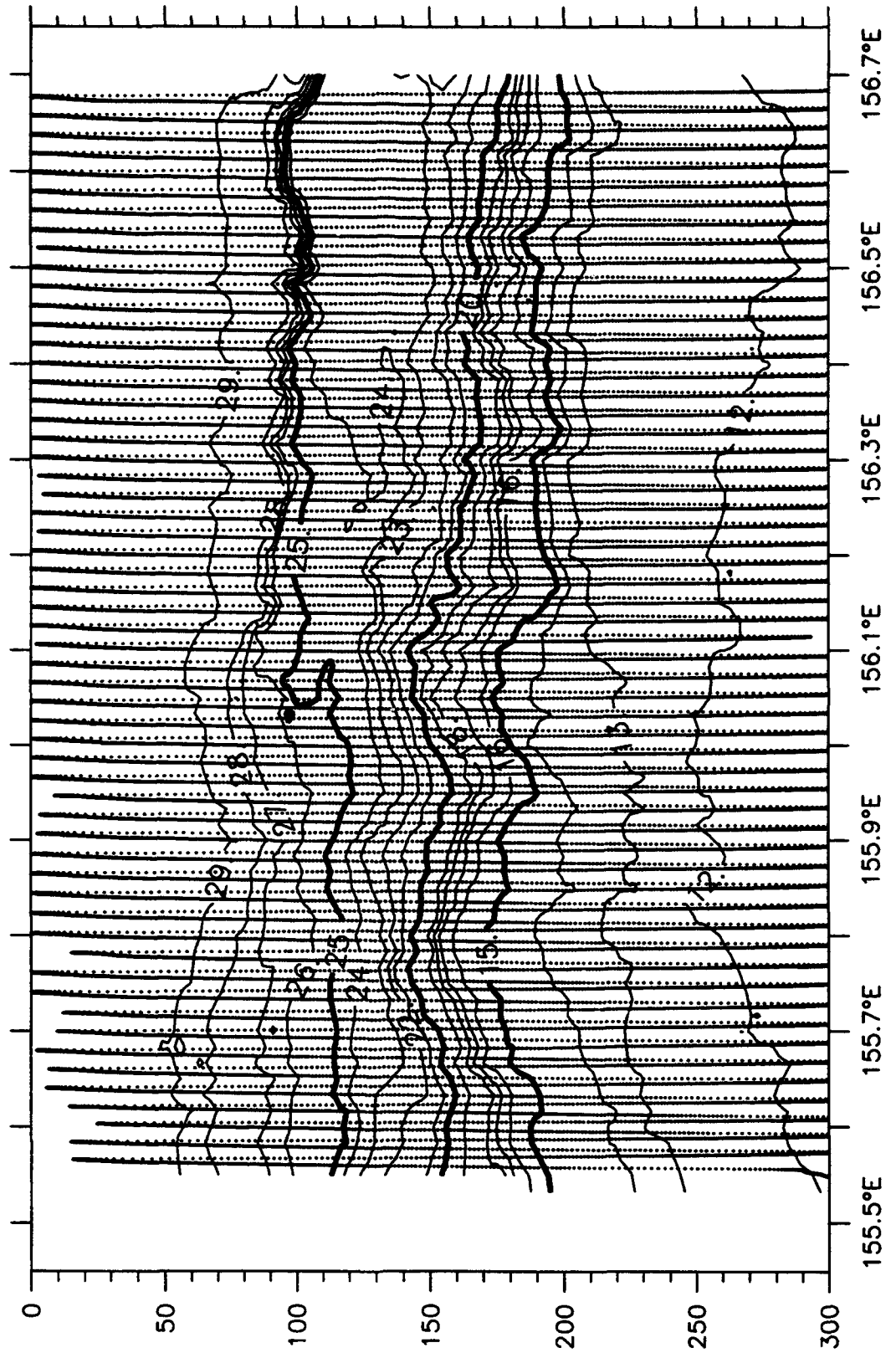
$T(^{\circ}\text{C})$ , W2E, 28 January 1993



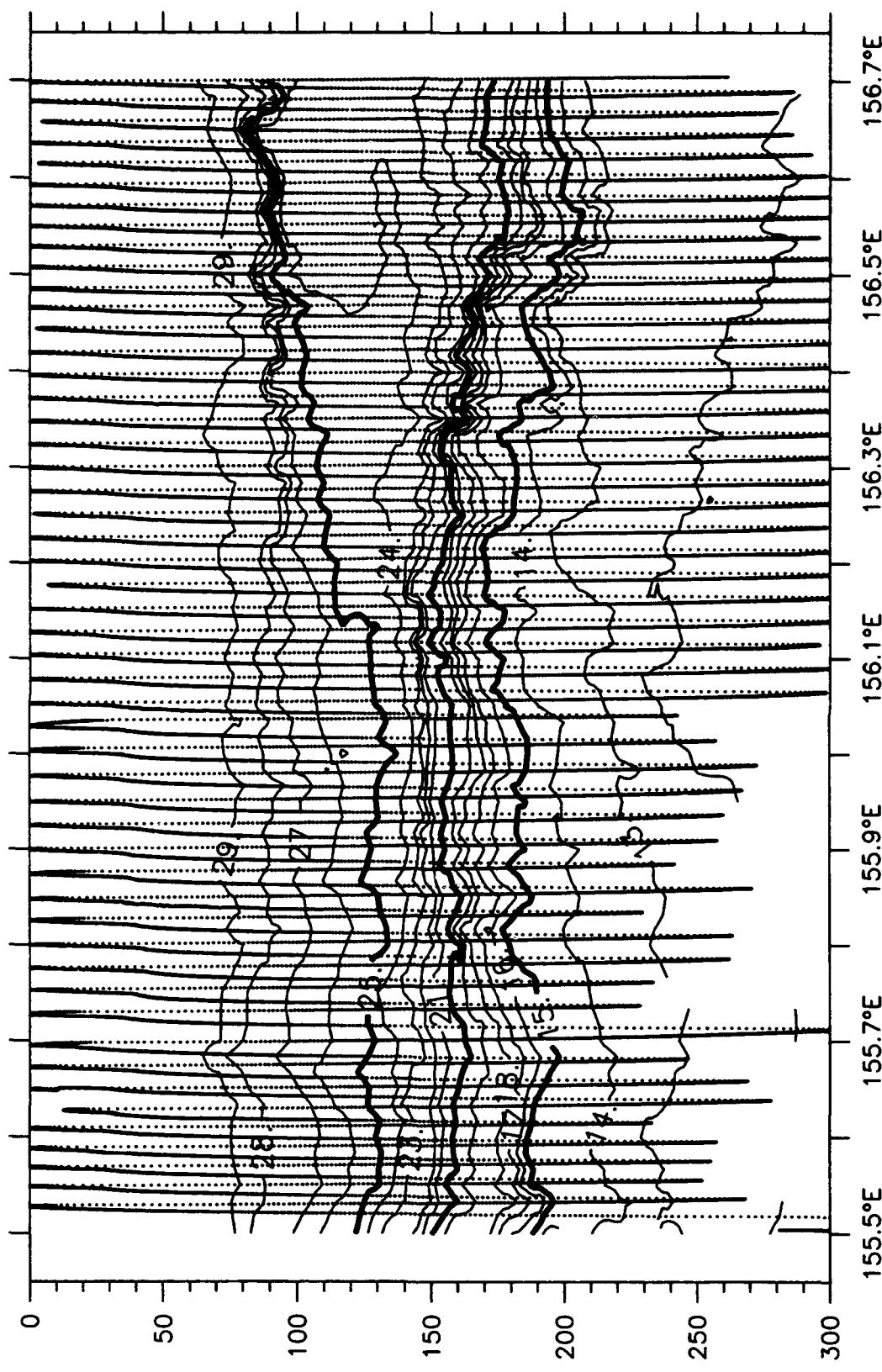


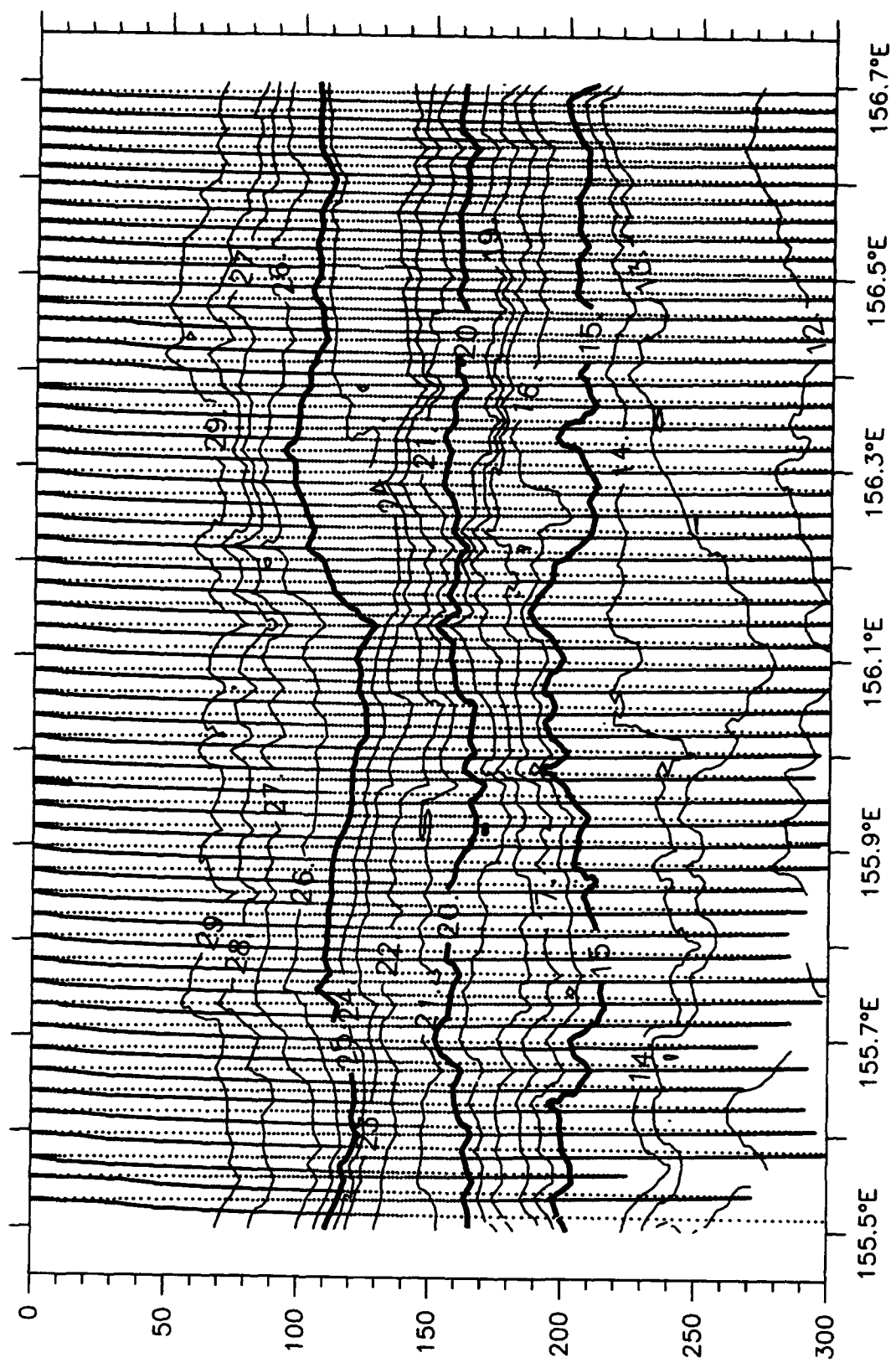


$T(^{\circ}\text{C})$ , W2E, 1 February 1993

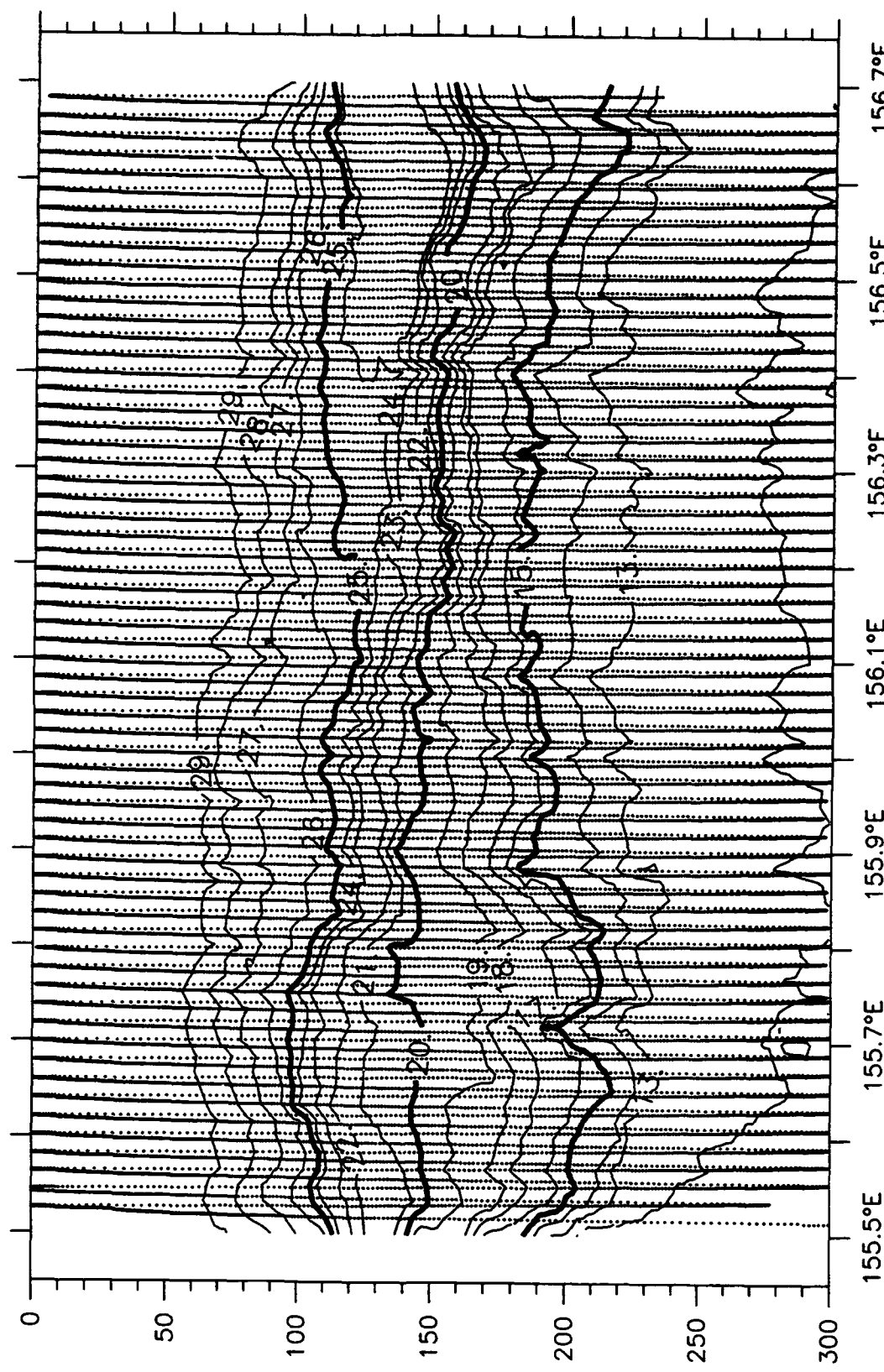


T( $^{\circ}$ C), W2E, 04 February 1993



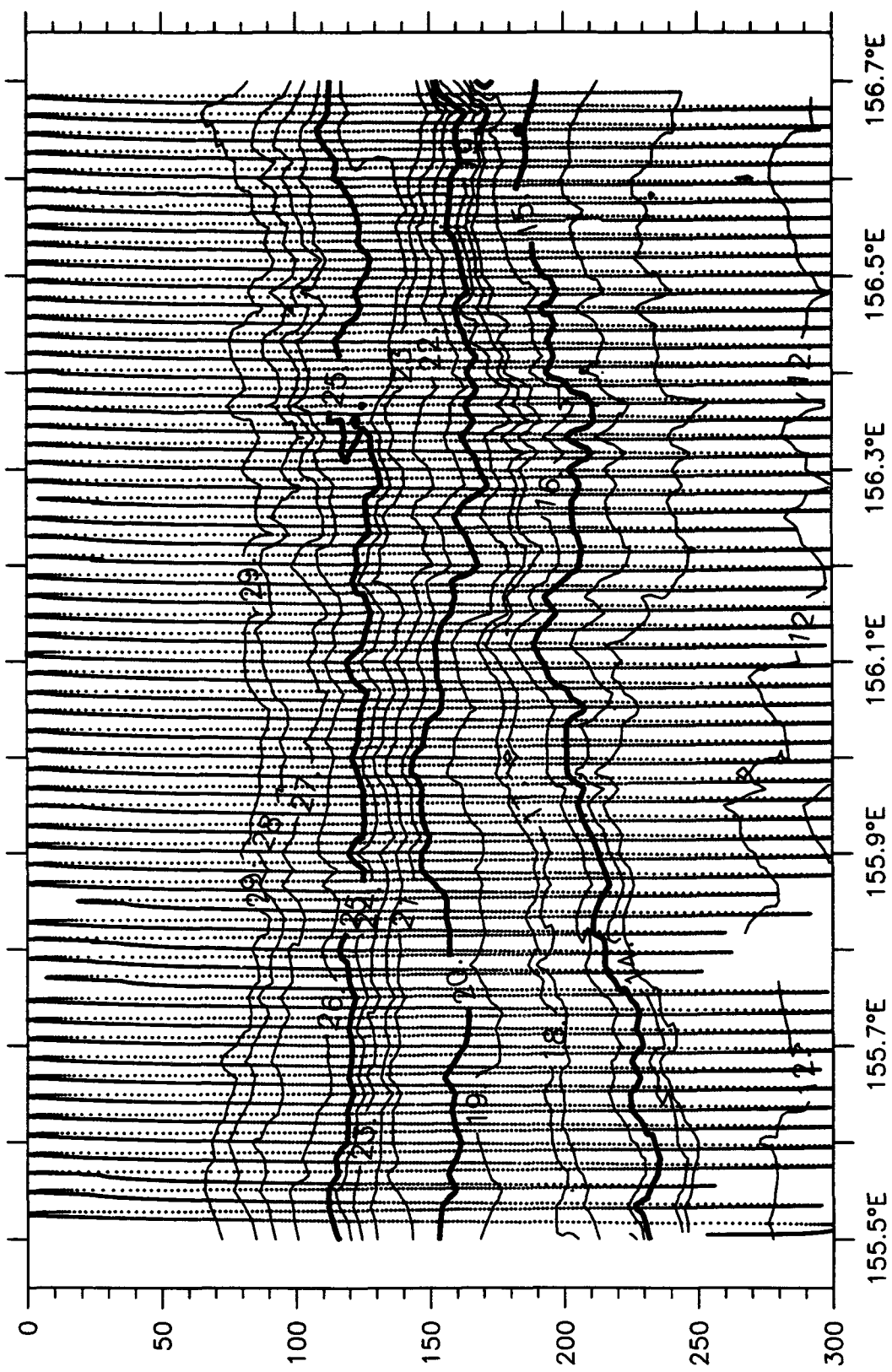


$T(^{\circ}\text{C})$ , W2E, 06 February 1993

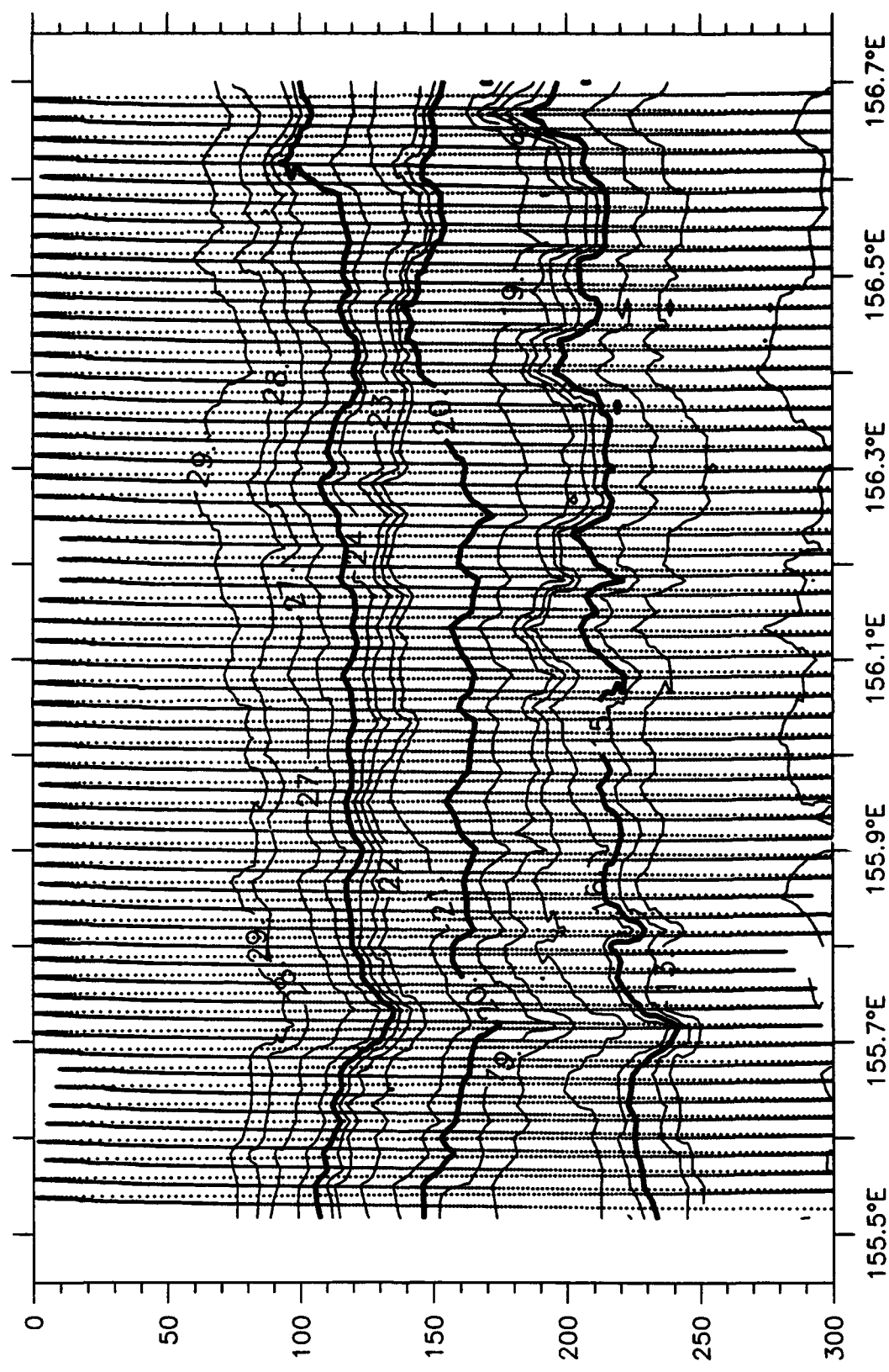


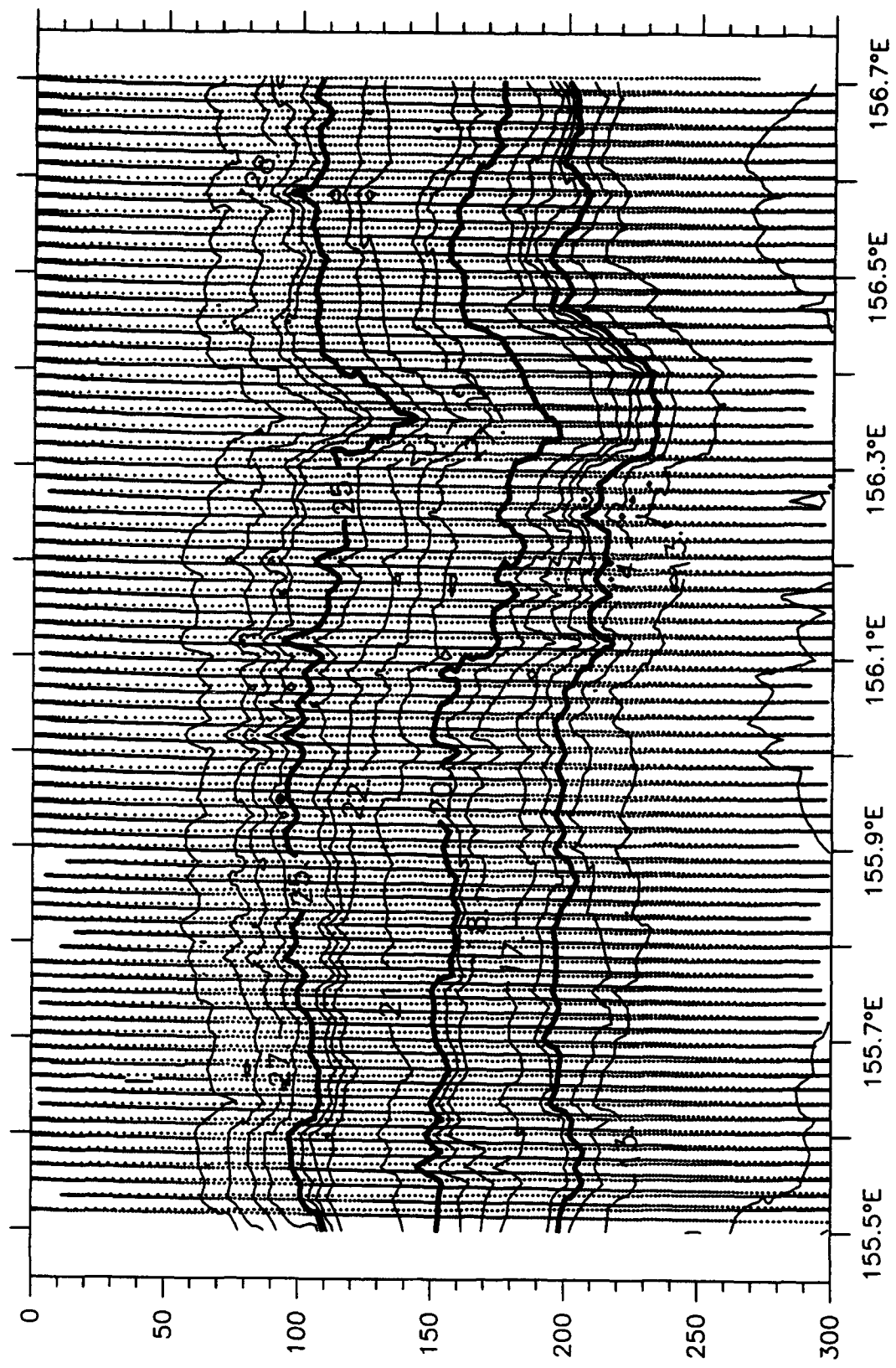
$T$  ( $^{\circ}\text{C}$ ), W2E, 08 February 1993

T( $^{\circ}$ C), W2E, 10 February 1993

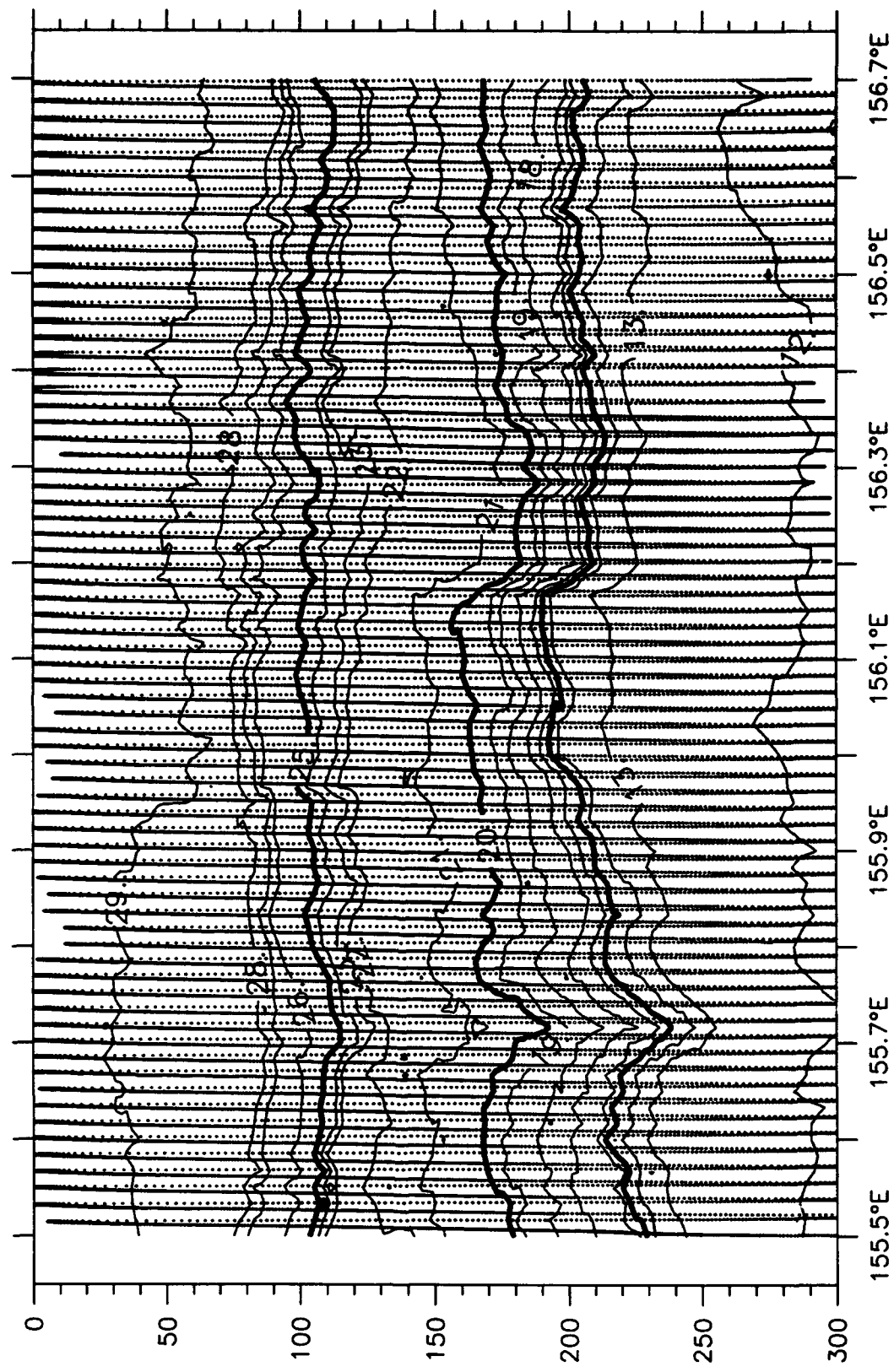


T( $^{\circ}$ C), W2E, 11 February 1993

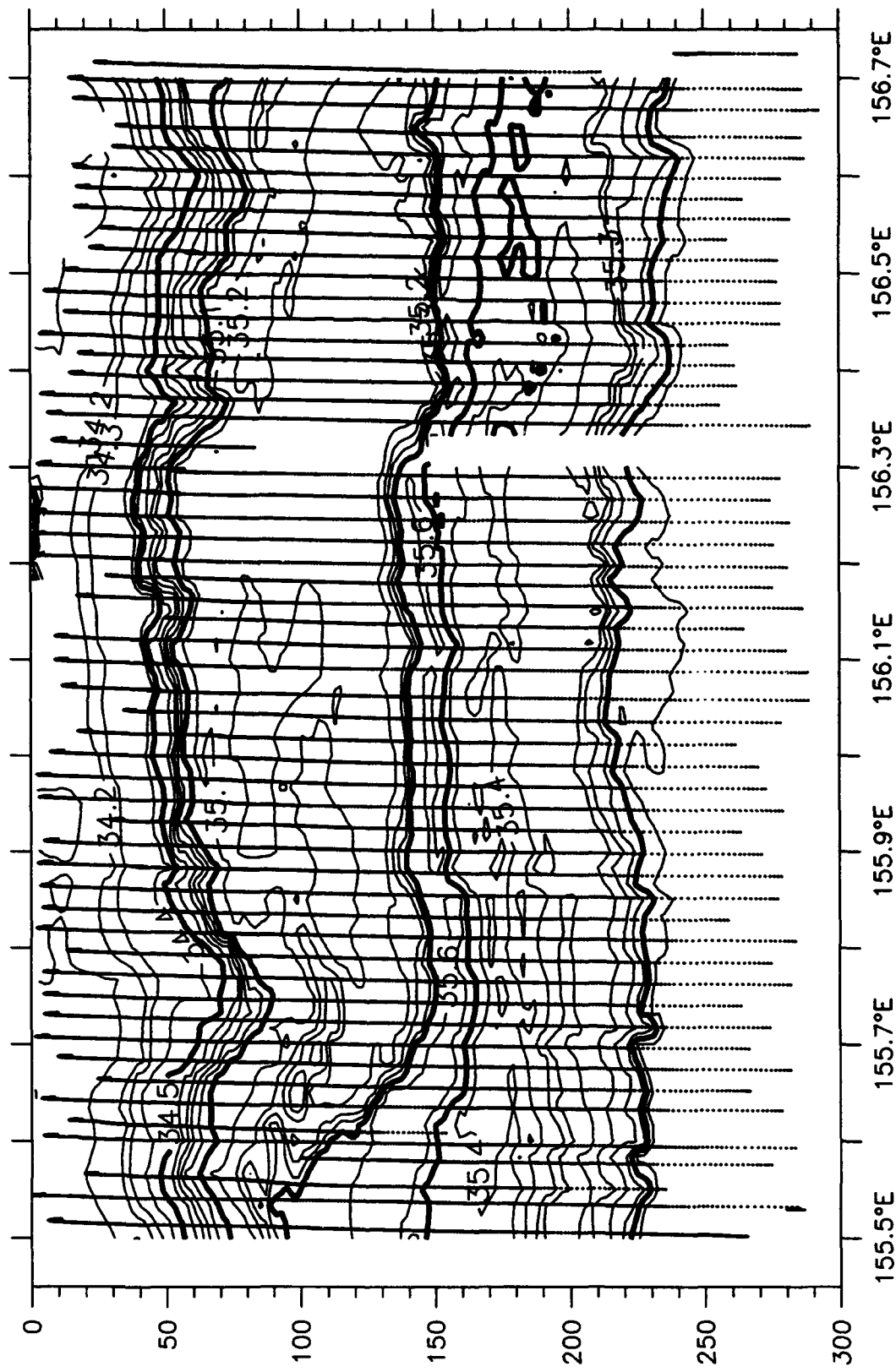




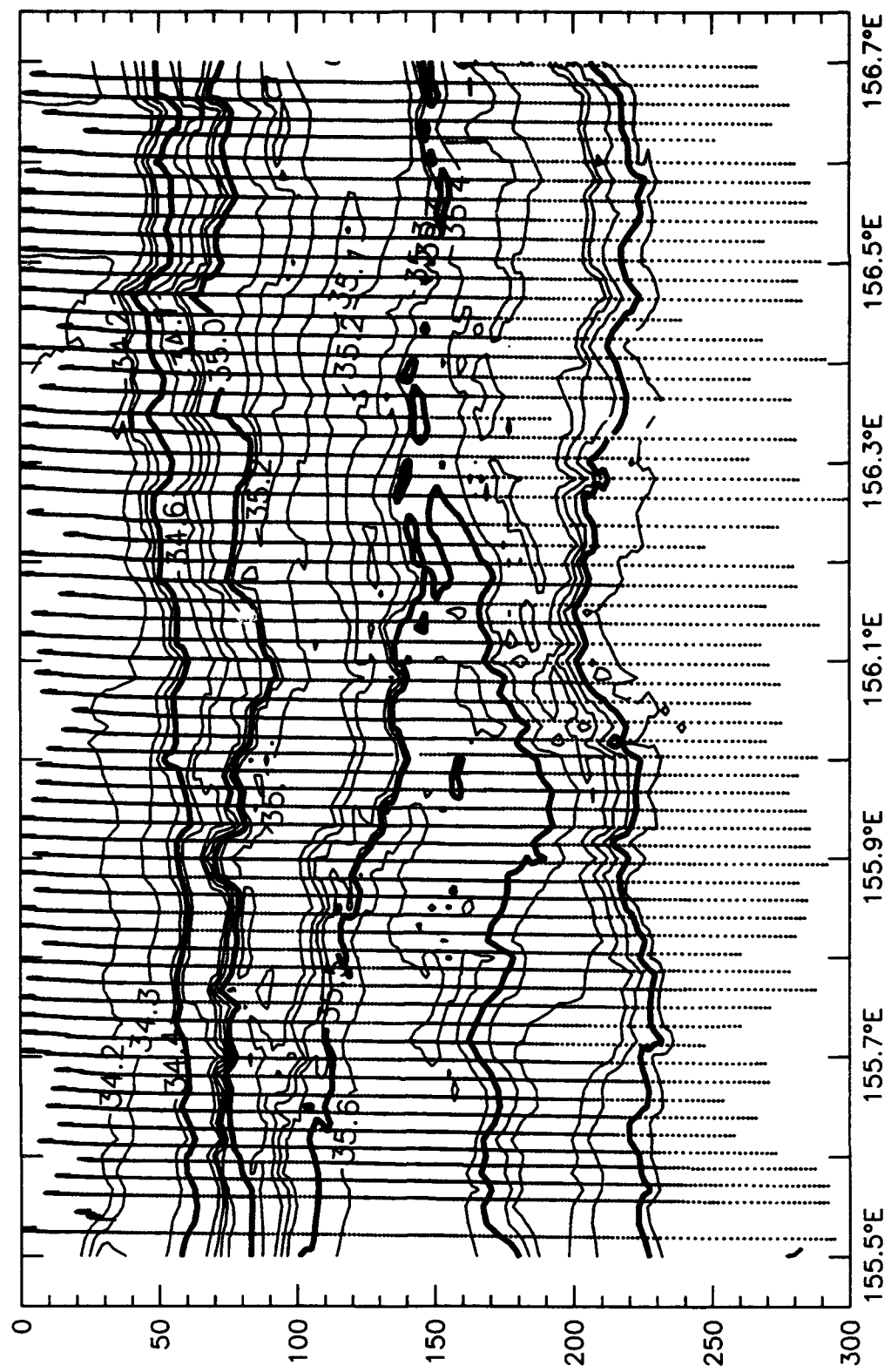
$T(^{\circ}\text{C})$ , W2E, 13 February 1993



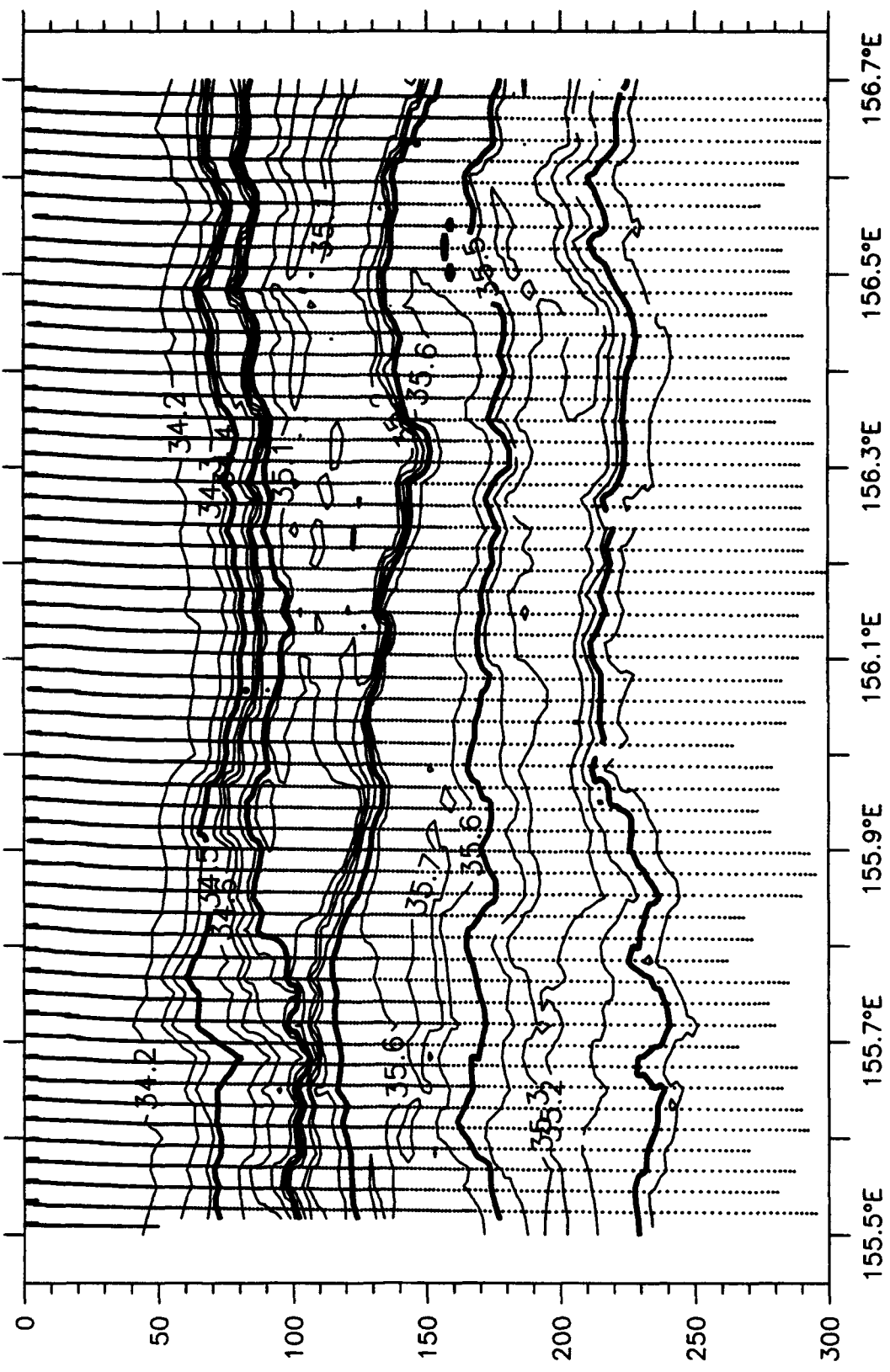
$T(^{\circ}\text{C})$ , W2E, 14 February 1993



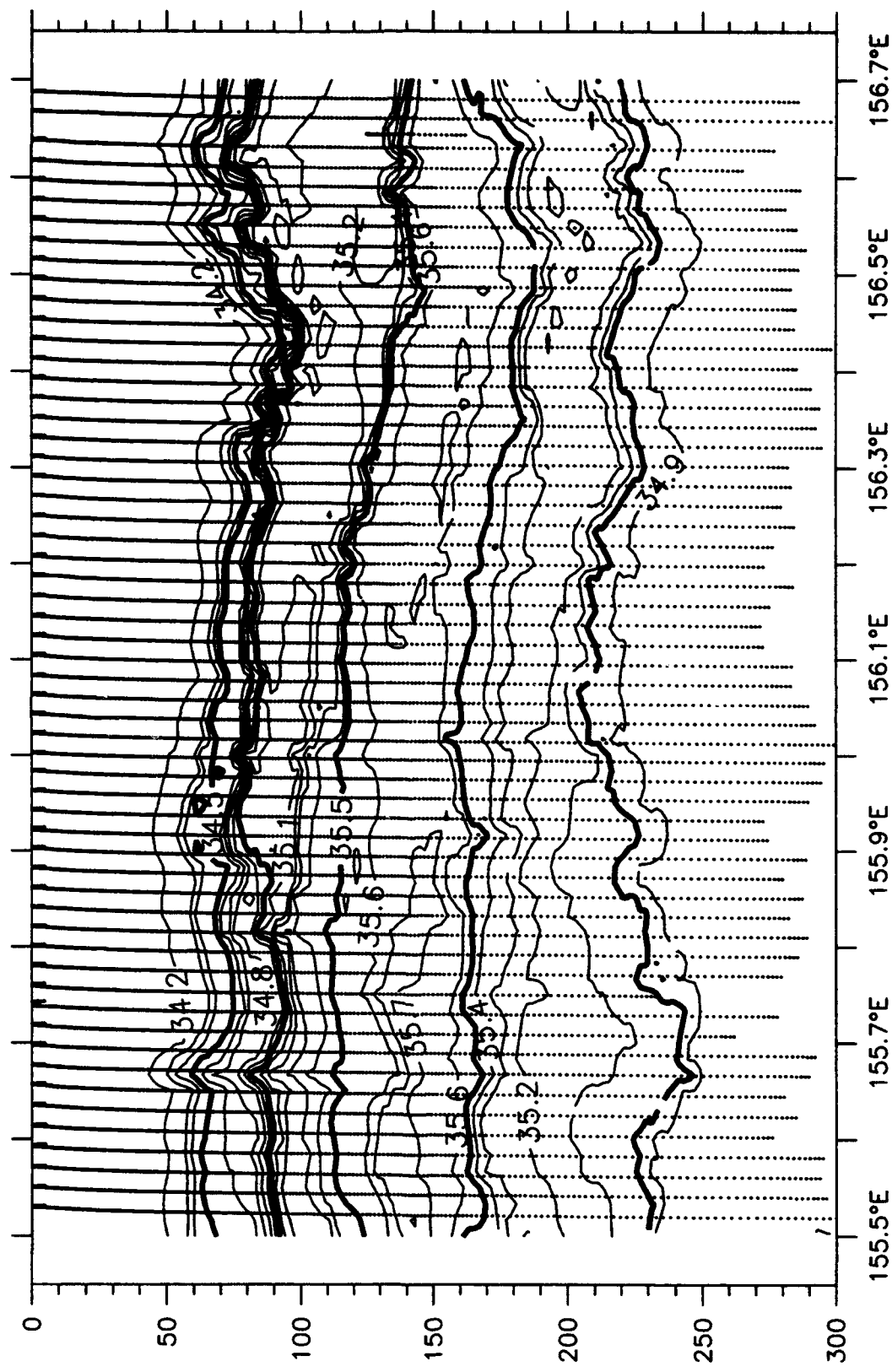
$S(\text{psu})$ , W2E, 28 January 1993



$S(\text{psu})$ , W2E, 29 January 1993

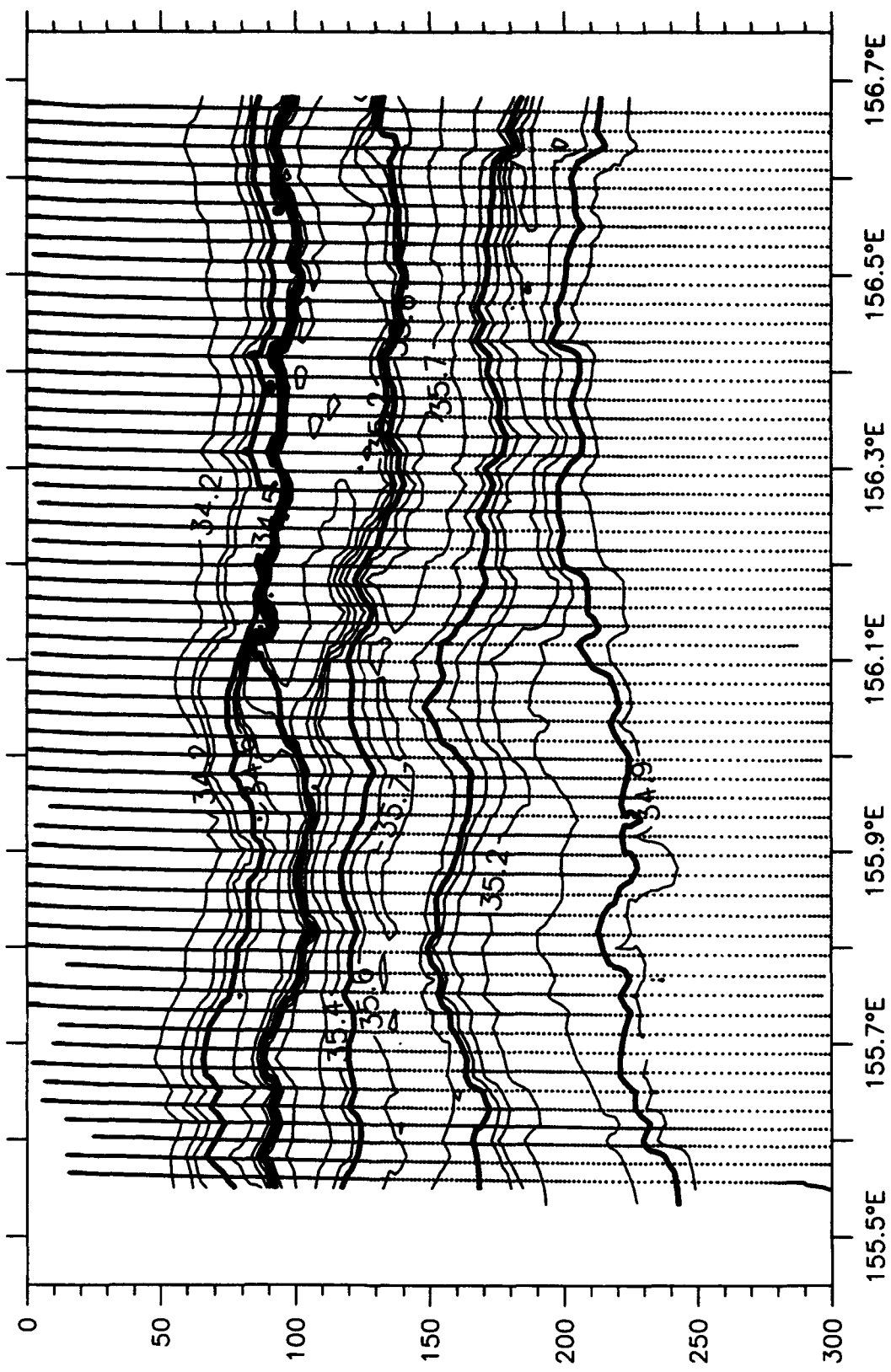


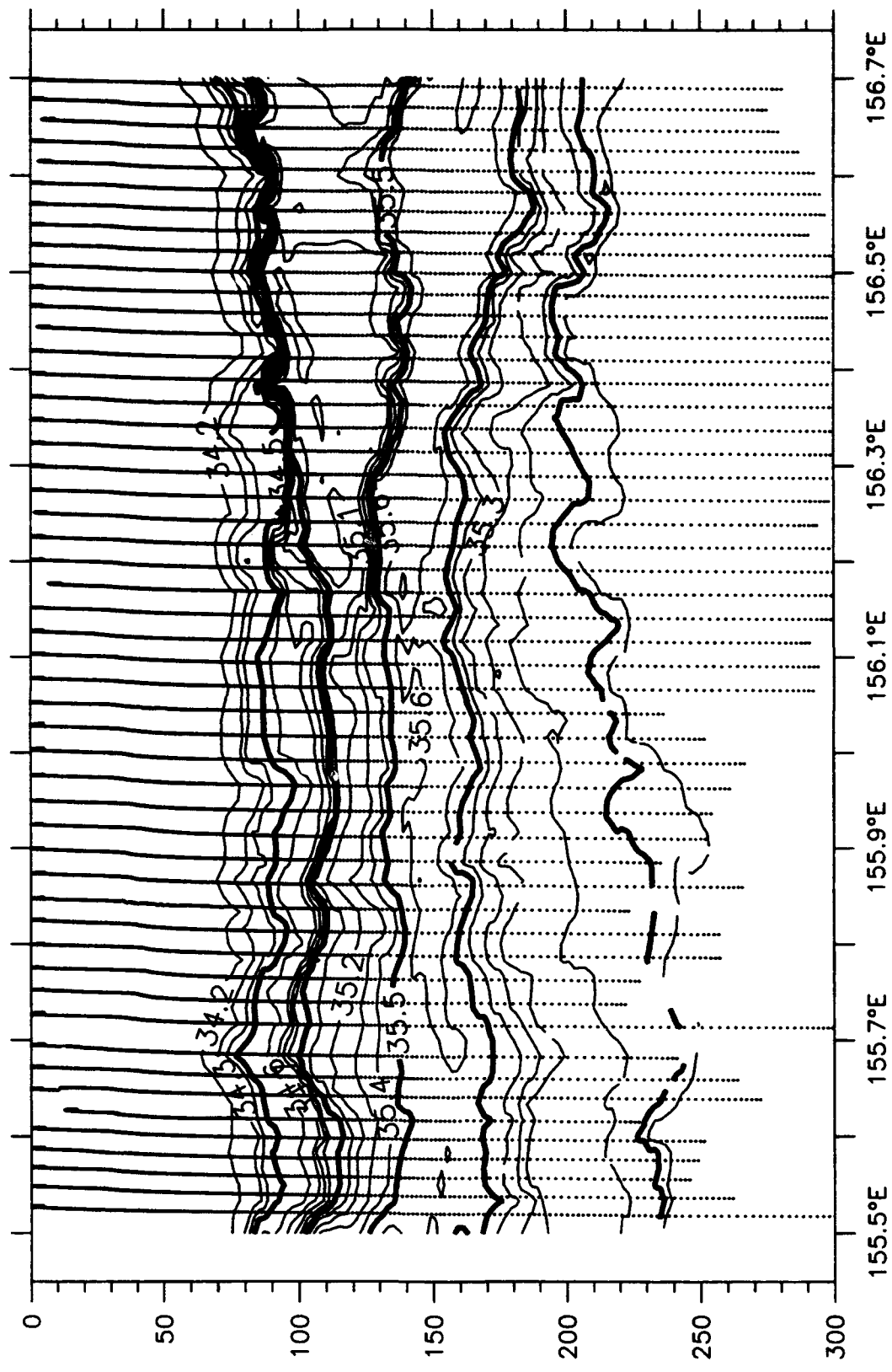
$S(\text{psu})$ , W2E, 31 January 1993



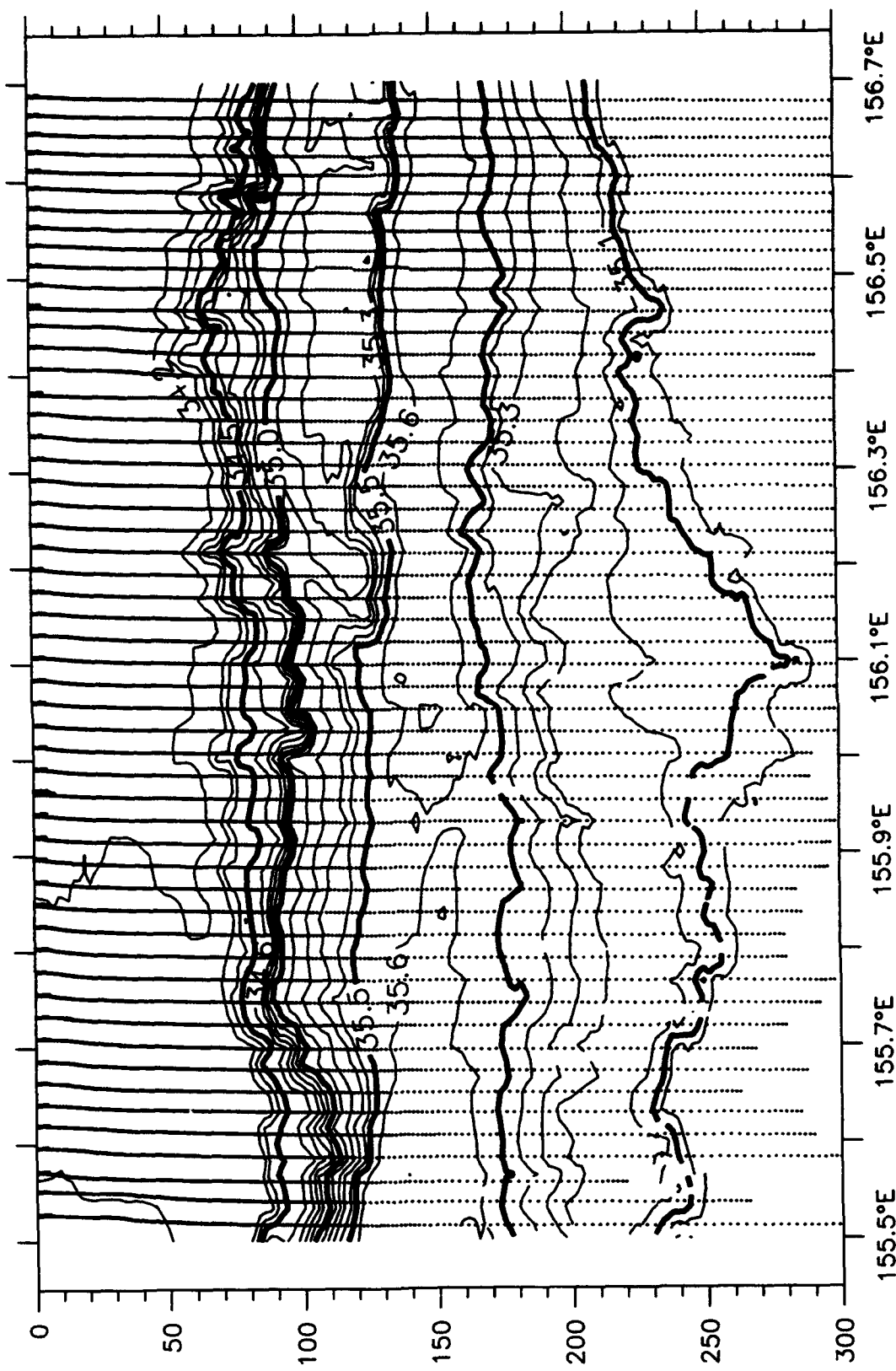
$S(\text{psu})$ , W2E, 1 February 1993

S(psu), W2E, 3 February 1993



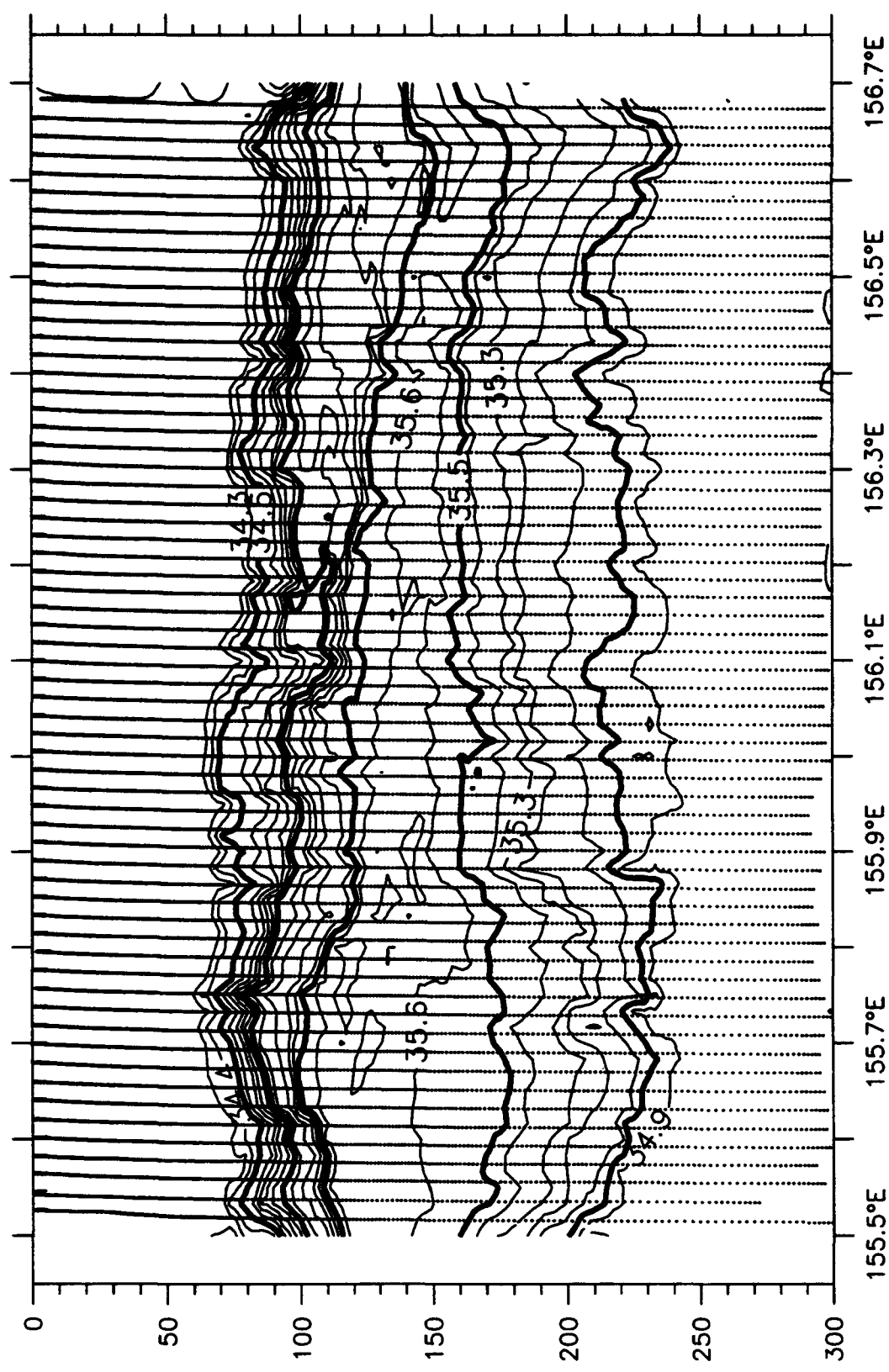


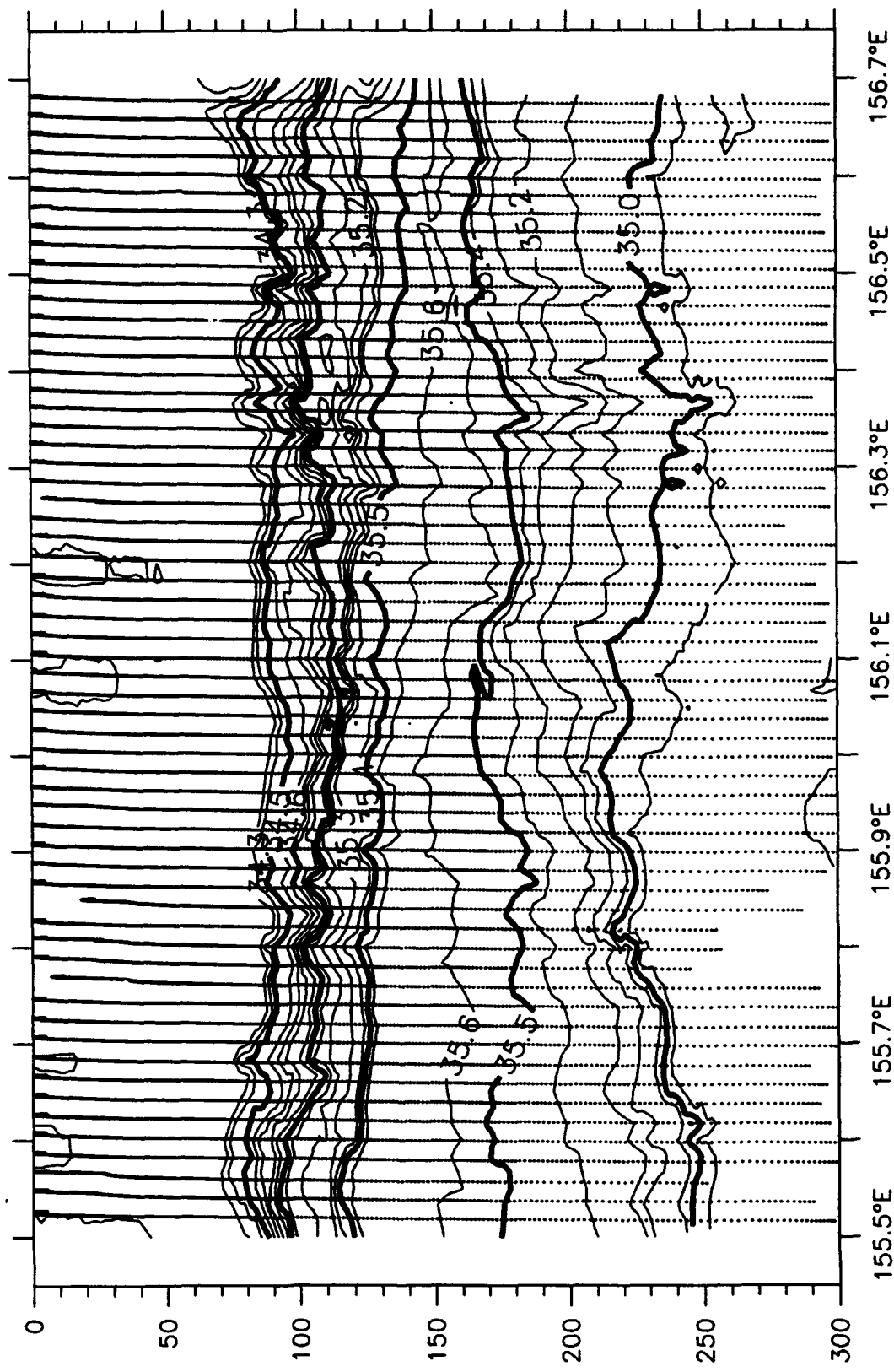
S(psu), W2E, 04 February 1993



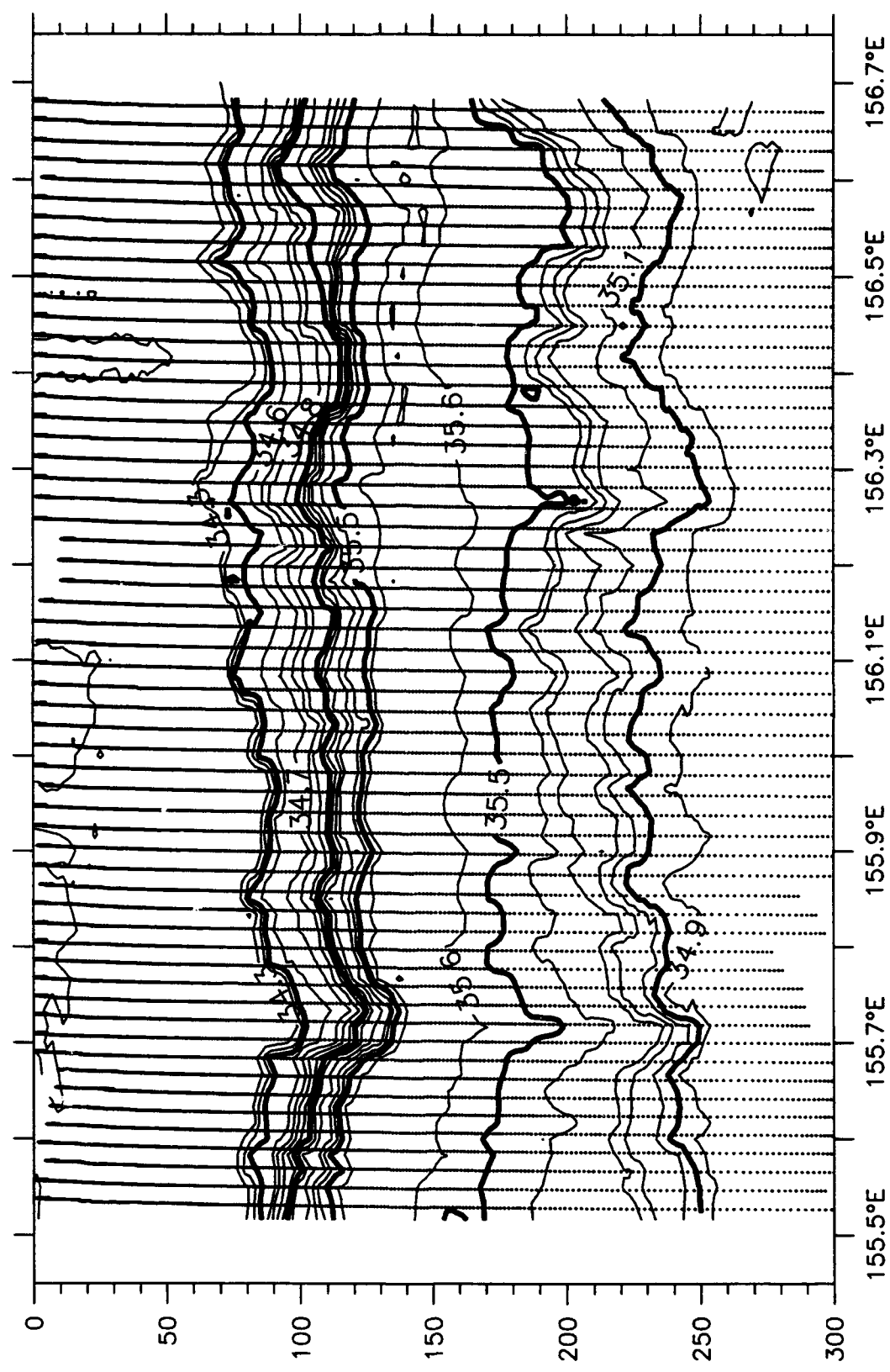
$S$ (psu), W2E, 06 February 1993

S(psu), W2E, 08 February 1993



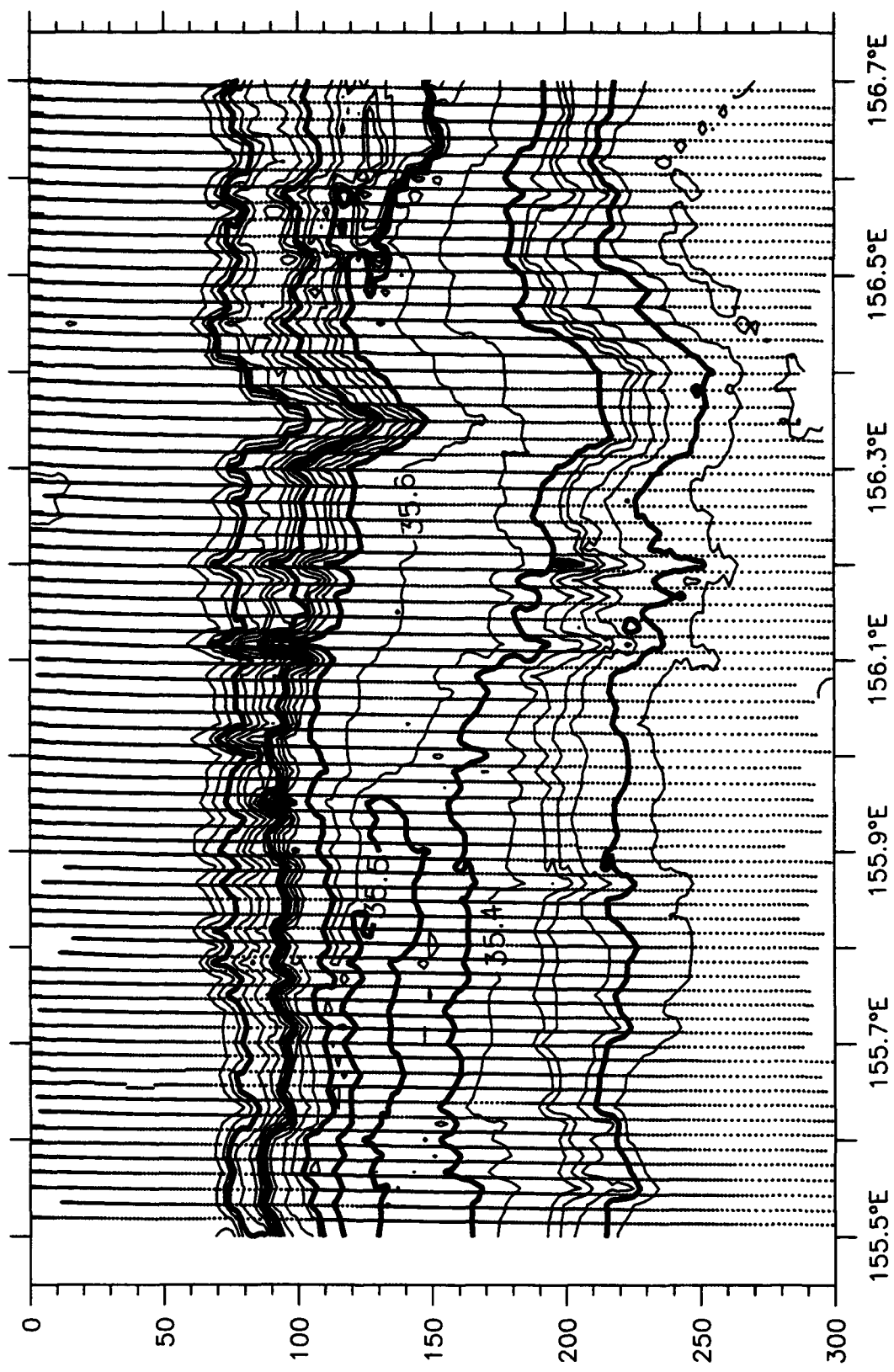


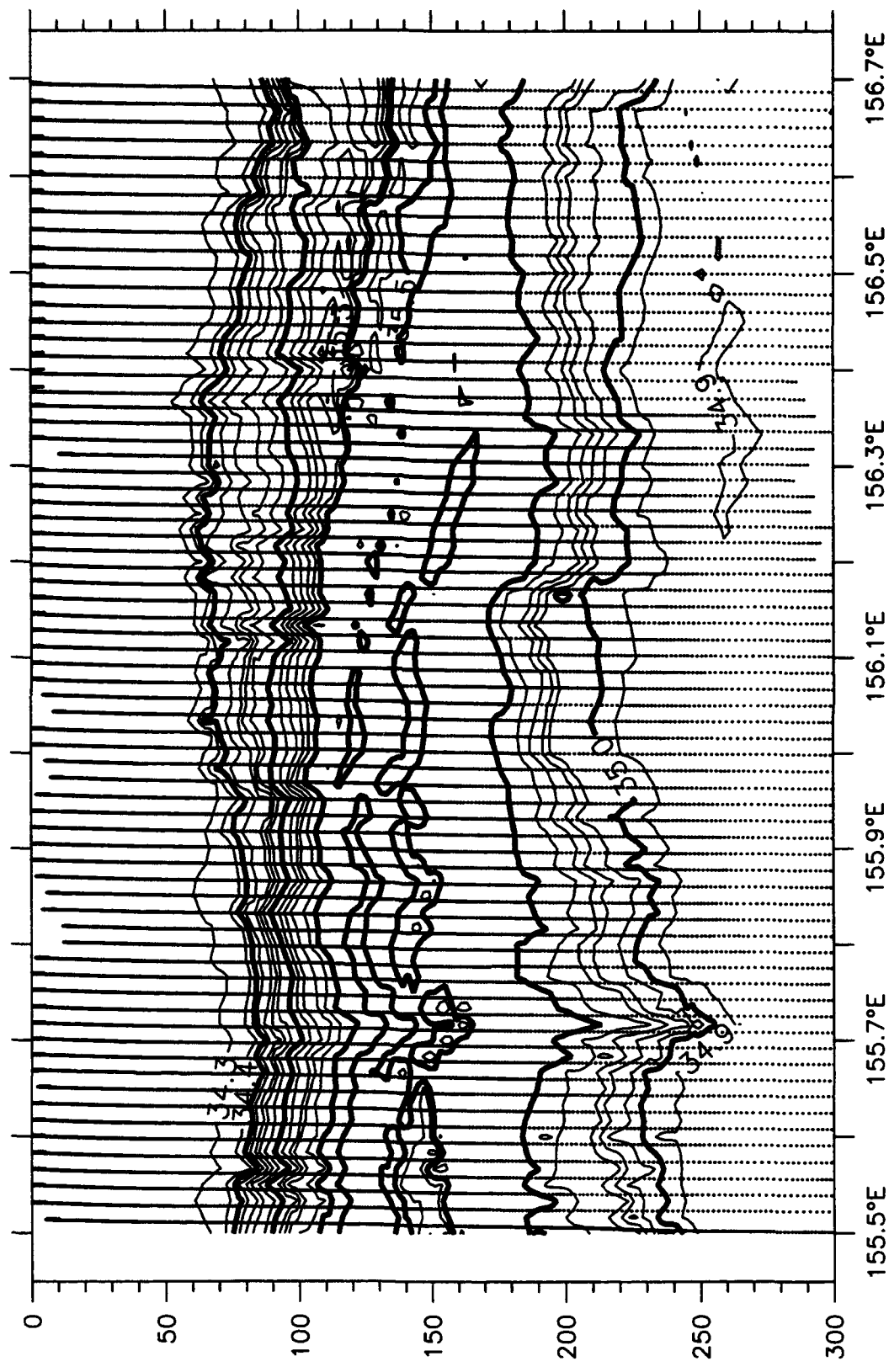
$S$ (psu), W2E, 10 February 1993



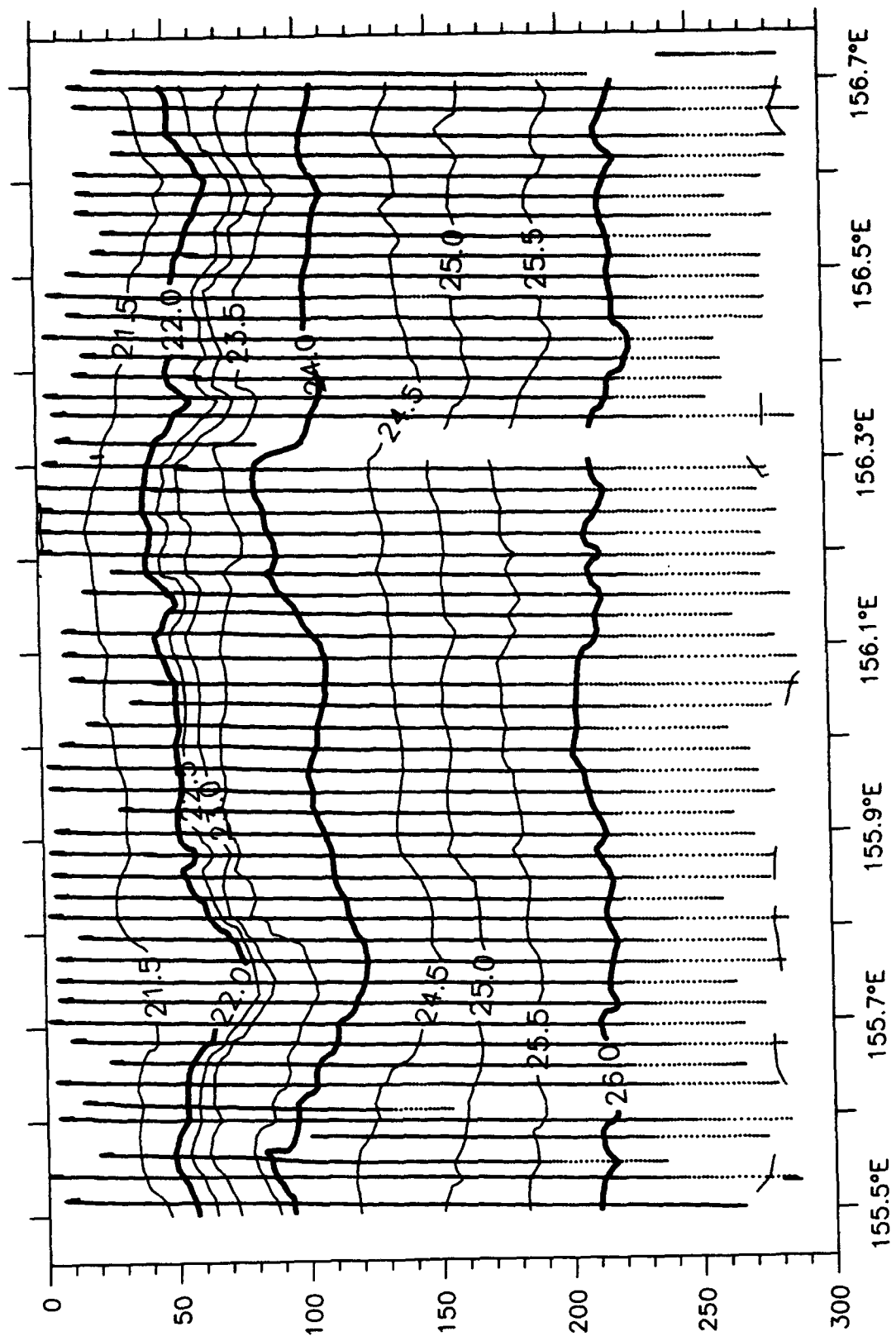
$S$ (psu), W2E, 11 February 1993

S(psu), W2E, 13 February 1993

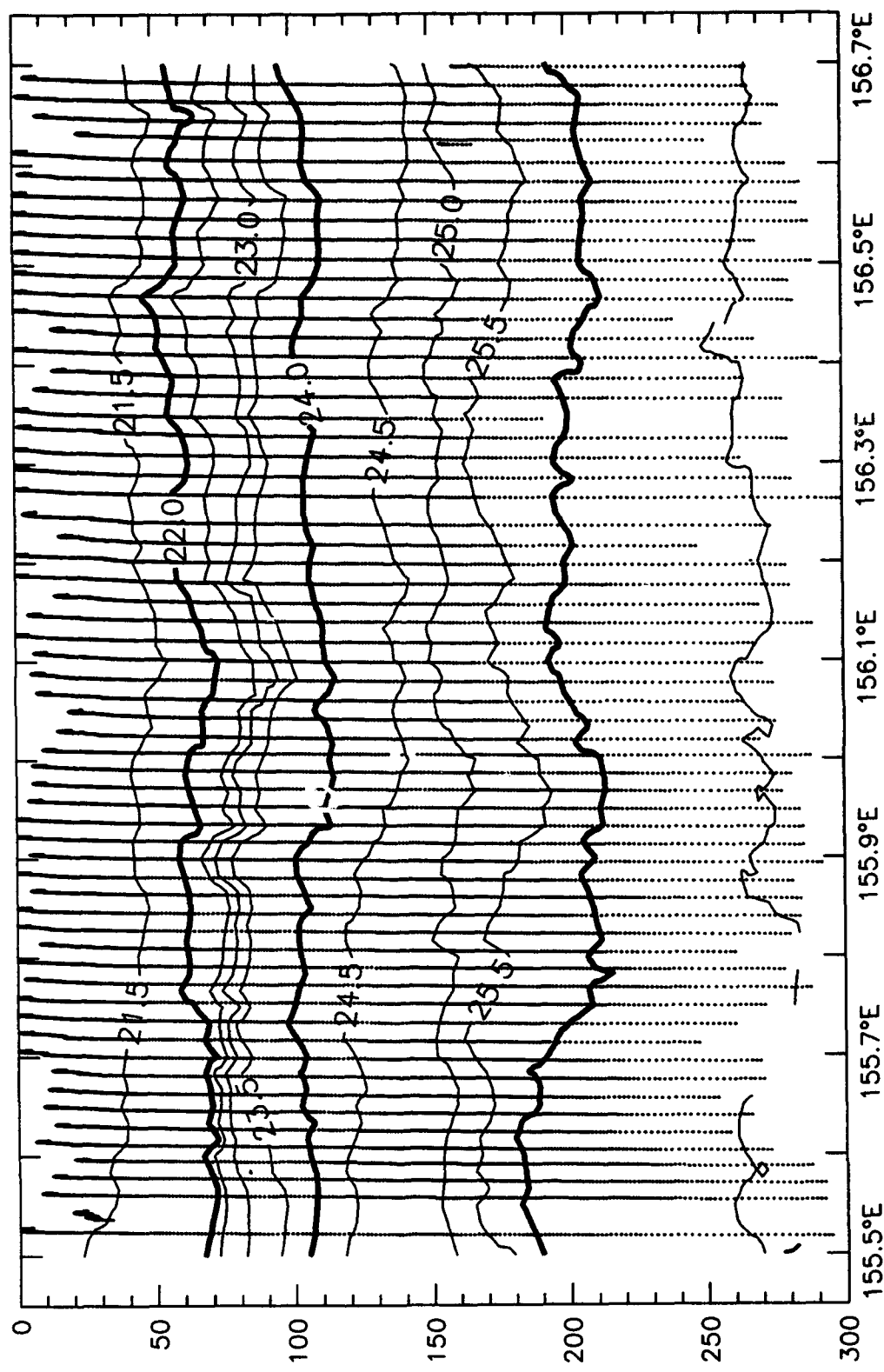




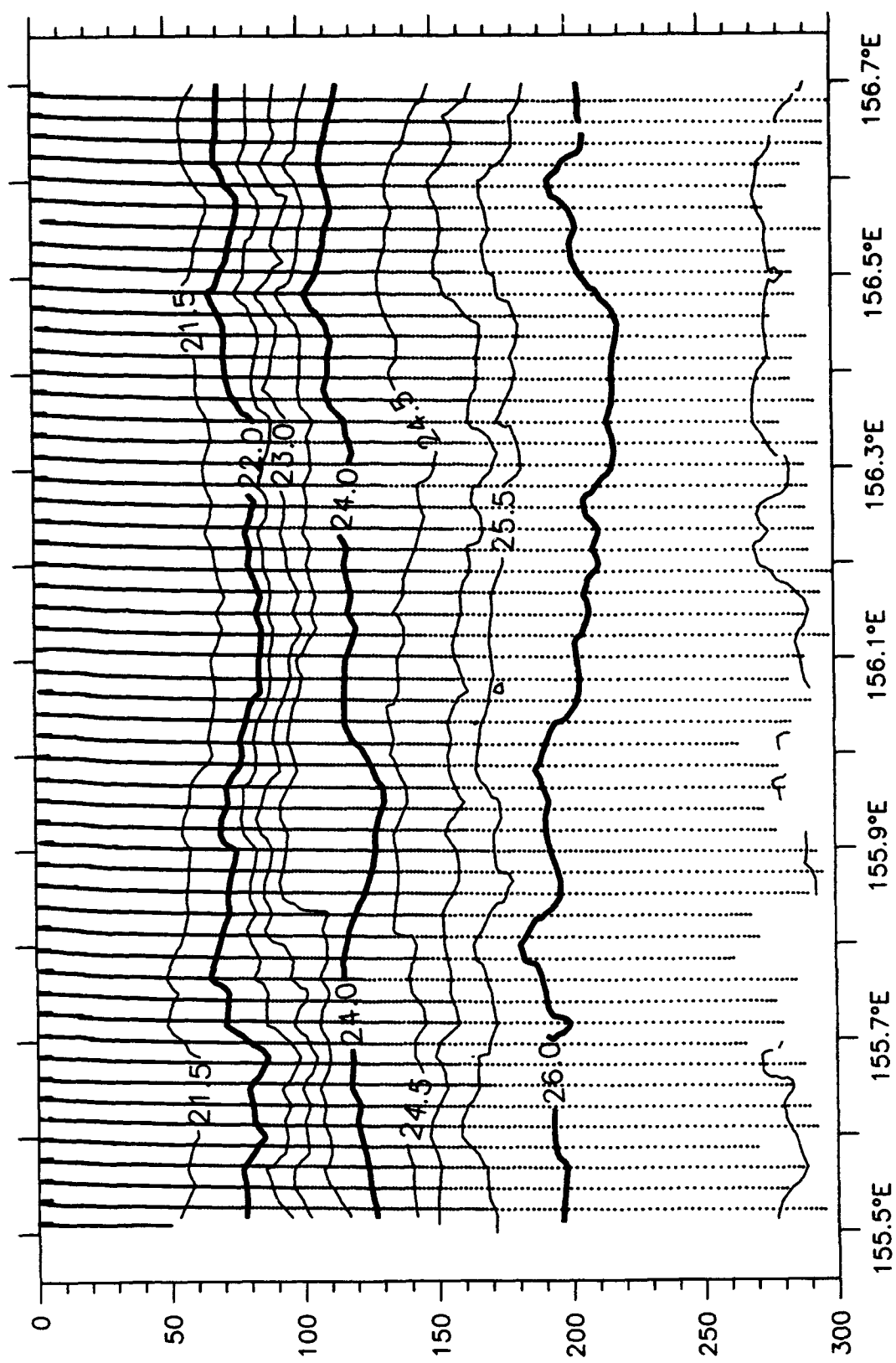
$S$ (psu), W2E, 14 February 1993



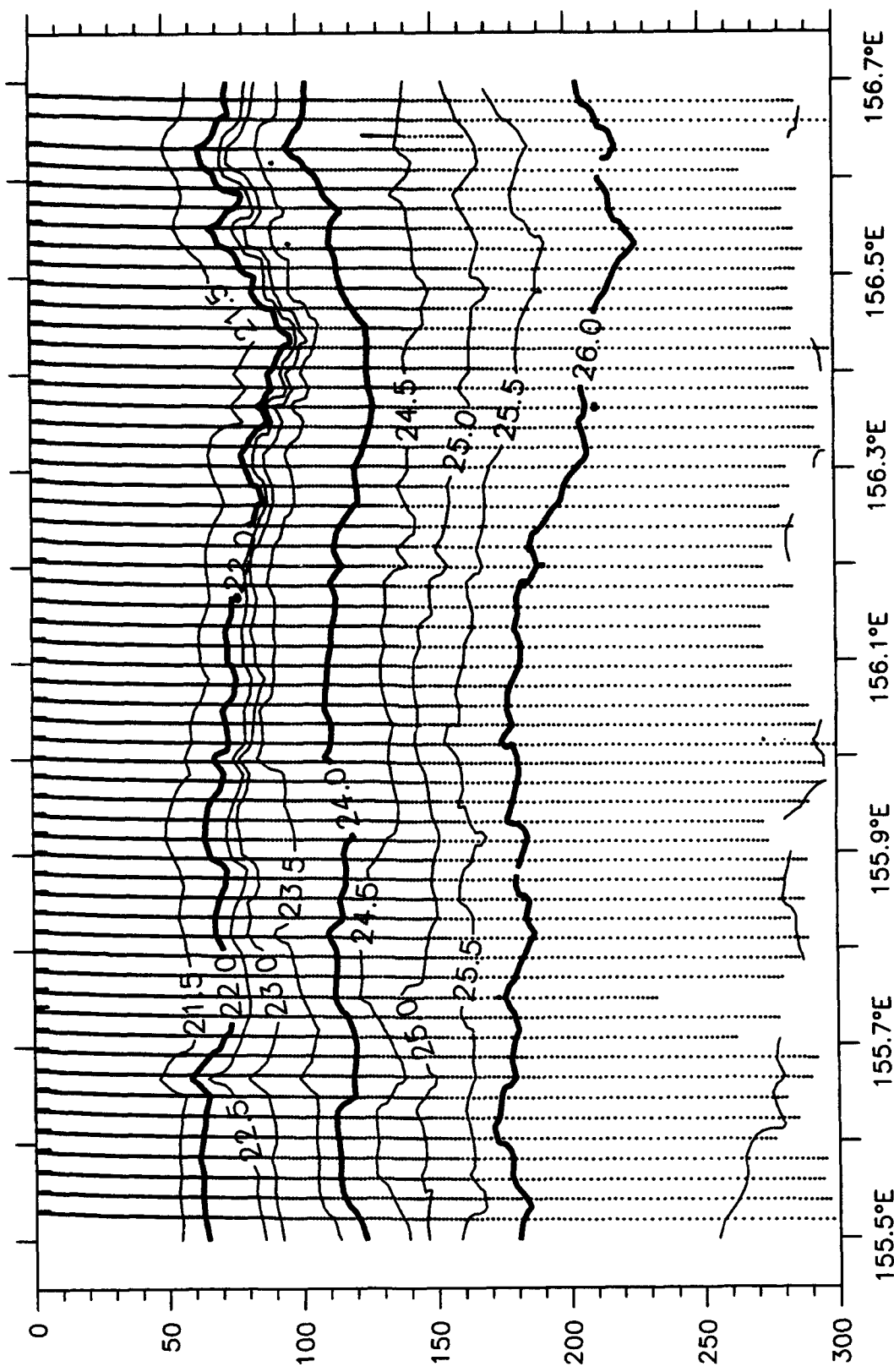
Sigma-t, W2E, 28 January 1993



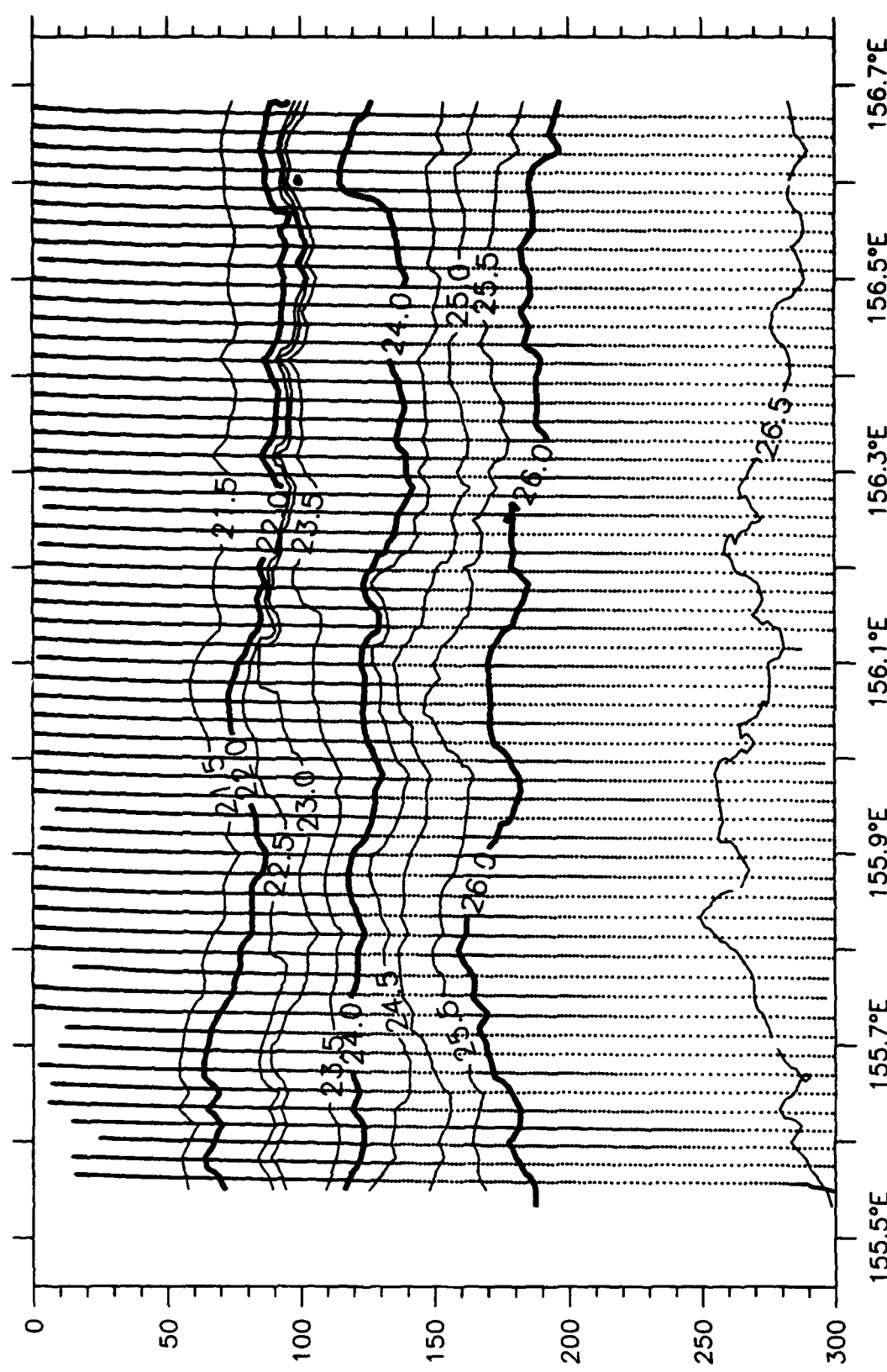
Sigma-t, W2E, 29 January 1993



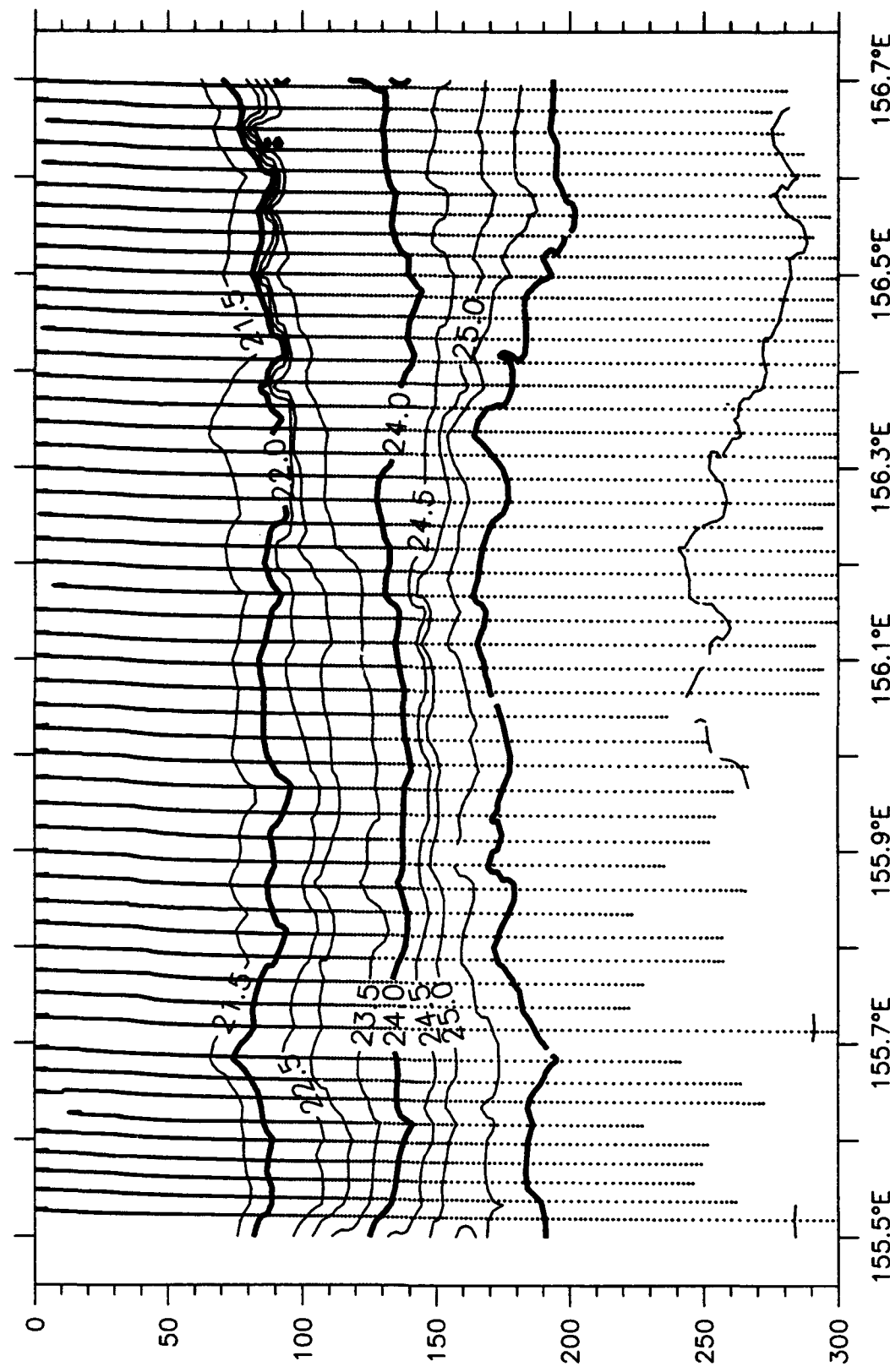
Sigma-t, W2E, 31 January 1993



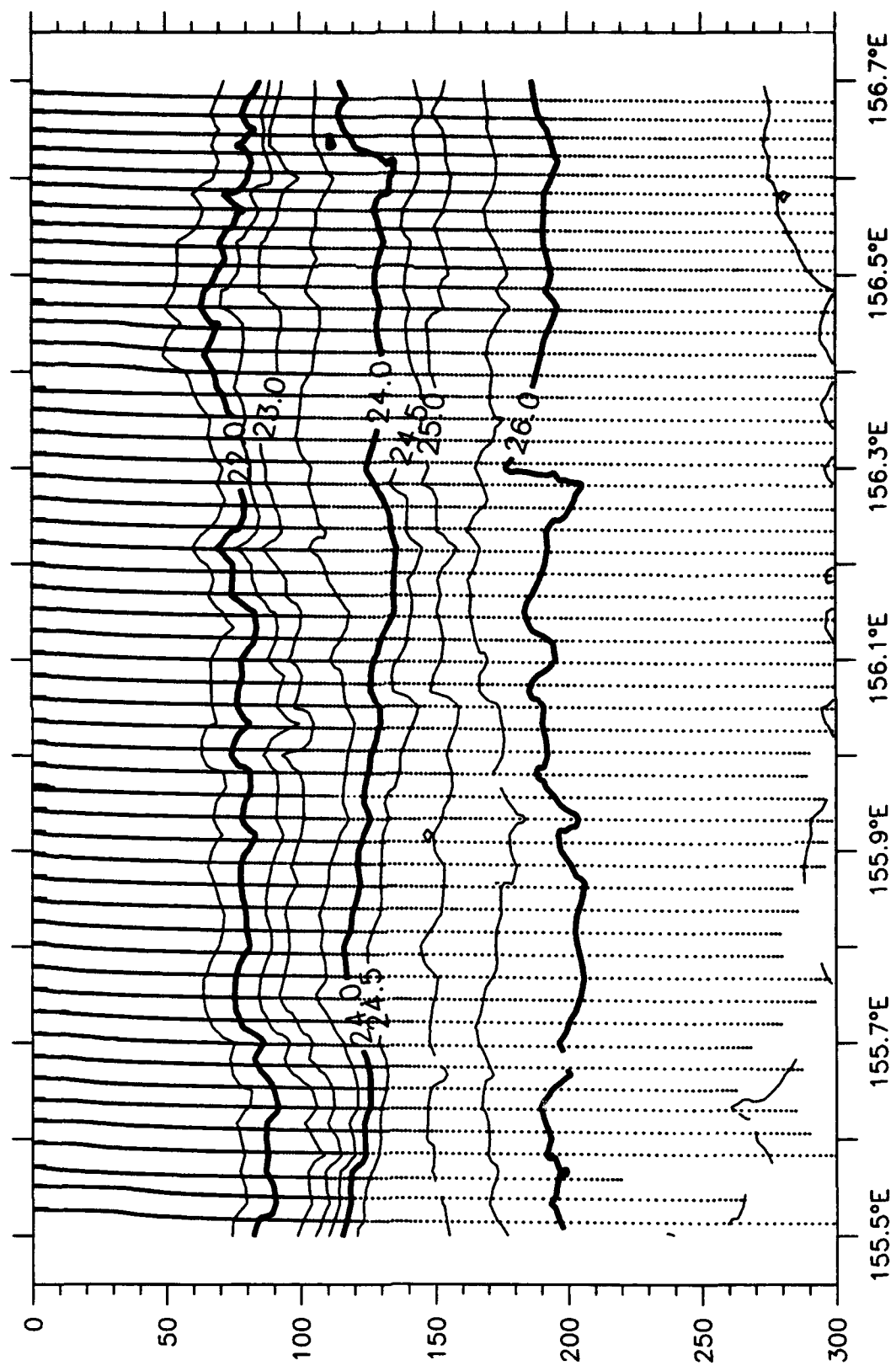
Sigma-t, W2E, 1 February 1993



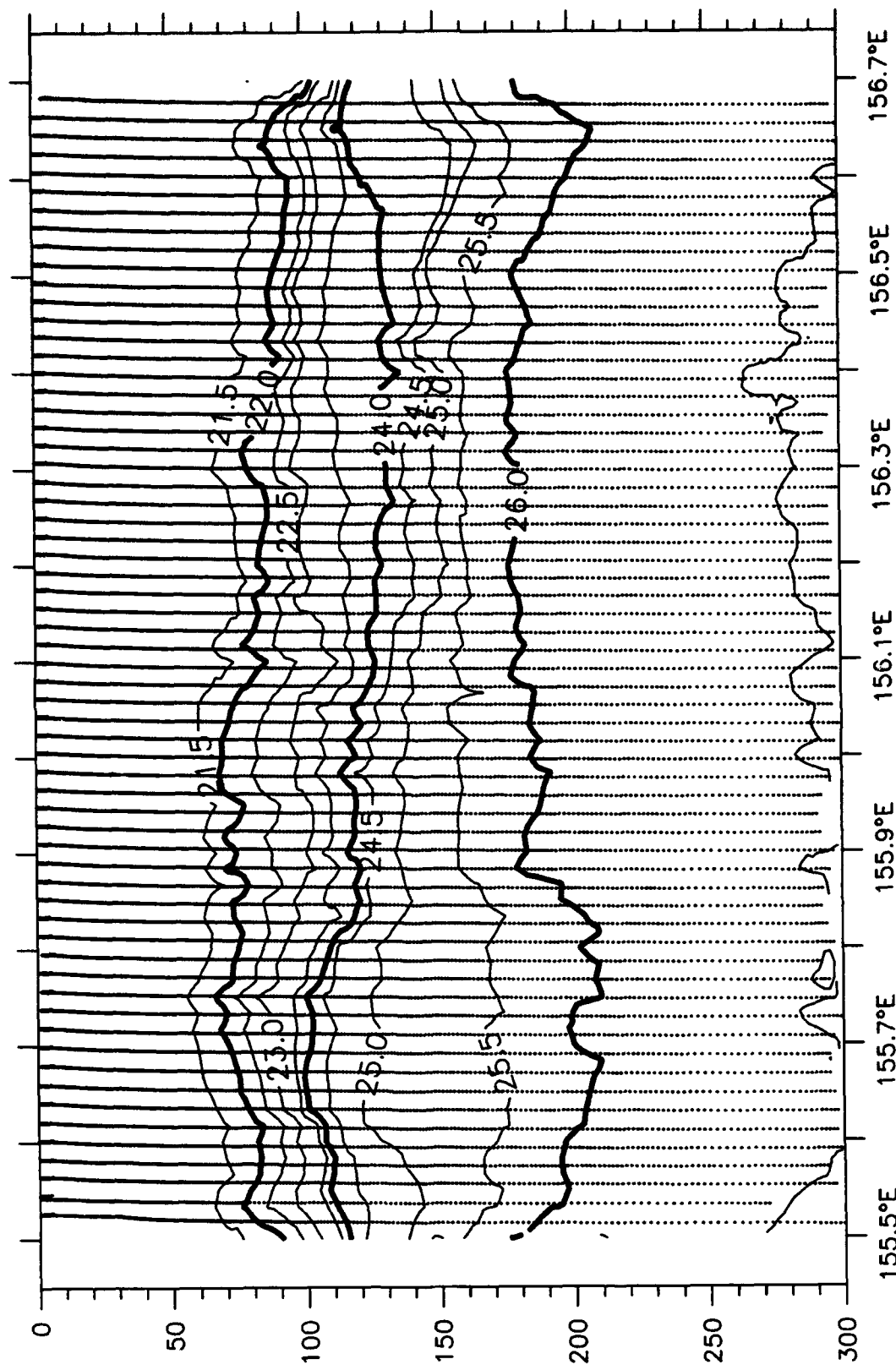
Sigma-t, W2E, 3 February 1993



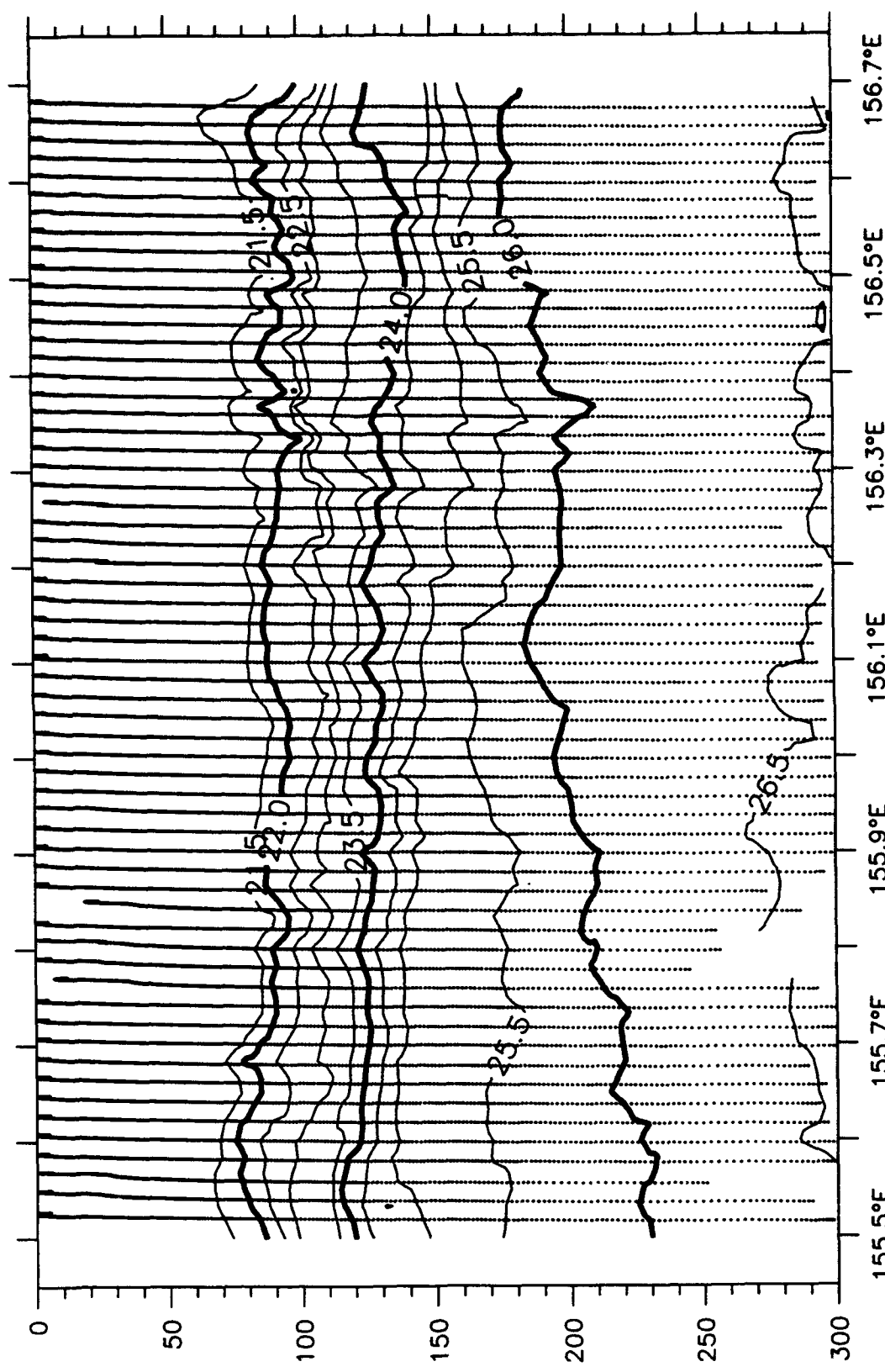
Sigma-t, W2E, 04 February 1993



Sigma-t, W2E, 06 February 1993

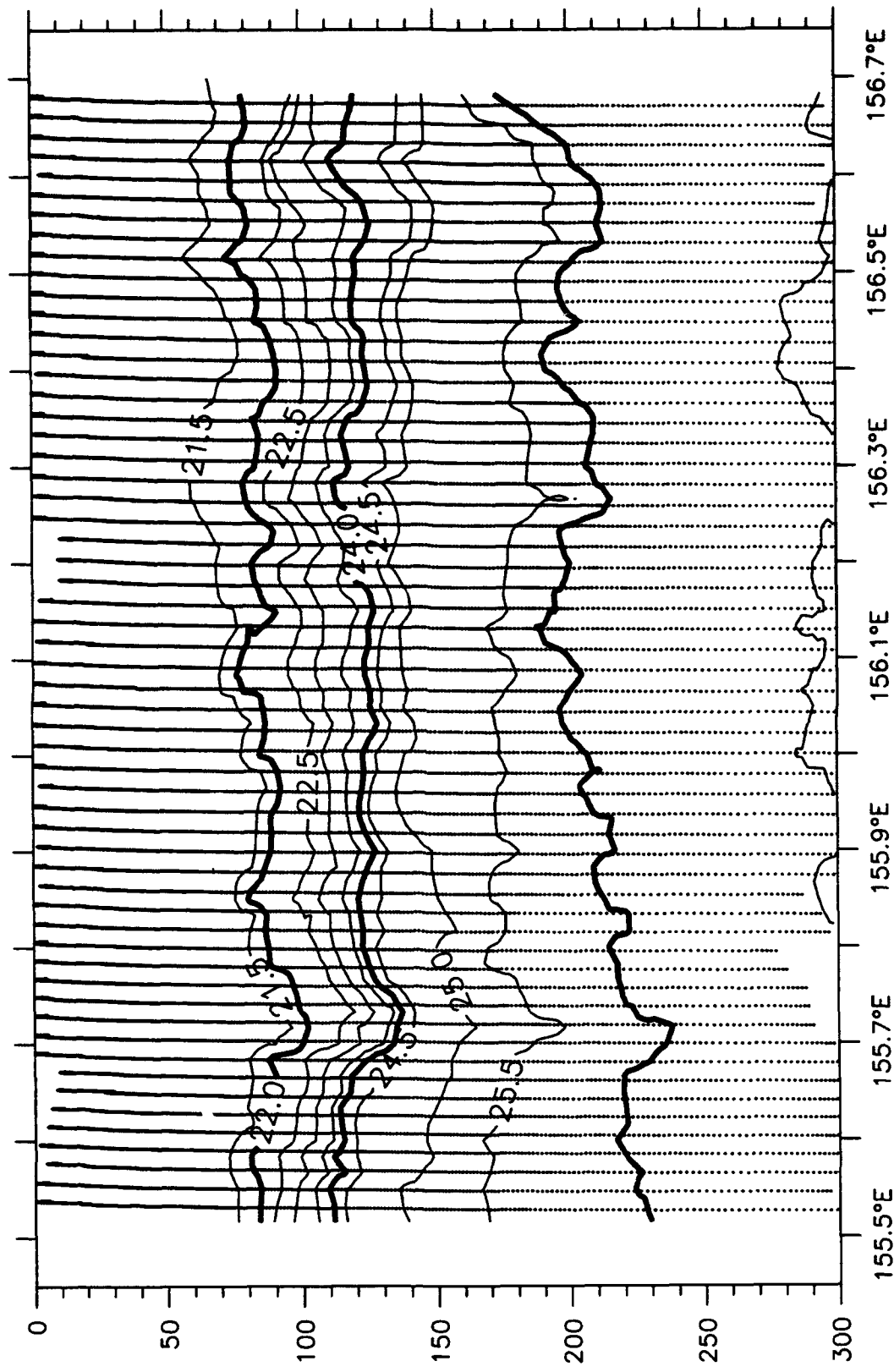


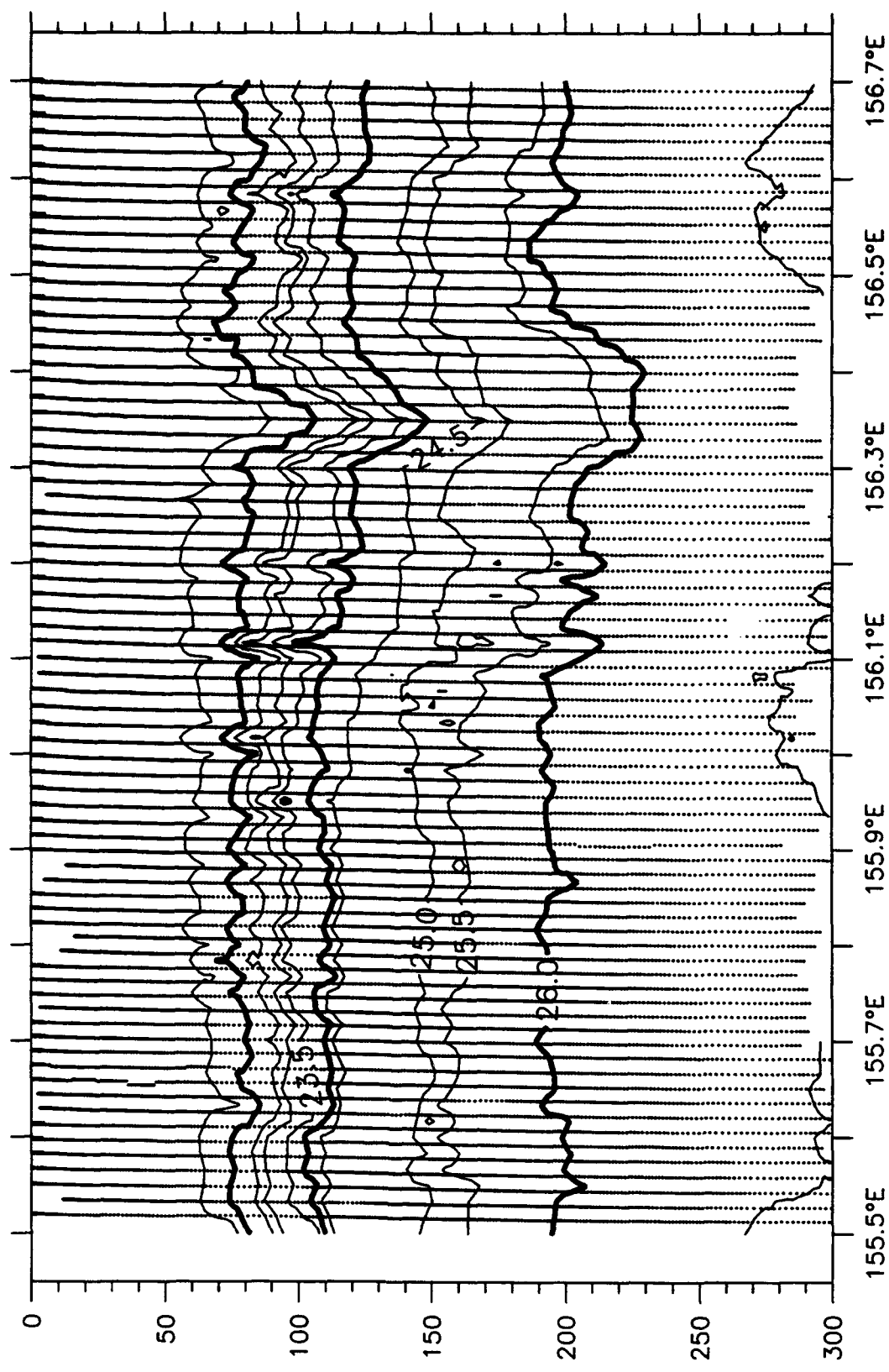
Sigma-t, W2E, 08 February 1993



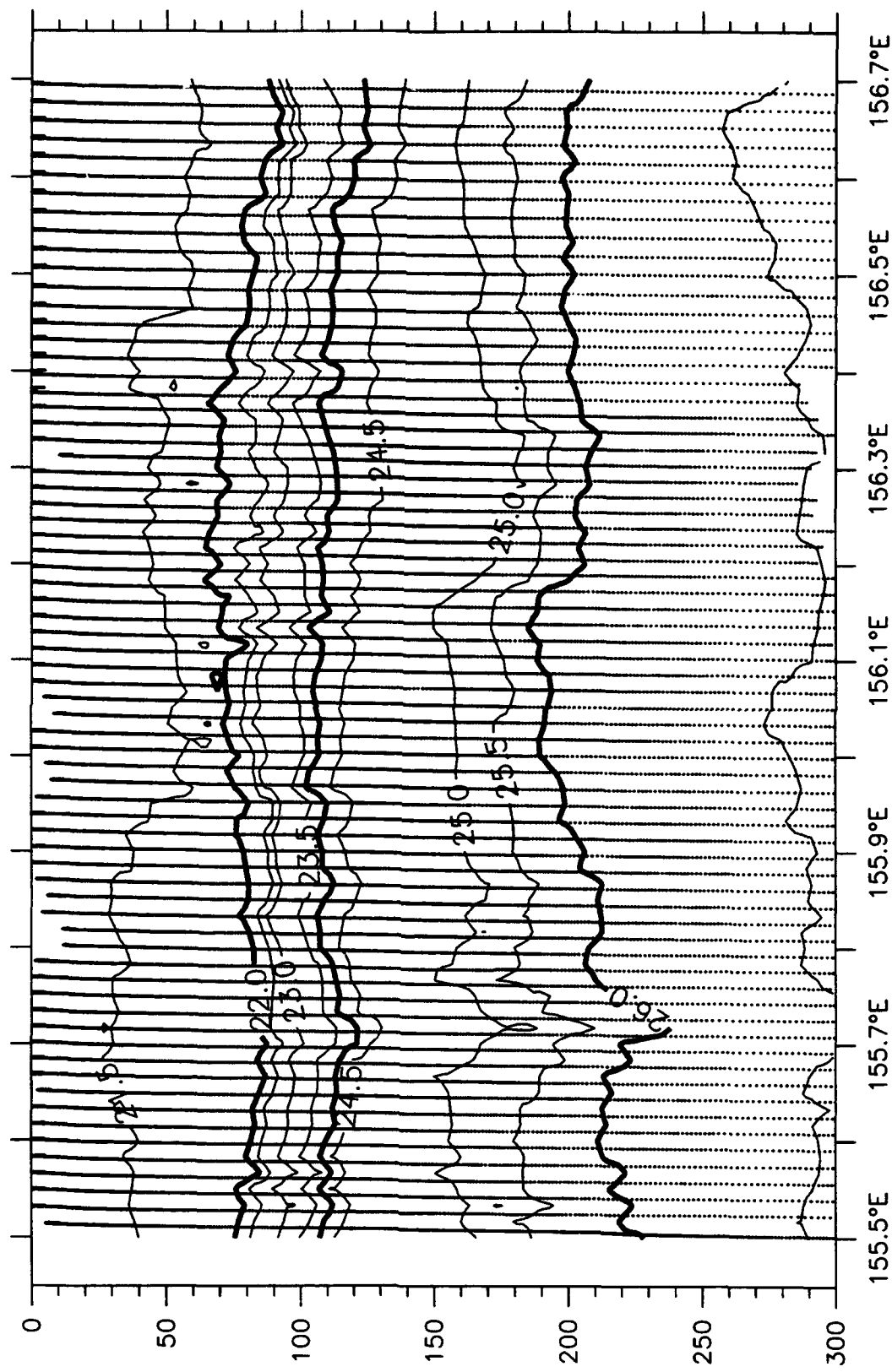
Sigma-t, W2E, 10 February 1993

Sigma-t, W2E, 11 February 1993

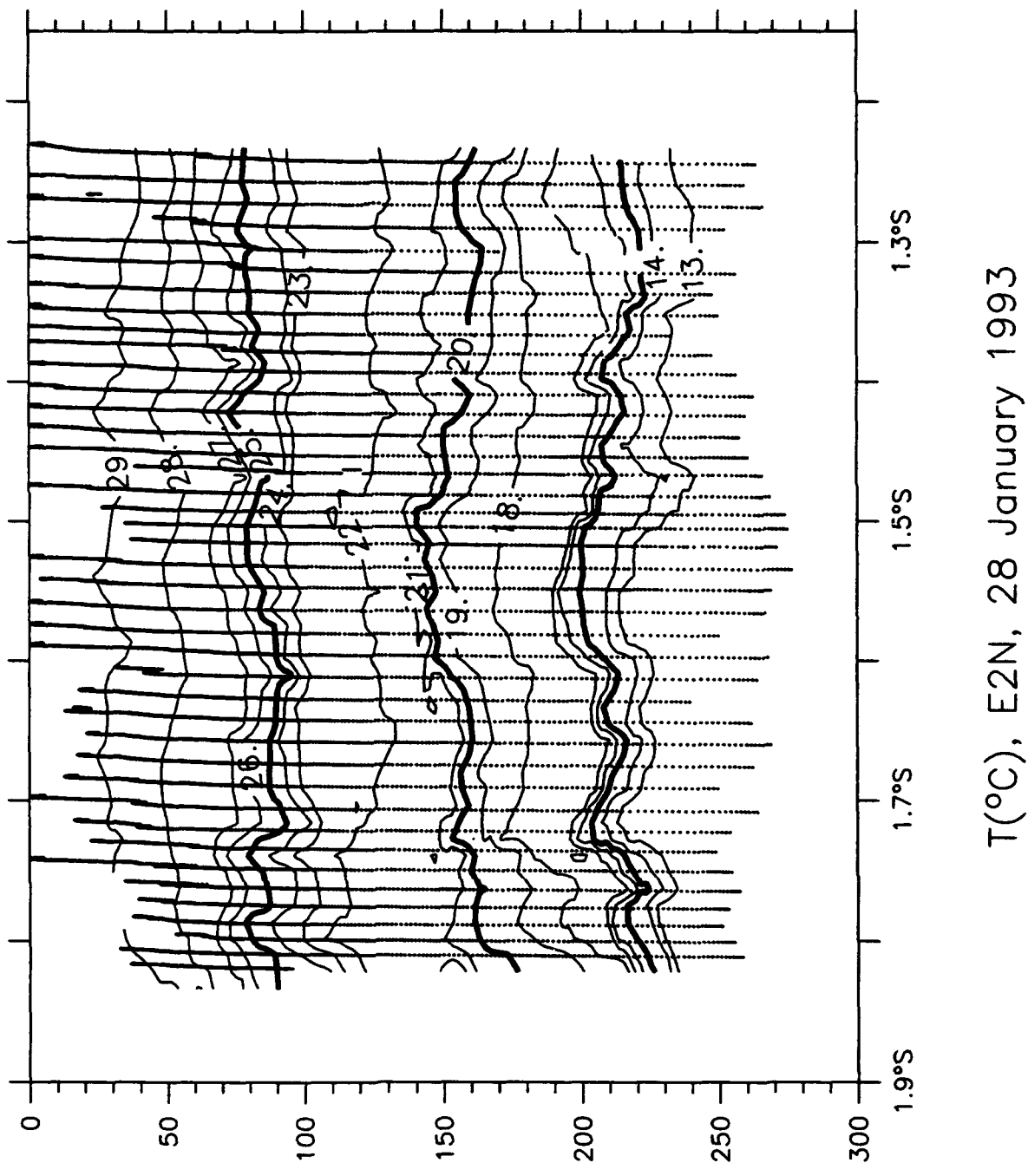


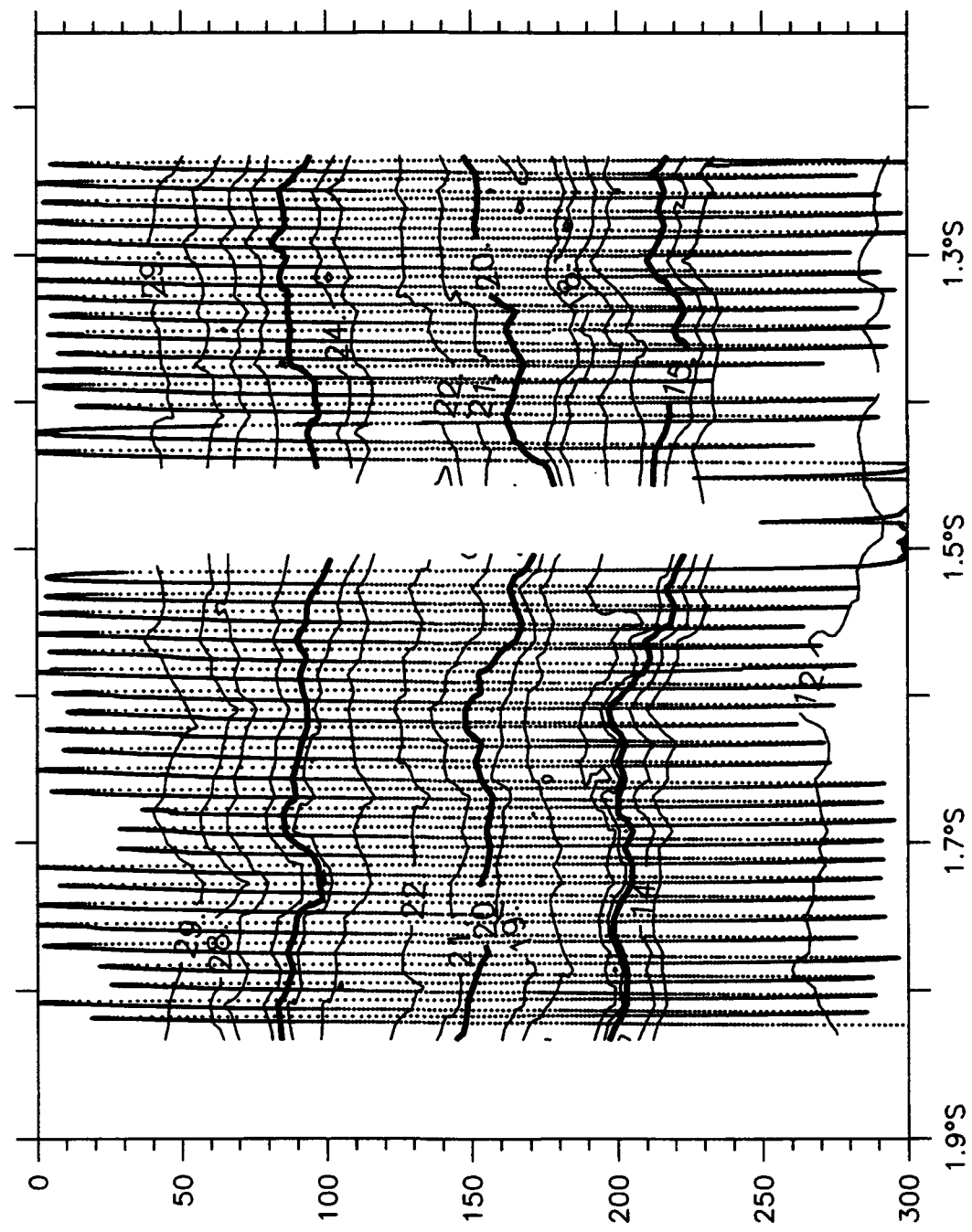


Sigma-t, W2E, 13 February 1993



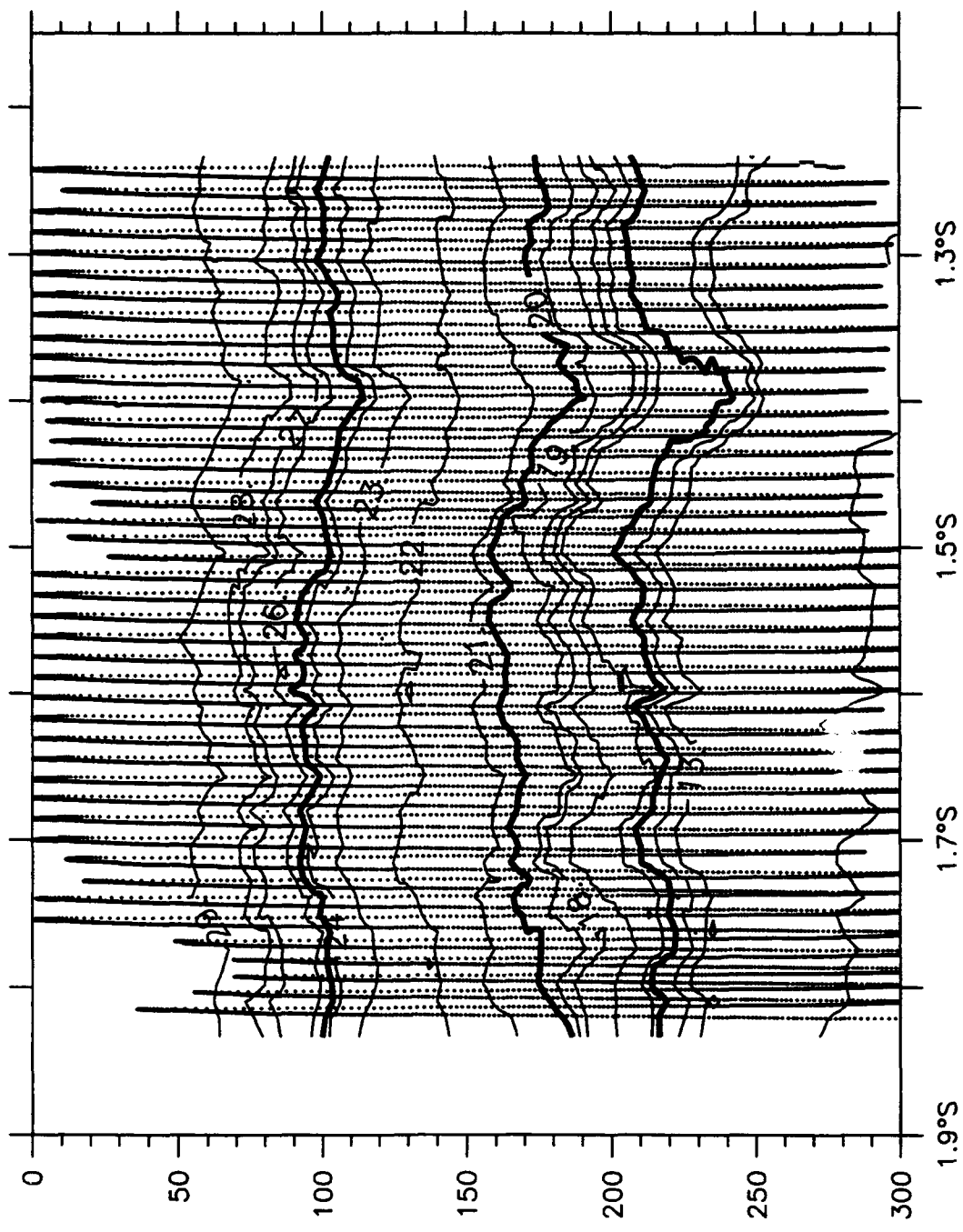
Sigma-t, W2E, 14 February 1993

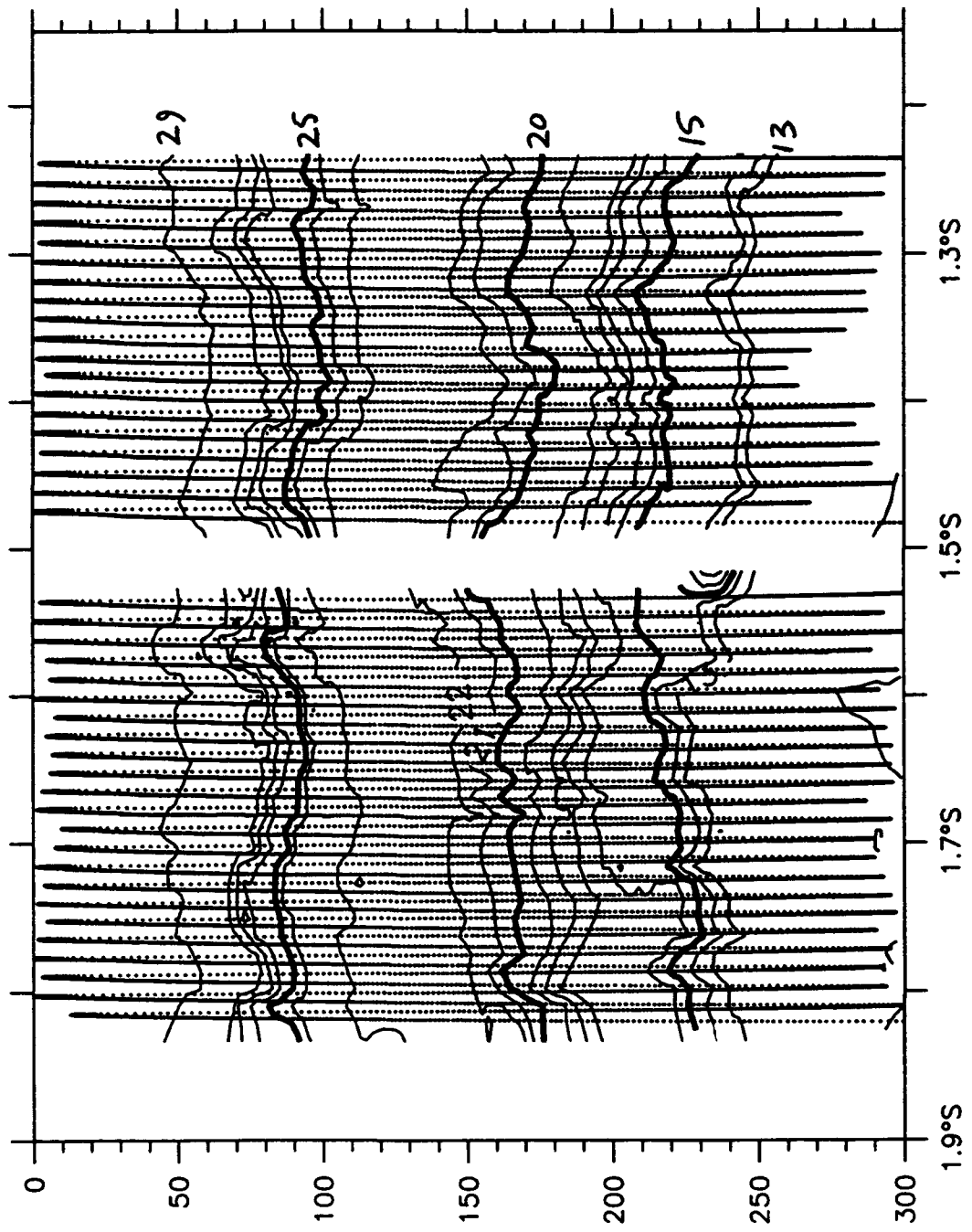




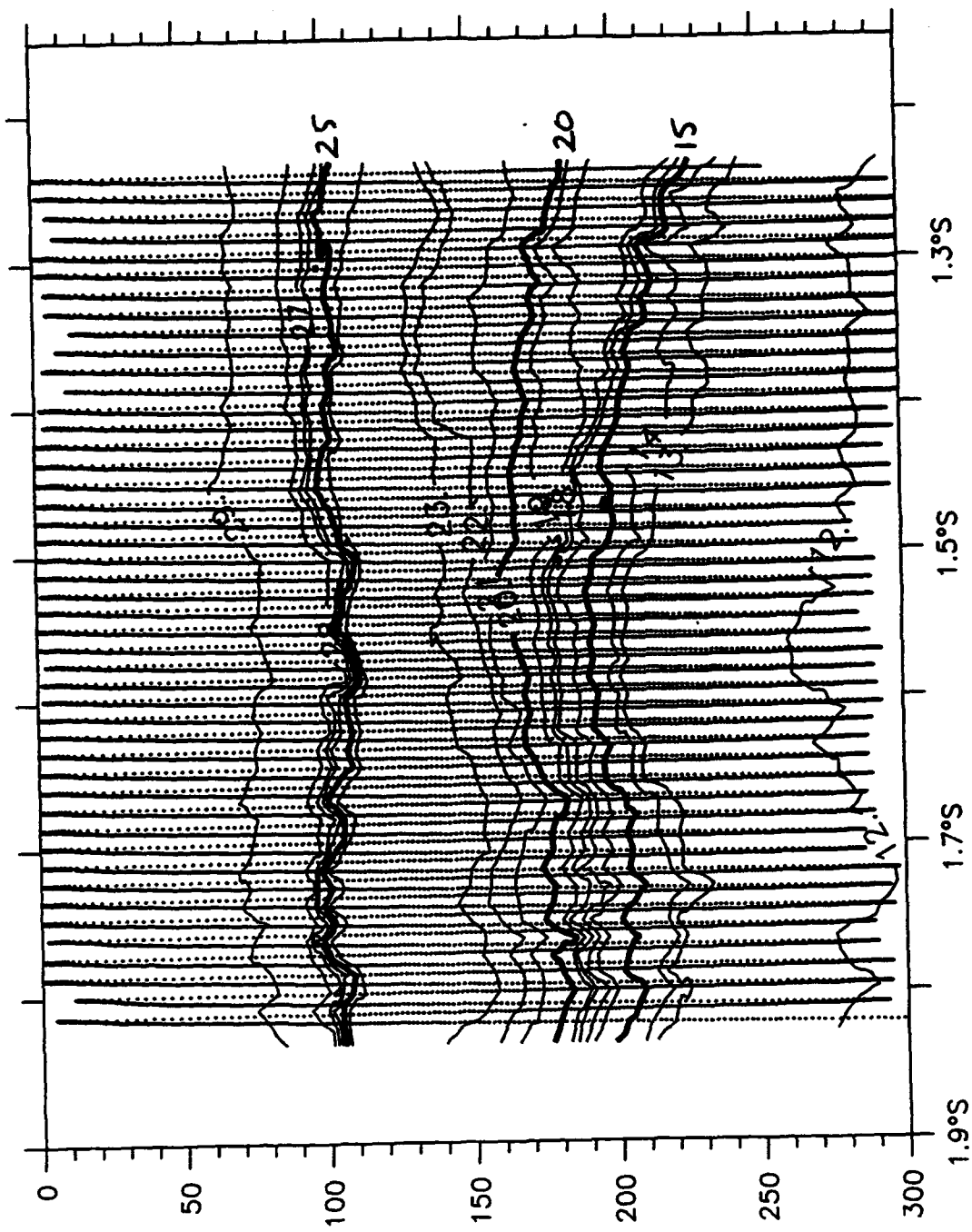
$T(\text{ }^{\circ}\text{C})$ , E2N, 30 January 1993

T( $^{\circ}$ C), E2N, 31 January 1993

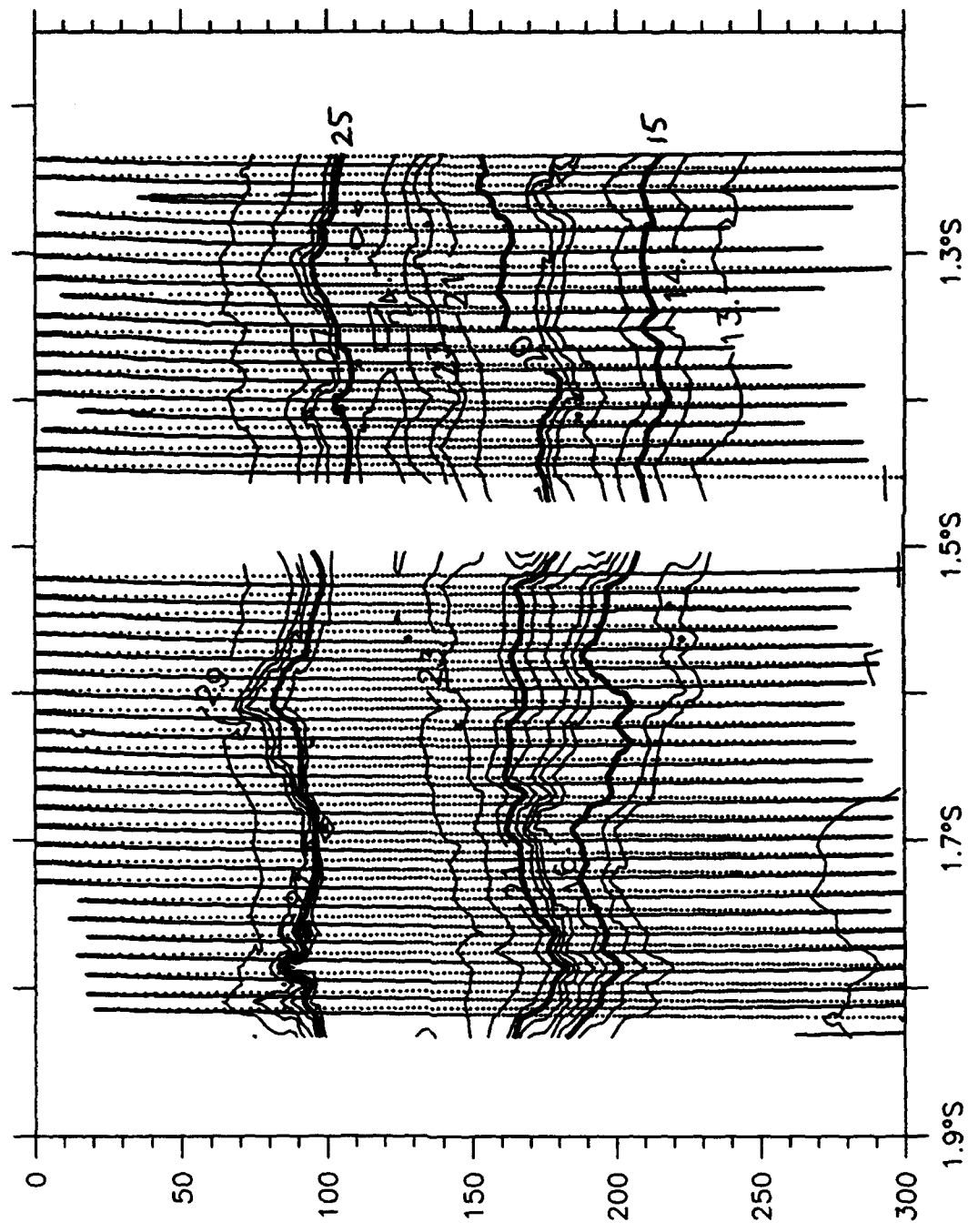




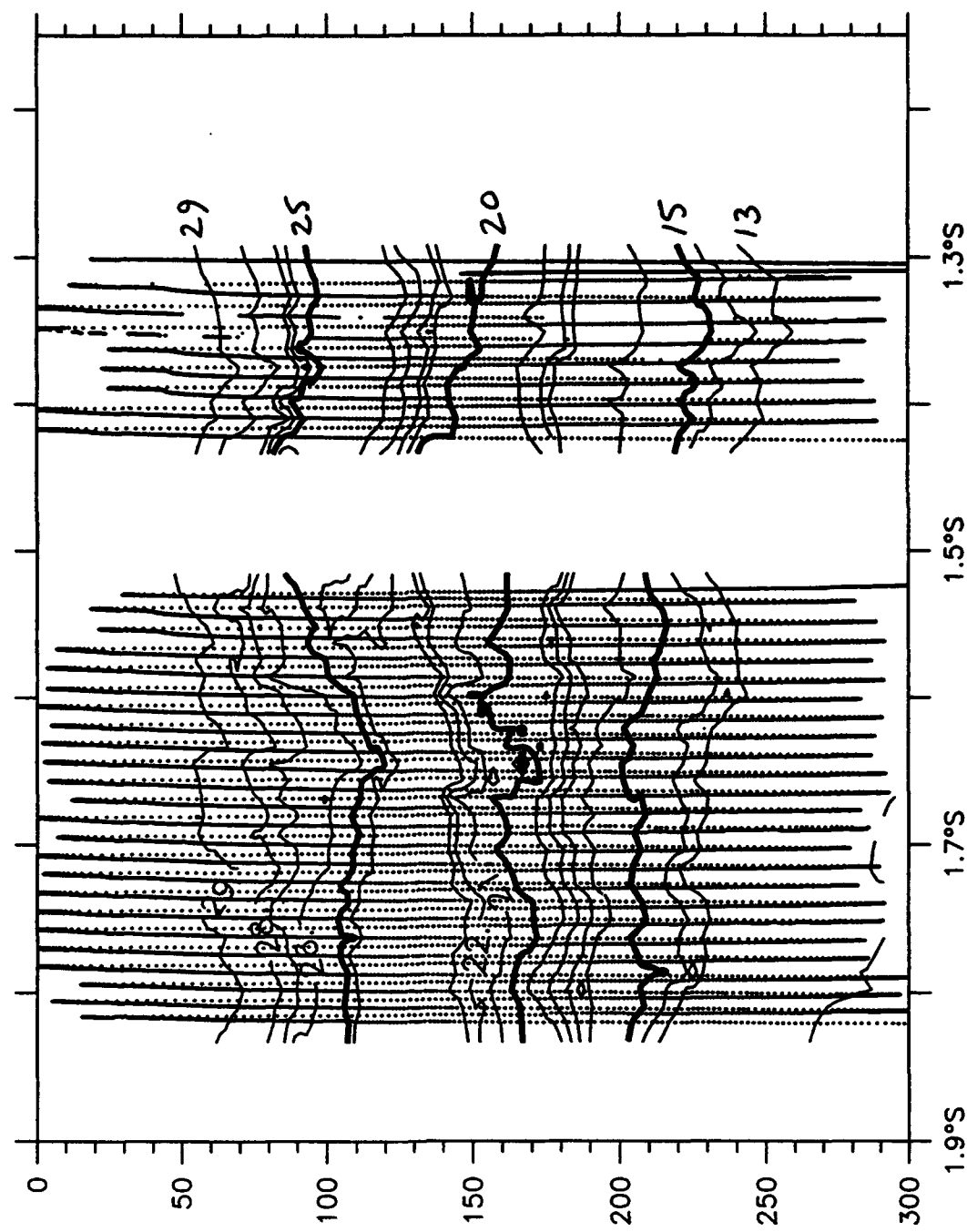
$T(\text{ }^{\circ}\text{C})$ , E2N, 1 February 1993



$T$  ( $^{\circ}\text{C}$ ), E2N, 3 February 1993

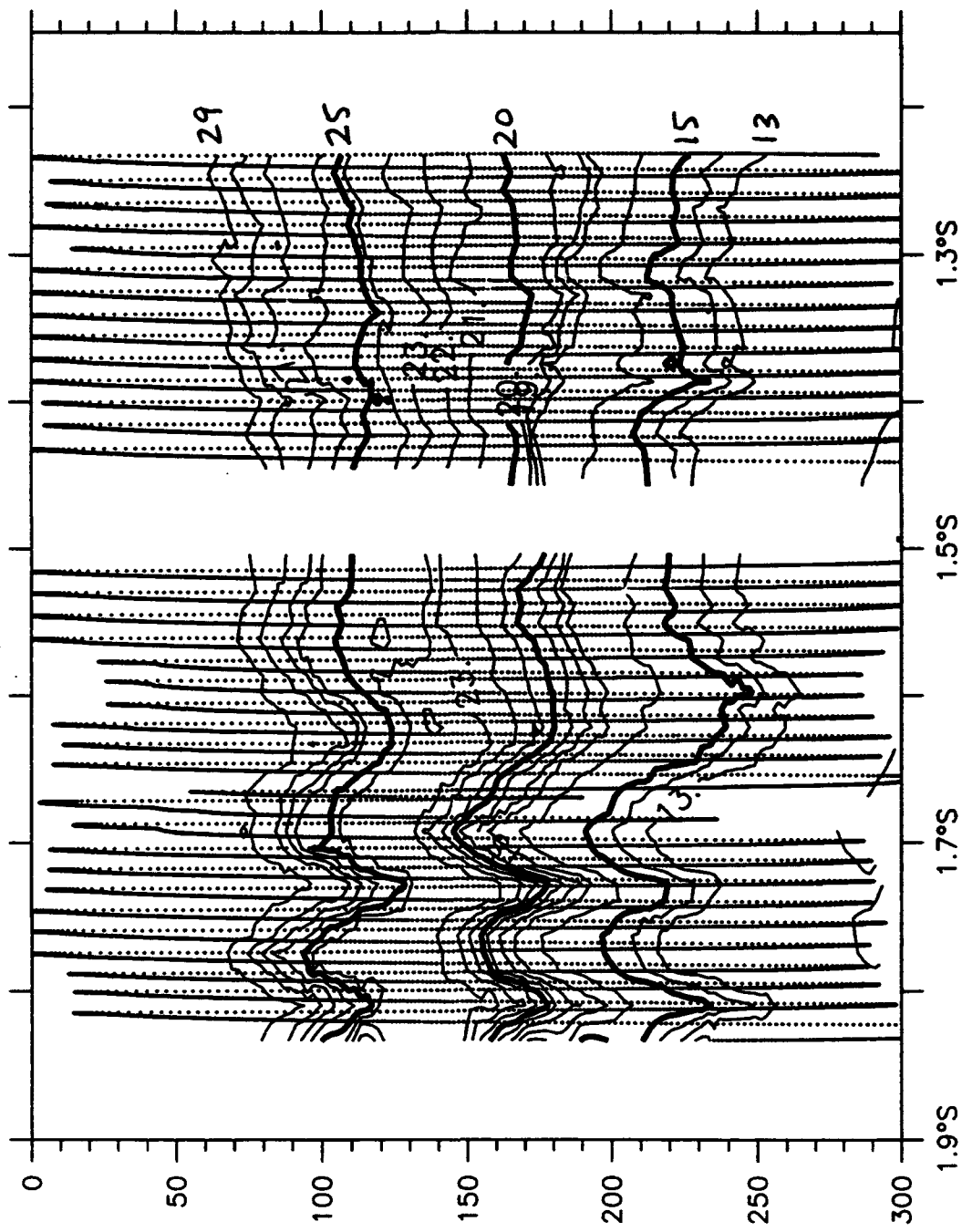


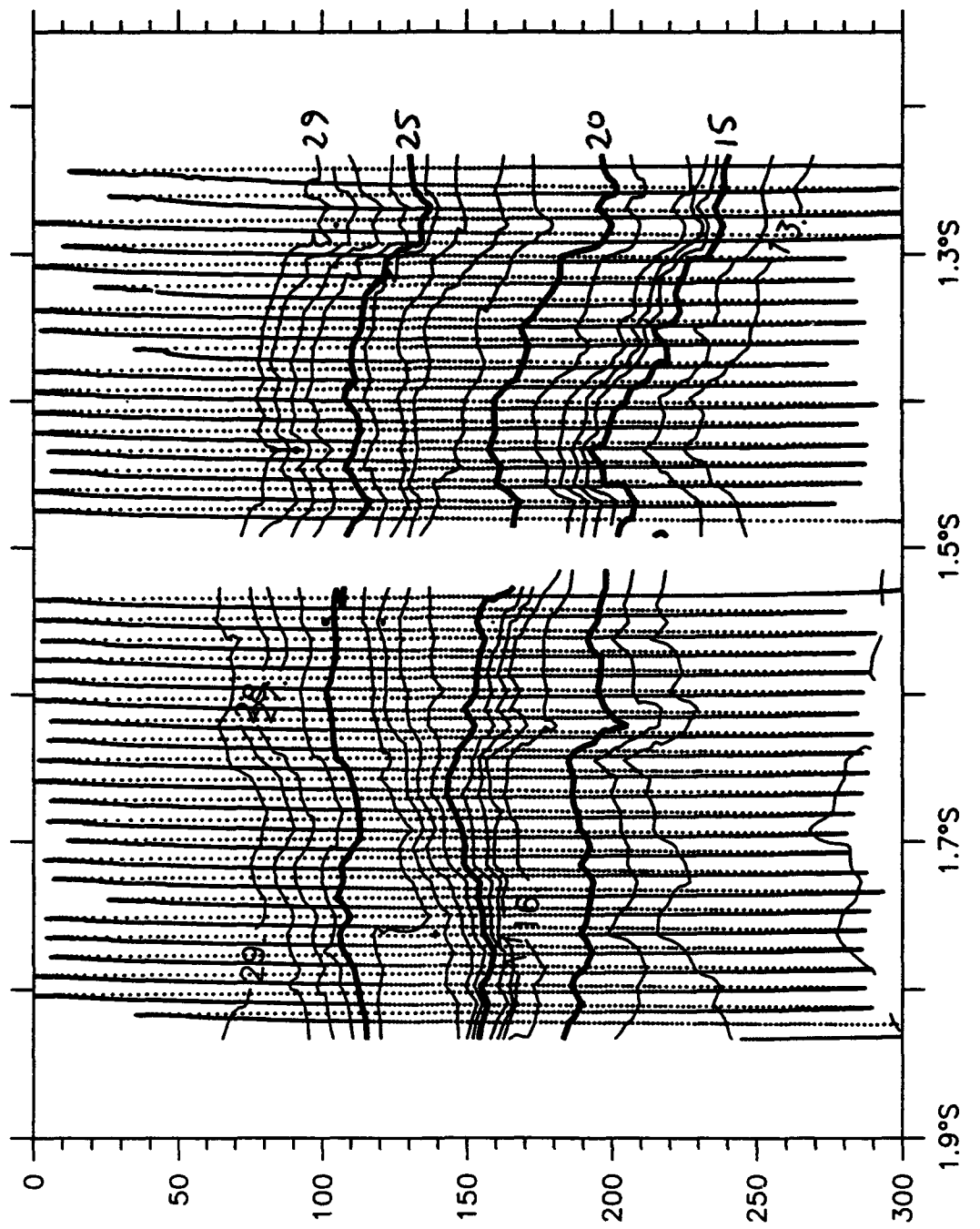
$T(^{\circ}\text{C})$ , E2N, 5 February 1993



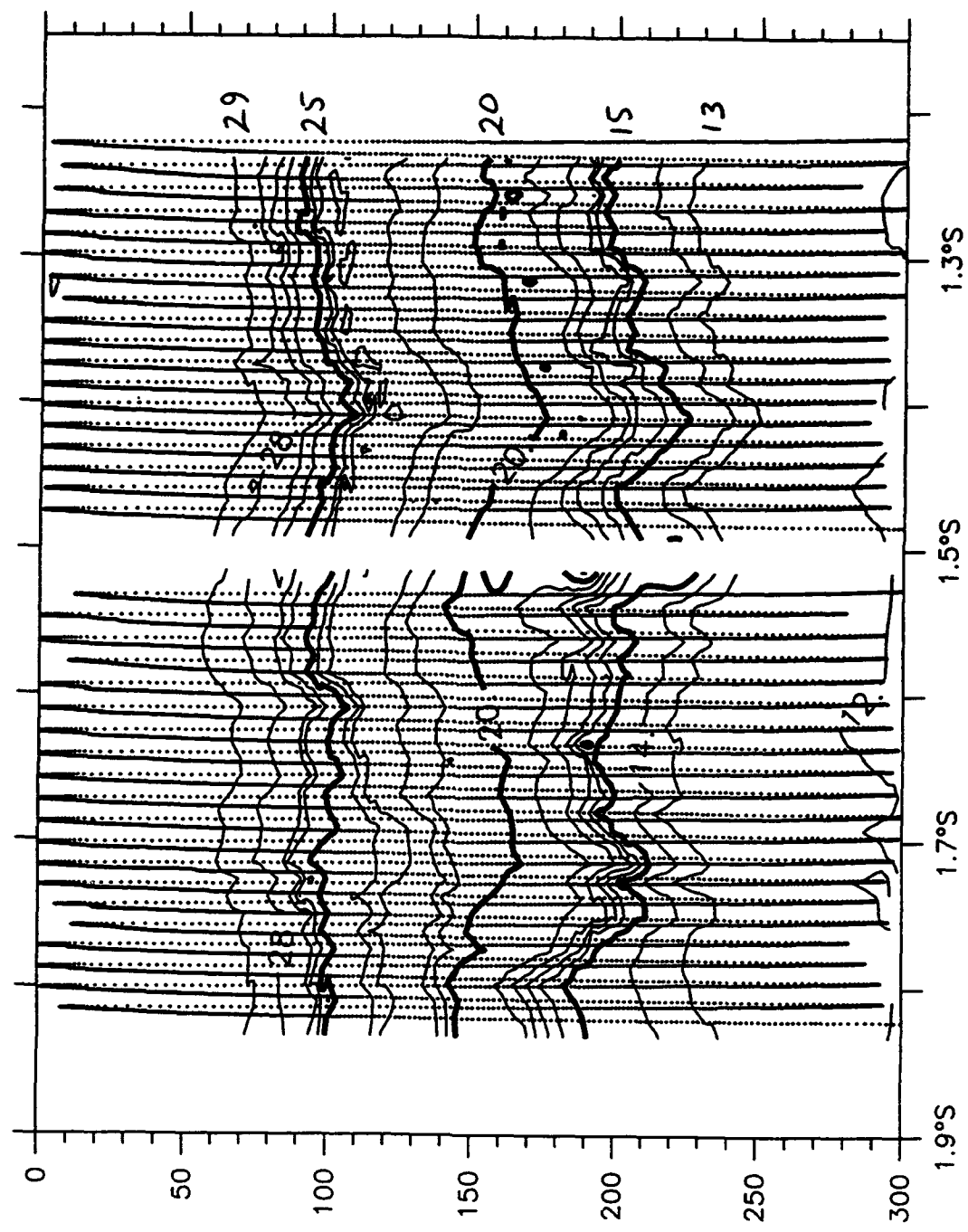
T( $^{\circ}$ C), E2N, 6 February 1993

T( $^{\circ}$ C), E2N, 9 February 1993

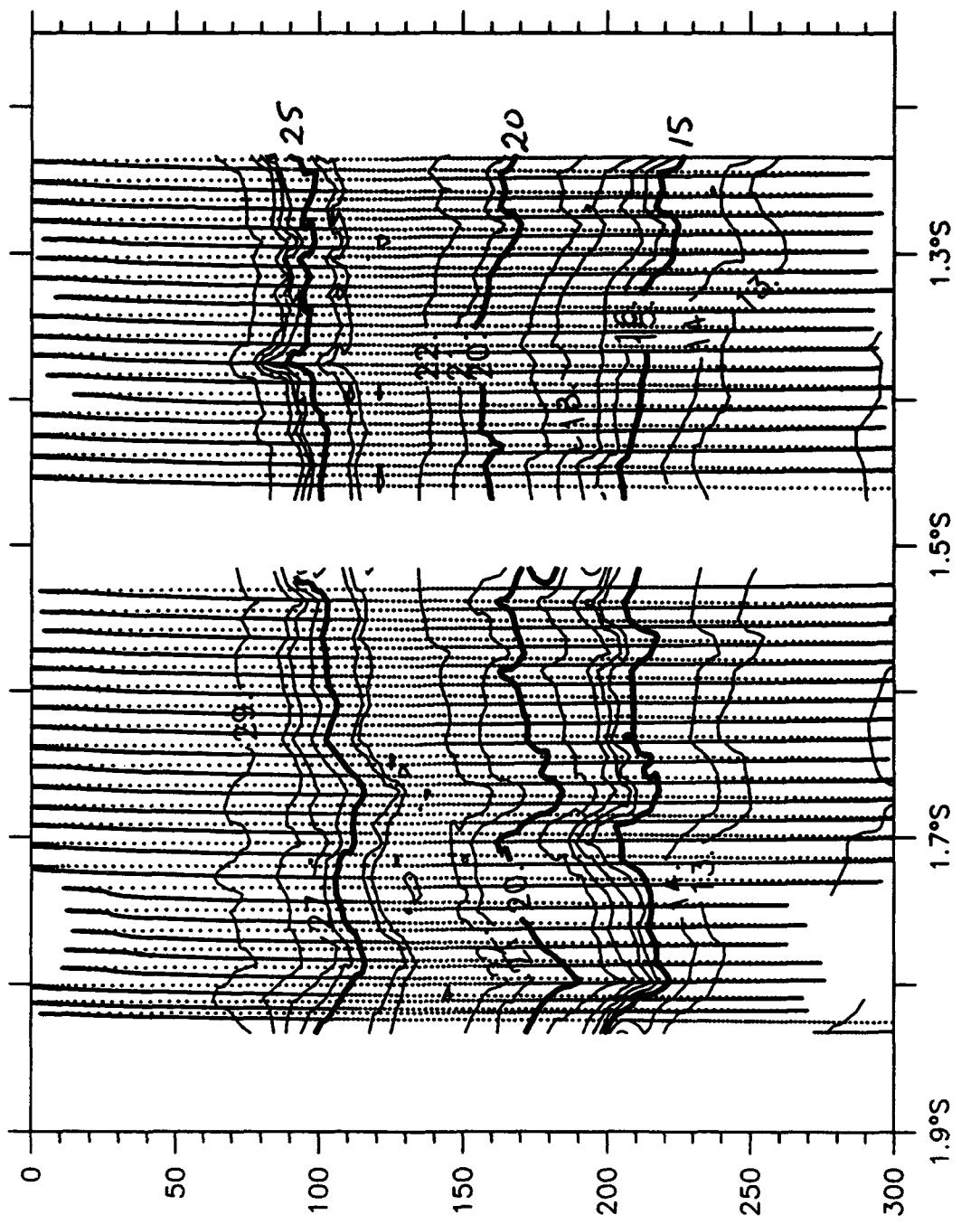




$T(^{\circ}\text{C})$ ,  $E2\text{N}$ , 10 February 1993

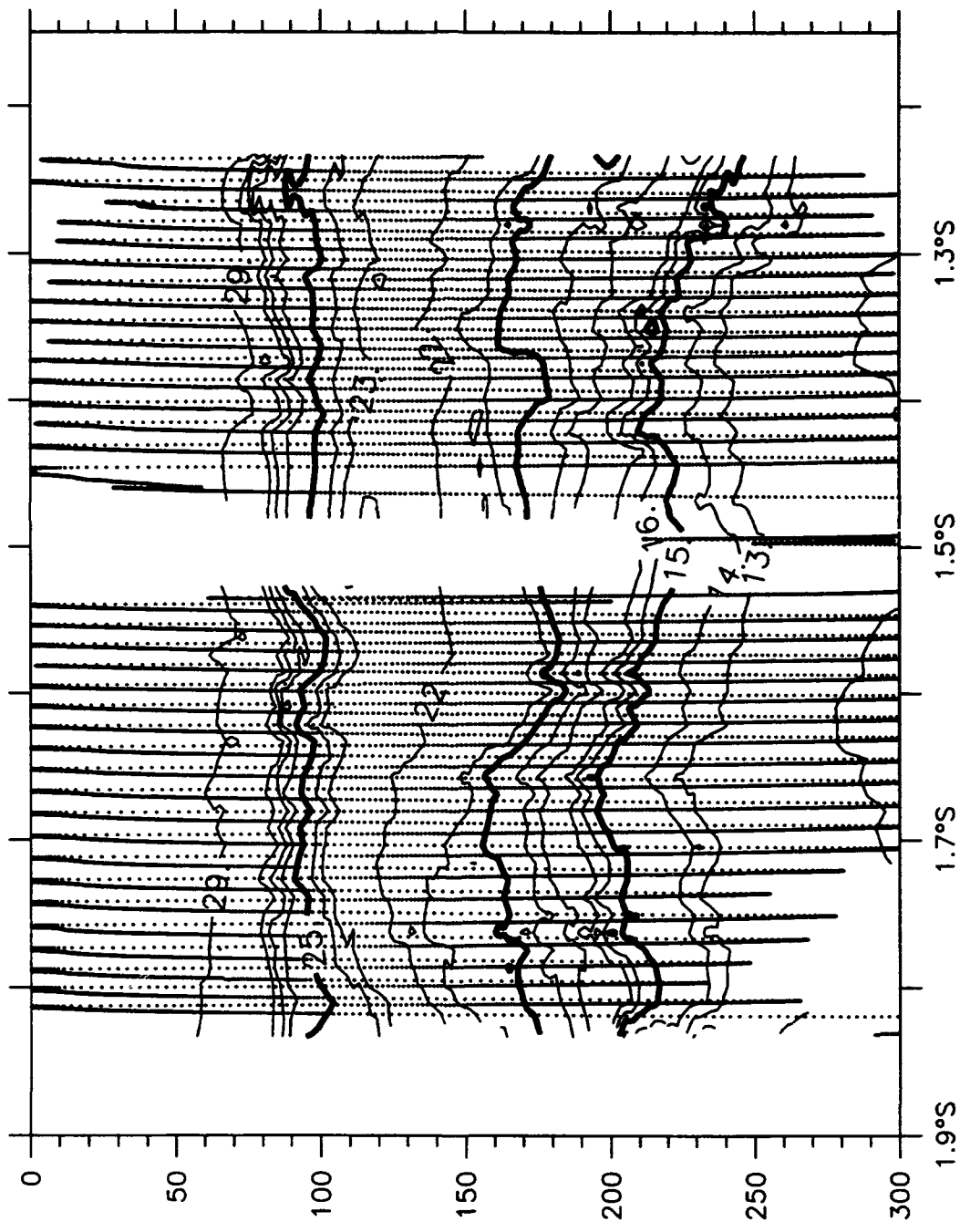


$T(^{\circ}\text{C})$ , E2N, 11 February 1993

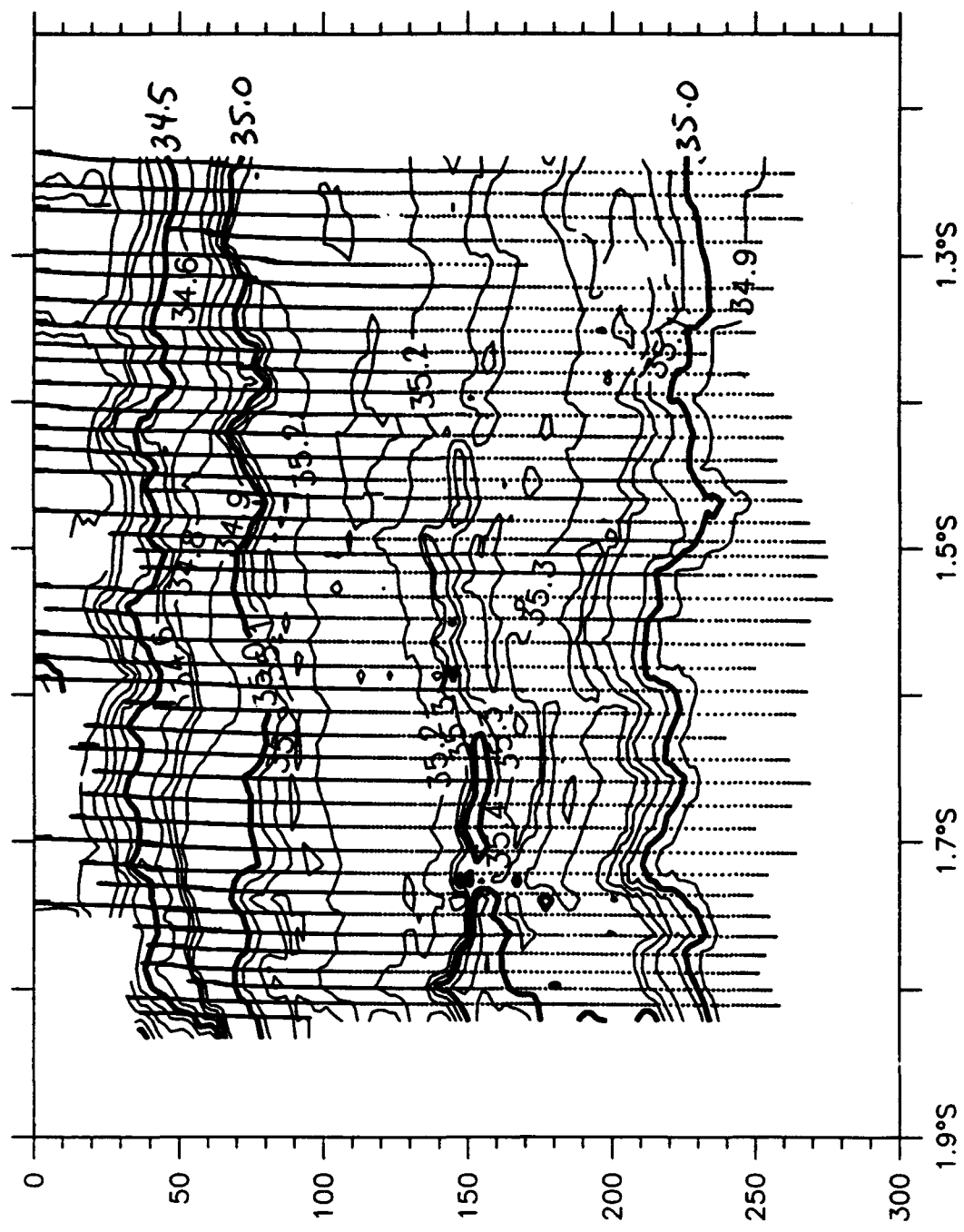


$T(^{\circ}\text{C})$ , E2N, 13 February 1993

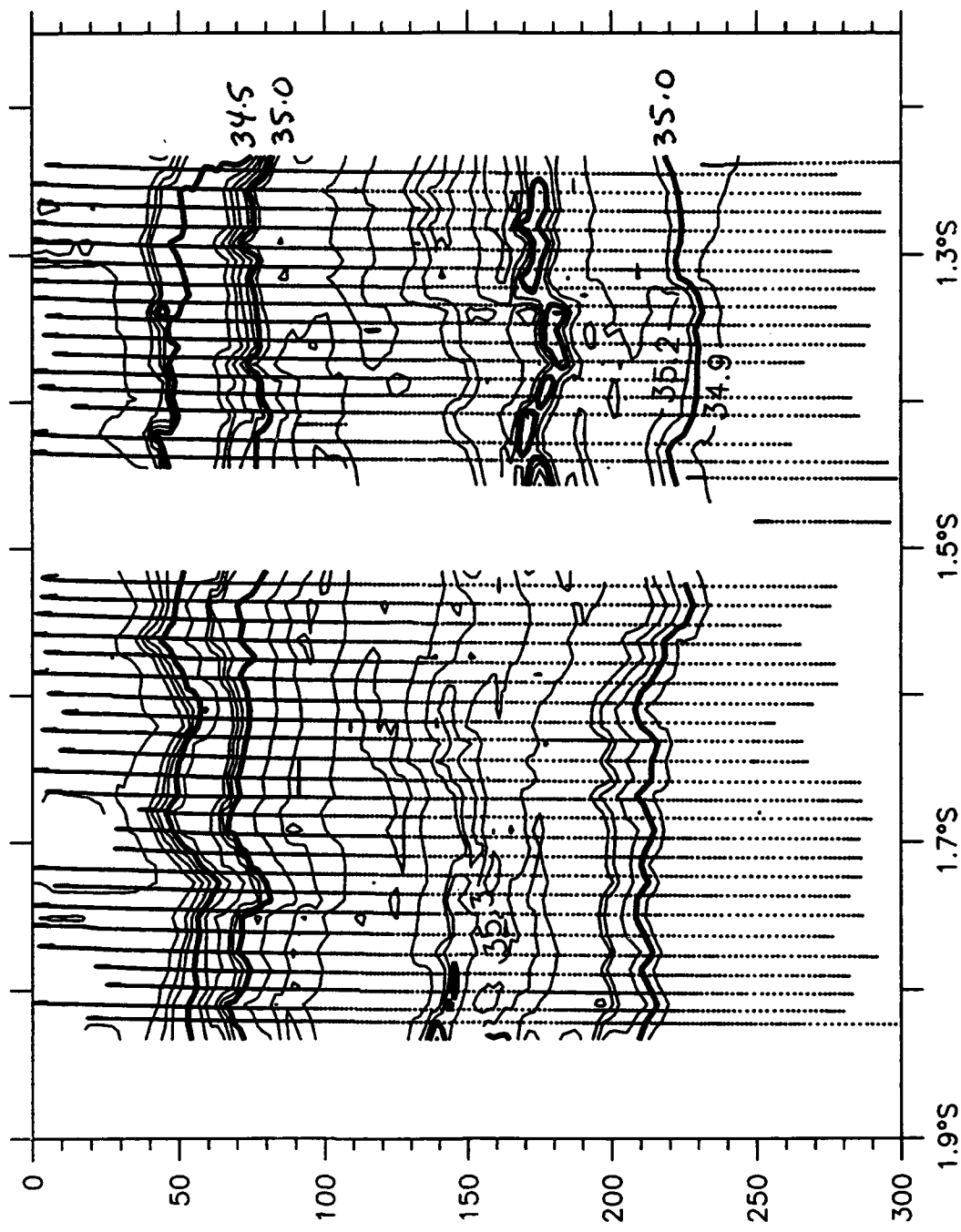
T( $^{\circ}$ C), E2N, 15 February 1993

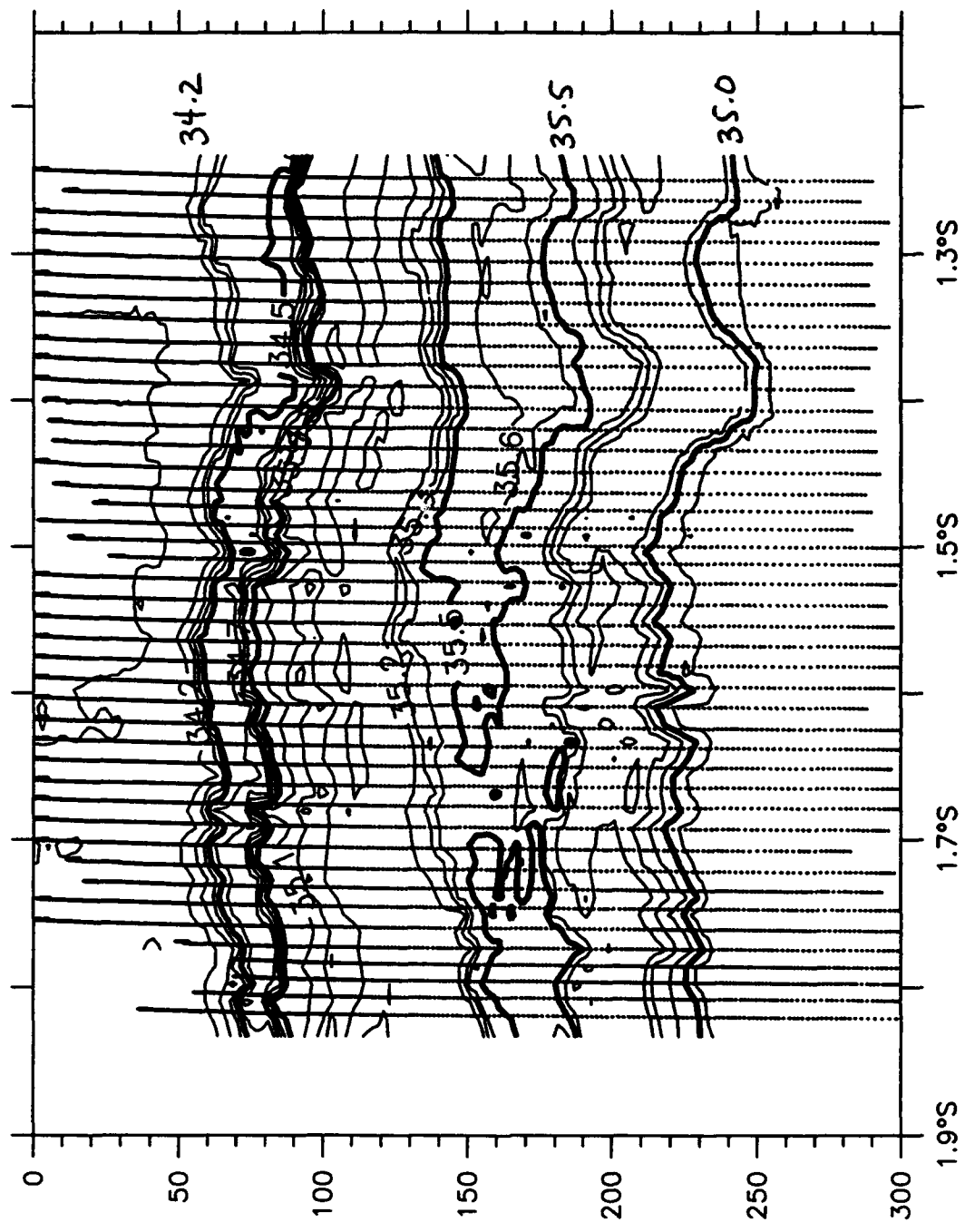


S(psu), E2N, 28 January 1993

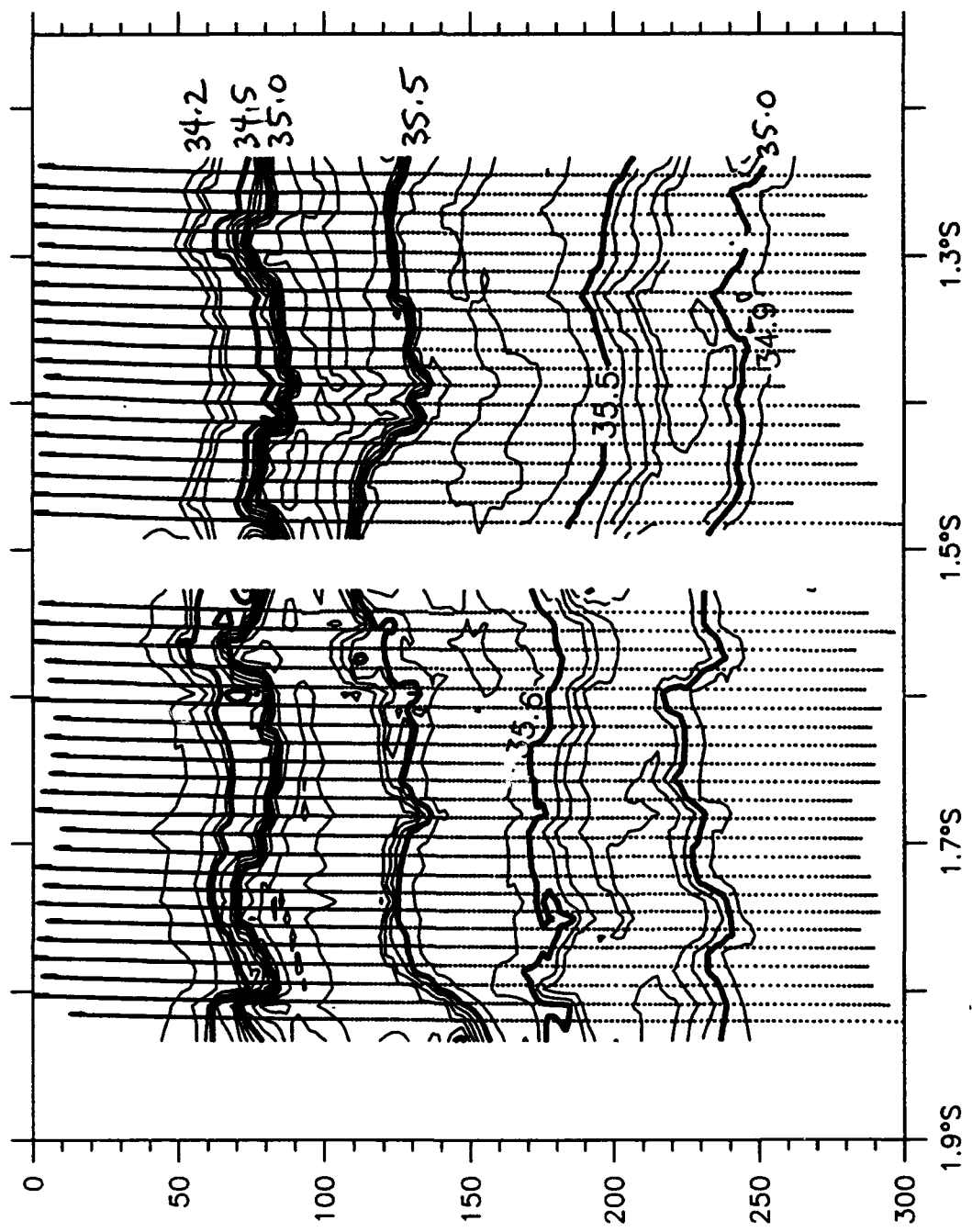


S(psu), E2N, 30 January 1993



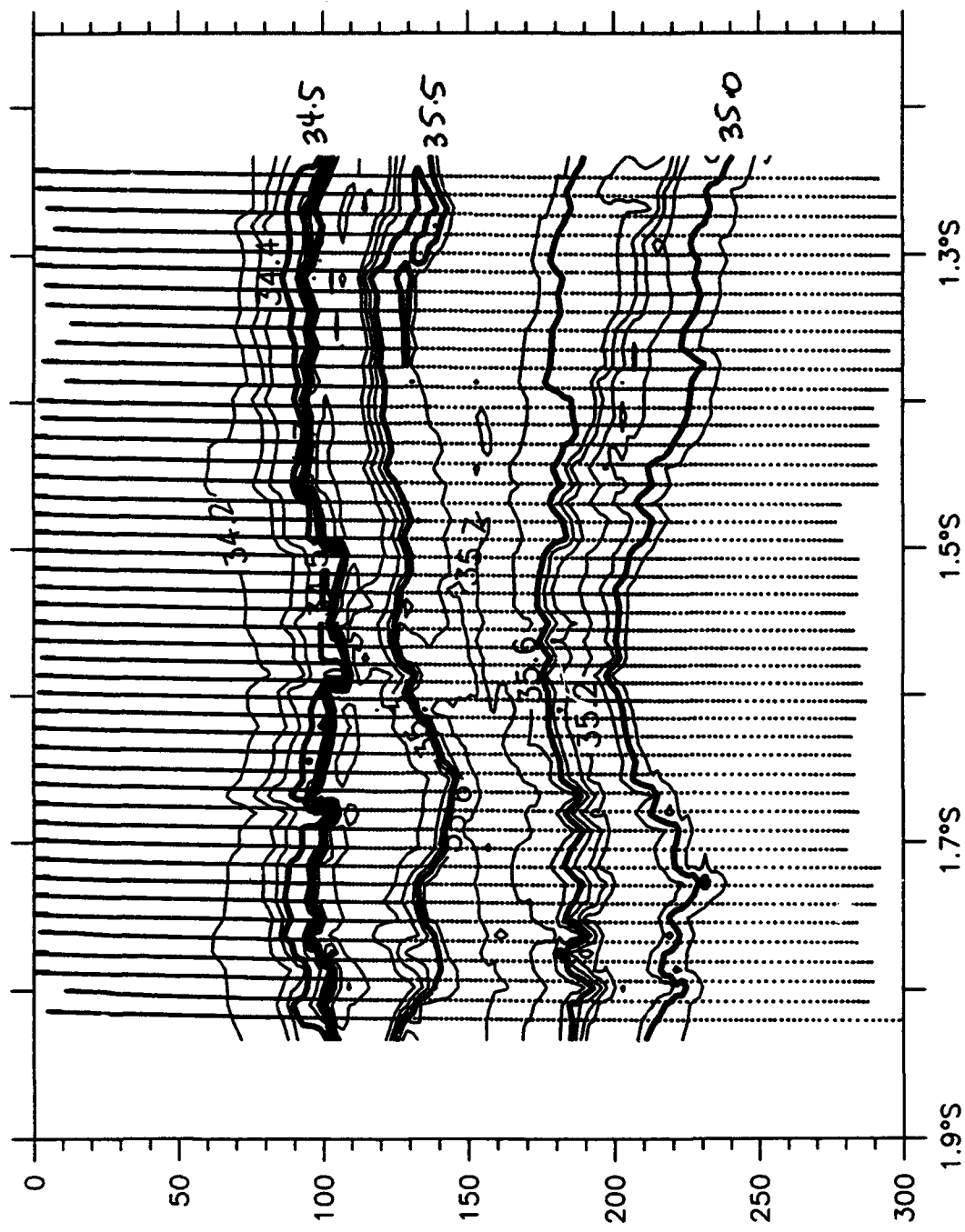


$S(\text{psu})$ , E2N, 31 January 1993

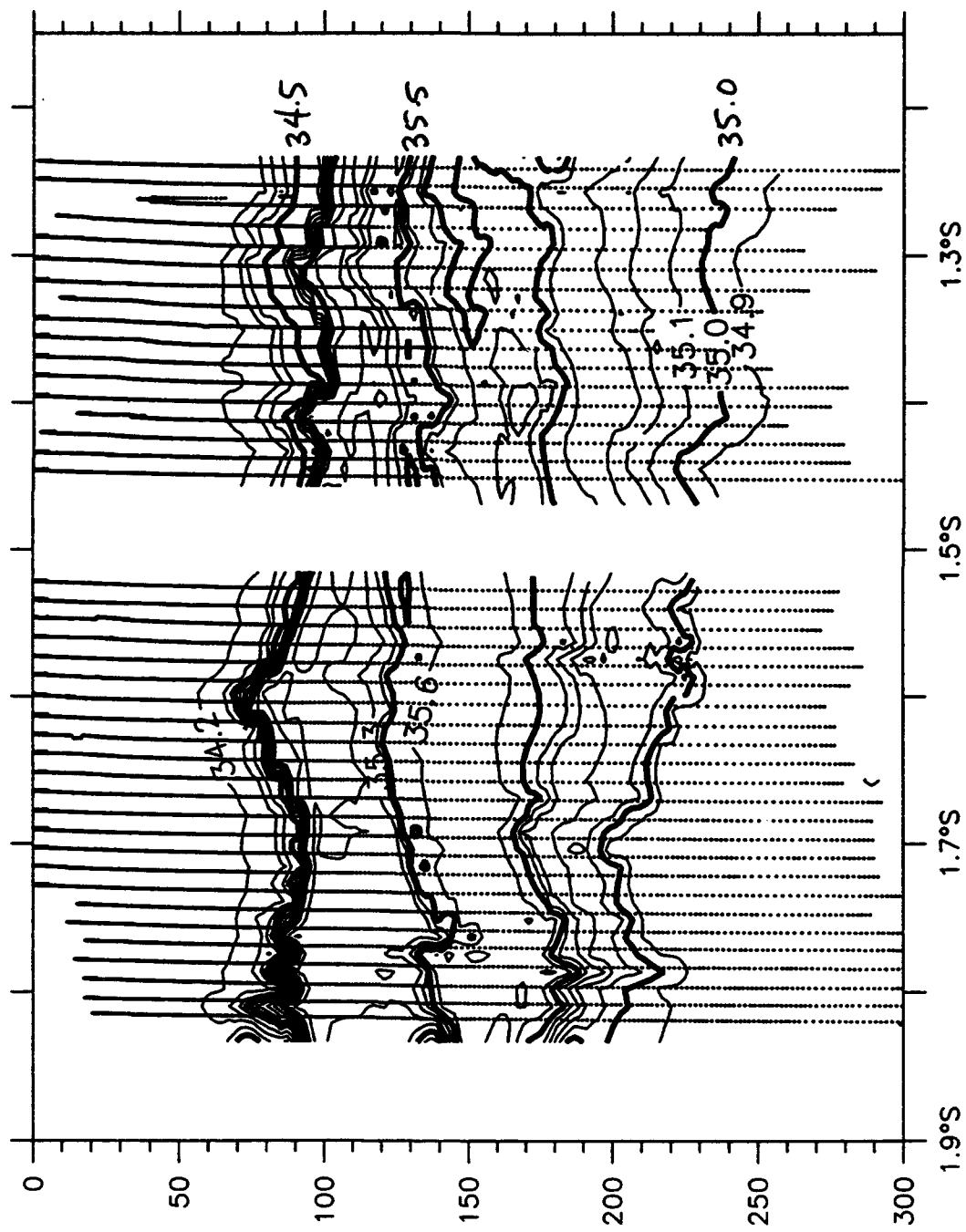


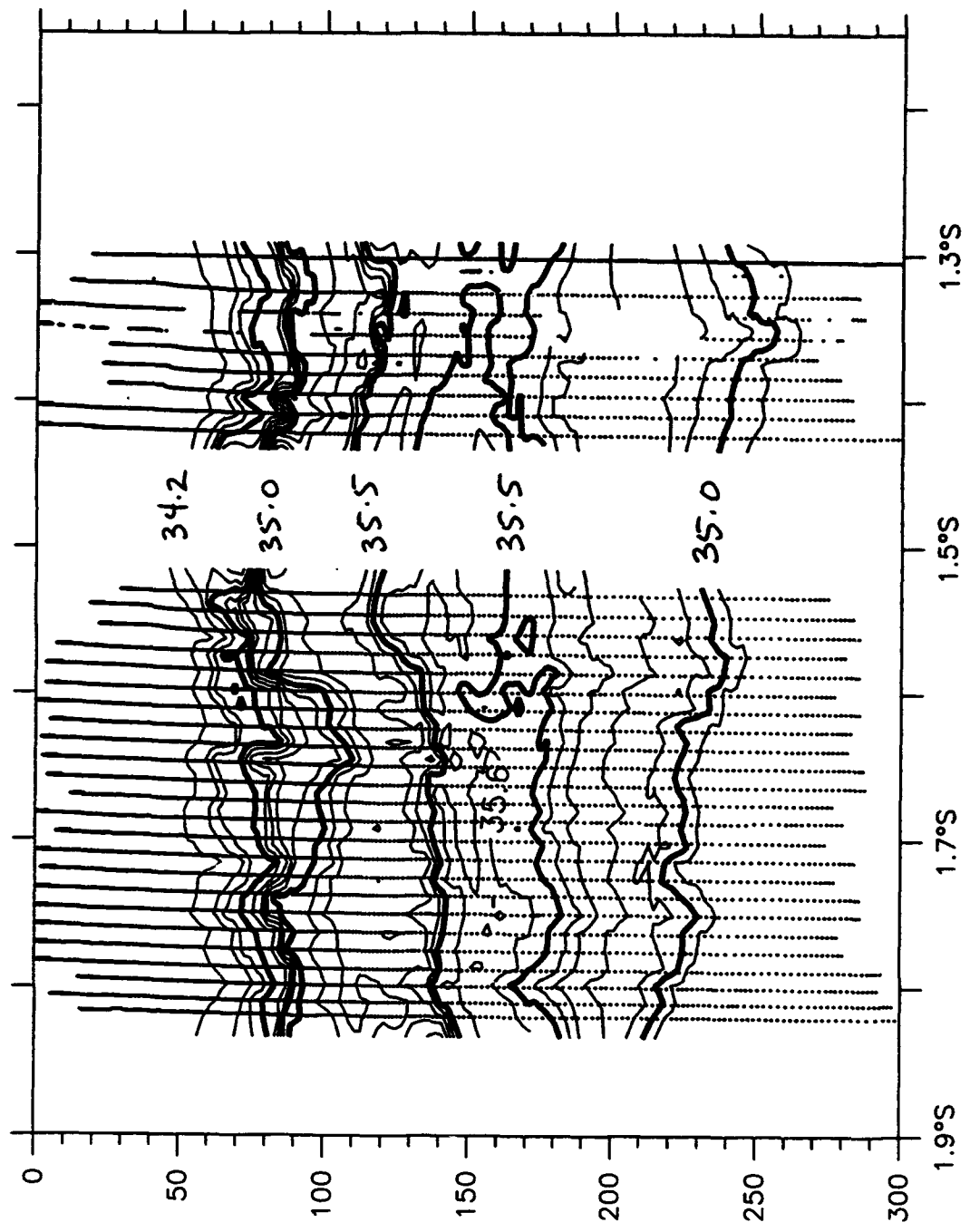
$S(\text{psu})$ , E2N, 1 February 1993

S(psu), E2N, 3 February 1993



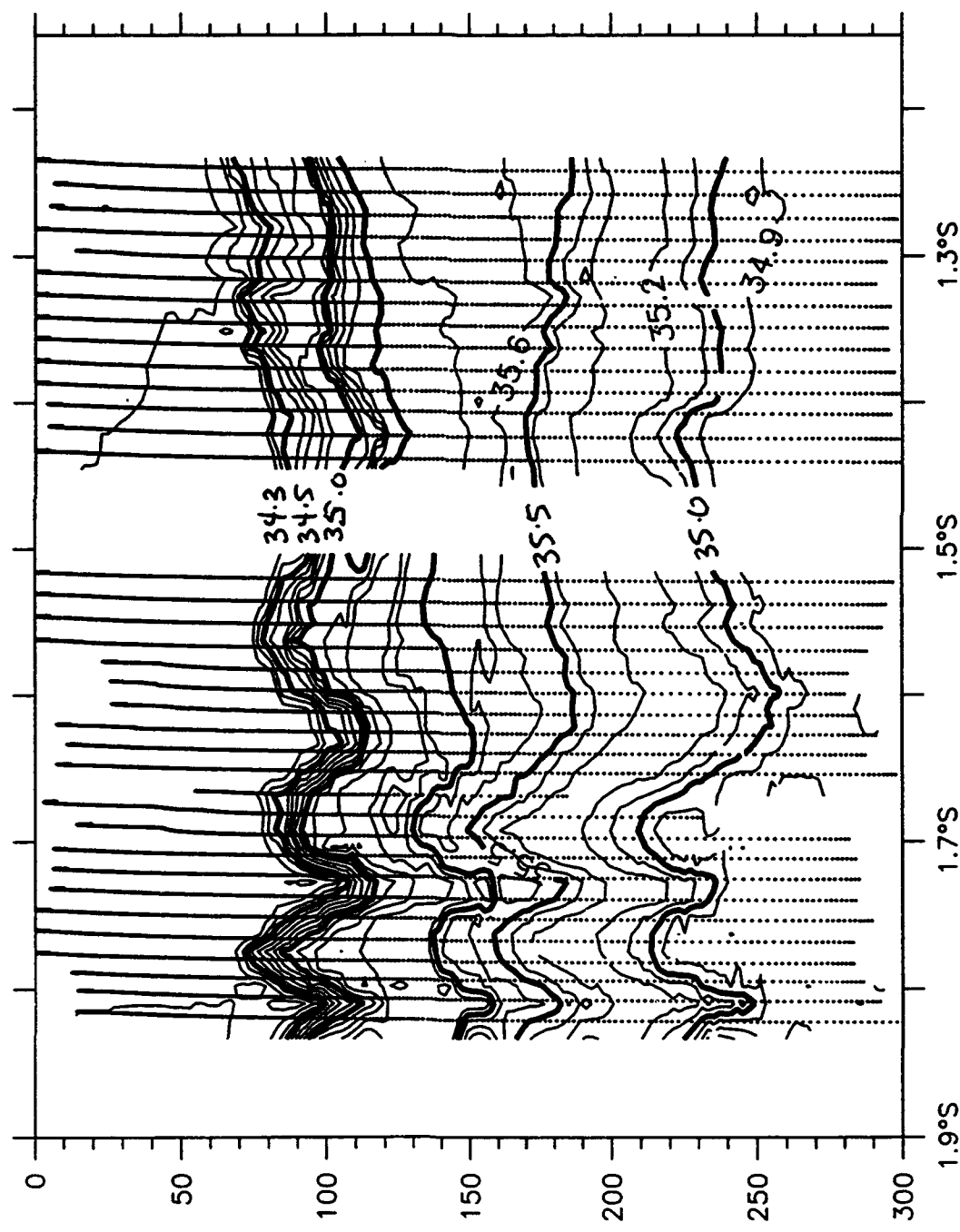
S(psu), E2N, 5 February 1993



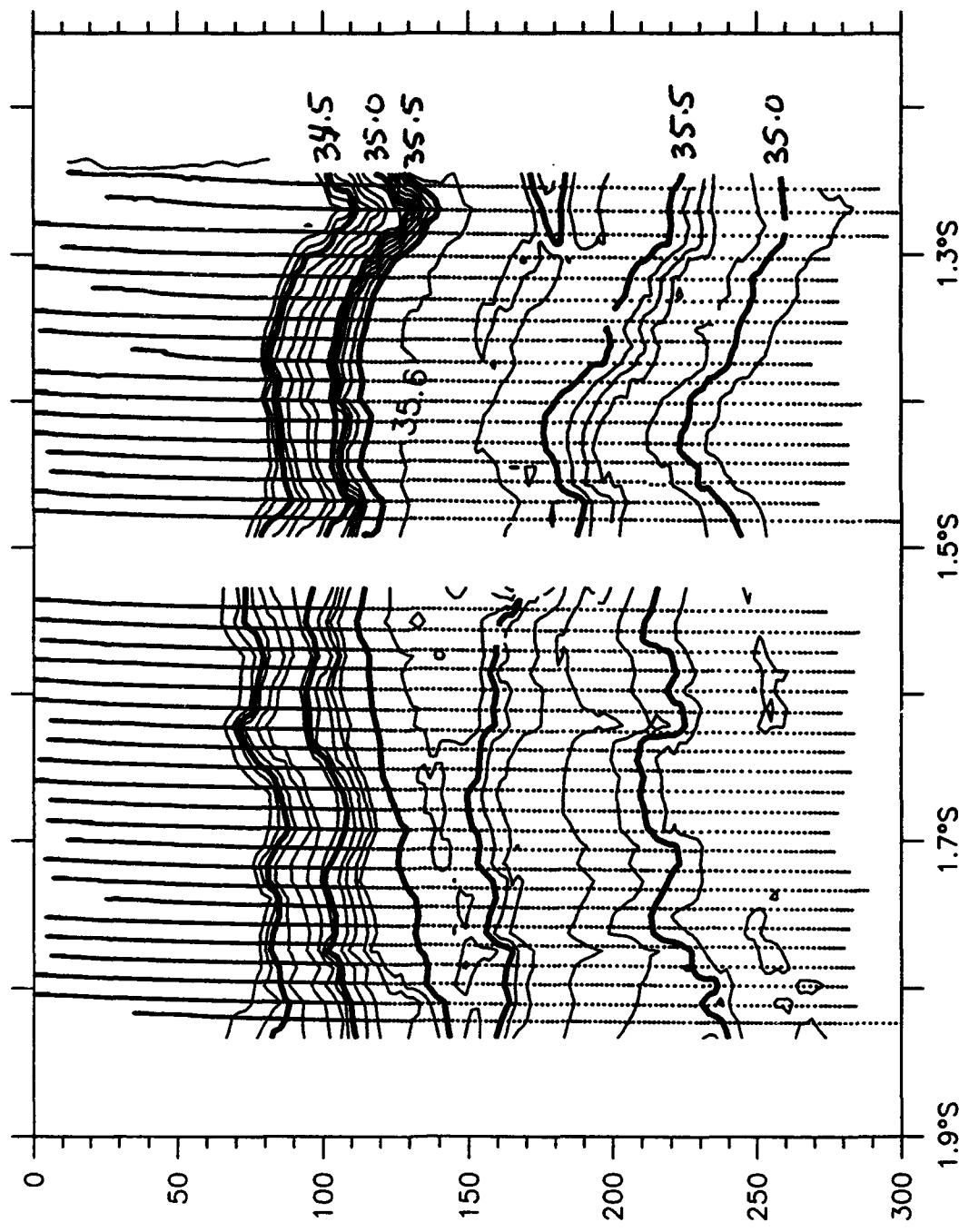


$S(\text{psu})$ , E2N, 6 February 1993

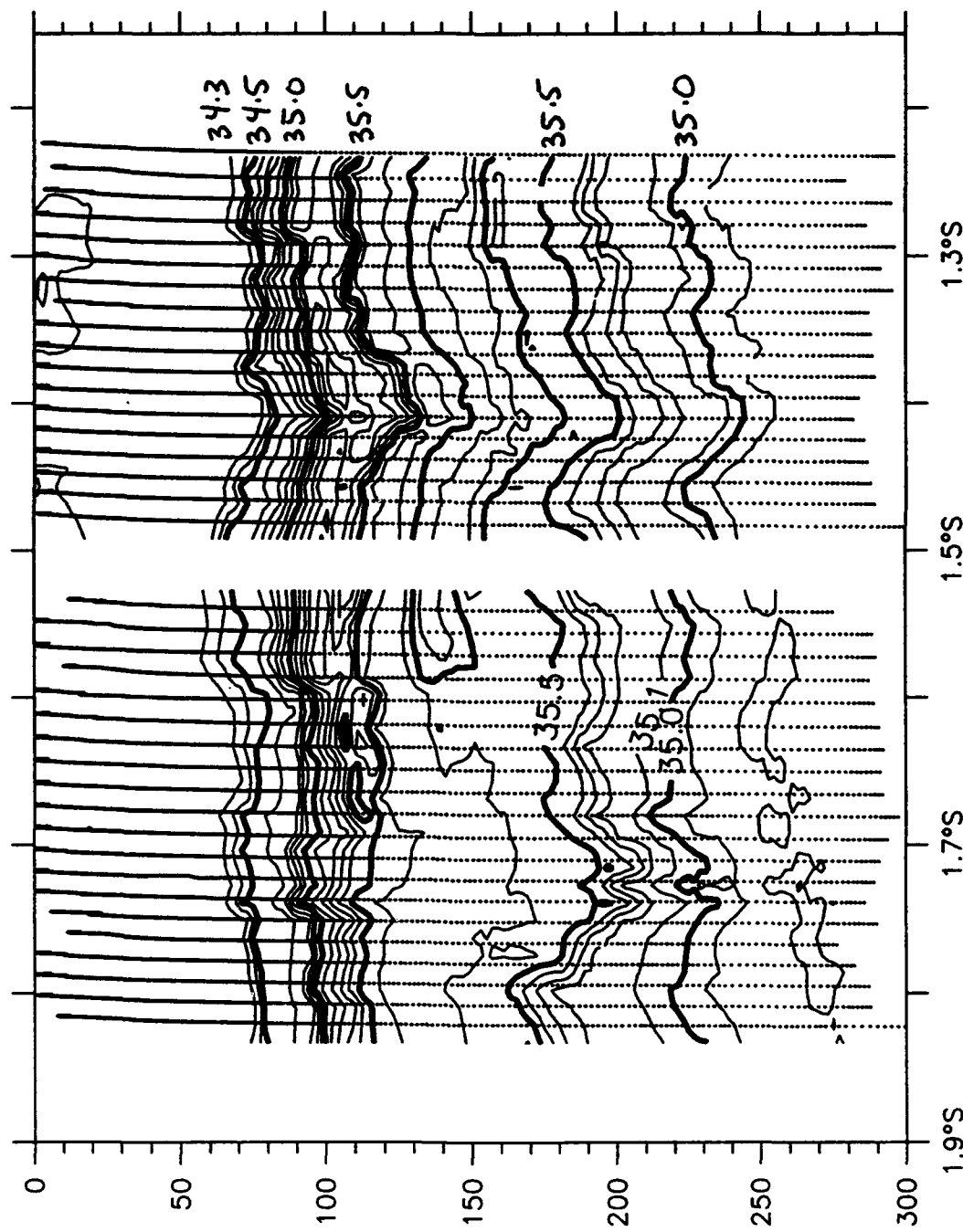
S(psu), E2N, 9 February 1993

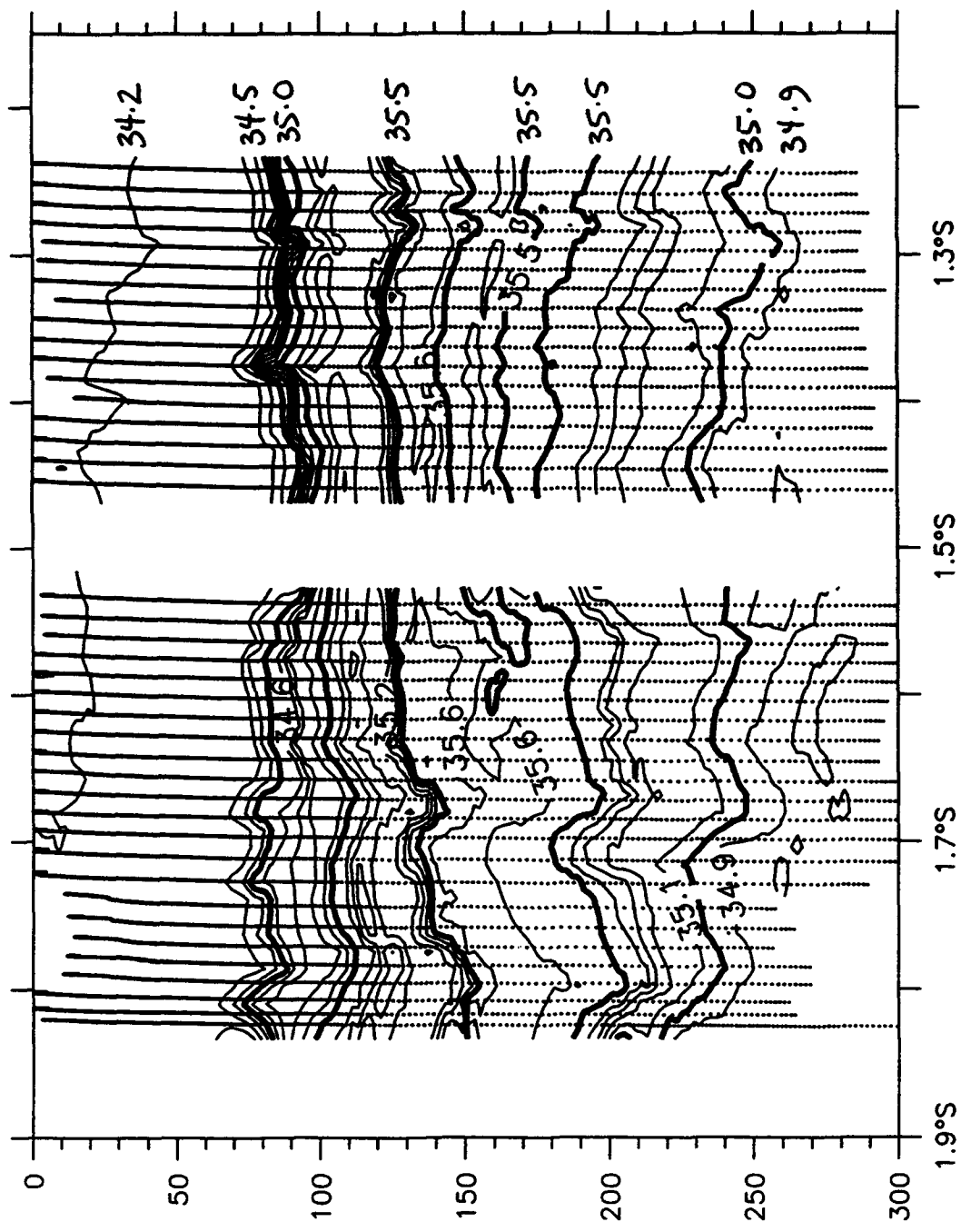


S(psu), E2N, 10 February 1993

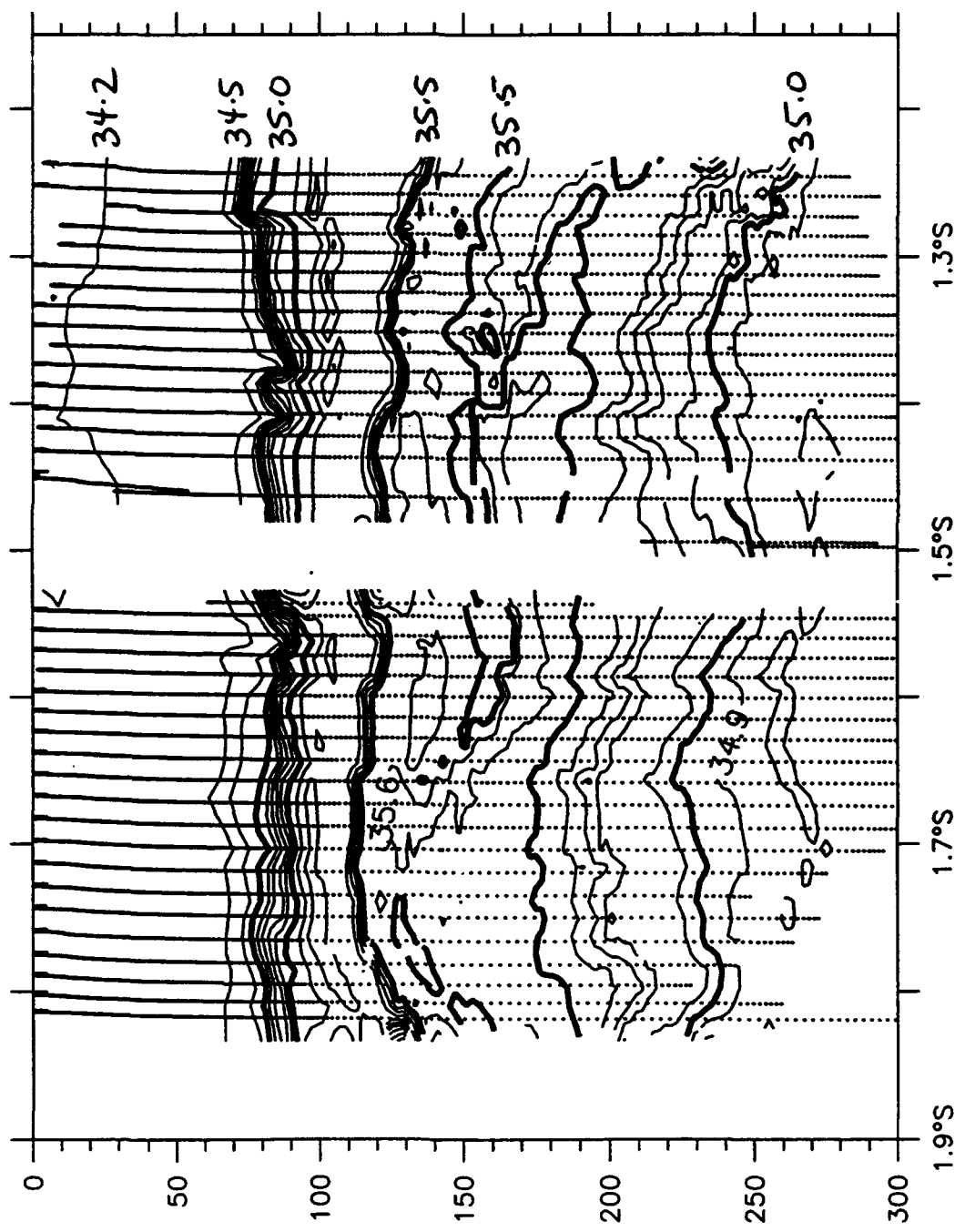


S(psu), E2N, 11 February 1993

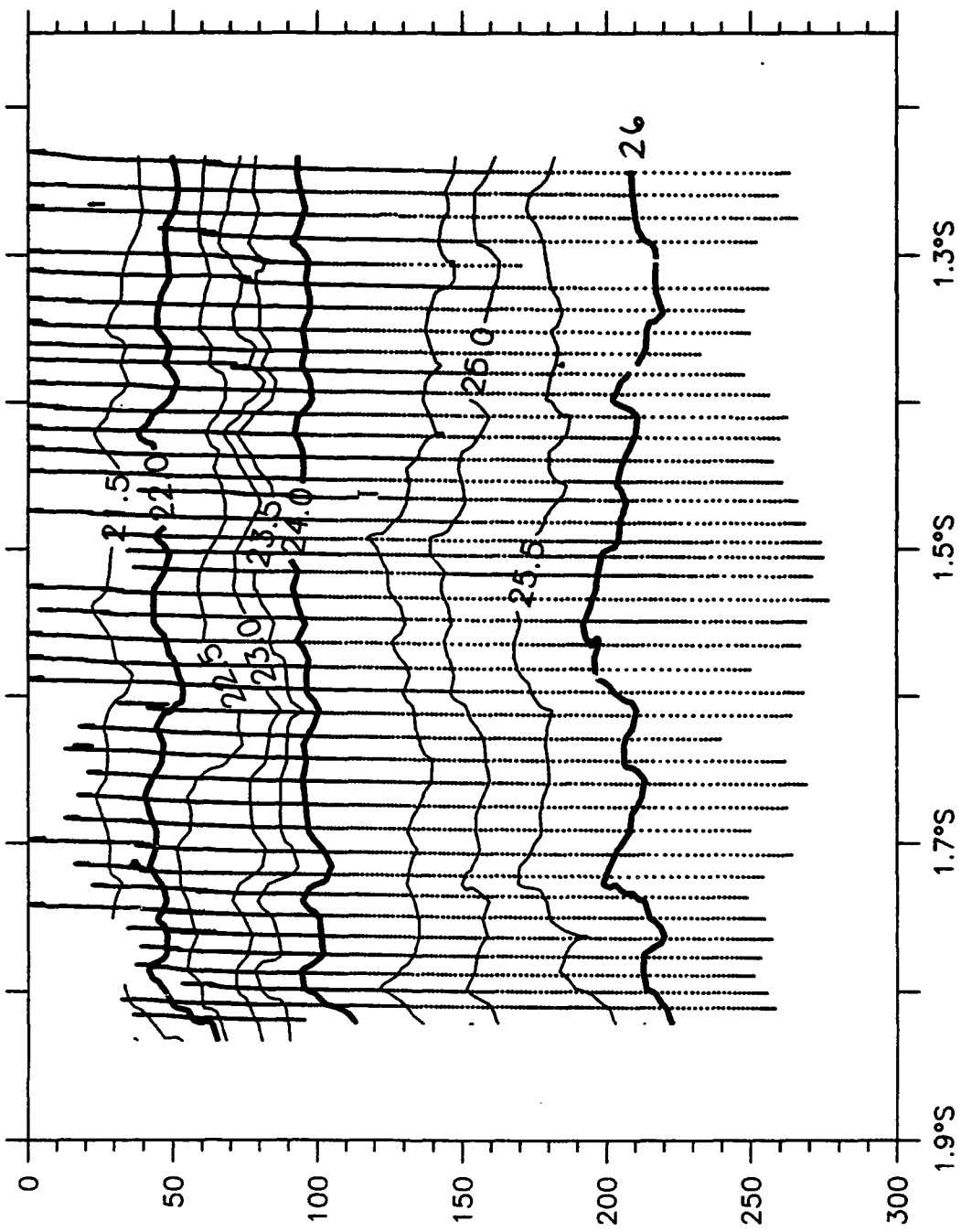




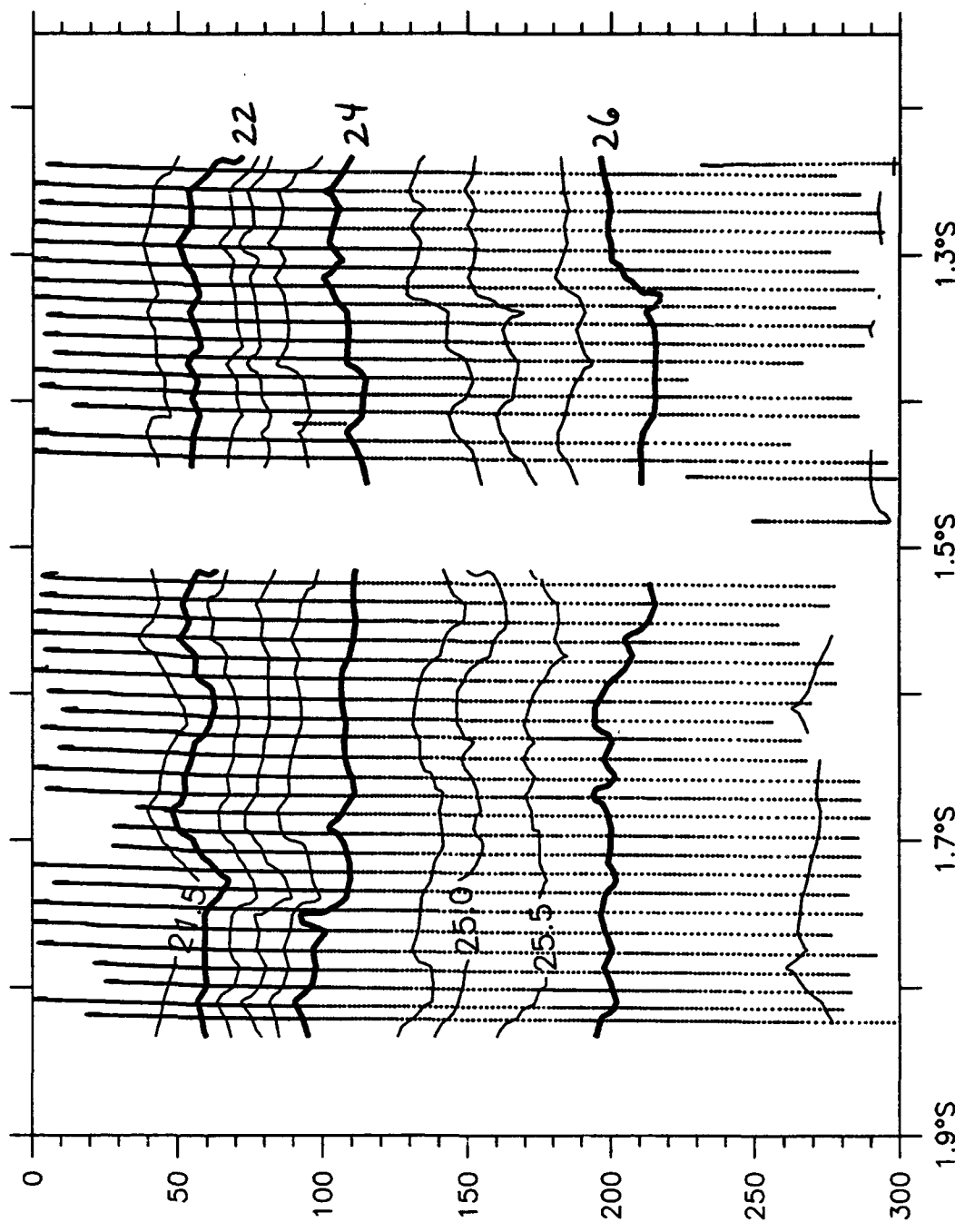
$S(\text{psu})$ , E2N, 13 February 1993



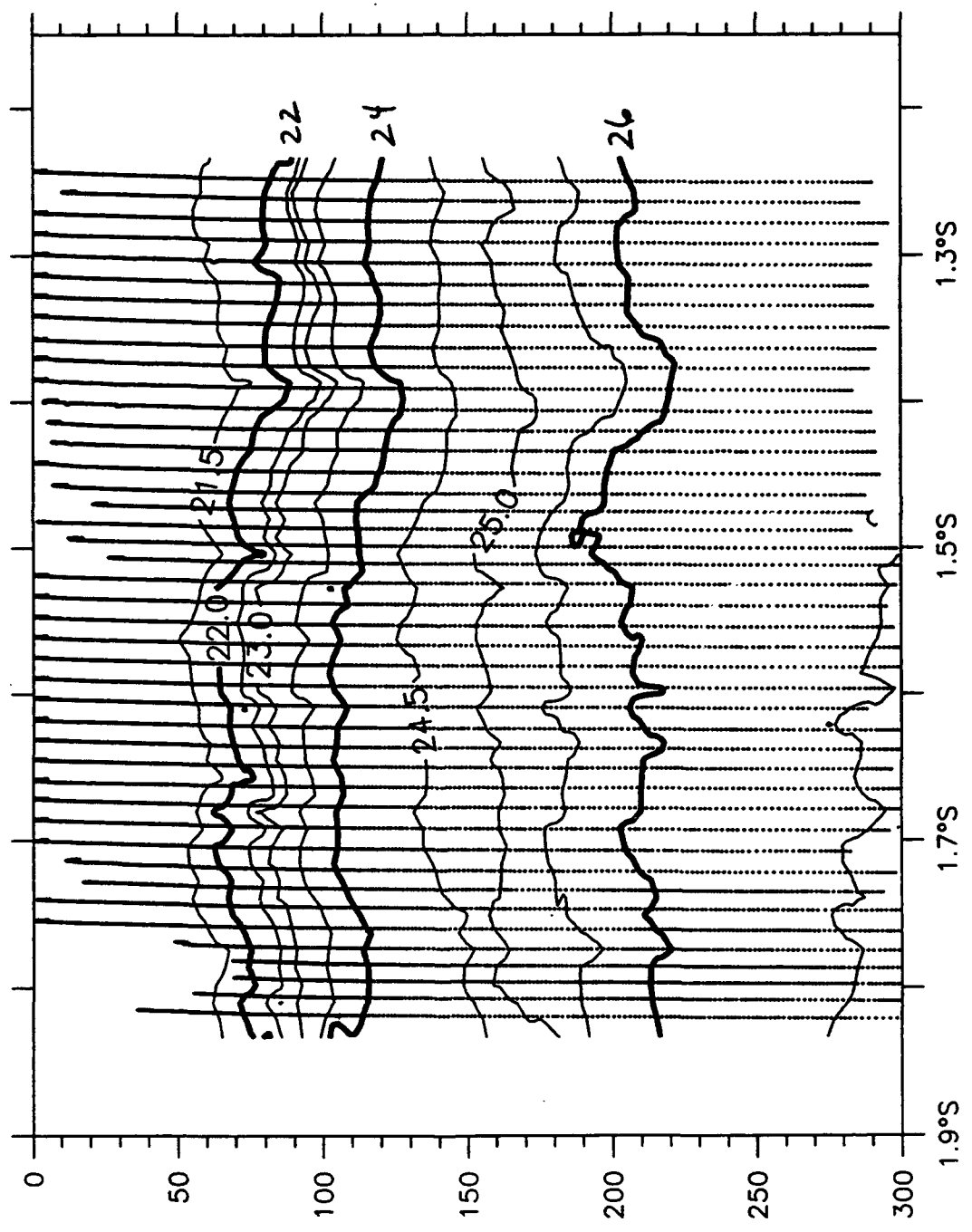
$S(\text{psu})$ , E2N, 15 February 1993



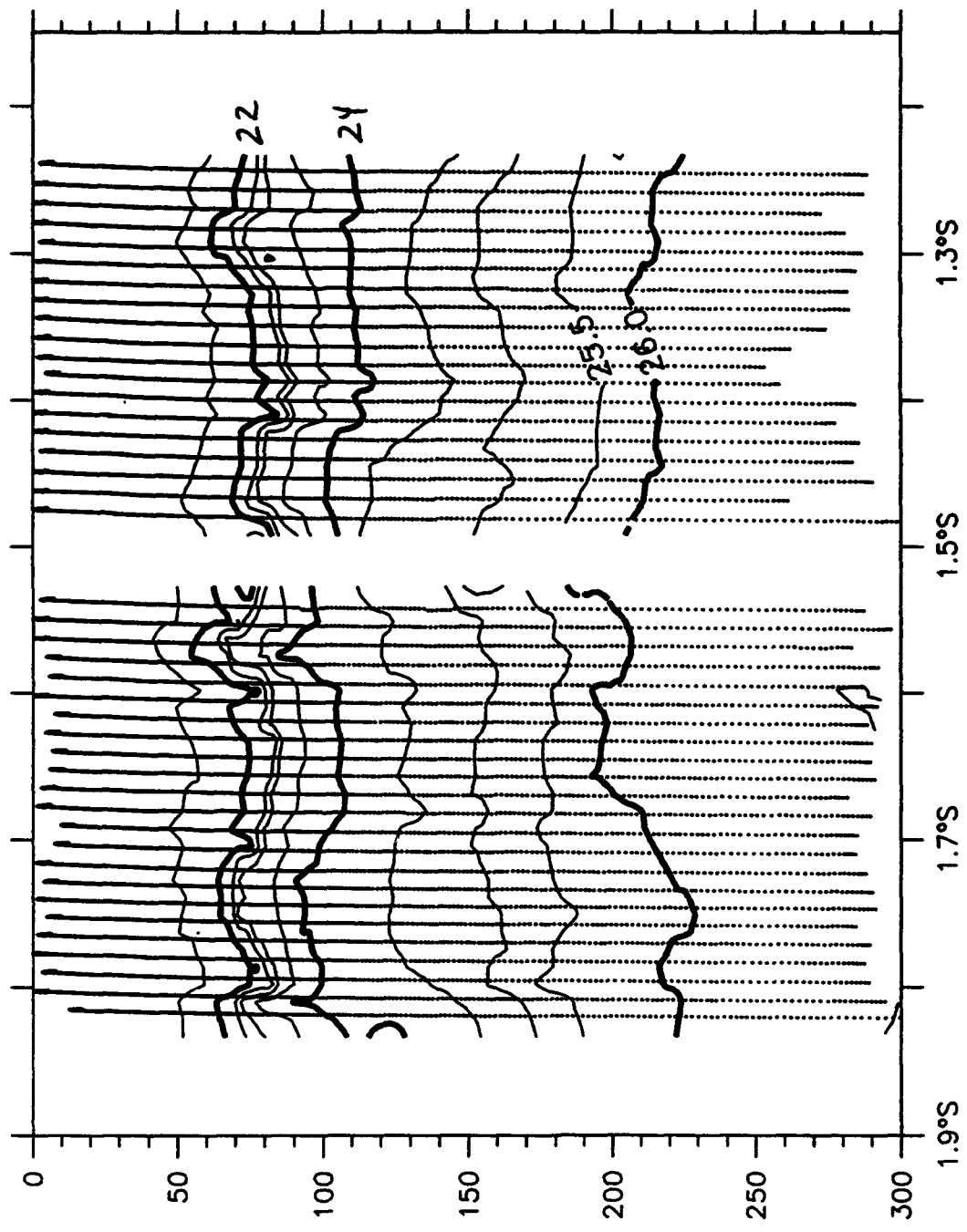
Sigma-t, E2N, 28 January 1993



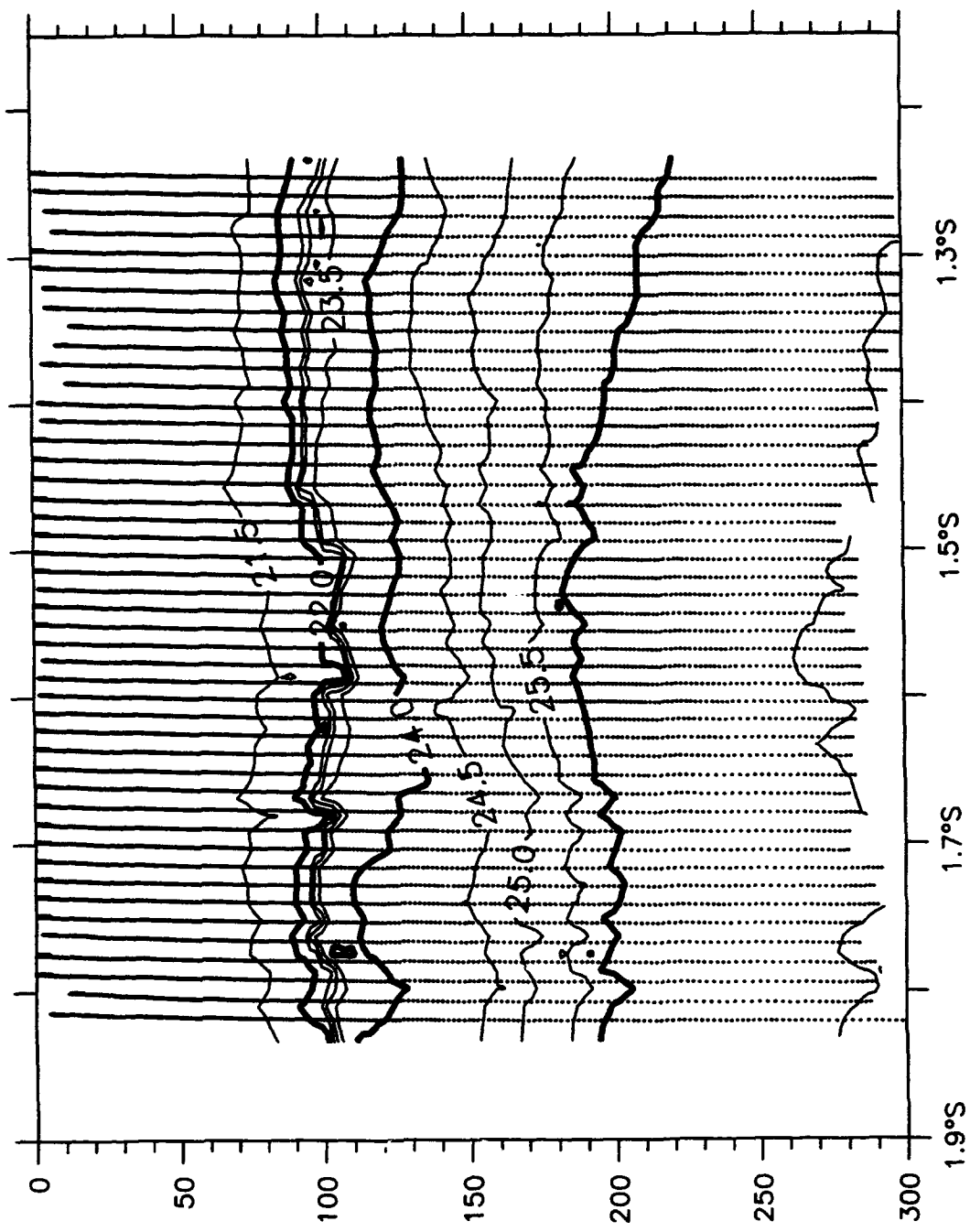
Sigma-t, E2N, 30 January 1993



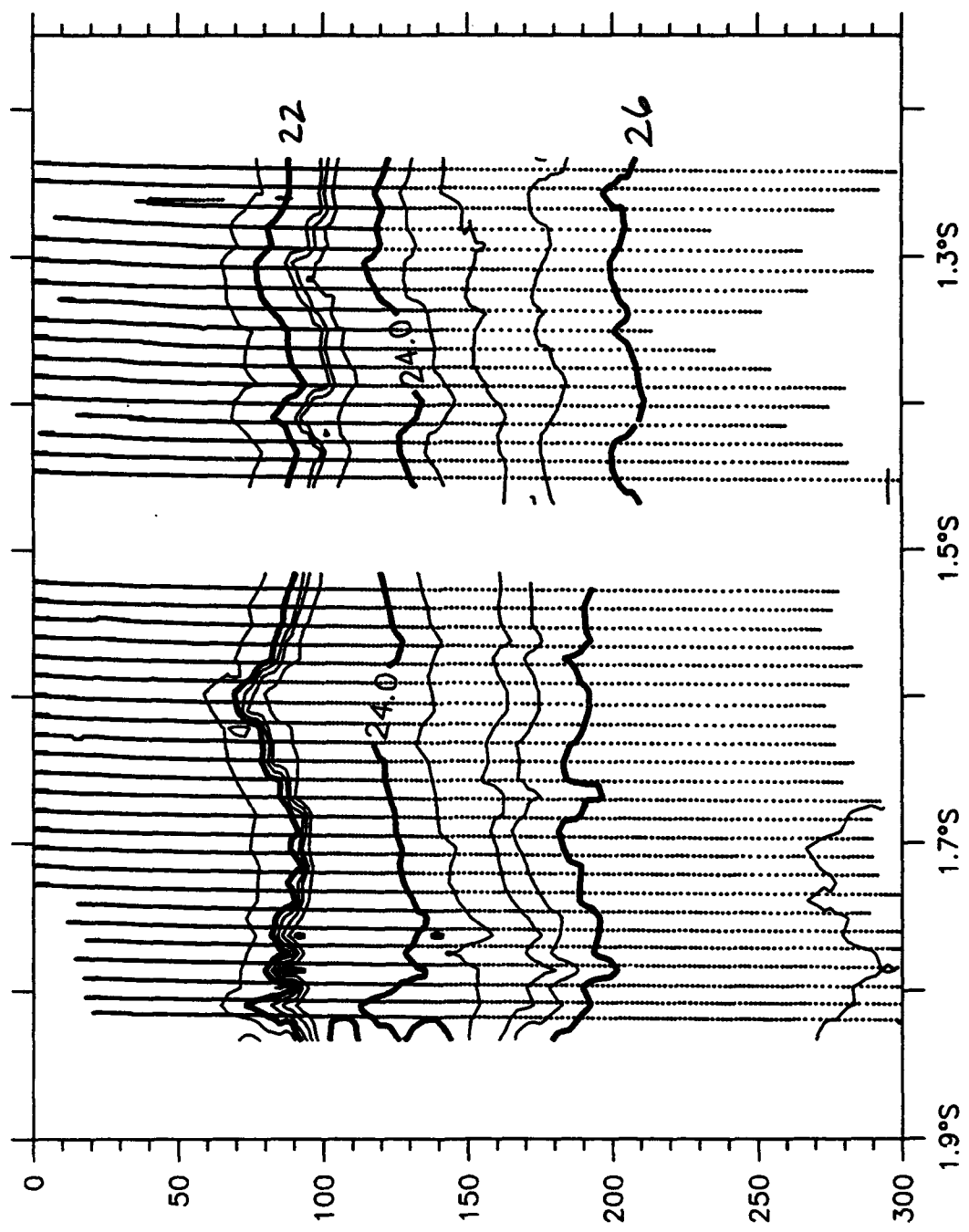
Sigma-t, E2N, 31 January 1993



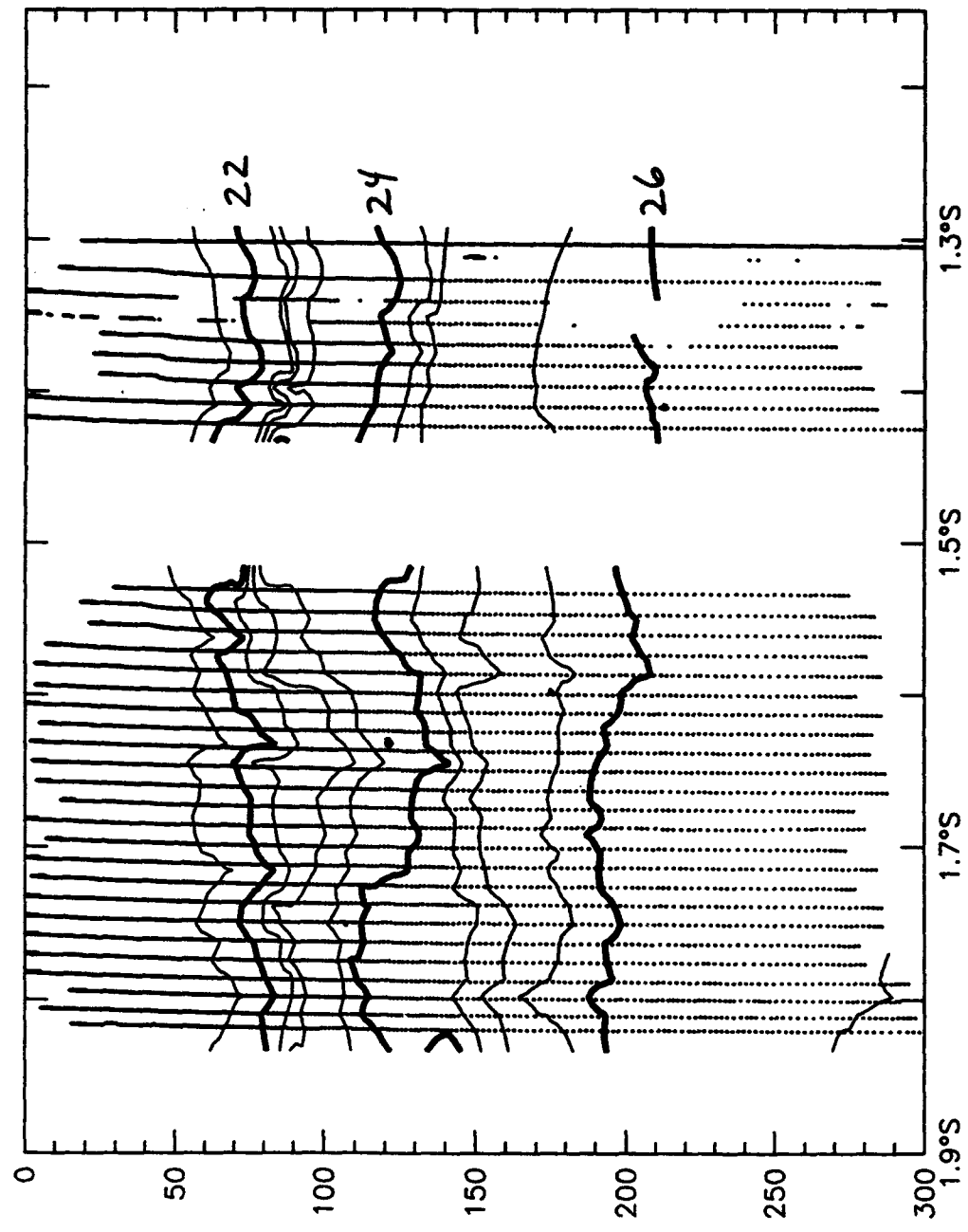
Sigma-t, E2N, 1 February 1993



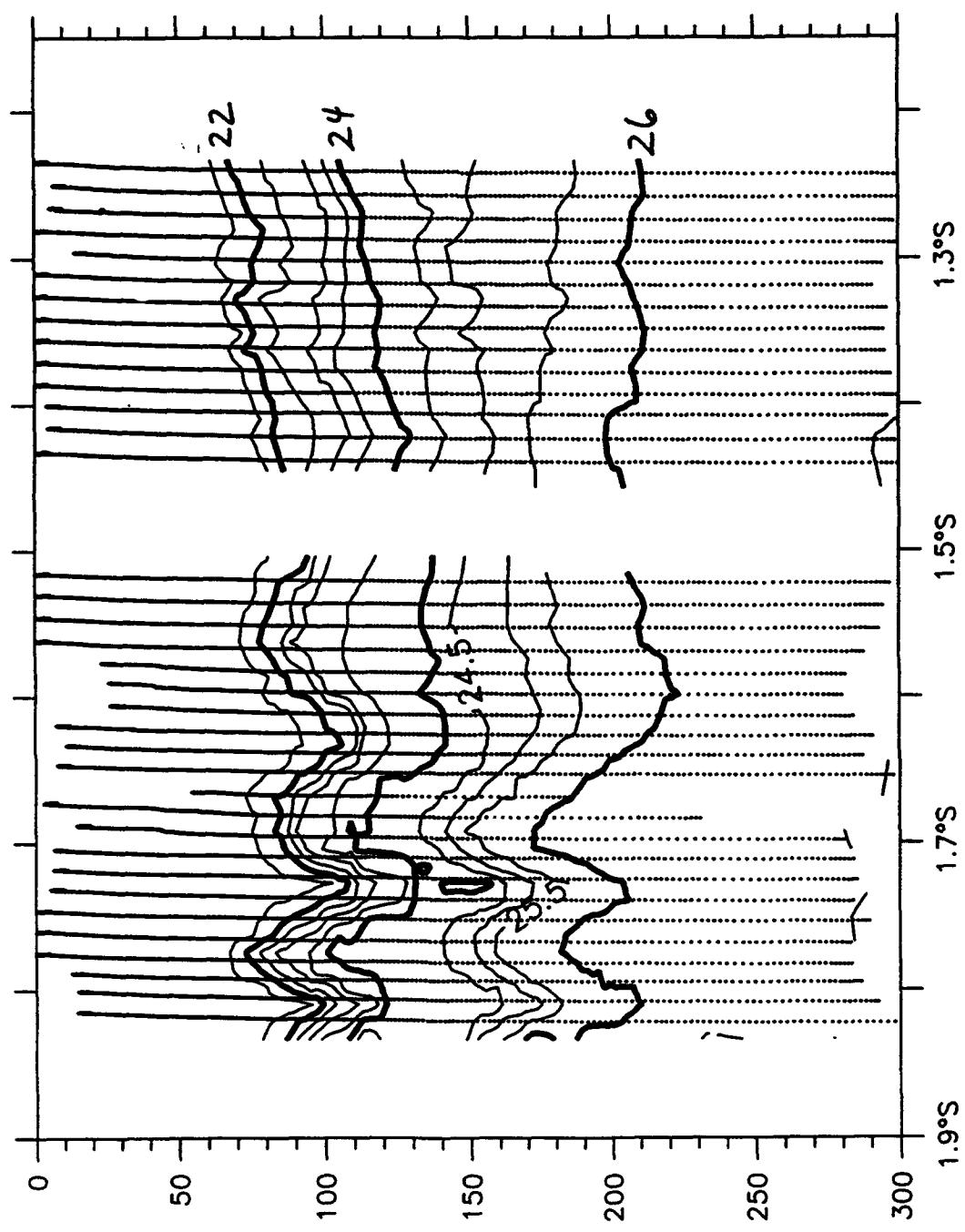
Sigma-t, E2N, 3 February 1993



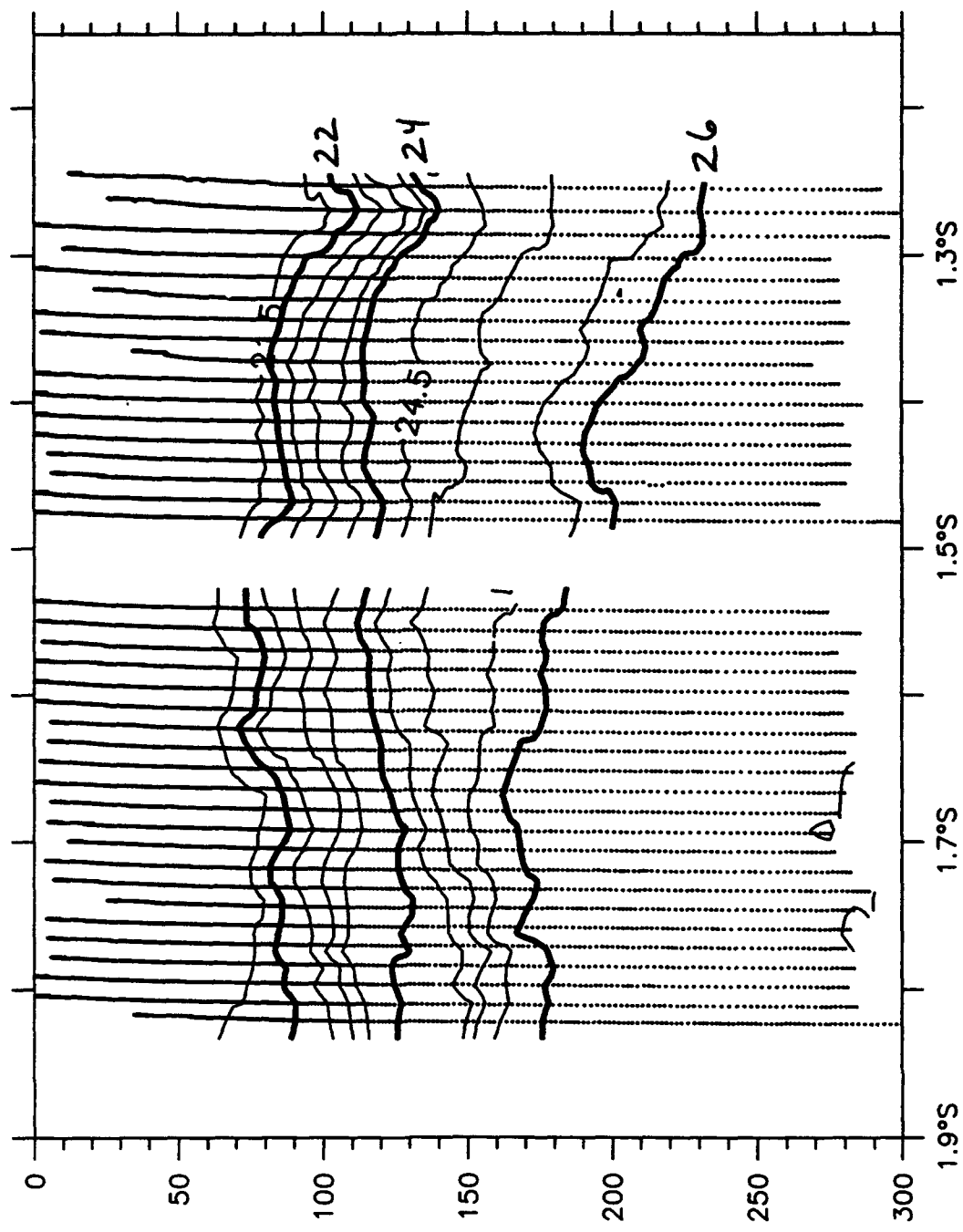
Sigma-t, E2N, 5 February 1993



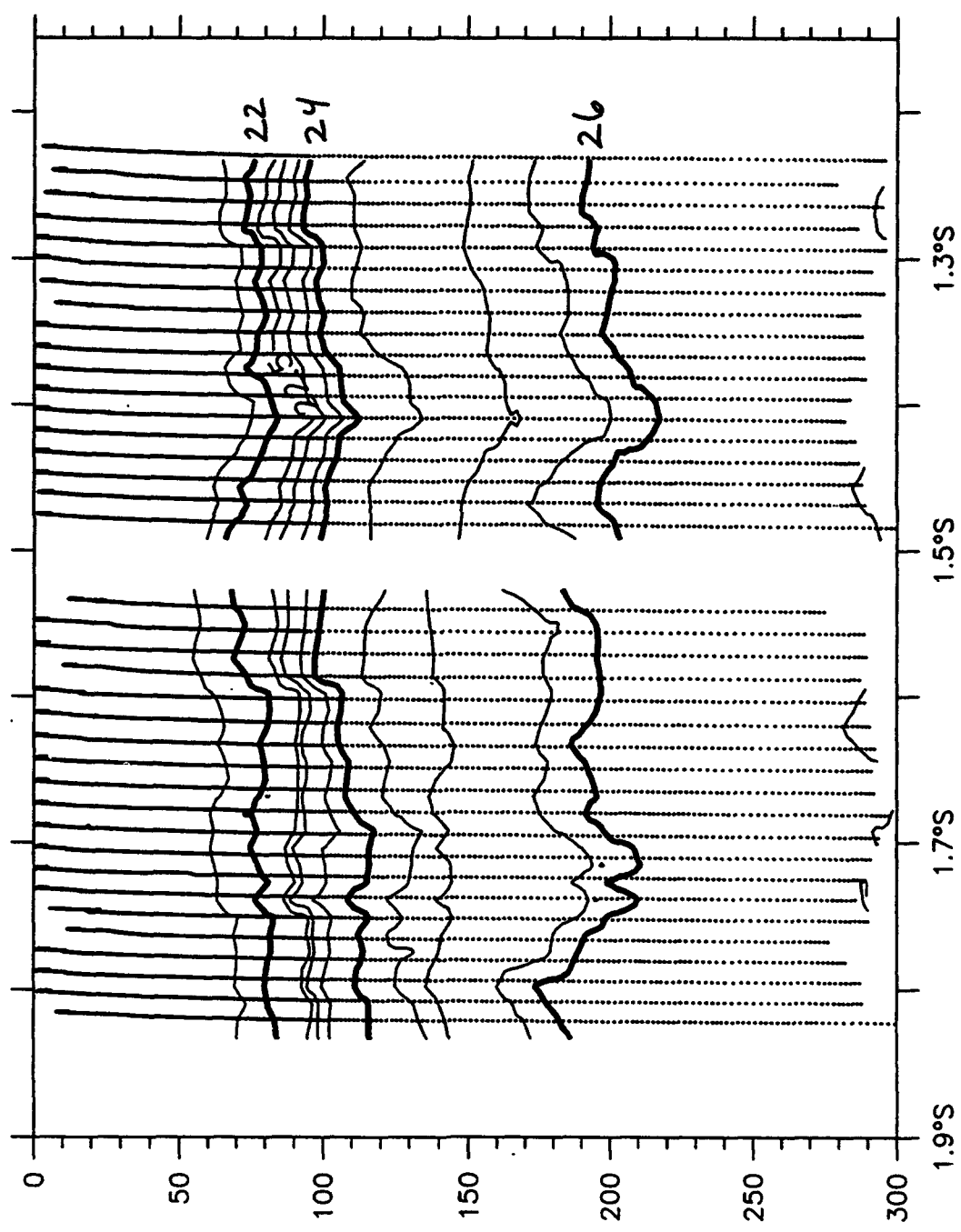
Sigma-t, E2N, 06 February 1993



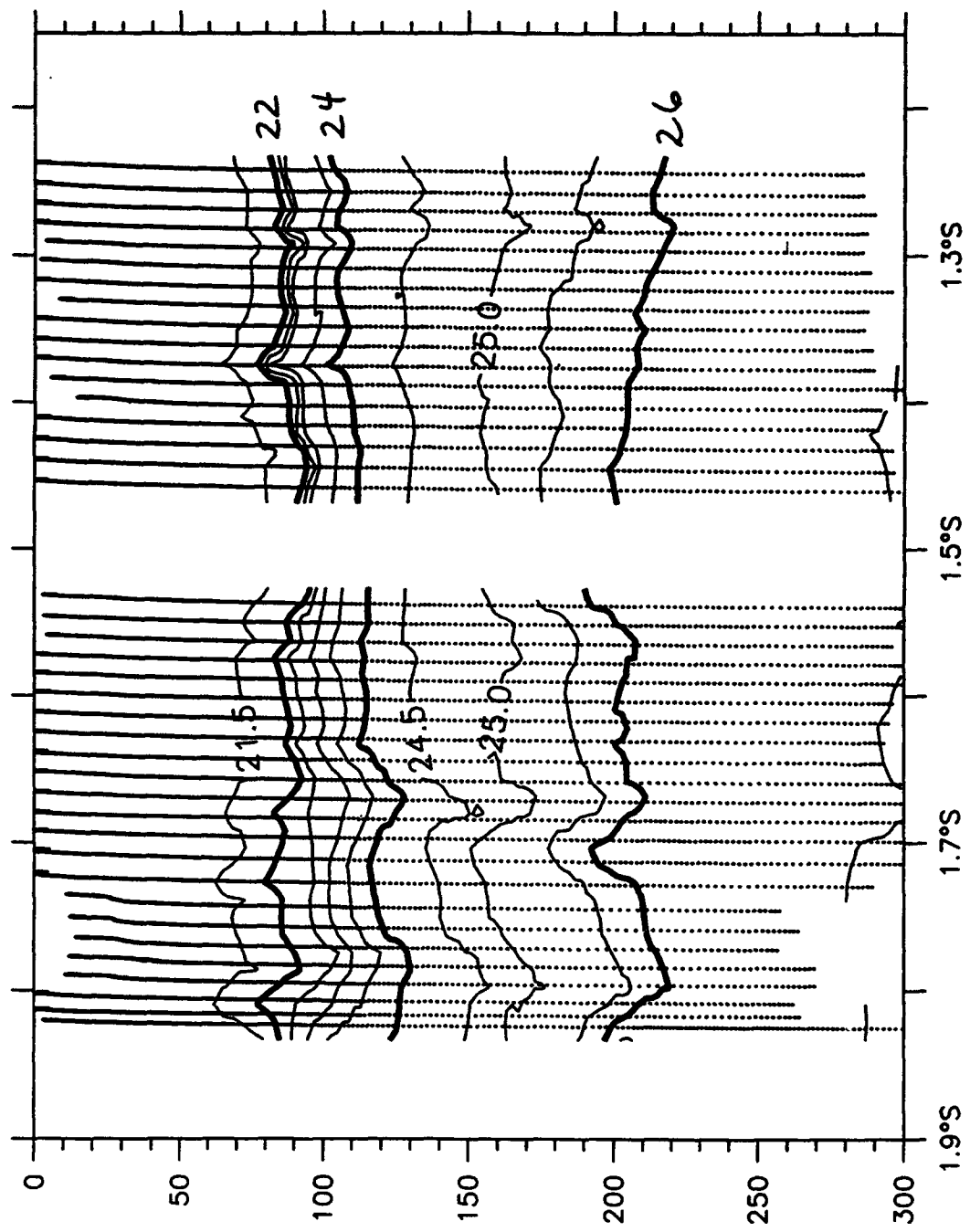
Sigma-t, E2N, 9 February 1993



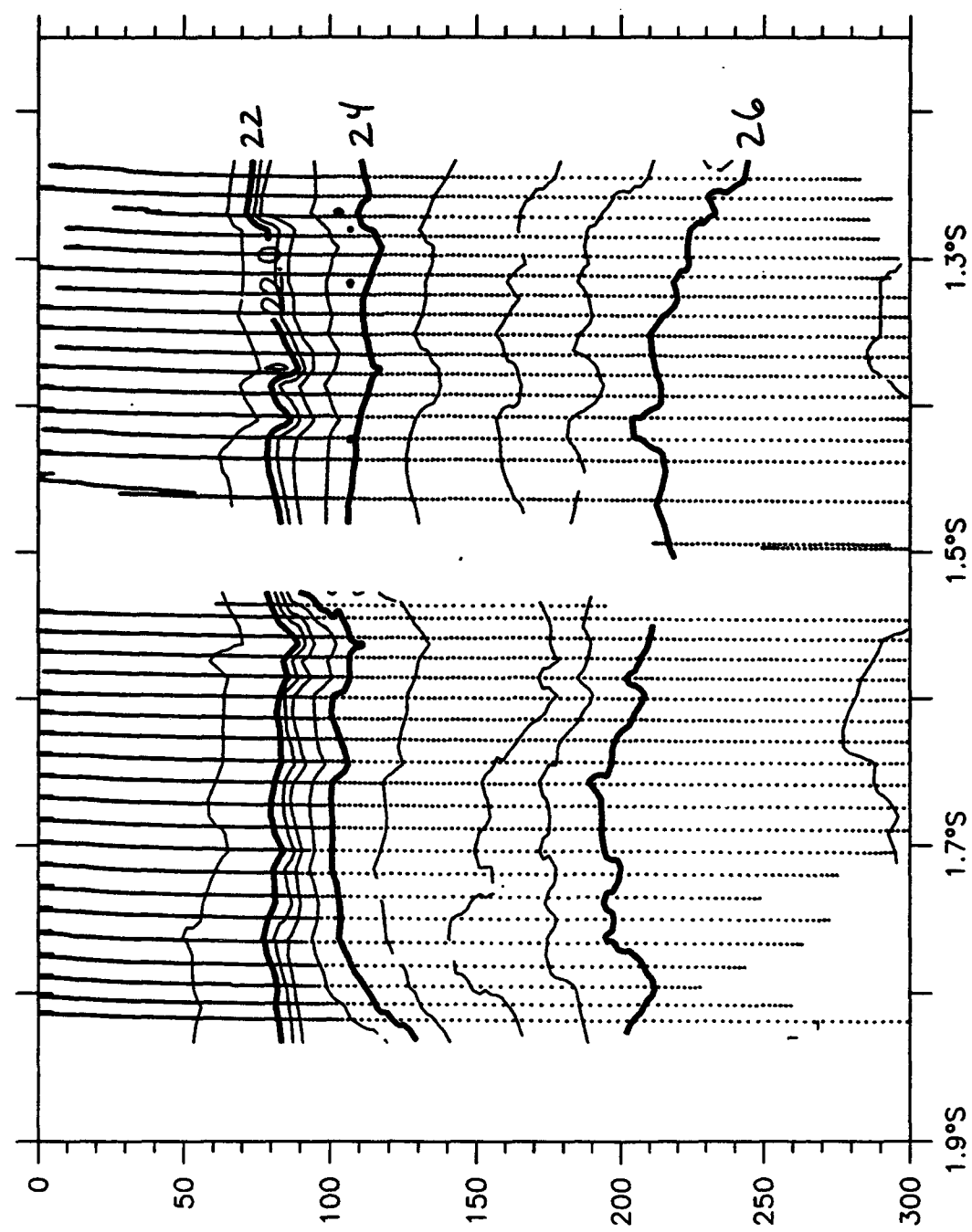
Sigma-t, E2N, 10 February 1993



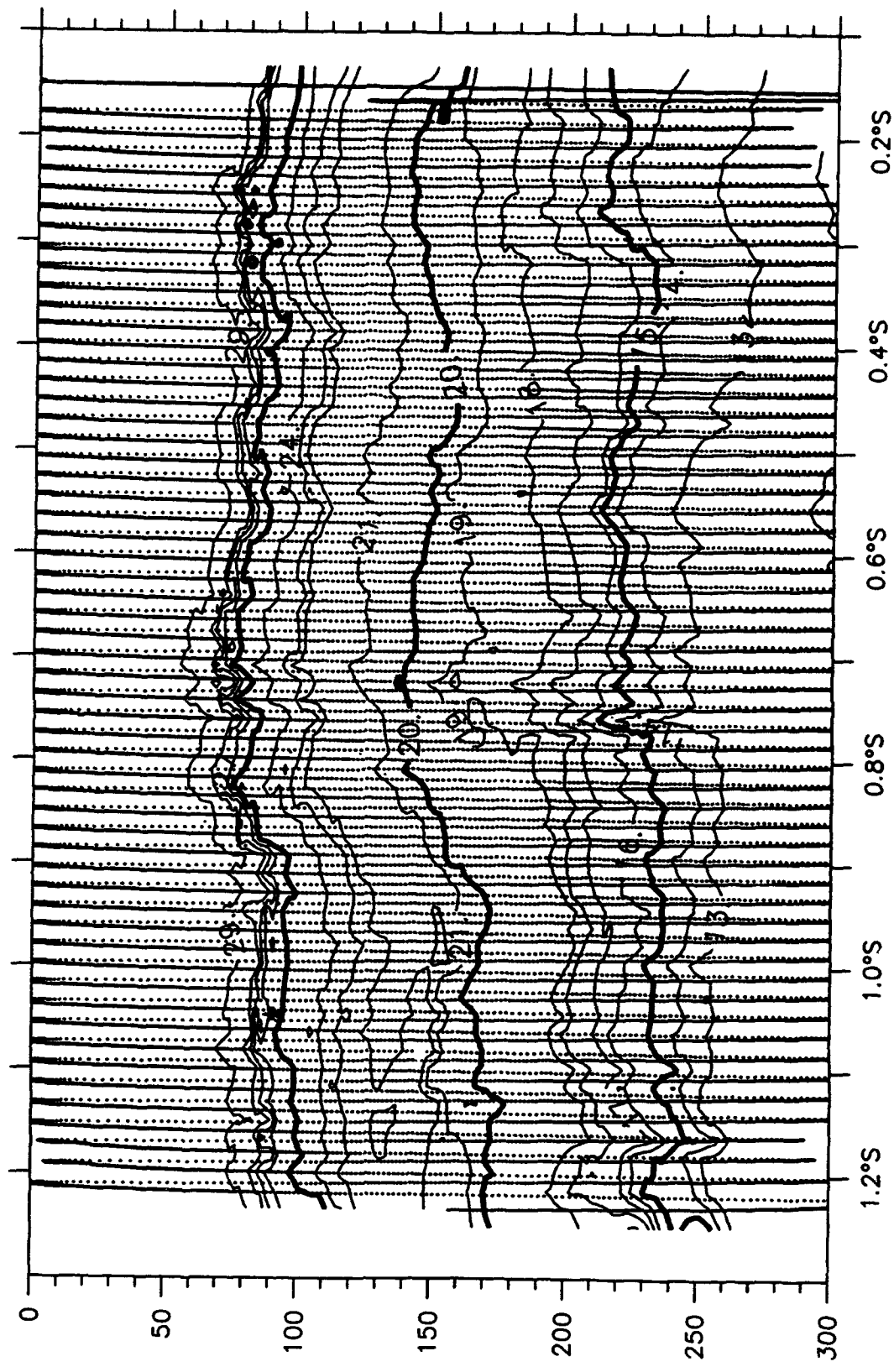
Sigma-t, E2N, 11 February 1993



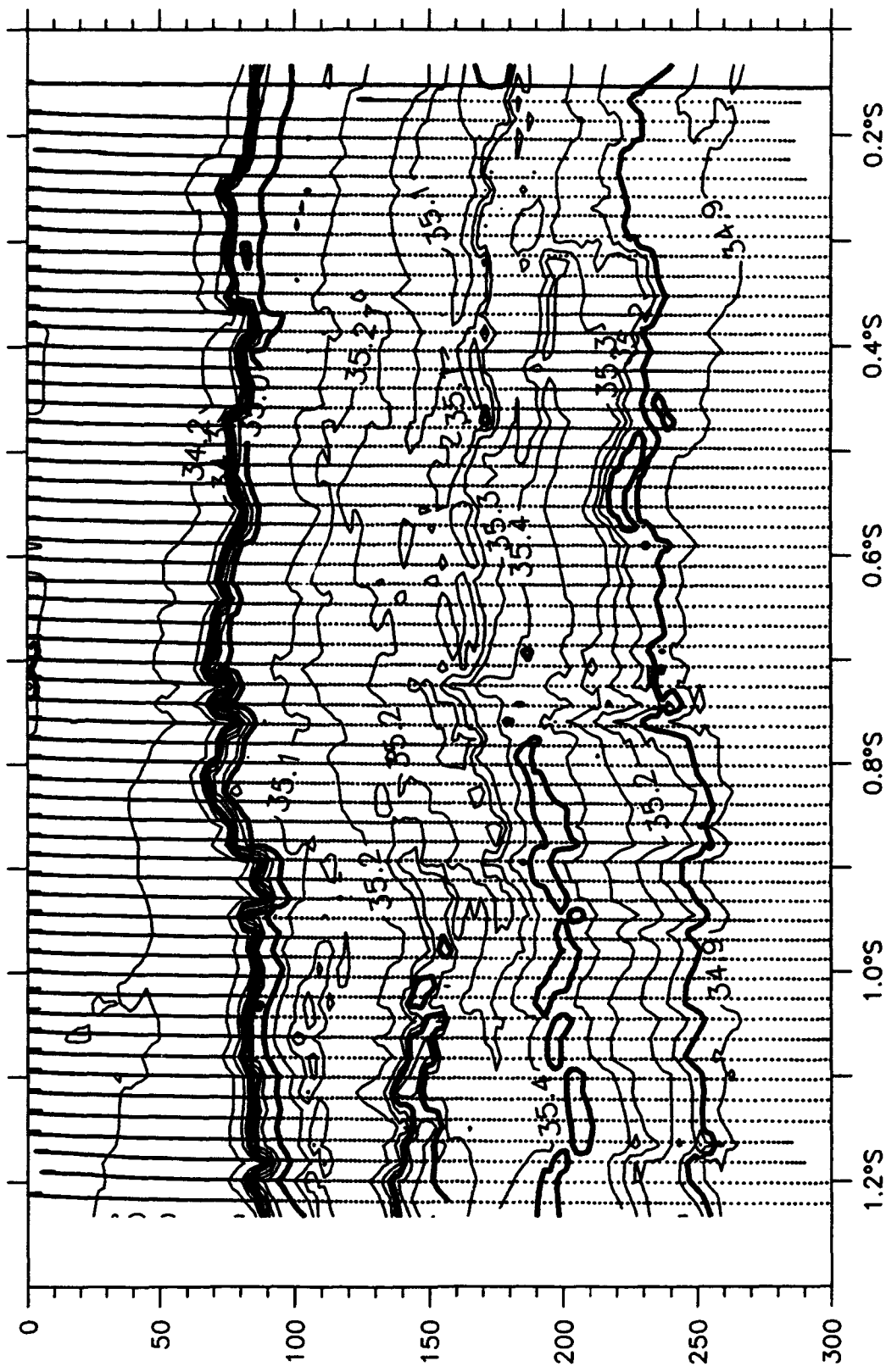
Sigma-t, E2N, 13 February 1993



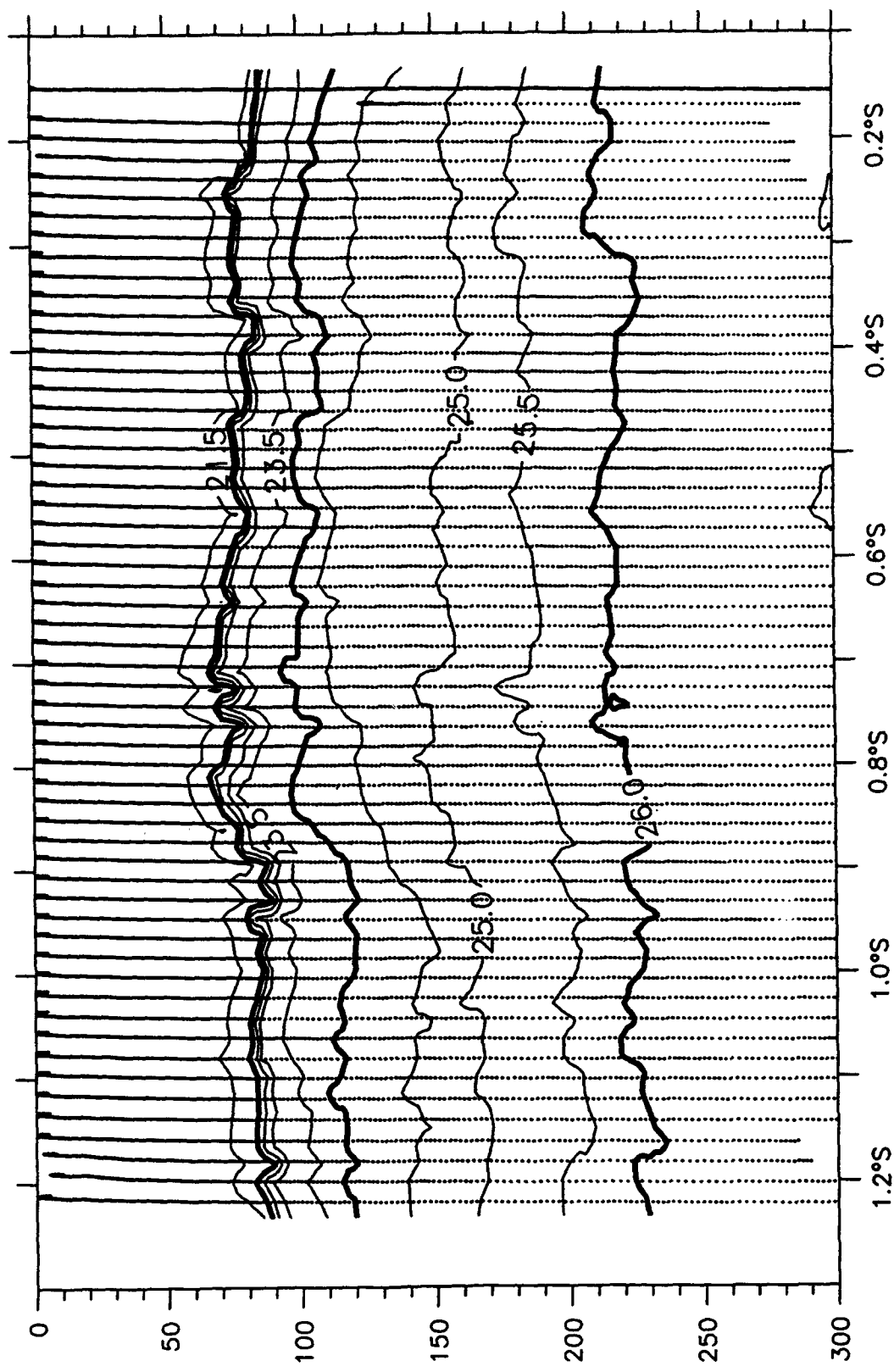
Sigma-t, E2N, 15 February 1993



$T$  ( $^{\circ}\text{C}$ ), SBN to Equator, 15 February 1993



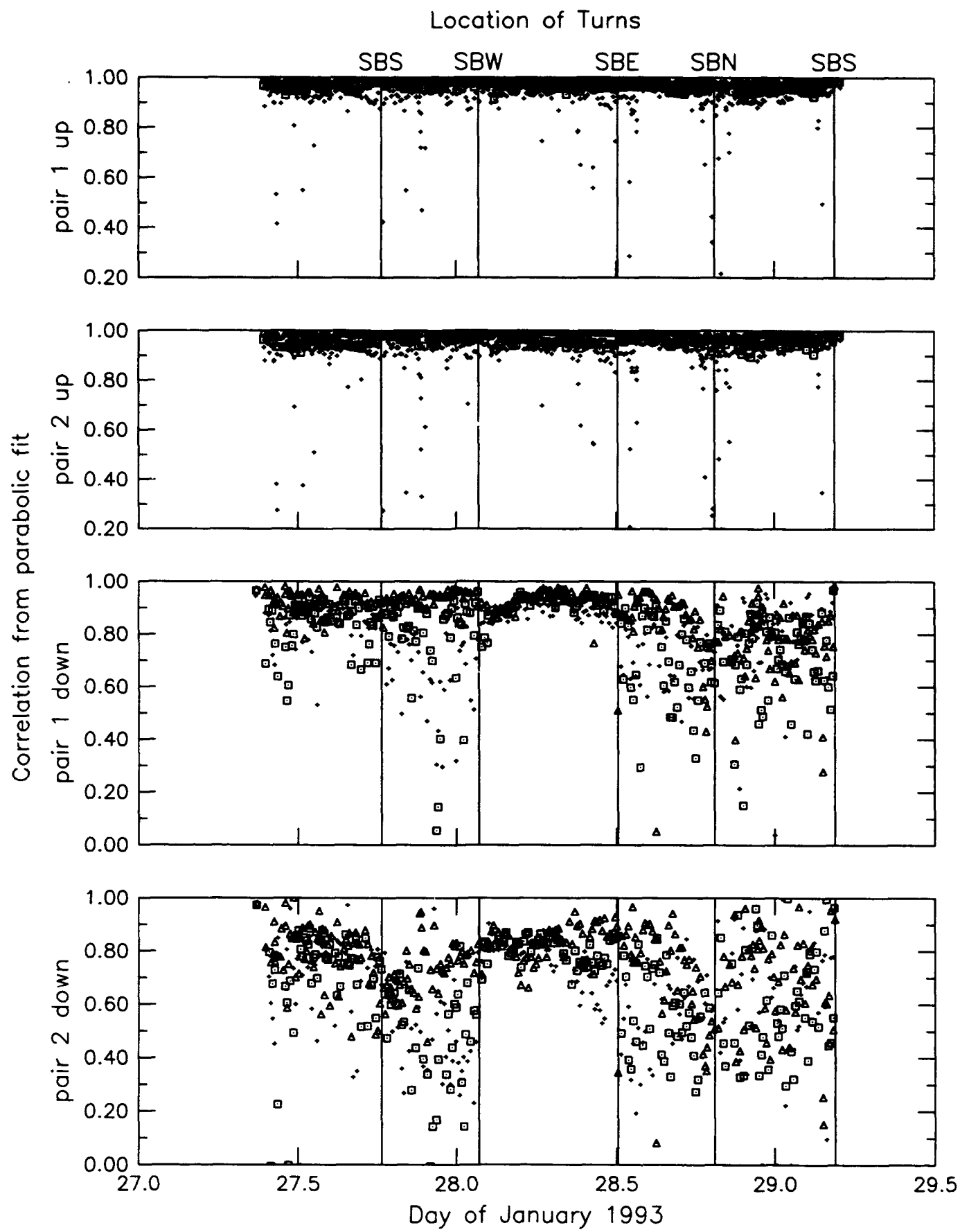
$S$ (psu), SBN to Equator, 15 February 1993



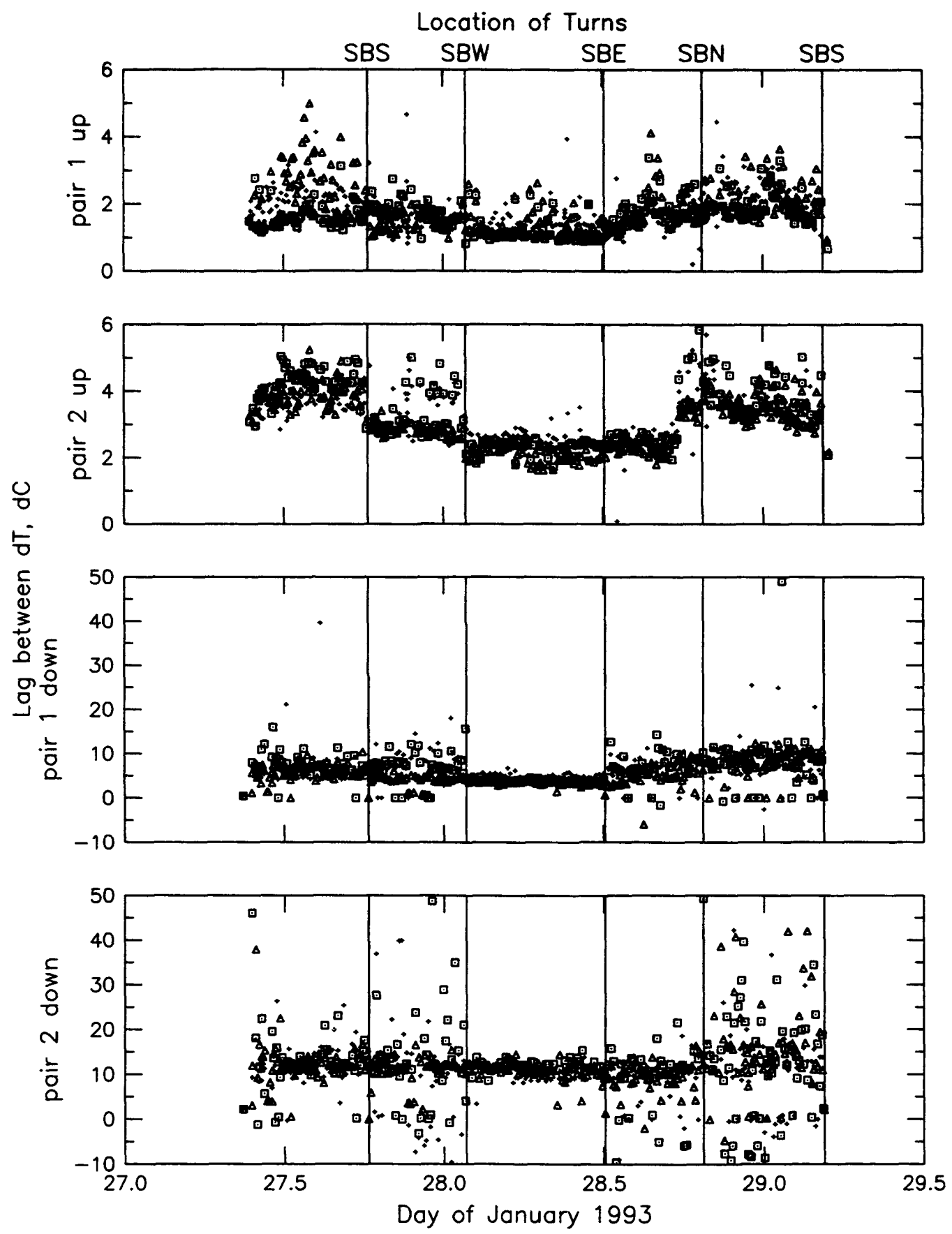
Sigma-t, SBN to Equator, 15 February 1993

**APPENDIX A:**

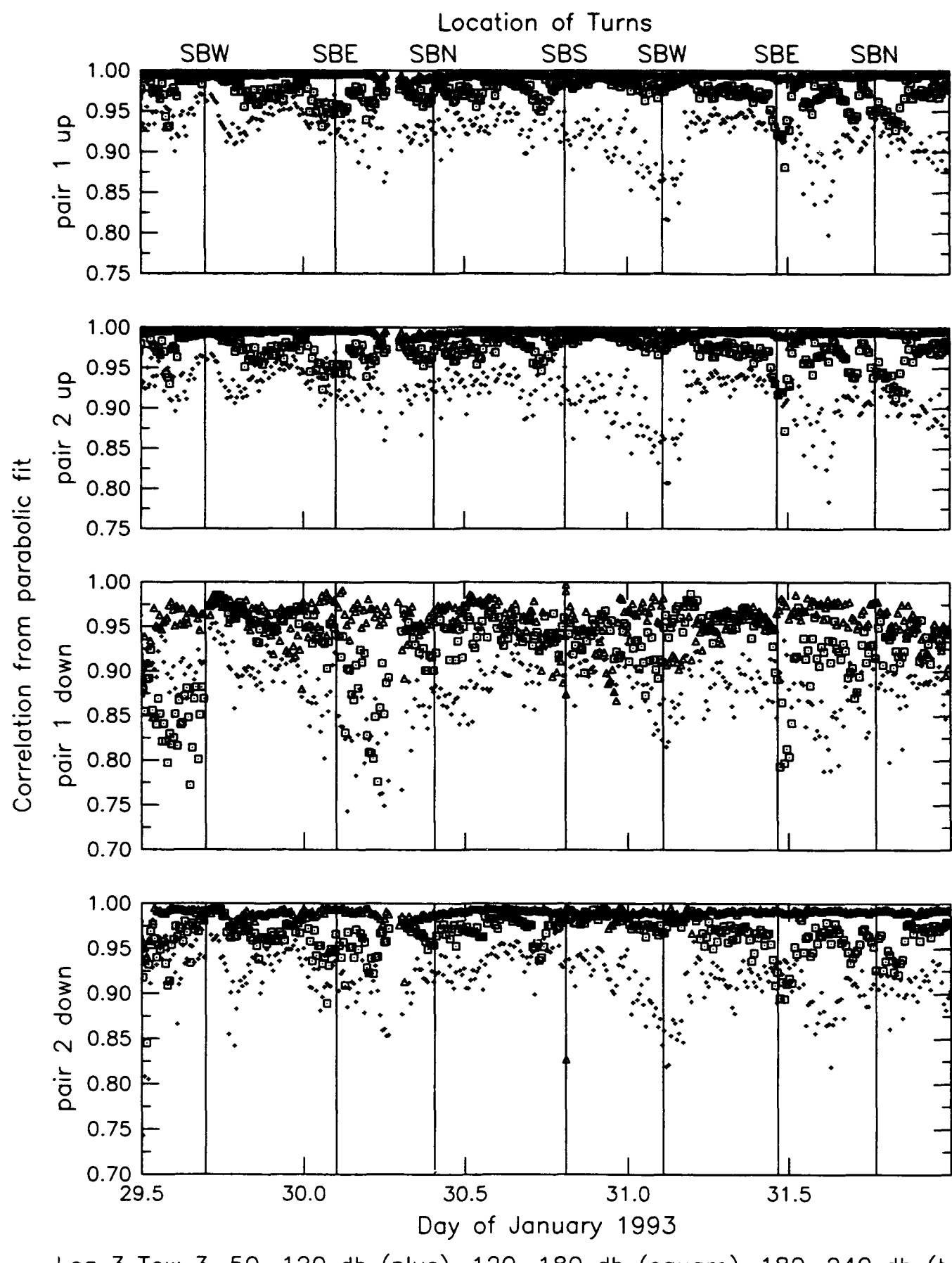
**Time Series of Lag of Maximum T/C Correlation  
for Seasoar Tows 2-6**

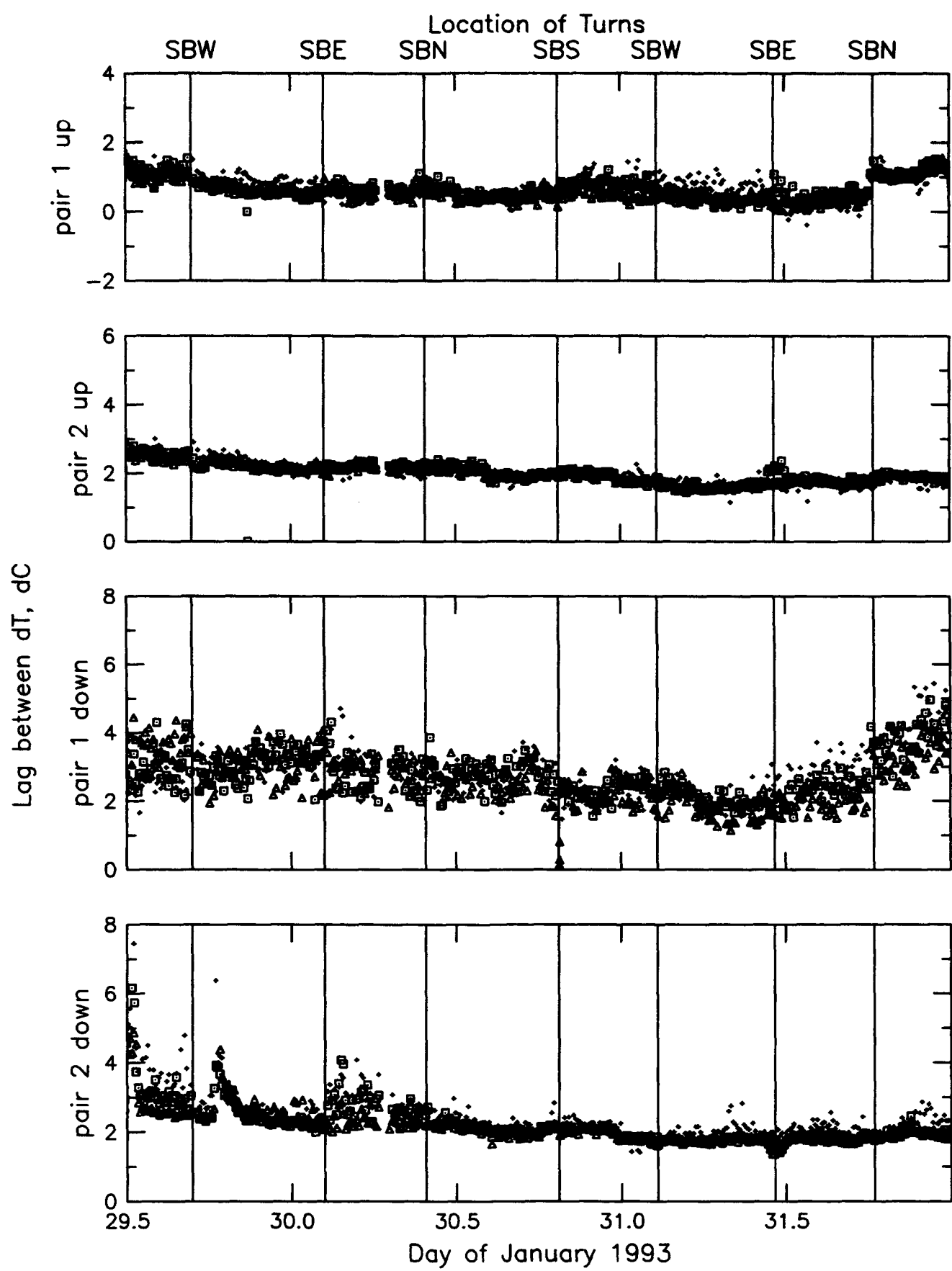


Leg 3 Tow 2, 50–120 db (plus), 120–180 db (square), 180–240 db (triangle)

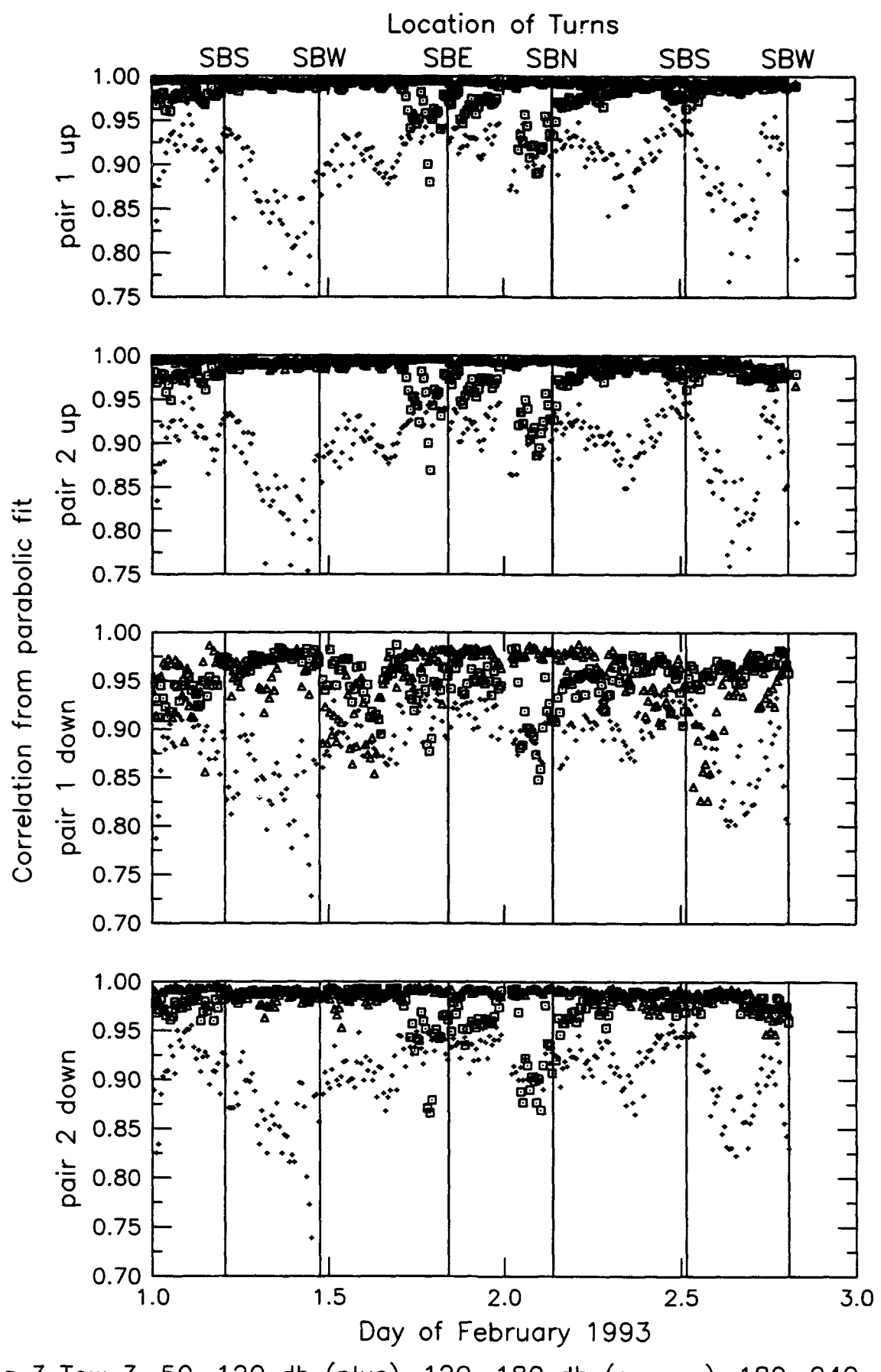


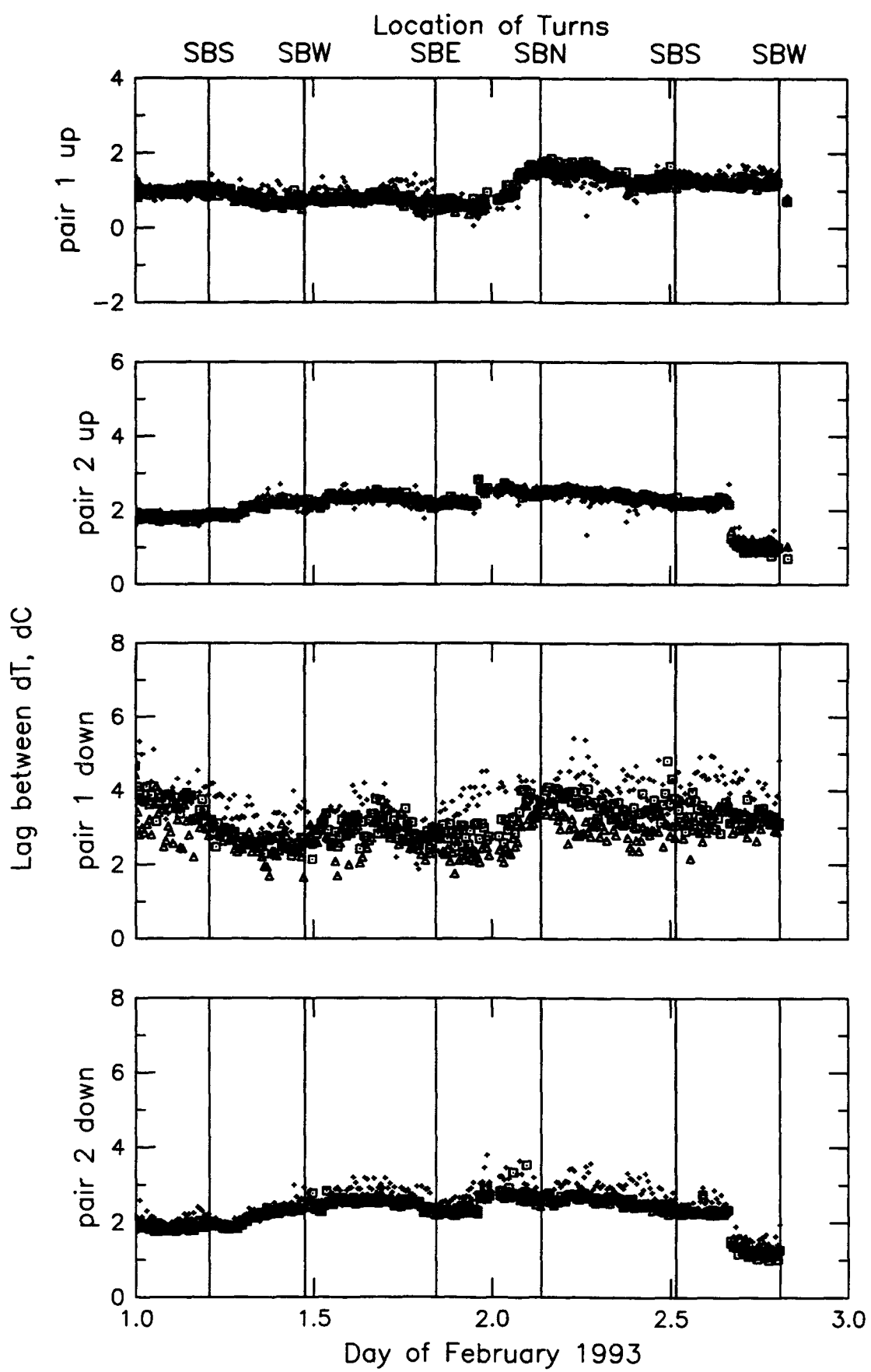
Leg 3 Tow 2, 50–120 db (plus), 120–180 db (square), 180–240 db (triangle)



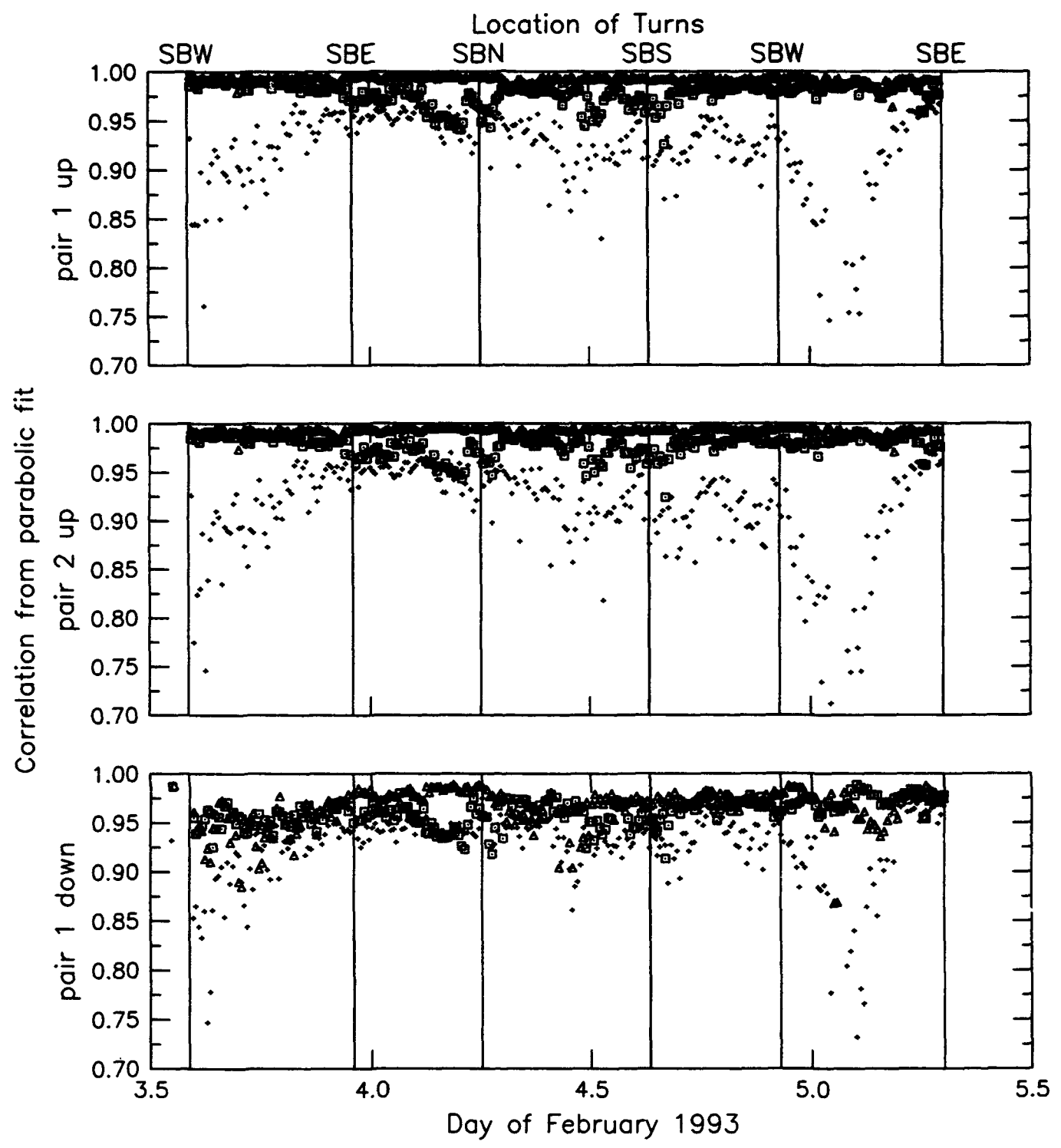


Leg 3 Tow 3, 50–120 db (plus), 120–180 db (square), 180–240 db (triangle)

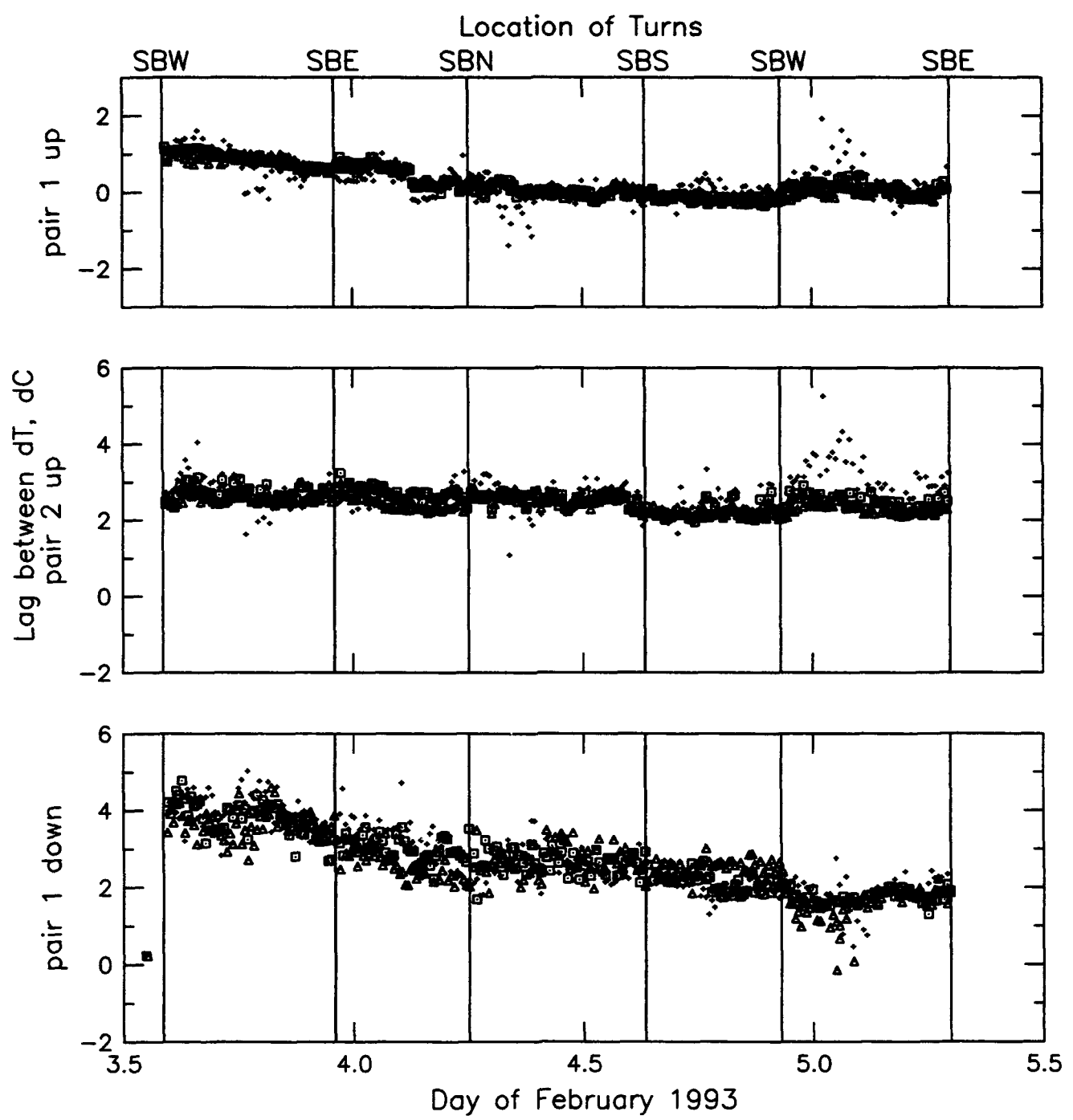




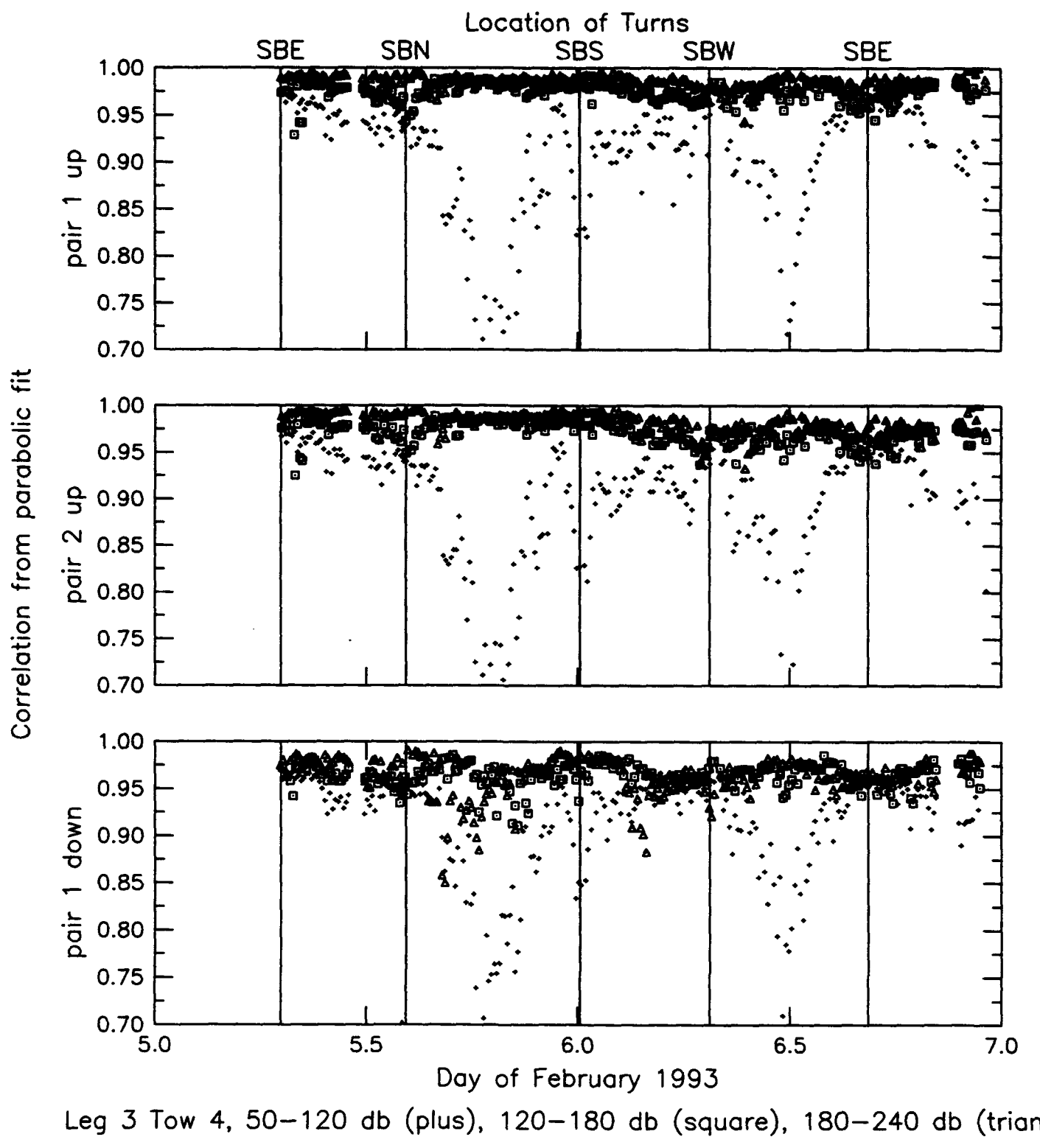
Tow 3 Leg 3, 50–120 db (plus), 120–180 db (square), 180–240 db (triangle)

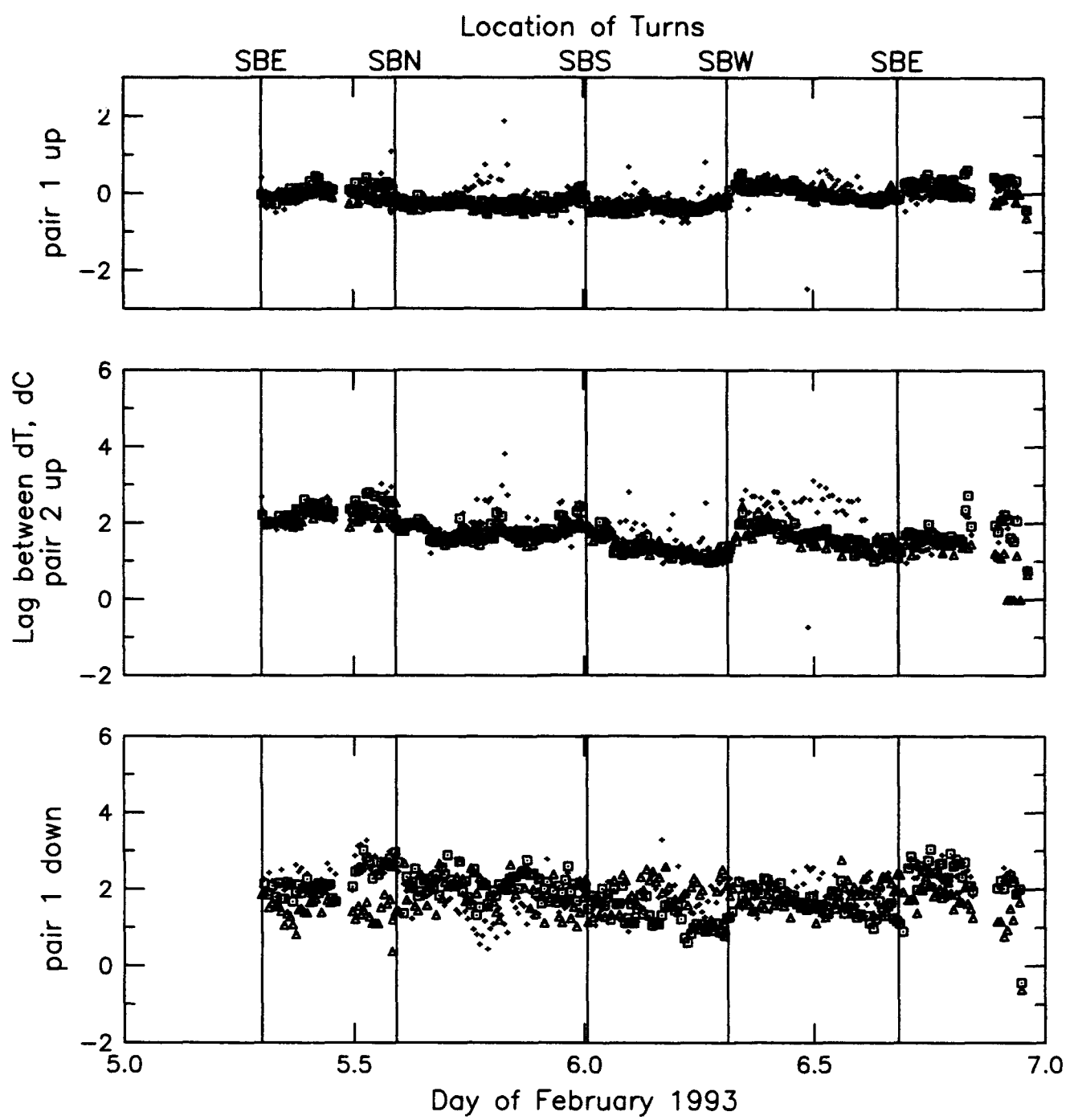


Leg 3 Tow 4, 50–120 db (plus), 120–180 db (square), 180–240 db (triangle)

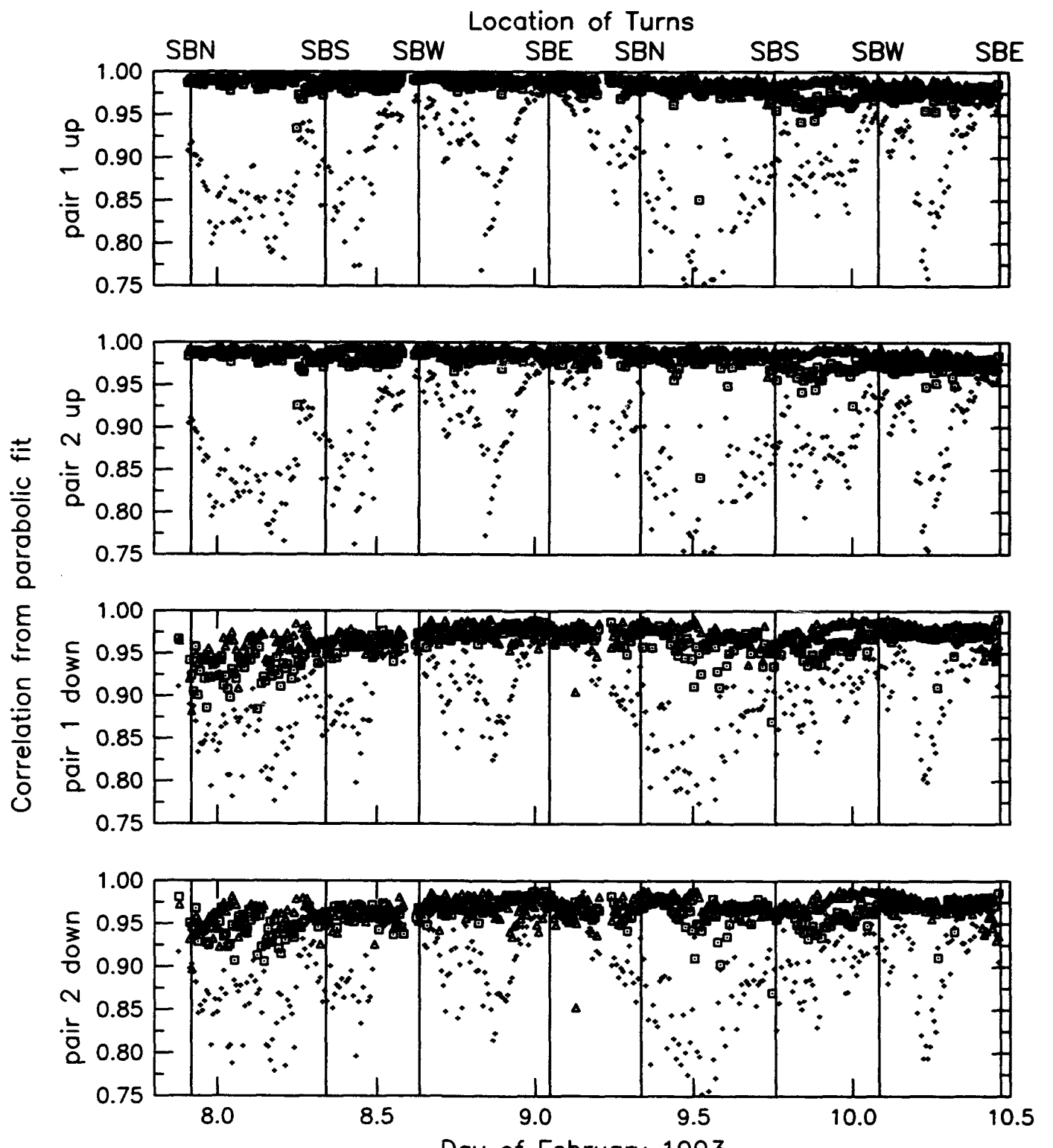


Leg 3 Tow 4, 50-120 db (plus), 120-180 db (square), 180-240 db (triangle)

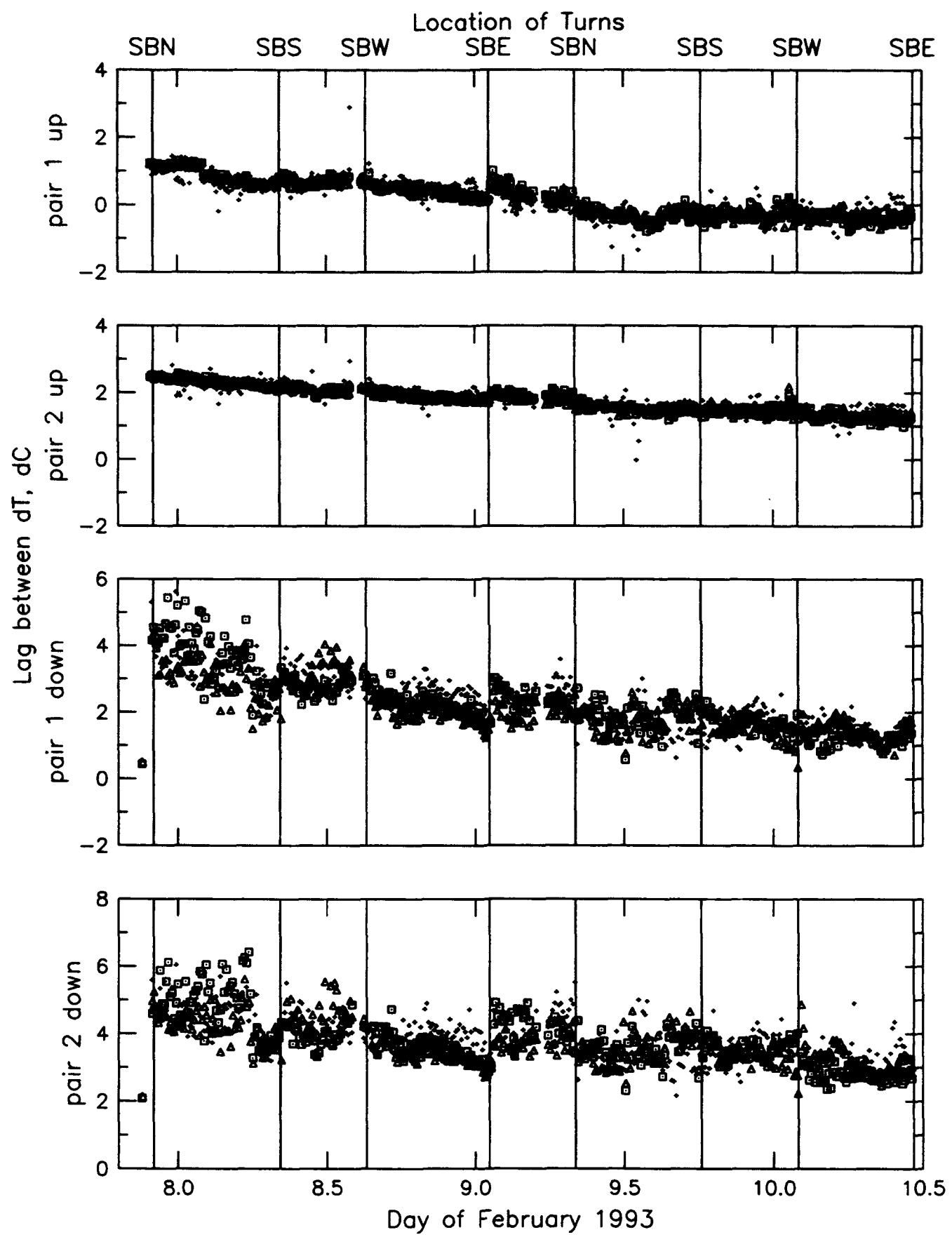


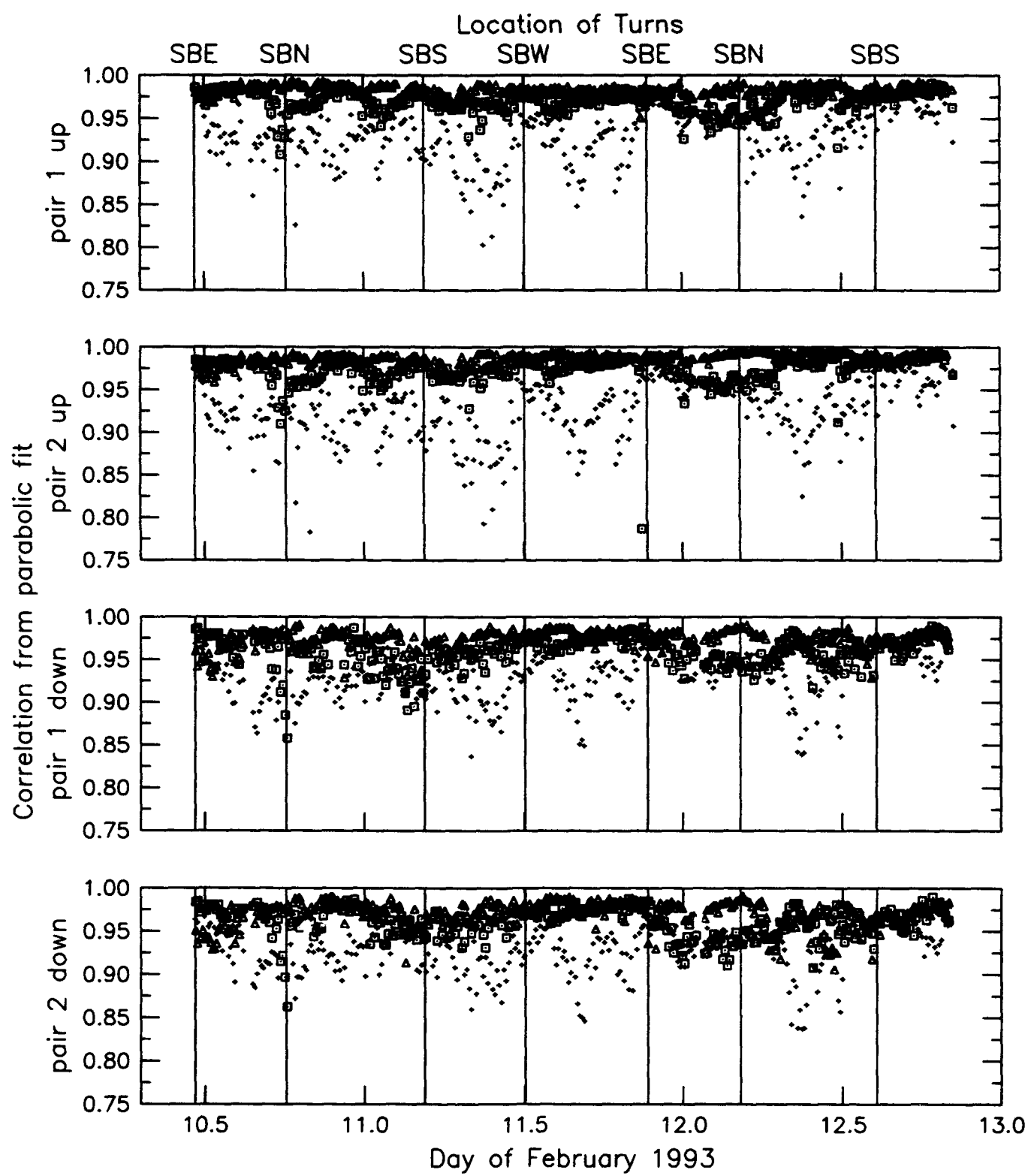


Leg 3 Tow 4, 50–120 db (plus), 120–180 db (square), 180–240 db (triangle)

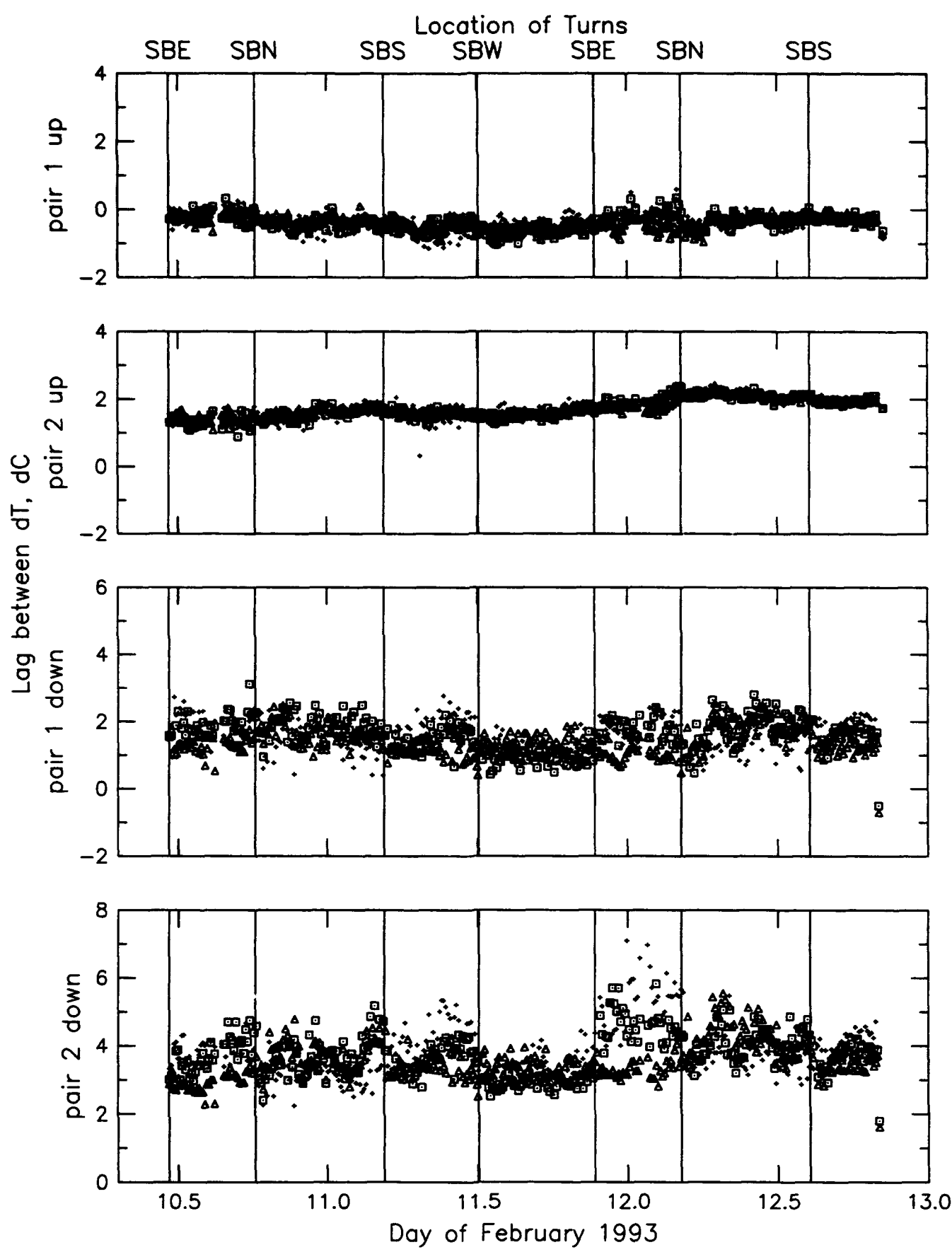


Leg 3 Tow 5, 50–120 db (plus), 120–180 db (square), 180–240 db (triangle)

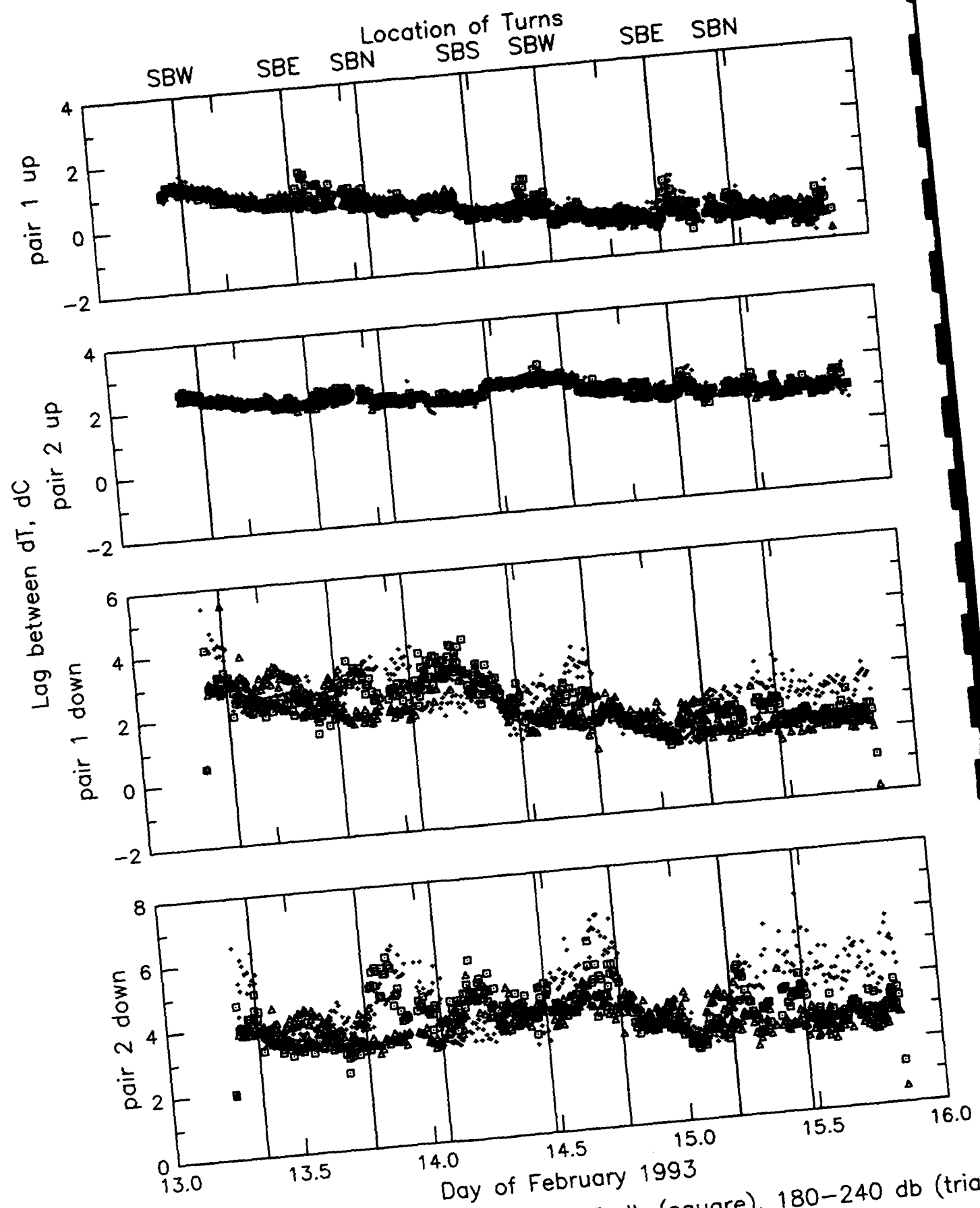




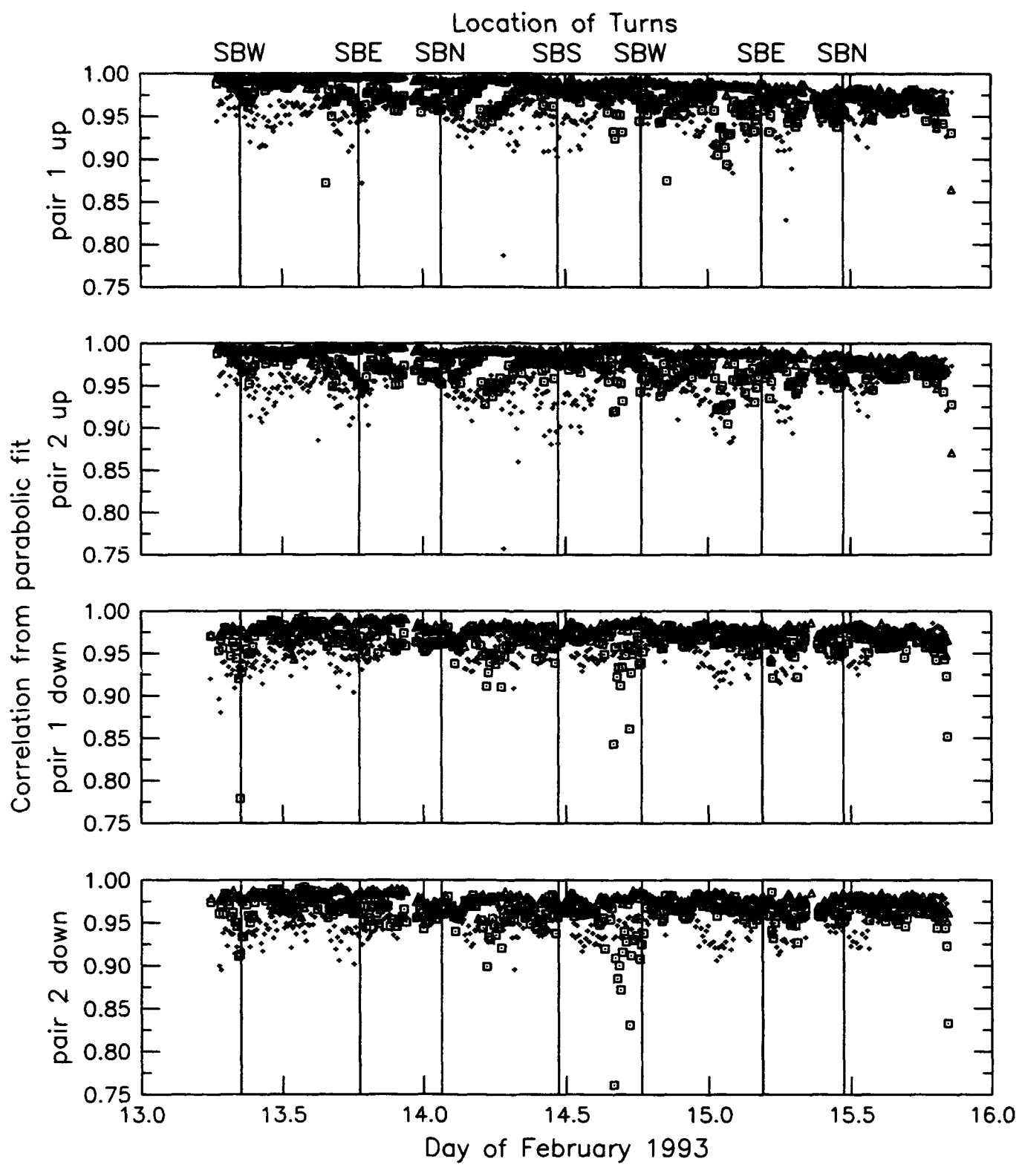
Leg 3 Tow 5, 50–120 db (plus), 120–180 db (square), 180–240 db (triangle)



Leg 3 Tow 5, 50–120 db (plus), 120–180 db (square), 180–240 db (triangle)



Leg 3 Tow 6, 50-120 db (plus), 120-180 db (square), 180-240 db (triangle)



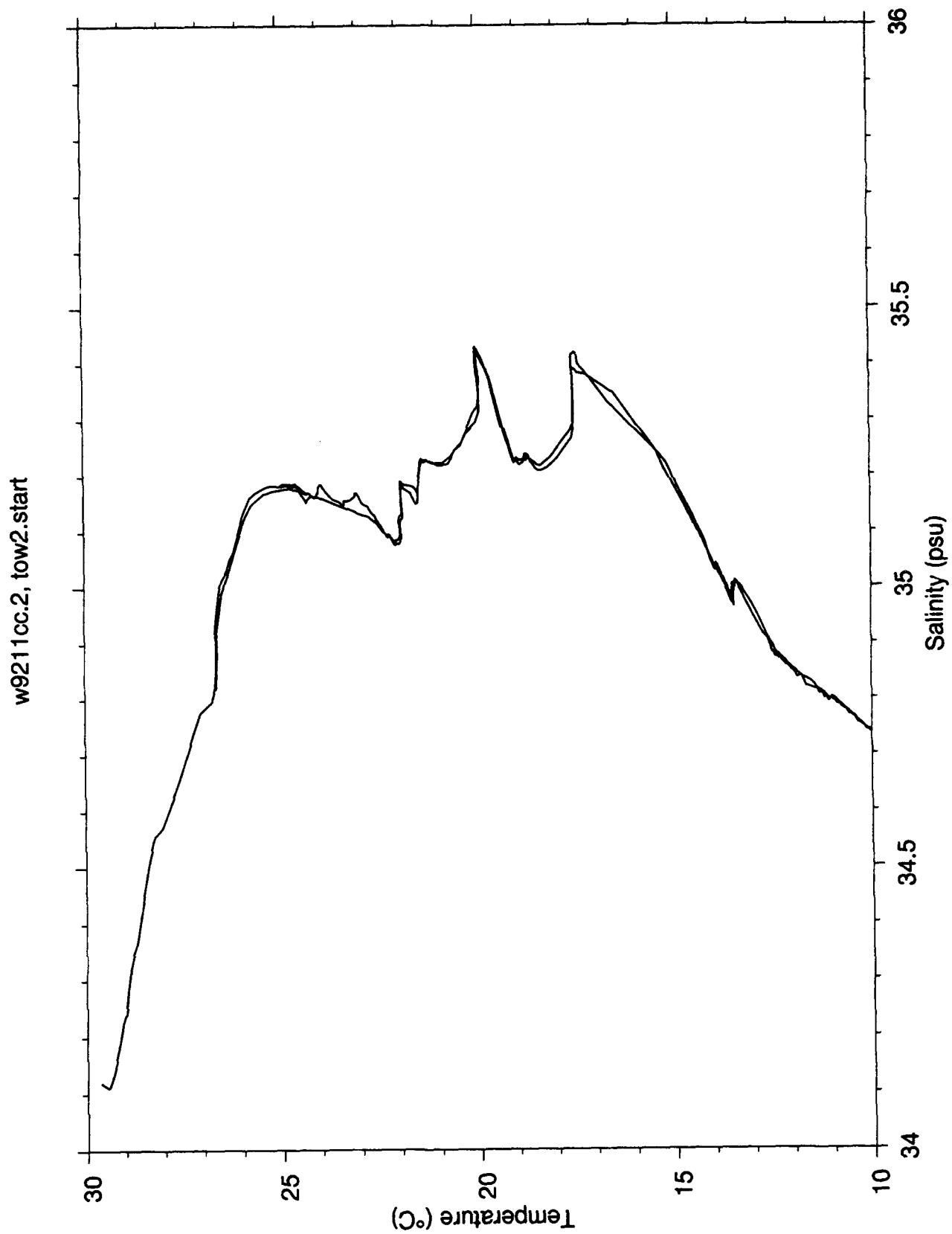
Leg 3 Tow 6, 50-120 db (plus), 120-180 db (square), 180-240 db (triangle)

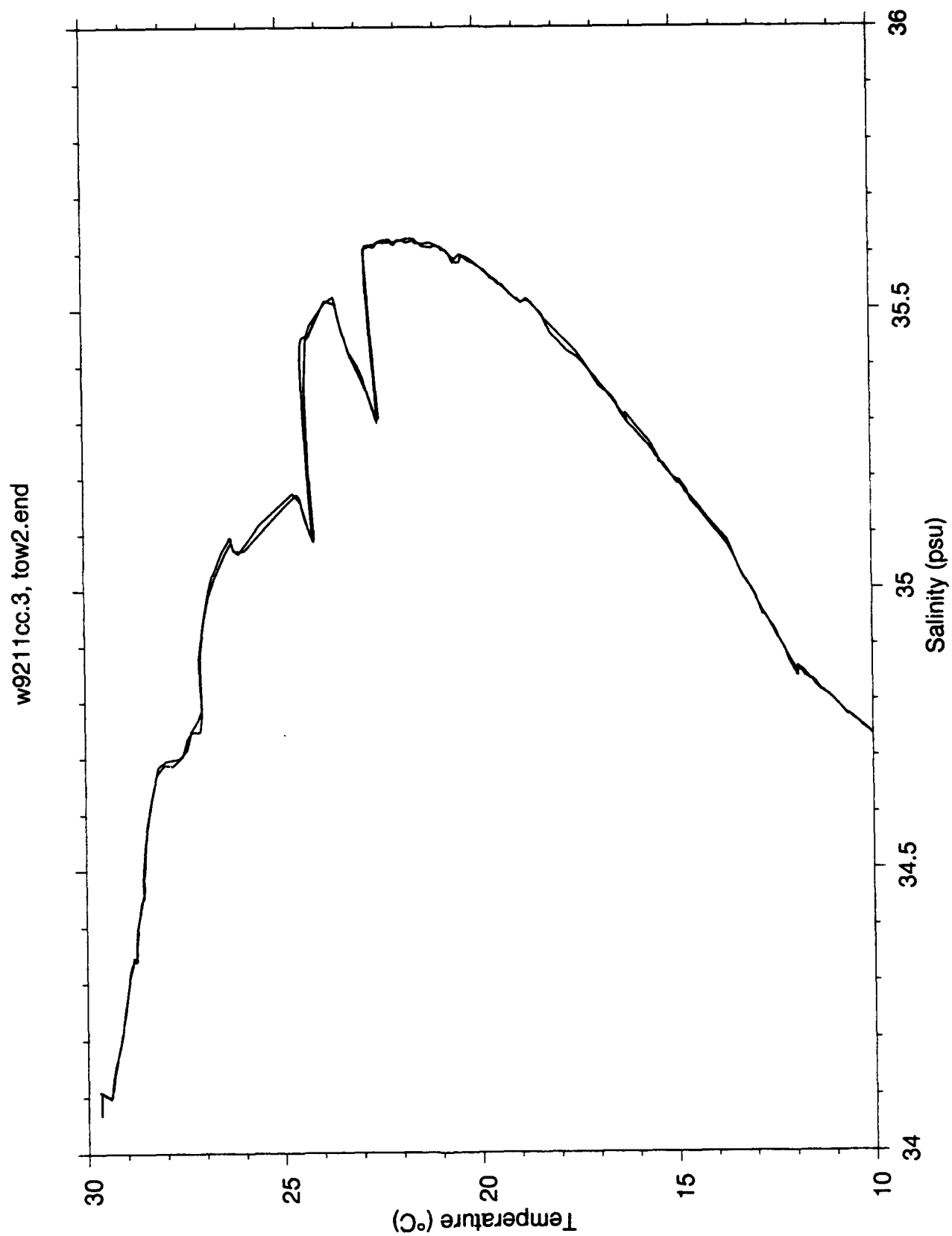


**APPENDIX B:**

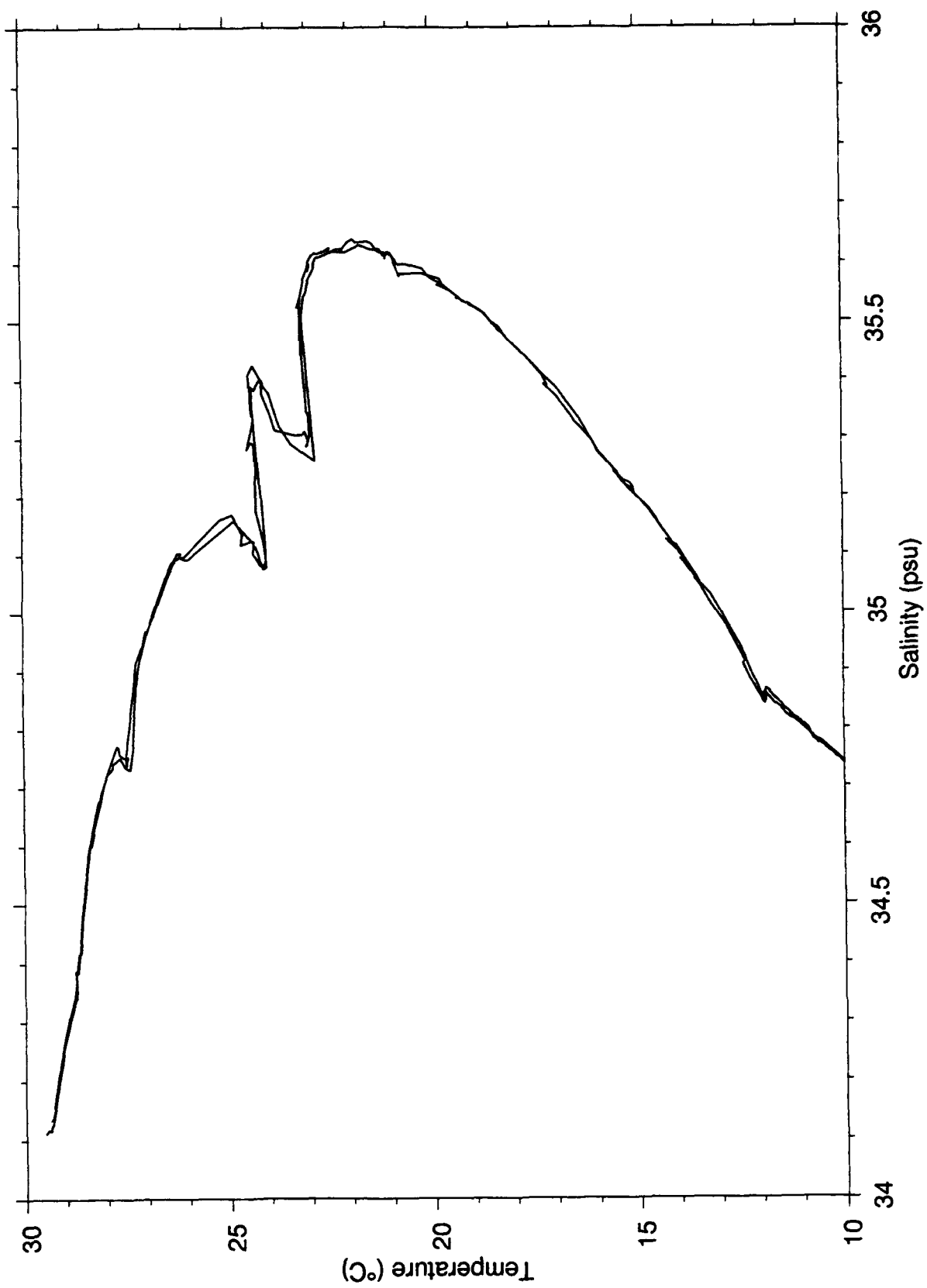
**T-S Diagrams from CTD and Seasoar**

**at Start and End of Tows 2-6.**

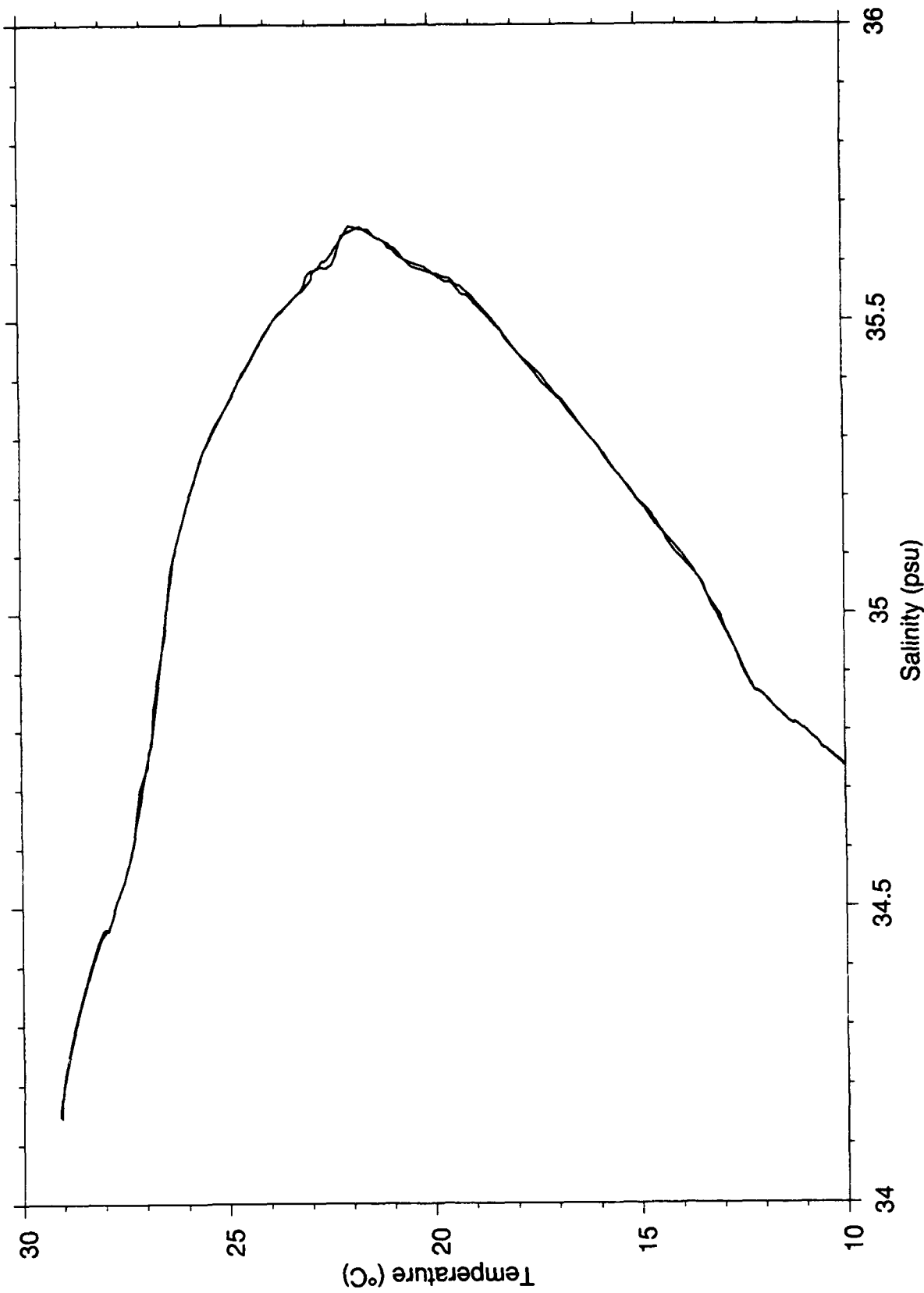




w9211cc.4, tow3 start

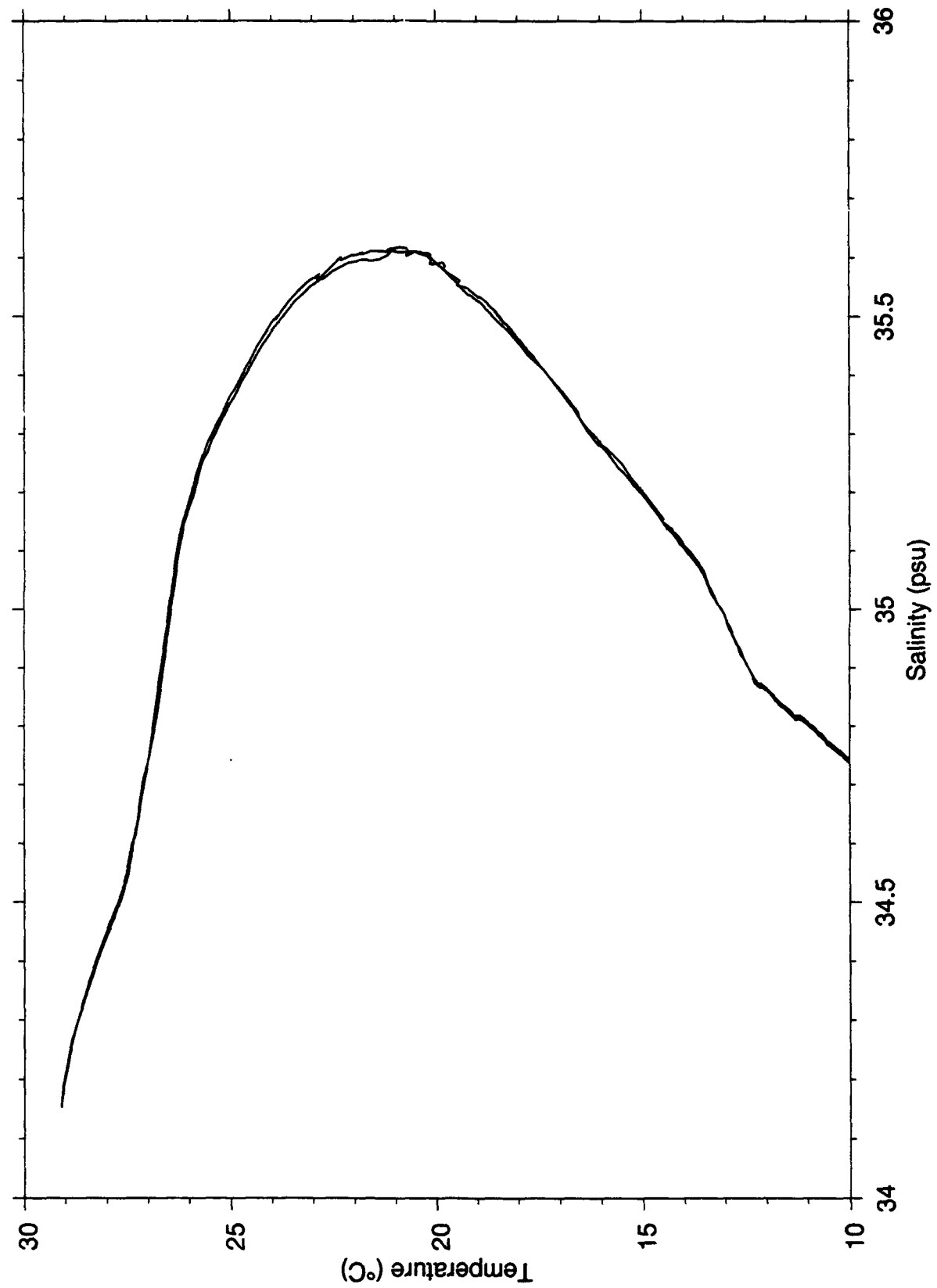


w9211cc.5, tow3.end

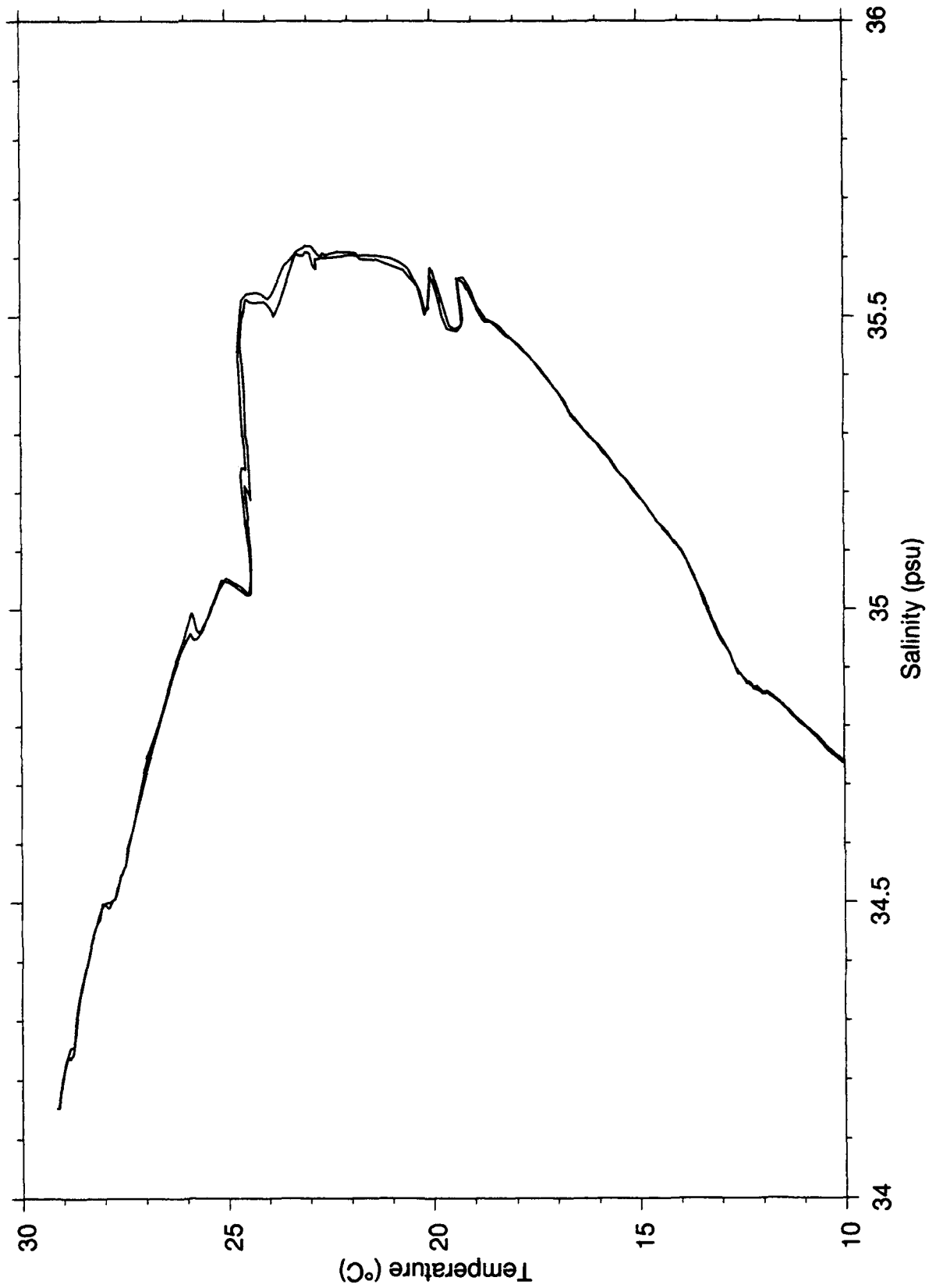


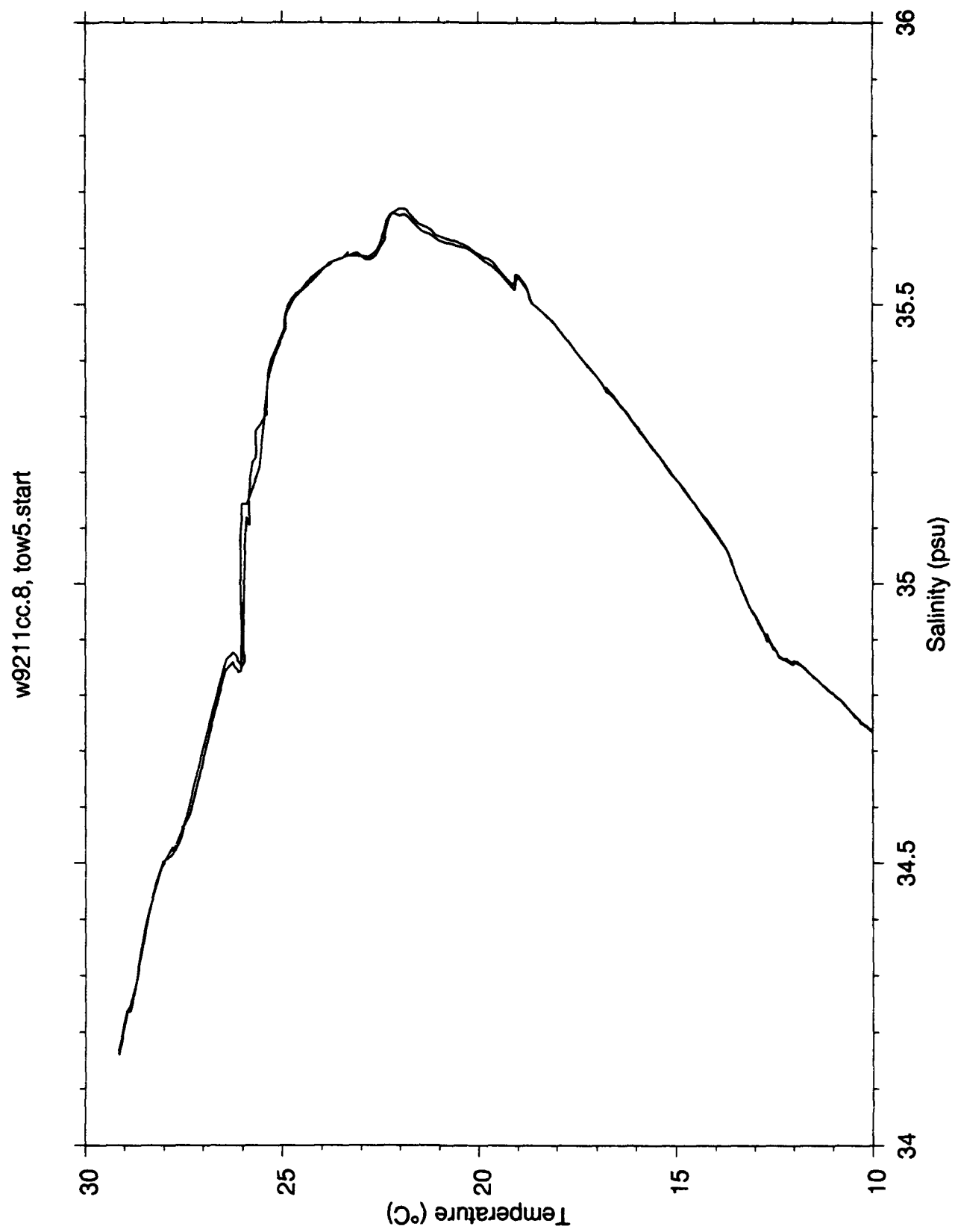
320

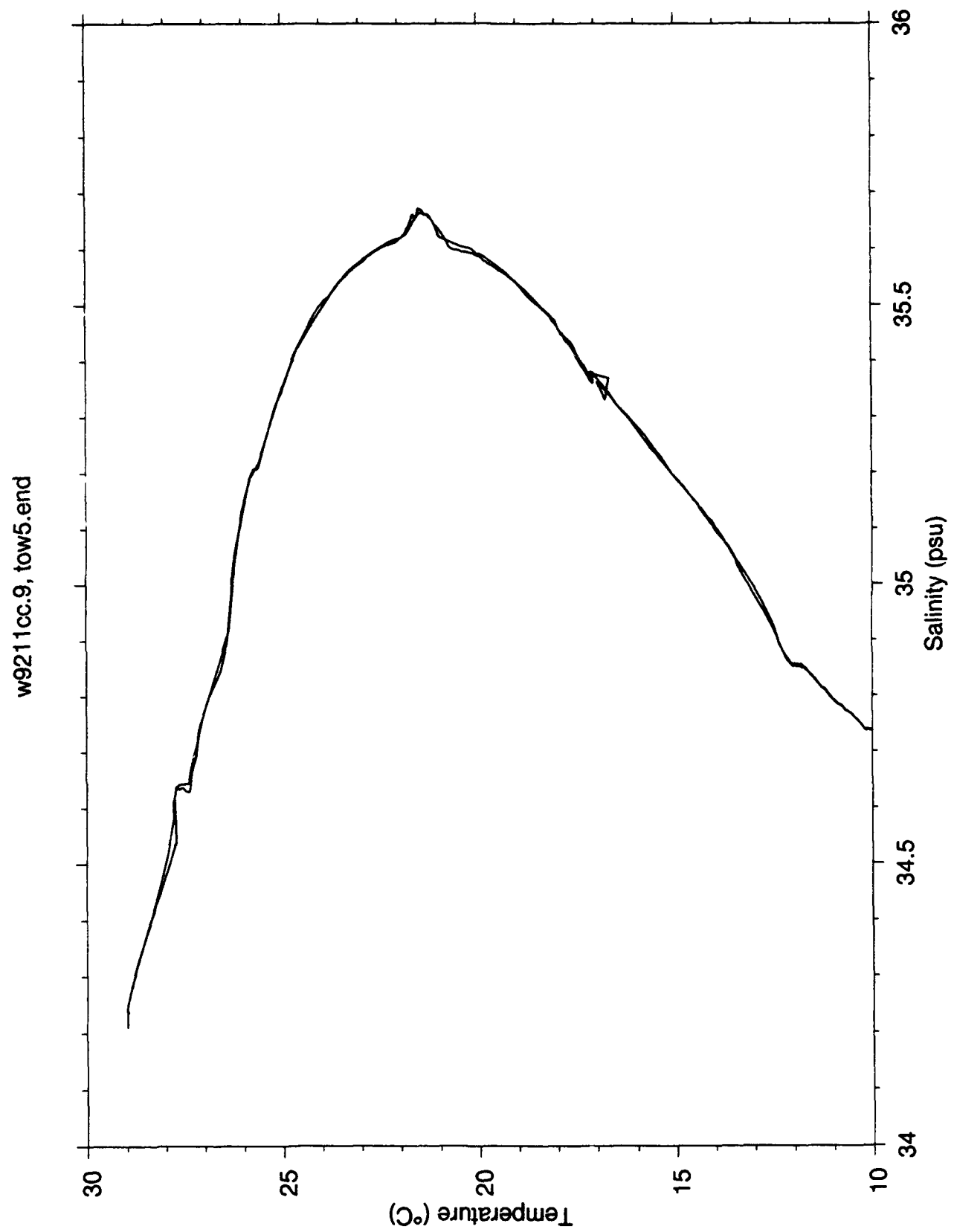
w9211cc.6, tow4.start



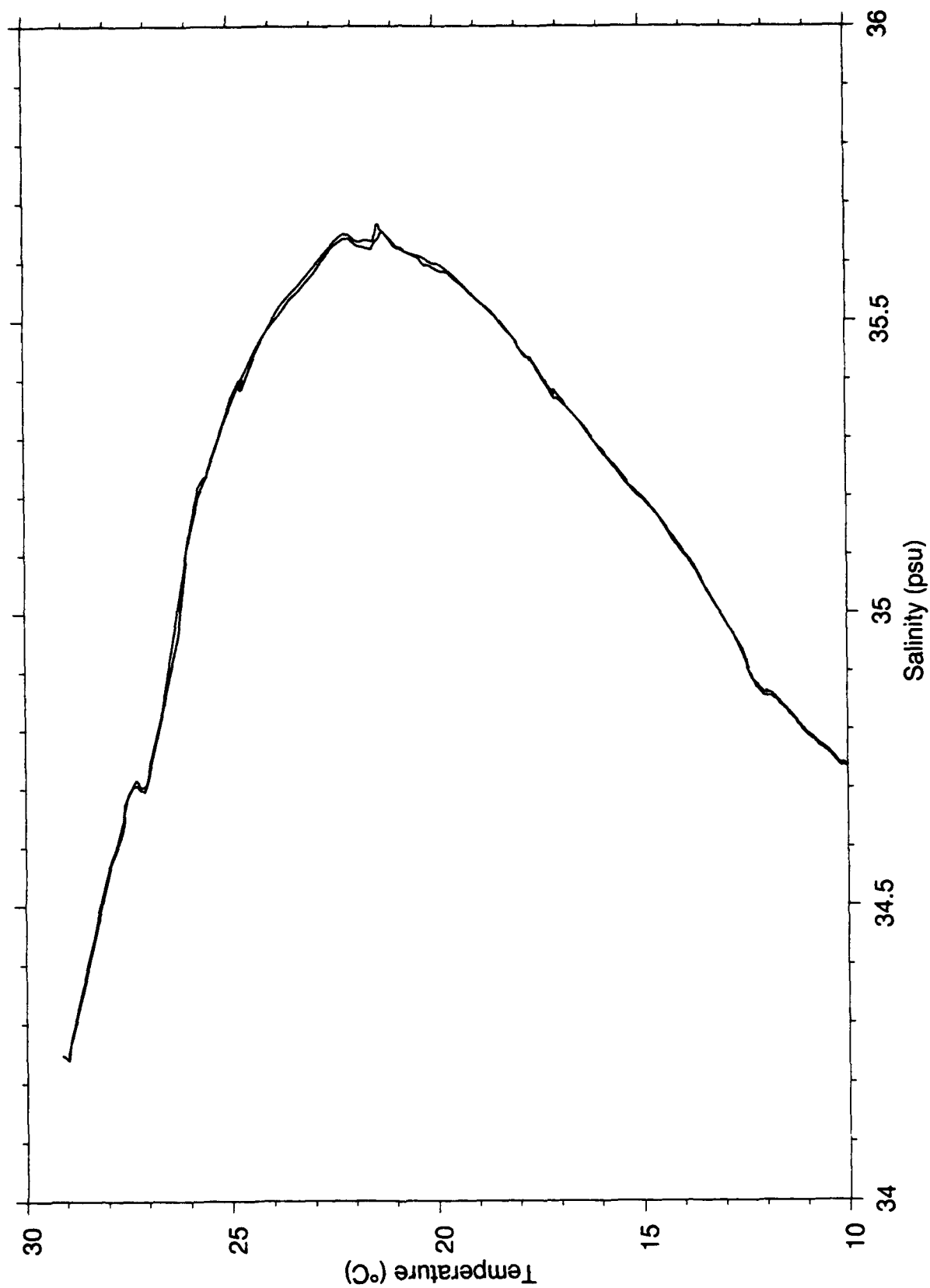
w9211cc.7, tow4.end







w9211cc.11, tow6.start



w9211cc.12, tow6.end

